

**COMPRESSIVE STRENGTH OF BRICKWORK MASONRY  
WITH SPECIAL REFERENCE TO  
CONCENTRATED LOAD**

by

**Mohammad H. Malek**

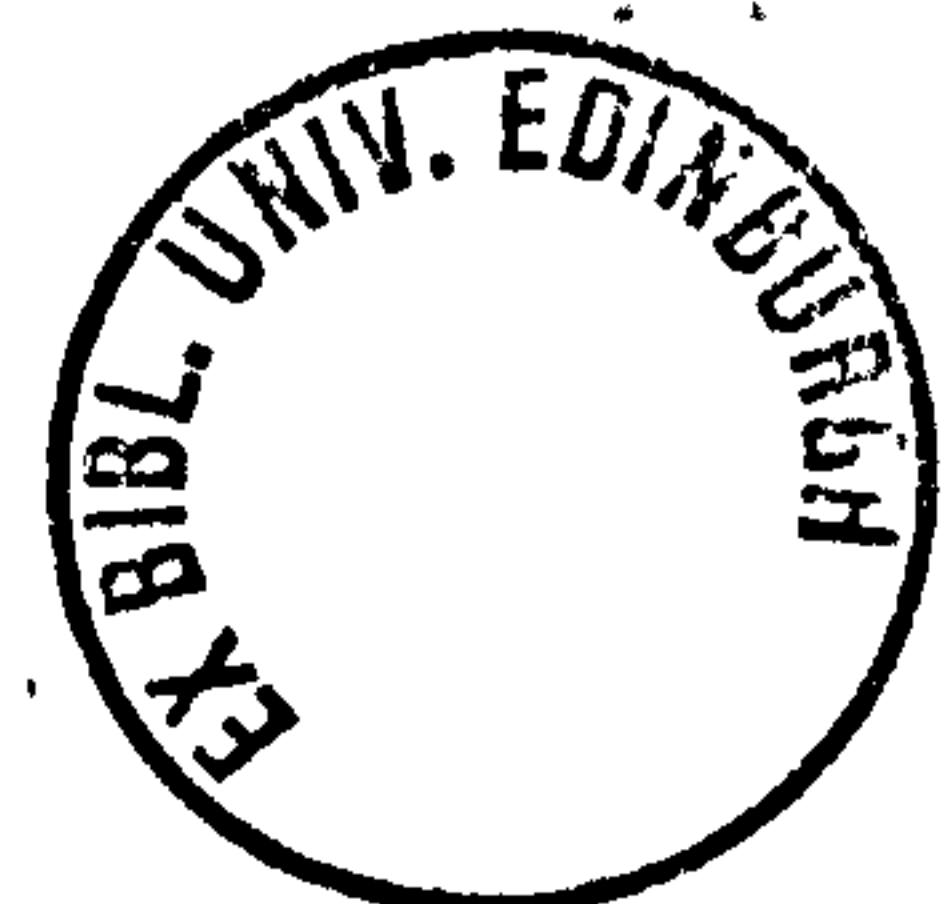
**B.Sc. Hons. (Edinburgh)**

Thesis submitted for the  
Degree of  
Doctor of Philosophy

**Department of Civil Engineering and Building Science**

**University of Edinburgh**

**October 1987**



## PREFACE

It is declared that the thesis has been composed by the author himself, and the work embodied in this thesis is the result of original research which has been carried out and achieved solely by him unless otherwise stated, and have not been submitted for a higher degree to any other University or Institution.

During the period of research two papers have been accepted for publication. The titles are as follows:

1. "Characteristic Compressive Strength of Brickwork Walls from Collected Test Results", *Masonry International*, No. 7, March 1986.
2. "Compressive Strength of Brickwork Masonry Under Concentrated Loading", *Proc. of the British Masonry Society*, No. 2, 1987.

Also the following papers and technical notes are being prepared and will be submitted for publication in referred journals:

1. "Failure Mechanism and Failure Envelope for Brickwork Masonry Under Concentrated Load".
2. "Comparative Study of Bearing Capacity of Clay and AAC Brickwork Masonry Under Concentrated Load".
3. "Characteristic Bearing Strength and Parameters Affecting the Compressive Strength of Brickwork Masonry Under Concentrated Load".
4. "Effect of Pre-compression on the Bearing Strength of Masonry Under the Action of Concentrated Load Transmitted Through Built-in-beam".

Edinburgh, October 1987

M.H. Malek

## ABSTRACT

This thesis presents a comprehensive experimental study for the behaviour of brickwork masonry subjected to concentrated load applied through a rigid steel bearing plate and investigates the enhancement in strength under this type of loading in relation to its uni-axial compressive strength. To normalize the bearing strength under partial load, a thorough investigation has been carried out to establish accurate values for the characteristic compressive strength of masonry based on the limit state theory. This has been achieved by analysing statistically the data collected on the crushing strength of full storey-height brickwork walls. Relationships for mean and characteristic strengths for brickwork wall and brickwork masonry have been derived in terms of unit brick crushing strength for two mortar mixes and wall thicknesses and also in terms of unit brick and mortar cube strengths for two brick masonry thicknesses. Previous investigations of the compressive strength of brickwork masonry under uniform and partial load together with the design rules given in various codes are reviewed. A complete experimental study of materials properties used in the present research including the detailed study of the behaviour of brickwork masonry under the action of concentrated load are presented. In all 338 brickwork panels constructed from seven different brick types and two mortar grades were tested of which 300 were subjected to concentrated loads and the remaining under uni-axial load. The test results together with the results of 56 specimens tested under concentrated load prior to this investigation with their crack pattern and failure mode are reported. The results are analysed statistically and design charts for the characteristic bearing strength of masonry for various loaded area ratios are obtained. The influence of parameters such as loaded area ratio, loading position, loading configuration, strength of constituent materials, masonry thickness, element aspect ratio and the effective area of brickwork on the bearing strength and enhancement factor are examined. A theoretical investigation into the stress distribution of brickwork masonry under concentrated loading by Finite Element method is reported assuming brickwork as a homogeneous continuum and as an assemblage of separate bricks and mortar joints. Linear elastic and nonlinear analyses are performed using a standard package. A mechanism of failure is proposed for masonry under partial load. Based on the results obtained experimentally failure envelopes are derived for two masonry thicknesses. Finally, design rules based on the outcome of this investigation are proposed.

## ACKNOWLEDGEMENTS

The author wishes to thank Professor A.W. Hendry for providing the opportunity to carry out this research under his personal supervision, and gratefully acknowledges the encouragement, understanding and assistance during this period.

Thanks are also due to Dr. S.R. Davies, Dr. R. Royles, Dr. B.P. Sinha and the technical staff of the Department of Civil Engineering and Building Science at the University of Edinburgh.

The Brick Development Association is thanked for its financial assistance.

Last but not least, thanks are also given to my parents, brothers and their family and all of my friends for their encouragement and continuous support.

## TABLE OF CONTENTS

<b>PREFACE</b>	<b>ii</b>
<b>ABSTRACT</b>	<b>iii</b>
<b>ACKNOWLEDGEMENTS</b>	<b>iv</b>
<b>TABLE OF CONTENTS</b>	<b>v</b>
<b>LIST OF FIGURES</b>	<b>ix</b>
<b>LIST OF TABLES</b>	<b>xviii</b>
<b>NOTATIONS</b>	<b>xxi</b>
<b>1 INTRODUCTION</b>	<b>1</b>
<b>2 CHARACTERISTIC COMPRESSIVE STRENGTH OF BRICKWORK MASONRY</b>	<b>8</b>
2.1 INTRODUCTION	8
2.2 CONCEPT OF CHARACTERISTIC STRENGTH	11
2.3 REVIEW OF PREVIOUS WORK	14
2.4 DETERMINATION OF CHARACTERISTIC COMPRESSIVE STRENGTH OF BRICKWORK WALLS	19
2.4.1 Introduction	19
2.4.2 Sorted Data	21
2.4.3 Statistical Model for the Determination of characteristic strength	21
2.4.4 Statistical Analysis of the Data	25
2.4.4.1 Wall strength in terms of unit brick strength	25
2.4.4.2 Wall strength in terms of unit brick and mortar cube strength	33
2.5 CHARACTERISTIC COMPRESSIVE STRENGTH OF MASONRY	39
2.6 DISCUSSIONS	46
2.7 CONCLUSIONS	48

<b>3</b>	<b>COMPRESSIVE STRENGTH OF MASONRY UNDER CONCENTRATED LOADING</b>	<b>55</b>
	3.1 INTRODUCTION	55
	3.2 REVIEW OF PREVIOUS RESEARCH	56
	3.3 CURRENT DESIGN GUIDES	67
	3.4 SUMMARY	74
<b>4</b>	<b>EXPERIMENTAL STUDY: MATERIALS PROPERTIES</b>	<b>75</b>
	4.1 INTRODUCTION	75
	4.2 PROPERTIES OF BRICKS	75
	4.2.1 Dimensions	75
	4.2.2 Density	75
	4.2.3 Water Absorption	76
	4.2.3.1 5-hour boiling test	76
	4.2.3.2 24-hour cold immersion test	76
	4.2.4 Compressive Strength	76
	4.2.5 Elastic Properties	76
	4.3 PROPERTIES OF MORTARS	77
	4.3.1 Proportioning and Materials	77
	4.3.1.1 Sand	88
	4.3.1.2 Cement	88
	4.3.1.3 Lime	88
	4.3.2 Density	88
	4.3.3 Compressive Strength	88
	4.3.4 Elastic Properties	88
	4.4 PROPERTIES OF BRICKWORK MASONRY	89
	4.4.1 Dimensions	89
	4.4.2 Density	89
	4.4.3 Compressive Strength	89
	4.4.4 Characteristic Compressive Strength	95
	4.4.5 Elastic Properties	95
	DISCUSION AND CONCLUSIONS	95
<b>5</b>	<b>EXPERIMENTAL STUDY: CONCENTRATED LOAD ON BRICKWORK</b>	<b>104</b>
	5.1 INTRODUCTION	104
	5.2 CONSTRUCTION OF BRICKWORK SPECIMENS	104
	5.2.1 Construction of Brickwork Walleτες	104
	5.2.2 Construction of Brickwork Control Specimens	104

TESTING EQUIPMENT	105
METHOD OF TESTING	106
5.4.1 Preparation of Specimens	106
5.4.2 Loading Conditions	106
5.4.3 Rate of Loading	108
5.4.4 Bearing Plates	108
5.5 TEST PROGRAMME	109
5.6 TEST RESULTS	109
<b>6 EXPERIMENTAL STUDY: ANALYSIS OF RESULTS</b>	<b>127</b>
6.1 INTRODUCTION	127
6.2 ENHANCEMENT FACTOR ( $\zeta$ )	127
6.3 CHARACTERISTIC BEARING STRENGTH OF MASONRY ( $f'_{cb}$ )	145
6.4 FACTORS AFFECTING THE BEARING STRENGTH	146
6.4.1 Loaded Area ratio	146
6.4.2 Masonry and its Constituent materials strengths	157
6.4.3 Masonry Thickness	157
6.4.4 Aspect Ratio	167
6.4.5 Loading Position	173
6.4.6 Loading Configuration	173
6.4.7 Type of Brick Unit	185
6.5 EFFECTIVE AREA CONTRIBUTING TO THE BEARING CAPACITY	185
6.5.1 Effective Length	185
6.5.2 Effective Thickness	186
6.5.3 Effective Area	186
6.6 MODE OF FAILURE	194
6.6.1 Strip Loading Configuration	194
6.6.2 Edge Loading Configuration	195
6.7 SUMMARY AND CONCLUSIONS	219
<b>7 STRESS DISTRIBUTION IN MASONRY UNDER CONCENTRATED LOAD</b>	<b>221</b>
7.1 INTRODUCTION	221
7.2 METHOD OF FINITE ELEMENT ANALYSIS	221
7.3 RESULTS OF FINITE ELEMENT ANALYSES	223
7.3.1 Concentric Position	223
7.3.1.1 Homogeneous	223
7.3.1.2 Non-homogeneous	224
7.3.1.3 Nonlinear analysis	225

Eccentric Position	225
SUMMARY AND CONCLUSIONS	226
<b>8 FAILURE MECHANISM, ENVELOPE AND DESIGN RECOMMENDATION</b>	<b>235</b>
8.1 FAILURE MECHANISM OF MASONRY UNDER CONCENTRATED LOAD	235
8.2 FAILURE ENVELOPE FOR MASONRY UNDER CONCENTRATED LOAD	239
8.3 DESIGN RECOMMENDATION	240
8.4 SUMMARY AND CONCLUSIONS	244
<b>9 GENERAL SUMMARY AND CONCLUSIONS</b>	<b>251</b>
9.1 GENERAL SUMMARY	251
9.2 GENERAL CONCLUSIONS	252
9.3 SUGGESTIONS FOR FURTHER RESEARCH	255
<b>REFERENCES</b>	<b>256</b>
<b>I APPENDIX A</b>	<b>264</b>
I.I METHOD OF CALCULATING CHARACTERISTIC COMPRESSIVE STRENGTH OF BRICKWORK MASONRY FROM SMALL NUMBER OF TEST RESULTS	264
I.II COLLECTED DATA	266
I.III STATISTICAL ANALYSIS OF BRICKWORK WALL STRENGTH IN TERMS OF UNIT BRICK STRENGTH	287
I.IV STATISTICAL ANALYSIS OF BRICKWORK WALL STRENGTH IN TERMS OF UNIT BRICK AND MORTAR CUBE STRENGTHS	301
I.V STATISTICAL ANALYSES OF MORTAR CUBE STRENGTHS	306
<b>II APPENDIX B</b>	<b>310</b>
II.I RESULTS OF TESTS ON BRICKWORK UNDER CONCENTRATED LOAD	310



## LIST OF FIGURES

### Chapter 1

- Fig. 1. 1- Typical concentrated load problems in brickwork masonry.  
Fig. 1. 2- Typical stress blocks under steel beam applying concentrated load.

### Chapter 2

- Fig. 2. 1- Variation of  $k$  with number of test specimens.  
Fig. 2. 2- Flow chart of statistical analysis.  
Fig. 2. 3- Plot of results for 102.5mm thick wall and mortar M(i).  
Fig. 2. 4- Plot of results for 102.5mm thick wall and mortar M(iii).  
Fig. 2. 5- Plot of results for 215.0mm thick wall and mortar M(i).  
Fig. 2. 6- Plot of results for 215.0mm thick wall and mortar M(iii).  
Fig. 2. 7- Plot of characteristic compressive strength for two mortar mixes and wall thicknesses.  
Fig. 2. 8- Mean compressive strength of 102.5mm thick walls.  
Fig. 2. 9- Characteristic compressive strength of 102.5mm thick walls.  
Fig. 2.10- Mean compressive strength of 215.0mm thick walls.  
Fig. 2.11- Characteristic compressive strength of 215.0mm thick walls.  
Fig. 2.12- Mean compressive strength of masonry,  $f_{mm}$ , 102.5mm thick.  
Fig. 2.13- Mean compressive strength of masonry,  $f_{mm}$ , 215.0mm thick.  
Fig. 2.14- Characteristic compressive strength of masonry,  $f_k$ , 102.5mm thick.  
Fig. 2.15- Characteristic compressive strength of masonry,  $f_k$ , 215.0mm thick.  
Fig. 2.16- Comparison between the characteristic compressive strengths of masonry,  $f_k$ , 102.5mm thick determined from the wall test results and the Code<sup>[1]</sup>.  
Fig. 2.17- Comparison between the characteristic compressive strengths of masonry,  $f_k$ , 215.0mm thick determined from the wall test results and the Code<sup>[1]</sup>.  
Fig. 2.18- Comparison between  $f_{mw}$  and  $f_{kw}$  derived from the test results of storey-height walls, 102.5mm thick and mortar designation M(i) with the  $f_k$  curves from the code<sup>[1]</sup>.  
Fig. 2.19- Comparison between  $f_{mw}$  and  $f_{kw}$  derived from the test results of storey-height walls, 102.5mm thick and mortar designation M(iii) with the  $f_k$  curves from the code<sup>[1]</sup>.  
Fig. 2.20- Comparison between  $f_k$  determined from storey-height wall and 4-brick stack bonded prism test results.

### **Chapter 3**

- Fig. 3. 1- Relation between enhancement factor and the length of loading plate (after Kirtschig *et al*<sup>[66]</sup>).
- Fig. 3. 2- Effective area under bearing (after Dai-Xin<sup>[69]</sup>).
- Fig. 3. 3- Method of load application (after Lind<sup>[74]</sup>).
- Fig. 3. 4- Different bearing types given by BS 5628<sup>[1]</sup>.
- Fig. 3. 5- Distribution of concentrated load for the three types of bearings (after BS 5628<sup>[1]</sup>).
- Fig. 3. 6- Loading application and notations (after CIB code<sup>[76]</sup>).
- Fig. 3. 7- Loading application and notations (after Swedish code<sup>[84]</sup>).

### **Chapter 4**

- Fig. 4. 1- Water absorption of bricks.
- Fig. 4. 2- Testing method for elastic properties of bricks.
- Fig. 4. 3- Vertical stress-strain relationship for brick units A to E.
- Fig. 4. 4- Vertical stress-lateral strains relationship for brick units A to E.
- Fig. 4. 5- Vertical-lateral strain relationship for brick units A to E.
- Fig. 4. 6- Grading curve for mortar sand.
- Fig. 4. 7- Vertical stress-strain relationship for mortar designations M(i) and M(iii).
- Fig. 4. 8- Vertical stress-lateral strain relationship for mortar designations M(i) and M(iii).
- Fig. 4. 9- Vertical-lateral strain relationship for mortar designations M(i) and M(iii).
- Fig. 4.10- Vertical stress-strain relationship for brickwork masonry specimens
- Fig. 4.11- Vertical stress-lateral strain relationship for brickwork masonry specimens.
- Fig. 4.12- Vertical-lateral strain relationship for brickwork masonry specimen.

### **Chapter 5**

- Fig. 5. 1- Strip loading configuration.
- Fig. 5. 2- Edge loading configuration.

### **Chapter 6**

- Fig. 6. 1- Bearing strength of masonry type A as a function of loaded area ratio under central strip loading ( $t = 102.5\text{mm}$ ).
- Fig. 6. 2- Bearing strength of masonry type B as a function of loaded area ratio under central strip loading ( $t = 102.5\text{mm}$ ).

- Fig. 6. 3- Bearing strength of masonry type C as a function of loaded area ratio under central strip loading ( $t = 102.5\text{mm}$ ).
- Fig. 6. 4- Bearing strength of masonry type D as a function of loaded area ratio under central strip loading ( $t = 102.5\text{mm}$ ).
- Fig. 6. 5- Bearing strength of masonry type E as a function of loaded area ratio under central strip loading ( $t = 102.5\text{mm}$ ).
- Fig. 6. 6- Bearing strength of masonry type F as a function of loaded area ratio under central strip loading ( $t = 102.5\text{mm}$ ).
- Fig. 6. 7- Bearing strength of masonry type F as a function of loaded area ratio under central strip loading ( $t = 215.0\text{mm}$ ).
- Fig. 6. 8- Bearing strength of masonry type G as a function of loaded area ratio under central strip loading ( $t = 102.5\text{mm}$ ).
- Fig. 6. 9- Bearing strength of masonry type G as a function of loaded area ratio under central strip loading ( $t = 215.0\text{mm}$ ).
- Fig. 6.10- Bearing strength of masonry type H as a function of loaded area ratio under central strip loading ( $t = 215.0\text{mm}$ ).
- Fig. 6.11- Bearing strength of masonry type L as a function of loaded area ratio under central strip loading ( $t = 102.5\text{mm}$ ).
- Fig. 6.12- Bearing strength of masonry type E as a function of loaded area ratio under intermediate strip loading ( $t = 102.5\text{mm}$ ).
- Fig. 6.13- Bearing strength of masonry type F as a function of loaded area ratio under intermediate strip loading ( $t = 102.5\text{mm}$ ).
- Fig. 6.14- Bearing strength of masonry type F as a function of loaded area ratio under intermediate strip loading ( $t = 215.0\text{mm}$ ).
- Fig. 6.15- Bearing strength of masonry type G as a function of loaded area ratio under intermediate strip loading ( $t = 102.5\text{mm}$ ).
- Fig. 6.16- Bearing strength of masonry type G as a function of loaded area ratio under intermediate strip loading ( $t = 215.0\text{mm}$ ).
- Fig. 6.17- Bearing strength of masonry type H as a function of loaded area ratio under intermediate strip loading ( $t = 215.0\text{mm}$ ).
- Fig. 6.18- Bearing strength of masonry type L as a function of loaded area ratio under intermediate strip loading ( $t = 102.5\text{mm}$ ).
- Fig. 6.19- Bearing strength of masonry type E as a function of loaded area ratio under end strip loading ( $t = 102.5\text{mm}$ ).
- Fig. 6.20- Bearing strength of masonry type F as a function of loaded area ratio under end strip loading ( $t = 102.5\text{mm}$ ).
- Fig. 6.21- Bearing strength of masonry type F as a function of loaded area ratio under end strip loading ( $t = 215.0\text{mm}$ ).

- Fig. 6.22- Bearing strength of masonry type G as a function of loaded area ratio under end strip loading ( $t = 102.5\text{mm}$ ).
- Fig. 6.23- Bearing strength of masonry type G as a function of loaded area ratio under end strip loading ( $t = 215.0\text{mm}$ ).
- Fig. 6.24- Bearing strength of masonry type H as a function of loaded area ratio under end strip loading ( $t = 215.0\text{mm}$ ).
- Fig. 6.25- Bearing strength of masonry type L as a function of loaded area ratio under end strip loading ( $t = 102.5\text{mm}$ ).
- Fig. 6.26- Bearing strength of masonry type M as a function of loaded area ratio under central edge loading ( $t = 215.0\text{mm}$ ).
- Fig. 6.27- Bearing strength of masonry type M as a function of loaded area ratio under intermediate edge loading ( $t = 215.0\text{mm}$ ).
- Fig. 6.28- Bearing strength of masonry type M as a function of loaded area ratio under end edge loading ( $t = 215.0\text{mm}$ ).
- Fig. 6.29- Bearing strength of brickwork masonry in terms of brick strength under central strip loading ( $A_r=0.10$ ).
- Fig. 6.30- Bearing strength of brickwork masonry in terms of brick strength under central strip loading ( $A_r=0.20$ ).
- Fig. 6.31- Bearing strength of brickwork masonry in terms of brick strength under central strip loading ( $A_r=0.30$ ).
- Fig. 6.32- Bearing strength of brickwork masonry in terms of brick strength under central strip loading ( $A_r=0.40$ ).
- Fig. 6.33- Mean bearing strength of brickwork masonry in terms of brick strength and loaded area ratio under central strip loading.
- Fig. 6.34- Characteristic bearing strength of masonry in terms of brick strength and loaded area ratio under central strip loading.
- Fig. 6.35- Enhancement factor in terms of brick strength and loaded area ratio under central strip loading.
- Fig. 6.36- Influence of loaded area ratio on enhancement factor under central strip loading.
- Fig. 6.37- Influence of loaded area ratio on enhancement factor under intermediate strip loading.
- Fig. 6.38- Influence of loaded area ratio on enhancement factor under end strip loading.
- Fig. 6.39- Influence of characteristic compressive strength of masonry on the bearing strength under central strip loading.
- Fig. 6.40- Influence of characteristic compressive strength of masonry on the bearing strength under intermediate strip loading.

- Fig. 6.41-** Influence of characteristic compressive strength of masonry on the bearing strength under end strip loading.
- Fig. 6.42-** Influence of characteristic compressive strength of masonry on the enhancement factor under central strip loading.
- Fig. 6.43-** Influence of characteristic compressive strength of masonry on the enhancement factor under intermediate strip loading.
- Fig. 6.44-** Influence of characteristic compressive strength of masonry on the enhancement factor under end strip loading.
- Fig. 6.45-** Effect of specimen thickness on the bearing strength of brickwork type F under central strip loading.
- Fig. 6.46-** Effect of specimen thickness on the bearing strength of brickwork type F under intermediate strip loading.
- Fig. 6.47-** Effect of specimen thickness on the bearing strength of brickwork type F under end strip loading.
- Fig. 6.48-** Effect of specimen thickness on the bearing strength of brickwork type G under central strip loading.
- Fig. 6.49-** Effect of specimen thickness on the bearing strength of brickwork type G under intermediate strip loading.
- Fig. 6.50-** Effect of specimen thickness on the bearing strength of brickwork type G under end strip loading.
- Fig. 6.51-** Effect of specimen thickness on the enhancement factor for brickwork type F under central strip loading.
- Fig. 6.52-** Effect of specimen thickness on the enhancement factor for brickwork type F under intermediate strip loading.
- Fig. 6.53-** Effect of specimen thickness on the enhancement factor for brickwork type F under end strip loading.
- Fig. 6.54-** Effect of specimen thickness on the enhancement factor for brickwork type G under central strip loading.
- Fig. 6.55-** Effect of specimen thickness on the enhancement factor for brickwork type G under intermediate strip loading.
- Fig. 6.56-** Effect of specimen thickness on the enhancement factor for brickwork type G under end strip loading.
- Fig. 6.57-** Influence of aspect ratio on the bearing strength of clay brickwork.
- Fig. 6.58-** Influence of aspect ratio on the enhancement factor for clay masonry.
- Fig. 6.59-** Influence of aspect ratio on the bearing strength of AAC brickwork.
- Fig. 6.60-** Influence of aspect ratio on the enhancement factor for AAC masonry.
- Fig. 6.61-** Effect of loading position on bearing strength of brickwork type E under strip loading ( $t=102.5\text{mm}$ ).

- Fig. 6.62-** Effect of loading position on bearing strength of brickwork type F under strip loading (t=102.5mm).
- Fig. 6.63-** Effect of loading position on bearing strength of brickwork type F under strip loading (t=215.0mm).
- Fig. 6.64-** Effect of loading position on bearing strength of brickwork type G under strip loading (t=102.5mm).
- Fig. 6.65-** Effect of loading position on bearing strength of brickwork type G under strip loading (t=215.0mm).
- Fig. 6.66-** Effect of loading position on bearing strength of brickwork type H under strip loading (t=215.0mm).
- Fig. 6.67-** Effect of loading position on bearing strength of brickwork type L under strip loading (t=102.5mm).
- Fig. 6.68-** Effect of loading position on bearing strength of brickwork type M under edge loading (t=215.0mm).
- Fig. 6.69-** Effect of loading position on enhancement factor for brickwork type E under strip loading (t=102.5mm).
- Fig. 6.70-** Effect of loading position on enhancement factor for brickwork type F under strip loading (t=102.5mm).
- Fig. 6.71-** Effect of loading position on enhancement factor for brickwork type F under strip loading (t=215.0mm).
- Fig. 6.72-** Effect of loading position on enhancement factor for brickwork type G under strip loading (t=102.5mm).
- Fig. 6.73-** Effect of loading position on enhancement factor for brickwork type G under strip loading (t=215.0mm).
- Fig. 6.74-** Effect of loading position on enhancement factor for brickwork type H under strip loading (t=215.0mm).
- Fig. 6.75-** Effect of loading position on enhancement factor for brickwork type L under strip loading (t=102.5mm).
- Fig. 6.76-** Effect of loading position on enhancement factor for brickwork type M under edge loading (t=215.0mm).
- Fig. 6.77-** Effect of loading configuration on the bearing strength of masonry under central loading position.
- Fig. 6.78-** Effect of loading configuration on the bearing strength of masonry under intermediate loading position.
- Fig. 6.79-** Effect of loading configuration on the bearing strength of masonry under end loading position.
- Fig. 6.80-** Effect of loading configuration on enhancement factor under central loading position.

- Fig. 6.81-** Effect of loading configuration on enhancement factor under intermediate loading position.
- Fig. 6.82-** Effect of loading configuration on enhancement factor under end loading position.
- Fig. 6.83-** Influence of unit brick type on enhancement factor under central strip loading.
- Fig. 6.84-** Influence of unit brick type on enhancement factor under intermediate strip loading:
- Fig. 6.85-** Influence of unit brick type on enhancement factor under end strip loading.
- Fig. 6.86-** Effective areas according to CEB<sup>[99]</sup>.
- Fig. 6.87-** Effective area according to DIN 1045<sup>[100]</sup>.
- Fig. 6.88-** Determination of the limiting value of the effective length contributing to the bearing strength of clay masonry under central strip load.
- Fig. 6.89-** Determination of the limiting value of the effective length contributing to the bearing strength of AAC masonry under central strip load.
- Fig. 6.90-** Determination of the limiting value of the effective thickness contributing to the bearing strength of clay masonry under central, intermediate and end strip loads.
- Fig. 6.91-** Typical failure mode and crack pattern for brickwork type A under central strip loading (t=102.5mm).
- Fig. 6.92-** Typical failure mode and crack pattern for brickwork type B under central strip loading (t=102.5mm).
- Fig. 6.93-** Typical failure mode and crack pattern for brickwork type C under central strip loading (t=102.5mm).
- Fig. 6.94-** Typical failure mode and crack pattern for brickwork type D under central strip loading (t=102.5mm).
- Fig. 6.95-** Typical failure mode and crack patter for brickwork type E under central strip loading (t=102.5mm).
- Fig. 6.96-** Typical failure mode and crack pattern for brickwork type F under central strip loading (t=102.5mm).
- Fig. 6.97-** Typical failure mode and crack pattern for brickwork type F under central strip loading (t=215.0mm).
- Fig. 6.98-** Typical failure mode and crack pattern for brickwork type G under central strip loading (t=102.5mm).
- Fig. 6.99-** Typical failure mode and crack pattern for brickwork type G

under central strip loading ( $t=215.0\text{mm}$ ).

Fig. 6.100- Typical failure mode and crack pattern for brickwork type E under intermediate strip loading ( $t=102.5\text{mm}$ ).

Fig. 6.101- Typical failure mode and crack pattern for brickwork type F under intermediate strip loading ( $t=102.5\text{mm}$ ).

Fig. 6.102- Typical failure mode and crack pattern for brickwork type F under intermediate strip loading ( $t=215.0\text{mm}$ ).

Fig. 6.103- Typical failure mode and crack pattern for brickwork type G under intermediate strip loading ( $t=102.5\text{mm}$ ).

Fig. 6.104- Typical failure mode and crack pattern for brickwork type G under intermediate strip loading ( $t=215.0\text{mm}$ ).

Fig. 6.105- Typical failure mode and crack pattern for brickwork type E under end strip loading ( $t=102.5\text{mm}$ ).

Fig. 6.106- Typical failure mode and crack pattern for brickwork type F under end strip loading ( $t=102.5\text{mm}$ ).

Fig. 6.107- Typical failure mode and crack pattern for brickwork type F under end strip loading ( $t=215.0\text{mm}$ ).

Fig. 6.108- Typical failure mode and crack pattern for brickwork type G under end strip loading ( $t=102.5\text{mm}$ ).

Fig. 6.109- Typical failure mode and crack pattern for brickwork type G under end strip loading ( $t=215.0\text{mm}$ ).

Fig. 6.110- Formation of wedge or cone under strip loading for AAC masonry.

Fig. 6.111- Typical failure mode and crack pattern for brickwork type M under central edge loading ( $t=215.0\text{mm}$ ).

Fig. 6.112- Typical failure mode and crack pattern for brickwork type M under intermediate edge loading ( $t=215.0\text{mm}$ ).

Fig. 6.113- Typical failure mode and crack pattern for brickwork type M under end edge loading ( $t=215.0\text{mm}$ ).

## **Chapter 7**

Fig. 7. 1- Results of linear finite element analysis under concentric concentrated load modelling brickwork as homogeneous material.

Fig. 7. 2- Linear homogeneous finite element analysis of brickwork under concentric concentrated load ( $A_r=0.05$ ).

Fig. 7. 3- Results of linear finite element analysis under concentric concentrated load modelling brickwork as non-homogeneous material.

Fig. 7. 4- Results of nonlinear finite element analysis under concentric concentrated load modelling masonry as homogeneous material.



- Fig. 7. 5-** Nonlinear finite element analysis of brickwork under concentric concentrated load ( $A_r=0.10$ ).
- Fig. 7. 6-** Results of linear finite element analysis of brickwork under eccentric concentrated load modelling masonry as homogeneous material.
- Fig. 7. 7-** Linear homogeneous finite element analysis of brickwork under eccentric concentrated load ( $A_r=0.05$ ).

## **Chapter 8**

- Fig. 8. 1-** State of stress in a brick and mortar joint within a stack bonded prism under uniform axial compressive load.
- Fig. 8. 2-** State of stress in a brick, mortar bed joint and perpend within a brickwork panel under uniform axial compressive load.
- Fig. 8. 3-** State of stress in an element and stress distributions on the centre line of brickwork masonry subjected to concentrated load.
- Fig. 8. 4-** Mean and characteristic curves for enhancement factor of 102.5mm thick masonry as a function of loaded area ratio for central, intermediate and end loading positions respectively.
- Fig. 8. 5-** Mean and characteristic curves for enhancement factor of 215.0mm thick masonry as a function of loaded area ratio for central, intermediate and end loading positions respectively.
- Fig. 8. 6-** Failure envelope for brick masonry 102.5mm in thickness.
- Fig. 8. 7-** Failure envelope for brick masonry 215.0mm in thickness.
- Fig. 8. 8-** Dispersion of concentrated load in brickwork masonry.
- Fig. 8. 9-** Effective area under bearing.
- Fig. 8.10-** Recommended design guide and its comparison with the experimental test results.
- Fig. 8.11-** Simulated design chart showing the effect of precompression on the enhancement factor of brickwork masonry under concentrated load.

## LIST OF TABLES

### Chapter 2

- Table 2. 1- Details of collected wall results.
- Table 2. 2- Comparison between the correlation coefficients of the best fit to the data.
- Table 2. 3- Equations of the mean wall strength curves.
- Table 2. 4- Correlation coefficients for the straightness of the normal probability plots.
- Table 2. 5- Equations of characteristic compressive strength of brickwork walls
- Table 2. 6- Characteristic compressive strength of walls ( $f_{kw}$ ).
- Table 2. 7- Relationship between mean wall, brick and mortar cube strengths.
- Table 2. 8- Equation of characteristic wall strength curves in terms of unit brick and mortar cube strengths for 102.5mm and 215.0mm thickness.
- Table 2. 9- Characteristic compressive strength of 102.5mm and 215.0mm walls.
- Table 2.10- Equation for characteristic compressive strength of masonry.
- Table 2.11- Mean compressive strength of masonry,  $f_{mm}$ , 102.5mm and 215.0mm thickness in  $Nmm^{-2}$ .
- Table 2.12- Characteristic compressive strength of masonry,  $f_k$ , 102.5mm and 215.0mm thickness in  $Nmm^{-2}$ .

### Chapter 4

- Table 4. 1- Dimensions of bricks.
- Table 4. 2- Density of bricks.
- Table 4. 3- Water absorption of bricks.
- Table 4. 4- Physical properties of brick type A.
- Table 4. 5- Physical properties of brick type B.
- Table 4. 6- Physical properties of brick type C.
- Table 4. 7- Physical properties of brick type D.
- Table 4. 8- Physical properties of brick type E.
- Table 4. 9- Physical properties of brick type F.
- Table 4.10- Physical properties of brick type G.
- Table 4.11- Elastic properties of brick units.
- Table 4.12- Sieve analysis of the sand.
- Table 4.13- Density of mortars.
- Table 4.14- Compressive strength of mortar cubes.
- Table 4.15- Elastic constants for mortar designations M(i) and M(iii).
- Table 4.16- Density of brickwork masonry.
- Table 4.17- Compressive strength of brickwork masonry under uniform load.

- Table 4.18- Characteristic compressive strength of brickwork masonry specimens.
- Table 4.19- Elastic properties of brickwork masonry.
- Table 4.20- Comparison between the values of  $f_{mm}$  and  $f_k$  determined experimentally and by the statistical methods of chapter 2.

## **Chapter 5**

- Table 5. 1- Details of the constructed wallette specimens.
- Table 5. 2- Dimensions of bearing plates.
- Table 5. 3- Details of testing programme.
- Table 5. 4- Results of mortar cubes tested after 7-days used for the constructions of brickwork types A, B, C and D.
- Table 5. 5- Results of mortar cubes tested after 28-days used for the constructions of brickwork types A, B, C and D.
- Table 5. 6- Results of mortar cubes tested after 28-days used for the construction of brickwork type E.
- Table 5. 7- Results of mortar cubes tested after 7-days used for the construction of brickwork types F and G.
- Table 5. 8- Results of tests on control specimens under uniform compressive load.
- Table 5. 9- Test results of 102.5mm thick masonry under central strip concentrated loading for brickwork type A.
- Table 5.10- Test results of 102.5mm thick masonry under central strip concentrated loading for brickwork type B.
- Table 5.11- Test results of 102.5mm thick masonry under central strip concentrated loading for brickwork type C.
- Table 5.12- Test results of 102.5mm thick masonry under central strip concentrated loading for brickwork type D.
- Table 5.13- Test results of 102.5mm thick masonry under central strip concentrated loading for brickwork type E.
- Table 5.14- Test results of 102.5mm thick masonry under intermediate strip concentrated loading for brickwork type E.
- Table 5.15- Test results of 102.5mm thick masonry under end strip concentrated loading for brickwork type E.
- Table 5.16- Test results of 102.5 and 215.0mm thick masonry under central, intermediate and end strip concentrated loading for brickwork type F.
- Table 5.17- Test results of 102.5 and 215.0mm thick masonry under central, intermediate and end strip concentrated loading for brickwork type G.
- Table 5.18- Test results of 102.5mm thick brickwork types F and G under

central strip concentrated load for varying length of specimens.

**Chapter 6**

**Table 6.1-** Equations of the mean and characteristic bearing strength of masonry and the ratios of enhancement factors for different loading positions.

**Table 6.2-** Equations for mean and characteristic bearing strength of brickwork in terms of brick strength for different loaded area ratios.

**Table 6.3-** Relationships for enhancement factor in terms of loaded area ratio.

**Chapter 8**

**Table 8.1-** Equations of the mean and 95% lower confidence limit curves for failure envelopes under various loading position and masonry thickness.

**Table 8.2-** Proposed reduction factor for the effect of precompression.

## NOTATIONS

<b>a</b>	Length of bearing plate
<b>A</b>	Total cross sectional area of specimen ( $=l.t$ )
<b><math>A_{cb}</math></b>	Loaded area ( $=a.b$ )
<b><math>A_e</math></b>	Effective area of specimen ( $=l_e.t_e$ )
<b><math>A_r</math></b>	Loaded area ratio ( $=A_{cb}/A$ )
<b><math>A_{re}</math></b>	Effective loaded area ratio ( $=A_{cb}/A_e$ )
<b>b</b>	Width of specimen
<b><math>C_v</math></b>	Coefficient of variation
<b>d</b>	Distance of centroid of loaded area to nearest edge
<b>E</b>	Modulus of elasticity of brickwork masonry
<b><math>E_b</math></b>	Modulus of elasticity of brick
<b><math>E_m</math></b>	Modulus of elasticity of mortar cube
<b><math>f_b</math></b>	Crushing strength of brick
<b><math>f_c</math></b>	Precompression
<b><math>f_{cb}</math></b>	Compressive strength of masonry under concentrated load
<b><math>f'_{cb}</math></b>	Characteristic bearing strength of masonry
<b><math>f_k</math></b>	Characteristic compressive strength of masonry
<b><math>f_{kp}</math></b>	Characteristic compressive strength of brick prism
<b><math>f_{kw}</math></b>	Characteristic compressive strength of masonry wall
<b><math>f_m</math></b>	Mortar cube crushing strength
<b><math>f_{mm}</math></b>	Mean masonry compressive strength
<b><math>f_{mw}</math></b>	Mean brickwork wall compressive strength
<b><math>f_w</math></b>	Compressive strength of brickwork wall
<b><math>F_c</math></b>	Load at appearance of first crack in masonry
<b><math>F_r</math></b>	Ratio of cracking load to the ultimate load at failure ( $=F_c/F_u$ )
<b><math>F_u</math></b>	Load at failure of specimen
<b>h</b>	Height of specimen
<b><math>h_e</math></b>	Effective height of specimen
<b>k</b>	Constant relating mean to the characteristic value
<b>K</b>	Constant
<b>l</b>	Length of specimen
<b><math>l_e</math></b>	Effective length of specimen
<b>M(i)</b>	Mortar designation (i), 1:0.25:3, cement:lime:sand mix by volume
<b>M(ii)</b>	Mortar designation (ii), 1:0.50:4.5, cement:lime:sand mix by volume
<b>M(iii)</b>	Mortar designation (iii), 1:1:6, cement:lime:sand mix by volume

<b>M(iv)</b>	<b>Mortar designation (iv), 1:2:9, cement:lime:sand mix by volume</b>
<b>n</b>	<b>Number of test samples</b>
<b>P</b>	<b>Concentrated load applied to bearing plate</b>
<b><math>Q_k</math></b>	<b>Characteristic load</b>
<b><math>Q_m</math></b>	<b>Mean of applied load</b>
<b><math>r^2</math></b>	<b>Correlation coefficient of the best fit to the data</b>
<b><math>R^2</math></b>	<b>Correlation coefficient of the normal probability plot</b>
<b><math>R_k</math></b>	<b>Characteristic strength</b>
<b><math>R_m</math></b>	<b>Mean strength</b>
<b><math>S_d</math></b>	<b>Standard deviation</b>
<b>t</b>	<b>Thickness of specimen</b>
<b><math>t_e</math></b>	<b>Effective thickness of specimen</b>
<b><math>t_q</math></b>	<b>Value of Student's t with unilateral probability q%</b>
<b>x, y, z</b>	<b>Axes of reference</b>
<b><math>\beta</math></b>	<b>Capacity reduction factor for the effect of slenderness</b>
<b><math>\nu</math></b>	<b>Poisson's ratio of brickwork masonry</b>
<b><math>\nu_b</math></b>	<b>Poisson's ratio of brick unit</b>
<b><math>\nu_m</math></b>	<b>Poisson's ratio of mortar cube</b>
<b><math>\gamma_f</math></b>	<b>Partial factor of safety for loads</b>
<b><math>\gamma_m</math></b>	<b>Partial factor of safety for material strength</b>
<b><math>\sigma</math></b>	<b>Average stress given by <math>P/l.t</math></b>
<b><math>\sigma_{cb}</math></b>	<b>Applied concentrated stress given by <math>P/a.b</math></b>
<b><math>\sigma_x</math></b>	<b>Stress in x direction</b>
<b><math>\sigma_y</math></b>	<b>Stress in y direction</b>
<b><math>\sigma_z</math></b>	<b>Stress in z direction</b>
<b><math>\xi</math></b>	<b>Reduction factor for the effect of precompression</b>
<b><math>\zeta</math></b>	<b>Enhancement factor</b>
<b><math>\zeta'</math></b>	<b>Enhancement factor at 95% lower limit</b>

## Chapter 1

### INTRODUCTION

There are many situations in the structural design of brickwork masonry where concentrated loads are applied to a supporting wall or piers as in the case of girder bearings, column bases, beam bearings, lintels, etc. These concentrated loads are usually applied locally and sometimes are accompanied with uniform precompressive load from above. Cases like these are common in practice and some typical examples are shown in Fig. 1.1.

In practice, a masonry wall at a particular floor level carries a concentrated load applied by the beams supporting floor slabs and direct compressive load from the brickwork placed above the wall. Where steel beams rest on either brickwork or concrete, it is common to consider that the bottom flanges tend to bend upwards, thus causing higher bearing stresses immediately beneath the web. The possibility of the bottom flanges of steel beams bending upwards would depend upon the loading, flange width and thickness, stiffness of the supporting material and workmanship in forming the bearing. The bearing stress distribution normal to the length of the beam could be almost rectangular for lightly loaded beams with narrow flanges of reasonable thickness, but for more heavily loaded beams with wide, thin flanges, the shape could be any one of the stress blocks shown in Fig. 1.2.(a). The distribution of bearing stress in the direction of the beam axis is dependent upon many factors such as: rotation at the end of the beam due to loading (this is usually the criterion); the length of the bearing; stiffness of the supporting material and the workmanship in forming the bearing. Typical stress blocks are shown in Fig. 1.2.(b).

However, most beams supporting floors carry their dead load before the brickwork above is placed and therefore, for dead loads only the ends of the beam will be free to rotate. On completion of the structure the rotation of the ends of the beam due to imposed loads including finishes would be restricted, and would be dependent upon relative stiffness of the interconnected members. The rotation of the ends of the beam is critical, and as the beam deflects, the contact area between the end of the beam and the supporting wall would decrease hence increasing the eccentricity of the loading. This would give rise to higher stresses, and non-uniform stress distribution under the beam. This condition would be difficult to analyse, and any adjustment of

the stress diagram is left to the discretion of the designer at present.

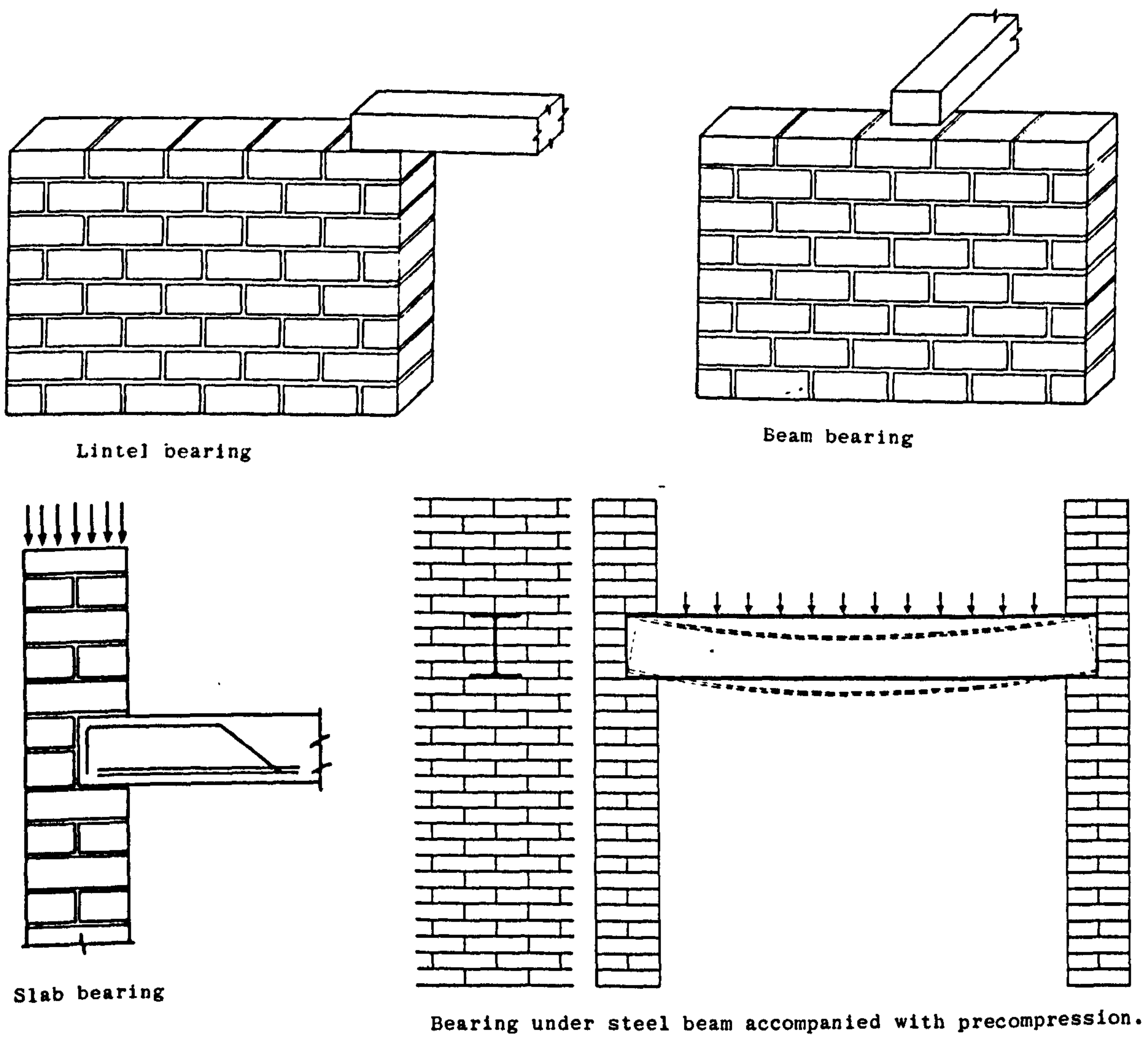


Fig. 1.1 - Typical concentrated load problems in brickwork masonry.



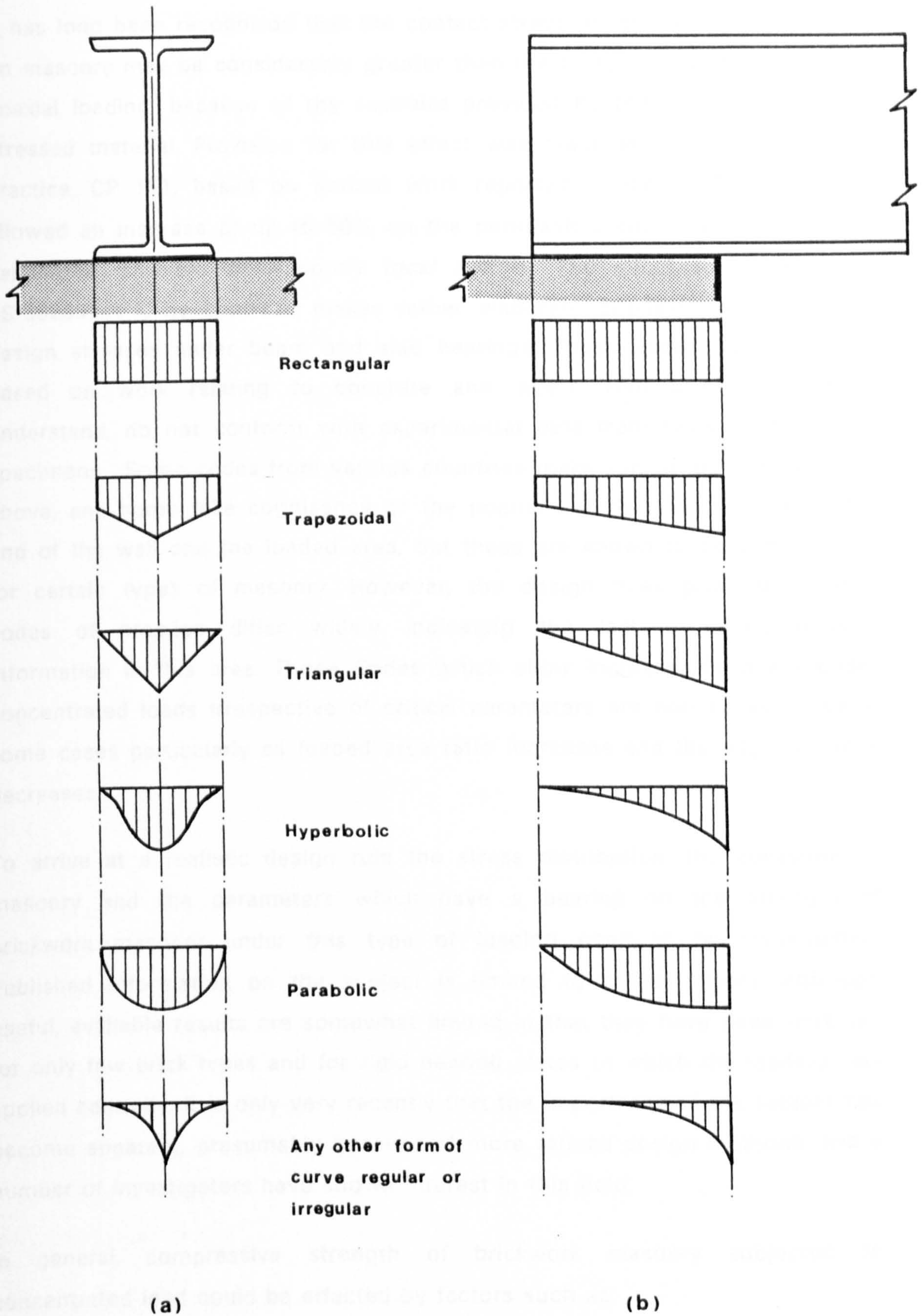


Fig. 1.2 - Typical stress blocks under steel beam applying concentrated load.

It has long been recognised that the contact stress under a concentrated load on masonry may be considerably greater than the compressive strength under uniaxial loading, because of the restraint provided by the surrounding lightly stressed material. Provision for this effect was made in the British Code of Practice, CP 111, based on limited work reported in the 1930's. This code allowed an increase of up to 50% on the permissible compressive stress for *"additional stresses of a purely local nature"*. The successor to CP 111, BS 5628:Part 1, by contrast, makes rather elaborate provisions for increased design stresses under beam and slab bearings. These appear to have been based on work relating to concrete and, apart from being difficult to understand, do not conform with experimental data from tests on brickwork specimens. Some codes from various countries make similar provisions to the above, and some take cognisance of the position of the load relative to the end of the wall and the loaded area, but these are known to be conservative for certain types of masonry. However, the design rules given by various codes of practice differ widely indicating the lack of comprehensive information in this area. Those Codes which allow increases in stress under concentrated loads irrespective of critical parameters are non-conservative in some cases particularly as loaded area ratio increases and the edge distance decreases.

To arrive at a realistic design rule the stress distribution, the behaviour of masonry and the parameters which have a bearing on the strength of brickwork masonry under this type of loading need to be investigated. Published information on the subject is limited to a few papers. Although useful, available results are somewhat limited in that they have been obtained for only few brick types and for rigid bearing plates to which the loading was applied centrally. It is only very recently that the importance of the subject has become apparent, presumably because of more refined design methods, and a number of investigators have shown interest in this field.

In general, compressive strength of brickwork masonry subjected to concentrated load could be effected by factors such as:

- the properties of brickwork masonry and its constituent materials;
- the ratio of bearing area to the cross-sectional area;
- the loading configuration;

- the loading position and the effect of edge distance;
- the type of units;
- the thickness of the element;
- the aspect ratio of the element;
- the effective cross-sectional area of the brickwork element;
- the angle of dispersion of the concentrated load;
- the presence of a perpend under the bearing;
- the ratio of unit height to bed joint thickness;
- the characteristics of the element by which the load is applied;
- the support conditions of the masonry and the effect of a spreader under the bearing;
- the degree of precompression;
- the rotation of the end of the element applying the concentrated load;
- the amount and positioning of reinforcement;
- the presence of a horizontal component of load and/or lateral restraining.

Although the variables involved are large in number, they are not all of equal significance. It is beyond the scope of this investigation to study all the parameters which may influence the bearing strength of brickwork masonry. However, the experimental program adopted in this investigation has eliminated some of the variables by assuming the case where the concentrated load is applied to a brickwork via a rigid bearing plate in contrast to a beam which is used in practice. This immediately eliminates the influence of parameters such as the stiffness and the end rotation of the beam applying the concentrated load.

In the present investigation the effect of the parameters listed below on the behaviour of brickwork masonry under concentrated load is considered.

**The properties of masonry and its constituent materials:** In total, seven brick strengths and two mortar mixes have been employed in this investigation. The effect of brick crushing strength on the bearing strength of brickwork masonry has been studied. Design charts for the characteristic compressive strength of

masonry under partial load for four ratios of loaded area have been obtained in terms of brick crushing strengths. To compare the compressive strengths under partial and uniaxial load, a thorough investigation has been carried out to establish accurate values for the characteristic compressive strengths of masonry,  $f_k$ . This has been achieved by analysing statistically the data collected on the crushing strength of full storey height brickwork walls. Relationships for mean and characteristic strengths for brickwork wall and brickwork masonry have been derived in terms of unit brick crushing strength; for two mortar mixes and wall thicknesses and also in terms of unit brick and mortar cube crushing strengths for two wall thicknesses.

**Loaded area ratio:** Ratios of bearing to the total cross-sectional areas of 0.05, 0.10, 0.15, 0.20, 0.30 and 0.40 have been considered. The loads have been applied through a rigid steel plate 25mm in thickness, cut to size corresponding to the above loaded area ratios.

**Loading configuration:** In the present investigation only strip loading configuration (where partial load is applied over the whole thickness of the specimen) has been considered. However, test results of bonded brickwork masonry specimens under edge or patch loading configuration (where partial load is applied over an area eccentric in the direction normal to the longitudinal axis) carried out by the author prior to this investigation have been reported here and compared with the present test results.

**Loading position:** The effect of loading position in terms of edge distance (the distance from the centroid of the bearing plate to the nearest edge of the specimen) has been investigated for central, intermediate and end positions.

**Effect of material:** Tests on bricks of two different materials, clay and lightweight autoclaved aerated concrete (AAC) were carried out to study the comparative effect on the bearing strength.

**Thickness of brickwork specimen:** Two masonry thicknesses, 102.5mm and 215.0mm were investigated for each type of unit; i.e. clay and AAC bricks.

**Aspect ratio:** The ratio of length to height of the elements tested were studied by keeping the height constant and varying the length of the specimens for the clay and AAC brickwork masonry.

**Effective area:** The effective length and width of specimen contributing to the bearing strength has been determined, giving rise to the effective area of the

masonry element.

In all, 338 brickwork wallettes were tested of which 300 were under concentrated loads and 38 under uniformly distributed axial load. Also the results of 56 specimens tested under concentrated strip and edge loading carried out at the Department of Civil Engineering at University of Edinburgh prior to this investigation the results of which have not previously been published have been included.

The above results have been used to carry out a comprehensive parameteric study of the behaviour of brickwork masonry subject to concentrated loads. Based on these results design recommendations have been proposed.

The structure of the thesis can be summarised as follows:

**Chapter 1:** Introduction, scope and aim of the present investigation.

**Chapter 2:** Derivation of a true values for the characteristic wall, ( $f_{kw}$ ) and masonry ( $f_k$ ) strengths statistically, based on the collected test results of full storey height brickwork walls.

**Chapter 3:** Literature review of previous investigations of compressive strength of masonry under concentrated loads and the design rules given by the current masonry codes.

**Chapter 4:** The experimental determination of the material properties from the representative samples of units, mortar and brickwork masonry.

**Chapter 5:** The experimental investigation of concentrated load on brickwork; construction, method of testing and the results of the wallette tests.

**Chapter 6:** The analysis of the results and the influence of the parameters studied on the bearing strength.

**Chapter 7:** Theoretical investigation into the stress distribution of brickwork masonry by the Finite Element analysis.

**Chapter 8:** Failure mechanism and envelopes for brickwork masonry applied through a rigid bearing plate with proposals for design rules.

**Chapter 9:** General summary and conclusions with recommendation for further research.

## Chapter 2

### CHARACTERISTIC COMPRESSIVE STRENGTH OF BRICKWORK MASONRY

#### 2.1. INTRODUCTION

The object of structural design is to obtain an economical structural solution for safety and serviceability and to ensure that a structure will fulfil its intended function throughout its design life.

There are three methods which use factors of safety as a criteria for achieving safe, workable structure, namely: the Permissible Stress method in which ultimate strengths of the materials are divided by a factor of safety to provide design stresses which are usually within the elastic range; the Load Factor method in which the working loads are multiplied by a factor of safety; and the Limit State method which multiplies the working loads by partial factors of safety and also divides the ultimate strength of the material by a further partial factor of safety.

The permissible stress method has proved to be a simple and useful method but it does have some serious disadvantages as it is based on an elastic stress distribution. It is not really applicable to a elasto-plastic material such as masonry, nor is it suitable when the deformations are not proportional to load.

The load factor method uses the ultimate strength of the materials in the calculations without applying factors of safety to the materials strength, thus it cannot directly take account of the variability of the materials, and also it cannot be used to calculate the deflections or cracking at working loads.

A more rational and flexible method of structural safety and serviceability is "limit state" which is probabilistically based. The aim is to achieve acceptable probabilities so that a structure or part of a structure would not reach a limit state when it would no longer fulfil the functions of its design.

Until recently, the code of practice for masonry structures ensured safety and serviceability of walls under compressive load by specifying permissible stresses for various types and combinations of materials. Basic compressive stresses for materials were given which had to be adjusted for the slenderness ratio of the element and the eccentricity of loading. These basic stresses were derived by obtaining the ultimate stresses from tests on walls

or piers and had been divided by an arbitrary factor of safety sufficiently large to avoid cracking at working loads. Thus, brickwork design has always been related to ultimate strength and to a serviceability limit state. In the current code <sup>[1]</sup>, the design of brickwork masonry is based on limit state theory. The two principal types of limit state are the Ultimate Limit State; of failure or collapse and Serviceability Limit State; of excessive deflection or cracking. Other limit states include; durability, vibration, fire resistance, fatigue, earthquake resistance, etc.

In order to prevent the structure from reaching a limit state, an acceptable probability of failure must be estimated of load variations on the structure, and variations in the strengths of constructional materials. Ideally, all the probable variations for limit state should be predicted from a sufficiently large number of statistically analysed data. However, at present only some of the relevant data is available, although it is still possible to implement the main principles of the limit state philosophy.

Variations in loads are those due to inherent variability of loads which can be allowed for by a "Characteristic Load ( $Q_k$ )," and variations due to other causes, which are covered by a "Partial Factor of Safety for loads ( $\gamma_f$ )."

Material strength variables are inherent variations in the material strength in its manufacture and quality, which can be allowed by a "Characteristic Strength ( $R_k$ )," and other uncertainties which are allowed for by a "Partial Safety Factor for material strength, ( $\gamma_m$ )."

The basic parameters and terminology in the consideration of structural safety in limit state theory was first published in 1964 <sup>[2]</sup>, and the method of applying the limit states approach to the design of structures is outlined in a publication of the International Organisation for Standardisation <sup>[3]</sup>.

The criteria for a satisfactory design is expressed in terms of design loading effects ( $S^*$ ) and design strengths ( $R^*$ ) such that:

$$R^* \geq S^* \quad (2.1)$$

Design loading effects are determined from the characteristic actions from the relationship;

$$S^* = \text{effects of } (\gamma_f Q_k) \quad (2.2)$$

where characteristic load,  $Q_k$  is defined in statistical terms by:

$$\begin{aligned} Q_k &= Q_m + k.S_d \\ Q_k &= Q_m ( 1 + k.C_v ) \end{aligned} \quad (2.3)$$

Similarly, design strengths of material  $R^*$  is defined by;

$$R^* = R_k / \gamma_m \quad (2.4)$$

where characteristic strength  $R_k$  is defined in statistical terms by:

$$\begin{aligned} R_k &= R_m - k.S_d \\ R_k &= R_m ( 1 - k.C_v ) \end{aligned} \quad (2.5)$$

The advantage with limit state approach is that the characteristic values and partial safety factors could be determined statistically for a given probability of failure, if loadings and strengths are expressed in statistical terms.

In the case of loads this has not been possible yet, so that characteristic values were determined on the basis of available evidence, which is the results from surveys of buildings in service. However, in the case of strengths of materials, laboratory test results can provide a statistical basis for determining the characteristic strengths.

Compressive testing of brickwork masonry based on large or small scale specimens has been carried out in various countries for well over half a century, and the factors which have a bearing on the compressive strength of masonry, and the phenomena which accompany compressive failure are now fairly well recognized.

Experimental investigations have shown factors such as; strength of unit, geometry of unit, strength of mortar, deformation characteristics of units and mortar, joint thickness, brickwork bonding, suction of units and water retentivity of mortar are of importance in determining the compressive strength of brick masonry, but are not all of equal significance.

Mechanism of compressive failure of masonry based either on Elastic strength or empirical theories which have been put forward and other published literatures related to masonry are reviewed and well documented elsewhere<sup>[4]</sup>.



## 2.2. CONCEPT OF CHARACTERISTIC STRENGTH

Characteristic strength takes into account the inherent variations in the material strength due to its quality and manufacturing. It is defined in statistical terms by equation 2.5.

However, the definition has been narrowed so that the characteristic strength is defined as a lower limit for strength below which only a small proportion of values likely to fall, and this proportion is taken as 5% in Britain.

Statistical properties of characteristic strength is based on the size of samples, i.e. large or small samples, and the object of defining characteristic strength in terms of mean and standard deviation of the samples, is to give it some probabilistic meaning. This type of probability statement can be made if the distribution of strength is completely characterized by these two parameters. The most frequent assumed distributions are Normal and Lognormal.

If the mean and standard deviation are based on a large sample, so that they are subject to negligible sampling error, then for normal distribution at 95% confidence limit the value of  $k$  would be equal to 1.645 and the characteristic strength is expressed as;

$$\begin{aligned} R_k &= R_m - 1.645 S_d \\ R_k &= R_m ( 1 - 1.645 C_v ) \end{aligned} \quad (2.6)$$

There has not been sufficient results available for a given case to determine the form of the distribution of strength, and so the tendency has been to assume strength is normally distributed. However, it may be arguable that when the coefficient of variation is large, (say greater than 20%), the lower tail of distribution may give unacceptably low values.

An alternative distribution would be lognormal, which gives less trouble in this respect and is obtained by assuming that the logarithms of the strengths are normally distributed. This has been found to give an acceptable fit to certain strength distributions.

Beech<sup>[5]</sup> assumed a value of 30 test results as a minimum for large samples and not less than 10 tests for small samples. He compared the values of 5% characteristic strengths for four types of distributions namely, Normal, Lognormal, Rectangular and Triangular, and determined what error was

introduced by assuming a normal distribution when the true distribution was lognormal. For this purpose he assumed the distributions to have the same mean and coefficient of variation and chose values for coefficient of variations of 0.1, 0.15 and 0.25 for good, average and poor standards respectively. In each case he calculated  $R_k/R_m$ , and the ratio of  $(R_k)_{\text{normal}}$  to  $(R_k)_{\text{lognormal}}$  and concluded that for these cases, the form of distribution makes comparatively little difference to the value of the characteristic strength at the same coefficient of variation. The greatest difference occurs with the lognormal distribution, which is skew, with the skewness increasing with the coefficient of variation. His results showed an error of 9% by assuming a normal distribution with the coefficient of variation of 0.25, and suggested that this is not very serious when fairly large material safety factors are being used in addition.

In the case of small samples, it has been suggested that the value of  $k$  needs to be greater than the value for large sample in order to give the characteristic value the same confidence level. As Beech<sup>[5]</sup> also stated the main difficulty affecting a national choice of  $k$  is that in repeated samples from the same population the values of mean and standard deviation vary owing to sampling errors, and these errors become considerable as the sample size decreases. Hence characteristic value will vary appreciably in repeated samples whatever the value of  $k$  is chosen.

Fisher's<sup>[6]</sup> fiducial limit method could be employed to determine the values of  $k$  for different sample sizes. It defines a lower limit below which a new value, randomly taken from a sample of  $n$ -measurements from a normal distribution, would be expected to occur with probability of  $q\%$ . It is calculated by  $R_m - k.S_d$ , such that;

$$k = t_q \cdot \sqrt{\{(n+1)/n\}} \quad (2.7)$$

where  $t_q$  is the value of Student's  $t$  with unilateral probability  $q\%$  and  $(n-1)$  degrees of freedom, taken from appropriate tables. If in the above definition of lower limit a value of 5 is substituted for  $q$ , the definition would be similar to that of characteristic value. The resulting value of  $k$  varies from 7.7328 to 1.645 for minimum of two measurements up to infinite number of measurements respectively, as shown in Fig. 2.1 and Table A1 in Appendix I.I.

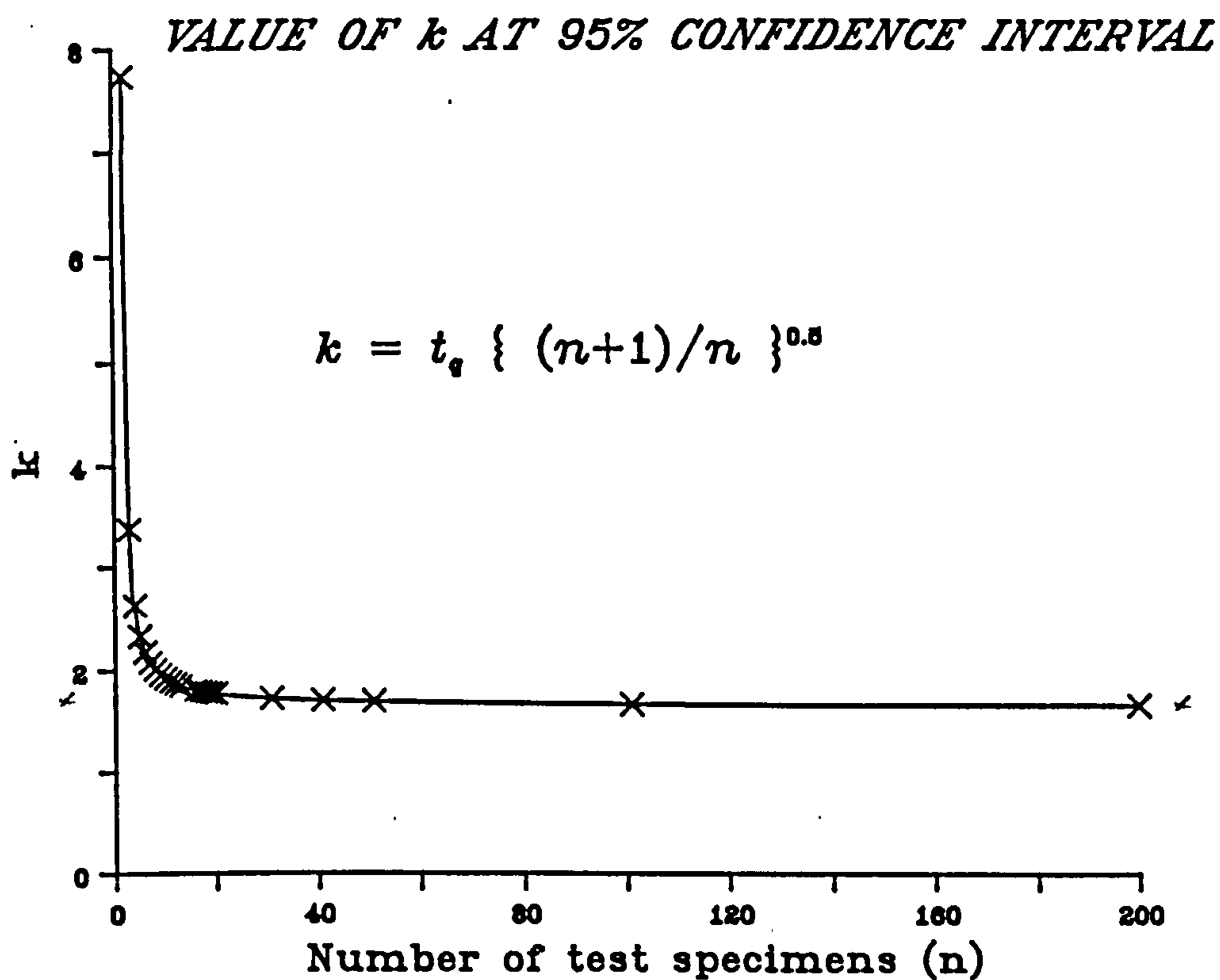


Fig. 2.1 - Variation of  $k$  with number of test specimens.

The difficulty of sampling variation still remains as repeated samples will give estimates of characteristic value that vary, and vary considerably for small samples. If repeated samples are taken from a known normal population and the characteristic values are calculated, then, as has been shown<sup>[5]</sup>, each characteristic value corresponds to a true probability  $q$  that a new value will be below it. Although  $q$  will not necessarily be 5%, in the long run the average of the value of  $q$  will be 5%.

Beech also investigated the variation of the estimated to the true characteristic strength by studying the variation of the ratio  $R = R_{k(\text{estimated})} / R_{k(\text{true})}$  in the case of repeated sampling from normal and lognormal distribution with known mean and standard deviation for sample sizes of 5, 10 and 20. The results showed that the mean value of  $R$  is less than unity and its standard deviation increases with coefficient of variation. For sample size 5 the the standard deviation of  $R$  reaches unacceptably high values.

On the basis of these results he recommended that the sample size should not be less than 10. Although  $R$  was found not to be normally distributed,

Beech suggested that it may be expected to approximate to normality as sample size increases.

Based on the above principles a method has been recommended for the calculation of characteristic compressive strength of masonry from small number of experimental test results. The details is outlined in Appendix I.I.

### 2.3. REVIEW OF PREVIOUS WORK

This section contains a literature survey of work carried out on the compressive strength of axially loaded brickwork. Experimental investigations which has led to empirical relationships between unit brick and brickwork strengths are reviewed, and, where appropriate, the results of tests on full storey-height brickwork walls have been collected for further statistical analysis in later sections.

Extensive experimental investigations have been carried out in this country by the Building Research Station, the British Ceramic Research Association and others since 1950's. Reference may be made to the publications of Morsy<sup>[7]</sup> and Monk<sup>[8]</sup> for information concerning work carried out prior to this date.

In 1950, Davey and Thomas<sup>[9]</sup> described the testing carried out at Building Research Station to determine, among other things, the relationship between the strengths of brick/mortar and brickwork. They point out the insignificant influence of the mortar upon the crushing strength of brickwork piers, and arising from the experimental results, advise against the use of a mortar stronger than is just necessary to give the requisite strength of brickwork. Using the data acquired in this investigation, Thomas<sup>[10]</sup> in 1953 criticised the conservative provisions contained in the Code of Practice CP 111:1948<sup>[11]</sup> "Structural Recommendations for Loadbearing Walls", especially in the use of high strength bricks. He suggested an increase of 50 to 75% in the permissible stresses in brickwork using high strength bricks. This brought about the revision of CP 111 in 1964.

The results<sup>[12]</sup> for full-scale, storey-height walls tested at BRS and BCRA up to 1960 have been collected, and are as shown in Tables A2-6 in Appendix I.II.

The first attempt to develop a theoretical expression for the strength of brickwork in compression was made by Haller<sup>[13]</sup> in 1960 on the assumption of elastic behaviour in brickwork. However, he was quick to admit the limitation of his formula, acknowledging the inelastic behaviour of brickwork approaching

failure. In the same paper, based upon results derived from some crushing tests on brickwork, he evolved an empirical expression which relates brickwork strength to strength of brick and mortar. His formula gave higher values for brickwork strength than the uniaxial strength of unit bricks.

Beginning in 1963, the Structural Clay Products Research Foundation in the United States began a series of brickwork tests designated as the "National Testing Program", the results of which were published in a series of SCPRF Research Reports. In report No.1<sup>[14]</sup> of the program, small scale specimens were tested to determine the influence of brick/mortar properties, and the thickness of joints on the strength of brickwork. Experimental data indicated that higher brickwork compressive strengths were associated with higher brick and mortar strengths, and that an inverse linear relationship existed between the brickwork compressive strength and the thickness of mortar joints. In report No.8<sup>[15]</sup> the results of 15 compressive test specimens of which five were column walls, 2.44m high, 0.61m in length and 115mm thick. The other ten test specimens were 5-brick high stack and running bond prisms. The mortar were 1:0.5:4.5 mix by volume with joint thickness of 10mm. The results are as shown in Table A7 in Appendix I.II. In report No.9<sup>[16]</sup> compressive, transverse and racking strength tests of 100mm brick walls have been investigated. Using three different strength of bricks, a total of 55 compressive test specimens, of which 40 were wall columns having heights of 0.90, 1.5, 2.4, 3.0, 3.6 and 4.5m, were tested as with the previous test procedures. The results are as shown in Table A8 in Appendix I.II. Report 10<sup>[17]</sup> investigated the effects of such variables such as method of bonding, strength of unit brick, type of mortar, thickness of joints, slenderness ratio and quality of workmanship on the compressive and transverse strength of nominal 200mm two-wythe brick walls. The results of reports<sup>[17,18]</sup> are included in Tables A9 and A10 in Appendix I.II.

In a number of crushing tests on storey-height brickwork walls in 1965, Prasan *et al* <sup>[19]</sup> observed that the mode of failure in brick walls under compression was by transverse splitting, and this suggested the importance of the tensile strength of brick and also of the properties of the horizontal mortar joints in determining the strength of brickwork. Increases in brickwork strength of over 60% were observed when every bed joint was reinforced horizontally. His results of crushing tests on storey-height brick walls are as shown in Table A11 in Appendix I.II.

Extending the above study, Bradshaw and Hendry<sup>[20]</sup> carried out further tests on the crushing strength of storey-height brick walls. The outcome of the tests were largely in agreement with earlier results. Empirical formulae derived from these tests suggested the strength of brickwork in compression to be proportional to the square root of the brick strength, and to the third or fourth root of the mortar cube strength. Also the results indicated that the single-leaf walls to be stronger than bonded walls when axially loaded. The results of the tests on full storey-height walls are summarised in Table A12 in Appendix I.II. Further tests were carried out by Bradshaw and Hendry<sup>[21]</sup> on storey-height, 263mm thick cavity walls. The results showed approximately 30% reduction in strength compared with two leaves of similar materials constructed and tested separately. The results are as shown in Table A13 in Appendix I.II.

The results of all loading tests on walls built and tested at the Building Research Station from 1935 to 1948 was reported by Simms<sup>[22]</sup>. The types of units used to build the test walls were clay bricks and blocks with perforations varying from 0 to 25% and perforated clay bricks with voids not exceeding 25%. The mortar used were 1:0.25:3 and 1:0:3, cement:lime:sand mix by volume. The results are represented in Table A14 , Appendix I.II.

McDowall *et al* <sup>[23]</sup> carried out tests on the strength of brick walls and wallettes in 1966, to determine the effects of brick type, wall size, wall thickness and workmanship on the strength of brickwork. The aim of this test program was to provide information for the committee of the Standards Association of Australia whom were preparing the first code of practice for brickwork in Australia. Only four full storey-height, 4.5-in thick walls were tested in conjunction with wallettes 4.5 and 9-in thick and four-brick high stack bond prisms. It was concluded that the thickness of wallettes did not affect the results and the wallettes gave a good measure of brickwork strength. However, the number of tests performed was not enough to draw definite conclusions. The results of this investigation is summarised in Table A15 in Appendix I.II.

The results of 30 storey-height walls tests was reported by Stedham<sup>[24]</sup> in 1968. The walls were nominally 1.35m in length, 2.475m in height and 225mm thick. They were tested after 28 days and the results are summarised in Table A16 in Appendix I.II.

A failure theory for the compressive strength of brickwork was formulated by

Sinha and Hendry<sup>[25]</sup> in 1966. The analysis assumed an elastic behaviour of brickwork, and predicted the compressive strength at first crack. In 1967, Hilsdorf<sup>[26]</sup> outlined a new approach towards the development of a failure criterion for brickwork in compression, in which the compressive strength of brickwork is determined by the interaction of the strength properties of brick and of mortar under their appropriate state of complex stresses. However, due to a lack of information concerning the behaviour of brick and mortar materials under combined stresses, the merit of this method of analysis was not apparent.

Sinha<sup>[27, 28]</sup> in 1968 devised a direct tensile test for one-sixth scale model bricks, and hence was able to relate the compressive strength of brickwork to the tensile strength of brick, a relationship which he found to be linear. Sinha and Hendry<sup>[29]</sup> also studied the effect of brickwork bonding on the load-bearing capacity of model-brick walls. It was concluded that for English, Flemish, Garden, Header and Stretcher bonding, the load bearing capacity of the model brickwork was not affected for different bonding pattern to any practical extent.

The performance of walls built of wire-cut bricks with and without perforations was comprehensively investigated by West *et al*<sup>[30]</sup> in 1968. The investigation showed that so long as the degree of perforation in bricks was low and the shape of the perforations did not result in points of stress concentration, brickwork built with perforated bricks performed under compression as well as those built with solid bricks. A total of 144 storey-height, single leaf walls constructed using mortar designation M(i) and M(iii) were tested under axial and eccentric loading. The results for axial loading are as shown in Tables A17-19 in Appendix I.II.

Morsy<sup>[7]</sup> also produced a formula for the compressive strength of brickwork which took into account the effect of the presence of vertical mortar joints in brickwork. Computations using this formula, which assumed elastic behaviour of brickwork, did not yield acceptable values.

Francis *et al*<sup>[31]</sup> developed a failure theory for stack bonded prisms which was partly based on the elastic theory and partly based on an arbitrary assumed linear failure envelope for brick under biaxial compression-tension. Since the behaviour of brickwork near ultimate stress is principally inelastic and stack bonded prism does not represent brickwork from bonding point of view, this approach is of doubtful value.

Astbury *et al* <sup>[32]</sup> reported the test results on 9-in and 4.5-in thick storey-height walls which were carried out by Structural Clay Products, British Ceramic Research Association and Building Research Station. A linear relationship was derived from the collected data and compared with the expression derived for the 9-in walls by Stedham<sup>[24]</sup>. The results reported are as shown in Table A20 in Appendix I.II.

The comparative strengths of walls built of standard and modular bricks were investigated by West *et al* <sup>[33]</sup>. The results of single-leaf walls of nominal storey-height (2.55m) and nominally 1.35m long are summarised in Table A21 in Appendix I.II. Also the results of tests on the compressive strength of calcium silicate brick walls under axial loading investigated by West *et al* <sup>[34]</sup> are presented in Tables A22-23 in Appendix I.II.

Attempts were made by Anderson<sup>[35]</sup> to correlate between minimum compressive strength of brick and minimum compressive strength of four-brick high stack bond prisms. Also the results of tests on six, single-leaf brick walls carried out by Base<sup>[36]</sup> are reported and comparison was made between the prism strength, wall strength and the tabulated values given in the Australian code<sup>[37]</sup> for the minimum ultimate strengths of brickwork. The results reported are represented in Table A24 in Appendix I.II.

An intensive test programme was undertaken by James in Australia during early 1970's. The first investigation<sup>[38]</sup> involved the testing of two types of locally produced bricks in a series of storey-height walls under differently applied compressive loading. This programme was extended to provide additional information on the relationship between the strength of storey-height walls and small brickwork specimens. The variables such as mortar mix and method of laying were kept constant. Three loading conditions were used being axial and eccentric loading with two eccentricities,  $e=t/6$  and  $t/3$ . A total of four walls were tested for each type of brick in axial loading and three walls were laid with each type of brick for each of two eccentric loading conditions. The walls were laid in the form of single-leaf panels, six stretchers wide and twenty-eight courses high with 10mm bed and perpendicular joints. Accompanying prisms were four-brick high stack bonded with mortar 1:1:6 mix by volume constructed of the standard bricks. His further work<sup>[39 - 46]</sup> was along the same lines and the cumulative results for the above reports are represented in Table A25 in Appendix I.II.

James's report<sup>[43]</sup> to the Standard Association of Australia contains useful



results on 16 different types of bricks in which 42 single-leaf storey-height walls and 774 four-brick high stack bond prisms were tested in axial compression, with the same procedures as mentioned above. The results are also presented in Table A25 in Appendix I.II.

Hilsdorf's<sup>[26]</sup> approach was developed by Khoo and Hendry<sup>[47]</sup> who investigated the behaviour of brick material under a state of biaxial compression-tension, and of mortar under a state of triaxial compression; these characteristics had to be assumed by Hilsdorf in the absence of direct experimental data. Based on the results of tests on a large number of specimens of brick with a wide range of crushing strength, they established an expression for the biaxial compression-tension strength envelope for brick. The effect of a confining pressure on the compressive strength of mortar for two mixes using a triaxial test cell<sup>[48]</sup> was also studied. On the basis of these studies a failure theory for brickwork was developed<sup>[47, 49]</sup>, and an analytical solution was proposed in terms of polynomials for the brick failure envelope and the mortar triaxial strength curve. Comparison of brickwork prism strengths calculated by the above theory showed reasonable agreement with experimental results.

## **2.4. DETERMINATION OF CHARACTERISTIC COMPRESSIVE STRENGTH OF BRICKWORK WALLS**

### **2.4.1. Introduction**

It is well understood that brickwork masonry will exhibit tensile cracking and failure in compression is by vertical splitting. The state of stress in a brick element within a brickwork wall under axial compressive force is a combination of vertical compression and bi-lateral tension. Bi-lateral tension is the result of the differential lateral strain between the mortar and the brick element. The mortar element consequently is in a state of tri-axial compression. In order to derive an expression for the strength of a brickwork wall, it would be logical to relate the mean wall strength to the variables involved.

The primary variables include the properties of the constituent materials, such as the compressive and tensile strengths of the brick unit, the tri-axial compressive strength of mortar cube and the slenderness ratio of the wall. The secondary variables could include the mortar/brick thickness ratio, the shape of units, percentage and geometry of perforations of the units, bonding

of the brickwork masonry and aspect ratio of the wall.

Strictly speaking, the strength of a particular wall is a function of the triaxial strengths of the component materials but as information about these properties is generally unavailable, attempts have been made to formulate the brickwork strength in terms of conventional unit brick strength for a particular mortar mix or mortar cube strength. It has been shown<sup>[4]</sup> that in these terms, brickwork strength varies roughly as a square root of the unit brick crushing strength and as the third or fourth root of the mortar cube strength.

The results show considerable scatter, indicating that these variables which are included in the expressions were insufficient. Introducing the tensile strength of the unit brick would most probably reduce the scatter and it will be shown later in this chapter that as the number of primary variables is increased, the better the correlation coefficient between the test results and the fitted regression becomes. However, an intensive survey of all the experimental results reported from tests on full storey-height brickwork walls (as mentioned in section 2.3) reveals that, presumably in the absence of a recognised test method, the tensile strength of unit bricks was not investigated.

Attention will therefore be confined to the estimation of wall strength with reference to a known brick strength; (even though the apparent compressive strength of bricks in a standard crushing test is not a direct measure of the strength of the unit in brickwork), and mortar mix which is common practice for design purposes. Various codes of practice provide tabular values for masonry strength from which wall strength can be determined on this basis.

This section determines statistically the relationship between wall strength and unit brick strength for a given mortar mix and wall thickness in the form:

$$f_{mw} = K_1 \cdot f_b^n \quad (2.8)$$

Also the relation between the wall strength and unit brick and mortar cube strengths for a particular wall thickness has been investigated statistically assuming a relationship in the form:

$$f_{mw} = K_2 \cdot f_m^l \cdot f_b^n \quad (2.9)$$

In each of these cases the characteristic wall strength,  $f_{kw}$  has been

determined statistically. Finally, the characteristic compressive strength of masonry,  $f_k$  will be determined by applying a modification factor to the  $f_{kw}$  values (see section 2.5).

#### 2.4.2. Sorted Data

The data used in the calculation of characteristic strength are the experimental results of tests on solid, single leaf storey-height, 102.5mm and 215.0mm thick walls, most of which were carried out in the U.K. with the addition of some Australian and American results for which brick types and test procedures were similar to those in Britain. These results are the sorted data taken from the tables in appendix I.II which have been reviewed in section 2.3.

A total of 646 wall test results with their corresponding unit brick and mortar cube strengths have been collected and sorted according to the wall thickness and corresponding mortar mixes, as shown in Table 2.1.

Wall thickness t (mm)	Mortar Designation				Total
	M(i)	M(ii)	M(iii)	M(iv)	
102.5	167	27	163	15	372
215.0	169	10	95	--	274
Total	336	37	258	15	646

Table 2.1 - Details of collected wall results.

#### 2.4.3. Statistical Model for the Determination of Characteristic Strength

A model has been put forward for the determination of characteristic strength statistically. Where there are sufficient wall test results for a given unit brick strength, one can calculate the mean wall strength and the standard deviation of the data and determine the type of distribution. The lower confidence interval could then be worked out. However, inspection of the data shows that there are not sufficient wall test results for a particular unit brick strength to determine the type of distribution.

The flow chart for the analysis of the data is shown in Fig. 2.2. This model is based on the general idea that given a set of data points, it is possible to establish the best fit to these data points using the method of least squares approximation. The equation of the fitted regression is determined and the

standard deviation of the best fit is calculated with respect to the data points. A lower confidence interval then could be calculated knowing the type of distribution which is possible to determine by statistical tests.

The first step is to determine the best fit between unit brick and wall compressive strength for a particular wall thickness and mortar designation. Primary analyses were carried out on the data for four types of fit, namely power, exponential, logarithmic and linear regressions by the method of least squares approximation. The correlation coefficients of the best fits were compared with the results shown in Table 2.2.

Wall thickness t (mm)	Mortar designation	$r^2$			
		linear	exponential	logarithmic	power
102.5	M(i)	0.429	0.426	0.466	0.506
	M(ii)	0.436	0.349	0.354	0.281
	M(iii)	0.426	0.417	0.439	0.452
	M(iv)	0.228	0.048	0.191	0.034
215.0	M(i)	0.431	0.449	0.370	0.419
	M(ii)	Brick strength is essentially constant.			
	M(iii)	0.424	0.493	0.398	0.479

Table 2.2 - Comparison between the correlation coefficients of the best fit to the data.

Upon this analysis it was found that the power curves gave the most consistent best fit to the data, hence the assumed equation 2.8.

A computerised statistical package called Minitab<sup>[50]</sup> was employed for the calculation and the analysis of the characteristic strength. The package is programmed to operate in first and higher order linear regression ( $Y=b_0+b_1X_1+b_2X_2+ \dots +b_kX_k$ ). Given a set of data, they are put in appropriate columns and with command "REGRESS", the regression equation is found by the least squares linear approximation for predicting Y from k predictors  $X_1, X_2, \dots, X_k$ . The values of the regression coefficients  $b_0, b_1, \dots, b_k$  are found by Minitab. The basic assumption of regression made by Minitab is that the data is of the form  $Y= B_0+B_1X_1+B_2X_2+ \dots + E$ , where the  $B_0, B_1, \dots$  are unknown "true" coefficients to be estimated by  $b_0, b_1, \dots$  and the E's are independent normal errors with mean equal to zero and standard deviation (sigma) which is defined by the square root of the mean squares of the error.

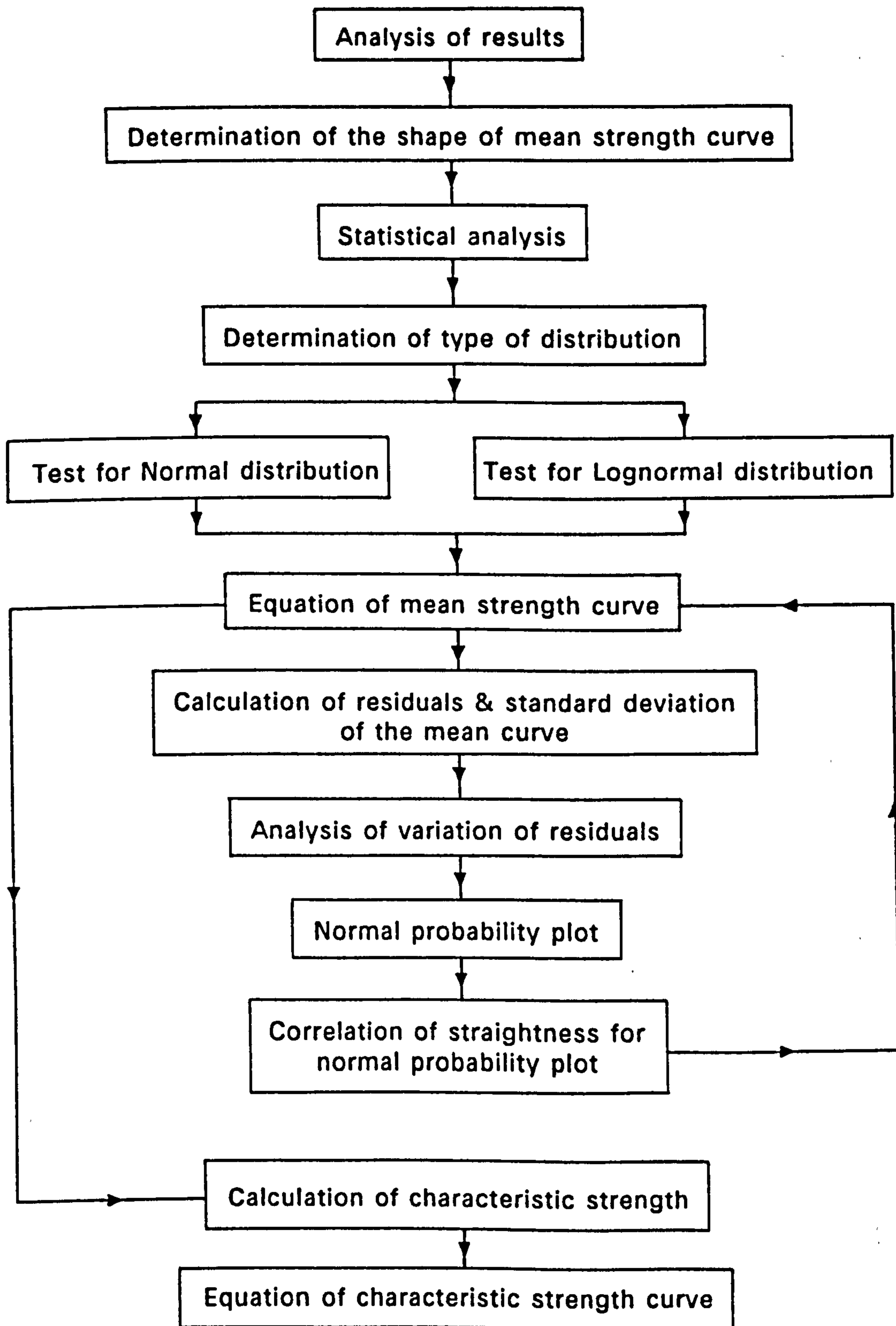


Fig. 2.2 - Flow chart of statistical analysis.

Since the data was shown to be best fitted by power curves, they were converted to logarithmic values such as;

$$\ln(f_{mw}) = \ln(K_1) + n[\ln(f_b)] \quad (2.10)$$

$$\ln(f_{mw}) = \ln(K_2) + n[\ln(f_b)] + l[\ln(f_m)] \quad (2.11)$$

Regression was carried out to establish the equation of the best fit, which gave the "mean strength curve". The residuals of the data points (being the difference of the individual brick wall results and the fitted mean strength curve values) were calculated and plotted against unit brick and wall strengths to establish the variation of the residuals.

To determine the type of distribution, normal probability plots were employed, in which were calculated the "normal score" for the data called "NSCORE". In a normal probability plot (i.e. plot of calculated residuals against the expected values of residuals of the wall strength from a normal probability distribution), if the sample is from a normal population, the points in the plot will probably fall roughly in a straight line. If the sample is from a non-normal population, the plot will show curvature. The "straightness" of the probability plot can be measured by the correlation coefficients ( $R^2$ ) of the points in the plot. A very high correlation coefficient is consistent with normality and a value of 0.97 has been suggested<sup>[50]</sup>. The hypothesis for normality could be rejected if the correlation falls below this value. This test could also be used to determine the correlation coefficient of the normal probability plot for lognormal distribution by entering logarithmic values of the data points, as compared to the data tested for normal distribution.

From the above test it is possible to determine whether the wall strengths are normally or lognormally distributed. The characteristic strength is then calculated by considering the standard deviation of the mean strength curve such that the characteristic curve for the 95% lower limit is given by;

$$f_{kw} = f_{mw} - k.S_d \quad (2.12)$$

$$\text{where } f_{mw} = K_1.f_b^n \text{ or } K_2.f_b^n.f_m^l$$

The package gives the standard deviation of the mean wall strength once the regression is performed. This has been found to be the standard deviation of the mean curve provided one predictor is used, i.e. if the mean wall strength

is a function of unit brick strength. However, when the mean wall strength is a function of two variables, unit brick and mortar cube strengths, the value of the standard deviation is unacceptably high. This has been overcome by calculating the standard deviation of the predicted value of wall strength from the standardized residuals (which are the residuals divided by the estimated standard deviations of those residuals). Analyses were carried out on all sets of data to compare the standard deviation obtained by the two above methods. The results were exactly the same for one variable functions and gave a more realistic value of standard deviation for the two variable functions.

A detailed input and output worksheet is given in Appendix I.III for the one variable function and in Appendix I.IV for two variable functions.

#### **2.4.4. Statistical analysis of the data**

Two types of analysis were carried out. The first analysis assumes a relationship in the form of equation 2.8 relating the mean wall strength as a function of unit brick strength for a particular mortar mix and wall thickness.

The second analysis assumes a relationship in the form of equation 2.9, relating the mean wall strength as function of unit brick and mortar cube strengths for a particular wall thickness. In both cases the characteristic wall strength was determined by performing tests on the data to establish the type of distribution (ref. to Appendix I.III & I.IV).

##### **2.4.4.1. Wall strength in terms of unit brick strength**

Expressions in the form of equation 2.8 have been assumed in this case and only the results of mortar designation M(i) and M(iii) for the two thicknesses have been analysed statistically, since the data for other mixes are insufficient.

As the results of statistical analysis, the strength of storey-height brickwork walls in terms of the corresponding unit brick strength are found to be represented by the expressions in Table 2.3.

The normal probability plots of residuals have been carried out to determine the type of distribution, (i.e. whether normal or lognormal). Table 2.4 shows the correlation coefficients of the straightness of the normal probability plot ( $R^2$ ) for normal and lognormal distributions.

The values obtained for  $R^2_{normal}$  satisfies the hypothesis for normality (except in the case of 215mm thick walls constructed with mortar designation M(iii) for which there were only 95 test results), and the wall strength may be taken to be normally distributed. The standard deviation of each mean strength curve was computed and since the distribution is normal, then the characteristic wall strength  $f_{kw}$  was calculated from equation 2.12 for the 95% confidence limit for corresponding mortar mixes and wall thicknesses as;

$$f_{kw} = f_{mw} - 1.645 S_d \quad (2.13)$$

Table 2.5 shows the equation of the characteristic curves and these curves have been plotted in Figs. 2.3 - 2.6 for comparison with the mean strength curves and the test results. Fig. 2.7 shows the calculated characteristic compressive strength curves for brickwork walls ( $f_{kw}$ ) for the two mortar designations and wall thicknesses. This has also been shown in tabular form in Table 2.6.

Wall thickness t (mm)	Mortar Designation	Equation of mean wall strength curve	$r^2$ (%)	$S_d$ of the curve
102.5	M(i)	$f_{mw} = 2.312f_b^{0.516}$	50.6	1.250
	M(iii)	$f_{mw} = 2.366f_b^{0.441}$	45.2	1.268
215.0	M(i)	$f_{mw} = 1.587f_b^{0.543}$	41.9	1.214
	M(iii)	$f_{mw} = 0.691f_b^{0.670}$	47.9	1.346

Table 2.3 - Equations of the mean wall strength curves.

Wall thickness t (mm)	Mortar designation	$R^2$	
		normal	lognormal
102.5	M(i)	0.994	0.987
	M(iii)	0.985	0.965
215.0	M(i)	0.987	0.990
	M(iii)	0.956	0.976

Table 2.4 - Correlation coefficient for the straightness of the normal probability plots.



Wall thickness t (mm)	Mortar designation	Equation of characteristic wall strength curve
102.5	M(i)	$f_{kw} = 1.601f_b^{0.516}$
	M(iii)	$f_{kw} = 1.602f_b^{0.441}$
215.0	M(i)	$f_{kw} = 1.153f_b^{0.543}$
	M(iii)	$f_{kw} = 0.424f_b^{0.670}$

Table 2.5 - Equations of characteristic compressive strength of brickwork walls.

$f_b$  Nmm <sup>-2</sup>	$f_{kw}$ (Nmm <sup>-2</sup> )			
	t=102.5mm		t=215.0mm	
	M(i)	M(iii)	M(i)	M(iii)
5	3.67	3.26	2.76	1.25
10	5.25	4.42	4.03	1.98
20	7.51	6.00	5.87	3.16
30	9.26	7.17	7.31	4.14
40	10.74	8.15	8.55	5.02
50	12.05	8.99	9.65	5.83
60	13.24	9.74	10.65	6.59
70	14.34	10.43	11.58	7.30
80	15.36	11.06	12.45	7.99
90	16.32	11.65	13.27	8.64
100	17.23	12.20	14.05	9.28
110	18.10	12.72	14.80	9.89
120	18.93	13.22	15.52	10.48

Table 2.6 - Characteristic compressive strength of walls ( $f_{kw}$ ).

**SINGLE LEAF WALL, 102.5mm THICK  
MORTAR DESIGNATION M(i)**

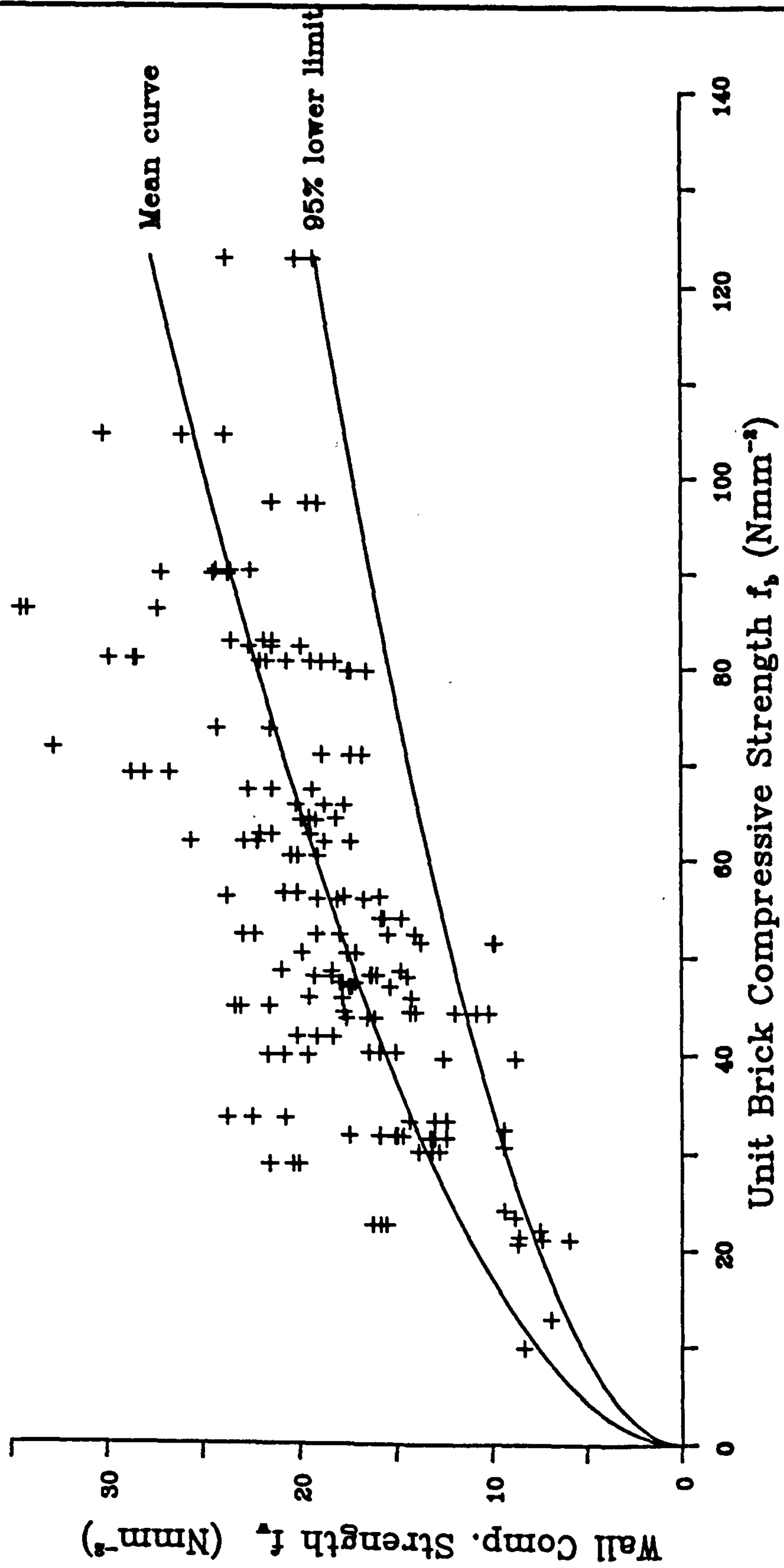


Fig. 2.3 - Plot of results for 102.5mm thick wall and mortar M(i).

**SINGLE LEAF WALL, 102.5mm THICK  
MORTAR DESIGNATION M(iii)**

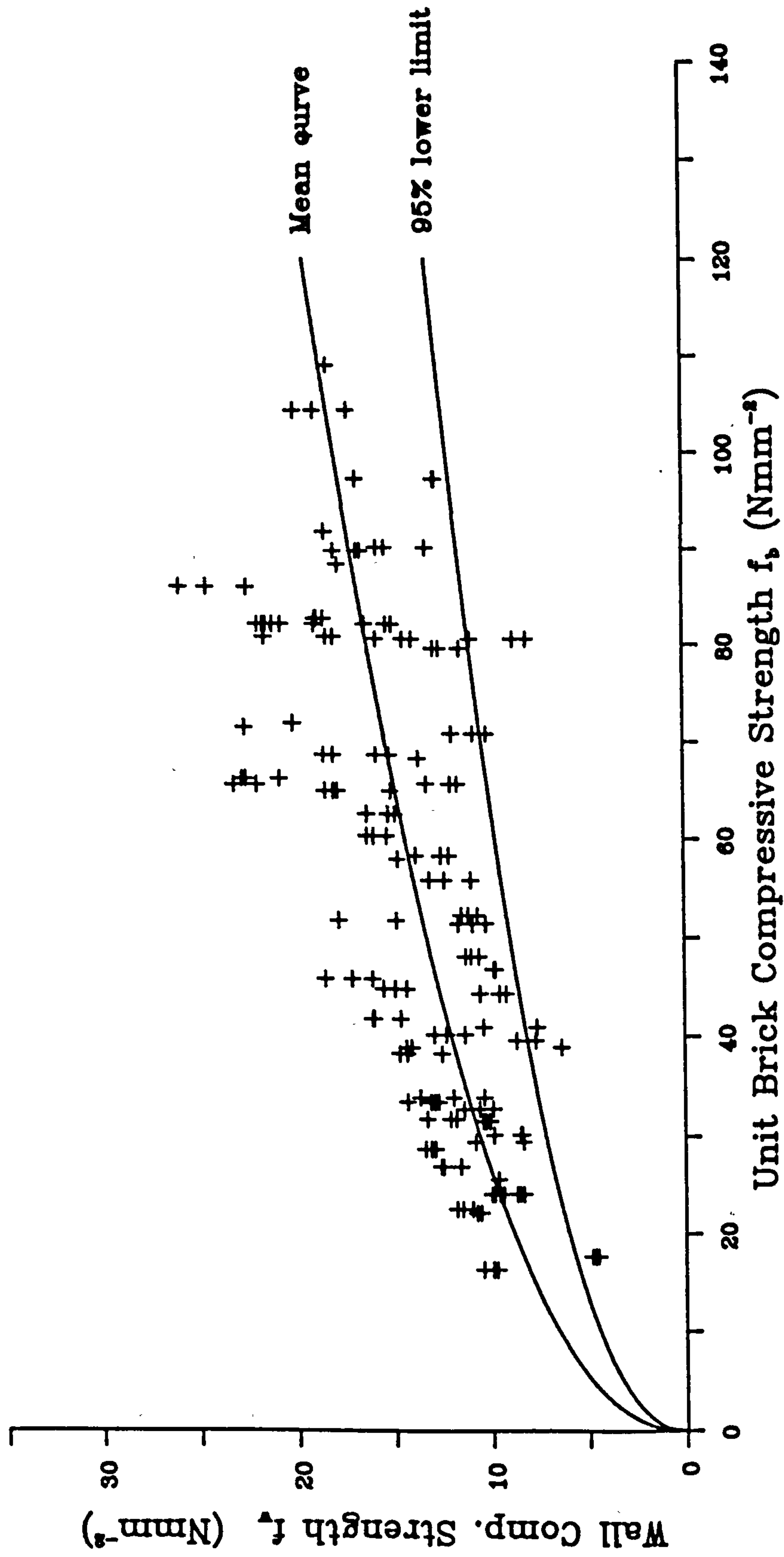


Fig. 2.4 - Plot of results for 102.5mm thick wall and mortar M(iii).

**BONDED WALL, 215.0mm THICK  
MORTAR DESIGNATION M(i)**

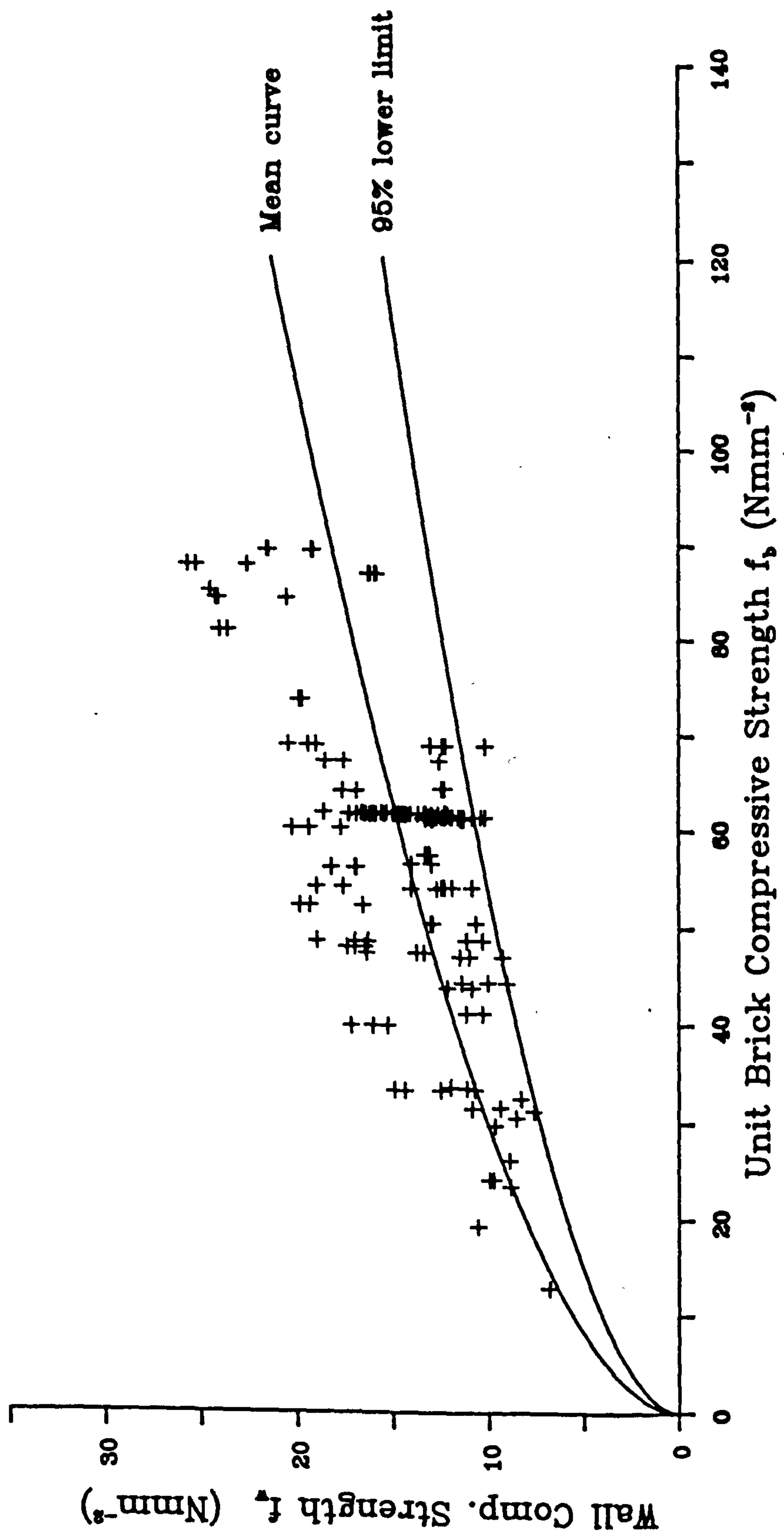


Fig. 2.5 - Plot of results for 215.0mm thick wall and mortar M(i).

**BONDED WALL, 215.0mm THICK  
MORTAR DESIGNATION M(iii)**

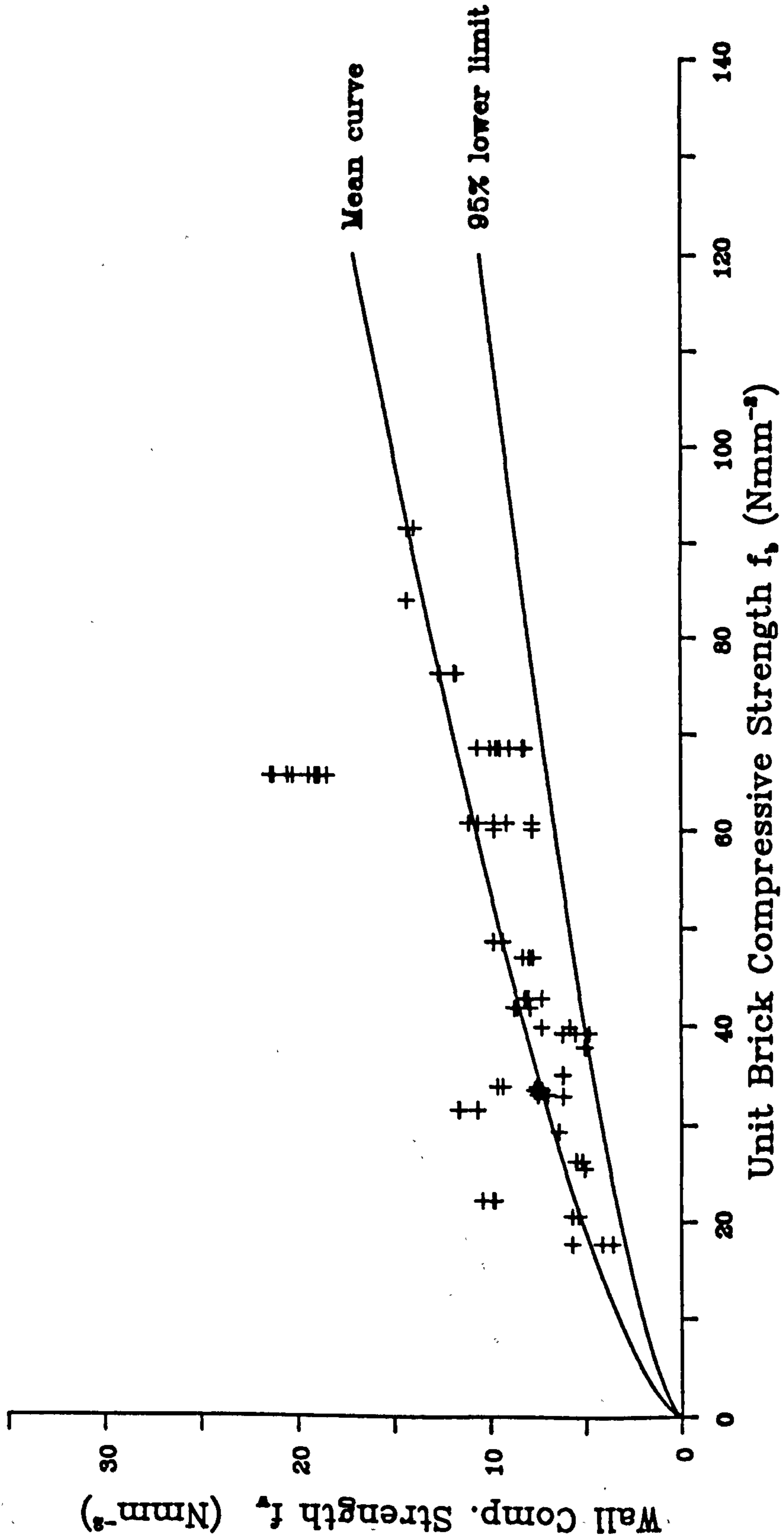


Fig. 2.6 - Plot of results for 215.0mm thick wall and mortar M(iii).

**CHARACTERISTIC COMPRESSIVE STRENGTH OF MASONRY WALL  
IN TERM OF UNIT BRICK STRENGTH**

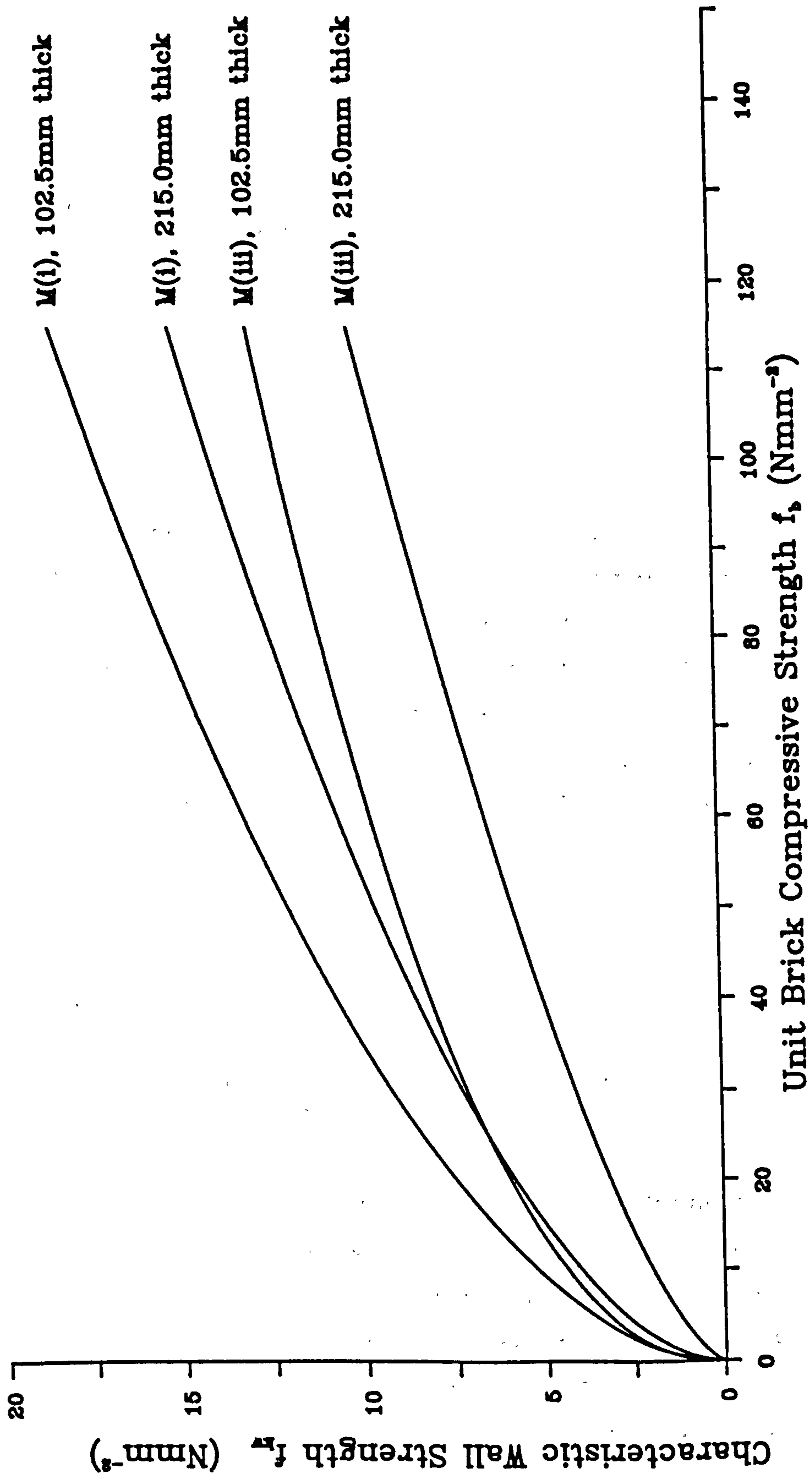


Fig. 2.7 - Plot of characteristic compressive strength of walls for two mortar mixes and wall thicknesses.

#### 2.4.4.2. Wall strength in terms of unit brick and mortar cube strengths

Since a considerable number of experimental test results have been collected, it is advantageous to analyse the data statistically to determine the relation between masonry wall, unit brick and mortar cube strengths. Expressions in the form of equation 2.9 have been assumed for the mean strength curve and hence the 95% lower confidence limit or the characteristic wall strength curve has been derived using the relevant standard deviation such that;

$$f_{kw} = K_3 \cdot f_m^l \cdot f_b^n \quad (2.14)$$

where  $f_{kw} = f_{mw} - 1.645 S_d$

$$f_{kw} = K_2 \cdot f_m^l \cdot f_b^n - 1.645 S_d$$

In all 364 test results for 102.5mm, and 272 test results for 215.0mm thick walls of which the mortar cube strengths were known have been analysed statistically and equations of the mean brickwork wall strength in terms of unit brick and mortar cube strengths have been determined for the two wall thicknesses. Table 2.7 summarises the results obtained.

Wall thickness t (mm)	Equation of the mean wall strength curve	r <sup>2</sup> (%)	S <sub>d</sub>	R <sup>2</sup>
102.5	$f_{mw} = 1.242 f_b^{0.531} \cdot f_m^{0.208}$	53.1	1.319	0.967
215.0	$f_{mw} = 0.334 f_b^{0.778} \cdot f_m^{0.234}$	62.8	1.302	0.996

Table 2.7 - Relationship between mean wall, brick and mortar cube strengths.

The cube strength for the four mortar mixes (i.e. mortar designations M(i), M(ii), M(iii) and M(iv)) were also analysed to obtain the mean cube strength and for other statistical information. The t-interval at 95% confidence interval were determined for each mix resulting in strengths of 14.7, 9.5, 4.7 and 1.5 Nmm<sup>-2</sup> for mortar designations M(i), M(ii), M(iii) and M(iv) respectively. The statistical analysis of the mortar cube strength are included in Appendix I.V.

The characteristic compressive strengths of brickwork walls were determined as before and the equations are as shown in Table 2.8. The results have been plotted by substituting the corresponding mortar cube strength at 95% confidence level for each mortar designation as shown in Figs. 2.8 - 2.11, and

in tabular form in Table 2.9.

Wall thickness t (mm)	Equation of characteristic wall strength curve
102.5	$f_{kw}=0.783f_b^{0.532}.f_m^{0.208}$
215.0	$f_{kw}=0.214f_b^{0.780}.f_m^{0.235}$

Table 2.8 - Equation of characteristic wall strength curves in terms of unit brick and mortar cube strengths for 102.5mm and 215.0mm thickness.

$f_b$  Nmm <sup>-2</sup>	$f_{kw}$ (Nmm <sup>-2</sup> )							
	t=102.5mm				t=215.0mm			
	M(i)	M(ii)	M(iii)	M(iv)	M(i)	M(ii)	M(iii)	M(iv)
5	3.2	2.9	2.5	2.0	1.4	1.3	1.1	0.8
10	4.7	4.3	3.7	2.9	2.4	2.2	1.9	1.4
20	6.7	6.2	5.3	4.2	4.2	3.8	3.2	2.4
30	8.4	7.6	6.6	5.2	5.7	5.2	4.4	3.3
40	9.7	8.9	7.7	6.1	7.2	6.5	5.5	4.2
50	11.0	10.0	8.7	6.8	8.5	7.7	6.5	5.0
60	12.1	11.0	9.5	7.5	9.8	8.9	7.5	5.7
70	13.1	12.0	10.4	8.2	11.1	10.0	8.5	6.5
80	14.1	12.9	11.1	8.8	12.3	11.1	9.4	7.2
90	15.0	13.7	11.8	9.3	13.5	12.1	10.3	7.9
100	15.9	14.5	12.5	9.9	14.6	13.2	11.2	8.5
110	16.7	15.2	13.2	10.4	15.7	14.2	12.0	9.9
120	17.5	16.0	13.8	10.9	16.8	15.2	12.9	9.9

Table 2.9 - Characteristic compressive strength of 102.5mm and 215.0mm walls.



**MEAN COMPRESSIVE STRENGTH OF FULL-STORY  
HEIGHT BRICKWORK WALL ( $f_{mw}$ ), 102.5mm THICK IN  
TERMS OF UNIT BRICK AND MORTAR CUBE STRENGTHS**

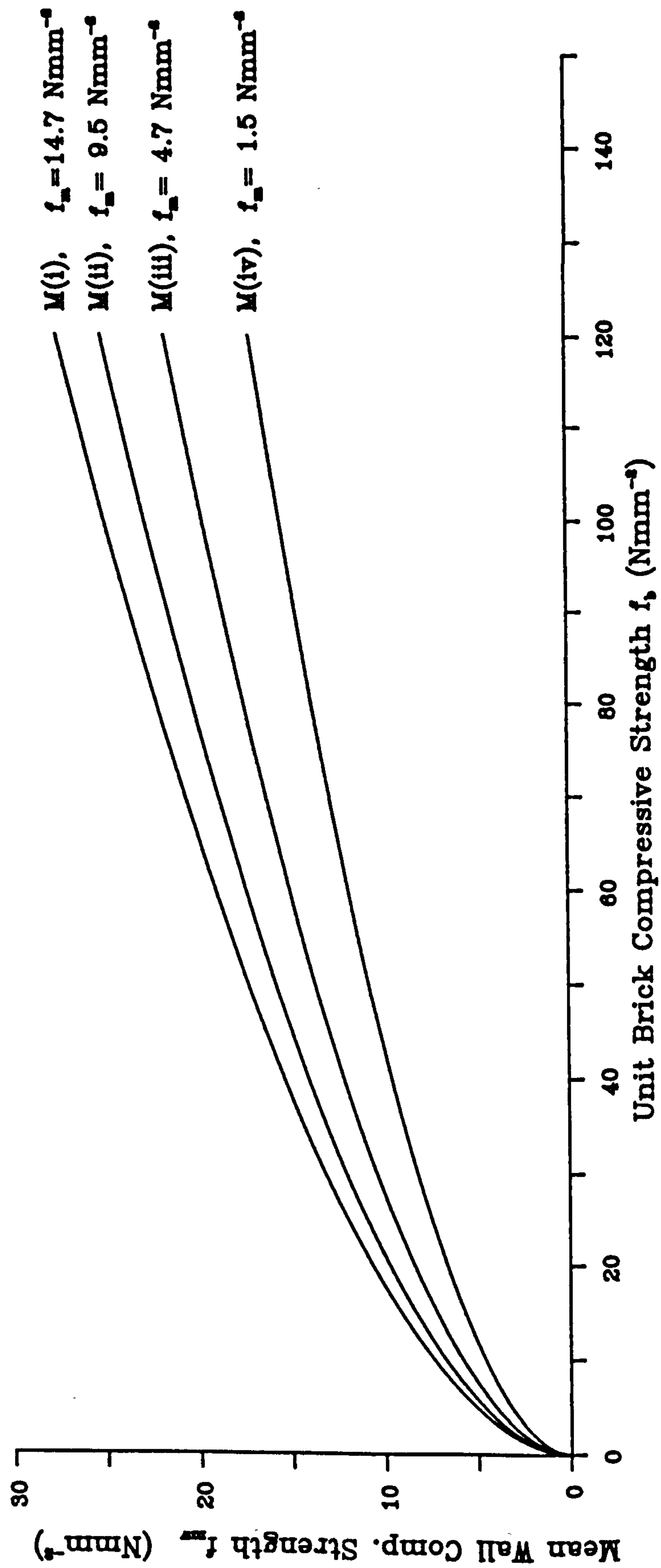


Fig. 2.8 - Mean compressive strength of 102.5mm thick walls.

**CHARACTERISTIC COMPRESSIVE STRENGTH OF FULL-STORY  
HEIGHT BRICKWORK WALL ( $f_{bw}$ ), 102.5mm THICK IN  
TERMS OF UNIT BRICK AND MORTAR CUBE STRENGTHS**

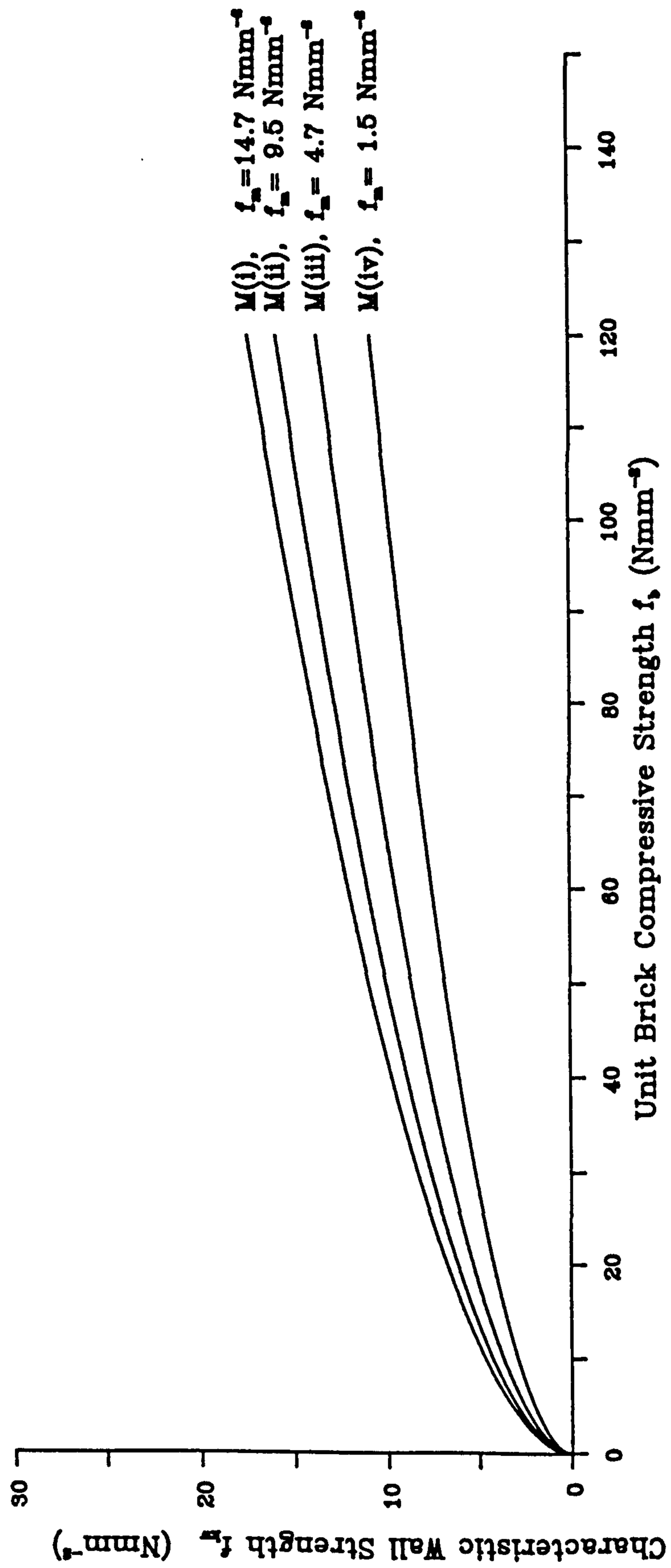


Fig. 2.9 - Characteristic compressive strength of 102.5mm thick walls.

**MEAN COMPRESSIVE STRENGTH OF FULL-STOREY  
HEIGHT BRICKWORK WALL ( $f_{mw}$ ), 215.0mm THICK IN  
TERMS OF UNIT BRICK AND MORTAR CUBE STRENGTHS**

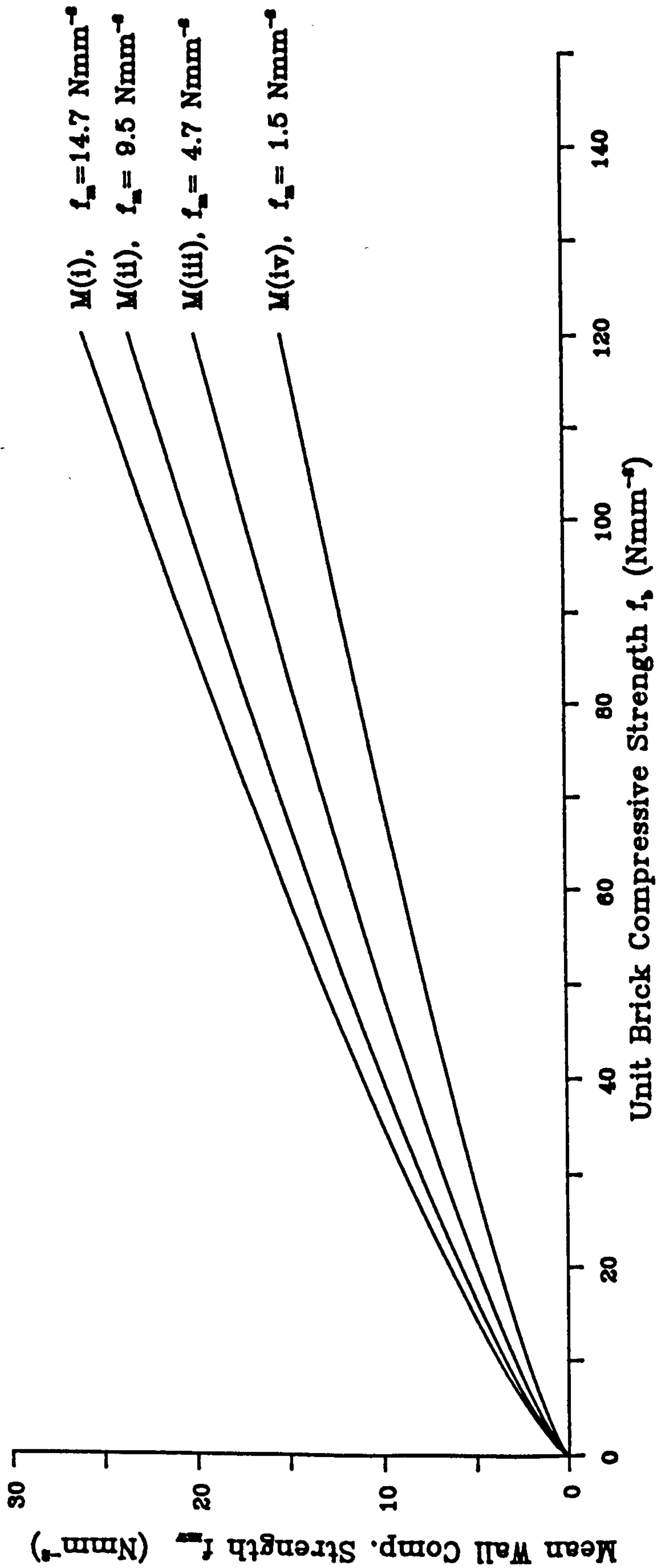


Fig. 2.10 - Mean compressive strength of 215.0mm thick walls.

**CHARACTERISTIC COMPRESSIVE STRENGTH OF FULL-STORY  
HEIGHT BRICKWORK WALL ( $f_{kw}$ ), 215.0mm THICK IN  
TERMS OF UNIT BRICK AND MORTAR CUBE STRENGTHS**

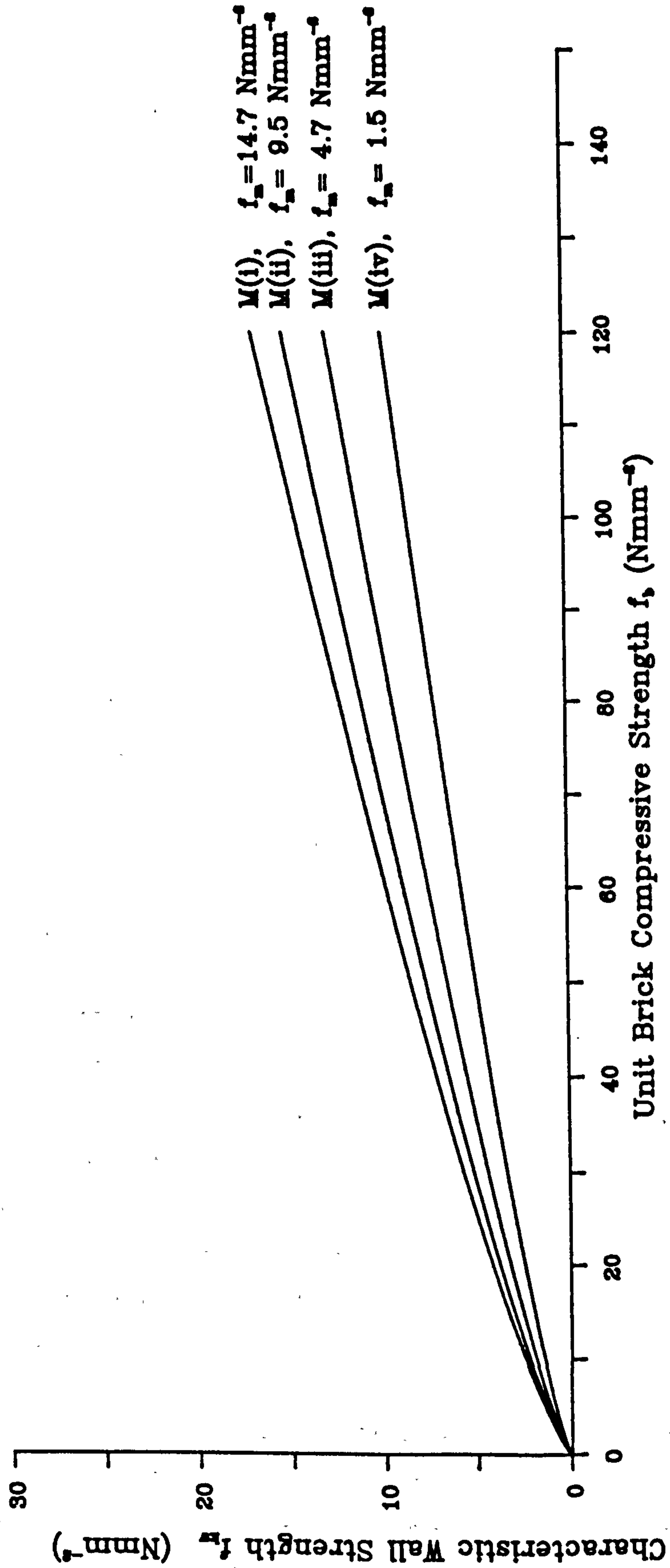


Fig. 2.11 - Characteristic compressive strength of 215.0mm thick walls.

## 2.5. CHARACTERISTIC COMPRESSIVE STRENGTH OF MASONRY

The strength of *masonry* is regarded as the strength of a brickwork specimen such that the effect of slenderness is negligible. There is no standard definition of a small specimen of which the strength would represent the masonry strength.

The 9-in brickwork cube was proposed in 1963 in Britain<sup>[51 - 54]</sup> as a basis for brickwork design, control and routine measure of quality. The intention was to use the cubes for measuring the compressive strength of brickwork once the correlation between storey-height walls and cubes were known. Upon further research, it was shown that the cubes yielded an unreliable method for measuring the compressive strengths, due to the fact that they do not simulate the characteristics of the full size brickwork masonry in compression. The factors which support this argument are: the mode of failure; initial splitting followed by shear<sup>[53 - 56]</sup> clearly indicating mixed stress patterns. The shape factor; the ratios of height to thickness and height to length is unity. Hence the strength of the cube is influenced by the effect of platens of testing machine. Strength ratio; in the large amount of work done to correlate cube and wall strengths<sup>[20, 30, 32, 53, 54]</sup>, cube strength was mostly two to three times the wall strength. This is a far higher ratio than obtained elsewhere<sup>[53, 58, 59]</sup>, using prisms of sufficient height.

An alternative to the British cube was a prism specimen. However, prism strength is not necessarily equal to compressive strength of bonded brickwork, but it has become common practice in certain countries to test for quality control and strength purposes, and as long as the height of the specimen is such that the platen effect is not significant, its strength is assumed to represent the masonry strength. The two most common small specimens are stack and running bonded prisms of different height to thickness ratios depending on its number of courses.

Research work in Australia<sup>[35]</sup>, where a stack bond prism is used as a basis for determining brickwork design strength, has indicated that the ratio of wall strength to prism strength (with  $h/t=3$ ) is on average 0.9. This ratio<sup>[57]</sup> has been shown to vary with the ratio of height to thickness of specimen ( $h/t$ ) from about 0.7 at  $h/t=2$  to 1.0 at  $h/t=5$ .

However, it is possible to arrive at mean and characteristic compressive strengths of masonry ( $f_{mm}$  and  $f_k$ ) from the wall strength already determined,

provided there exists a set of true reduction factors for slenderness<sup>[32]</sup> such that:

$$f_{mw} = \beta \cdot f_{mm} \quad (2.15)$$

$$\text{or } f_{mm} = (K_2/\beta) \cdot f_m \cdot f_b^n$$

$$f_{kw} = \beta \cdot f_k \quad (2.16)$$

$$\text{or } f_k = (K_3/\beta) \cdot f_m \cdot f_b^n$$

The slenderness ratio ( $h_{ef}/t_{ef}$ ) for the walls analysed in previous section were on average 18.0 and 9.0 for 102.5mm and 215.0mm thickness respectively. The values given in BS 5628:table 7<sup>[11]</sup> for  $\beta$  are used here which are equal to 0.770 and 0.985 for slenderness ratios of 18.0 and 9.0 respectively.

The equations for mean and characteristic compressive strengths of masonry for the two wall thicknesses are as shown in Table 2.10 and by substituting the appropriate values of cube strength for a particular mortar designation, sets of curves are produced representing  $f_{mm}$  and  $f_k$  values in terms of unit brick strength ( $f_b$ ) for a particular mortar designation and wall thickness. These curves are represented in Figs. 2.12, 2.13, 2.14 and 2.15 and in tabular forms in Tables 2.11 and 2.12.

Masonry thickness t (mm)	Equation of mean compressive strength of masonry ( $f_{mm}$ )	Equation of characteristic compressive strength of masonry ( $f_k$ )
102.5	$f_{mm} = 1.613 f_b^{0.531} \cdot f_m^{0.208}$	$f_k = 1.017 f_b^{0.532} \cdot f_m^{0.208}$
215.0	$f_{mm} = 0.339 f_b^{0.778} \cdot f_m^{0.234}$	$f_k = 0.217 f_b^{0.780} \cdot f_m^{0.235}$

Table 2.10 - Equation for mean and characteristic compressive strength of masonry.

**MEAN COMPRESSIVE STRENGTH OF MASONRY ( $f_{mm}$ ),  
102.5mm THICK**

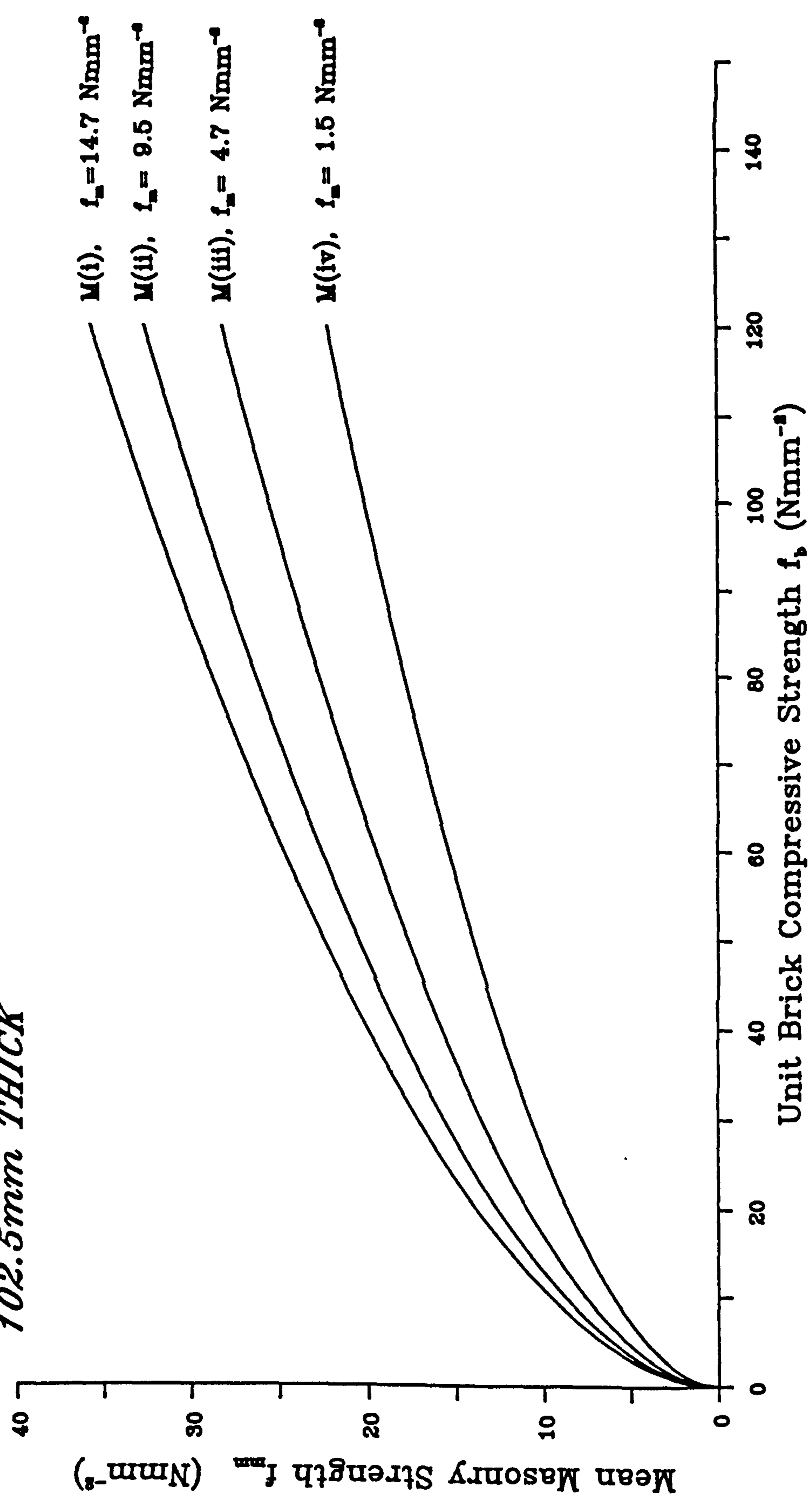


Fig. 2.12 - Mean compressive strength of masonry,  $f_{mm}$ , 102.5mm thick.

**MEAN COMPRESSIVE STRENGTH OF MASONRY ( $f_{mm}$ ),  
215.0mm THICK**

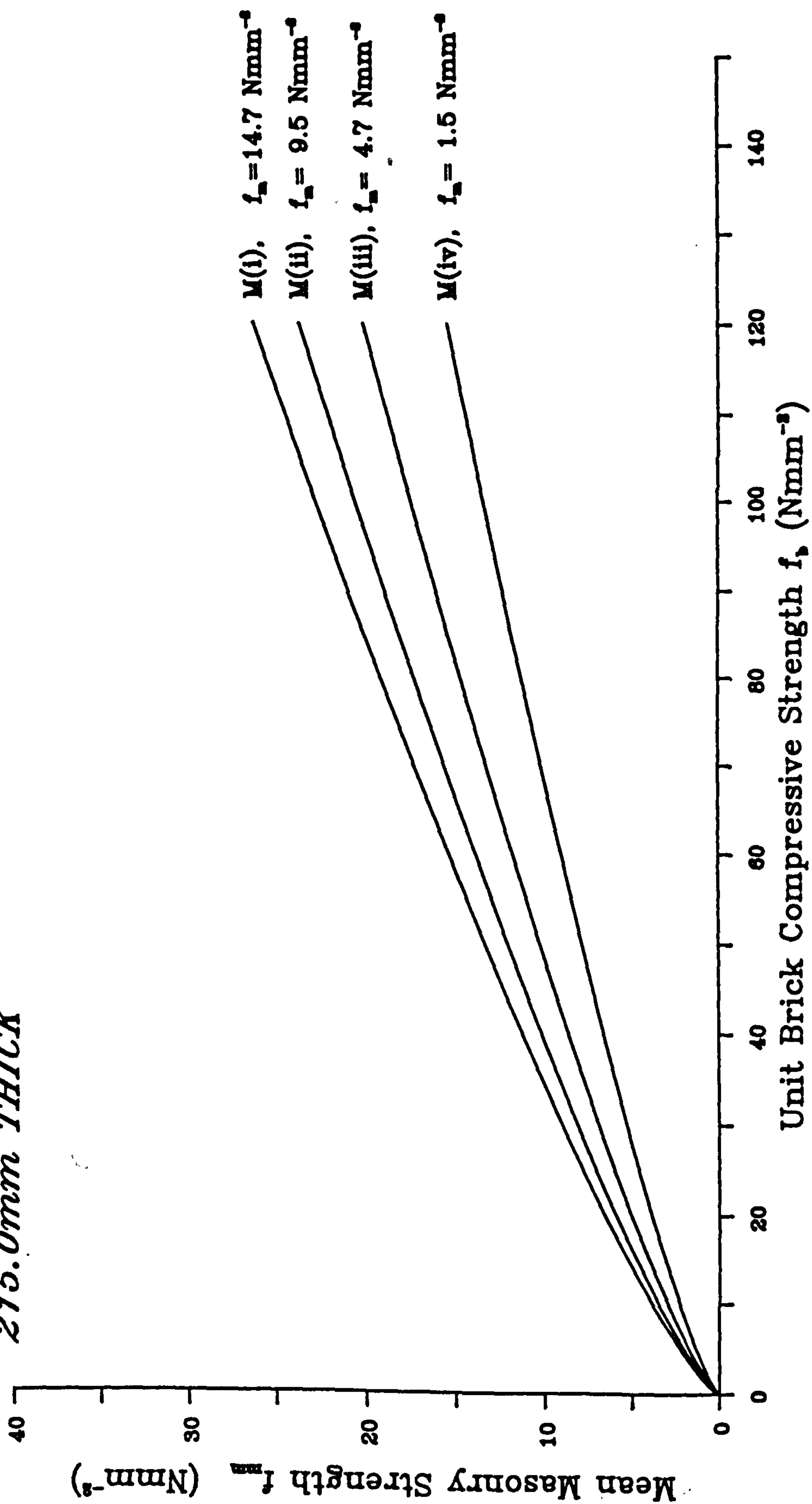


Fig. 2.13 - Mean compressive strength of masonry,  $f_{mm}$ ,  
215.0mm thick.



**CHARACTERISTIC COMPRESSIVE STRENGTH OF MASONRY  
( $f_k$ ), 102.5mm THICK**

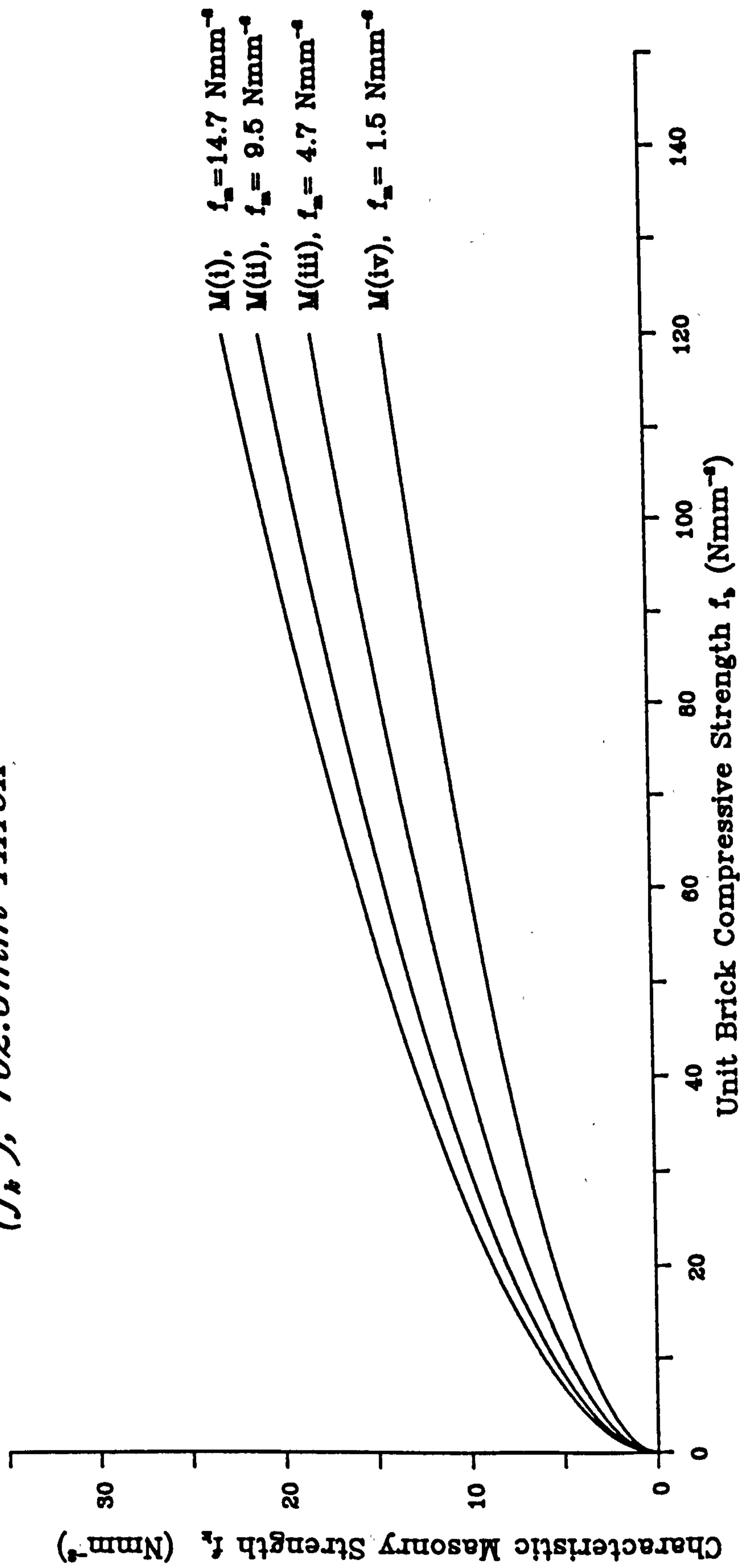


Fig. 2.14 - Characteristic compressive strength of masonry,  $f_k$ , 102.5mm thick.

**CHARACTERISTIC COMPRESSIVE STRENGTH OF MASONRY**  
*( $f_k$ ), 215.0mm THICK*

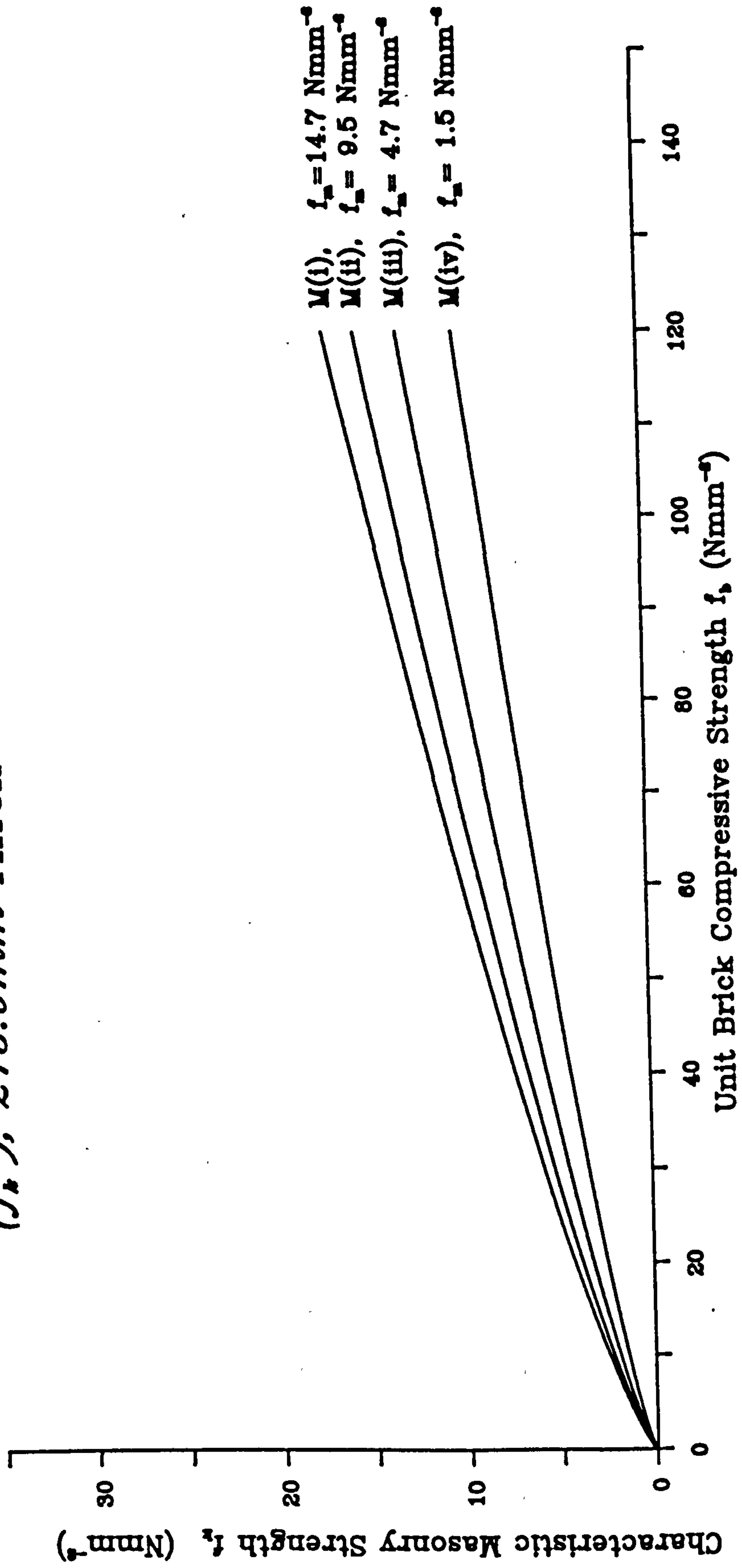


Fig. 2.15 - Characteristic compressive strength of masonry,  $f_k$ , 215.0mm thick.

$f_b$	$f_{mm}$ (Nmm <sup>-2</sup> )							
	t=102.5mm				t=215.0mm			
	M(i)	M(ii)	M(iii)	M(iv)	M(i)	M(ii)	M(iii)	M(iv)
10	9.6	8.7	7.6	6.0	3.8	3.4	2.9	2.2
20	13.8	12.6	10.9	8.6	6.5	5.9	5.0	3.8
30	17.2	15.7	13.5	10.7	9.0	8.1	6.9	5.3
40	20.0	18.3	15.8	12.4	11.2	10.1	8.6	6.6
50	22.5	20.6	17.8	14.0	13.3	12.0	10.2	7.8
60	24.8	22.7	19.6	15.4	15.4	13.9	11.8	9.0
70	26.9	24.6	21.2	16.8	17.3	15.6	13.3	10.2
80	28.9	26.4	22.8	18.0	19.2	17.4	14.7	11.3
90	30.8	28.1	24.3	19.1	21.1	19.0	16.1	12.4
100	32.5	29.7	25.7	20.2	22.9	20.6	17.5	13.4
110	34.2	31.3	27.0	21.3	24.6	22.2	18.9	14.5
120	35.8	32.7	28.3	22.3	26.4	23.8	20.2	15.5

Table 2.11 - Mean compressive strength of masonry,  $f_{mm}$ , 102.5mm and 215.0mm thickness in Nmm<sup>-2</sup>.

$f_b$	$f_k$ (Nmm <sup>-2</sup> )							
	t=102.5mm				t=215.0mm			
	M(i)	M(ii)	M(iii)	M(iv)	M(i)	M(ii)	M(iii)	M(iv)
5	4.2	3.8	3.3	2.6	1.4	1.3	1.1	0.8
10	6.1	5.5	4.8	3.8	2.5	2.2	1.9	1.4
20	8.8	8.0	6.9	5.4	4.2	3.8	3.2	2.5
30	10.9	9.9	8.6	6.8	5.8	5.2	4.4	3.4
40	12.7	11.6	10.0	7.9	7.2	6.5	5.5	4.2
50	14.3	13.0	11.2	8.9	8.6	7.8	6.6	5.1
60	15.7	14.3	12.4	9.8	9.9	9.0	7.6	5.8
70	17.1	15.6	13.4	10.6	11.2	10.1	8.6	6.6
80	18.3	16.7	14.4	11.4	12.4	11.2	9.5	7.3
90	19.5	17.8	15.4	12.1	13.6	12.3	10.4	8.0
100	20.6	18.8	16.3	12.8	14.8	13.4	11.3	8.7
110	21.7	19.8	17.1	13.5	16.0	14.4	12.2	9.3
120	22.7	20.7	17.9	14.1	17.1	15.4	13.1	10.0

Table 2.12 - Characteristic compressive strength of masonry,  $f_k$ , 102.5mm and 215.0mm thickness in Nmm<sup>-2</sup>.

## 2.6. DISCUSSIONS

Sections 2.3 and 2.4.2 reports the published results on full storey-height brickwork wall. It should be pointed out that no distinction has been made between the conditions of end fixity of the walls from the point of view of the loading application. The tests carried out in the earlier times on walls were by means of knife edge loading, whereas the latter tests were conducted to try to simulate the conditions in practice of which the walls were tested between thick concrete plinths. Inspection of the results shows there is not a significant difference taking into account the variation in the strength of brickwork. However, if the distinction had to be made the number of test results would have not been sufficient in order to carry out the statistical analyses.

The results obtained from the two analyses outlined in sections 2.4.4.1 and 2.4.4.2, show good agreement. Comparing the results obtained as shown in Tables 2.6 and 2.9, shows there is little difference in the value for  $f_{kw}$ . However, this small difference in value for  $f_{kw}$  could be explained by the fact that in the first analysis,  $f_{kw}$  is given in terms of  $f_b$  only for a particular mortar mix, whereas in the second analysis,  $f_{kw}$  is given as a function of  $f_b$  and  $f_m$ , where values for the mortar cube strength are the characteristic values obtained from the mean cube strengths.

Provided that all the primary variables were included, it would have been possible to demonstrate that homogeneity of the expressions would have been satisfied. However, due to the lack of tensile strength of brick units in the results the sum of indices, as in equation 2.8 is  $0.67 \geq (l) \geq 0.44$ , and for expression in the form of equation 2.9 is  $1.01 \geq (l+n) \geq 0.74$ . Furthermore it is arguable that the constant coefficients  $K_1$  and  $K_2$  given in the equations are themselves a function of strength to some power. It is also worthy to note that better correlation coefficients are attained for the best fit if the number of primary variables is increased. This is evident by comparing the values obtained for  $r^2$  in Tables 2.3 and 2.7.

The 95% confidence interval or the characteristic compressive strength of mortar cubes are 14.7, 9.5, 4.7 and 1.5  $\text{Nmm}^{-2}$  for mortar designations M(i), M(ii), M(iii) and M(iv) respectively compared to the values of 16.0, 6.5, 3.6 and 1.5  $\text{Nmm}^{-2}$  given as the minimum values of mortar-cube strength in the code<sup>[1]</sup>.

In the two analyses of walls the ratios of  $f_{kw}/f_{mw}$  were found to be on average 0.64 and 0.68 assuming expressions in the form of equations 2.9 and 2.8 respectively. Also the ratio of  $f_k/f_{mm}$  based on equations 2.15 and 2.16 were found to be 0.64. However, in a recent paper, research work in China<sup>[58]</sup> has shown that this ratio is equal to 0.72. This is because the coefficient of variation of the masonry is taken as 17%.

In section 2.5 mean and characteristic compressive strengths of masonry, ( $f_{mm}$  and  $f_k$ ), have been calculated based on the values given in the code<sup>[1]</sup> for the capacity reduction factor for walls allowing for the effect of slenderness ( $\beta$ ). This, however, could be done with any set of values for  $\beta$ .

Comparison has been made between the values for the characteristic compressive strength of masonry,  $f_k$ , as obtained in section 2.5 and the BS 5628<sup>[1]</sup>. These are graphically shown in Figs. 2.16 and 2.17 for the two masonry thicknesses respectively. From these graphs it can be seen that the code<sup>[1]</sup> values for  $f_k$  are higher, particularly for bonded masonry. This, however, could be explained by the fact that the values of  $f_k$  given in BS 5628:Part1<sup>[1]</sup>; table 2(a) or fig. 1(a) for bonded masonry are the mean strength of British test results of single leaf walls for a particular mortar designation. This is evident from Figs. 2.18 and 2.19 of which they show the comparison between the  $f_k$  values from the code<sup>[1]</sup> for two masonry thicknesses and the test results of storey-height walls for mortar designations M(i) and M(iii) respectively.

However, the validity of the  $f_k$  values given in BS 5628<sup>[1]</sup> is questionable. The factors which support this argument are:

- No statistical evidence for the derivation of  $f_k$  values given in the code exists. It is believed to be based on the test results of storey-height walls which originated from CP 111<sup>[11]</sup>.
- $f_k$  values given by the code are mean and not characteristic values as shown by Figs. 2.18 and 2.19.
- $f_k$  values given in table 2(a) of the code is for bonded masonry, and in case of *narrow brick walls* (i.e. where the thickness of the wall is equal to the width of a standard format brick,  $t=102.5\text{mm}$ ), clause 23.1.2 of the code<sup>[1]</sup> states that "the values of  $f_k$  obtained from table 2(a) may be multiplied by 1.15". Hence increasing the  $f_k$  values further.
- It is well known that single leaf brick wall is stronger than bonded wall, Therefore, the values for  $f_k$  in table 2(a) of the code<sup>[1]</sup> does not represent the strength of bonded masonry, since it is the average strength of single leaf, 102.5mm thick

walls being tested in U.K. Furthermore, they need to be adjusted to represent masonry strength in contrast to wall strength.

As a comparison, Fig. 2.20 has been included, which is a plot of 389 test results of four-brick high stack bonded prisms, 102.5mm thick constructed with mortar designation M(iii). The characteristic compressive strength of the prism,  $f_{kp}$ , was determined as before. On the same graph the values for characteristic compressive strength of masonry,  $f_k$ , derived from the wall test results, has been plotted for the same masonry thickness and mortar designation.  $f_k$  values are 40% lower on average than  $f_{kp}$  values. This, however, may be explained as being due to the different  $h/t$  ratios. In the case of four-brick high stack bonded prisms  $h/t=3$ , whereas in the case of  $f_k$  values, the code<sup>[1]</sup> gives a value of 1.0 for  $\beta$  when  $h_{ef}/t_{ef} = 8$  (or  $h/t=10$ ). To compare the two curves one has to be modified by another reduction factor to adjust for the slenderness.

## 2.7. CONCLUSIONS

Relationships of the form  $K.f_b^n$  and  $K.f_m^l.f_b^n$  have been established for mean and characteristic brickwork wall strengths for specific mortar grades and strengths and two wall thicknesses by statistical analysis of wall test results.

The constants and indices in the above formulae depend on the mortar mix and also on the type of wall, i.e. whether the wall thickness is equal to the unit thickness or is of bonded construction.

The test results were found to be consistent with normal distribution in statistical terms. This is especially true when large number of test data is available, i.e. as number of test results increase, the distribution of strength tends to normality.

The characteristic strength of mortar cubes were found to be 14.7, 9.5, 4.7 and 1.5  $\text{Nmm}^{-2}$  for mortar designations M(i), M(ii), M(iii) and M(iv) respectively.

The characteristic compressive strength of various types of masonry ( $f_k$ ) has been derived from the wall strength relationships by applying a correction to allow for the effect of slenderness ratio on the basis of the reduction factors given in BS 5628:Part 1:table 7<sup>[1]</sup>.

A limited comparison between characteristic compressive strengths derived

from wall tests and from prism tests indicates that the latter gives a high value for  $f_k$ . This may be due to discrepancies in correcting for slenderness effects.

**COMPARISON BETWEEN CHARACTERISTIC COMPRESSIVE STRENGTH  
OF MASONRY ( $f_k$ ), 102.5mm THICK OBTAINED FROM  
WALL TEST RESULTS AND BS 5628 CODE**

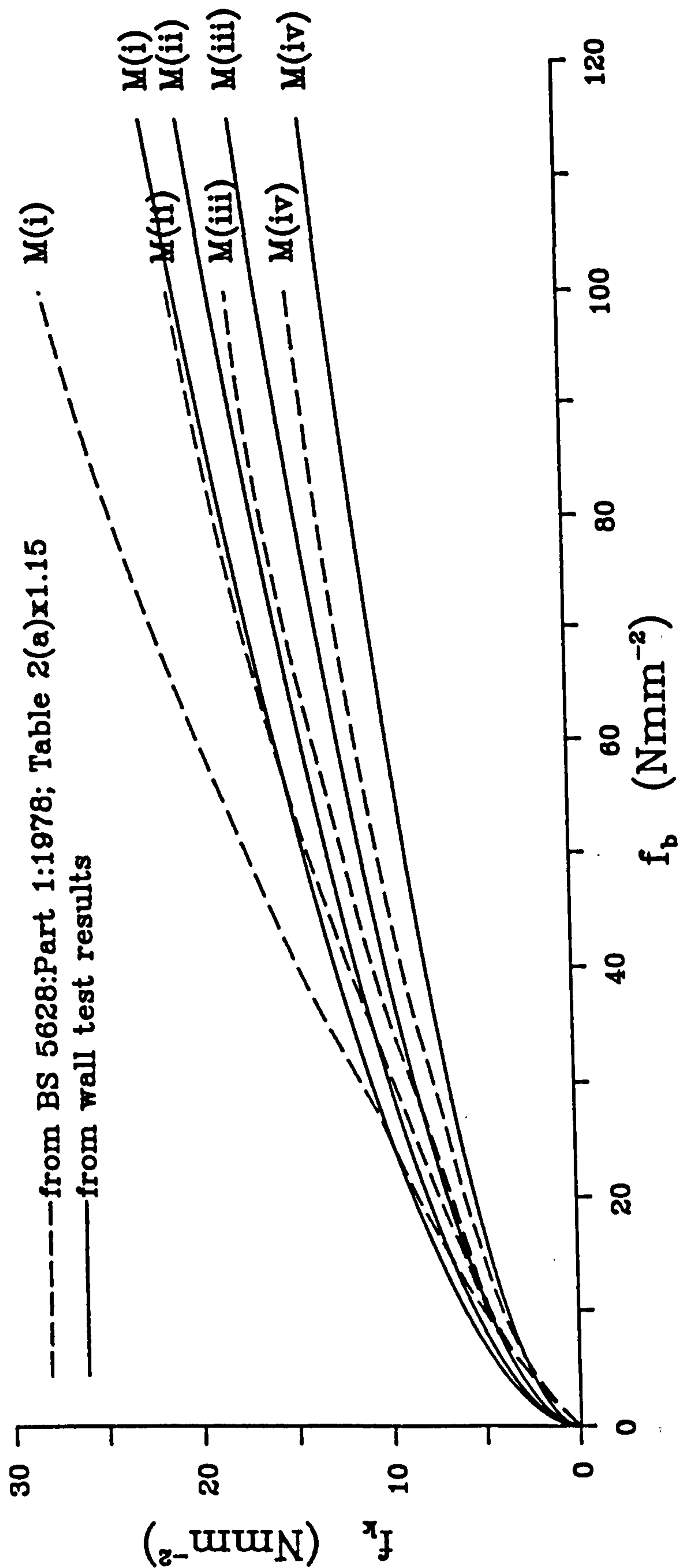


Fig. 2.16 - Comparison between the characteristic compressive strengths of masonry,  $f_k$ , 102.5mm thick determined from the wall test results and the Code<sup>(1)</sup>.



**COMPARISON BETWEEN CHARACTERISTIC COMPRESSIVE STRENGTH  
OF MASONRY ( $f_k$ ), 215.0mm THICK OBTAINED FROM  
WALL TEST RESULTS AND BS 5628 CODE**

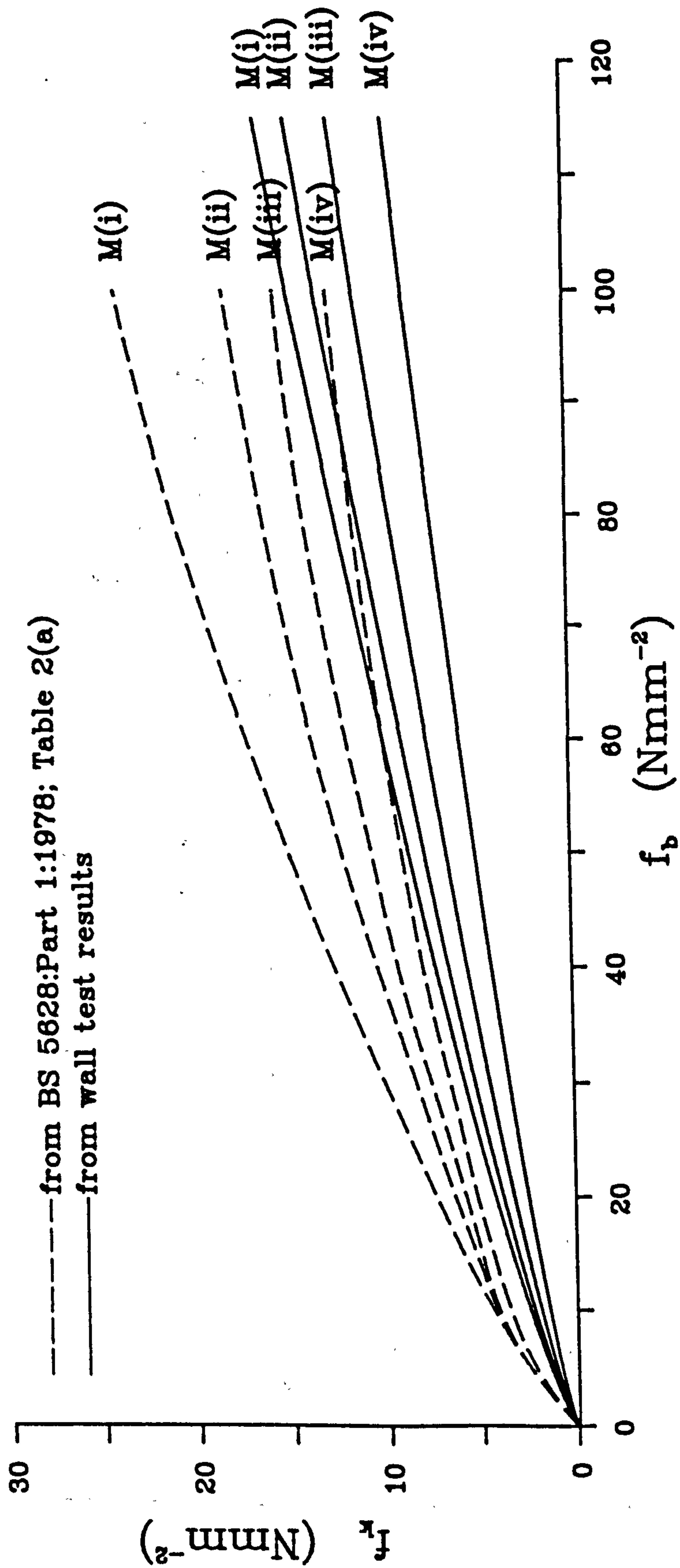
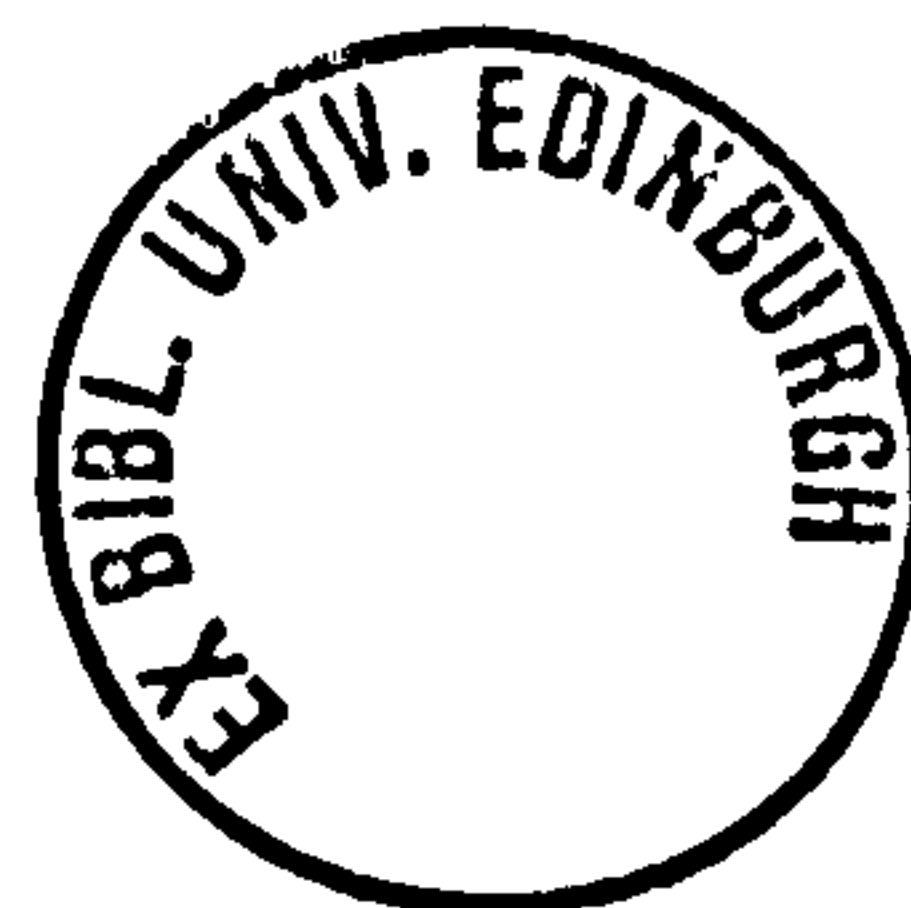


Fig. 2.17 - Comparison between the characteristic compressive strengths of masonry,  $f_k$ , 215.0mm thick determined from the wall test results and the Code<sup>[1]</sup>.



**COMPARISON BETWEEN  $f_{mw}$  and  $f_{kw}$  DETERMINED FROM  
WALL TEST RESULTS, 102.5mm THICK, MORTAR M(i)  
AND THE  $f_k$  FROM BS 5628**

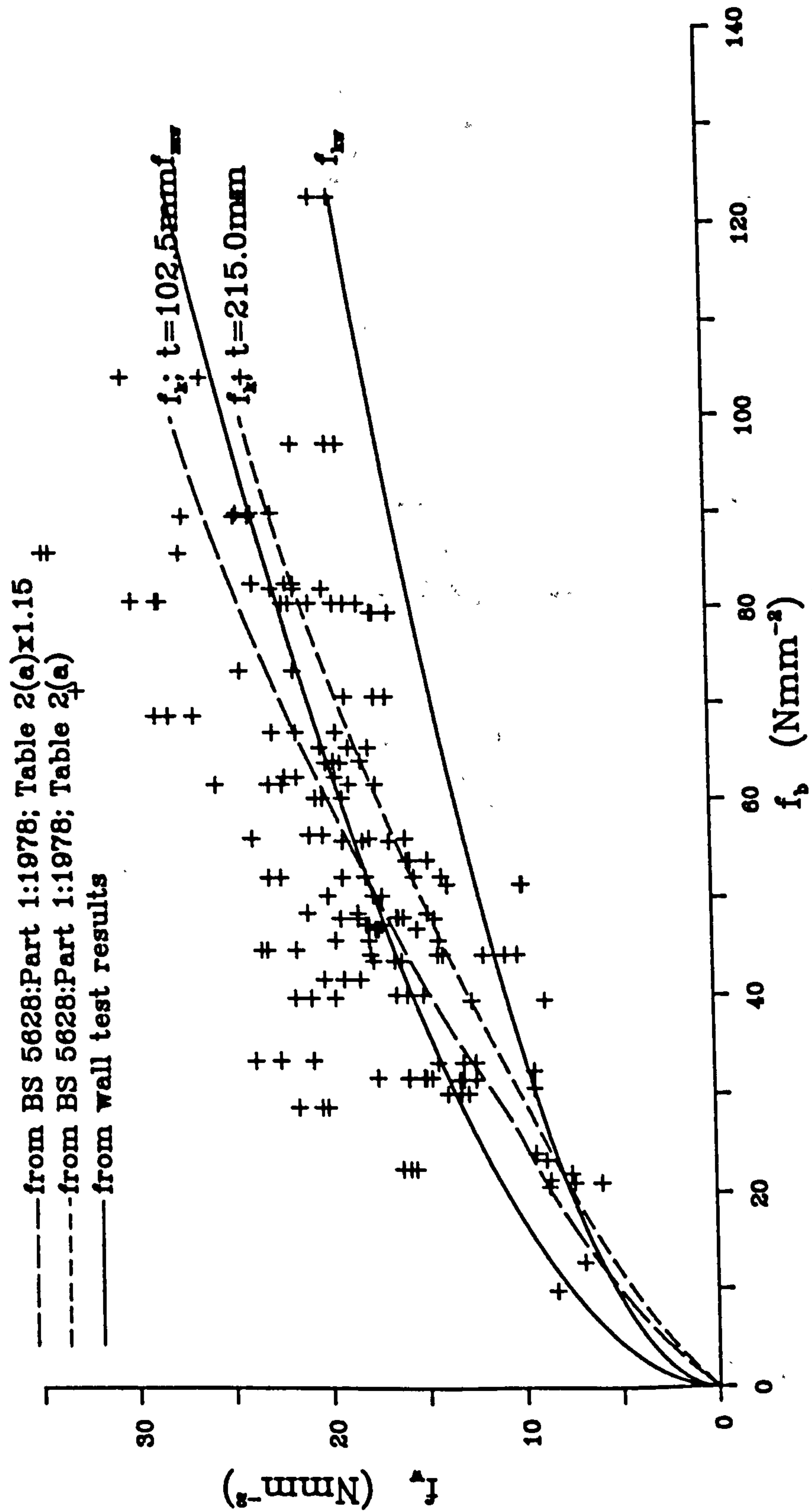


Fig. 2.18 - Comparison between  $f_{mw}$  and  $f_{kw}$  derived from the test results of storey-height walls, 102.5mm thick and mortar designation M(i) with the  $f_k$  curves from the Code<sup>[1]</sup>.

**COMPARISON BETWEEN  $f_{mw}$  and  $f_{kw}$  DETERMINED FROM  
WALL TEST RESULTS, 102.5mm THICK, MORTAR M(ii)  
AND THE  $f_k$  FROM BS 5628**

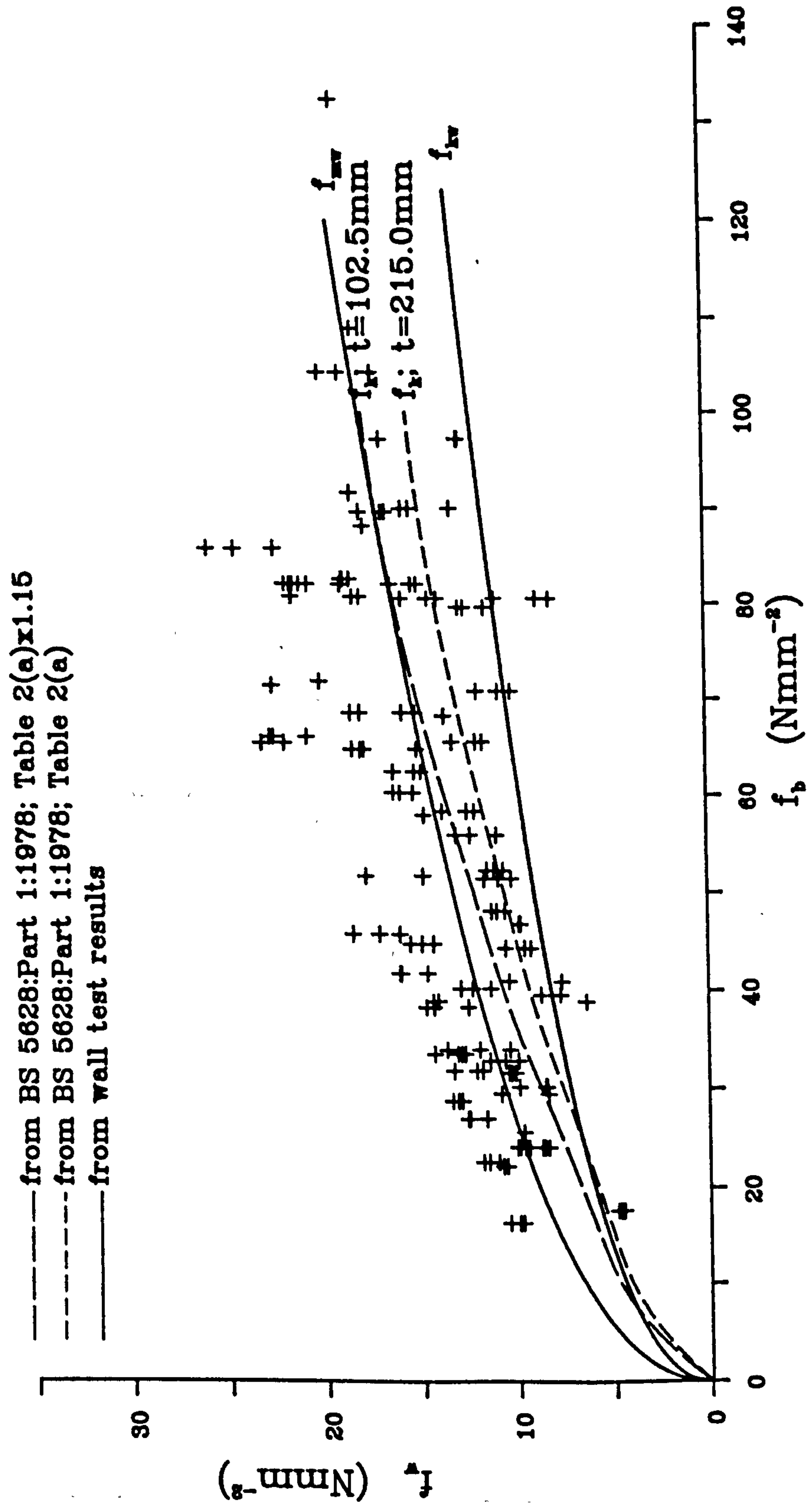


Fig. 2.19 - Comparison between  $f_{mw}$  and  $f_{kw}$  derived from the test results of storey-height walls, 102.5mm thick and mortar designation M(ii) with the  $f_k$  curves from the Code<sup>[1]</sup>.

**COMPARISON BETWEEN CHARACTERISTIC COMPRESSIVE STRENGTH OF  
MASONRY ( $f_k$ ) AND CHARACTERISTIC COMPRESSIVE STRENGTH  
OF FOUR-BRICK HIGH STACK BONDED PRISM ( $f_{kp}$ ),  
102.5mm THICK, MORTAR DESIGNATION M(iii).**

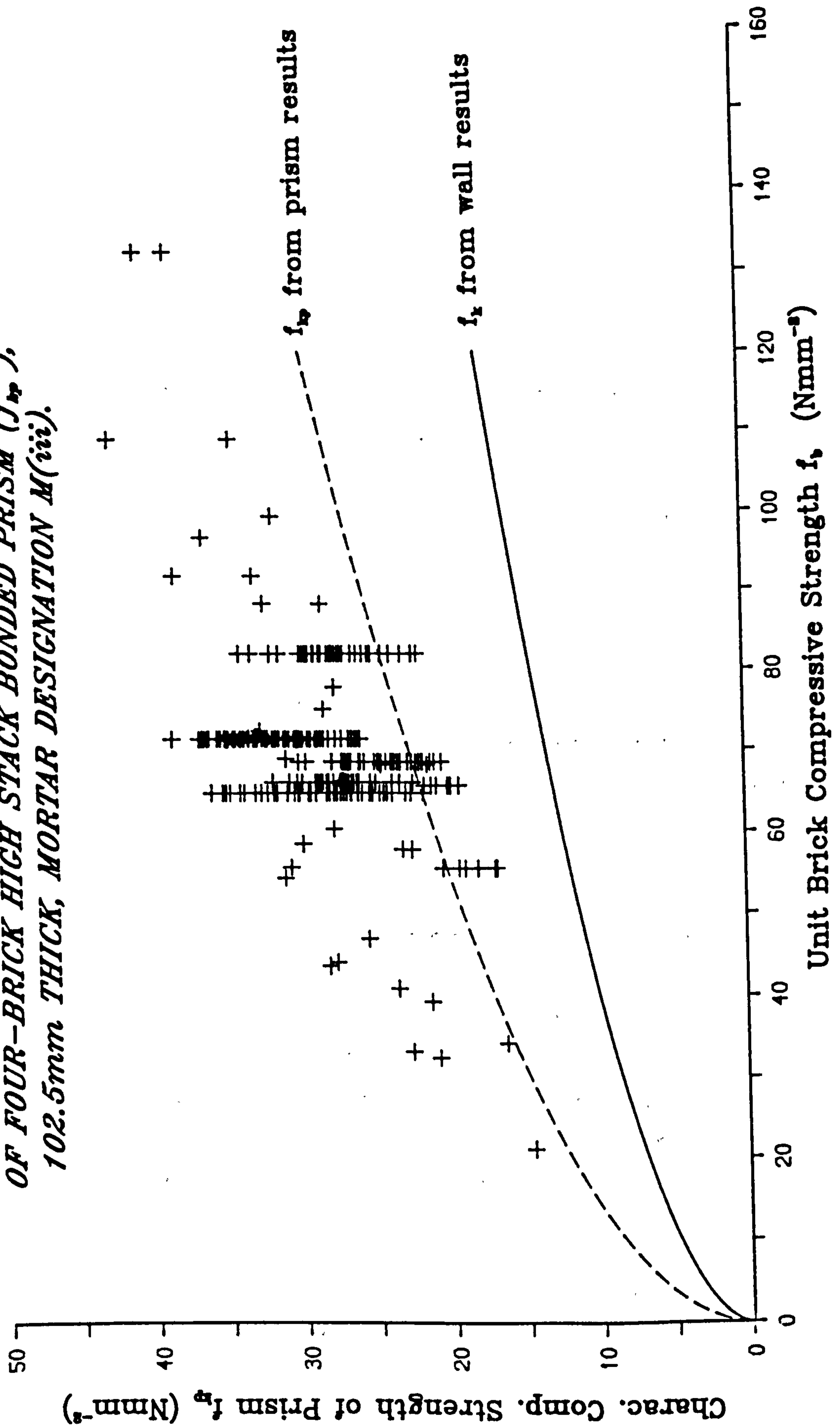


Fig. 2.20 - Comparison between  $f_k$  determined from storey-height wall and 4-brick high stack bonded prism test results.

## Chapter 3

### COMPRESSIVE STRENGTH OF MASONRY UNDER CONCENTRATED LOADING

#### 3.1. INTRODUCTION

The ability of masonry to withstand higher direct stresses over confined areas has been known for a considerable time. The problem of the application of a concentrated force to the boundary of a brickwork structure is one which presents almost insuperable difficulties for the solution of the stress distribution. The reason for these difficulties are many, and include the non-homogeneity of brickwork, the anisotropic structure of the brickwork, and the difficulty in obtaining the deformation properties of the brick, mortar and brickwork.

The earlier classical solutions of stress distribution theory were based on results given by the mathematical theory of elasticity for the simplest case of loading a solid homogeneous, linear elastic, isotropic, semi-infinite medium assuming the material is weightless. Other investigators have produced more exact solutions in two and three dimensions based on the theory of elasticity. A detailed survey is given elsewhere<sup>[59]</sup>.

Considerable amount of theoretical and experimental work has been carried out on the bearing capacity of concrete loaded over a limited area. The theoretical investigations have been based mainly on the Coulomb/Mohr theory of rupture which envisages failure as a sliding action along planes inclined to the direction of the principal stress. Resistance to sliding is brought about by the shearing strength or internal cohesion of the material and by a resistance due to internal friction which is proportional to the normal stress on the shear plane.

Large numbers of tests have been carried out on unreinforced concrete cubes and prisms by various investigators. The bulk of the results have been collected and analysed by Williams<sup>[60]</sup>, to study the influence of variables such as specimen depth, geometry of loaded area, loading and support media, concrete properties, size of aggregate, horizontal component of load and effective area on the ratio of bearing strength to the characteristic cube compressive strength of concrete.

Concrete is however, a relatively homogeneous material compared with brickwork, and any loading on a concrete structure may be considered to be distributed in such a way that it is not affected by any one aggregate particle. Theoretical solutions proposed were all based on the supposition that the loaded material behaves in a homogeneous, isotropic, and elastic manner. The comparison of the theoretical and experimental strain distributions has shown that concrete satisfies these criteria, the form of the experimental strain distribution being similar to those of the advanced theoretical analyses.

With brickwork it is likely that a concentrated load will only be applied to a relatively small number of bricks, and hence the individual brick properties will have a considerable effect. The effect of the mortar beds on the strain distribution is very difficult to determine experimentally. If the deformation properties of the brick and mortar were similar, the vertical strain distribution would not be greatly affected by the mortar layers. The horizontal strain distribution is however, influenced by the difference in the deformation properties of the two materials, and vertical jointing of the composite material will also have an effect.

In this situation any solution based on the theory of elasticity will be of doubtful validity, under-estimating the tensile stresses which are in fact developed. The only analytical tool likely to be useful will be the finite element method.

In this chapter, the previous research work carried out on the compressive strength of brickwork masonry under concentrated load will be reviewed and the design guides given in various codes of practice are summarised.

### **3.2. REVIEW OF PREVIOUS RESEARCH**

The first known series of tests<sup>[61 - 63]</sup> were carried out during the 1930's by the Masonry Sectional Committee of the Institute of Structural Engineers on the safe bearing pressure on brickwork carrying a heavy load applied through a steel plate bedded directly onto the brickwork. This investigation tried to determine the effect of using bearing plates of different thicknesses beneath the load; of using stronger bricks in the top courses; and of building in the section through which the load was applied to the bearing plate (an "I"-section). The investigation also covered the effect of slenderness ratio and the deflection of the lintel applying the load.

The results obtained indicated that as the wall length/bearing plate length ratio decreases the failure stress also decreases, and either building-in the joist or increasing the plate thickness from 12.5 to 25.0mm raises the resistance roughly by 30% over that of brickwork carrying the joist direct. The number of specimens tested was small and no definite design guide was proposed. However, the committee concluded that permissible stresses should not be increased, although results indicated that well built brickwork, even in thin walls, acts as a unified mass, and is capable of sustaining load considerably greater than those permitted in the CP 111:1936<sup>[11]</sup>. Two reasons were given for this decision. The first was the rigid foundation they had adopted, and the second, the high quality of workmanship in the specimens constructed. It was also concluded that thin bearing plates were of little use, as was the provision of stronger bricks in only a few courses below the load. Building the beam into the wall was, however, considered to increase the load capacity of the wall. No comment is made about the effectiveness of rigid bearing plates although their tests indicated that these increases the load capacity of the wall. The effect of the wall height on the resistance to eccentric loading was not found to be important in the tests conducted (i.e.  $H/t=10.7$ ), although strains measured on the wall faces were found to indicate much higher compression on the more heavily loaded faces.

A report was put forward by Building Research Station<sup>[64]</sup> in 1956, in which it described a laboratory investigation of the behaviour of some brick piers and walls under concentrated loading. The object of the work was to obtain test data to be used in future revision of building regulations. Tests were made on storey-height piers and slender walls and axial load was applied over all or part of the area of the specimen.

Concentric central and strip loading configurations were investigated using piers and the results obtained showed clearly the increase in stress under the contact area as the percentage of the loaded area decreased. The mode of failure in the piers under a uniform load was by vertical cracks followed by crushing of the brickwork in the lower portion of the pier. However, when subjected to concentrated loading vertical cracks were visible at loads ranging from 80-95% of the ultimate load. These vertical splitting cracks were confined to the upper half of the height of the pier and were followed at failure by local crushing under the load plate.

Walls were utilized to study the effect of central strip with single or double,

and end loading configurations. The results again showed that as bearing area decreases the enhancement factor increases. In the case of end strip loading this increase in stress was shown to be smaller than in the case of central strip loading. Again failure occurred after the formation of vertical cracks which passing through both brick and mortar joints, extending from one edge of the load plate usually to about mid-height of the wall. This form of cracking was observed in all the specimens tested irrespective of the position of the load plate with respect to the bond of brickwork. However, walls subjected to the concentrated loads from two symmetrically disposed load plates, vertical cracks formed usually under one load plate, and at failure some of these extended the full height of the wall with local crushing occurring under one load plate.

It was concluded that, where a centrally disposed load does not cover the whole area of the pier, the 50% increase in stress allowed in building regulations is not applicable when the ratio of the area loaded to the total cross-sectional area is greater than 0.33. On the other hand this increase could be at least doubled when the ratio is less than 0.125. As regards to concentrated loading on slender brick wall, an inference from the tests is that no increase in stress is warranted if more than one-half of the wall length is loaded. For more concentrated loading away from the ends of the wall, when load can be disposed on both sides of a load plate the increase in stress under contact areas may be doubled when the loaded area ratio is less than 0.125; where, however, the local load can be disposed on one side, as in lintels, the increase in stress of 50% is justified.

The failure stresses, strain distribution, and failure modes of full-scale brickwork piers, subjected to stress concentrations were investigated by Rutherford<sup>[59]</sup>. The bearing plate length was varied; central, intermediate and end positions of loading were considered for the strain distributions. He also studied the failure stresses, strain distributions, and mode of failure of model brickwork piers, 1/6th and 1/3rd scale. A large number of model piers were tested, increasing the range of bearing plate length used in comparison to the full-scale. The structural behaviour of 1/3rd-scale model cavity walls subjected to eccentric loading of various types were also investigated by studying the strain distribution on the faces of the two leaves, across the leaves and the lateral deflections of the leaves of the wall. The results of this experimental investigation was published<sup>[65]</sup>, which concluded:



- "Bulbs" of compressive strain existed under concentrated loads and although the vertical strains were contained within a 45 degrees fan drawn from the ends of bearing plate they were not uniformly distributed on horizontal planes within these limits.
- Failure of the brickwork under a concentrated load may take place by vertical splitting at some distance below the loaded area, by horizontal "tearing" at the surface or by spalling of the brickwork under the load.
- For both end and centrally applied loadings the failure stress increased as the bearing plate length was reduced. However, above  $A_r=0.17$  the effect is not pronounced.
- Central bearing plate tests (for 1/3rd and 1/6th-scales) had a failure stress of 1.3 times the end-bearing failure stress, for the same bearing plate.
- One-third scale tests showed that end distance is a critical factor, i.e. there is rapid increase from end failure stress to 1.3 (end failure stress) as the edge distance is increased.
- The load was in all cases transmitted through a rigid bearing plate. When very short bearing plate length were used, simulating extreme concentrations, high failure stresses were obtained, particularly when the load was transmitted away from the end of the member.

Kirtschig *et al* <sup>[66]</sup> investigated the partial surface load on masonry. The experimental tests were confined to four brick types (hollow brick, sand lime brick, hollow block and concrete brick) and mortar grade of II and IIa (cement-lime mortar with mean compressive strength of 2.5 and 5.0 Nmm<sup>-2</sup> respectively) and mortar grade III (cement mortar with mean compressive strength of 10 Nmm<sup>-2</sup>). Wall specimens were 1m high and 1m in length and 0.24m in thickness. Central strip, end strip and central patch loading configurations were chosen and also a series of columns 0.24m x 0.24m and 0.625m in height were tested under central strip and middle concentric loading configurations. In each case a control specimen was tested under uniform load applied over the whole cross section. An expression was proposed in the form:

$$\beta_1 = (1 + \alpha) \beta_0 \quad (3.1)$$

$$\beta_1 / \beta_0 = (1 + \alpha) = \alpha_T \quad (3.2)$$

where  $B_0$  is the masonry compressive strength under uniform load,  
 $B_1$  is the masonry compressive strength under partial load,  
 $\alpha$  is a constant with a value greater than zero,  
 $\alpha_T$  is the enhancement factor.

Enhancement factors were calculated based on the experimental results and were plotted against the length of loading plate ( $l_1$ ). The results are reproduced and is as shown in Fig. 3.1.

However, it was suggested that from the evidence of test results the values for  $\alpha_T$  could not be identified as being dependent on the type of unit nor the strength of the mortar. As it can be seen from Fig. 3.1, the test results have a very large dispersion. The value of  $\alpha_T$  become smaller as the length of the loaded area increases and shows a sharp increase as the length of the loaded area decreases, with the exception of end strip loading configuration. The magnitude of the values of  $\alpha_T$  is dependent to a very large extent on the type of loading.

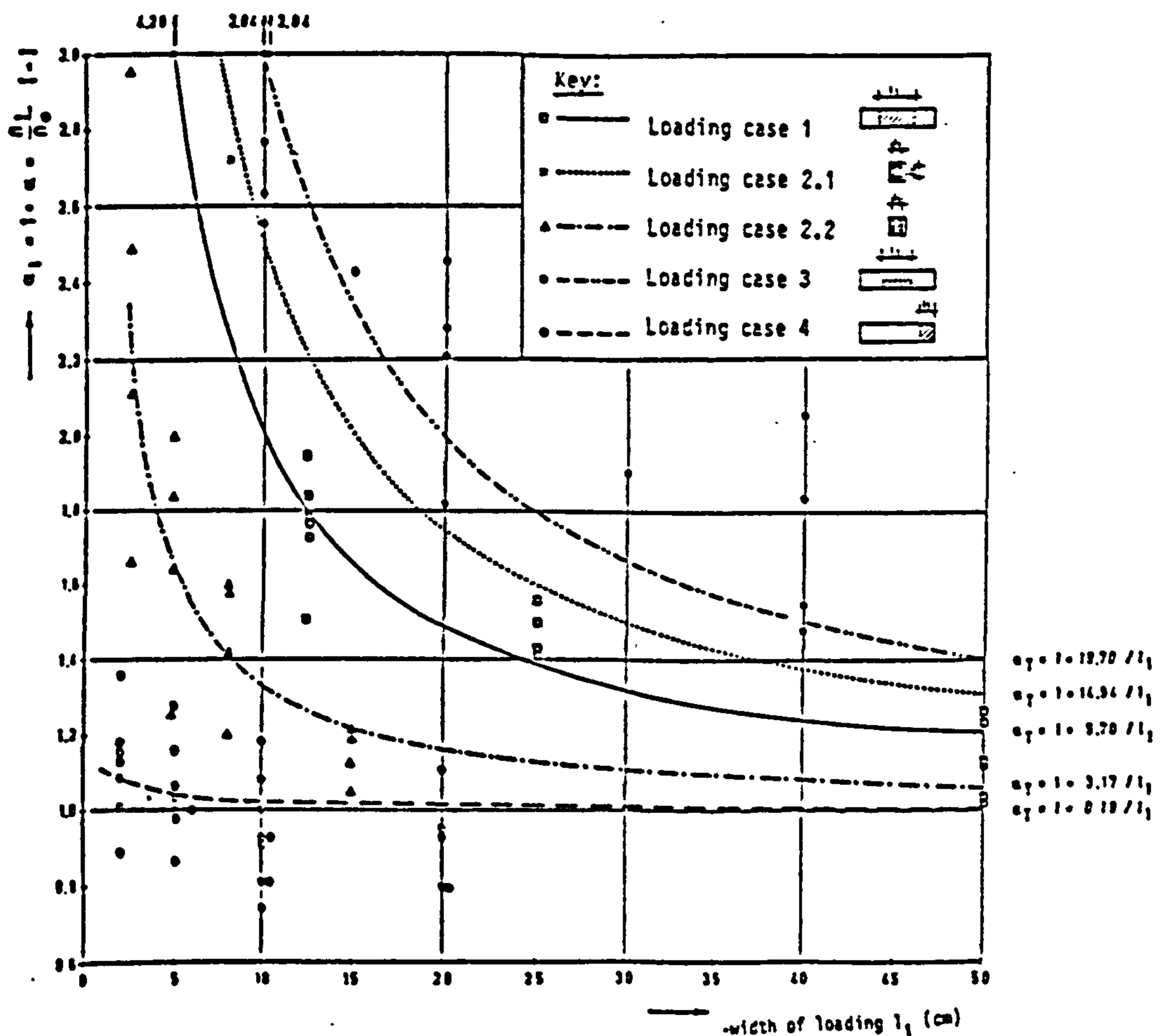


Fig. 3.1 - Relation between enhancement factor and the length of loading plate (after Kirtschig *et al*<sup>[66]</sup>).

Equations in the form:

$$\alpha_T = 1 + b/l_1 \quad (3.3)$$

where  $b$  is a constant dependent on the type of loading,  
and  $l_1$  is the length of loading plate.

were obtained for the test results for each type of loading as shown in Fig. 3.1. An attempt was also made to relate the enhancement factor not only to the type of loading but also to incorporate the edge distance. Expression in the form:

$$\alpha_T = 1 + \{ b(a/l_1) + 1 \} / l \quad (3.4)$$

where  $a$  is the length of wall from the edge of the loaded area to the nearest edge of the wall,  
and  $l$  is effective length of the wall assumed to be equal to  $(l_1+2a)$ .

Equations were derived for central strip loading configurations based on the results of the wall and column tests and also in the case of central patch loading on walls. A conservative approximation was borne from these equations such that:

$$\alpha_T = 1.0 + 0.1 a/l_1 \quad (3.5)$$

which was intended for use in a draft for "engineer-designed masonry" in the Federal Republic of Germany (Refer to section 3.3). However, these expressions are approximate and are based on a small number of test results. They are not therefore statistically valid.

A limited number of tests on clay brick specimens were carried out by the author<sup>[67]</sup> in 1981 and the test programme was extended throughout the year by Professor Hendry at the Department of Civil Engineering at Edinburgh University. These results were not published though they showed the influence of variables such as constituent material strengths, specimen thickness, ratio of bearing area to the total cross-sectional area, loading configuration, and the effect of edge distance on the compressive strength of brickwork under concentrated loading. The results are summarised in Appendix II.

In China, Dai-Xin<sup>[68]</sup> investigated the bearing strength of brick masonry

specimens 240mm and 370mm thick. The loading configurations were such that concentrated load was applied through a bearing plate at the middle and end of a pier and also at the corner of a wall with return. The aim of this investigation was to examine the recommendation given in the Chinese code<sup>[69]</sup> as given by equation 3.14 in section 3.3. The main variable investigated was the ratio of cross-sectional area to the loaded area. Also the effect of reinforcing the bed joint and bracing the specimen using brackets and bolts on a few test specimens was studied. He concluded that failure due to development of vertical cracks is a basic failure mode of brick masonry under local loading. Splitting failure may happen when the ratio of specimen cross-sectional area to the loaded area is large (larger than 10 for piers under concentric central loading or 9 for walls under central edge loading). A local failure within the loading area may occur when the strength of brick unit is very low. He proposed the following formula for the design of masonry under uniform local loading based on the experimental work.

$$K N_c \leq \psi A_c R \quad (3.6)$$

$$\text{where } \psi = 1 + \omega \{(A_0/A_c) - 1\}^{0.5} \quad (3.7)$$

for  $\omega=0.708$  for concentric central bearing, and  $\omega=0.364$  for a central patch, end and the corner bearing, and suggested the upper limit of  $\psi$  is 3.0 and 2.0 for the former and latter respectively.

where	$N_c$	is the bearing load,
	$K$	a constant
	$\psi$	strength coefficient (or enhancement factor),
	$\omega$	a constant related to the type of loading,
	$A_c$	loaded area,
	$R$	bearing strength under local load,
	$A_0$	effective area (see Fig. 3.2).

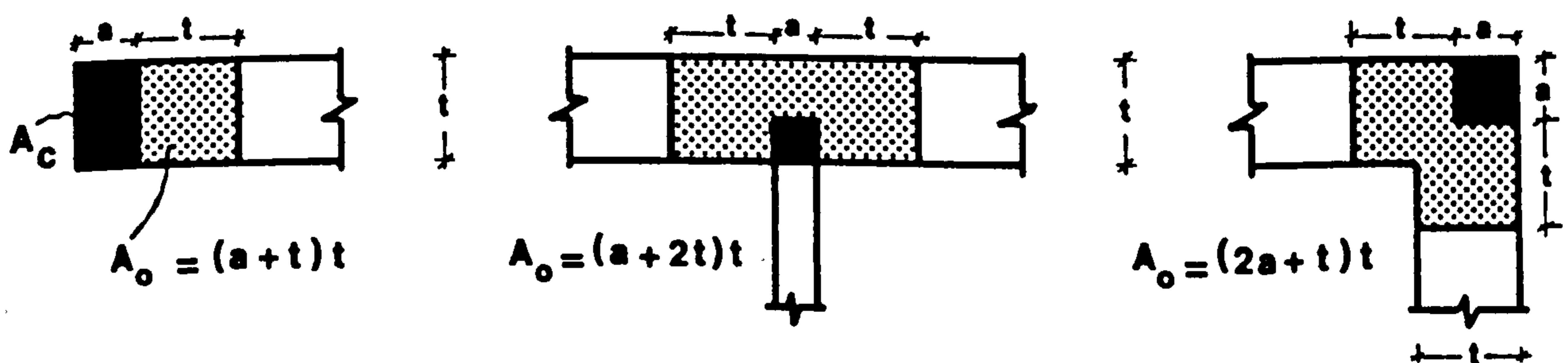


Fig. 3.2 - Effective area under bearing (after Dai-Xin<sup>[69]</sup>).

Two dimensional elastic finite element analyses were used by Ali *et al*<sup>[70]</sup> to

carry out a preliminary study of stress distribution in masonry walls subjected to concentrated load. One analysis assumed masonry to be a homogeneous continuum, the other treated bricks and joints separately. The influence of various parameters such as loaded area ratio, loading position, modular ratio and effect of parallel loading on the stress distribution was studied. A follow up<sup>[71]</sup> to this investigation used three dimensional elastic finite element analyses to determine the limitations of a simple two dimensional analysis in above, and for concentrically and eccentrically loaded walls the influence of variables mentioned above were studied. However, the authors admit that studies of this type, although not being able to reproduce material non-linearities or predict failure, would provide useful guidance for the design of masonry walls subjected to concentrated loads. In the three dimensional analysis, homogeneous, isotropic elastic behaviour were considered for the material. This analysis showed that the concentration ratio in the direction of the wall thickness is the critical factor and as long as this ratio approaches unity (i.e. strip loading as compared to patch loading) a two dimensional analysis would be representative of the three dimensional analysis. A number of conclusions were drawn from this study:

- When a concentrated load is applied so that its area of contact extends across at least 75% of the wall thickness, the influence of stresses in a direction through the wall thickness will be negligible, and a two dimensional analysis will suffice. In other cases, a three dimensional analysis is required.
- A finite element model which treats bricks and joints separately is more effective, since it reflects the influence of varying stiffness of its constituents. This was particularly important in the study of the transverse tensile stresses, where peak stresses were always greater than those predicted in the homogeneous wall.
- Concentrated load tests should recognise the important influence of the method of load application on the stress distributions within the wall. Significant variations will occur if the load is applied through a flexible rather than a stiff loading plate.
- The transverse tensile stresses (which would initiate cracking and failure) significantly increase with decreasing loaded area ratio.
- The concentration of vertical stress beneath the loaded area increases as the loaded area decreases. The dispersion of concentrated load occurs at an angle of approximately 30 degrees. An average stress at any level calculated on the basis of a 45 degrees dispersion gives a reasonable

approximation of the stress distribution, although underestimating the peak stress.

- As the ratio of brick/mortar stiffness increases, the transverse tensile stresses increase in the brick and the vertical joints, and decrease in the bed joints. A similar effect is observed as the ratio of the brick thickness to the joint thickness is increased.
- As the concentrated load is applied closer to the edge of the wall, transverse tensile stresses markedly increase.
- The presence of brick, (or bricks), with high stiffness in the region directly beneath the load will increase the magnitude of local peak transverse tensile stresses and thus potentially reduce the wall capacity.

A theory was put forward by Mann *et al*<sup>[72]</sup> for obtaining the enhancement factor. Assuming brickwork as a homogeneous material, expressions for the maximum horizontal tensile cracking force and the height where this force acts were given. It was argued that this horizontal tensile force occurring in the homogeneous wall cannot be applied as such to masonry walling. The reasons given were that the tensile cracking forces are interrupted by the vertical butt joints and also tensile stresses occur in the bricks caused by varying transverse strain between bricks and mortar. Therefore, these tensile cracking stresses cannot run continuously over the height of the wall as the vertical butt joints cannot take up tensile forces. So it was assumed that only bricks transfer tensile forces and as bricks only exist in every second course in the area of the butt joints, the tensile cracking forces in the brick must be doubled. Two expressions were formulated for the enhancement factor and it was suggested that the smaller of the two values is decisive. Comparisons were made between the calculated values by this theory and with a limited number of test results and the values given in accordance with the German masonry standard DIN 1053:Part 2<sup>[73]</sup>. It was concluded that the enhancement factor from the DIN are on the safe side compared to the results from the theory and test results. However, due to the assumptions and lack of satisfactory explanations this theory is of little value.

Lind<sup>[74]</sup> conducted a series of tests with the aim of developing a method of calculating the edge strength of masonry. Three types of units namely clay bricks/blocks, calcium silicate bricks and gas concrete blocks were used to construct walls with nominal dimensions 625x490x115mm (hxlxt) with brick units and 750x490x120mm for block units using mortar class of IIa and III

according to DIN 1053<sup>[73]</sup>. The load application was made by means of a semi-circle device and by means of a flat bearing plate on a partial surface of the wall, assuming a triangular and rectangular stress distributions respectively (see Fig. 3.3).

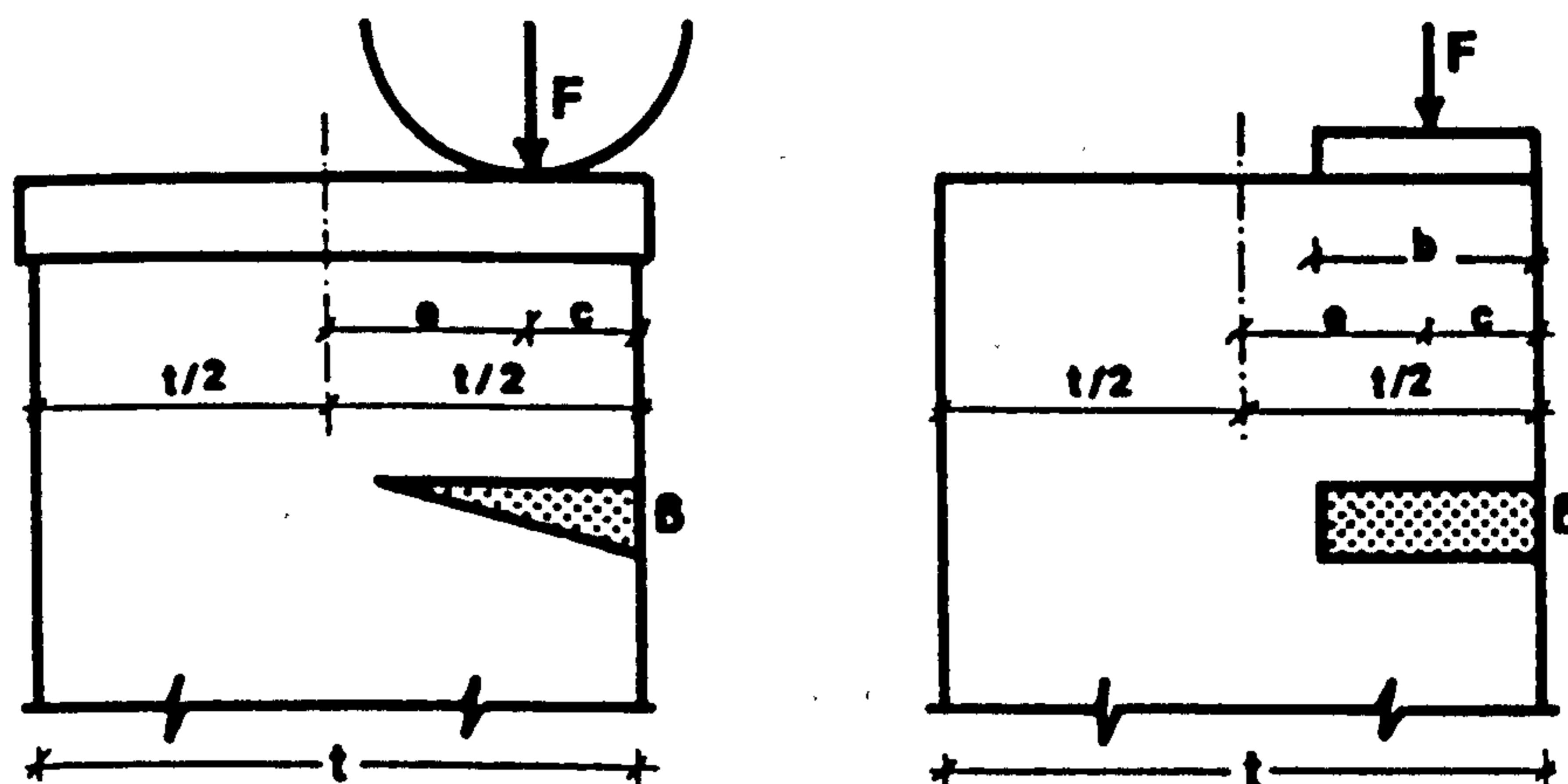


Fig. 3.3 - Method of load application (after Lind<sup>[74]</sup>).

The results showed value of 1 for enhancement factor  $\omega$ , for  $0.20 \geq e/t \geq 0.0$  ( $e$  is the eccentricity of loading normal to the longitudinal direction of the wall) and increases from 1 to a value of 1.25 for  $0.50 \geq e/t \geq 0.2$  for brickwork and  $\omega=1$  for  $0.25 \geq e/t \geq 0.0$  and increases to a value 2.0 for  $0.50 \geq e/t \geq 0.25$  for blockwork.

However it was concluded that:

- The evaluation of masonry tests with walls having applied load near the edges has shown that edge stresses can be attained in masonry which are many times higher than the concentric failure stress.
- In a comparison of brick sizes, it was found there was hardly any difference between two and three blocks high prisms.
- Walls of standard size brick however tended to have lower edge failure loads than two blocks high prisms.
- Vertically perforated clay bricks or blocks reached somewhat higher edge stress values than calcium silicate bricks, which is to be explained by the perforation pattern.
- The increase in edge load strength of gas concrete block masonry is significantly lower with increasing eccentricity of the load than with other types of brick or block.
- An improvement in mortar strength does not increase the edge strength in relation to the corresponding concentric failure stress.

Most recently, experimental investigation has been carried out at Building Research Station<sup>[75]</sup> in which some of 34 half storey high walls, 1.8m in length have been tested under concentrated load. The main test variables investigated were the area of the concentrated load (as a proportion of the total wall area) and the position of the load on the wall. The wall specimens were built mainly from low strength autoclaved aerated concrete blocks set in 1:2:9 cement-lime mortar. Also, selected experiments were repeated on walls built from stronger dense concrete blocks, both in 1:1:6 mortar.

It was concluded that:

- The strength enhancement under a concentrated load has been shown to be an approximately constant ratio of the compressive strength  $f_k$  of the wall material, with a small tendency for a reduction of enhancement with increase of  $f_k$ .
- A precise value of the ratio of  $f_{cb}$  to  $f_k$  depends upon the area of the concentrated load and its proximity to the centre of the wall. For a loaded area of around 8% of the wall area applied over full thickness at the centre of a wall, the enhancement factor is 1.9.
- A more general equation for determining the strength enhancement under a concentrated load applied over full thickness of a 200mm thick AAC block is:

$$f_{cb}/f_k = 1 + 0.44(a/l) - 0.04(a/l)^2 \quad (3.8)$$

where  $a$  is the length of bearing plate,  
and  $l$  is the length of the wall.

provided that the area of the load is not greater than  $1.65t^2$ .

- The mode of failure of a masonry wall appeared to be a function of the area of the concentrated load and its point of application on the wall. For a load of 8% of wall area over the full thickness at the centre of a wall (central strip) of any of the materials tested, the failure initiated by a tensile crack along a vertical line under the centre point of the load, culminating in local crushing under the load. For an increased area of load of 25%, the final failure was instead by more extensive cracking and crushing in the 200mm AAC block walls tested. For a further increased area of load of 50% applied at the centre of a 200mm AAC block wall, the failure mode was very similar to that obtained in a wall loaded over the full area.
- The angle of load dispersion for the above loads appeared to be a function of their area, seemingly being the lines of



slope of 2:1 and 3:1 for the 8% and 25% areas respectively. The cut-off line for load dispersion appears to be at about half the height from the top.

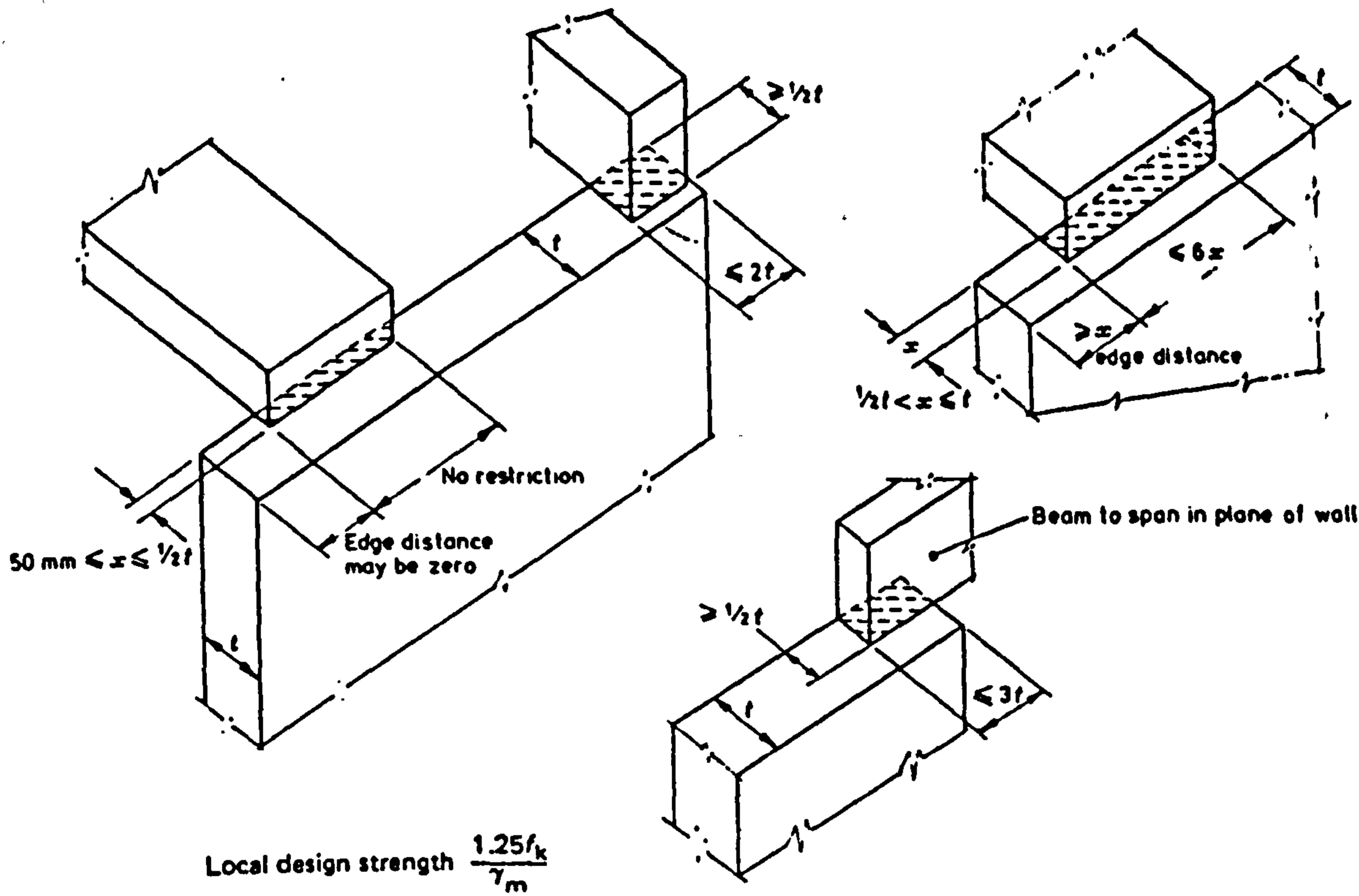
- Where loads were applied to the edge of the walls there was some load spreading on one side of the load when its area was 8%, resulting in the strength enhancement of around 35%. Loads of 25% and 50% areas produces high local tensile stresses and it behaves more as a pier than a wall, resulting in a drop of compressive strength below the characteristic compressive strength by a mean figure of 18%.

### 3.3. CURRENT DESIGN GUIDES

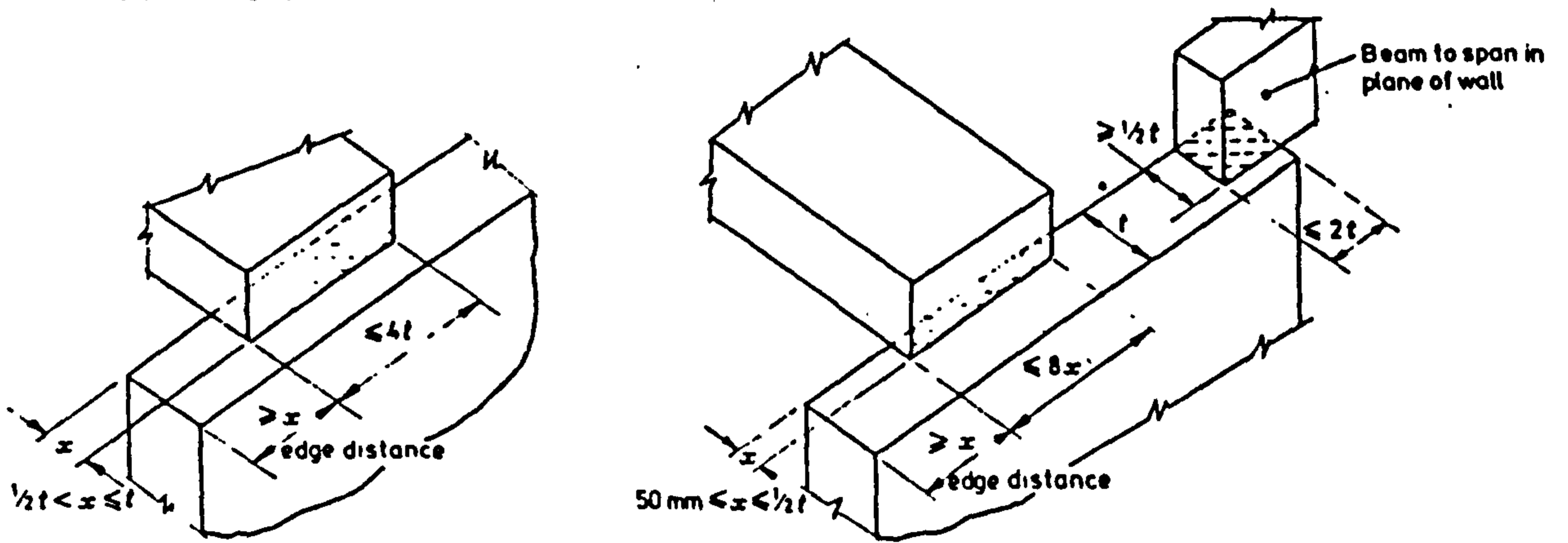
It has long been recognised that the contact stress under a concentrated load on masonry may be considerably greater than the compressive strength under uniaxial loading. Provision for this effect was made in the British Code of Practice, CP 111<sup>[11]</sup>, based on early work reported in the 1930's<sup>[61 - 63]</sup> and 1950's<sup>[64]</sup>. This code allowed an increase of up to 50% on the permissible compressive stress for "additional stresses of a purely local nature".

The successor to CP 111<sup>[11]</sup>, BS 5628:Part1<sup>[1]</sup>, by contrast, makes rather elaborate provisions for increased design stresses under beam and slab bearings. It permits increases in local stresses beneath the bearing of a concentrated load of a purely local nature, such as beams, columns, lintels, etc. provided either that the element applying the load is sensibly rigid, or that a suitable spreader is introduced. It states that the concentrated load may be assumed to be uniformly distributed over the area of the bearing, except in the special case of a spreader located at the end of a wall and spanning in its plane (bearing type 3, see Fig. 3.4(c)), and dispersed in two planes within a zone contained by lines extending downwards at 45 degrees from the edges of the loaded area. An increase of 25%, 50% and 100% has been suggested for bearing types 1, 2 and 3 respectively and states that the effect of the local load combined with stresses due to other loads (see Fig. 3.5(a)), should be checked at the bearing and at a distance of 0.4h below the bearing.

These rules appear to have been based on work relating to concrete and apart from being difficult to understand, do not conform with experimental data from tests on brickwork specimens.



(a) Bearing type 1



(b) Bearing type 2

(c) Bearing type 3

Distribution of stress under the spreader should be based on an acceptable elastic theory. Maximum stress should not exceed  $\frac{2f_k}{\gamma_m}$ .

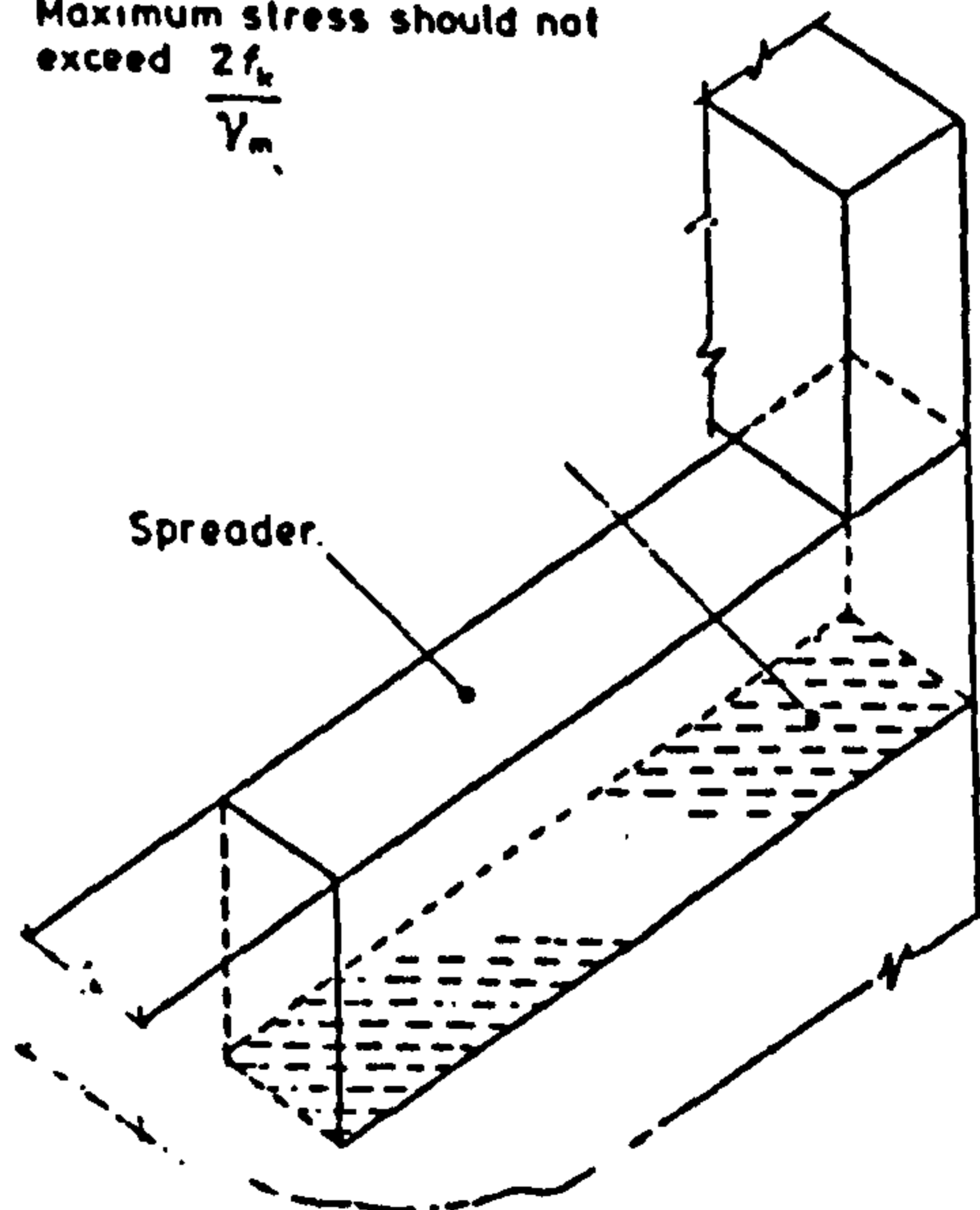
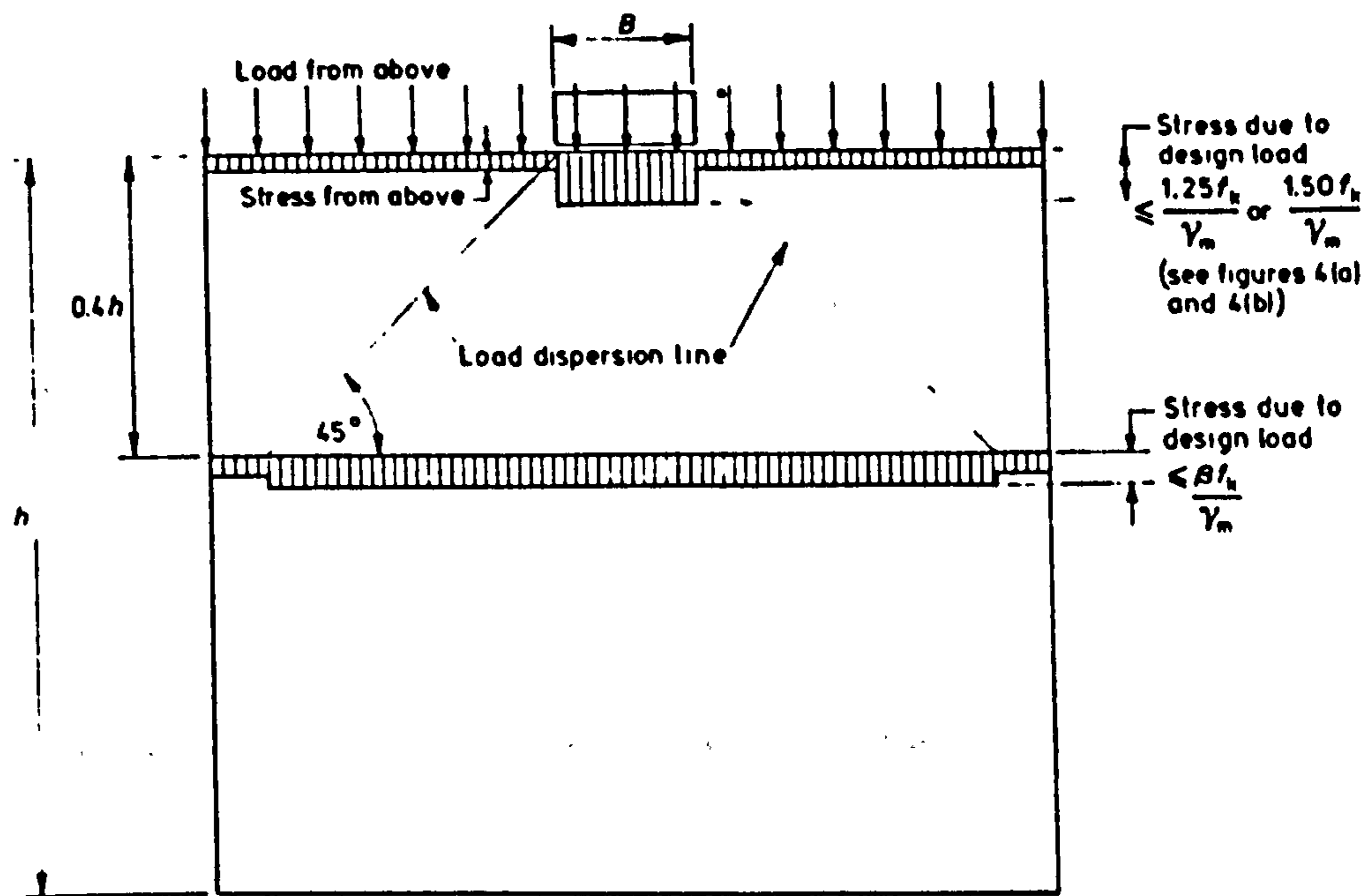
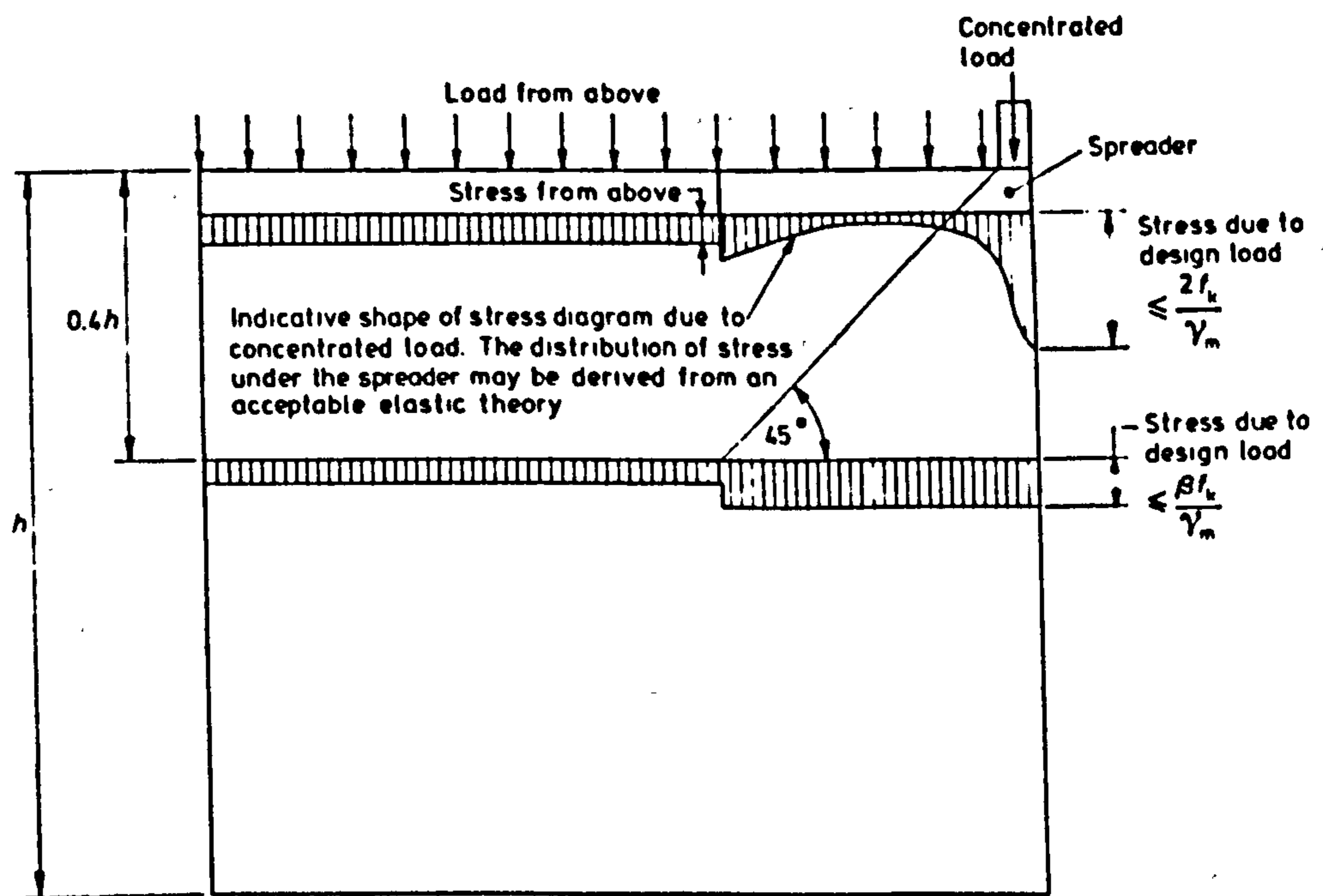


Fig. 3.4 - Different bearing types given by BS 5628<sup>(1)</sup>.



Stress due to design load to be compared with design strength as indicated above.

(a) Load distribution for bearing types 1 and 2



Stress due to design load to be compared with design strength as indicated above.

(b) Load distribution for bearing type 3

Fig. 3.5 - Distribution of concentrated load for the three types of bearings. (after BS 5628<sup>[1]</sup>).

The CIB Recommendations for Masonry Structures<sup>[76]</sup> give, in an appendix, a simpler provision for concentrated loading which takes cognisance of the position of the load relative to the end of the wall but which is known to be conservative for certain types of masonry.

It states when a beam or other structural member imposes a concentrated load on a wall the design compressive strength  $\sigma_1$  of the masonry may be taken as:

$$\sigma_1 = f_k/\gamma_m \{ 1 + 0.1(a_1/l_1) \} \leq 1.5 f_k/\gamma_m \quad (3.9)$$

and the design compressive strength may only be varied from  $f_k/\gamma_m$  if  $A_1 \leq 2t^2$  and  $e \leq t/6$  (see Fig.3.6).

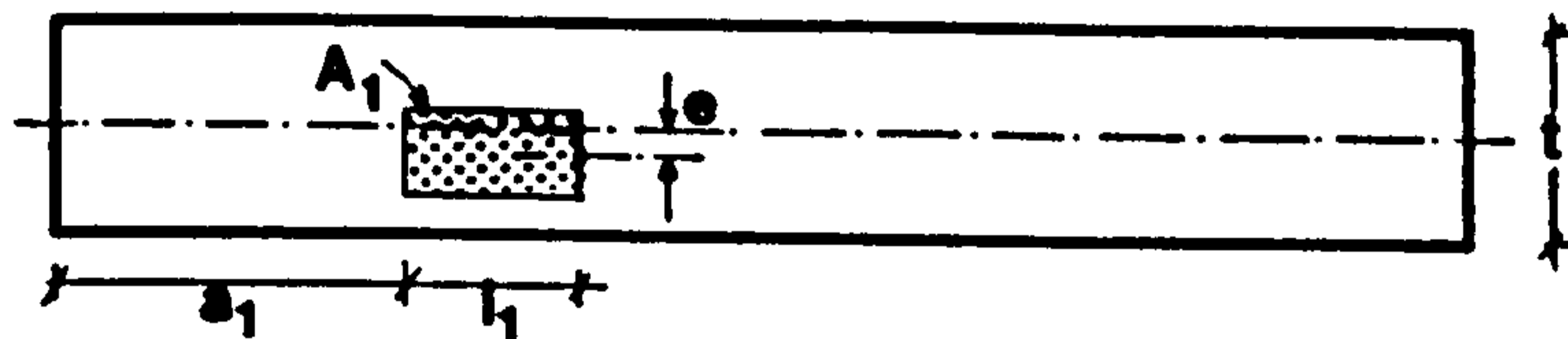


Fig. 3.6 - Loading application and notations (after CIB code<sup>[76]</sup>).

The German Code<sup>[73]</sup> makes similar allowances as above and also states that if walls are stressed by concentrated loads the absorption of the tensile splitting loads is to be assured by design measures or can be taken up by the tensile strength of the masonry bonding, by reinforcing or by reinforced concrete designs. If the absorption of the tensile splitting loads is assured by design measures, the distribution of pressure under concentrated loads within the masonry may be set at less than 60 degrees, and areas of wall subjected to greater stress may be constructed to a higher masonry quality. In the case of perforated and cellular blocks it suggests that the load be transmitted through bearing plates.

The Russian Code<sup>[77]</sup> states that masonry must be calculated for local compression when loads are applied to only part of the cross-section (i.e. masonry supporting frames, beams, purlins, arches, floor panels, columns, etc.) and the bearing capacity of masonry in local compression is determined by character of the pressure distribution. This code does not make any allowance for the increase in stress enhancement but it outlines construction requirements for masonry subjected to concentrated load. These are:

- A layer of mortar not more than 15mm thick shall be provided under member supports to transmit local loads to the masonry. The "dry" placing of these members or of distribution pads onto the masonry is prohibited.
- In locations of concentrated load, where required by calculations, load distribution pads shall be provided of thickness equal to a multiple of the masonry course thickness but not less than 140mm, and reinforced by two meshes by calculation, but not less than 0.5% reinforcing in each direction.
- For the support of girders, roof beams, crane girders, etc., on pilasters a tie into the main wall consisting of a distribution pad shall be provided on the supporting part of the masonry.
- Where concentrated edge loads exceeds 80% of the design capacity of the masonry in bearing, the supporting part of the masonry shall be reinforced by mesh located in not less than the three upper horizontal joints. To transfer large concentrated loads to the pilasters (e.g. to support girders and roof beams) the position of masonry within 1 to 1.2m below the distribution pads shall be reinforced by mesh. The mesh must connect the supporting parts of the pilasters to the main part of the wall.

The American Codes<sup>[78 - 81]</sup> give allowable bearing stress  $F_{br}$  in terms of specified compressive strength of masonry at the age of 28 days, ( $f'_m$ ) such that;

$$\text{On full area, } F_{br} = 0.26 f'_m \quad (3.10)$$

$$\text{On 1/3rd area or less, } F_{br} = 0.38 f'_m \quad (3.11)$$

This increase applies only when the least distance between the edges of the unloaded areas is a minimum of one fourth of the parallel side dimension of the loaded area. The allowable bearing stresses on a reasonably concentric area greater than one third but less than the full area shall be interpolated between the values of the above equations.

With regard to the distribution of concentrated vertical loads in wall, it suggests that the length of wall, laid up in running bond, which may be considered capable of working at the maximum allowable compressive stress to resist vertical concentrated loads, shall not exceed the centre-to-centre distance between such loads, nor the width of bearing area plus four times the wall thickness. Concentrated vertical loads shall not be assumed

distributed across continuous vertical mortar or control joints unless elements designed to distribute concentrated vertical loads are employed. However in the case of concrete masonry the American Concrete Institute's Code<sup>[82]</sup> makes similar allowances except the bearing stress ( $F_a$ );

$$\text{On full area, } F_a = 0.25 f'_m \quad \text{with max. } 6.21 \text{ Nmm}^{-2} \quad (3.12)$$

$$\text{On 1/3rd area or less } F_a = 0.37 f'_m \quad \text{with max. } 8.27 \text{ Nmm}^{-2} \quad (3.13)$$

The Canadian Code<sup>[83]</sup> also states where a vertical load is supported on a masonry surface and the ratio of the loaded surface to the total surface is not more than 1:3, the allowable bearing stress,  $f_b=0.25f'_m$ , stipulated in the tables for different types of masonry given in this code, may be increased to  $0.375f'_m$ , provided the least distance between the edges of the loaded and unloaded surfaces is at least one-quarter of the length of the edge of the loaded area perpendicular to such least distance. The allowable bearing stress on a reasonably concentric area greater than one-third the full area may be interpolated between the values given.

The Chinese Code<sup>[69]</sup> adopts the formula for the strength coefficient  $\psi$  of bearing strength of brickwork masonry as:

$$\psi = \{ A_o/A_c \}^{0.5} \quad (3.14)$$

where  $A_o$  is the calculating area affecting on bearing strength and  $A_c$  is the local bearing area (refer to Fig. 3.2). This expression was derived based on the principle of ultimate balance and the theory of assumed "hoop strength" and has been adopted in the concrete code. However an expression similar to Equations 3.6 and 3.7 have been recommended for the calculation of bearing strength of brickwork masonry under concentrated loading.

In the Swedish Code<sup>[84]</sup>, local pressure is considered to occur when the length of the contact area in the longitudinal direction of the wall, is less than twice the thickness of the wall or one third of its length. The local pressure  $\sigma_1$  must not exceed:

$$\sigma_1 \leq 1.5 \sigma_o \cdot l_a \cdot l_b / a \cdot b \quad (3.15)$$

where  $\sigma_o$  compressive strength of wall,  
 $a$  length of concentrated load,

- b breadth of concentrated load,
- $l_a$  distance from centre of load to end of wall,
- $l_b$  distance from centre of load to nearest face of wall,  
(ref. to Fig. 3.7).

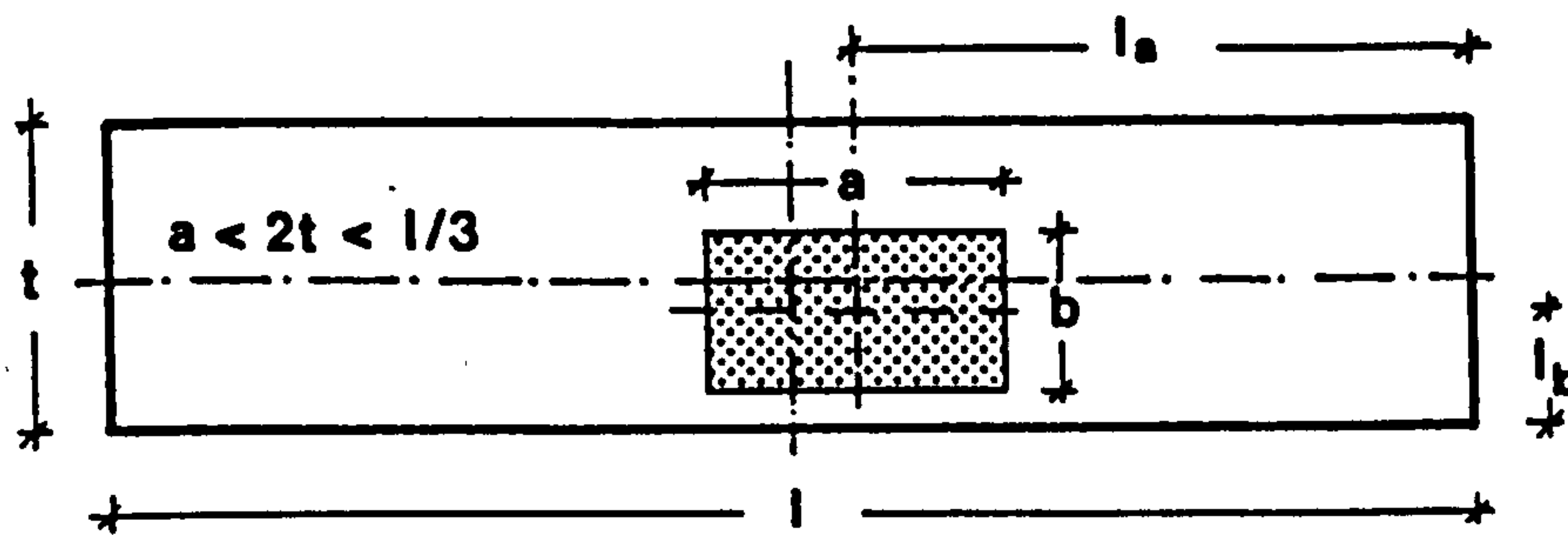


Fig. 3.7 - Loading application and notations (after Swedish Code<sup>[84]</sup>).

In the Australian Brickwork Code<sup>[85]</sup> a 50% increase in stress is permitted irrespective of the loaded area ratio. When loading is transmitted through brick masonry, the angle of dispersion of the loading is taken as 45° from the direction of such loading.

The Australian Blockwork Code<sup>[86]</sup> allows an increase of 85% in stress provided the supporting area projects beyond the loaded area on at least two opposite sides. In such a case the stress is assumed to be distributed through a cone contained within the supporting wall or pier, at slopes of 45° from the vertical.

The provision of the latest Code draft<sup>[87]</sup> follows the German provision as far as loaded area ratio is concerned and have used the following relationship:

$$K_d = 0.9 + 0.1 A_{dm}/A_{ds} \text{ or } 1.50 \text{ whichever is less} \quad (3.16)$$

- where
- $K_d$  magnification factor
  - $A_{dm}$  the maximum area of dispersion of the concentrated load in the member
  - $A_{ds}$  the area of dispersion of the concentrated load at the design cross-section under consideration.

In addition, if a load is applied within one eighth of the wall height from the end of the wall, no increase in stress is permitted.

### 3.4. SUMMARY

A review of literature relevant to this investigation has been presented in this chapter. From the literature review, it is clear that much remains unknown about the concentrated load problem. *Experimental investigations* have shown the importance of parameters such as loaded area ratio, edge distance and loading configuration in accessing the enhancement factor and their influence on the bearing strength of brickwork masonry partially loaded. In most cases they have not been comprehensive because of the large number of variables involved. They seemed to illustrate the parameters which can be critical and to illustrate that significant strengthening does occur beneath concentrated loads in many cases.

Theoretical investigations have been limited to linear elastic finite element analysis with no attempt to model non-linear material characteristics or failure. Attempt is being made by Ali and Page in Australia to develop a non-linear finite element program based on non-linear fracture model of masonry for the analysis of the in-plane behaviour of masonry subjected to concentrated load. If a suitable finite element model could be developed to predict the failure of masonry subject to concentrated loads, a large number of tests could be simulated using this type of analysis and the significance of the parameters influencing the bearing strength could be studied.

Design rules given in codes of practice from various countries differ widely indicating the lack of comprehensive information in this area. Those codes which allow increases in stress under concentrated load irrespective of critical parameters are non-conservative in some cases, particularly as the loaded area ratio increases and the edge distance decreases.



## Chapter 4

### EXPERIMENTAL STUDY: MATERIALS PROPERTIES

#### 4.1. INTRODUCTION

The existence of a masonry structure depends not only on the form of the structure as a whole but ultimately on the properties of individual materials; brick units and mortar as jointing material. Therefore, it is necessary to determine the characteristics of the materials involved before considering the structural behaviour of the material in a structural element.

The properties of brickwork are influenced by variables such as type and physical properties of bricks, type of mortar, physical properties of the sand, lime and cement used for the mortar, curing, workmanship, thickness of brickwork element and the bed joint.

In order to keep the scope of this investigation within reasonable limits, the variables such as joint thickness, curing, workmanship and the mortar's constituent materials were kept constant. The properties of the component masonry materials are documented in this chapter.

#### 4.2. PROPERTIES OF BRICKS

The bricks employed in this investigation are lettered from A to G. Bricks A, B, C, and D are clay bricks and were manufactured by Steetly Bricks Limited in North Staffordshire. Bricks lettered E and F were manufactured locally and are Scottish clay, Engineering Class A and B respectively. Brick G is a lightweight autoclaved aerated concrete (AAC) brick.

##### 4.2.1. Dimensions

Determination of dimensions was based on the overall measurement of 24-bricks placed in contact in a straight line upon a flat (level) surface in accordance with BS 3291:fig.1<sup>[88]</sup>. The dimensions for the seven types of bricks are as shown in Table 4.1.

##### 4.2.2. Density

The density of each brick type has been calculated from a sample of ten units and the results are presented in Table 4.2.

### 4.2.3. Water Absorption

#### 4.2.3.1. 5-hour boiling test

Samples of ten bricks were dried in a ventilated oven at 110°C. When cooled, they were weighed to an accuracy of 0.1% of the mass of the units and tested for 5-hour boiling test in accordance to the procedure outlined in the BS 3291:1974<sup>[88]</sup>. The results are as shown in Table 4.3.

#### 4.2.3.2. 24-hour cold immersion test

24-hour cold immersion test were carried out on sample of ten bricks in accordance to the procedure given in BS 3291<sup>[88]</sup>. The mean of absorption results are calculated to the nearest 0.1% of the dry mass of the units and the rate of water absorption for the units are presented graphically in Fig. 4.1.

### 4.2.4. Compressive Strength

Ten samples were taken from brick stock piles in accordance with BS 3291<sup>[88]</sup> and tested according to the same specification. The bricks were immersed in water for 24 hours at room temperature, and the least bed face area was measured to the nearest 1mm, before testing for compressive strength. Specimens were tested between two 3mm plywood sheets whose linear dimensions, length and width were 220mm x 110mm; each sheet was used once only. The initial loading was applied at the rate of 35 Nmm<sup>-2</sup>min<sup>-1</sup>, till about half the expected maximum load and then reduced approximately to 15 Nmm<sup>-2</sup>min<sup>-1</sup>, until the maximum failure load was reached. The results are presented in Tables 4.4 to 4.10.

### 4.2.5. Elastic Properties

There is no recognised test method to determine the elastic modulus of a brick unit. This is due to the difficulty of obtaining an accurate reading of the strains which are set up in the unit under axial compressive load. This difficulty arises due to the geometry of the unit and the pattern of the perforations. Some investigators have overcome this by cutting a test piece from a single solid brick such that the ratio of height to width of the test piece is large enough that the platen effect would become insignificant, and strain readings were taken using strain gauges. This method might be feasible provided a test specimen can be cut from a brick unit in the direction in which strain measurements are required. Others have tried to measure the strain on

a brick unit were the load was applied through wire brushes or frictionless pads to compensate for the platen effect.

However, in this investigation the brick units were all perforated bricks with exception of type G (AAC brick), and a chance of obtaining a test piece large enough was slim. In this case a test method was devised so that the elastic modulus and Poisson's ratio could be obtained (see Fig. 4.2(a) and (b)). In order to eliminate the restraint induced by the platen of the testing machine on the test specimen, two other bricks from the same batch were placed on the top and underneath the test specimen. No bonding was used between the interfaces, and the bed faces of the bricks were machine cut to a high standard such that the surfaces were all levelled with each other and were highly smooth in order to eliminate the friction as far as possible at the interfaces (refer to Fig. 4.2(b)). The purpose of a brick at each end was to transfer the load to the middle brick (test specimen) which will be free from the restraint caused by the platens of testing machine and because of smooth interfaces no friction would be set up, hence allowing the test specimen to expand laterally.

Wire strain gauges; rosette type (see Fig. 4.2(c)) were mounted at the middle of each face and the vertical and lateral strain measurements were read at each stress level by a Sangamo strain meter.

The plots of vertical stress-strain, vertical stress-lateral strain and vertical-lateral strains are shown in Figs. 4.3 to 4.5 respectively. The values obtained for *apparent* initial tangent modulus, *apparent* secant modulus at 3/4 of maximum stress and Poisson's ratio based on the linear portion of vertical-lateral strains curve are as shown in Table 4.11.

### 4.3. PROPERTIES OF MORTARS

#### 4.3.1. Proportioning and Materials

Two grades of mortar were used for the construction of the test specimens. A mortar designation M(i); 1:1/4:3 Portland cement:lime:sand, mix by volume was used for the construction of brickwork types A, B, C, D and E, of which the specimens were tested after 28 days. A mortar designation M(iii); 1:1:6 rapid hardening cement:lime:sand, mix by volume was used for the construction of brickwork types F and G which were tested after 7 days (see chapter 5).

Brick type	Dimensions of 24-bricks (mm)			Dimensions of single brick (mm)		
	length	width	height	length	width	height
A	5160	2460	1604	215.0	102.5	66.8
B	5204	2468	1574	216.8	102.8	65.6
C	5222	2450	1602	217.6	102.1	66.8
D	5208	2418	1620	217.0	100.8	67.5
E	5203	2480	1590	216.8	103.3	66.3
F	5216	2478	1580	217.3	103.3	65.8
G	5165	2415	1548	215.2	100.6	64.5

Table 4.1 - Dimensions of bricks.

Brick type	Density ( $\text{kgm}^{-3}$ )	
	dry	fully saturated
A	1843.3	1922.1
B	1714.2	1757.9
C	1627.1	1713.7
D	1383.2	1577.8
E	1718.7	1835.6
F	1737.6	1876.7
G	879.9	1433.1

Table 4.2 - Density of bricks.

Brick type	Water absorption (% by weight)	
	5-hrs. boiling test	24-hrs. cold immersion test
A	4.28	2.98
B	2.55	2.54
C	5.32	4.42
D	14.07	11.47
E	6.81	6.04
F	8.01	7.61
G	62.87	24.11

Table 4.3 - Water absorption of bricks.

# RATE OF WATER ABSORPTION OF BRICKS

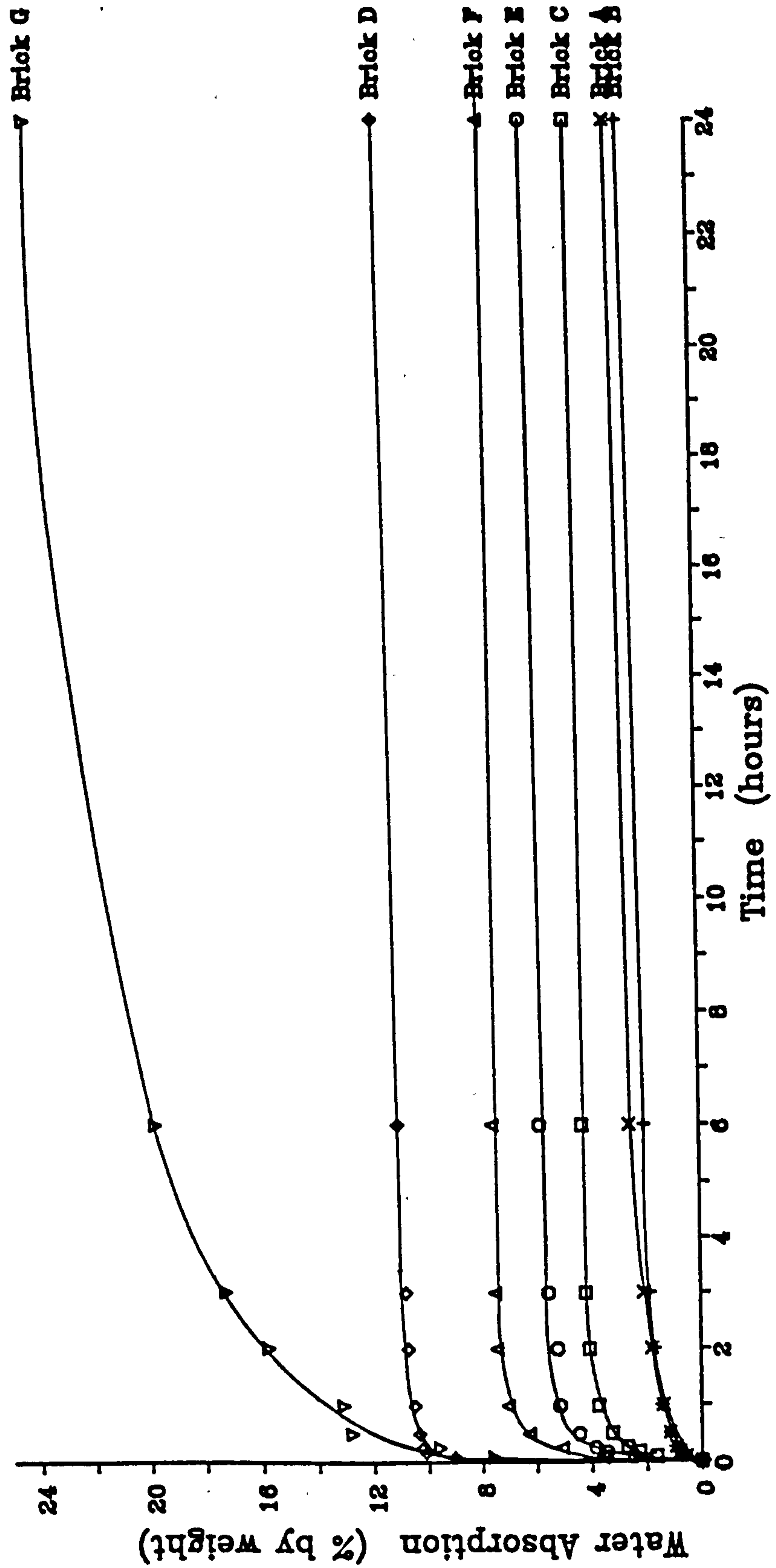


Fig. 4.1 - Water absorption rate of bricks.

Brick Ref. No.	Dimension (mm)				Least bed area (mm <sup>2</sup> )	Ult. load (kN)	Comp. strength (Nmm <sup>-2</sup> )
	Top bed		Bottom bed				
	length	width	length	width			
A 1	215.0	102.5	215.0	101.0	21715.00	1830	84.27
A 2	215.0	101.5	215.0	102.5	21771.75	1960	90.02
A 3	215.0	102.0	215.0	102.0	21930.00	1910	87.10
A 4	215.0	102.0	215.0	101.0	21715.00	2050	94.40
A 5	213.0	101.0	213.0	101.0	21513.00	1890	87.85
A 6	214.0	102.0	214.0	100.0	21400.00	1960	91.59
A 7	215.0	101.0	213.5	102.5	21715.00	1880	86.58
A 8	213.0	102.0	215.0	101.0	21715.00	2070	95.33
A 9	214.0	102.0	215.0	100.0	21500.00	1840	85.58
A10	215.0	102.5	214.0	101.0	21614.00	2120	98.08
Mean	214.35	101.85	214.45	101.20	21658.88	1951.0	90.08
S <sub>d</sub>	0.82	0.53	0.76	0.89	154.34	100.0	4.63
C <sub>v</sub> (%)	0.38	0.52	0.36	0.88	0.71	5.1	5.10

Table 4.4 - Physical properties of brick type A.

Brick Ref. No.	Dimension (mm)				Least bed area (mm <sup>2</sup> )	Ult. load (kN)	Comp. strength (Nmm <sup>-2</sup> )
	Top bed		Bottom bed				
	length	width	length	width			
B 1	216.0	102.0	217.0	101.0	21917.00	1790	81.67
B 2	216.0	103.0	215.0	103.0	22145.00	1980	89.41
B 3	217.0	101.0	217.0	101.0	21917.00	1770	80.76
B 4	215.0	101.0	215.0	100.0	21500.00	1830	85.12
B 5	213.0	102.0	214.0	102.0	21726.00	1785	82.16
B 6	215.0	103.0	216.0	102.0	22032.00	1745	79.20
B 7	214.0	101.0	215.0	101.0	21614.00	1835	84.90
B 8	216.0	101.0	216.0	101.0	21816.00	1722	78.93
B 9	214.0	101.0	215.0	101.0	21614.00	1785	82.59
B10	216.0	102.0	217.0	102.0	22032.00	1779	80.75
Mean	215.20	101.70	215.70	101.40	21831.30	1802.1	82.55
S <sub>d</sub>	1.23	0.82	1.06	0.84	213.22	71.0	3.18
C <sub>v</sub> (%)	0.57	0.81	0.49	0.83	0.98	3.9	3.85

Table 4.5 - Physical properties of brick type B.

Brick Ref. No.	Dimension (mm)				Least bed area (mm <sup>2</sup> )	Ult. load (kN)	Comp. strength (Nmm <sup>-2</sup> )
	Top bed		Bottom bed				
	length	width	length	width			
C 1	218.0	102.0	218.0	102.0	22236.00	1340	60.26
C 2	220.0	102.0	218.0	102.0	22236.00	1325	59.59
C 3	218.0	102.0	219.0	101.0	22119.00	1450	65.55
C 4	219.0	102.0	219.0	101.0	22119.00	1255	56.74
C 5	217.0	102.0	220.0	102.0	22134.00	1380	62.35
C 6	218.0	101.0	219.0	101.0	22018.00	1565	71.08
C 7	220.0	102.0	219.0	102.0	22338.00	1290	57.75
C 8	216.0	102.0	216.0	101.0	21816.00	1410	64.63
C 9	216.0	101.0	216.0	101.0	21816.00	1450	66.46
C10	216.0	101.0	216.0	101.0	21816.00	1310	60.05
Mean	217.80	101.70	218.00	101.40	22064.80	1377.5	62.45
S <sub>d</sub>	1.55	0.48	1.49	0.52	192.01	93.1	4.45
C <sub>v</sub> (%)	0.71	0.47	0.68	0.51	0.87	6.76	7.13

Table 4.6 - Physical properties of brick type C.

Brick Ref. No.	Dimension (mm)				Least bed area (mm <sup>2</sup> )	Ult. load (kN)	Comp. strength (Nmm <sup>-2</sup> )
	Top bed		Bottom bed				
	length	width	length	width			
D 1	217.0	100.0	220.0	100.0	21700.00	515.0	23.73
D 2	218.0	100.0	218.0	101.0	21800.00	660.0	30.28
D 3	218.0	100.0	217.0	101.0	21800.00	580.0	26.61
D 4	216.0	99.0	215.0	100.0	21384.00	655.0	30.63
D 5	218.0	99.0	217.0	101.0	21582.00	650.0	30.12
D 6	218.0	100.0	217.0	101.0	21800.00	630.0	28.90
D 7	218.0	101.0	217.0	100.0	21700.00	520.0	23.96
D 8	219.0	99.0	218.0	99.0	21582.00	560.0	25.95
D 9	218.0	100.0	218.0	99.0	21582.00	670.0	31.04
D10	218.0	100.0	215.0	101.0	21715.00	800.0	36.84
Mean	217.80	99.80	217.20	100.30	21664.50	624.0	28.81
S <sub>d</sub>	0.79	0.63	1.48	0.82	133.02	84.8	3.93
C <sub>v</sub> (%)	0.36	0.63	0.68	0.82	0.61	13.6	13.64

Table 4.7 - Physical properties of brick type D.

Brick Ref. No.	Dimension (mm)				Least bed area (mm <sup>2</sup> )	Ult. load (kN)	Comp. strength (Nmm <sup>-2</sup> )
	Top bed		Bottom bed				
	length	width	length	width			
E 1	215.0	101.5	215.0	102.0	21822.50	2090	95.77
E 2	215.5	101.0	214.5	101.0	21644.50	1990	91.86
E 3	215.0	102.0	214.5	102.0	21879.00	2155	98.50
E 4	214.0	100.5	214.0	101.0	21507.00	2020	93.92
E 5	215.0	101.0	215.5	100.5	21657.75	2130	98.35
E 6	215.0	100.5	215.0	101.0	21607.50	1930	89.32
E 7	214.0	101.0	214.0	101.0	21614.00	2045	94.61
E 8	215.0	102.0	214.0	101.0	21614.00	1775	82.12
E 9	215.0	101.0	215.0	101.0	21715.00	1840	84.73
E10	215.0	100.0	215.0	100.0	21500.00	2040	94.88
Mean	214.85	101.05	214.65	101.05	21656.13	2001.5	92.41
S <sub>d</sub>	0.42	0.64	0.53	0.60	121.79	122.1	5.49
C <sub>v</sub> (%)	0.20	0.64	0.25	0.59	0.56	6.1	5.94

Table 4.8 - Physical properties of brick type E.

Brick Ref. No.	Dimension (mm)				Least bed area (mm <sup>2</sup> )	Ult. load (kN)	Comp. strength (Nmm <sup>-2</sup> )
	Top bed		Bottom bed				
	length	width	length	width			
F 1	217.0	102.0	217.0	103.0	22134.00	1735	78.39
F 2	217.0	102.0	217.0	102.0	22134.00	1640	74.09
F 3	216.0	102.0	216.0	102.0	22032.00	1702	77.25
F 4	218.0	102.5	218.0	102.5	22345.00	1782	79.75
F 5	216.0	102.5	218.0	103.0	22140.00	1785	80.62
F 6	215.0	101.5	215.0	101.5	21822.50	1960	89.82
F 7	215.0	101.5	215.0	102.0	21822.50	2080	95.31
F 8	216.0	101.0	215.0	101.0	21715.00	1840	84.73
F 9	216.0	101.5	217.0	101.5	21924.00	1780	81.19
F10	215.0	102.5	215.0	102.5	22037.50	1700	77.14
Mean	216.10	101.90	216.30	102.10	22010.66	1800.4	81.83
S <sub>d</sub>	0.99	0.52	1.25	0.66	190.28	131.6	6.45
C <sub>v</sub> (%)	0.46	0.51	0.58	0.64	0.86	7.31	7.89

Table 4.9 - Physical properties of brick type F.

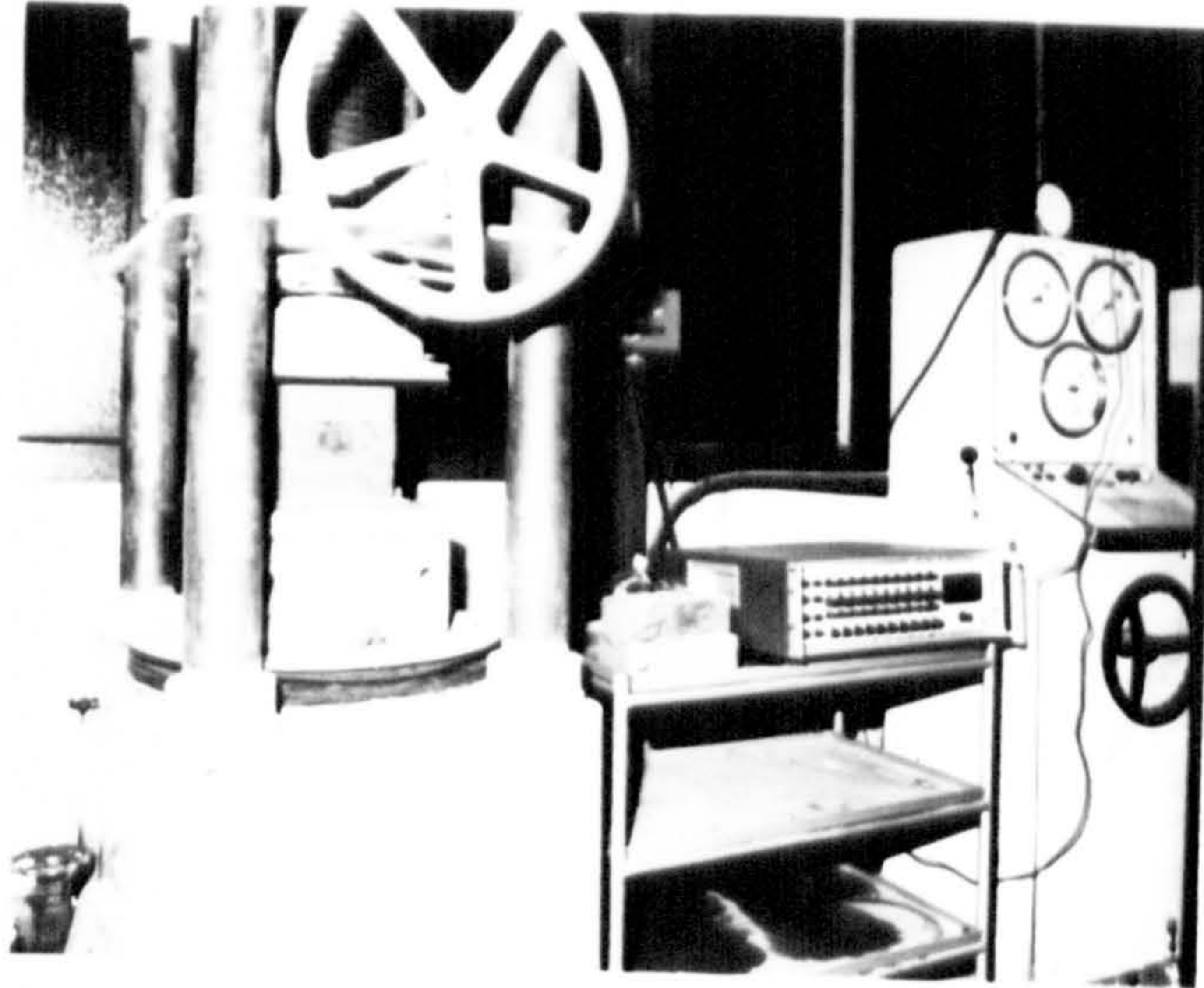


Brick Ref. No.	Dimension (mm)				Least bed area (mm <sup>2</sup> )	Ult. load (kN)	Comp. strength (Nmm <sup>-2</sup> )
	Top bed		Bottom bed				
	length	width	length	width			
G 1	212.0	98.0	212.0	98.0	20776.00	80.0	3.85
G 2	212.0	100.5	215.0	100.0	21306.00	90.0	4.22
G 3	213.5	99.0	214.0	99.0	21136.50	103.0	4.87
G 4	214.0	98.0	214.0	98.0	20972.00	93.0	4.43
G 5	214.0	98.0	213.0	98.0	20874.00	92.5	4.43
G 6	216.0	99.0	215.0	99.0	21285.00	94.0	4.42
G 7	214.0	99.0	213.0	99.0	21087.00	98.5	4.67
G 8	214.0	98.0	213.0	98.0	20874.00	99.5	4.77
G 9	213.0	100.0	213.0	100.0	21300.00	97.5	4.58
G10	213.0	98.0	213.0	98.0	20874.00	92.0	4.41
Mean	213.55	98.75	213.50	98.70	21047.45	94.0	4.47
S <sub>d</sub>	1.17	0.92	0.97	0.82	203.23	6.35	0.30
C <sub>v</sub> (%)	0.55	0.93	0.46	0.83	0.97	6.76	6.86

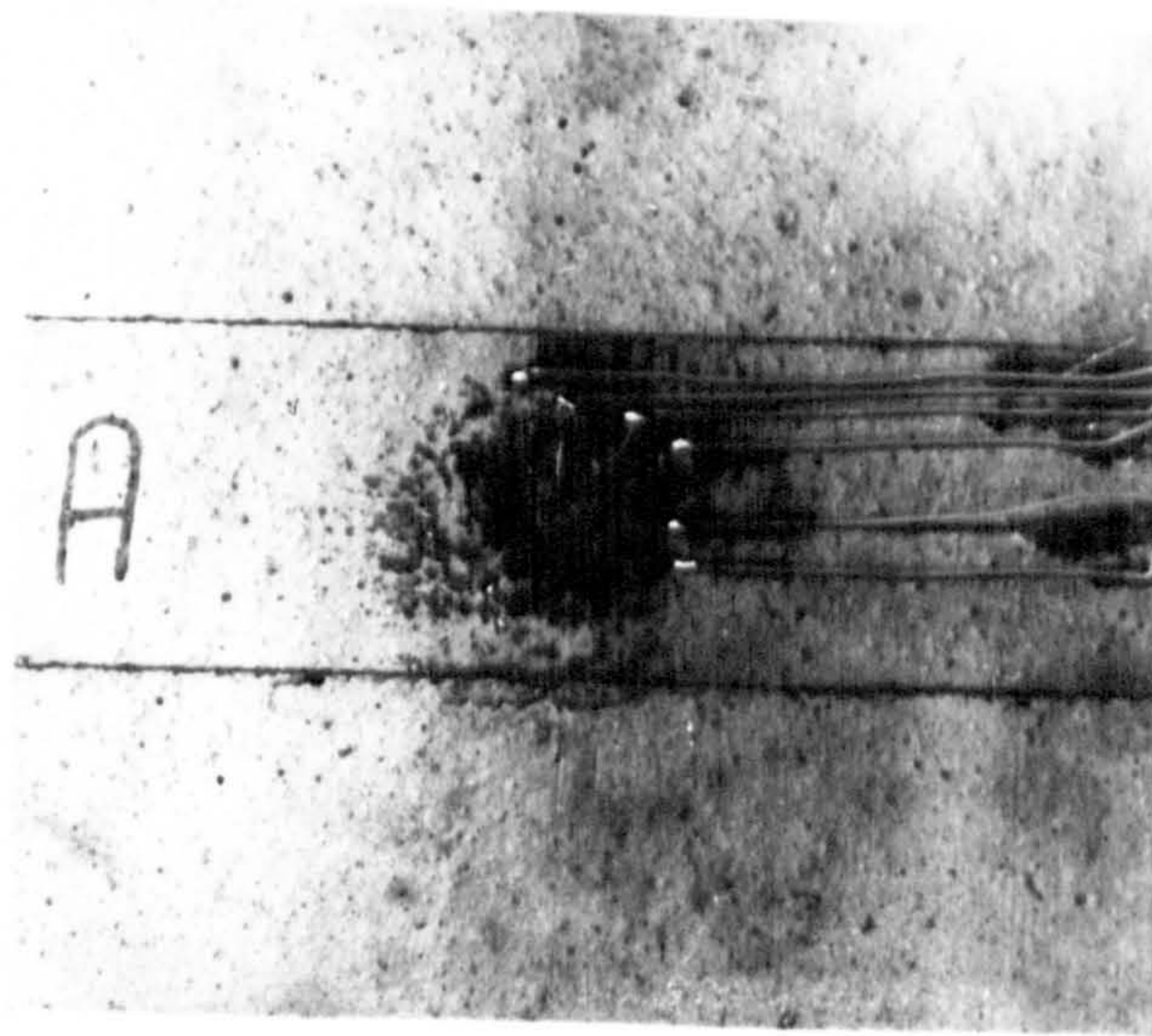
Table 4.10 - Physical properties of brick type G.

Brick type	f <sub>b</sub> (Nmm <sup>-2</sup> )	Init. tangent modulus (kNmm <sup>-2</sup> )	Secant modulus at 3/4 of max. stress (kNmm <sup>-2</sup> )	Poisson's ratio
A	90.08	84.850	89.184	0.13
B	82.55	85.304	89.211	0.16
C	62.45	67.945	72.108	0.12
D	28.81	47.935	51.820	0.15
E	92.41	65.383	64.548	0.12

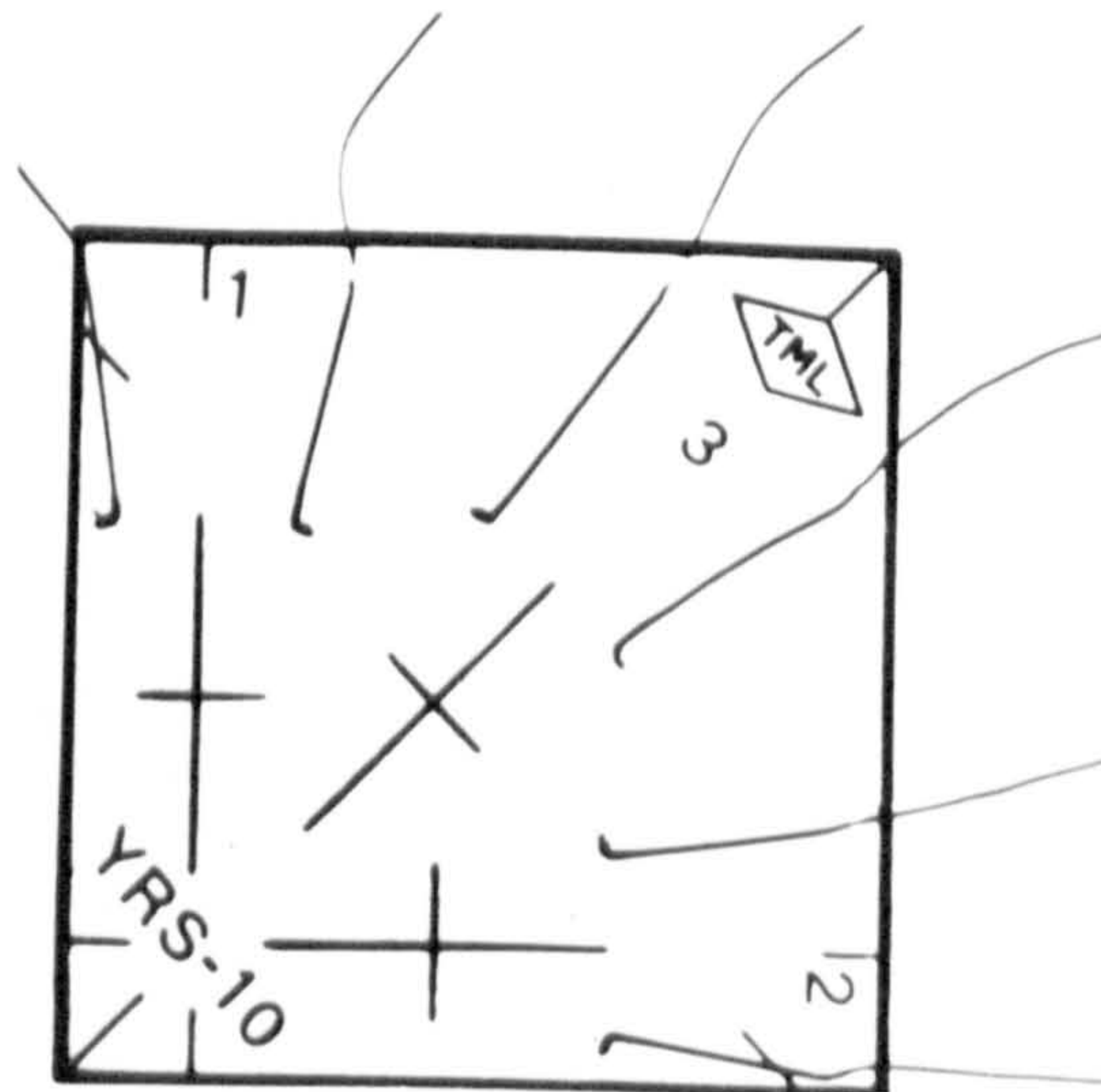
Table 4.11 - Elastic properties of brick units.



(a) - Test set up.



(b) - Brick test specimen.



(c) - Rosette wire strain gauge.

Fig. 4.2 - Testing method for elastic properties of bricks.

**VERTICAL STRESS-STRAIN RELATIONSHIP  
OF BRICK UNITS**

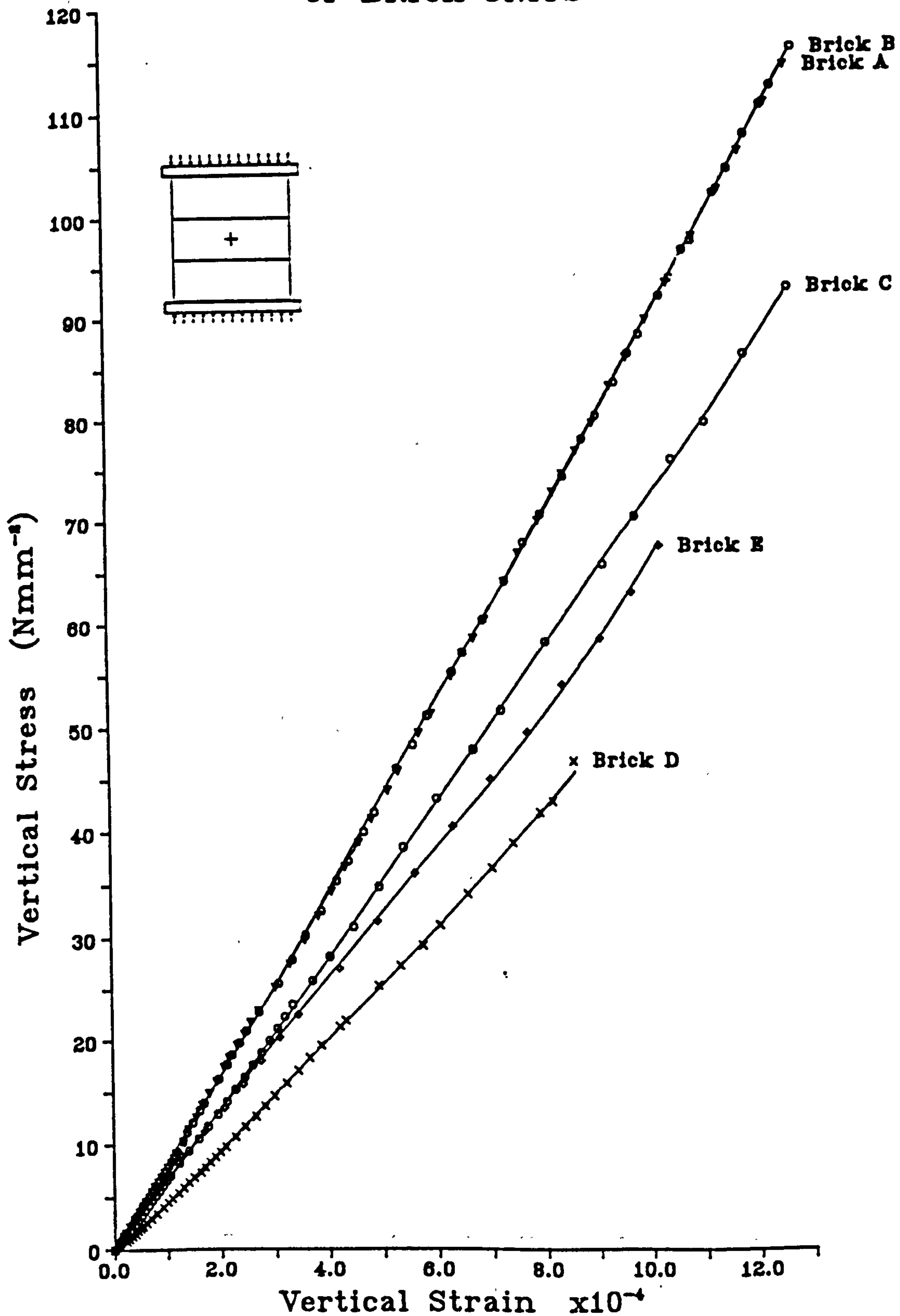


Fig. 4.3 - Vertical stress-strain relationship for brick units A to E.

**VERTICAL STRESS-LATERAL STRAIN  
RELATIONSHIP OF BRICK UNITS**

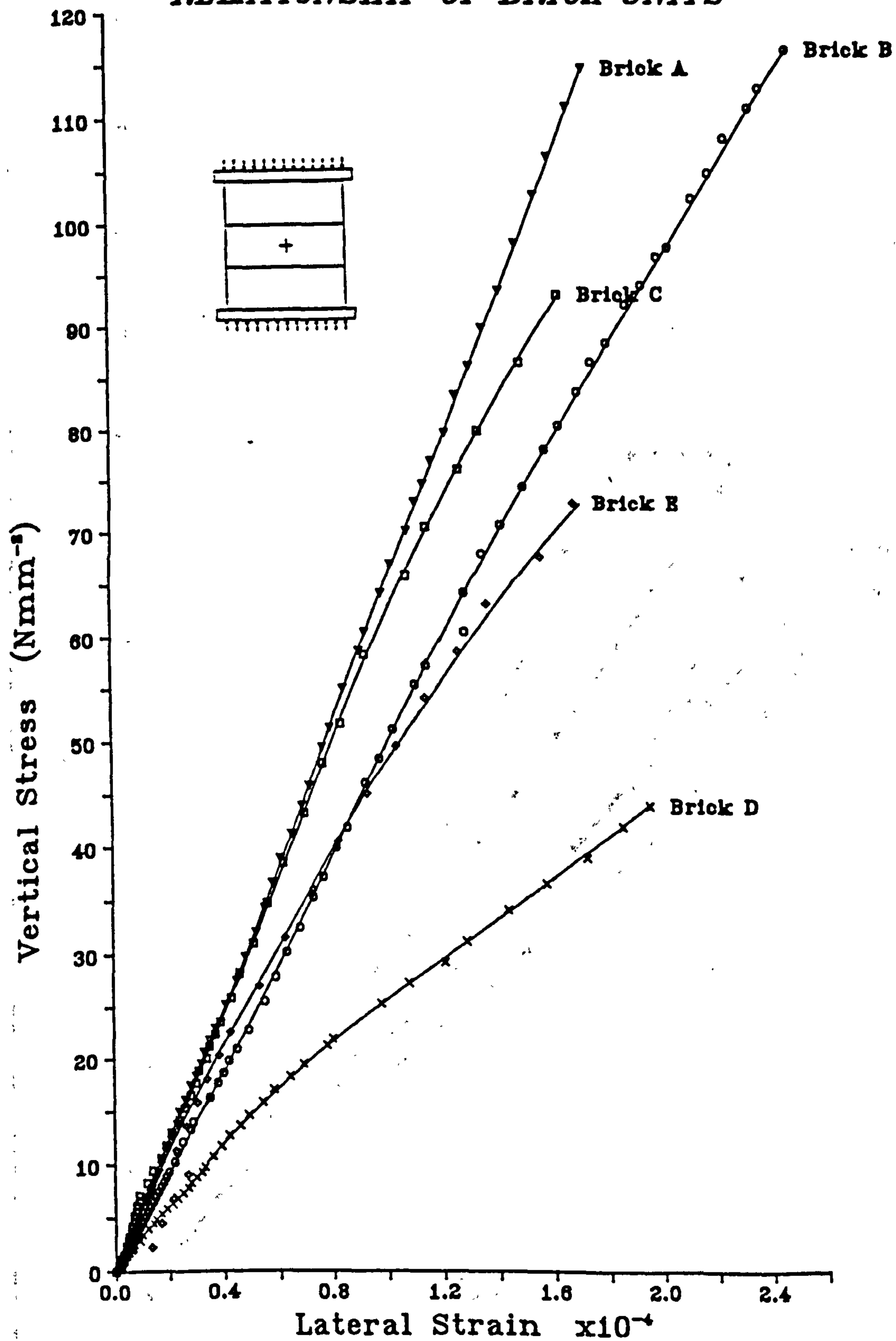


Fig. 4.4 - Vertical stress-lateral strain relationship for brick units A to E.

**VERTICAL-LATERAL STRAINS RELATIONSHIP  
OF BRICK UNITS**

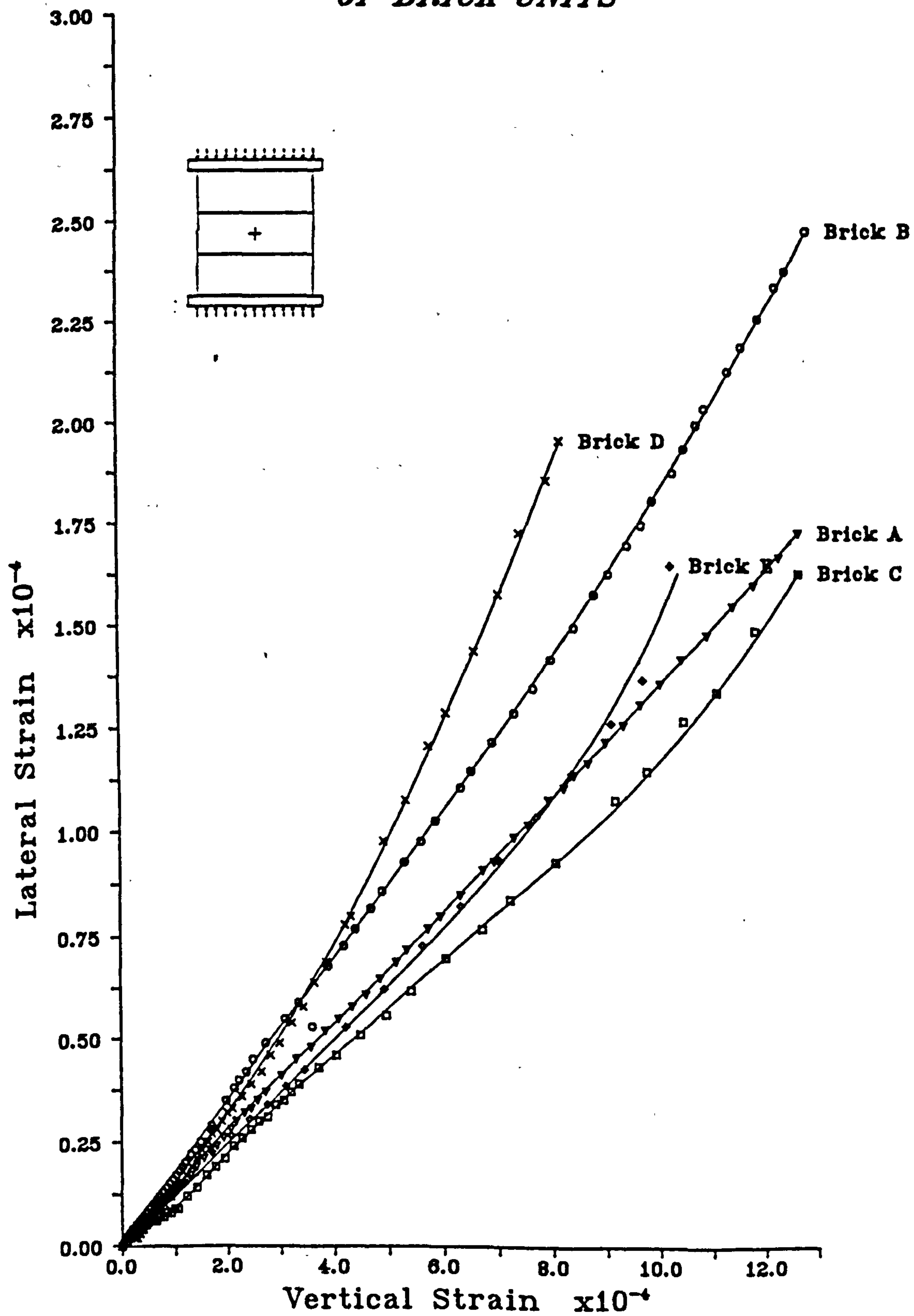


Fig. 4.5 - Vertical-lateral strain relationship for brick units A to E.

#### **4.3.1.1. Sand**

Local Scottish building sand was used throughout the investigation. It was said to be suitable for construction of unreinforced brickwork masonry. The grading of the sand is shown in Table 4.12 and illustrated in Fig. 4.6. It was carried out in accordance with the procedure laid in BS 1200<sup>[80]</sup>. The grading of the sand was found to lie within the limits proposed by BS 1200:table 1<sup>[89]</sup> for type S and G sand.

#### **4.3.1.2. Cement**

Ordinary Portland cement (Scottish Blue Circle) was used for the mortar designation M(i), which was found to be in accordance with the requirements of BS 12<sup>[90]</sup>.

Rapid hardening cement conforming to BS 12<sup>[90]</sup> was used for the mortar designation M(iii) where higher early strength was required.

#### **4.3.1.3. Lime**

White powdered high quality hydrated lime, (Limbox) manufactured by ICI, with 96.5% calcium hydroxide was used throughout in all batches of mortar. It was found to be in accordance with the requirements of BS 890<sup>[91]</sup>.

#### **4.3.2. Density**

Density was calculated for the designation M(i) and M(iii) from the mortar cubes. The results are presented in Table 4.13.

#### **4.3.3. Compressive Strength**

102mm mortar cubes were made and cured hydraulically in accordance with the procedures given in BS 5628<sup>[1]</sup> and BS 4551<sup>[92]</sup> for each mortar grade. In the case of mortar designation M(i) half of the test cubes were tested at the age of 7 days and the other half at the age of 28 days. The results are as shown in Table 4.14, and are found to comply with the requirements given in BS 5628:table 1<sup>[1]</sup>.

#### **4.3.4. Elastic Properties**

152mm cubes were cast for mortar designation M(i) and M(iii) for the purpose of strain readings. The constituent materials were the same as before for the two mortar grades. The axial and lateral strains were measured on the centre

lines of four faces of the cubes using 100mm Demec gauge with gauge constant of  $1.61 \times 10^{-5}$ .

The plots of vertical stress-strain, vertical stress-lateral strain and vertical-lateral strains for the two mortar designations are as shown in Figs. 4.7 to 4.9 respectively. The *apparent* initial tangent modulus, *apparent* secant modulus at 3/4 maximum stress and Poisson's ratio based on the linear portion of vertical-lateral strains curve are presented in Table 4.15.

#### 4.4. PROPERTIES OF BRICKWORK MASONRY

Brickwork masonry specimens constructed using brick types A, B, C, D and E with mortar grade M(i) are designated as brickwork types A, B, C, D and E respectively, and those constructed using brick types F and G with mortar grade M(iii) are designated as brickwork types F and G respectively.

##### 4.4.1. Dimensions

All the specimens were three stretchers in length, eight courses high and either single leaf or bonded with nominal dimensions; 665mm in length, 590mm in height and either 102.5mm or 215.0mm in thickness.

##### 4.4.2. Density

The density of the brickwork masonry was calculated based on at least 40 test specimens. Each specimen was weighed and the dimensions were measured accurately. The resulting densities for brickwork are presented in Table 4.16.

##### 4.4.3. Compressive Strength

To obtain the compressive strength of the brickwork masonry two identical test panels with nominal dimensions 590mm in height, 665mm in length and 102.5mm in thickness were tested under uniform axial compression for brickwork types A, B, C, D and E. Four specimens of brickwork type F were tested for each of the two thickness; 102.5mm and 215.0mm. In the case of brickwork type G (AAC brickwork), ten specimens were tested for each thickness.

These control specimens were built by the same bricklayer under the same conditions as the rest of the test specimens. The results of these control specimen tests are summarized in Table 4.17, and detailed results are presented in chapter 5.

BS sieve No.	Sieve aperture (mm)	%passing (by wt.)
3/16"	5.000	99.83
7	2.360	98.73
14	1.180	96.69
25	0.600	92.75
52	0.300	35.68
100	0.150	5.01
200	0.075	0.89

Table 4.12 - Sieve analysis of the sand.

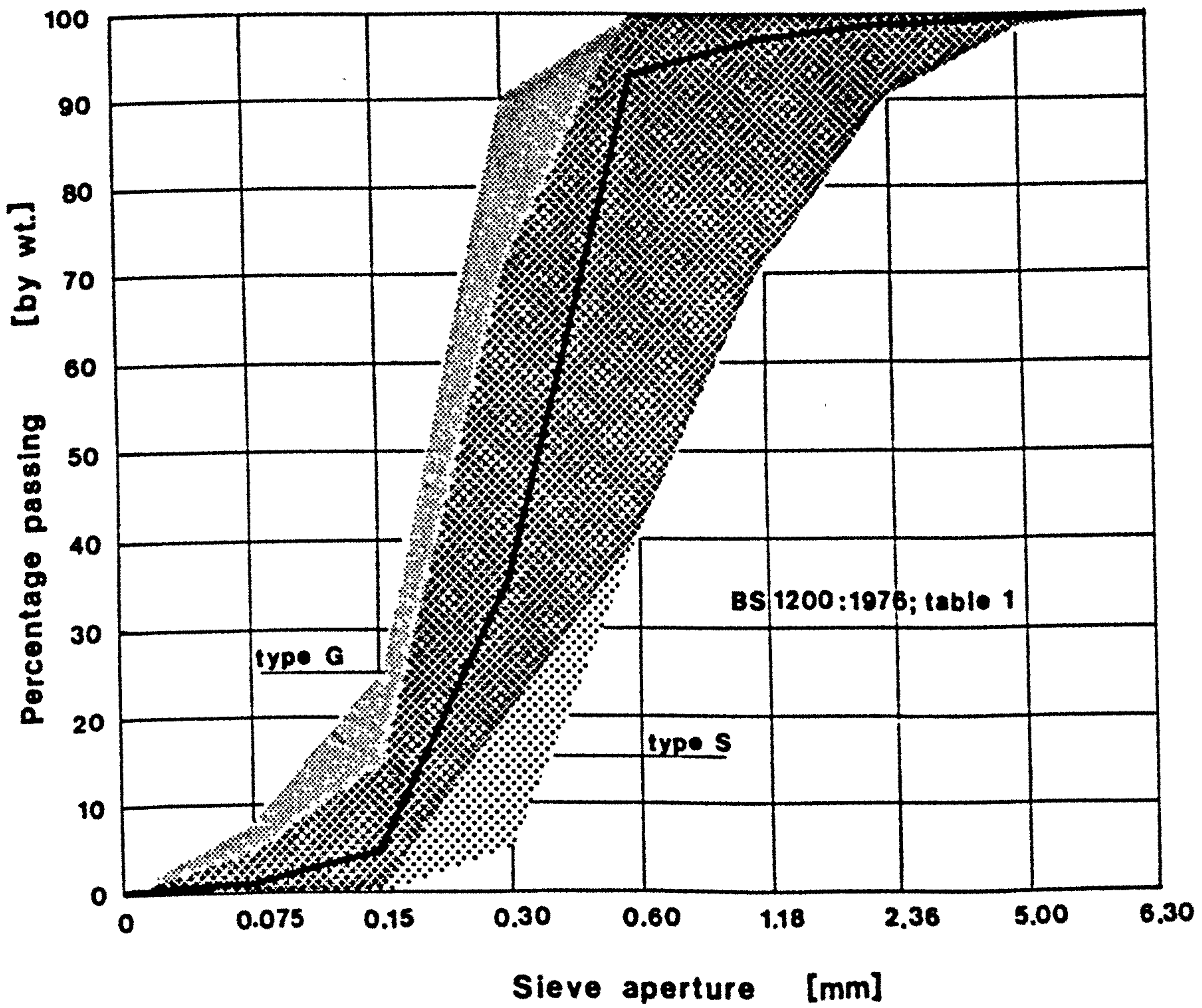


Fig. 4.6 - Grading curve for mortar sand.



Mortar designation	Age (days)	No. of samples	Density ( $\text{kgm}^{-3}$ )			$S_d$ ( $\text{kgm}^{-3}$ )	$C_v$ (%)
			average	maximum	minimum		
M(i) <sup>1</sup>	7	30	2082.50	2107.98	2040.13	19.80	0.95
M(i) <sup>1</sup>	28	30	2085.27	2148.49	2044.84	21.90	1.05
M(i) <sup>2</sup>	28	29	2159.74	2205.00	2126.00	22.12	1.02
M(iii) <sup>3</sup>	7	84	2031.29	2078.62	1868.85	43.28	2.13

- 1 mortar used for the construction of brickwork types A, B, C & D.
- 2 mortar used for the construction of brickwork type E.
- 3 mortar used for the construction of brickwork types F & G.

Table 4.13 - Density of mortars.

Mortar designation	Age at test (days)	No. of samples	$f_m$ ( $\text{Nmm}^{-2}$ )	$S_d$ ( $\text{Nmm}^{-2}$ )	$C_v$ (%)	$f_m$ from BS 5628:tab.1 ( $\text{Nmm}^{-2}$ )
M(i) <sup>1</sup>	7	30	12.24	1.84	15.02	10.7 <sup>4</sup>
M(i) <sup>1</sup>	28	30	17.61	2.23	12.66	16.0
M(i) <sup>2</sup>	28	29	27.42	3.25	11.86	16.0
M(iii) <sup>3</sup>	7	84	4.21	1.08	25.60	3.6 <sup>5</sup>

- 1 mortar used for the construction of brickwork types A, B, C & D.
- 2 mortar used for the construction of brickwork type E.
- 3 mortar used for the construction of brickwork types F & G.
- 4 suggested strength at 7-days is 2/3 of strength at 28-days.
- 5 equivalent strength at 28-days.

For more detailed results refer to Tables 5.4 to 5.7.

Table 4.14 - Compressive strength of mortar cubes.

Mortar designation	Age at test (days)	Init. tangent modulus ( $\text{kNmm}^{-2}$ )	Secant modulus at 3/4 of max. stress ( $\text{kNmm}^{-2}$ )	Poisson's ratio
M(i)	28	44.513	17.725	0.30
M(iii)	7	1.480	1.303	0.10

Table 4.15 - Elastic constants for mortar grade M(i) and M(iii).

*VERTICAL STRESS-STRAIN RELATIONSHIP  
OF MORTAR DESIGNATIONS M(i) AND M(iii)*

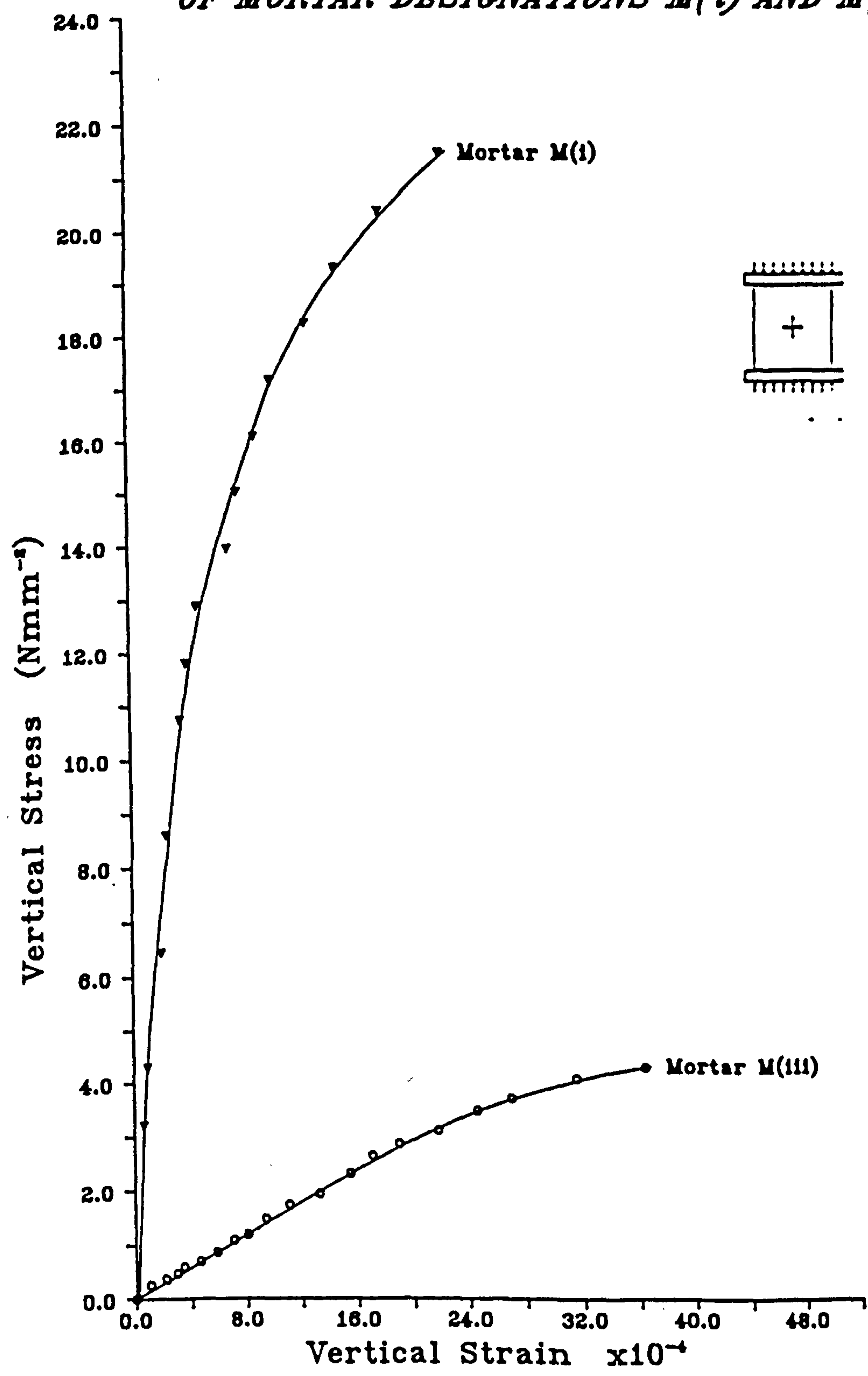


Fig. 4.7 - Vertical stress-strain relationship for mortar designations M(i) and M(iii).

**VERTICAL STRESS-LATERAL STRAIN  
RELATIONSHIP FOR MORTAR DESIGNATIONS  
M(i) AND M(iii)**

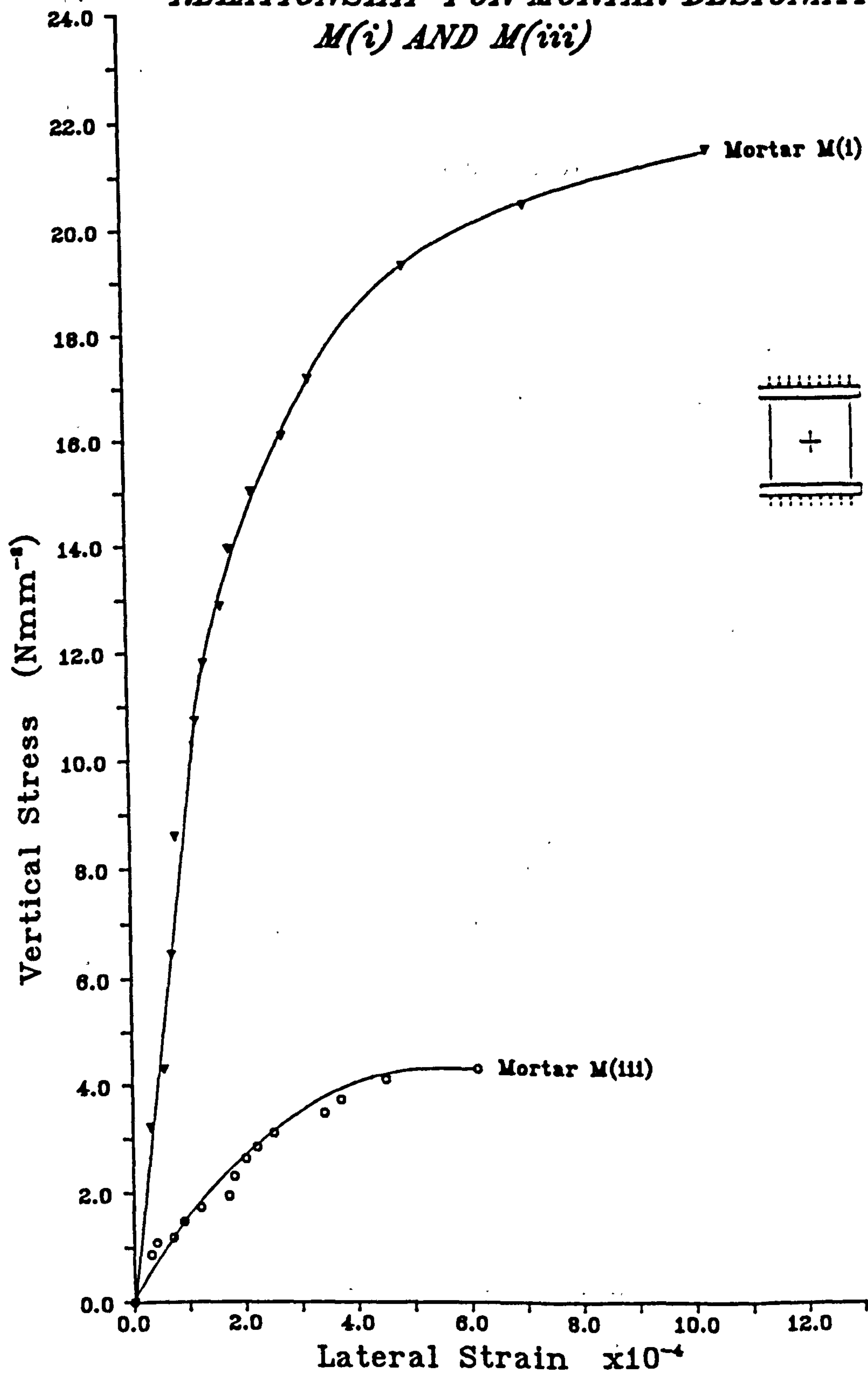


Fig. 4.8 - Vertical stress-lateral strain relationship for mortar designations M(i) and M(iii).

**VERTICAL-LATERAL STRAINS RELATIONSHIP  
OF MORTAR DESIGNATIONS M(i) AND M(iii)**

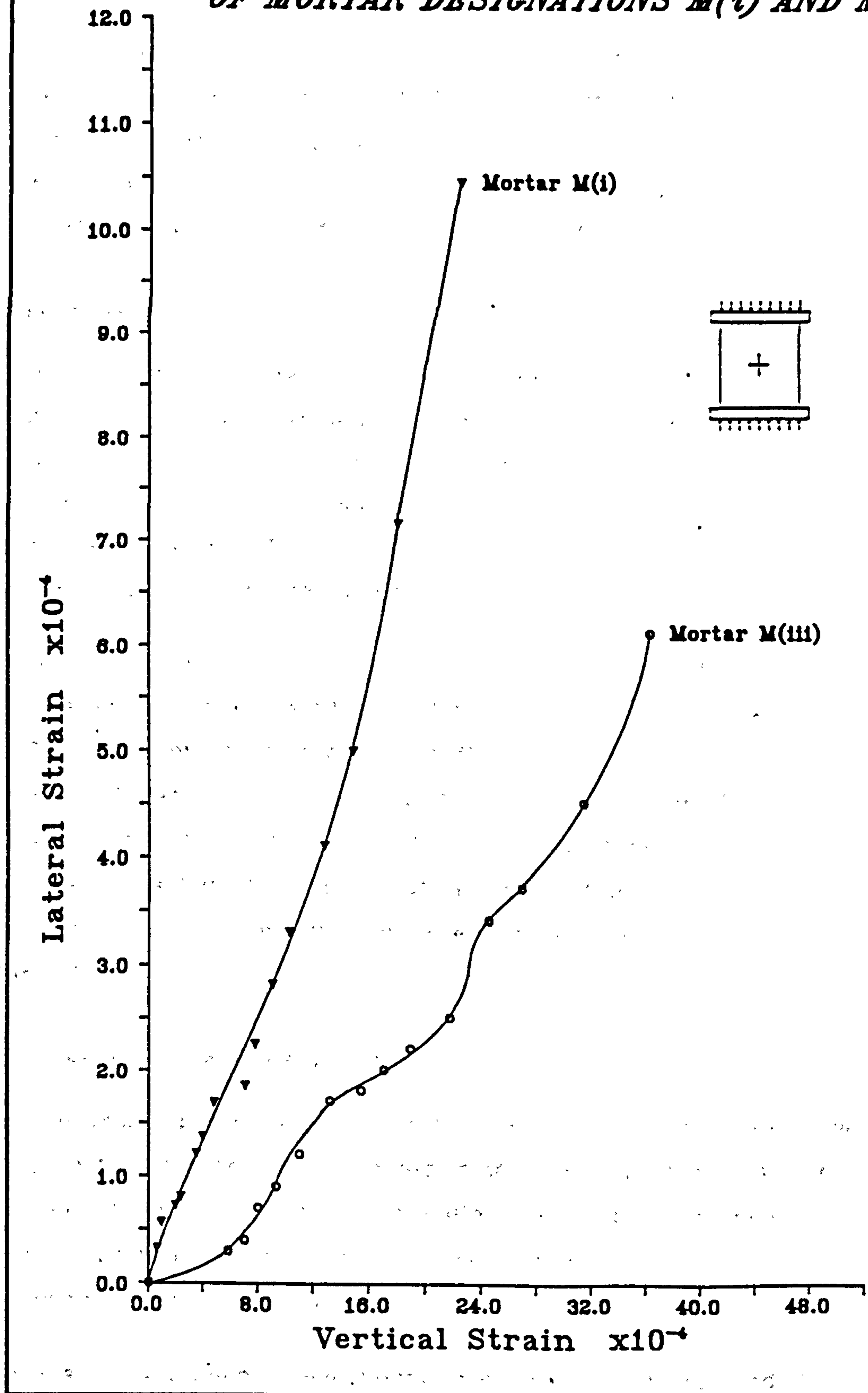


Fig. 4.9 - Vertical-lateral strains relationship for mortar designations M(i) and M(iii).

#### 4.4.4. Characteristic Compressive Strength

The characteristic compressive strengths of masonry,  $f_k$ , have been obtained from Table 2.12, section 2.5, for clay units depending on the thickness of the test specimen, mortar mix and the crushing strength of the brick units. In the case of AAC brick, since Table 2.12 does not represent concrete bricks, the  $f_k$  values for the two thicknesses have been calculated based on the method outlined in Appendix I.I. The results are as shown in Table 4.18 together with the values given for  $f_k$  in BS 5628:table 2(a)<sup>[1]</sup> for comparison.

#### 4.4.5. Elastic Properties

Specimens with nominal dimensions 665mm in length, 590mm in length and 102.5mm in thickness were utilized for the strain measurements. Three axial strain readings were taken on each side of the specimen; in the middle and near the ends using 12in Demec gauge with gauge constant of  $6.66 \times 10^{-6}$  for brickwork types A, B, C, D, E and F. The plots of axial stress-strain relationships are presented in Fig. 4.10.

Two lateral strain readings were taken on each side of the specimen in the middle two courses using 24in Demec gauge with a gauge constant of  $3.33 \times 10^{-6}$  for brickwork types A, B, C, D, E and F. The vertical stress-lateral strain and vertical-lateral strains relationships are graphically presented in Figs. 4.11 and 4.12. The values obtained for *apparent* initial tangent modulus, *apparent* secant modulus at 3/4 of maximum stress and Poisson's ratio based on the linear portion of lateral-vertical strains curve are as shown in Table 4.19.

### 4.5. DISCUSSION AND CONCLUSION

The physical properties of bricks, mortars and brickwork used in this investigation has been documented in this chapter. Ideally the most accurate method of determining the deformation constants is to measure the stress and the corresponding strain at a point within the specimens. This has been found to be difficult in practice.

Results of experimental investigations on elastic modulus and Poisson's ratio of brick units are limited. But the elastic modulus of brickwork have been studied by number of investigators and suggestions have been made that the elastic modulus of masonry is approximately 700 to 1000 times its characteristic strength.

Brickwork type	Brickwork density (kgm <sup>-3</sup> )	S <sub>d</sub> (kgm <sup>-3</sup> )	C <sub>v</sub> (%)
A	2168.29	20.85	0.96
B	1981.85	22.66	1.14
C	1931.63	23.01	1.19
D	1687.46	20.59	1.22
E	2110.09	29.69	1.41
F	2040.77	23.72	1.16
G	1093.03	49.35	4.51

Table 4.16 - Density of brickwork masonry.

Brickwork type	t (mm)	Mortar designation	f <sub>m</sub> (Nmm <sup>-2</sup> )	f <sub>b</sub> (Nmm <sup>-2</sup> )	Mean b.w. comp. strength (Nmm <sup>-2</sup> )
A	102.5	M(i)	17.61	90.08	31.42
B	102.5	M(i)	17.61	82.55	27.91
C	102.5	M(i)	17.61	62.45	17.50
D	102.5	M(i)	17.61	28.81	13.63
E	102.5	M(i)	27.42	92.41	31.90
F	102.5	M(iii)	4.21	81.83	15.22
F	215.0	M(iii)	4.21	81.83	12.26
G	102.5	M(iii)	4.21	4.47	2.17
G	215.0	M(iii)	4.21	4.47	2.04

Note: full detailed results in chapter 5, Table 5.8.

Table 4.17 - Compressive strength of brickwork masonry under uniform load.

Brickwork type	t (mm)	Mortar designation	$f_b$ (Nmm <sup>-2</sup> )	$f_k^1$ (Nmm <sup>-2</sup> )	$f_k$ BS 5628 (Nmm <sup>-2</sup> )
A	102.5	M(i)	90.08	19.50	25.7
B	102.5	M(i)	82.55	18.60	24.4
C	102.5	M(i)	62.45	16.00	20.2
D	102.5	M(i)	28.81	10.60	11.0
E	102.5	M(i)	92.41	19.70	26.2
F	102.5	M(iii)	81.83	14.60	16.1
F	215.0	M(iii)	81.83	9.70	14.0
G	102.5	M(iii)	4.47	1.68 <sup>2</sup>	2.4
G	215.0	M(iii)	4.47	1.73 <sup>2</sup>	2.7

- 1  $f_k$  values from Table 2.12, section 2.5.  
2  $f_k$  values calculated according to the method outlined in Appendix I.I.

Table 4.18 - Characteristic compressive strength of brickwork masonry specimens.

Brickwork type	$f_k$ (Nmm <sup>-2</sup> )	Init. tangent modulus (kNmm <sup>-2</sup> )	Secant modulus at 3/4 of max. stress (kNmm <sup>-2</sup> )	Poisson's ratio
A	19.50	9.843	18.648	0.24
B	18.60	11.088	14.571	0.10
C	16.00	17.368	15.212	0.14
D	10.60	9.480	9.299	0.10
E	19.70	31.274	22.219	0.18
F	14.60	21.949	11.287	0.20

Table 4.19 - Elastic properties of brickwork masonry.

**VERTICAL STRESS-STRAIN RELATIONSHIP  
OF BRICKWORK SPECIMENS**

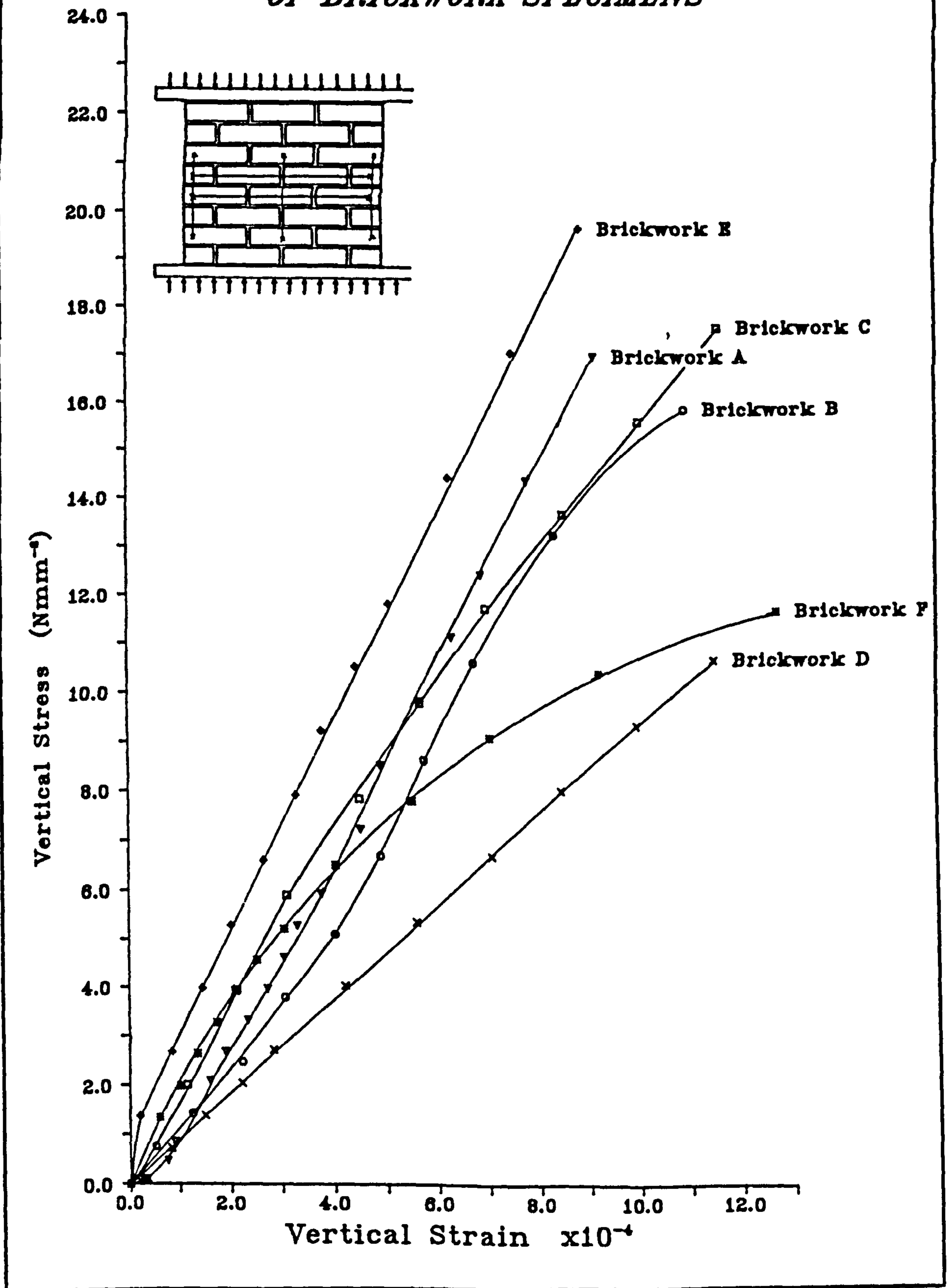


Fig. 4.10 - Vertical stress-strain relationship for brickwork masonry specimens.



**VERTICAL STRESS-LATERAL STRAIN  
RELATIONSHIP OF BRICKWORK SPECIMENS**

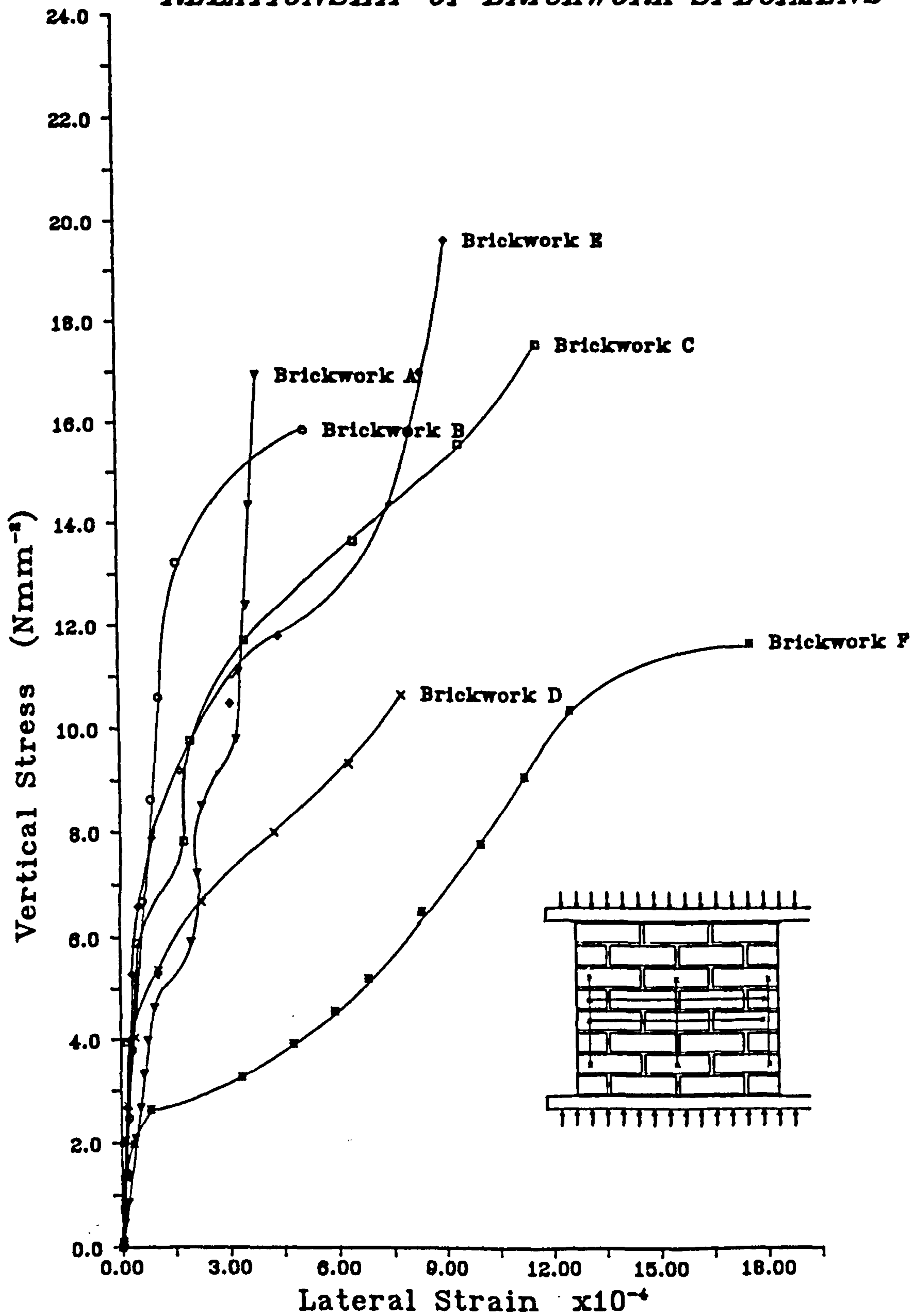


Fig. 4.11 - Vertical stress-lateral strain relationship for brickwork masonry specimens.

**VERTICAL-LATERAL STRAINS RELATIONSHIP  
OF BRICKWORK SPECIMENS**

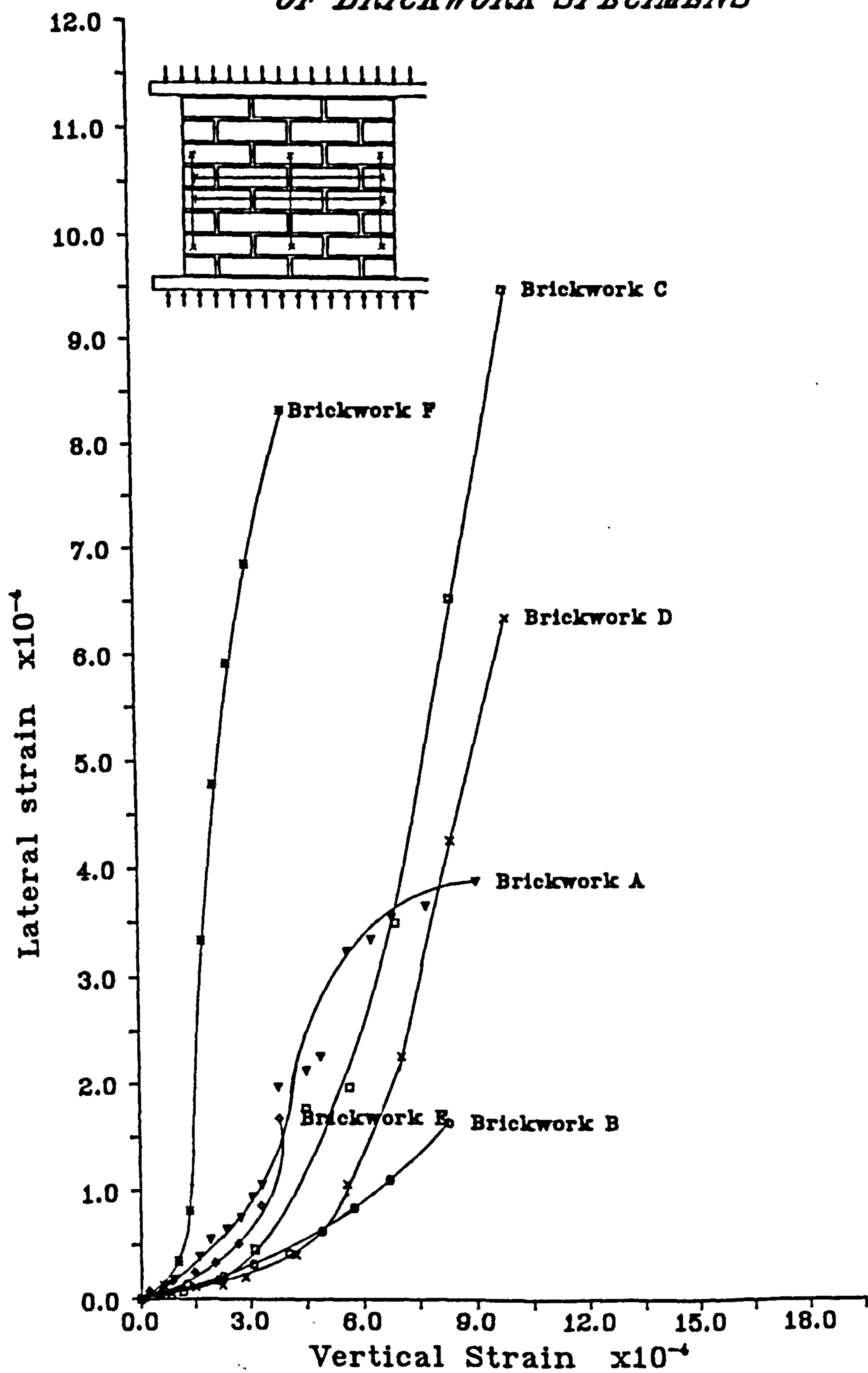


Fig. 4.12 - Vertical-lateral strains relationship for brickwork masonry specimens.

The vertical stress-strain relationship for brickwork in compression to failure has been determined by Powell and Hodgkinson<sup>[93]</sup>. The stress was related to the strain on a dimensionless basis in a parabolic form. Even though there was some variation of results between specimens of the same materials, it was found to be in good agreement with the results reported by Turnsek and Cacovic<sup>[94]</sup>.

Sinha and Pedreschi<sup>[95]</sup> investigated the elastic properties of brickwork prisms in three directions. It was concluded that the modulus of elasticity of brickwork increases with increase in compressive strength of brickwork ( $\sigma_m$ ), and the results yielded a relationship in the form:

$$E = 1180 \sigma_m^{0.83} \quad (4.1)$$

Warren and Lenczner<sup>[96]</sup> have proposed the following formula for elastic modulus of brickwork for bricks laid in mortar designation M(i);

$$E = ( 5.171 f_b^{0.5} - 19.158 ) \times 10^3 \quad (4.2)$$

Ameny *et al*<sup>[97]</sup> were able to predict the elastic deformation of masonry from the characteristics of the component unit and mortar. To investigate the elastic properties of bricks; (dry pressed giant units that are specifically designed for use in reinforced masonry with dimensions 390x190x90mm) small specimens 35x35x90mm were cut from the whole brick. Strains were registered using foil-type strain gauges. The stress-strain curves were found to have an initial linear portion and had a definite indication of non-homogeneity. Poisson's ratio was calculated in the linear stress-strain range resulting in values between 0.07 to 0.14. The stress-strain curves for mortar cylinders (76mm diameter x 152mm) were found to be non-linear. The non-linearity changed for different mortar grades. Poisson's ratio was shown to increase with applied stress. The stress-strain curves for masonry prisms had an initial linear portion, with subsequent non-linear behaviour to failure. It was shown that with weaker mortars the elastic modulus of masonry will be highly affected by the type of units. Also, depending on the kind of unit used, the mortar type may significantly affect the masonry elastic modulus. It was concluded that the simple theoretical models can give reasonable estimates of the short term deformation of brickwork.

However, it is evident from Figs. 4.3, 4.7 and 4.10 that the deformation characteristics are non-linear for brickwork and its constituent materials. The vertical stress-strain curves are found to have an initial linear portion. In the case of brick units the gradient of the curves increases with level of stressing. Whereas in the case of mortars the gradients decrease with applied load. This is also true for brickwork masonry types C, D, E and F. However, brickwork types A and B show the same behaviour as the brick units which might be due to the properties of the units.

Figs. 4.4, 4.8 and 4.11 are the plots of vertical stress-lateral strain under axial compressive load for brick units, mortar grades and brickwork respectively. Again there is an initial linear portion with subsequent non-linearity with increasing level of stress.

Figs. 4.5, 4.9 and 4.12 show the plots of vertical-lateral strains under axial compressive load. Again there is an initial linear portion and the Poisson's ratio increases with the level of stressing. This is clearly shown in Fig. 4.5.

It is worth mentioning that the shapes of the curves in Fig. 4.9 for mortar grade M(iii) and Figs. 4.11 and 4.12 are S shape. This could be explained due to the formation of vertical cracks in the specimens, especially in the case of brickwork masonry specimens where failure under uniform compressive load is by vertical splitting of the specimen. Hence the increase in lateral strain, and the shape of curves for vertical stress-lateral strain and lateral-vertical strains. The change of gradient actually shows the occurrence of a major crack in the specimen.

The method used for the determination of deformation behaviour of brick units in section 4.2.5 does not give actual values for the deformation constants because of the non-uniformity of stress at a section in the unit due to the presence of perforations. Since the holes do not transfer stress, stress concentrations are set up around the perforations. Therefore, it is accepted by the author that the values given in Tables 4.11, 4.15 and 4.19 are apparent values for the elastic properties of brickwork masonry and its component, brick unit and mortar.

Table 4.17 gives the mean brickwork masonry compressive strength under uniform load,  $f_{mm}$ , obtained experimentally and Table 4.18 contains the values for the characteristic compressive strength of brickwork masonry,  $f_k$ , determined from Table 2.12 in section 2.5. To compare the experimental

results with the results obtained from the collected wall test results reported in chapter 2, Table 4.20 has been constructed. From the two methods of analysis covered in sections 2.4.4.1 and 2.4.4.2 it is possible to work out the values for  $f_{mm}$  and  $f_k$  from equations 2.15 and 2.16 (in chapter 2) and comparison could be made between the values of  $f_{mm}$  by the two statistical method of analysis and the experimental values. Comparison could also be made for the values of  $f_k$  obtained from the results in sections 2.4.4.1, 2.4.4.2, 2.5 and the code values.

As Table 4.20 shows that there exists good agreement between the values of  $f_{mm}$  determined statistically and the experimental results, which in turn endorses the validity of the  $f_k$  values. Also close agreement could be seen between the values of  $f_k$  obtained from the three statistical methods of analysis. The small difference is due to the mortar cube strength, as discussed in chapter 2.

$f_b$ ( $Nmm^{-2}$ )	$t$ (mm)	Mortar desig.	Section 2.4.4.1		Section 2.4.4.2		Sect 2.5	Experi.	BS 5628
			$f_{mm}$ ( $Nmm^{-2}$ )	$f_k$ ( $Nmm^{-2}$ )	$f_{mm}$ ( $Nmm^{-2}$ )	$f_k$ ( $Nmm^{-2}$ )	$f_k$ ( $Nmm^{-2}$ )	$f_{mm}$ ( $Nmm^{-2}$ )	$f_k$ ( $Nmm^{-2}$ )
90.08	102.5	M(i)	30.63	21.21	31.96	20.24	19.50	31.42	25.90
82.55	102.5	M(i)	29.28	20.27	30.52	19.32	18.60	27.91	24.90
62.45	102.5	M(i)	25.35	17.55	26.31	16.66	16.00	17.50	20.10
28.81	102.5	M(i)	17.01	11.78	17.45	11.04	10.60	13.63	11.20
92.41	102.5	M(i)	31.03	21.49	35.53	22.50	19.70	31.90	27.10
81.83	102.5	M(iii)	21.43	14.51	22.55	14.28	14.60	15.22	24.10
81.83	215.0	M(iii)	13.42	8.23	14.61	9.46	9.70	12.26	21.00
4.47	102.5	M(iii)					1.68	2.17	2.40
4.47	215.0	M(iii)					1.73	2.04	2.40

Table 4.20 - Comparison between the values of  $f_{mm}$  and  $f_k$  determined experimentally and by the statistical methods of chapter 2.

## Chapter 5

### EXPERIMENTAL STUDY: CONCENTRATED LOAD ON BRICKWORK

#### 5.1. INTRODUCTION

The full-scale tests carried out investigate the bearing strength of brickwork wallettes when subjected to concentrated loading through mild steel bearing plates at various positions along the wall. The investigation covered the effect of loaded area ratio, edge distance, loading position and configurations, wall thickness, effective length of wall, brick unit and mortar strengths.

The construction, curing, preparation of test specimens and the method of testing together with the test programme and the results are documented in this chapter.

#### 5.2. CONSTRUCTION OF BRICKWORK SPECIMENS

##### 5.2.1. Construction of Brickwork Wallettes

The wallettes were constructed in Old English or stretcher bond and were three stretchers long and eight courses high. Seven strengths of bricks and two mortar grades (refer to section 4.2 and 4.3) were used to built the wallettes. The nominal dimensions were; 665mm in length, 590mm in height; some were 102.5mm and some 215.0mm in thickness. Mortar beds were 10mm and all perpends and bed joints were completely filled with mortar.

The wallettes were constructed on a flat surface by an experienced bricklayer, who checked mortar bed thickness using a graduated batten, and who plumbed and levelled the wallettes. Wallettes were left undisturbed after construction to cure in the laboratory.

In all, 300 brickwork wallettes were constructed for the investigation under concentrated loading, and the details are as shown in Table 5.1.

##### 5.2.2. Construction of Brickwork Control Specimens

Apart from the 300 test specimens outlined in previous section, 38 auxiliary control specimens were built and tested under uniform compressive load, (refer to Table 5.1) for the determination of their respective wallette compressive strength of which the results were reported in section 4.4.3 and Table 4.17. More detailed results will be given in section 5.6. These control

specimens had nominal dimensions 590mm in height, 665mm in length and 102.5mm in thickness for brickwork types A to G, constructed from the same constituent materials as in their respective wallettes type. In addition for brickwork types F and G, control specimens were also constructed in the same height and length with 215.0mm thickness.

No. o specimens	Brick type	Mortar designation	t (mm)	Age at test
40 <sup>1</sup>	A	M(i) <sup>3</sup>	102.5	28
40 <sup>1</sup>	B	M(i) <sup>3</sup>	102.5	28
40 <sup>1</sup>	C	M(i) <sup>3</sup>	102.5	28
40 <sup>1</sup>	D	M(i) <sup>3</sup>	102.5	28
56 <sup>1</sup>	E	M(i) <sup>3</sup>	102.5	28
18 <sup>1</sup>	F	M(iii) <sup>4</sup>	102.5	7
18 <sup>1</sup>	F	M(iii) <sup>4</sup>	215.0	7
18 <sup>1</sup>	G	M(iii) <sup>4</sup>	102.5	7
18 <sup>1</sup>	G	M(iii) <sup>4</sup>	215.0	7
6 <sup>1,5</sup>	F	M(iii) <sup>4</sup>	102.5	7
6 <sup>1,5</sup>	G	M(iii) <sup>4</sup>	102.5	7
2 <sup>2</sup>	A	M(i) <sup>3</sup>	102.5	28
2 <sup>2</sup>	B	M(i) <sup>3</sup>	102.5	28
2 <sup>2</sup>	C	M(i) <sup>3</sup>	102.5	28
2 <sup>2</sup>	D	M(i) <sup>3</sup>	102.5	28
2 <sup>2</sup>	E	M(i) <sup>3</sup>	102.5	28
4 <sup>2</sup>	F	M(iii) <sup>4</sup>	102.5	7
4 <sup>2</sup>	F	M(iii) <sup>4</sup>	215.0	7
10 <sup>2</sup>	G	M(iii) <sup>4</sup>	102.5	7
10 <sup>2</sup>	G	M(iii) <sup>4</sup>	215.0	7

- 1 Concentrated load applied partially over a limited area  
2 Uniformly distributed load applied over the whole area  
3 Mortar 1:1/4:3 Portland cement:lime:sand mix by volume  
4 Mortar 1:1:6 rapid hardening cement:lime:sand mix by volume  
5 length varied from one stretcher to six stretchers long

Table 5.1 - Details of the constructed wallette specimens.

### 5.3. TESTING EQUIPMENT

Brick units were crushed between two 3mm thick plywood sheets in a 2.5MN capacity Dennison compression machine. The mortar cubes were tested in a 2MN Avery-Denison testing machine.

The control and test specimens were tested in a 1MN capacity Avery Universal compression machine. Load was transmitted by means of the upper platen of the compression testing machine, which had a ball seating to allow for the possibility of the loading plate being slightly off level.

## **5.4. METHOD OF TESTING**

### **5.4.1. Preparation of Specimens**

The constructed brickwork specimens were measured, weighed accurately and numbered. They were placed on a 25mm thick steel base plate. A 3mm thick plywood sheet, which extended 10mm out from each side of the specimen, was inserted between the steel base plate and the base of the wallette. The top surface was sanded and flattened before placing in the testing machine. The wallettes were positioned in the testing machine such that the centre of the upper platen coincided with the centre point of the bearing plate ensuring that the load would be applied axially.

In the case of control specimens, uniform load was transmitted through a 150mm thick steel plate (thought to be sufficiently rigid as to ensure uniform loading) covering the entire cross-sectional area. In the case of test specimens, concentrated load was applied partially to the surface of the brickwork specimens via a 25mm thick steel bearing plate.

The steel bearing plates were mounted on top of the brickwork specimens, using freshly made dental plaster. Before the plaster was set, a small increment of load was applied to the bearing plate by means of the upper platen of the testing machine to level the bearing plate and fill up the pores beneath the bearing plate. It also ensured an even bedding for the bearing plates on the top surface of the brickwork specimens. This was thought to be necessary, since stress concentrations would occur if the specimen was not perfectly level, and also it would hold the bearing plates in position. Then the load was released and the specimen was left for few minutes allowing the plaster to dry before the testing commenced.

### **5.4.2. Loading Conditions**

In general one distinct loading configuration was investigated. This was **strip loading**, where the load was applied partially over a limited area of a wall covering its entire thickness. This in turn was applied concentrically or eccentrically with respect to the centre of the wall in the longitudinal direction. The concentric partial case is termed **central strip loading** and eccentric case is either **intermediate strip** (where the load is applied at quarter point of the length of the wallettes) or **end strip loading** (where the load is applied at the end of the wallette), see Fig. 5.1.



In the earlier work<sup>[67]</sup> the results of which are presented in Appendix II.I, in addition to strip loading, **edge** or **patch** loading configurations, where *concentrated load* is applied partially over an area of wall eccentrically in the direction normal to the longitudinal direction, were also investigated experimentally. These in turn were applied concentrically or eccentrically with respect to the centre of the wall in the longitudinal direction as shown in Fig. 5.2.

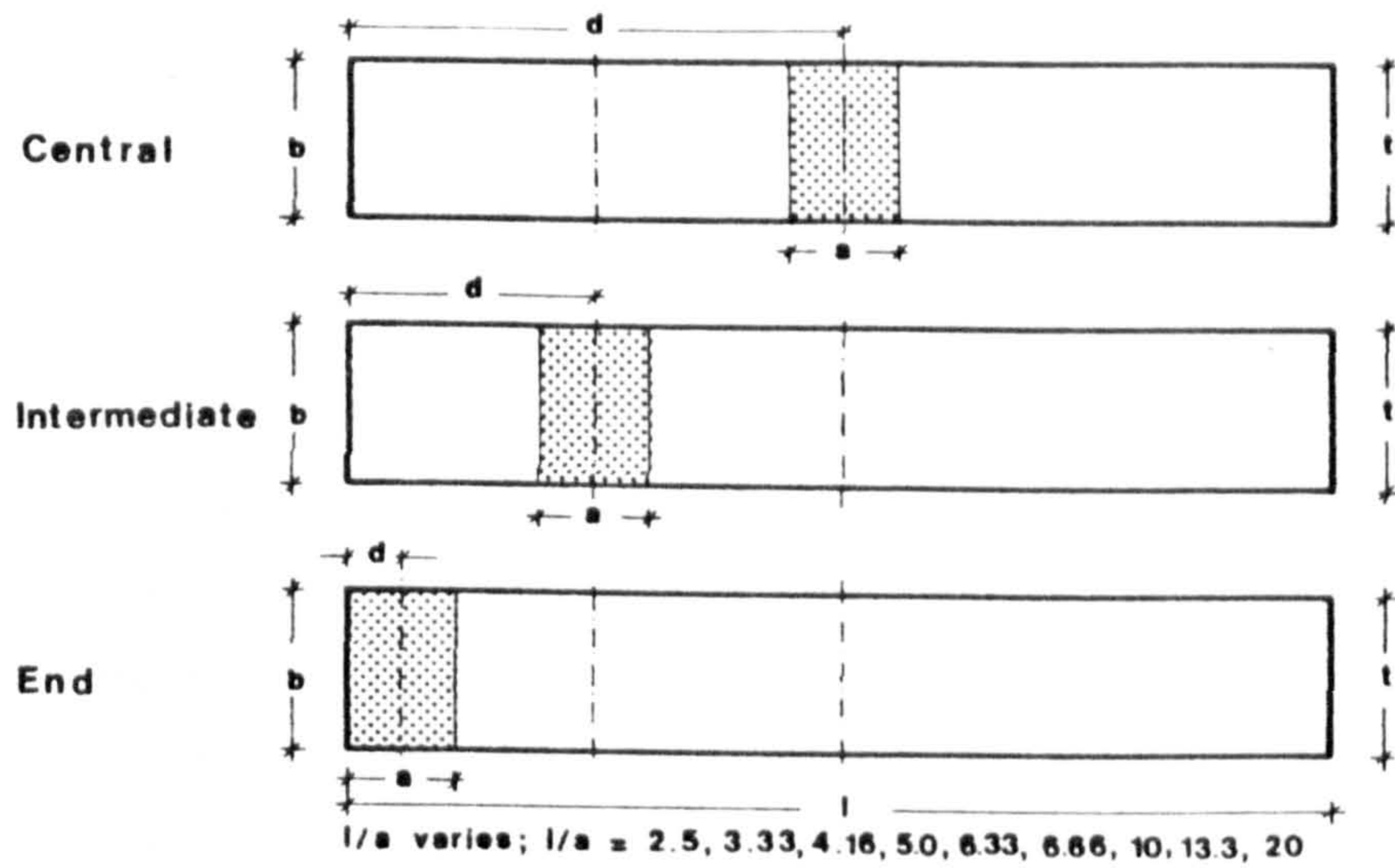


Fig. 5.1 - Strip loading configuration.

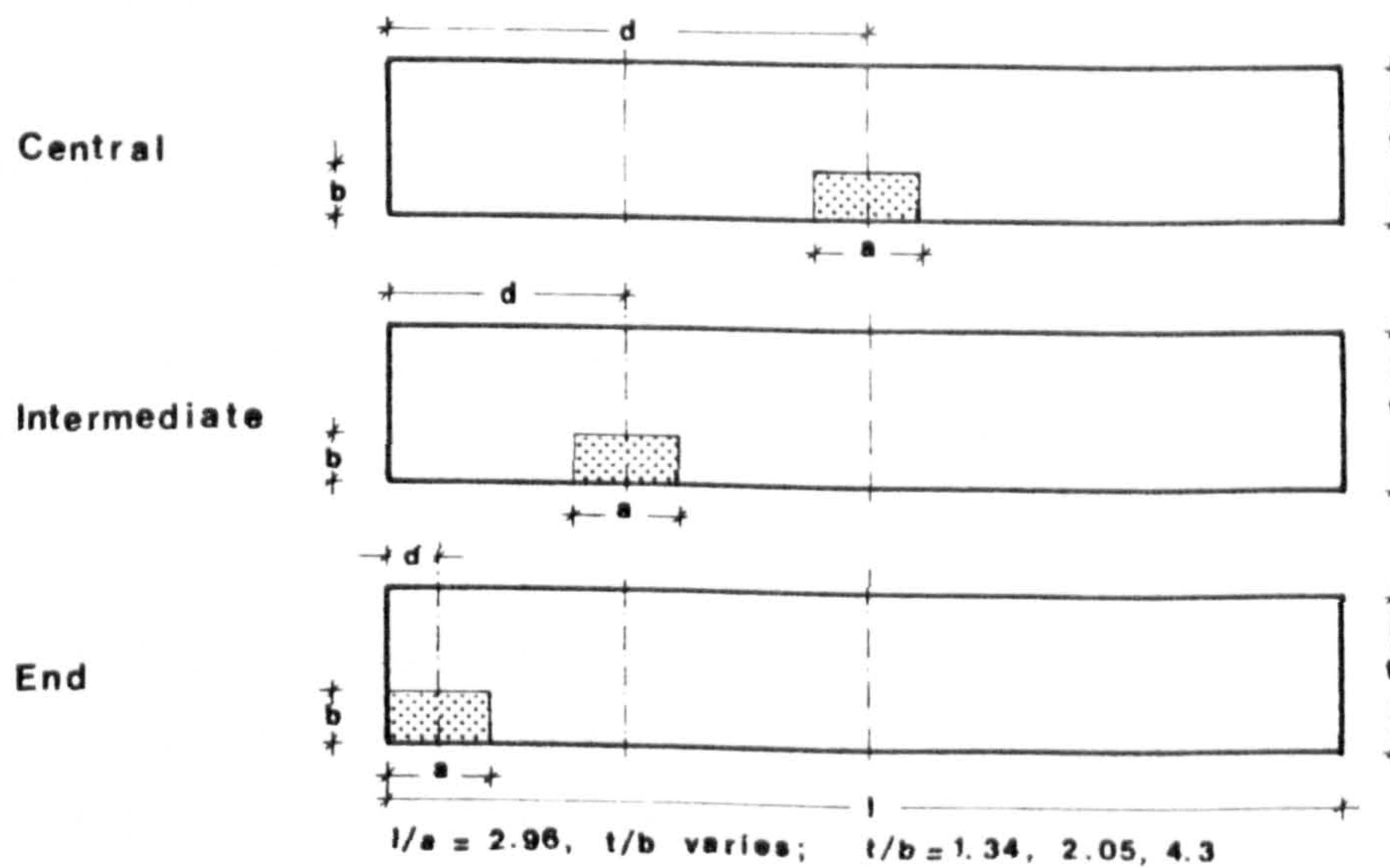


Fig. 5.2 - Edge loading configuration.

### 5.4.3. Rate of Loading

BS 3921:1974<sup>[88]</sup> recommends a rate of loading of up to  $35 \text{ Nmm}^{-2}\text{min}^{-1}$  initially for brick units. When half the expected maximum load has been reached this loading rate should be reduced to  $15 \text{ Nmm}^{-2}\text{min}^{-1}$  and maintained until the maximum failure load is reached. In the foregoing experiments the units were crushed under uniform load at the rate of  $15 \text{ Nmm}^{-2}\text{min}^{-1}$  throughout.

BS 4551:1980<sup>[92]</sup> recommends that the rate of loading for the determination of compressive strength of mortar cubes be within the range  $0.03$  to  $0.1 \text{ Nmm}^{-2}\text{sec}^{-1}$ , until failure occurs. This procedure were adopted during the testing of mortar cubes.

BS 5628:Part 1:1978<sup>[11]</sup> recommends a rate of loading of  $1 \text{ Nmm}^{-2}\text{min}^{-1}$  for brickwork test panels under uniform load. This loading rate was applied to the control specimens which were tested under uniform compressive load. However, since this loading rate was difficult to attain in practice under concentrated load, the maximum loading rate in this case was set to  $15 \text{ Nmm}^{-2}\text{min}^{-1}$ . The practical range reached during the testing was from  $2.5$  to  $14 \text{ Nmm}^{-2}\text{min}^{-1}$ . The loading rate for each particular case is presented in the tables of results in section 5.6.

### 5.4.4. Bearing Plates

Dimensions of bearing plates used through this investigation (see Table 5.2) are referred to as type I to XI. Bearing plates with reference number XII to XX are those used in the earlier investigation by the author<sup>[67]</sup> and Professor Hendry.

Bearing plates I to VI corresponds to  $A_r$  equal to 0.05, 0.10, 0.15, 0.20, 0.30 and 0.40 respectively with respect to the nominal cross-sectional area of the test specimens, 102.5mm in thickness. Bearing plates VII, VIII and IX correspond to  $A_r$  equal to 0.05, 0.10 and 0.15 respectively with respect to the nominal cross-sectional area of test specimens 215.0mm in thickness.

All the bearing plates were mild steel, 25mm thick plate machine cut to the required dimensions. They were considered to be rigid enough to transmit the load, due to their respective dimensions.

## 5.5. TEST PROGRAMME

A summary of the test programme is presented in Table 5.3. Brickwork types A, B, C and D were utilized to study the effect of brick unit strength and percentage of area loaded on the compressive strengths of brickwork wallettes 102.5mm in thickness under central strip concentrated load.

Brickwork type E was utilized to study the effect of edge distance using three loading positions; central intermediate and end strip loading, for various ratios of loaded areas.

Brickwork types F and G were utilized to do a comparative study on the effect of type of brick unit and the thickness of specimens and their influence on the compressive strength of masonry under central, intermediate and end strip concentrated load.

## 5.6. TEST RESULTS

The results of tests on the crushing strength of brick units and other physical properties are covered in section 4.2.

The results of mortar cubes tested for the determination of mortar cube strength designations M(i) and M(iii) at the ages of 7 and 28 days are presented in Tables 5.4 to 5.7, and the summary is as shown in Table 4.14.

The results of tests on the crushing strength of brickwork control specimens are presented in Table 5.8. In the case of brickwork types A to F inclusive the characteristic compressive strength,  $f_k$ , have been determined from Table 2.12, section 2.5, whereas in the case of brickwork type G (AAC brickwork) the  $f_k$  has been determined from the method outlined in Appendix I.I.

The results of tests on brickwork specimens 102.5mm in thickness under central strip load with loaded area ratios of 0.1, 0.2, 0.3 and 0.4 for brickwork types A, B, C, D are as shown in Tables 5.9, 5.10, 5.11 and 5.12 respectively. Table 5.13 presents the results of tests on brickwork type E under central strip concentrated load for loaded area ratio of 0.05. The results of tests on brickwork type E, 102.5mm in thickness, for loaded area ratios of 0.05, 0.10, 0.15, 0.20, 0.30 and 0.40 under intermediate strip and end strip concentrated load are as shown in Tables 5.14 and 5.15 respectively. The results of tests under central, intermediate and end strip concentrated load, for brickwork types F and G, for thicknesses of 102.5 and 215.0mm are presented in

Tables 5.16 and 5.17. The results of tests on 102.5mm thick brickwork types F and G under central strip concentrated load with the length of the specimen as a variable for two sizes of bearing plates are as shown in Table 5.18. In each case the enhancement factor, ( $\zeta = f_{cb}/f_k$ ) and the ratio of cracking load to the ultimate load at failure, ( $F_r = F_c/F_u$ ) have been calculated and are as shown in Tables 5.9 to 5.18.

Plate Ref. No.	Dimension of bearing plate (mm)			
	length (a)	breadth (b)	thickness (c)	
I	1	33.2	102.5	25.0
II	1	66.5	102.5	25.0
III	1	99.7	102.5	25.0
IV	1	133.0	102.5	25.0
V	1	199.5	102.5	25.0
VI	1	266.0	102.5	25.0
VII	1	33.2	215.0	25.0
VIII	1	66.5	215.0	25.0
IX	1	99.7	215.0	25.0
X	1	100.0	102.5	25.0
XI	1	225.0	100.0	25.0
XII	2	215.0	50.0	25.0
XIII	2	215.0	105.0	25.0
XIV	2	215.0	160.0	25.0
XV	1	50.0	215.0	25.0
XVI	1	105.0	215.0	25.0
XVII	1	160.0	215.0	25.0
XVIII	1	50.0	102.5	25.0
XIX	1	105.0	102.5	25.0
XX	1	160.0	102.5	25.0

1 Strip loading  
2 Edge loading

Table 5.2 - Dimensions of bearing plates.

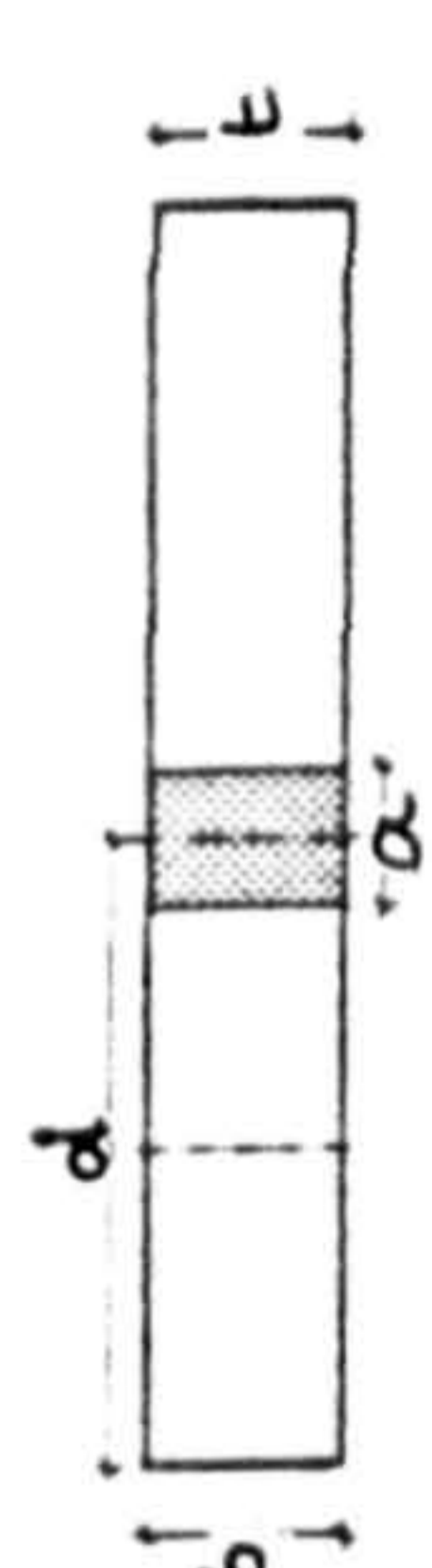
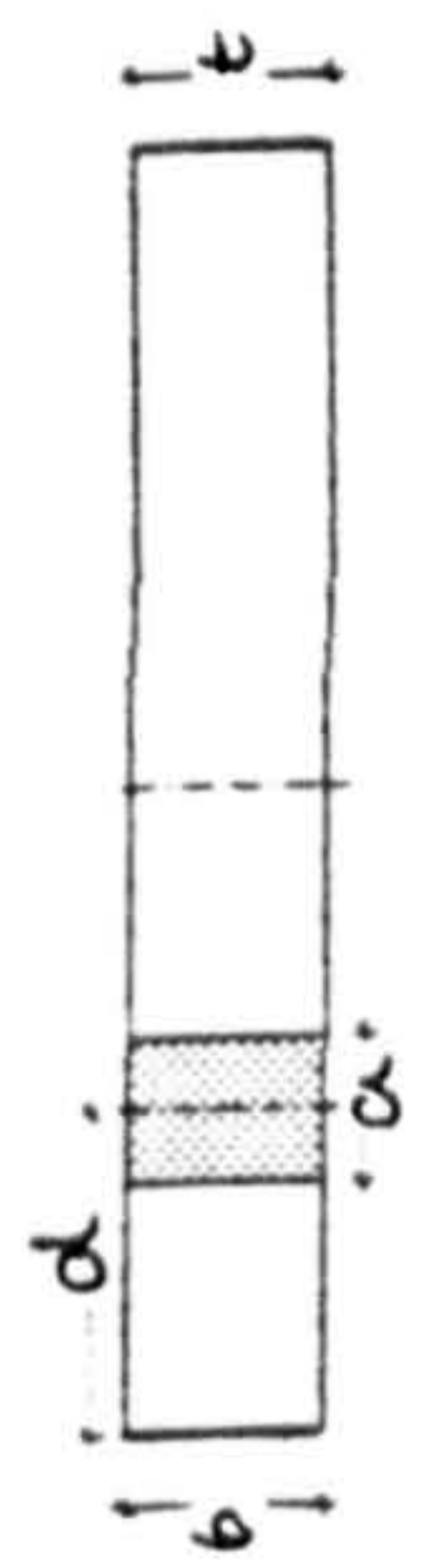
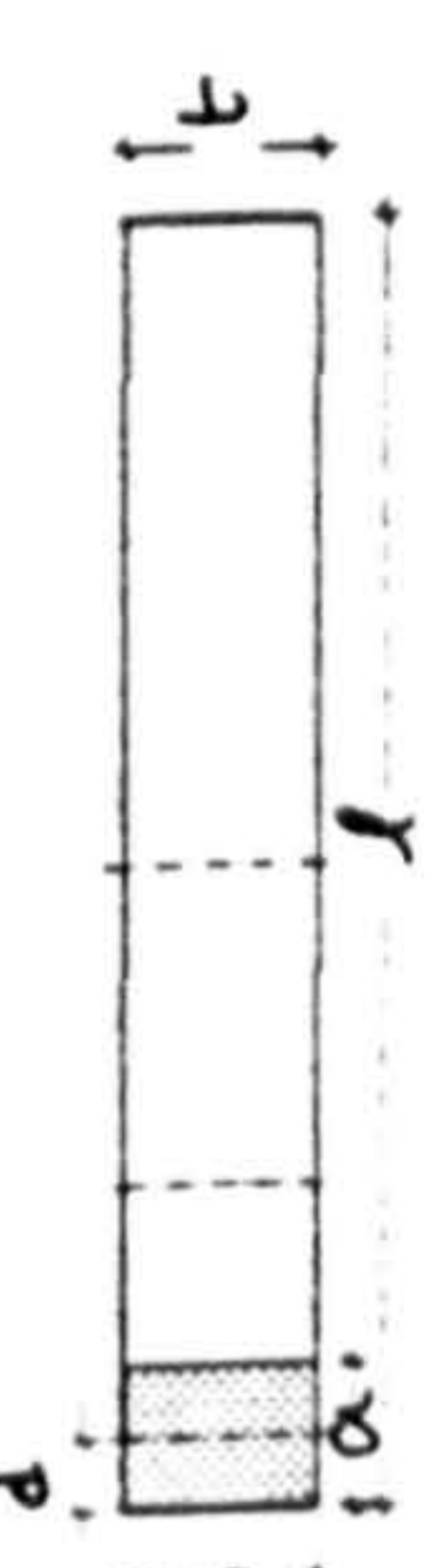
Loading type and configuration	t (mm)	Mortar desig.	$f_b$ (Nmm <sup>-2</sup> )	$f_k$ (Nmm <sup>-2</sup> )	$A_r$	l/a	t/b	d/l	n
<b>Central Strip</b> 	102.5	M(i)	90.04	19.50	0.10	10.00	1.0	0.500	10
					0.20	5.0			10
					0.30	3.3			10
					0.40	2.5			10
		82.55	18.60	0.10	10.0	10			
				0.20	5.0	10			
				0.30	3.3	10			
				0.40	2.5	10			
		62.45	16.00	0.10	10.0	10			
				0.20	5.0	10			
				0.30	3.3	10			
				0.40	2.5	10			
	28.80	10.60	0.10	10.0	10				
			0.20	5.0	10				
			0.30	3.3	10				
			0.40	2.5	10				
	92.40	19.60	0.05	20.0	5				
			0.10	10.0	2				
			0.15	6.6	2				
			0.40	2.5	2				
M(iii)	81.83	14.60	0.05	20.0	2				
			0.10	10.0	2				
			0.15	6.6	2				
			0.40	2.5	2				
4.47	1.68	0.05	20.0	2					
		0.10	10.0	2					
		0.15	6.6	2					
		0.40	2.5	2					
215.0	M(iii)	81.83	9.70	0.05	20.0	2			
				0.10	10.0	2			
				0.15	6.6	2			
				0.40	2.5	2			
4.47	1.73	0.05	20.0	3					
		0.10	10.0	2					
		0.15	6.6	2					
		0.40	2.5	2					
<b>Intermediate Strip</b> 	102.5	M(i)	92.40	19.60	0.05	20.0	1.0	0.250	5
					0.10	10.0			5
					0.15	6.6			5
					0.20	5.0			5
					0.30	3.3			5
					0.40	2.5			5
	M(iii)	81.83	14.60	0.05	20.0	2			
				0.10	10.0	2			
				0.15	6.6	2			
	4.47	1.68	0.05	20.0	2				
			0.10	10.0	2				
			0.15	6.6	2				
215.0	M(iii)	81.83	9.70	0.05	20.0	2			
				0.10	10.0	2			
				0.15	6.6	2			
				0.40	2.5	2			
4.47	1.73	0.05	20.0	2					
		0.10	10.0	2					
		0.15	6.6	2					
		0.40	2.5	2					
<b>End Strip</b> 	102.5	M(i)	92.40	19.60	0.05	20.0	1.0	0.025	10
					0.10	10.0		0.050	10
					0.15	6.6		0.075	9
					0.20	5.0		0.100	10
					0.30	3.3		0.150	5
					0.40	2.5		0.200	1
	M(iii)	81.83	14.60	0.05	20.0	0.025	3		
				0.10	10.0	0.050	2		
				0.15	6.6	0.075	2		
	4.47	1.68	0.05	20.0	0.025	2			
			0.10	10.0	0.050	2			
			0.15	6.6	0.075	2			
215.0	M(iii)	81.83	9.70	0.05	20.0	0.025	2		
				0.10	10.0	0.050	2		
				0.15	6.6	0.075	2		
				0.40	2.5	0.025	4		
4.47	1.73	0.05	20.0	0.025	4				
		0.10	10.0	0.050	3				
		0.15	6.6	0.075	2				
		0.40	2.5	0.075	2				

Table 5.3 - Details of testing programme.

Cube ref. No.	Age at test (days)	Wet weight (gm)	Mortar density ( $\text{kgm}^{-3}$ )	Ultimate load (kN)	Compressive strength ( $\text{Nmm}^{-2}$ )
M 1	8	2234	2105	156	14.99
M 4	7	2266	2135	132	12.69
M 5	7	2220	2092	100	9.61
M 9	7	2196	2069	117	11.25
M13	7	2216	2088	142	13.65
M14	7	2197	2070	106	10.19
M15	7	2199	2072	107	10.28
M18	7	2205	2078	167	16.05
M19	7	2165	2040	108	10.38
M20	7	2187	2061	127	12.21
M24	7	2219	2091	98	9.42
M25	7	2206	2079	115	11.05
M28	7	2225	2097	105	10.09
M29	7	2218	2090	107	10.28
M30	7	2235	2106	127	12.21
M34	7	2211	2083	144	13.84
M35	7	2200	2073	146	14.03
M36	7	2193	2067	133	12.78
M40	7	2205	2078	143	13.74
M41	7	2205	2078	138	13.26
M42	7	2185	2059	129	12.40
M46	7	2235	2106	157	15.09
M47	7	2214	2086	97	9.32
M48	7	2213	2085	125	12.01
M52	7	2172	2047	115	11.05
M53	7	2237	2108	134	12.88
M54	7	2236	2107	157	15.09
M58	7	2207	2080	128	12.30
M59	7	2193	2067	127	12.21
M60	7	2205	2078	135	12.98
Mean			2082.50		12.24
S <sub>d</sub>			19.74		1.84
C <sub>v</sub> (%)			0.95		15.02

Mortar 1:1/4:3 Portland cement:lime:sand mix by volume.

Cube dimensions =  $102 \times 102 \times 102 \text{ mm}^3$ .

BS 5628 - mean compressive strength of preliminary laboratory test at the age of 7-days (2/3 of strength at 28-days) is given as  $10.7 \text{ Nmm}^{-2}$ .

Table 5.4 - Results of mortar cubes tested after 7-days used for the constructions of brickwork types A, B, C, and D.

Cube ref. No.	Age at test (days)	Wet weight (gm)	Mortar density ( $\text{kgm}^{-3}$ )	Ultimate load (kN)	Compressive strength ( $\text{Nmm}^{-2}$ )
M 2	28	2236	2107	200	19.22
M 3	28	2280	2148	215	20.67
M 6	28	2224	2096	193	18.55
M 7	28	2249	2119	180	17.30
M 8	28	2249	2119	156	14.99
M10	28	2213	2085	187	17.97
M11	28	2237	2108	228	21.91
M12	28	2194	2067	150	14.42
M16	28	2183	2057	150	14.42
M17	28	2196	2069	164	15.76
M21	28	2200	2073	173	16.63
M22	28	2203	2076	184	17.69
M23	28	2208	2081	194	18.65
M26	28	2170	2045	140	13.46
M27	28	2183	2057	155	14.90
M31	28	2222	2094	210	20.18
M32	28	2215	2087	184	17.69
M33	28	2230	2101	212	20.38
M37	28	2202	2075	201	19.32
M38	28	2188	2062	157	15.09
M39	28	2206	2079	194	18.65
M43	28	2192	2066	190	18.26
M44	28	2190	2064	175	16.82
M45	28	2202	2075	190	18.26
M49	28	2228	2099	172	16.53
M50	28	2219	2091	146	14.03
M51	28	2210	2083	185	17.78
M55	28	2228	2099	213	20.47
M56	28	2215	2087	190	18.26
M57	28	2215	2087	210	20.18
Mean			2085.20		17.61
S <sub>d</sub>			21.78		2.23
C <sub>v</sub> (%)			1.04		12.66

Mortar 1:1/4:3 Portland cement:lime:sand mix by volume.

Cube dimensions =  $102 \times 102 \times 102 \text{ mm}^3$ .

BS 5628 - mean compressive strength of preliminary laboratory test at the age of 28-days is given as  $16.0 \text{ Nmm}^{-2}$ .

Table 5.5 - Results of mortar cubes tested after 28-days used for the constructions of brickwork typs A, B, C, and D.

Cube ref. No.	Age at test (days)	Wet weight (gm)	Mortar density ( $\text{kgm}^{-3}$ )	Ultimate load (kN)	Compressive strength ( $\text{Nmm}^{-2}$ )
ME 1	28	2268	2137	284.0	27.30
ME 2	28	2285	2153	258.0	24.80
ME 3	28	2256	2126	290.0	27.87
ME 4	28	2273	2142	285.5	27.44
ME 5	28	2305	2172	320.9	30.76
ME 6	28	2300	2167	342.0	32.87
ME 7	28	2279	2148	330.0	31.72
ME 8	28	2299	2166	320.0	30.76
ME 9	28	2283	2151	345.0	33.16
ME10	28	2335	2200	270.0	25.95
ME11	28	2328	2194	276.0	26.53
ME12	28	2301	2168	325.0	31.24
ME13	28	2304	2171	328.0	31.53
ME14	28	2289	2157	284.0	27.30
ME15	28	2256	2126	284.0	27.30
ME16	28	2308	2175	277.0	26.62
ME17	28	2316	2182	275.0	26.43
ME18	28	2323	2189	296.0	28.45
ME19	28	2307	2174	327.0	31.43
ME20	28	2340	2205	320.0	30.76
ME21	28	2298	2165	230.0	22.11
ME22	28	2267	2136	250.0	24.03
ME23	28	2265	2134	243.0	23.36
ME24	28	2277	2146	243.0	23.36
ME25	28	2259	2129	253.0	24.32
ME26	28	2302	2169	238.0	22.88
ME27	28	2295	2163	255.0	24.51
ME28	28	2265	2134	265.0	25.47
ME29	28	2283	2151	260.0	24.99
Mean			2159.74		27.42
S <sub>d</sub>			22.12		3.25
C <sub>v</sub> (%)			1.02		11.86

Mortar 1:1/4:3 Portland cement:lime:sand mix by volume.

Cube dimensions = 102x102x102 mm<sup>3</sup>.

BS 5628 - mean compressive strength of preliminary laboratory test at the age of 28-days is given as 16.0 Nmm<sup>-2</sup>.

Table 5.6 - Results of mortar cubes tested after 28-days used for the constructions of brickwork type E.



Cube ref. No.	Age at test (days)	Wet weight (gm)	Mortar density (kgm <sup>-3</sup> )	Ultimate load (kN)	Compressive strength (Nmm <sup>-2</sup> )
MF 1	7	2137	2014	52.0	5.03
MF 2	7	2122	2000	48.5	4.70
MF 3	7	2122	2000	49.5	4.80
MF 4	7	2108	1986	51.0	4.94
MF 5	7	2122	2000	50.0	4.84
MF 6	7	2128	2005	49.0	4.75
MF 7	7	2122	2000	41.0	3.94
MF 8	7	2141	2018	41.0	3.94
MF 9	7	2137	2014	42.5	4.08
MF10	7	2130	2007	41.5	3.99
MF11	7	2110	1988	41.5	3.99
MF12	7	2102	1981	42.5	4.08
MF13	7	2111	1989	51.5	4.99
MF14	7	2108	1986	50.5	4.89
MF15	7	2098	1977	49.5	4.80
MF16	7	2119	1997	49.0	4.75
MF17	7	2095	1974	49.0	4.75
MF18	7	2111	1989	51.5	4.99
MF19	7	2100	1979	25.0	2.42
MF20	7	2110	1988	24.0	2.33
MF21	7	2100	1979	25.0	2.42
MF22	7	2088	1968	24.0	2.33
MF23	7	2098	1977	25.0	2.42
MF24	7	2100	1979	24.0	2.33
MF25	7	2134	2011	42.0	4.07
MF26	7	2146	2022	42.5	4.12
MF27	7	2130	2007	42.7	4.14
MF28	7	2136	2013	42.5	4.12
MF29	7	2152	2028	43.2	4.19
MF30	7	2149	2025	42.0	4.07
MF31	7	2141	2018	44.0	4.26
MF32	7	2136	2013	46.0	4.46
MF33	7	1972	1858	50.0	4.84
MF34	7	1960	1847	50.0	4.84
MF35	7	1968	1854	51.5	4.99
MF36	7	1971	1857	50.5	4.89
MF37	7	2136	2013	42.0	4.07
MF38	7	2127	2004	42.0	4.07
MF39	7	2137	2014	42.5	4.12
MF40	7	2125	2002	41.5	4.02
MF41	7	2130	2007	42.0	4.07
MF42	7	2130	2007	42.0	4.07
MF43	7	2180	2054	61.0	5.91
MF44	7	2167	2042	57.5	5.57
MF45	7	2163	2038	59.0	5.72
MF46	7	2179	2053	62.0	6.01
MF47	7	2144	2020	59.5	5.76
MF48	7	2172	2047	58.5	5.67
MF49	7	2159	2034	62.5	6.05
MF50	7	2169	2044	65.0	6.30
MF51	7	2162	2037	65.0	6.30
MF52	7	2168	2043	63.0	6.10
MF53	7	2153	2029	63.0	6.10
MF54	7	2162	2037	63.0	6.10
MF55	7	2170	2045	40.0	3.88
MF56	7	2156	2032	41.5	4.02
MF57	7	2146	2022	42.0	4.07
MF58	7	2159	2034	41.5	4.02
MF59	7	2164	2039	42.0	4.07
MF60	7	2160	2035	41.5	4.02
MF61	7	2182	2056	44.0	4.26
MF62	7	2184	2058	46.5	4.50
MF63	7	2140	2017	37.5	3.63
MF64	7	2146	2022	37.0	3.58
MF65	7	2163	2038	35.5	3.44
MF66	7	2163	2038	35.5	3.44
MF67	7	2140	2017	32.5	3.15

MF68	7	2178	2052	42.0	4.07
MF69	7	2147	2023	33.5	3.25
MF70	7	2159	2034	45.0	4.36
MF71	7	2180	2054	33.0	3.20
MF72	7	2169	2044	43.0	4.17
MF73	7	2170	2045	46.0	4.46
MF74	7	2142	2018	42.5	4.12
MF75	7	2174	2049	44.0	4.26
MF76	7	2180	2054	43.0	4.17
MF77	7	2180	2054	43.0	4.17
MF78	7	2132	2009	45.0	4.36
MF79	7	2102	1981	25.0	2.42
MF80	7	2088	1968	20.0	1.94
MF81	7	2086	1966	22.0	2.13
MF82	7	2087	1967	24.0	2.33
MF83	7	2122	2000	22.0	2.13
MF84	7	2104	1983	20.0	1.94
Mean			2031.29		4.21
S <sub>d</sub>			43.28		1.08
C <sub>v</sub> (%)			2.13		25.60

Mortar 1:1:6 rapid hardening cement:lime:sand mix by volume.

Cube dimensions = 102x102x102 mm<sup>3</sup>.

BS 5628 - equivalent mean compressive strength of preliminary laboratory test at the age of 28-days is given as 10.7 Nmm<sup>-2</sup>.

Table 5.7 - Results of mortar cubes tested after 7-days used for the constructions of brickwork types F and G.

Wall No.	Age at test (days)	Specimen dimension h x l x t (mm)	Mortar designation	$f_m$ ( $Nmm^{-2}$ )	$f_b$ ( $Nmm^{-2}$ )	Ultimate load (kN)	Masonry strength ( $Nmm^{-2}$ )	Mean and characteristic strength ( $Nmm^{-2}$ )
A41	28	596x668x102.5	M(i)	17.61	90.08	2156	31.48	mean=31.42 $f_k^1=19.50$
A42	28	590x665x103.0	M(i)	17.61	90.08	2148	31.36	
B41	28	587x665x101.5	M(i)	17.61	82.55	1897	28.10	mean=27.91 $f_k^1=18.60$
B42	28	595x668x102.0	M(i)	17.61	82.55	1889	27.72	
C41	28	600x673x102.0	M(i)	17.61	62.45	1204	17.54	mean=17.50 $f_k^1=16.00$
C42	28	595x668x101.5	M(i)	17.61	62.45	1185	17.47	
D41	28	593x665x101.0	M(i)	17.61	28.81	928	13.81	mean=13.63 $f_k^1=10.60$
D42	28	594x666x101.5	M(i)	17.61	28.81	909	13.44	
E57	28	594x668x102.0	M(i)	27.42	92.41	2182	32.02	mean=31.90 $f_k^1=19.70$
E58	28	595x666x102.5	M(i)	27.42	92.41	2169	31.77	
F37	7	608x670x102.5	M(iii)	4.21	81.83	1203	17.51	mean=15.22 $f_k^1=14.60$
F38	7	610x672x102.5	M(iii)	4.21	81.83	983	14.27	
F39	7	605x672x102.5	M(iii)	4.21	81.83	1001	14.53	
F40	7	598x670x102.0	M(iii)	4.21	81.83	998	14.60	
F41	7	609x668x218.0	M(iii)	4.21	81.83	1666	11.44	mean=12.26 $f_k^1=9.70$
F42	7	610x675x219.0	M(iii)	4.21	81.83	1754	11.86	
F43	7	600x674x217.0	M(iii)	4.21	81.83	1798	12.29	
F44	7	600x673x219.0	M(iii)	4.21	81.83	1983	13.45	
G37	7	600x678x 99.0	M(iii)	4.21	4.47	128	1.91	mean=2.173 $S_d=0.2795$ $C_v=12.86\%$ $f_k^2=1.68$
G38	7	595x660x100.0	M(iii)	4.21	4.47	117	1.77	
G56	7	600x670x100.0	M(iii)	4.21	4.47	134	2.00	
G57	7	600x670x100.0	M(iii)	4.21	4.47	147	2.19	
G58	7	600x665x100.0	M(iii)	4.21	4.47	148	2.23	
G59	7	600x673x 99.0	M(iii)	4.21	4.47	174	2.61	
G60	7	600x672x100.0	M(iii)	4.21	4.47	152	2.26	
G61	7	600x665x100.0	M(iii)	4.21	4.47	169	2.54	
G62	7	600x680x 99.0	M(iii)	4.21	4.47	127	1.89	
G63	7	600x679x100.0	M(iii)	4.21	4.47	158	2.33	
G39	7	590x675x210.0	M(iii)	4.21	4.47	247	1.74	mean=2.038 $S_d=0.1578$ $C_v=7.74\%$ $f_k^2=1.73$
G40	7	590x668x210.0	M(iii)	4.21	4.47	297	2.12	
G64	7	590x670x215.0	M(iii)	4.21	4.47	298	2.07	
G65	7	590x660x216.0	M(iii)	4.21	4.47	304	2.13	
G66	7	590x674x215.0	M(iii)	4.21	4.47	298	2.06	
G67	7	590x670x215.0	M(iii)	4.21	4.47	288	2.00	
G68	7	590x674x215.0	M(iii)	4.21	4.47	258	1.78	
G69	7	590x675x215.0	M(iii)	4.21	4.47	329	2.27	
G70	7	590x672x216.0	M(iii)	4.21	4.47	300	2.07	
G71	7	590x670x215.0	M(iii)	4.21	4.47	295	2.05	

1  $f_k$  from Table 2.12, section 2.5.

2  $f_k$  calculated by the method outlined in Appendix I.I.

Table 5.8 - Results of tests on control specimens under uniform compressive load.

Wall No.	Age at test (days)	Wall dimens. h x l x t (mm)	Plate dimens. a x b (mm)	Edge dist. d (mm)	$A_r$	d/l	b/t	l/a	$f_{cb}$ (Nmm <sup>-2</sup> )	$\zeta$	$F_r$
A 1	28	590x665x102.5	66.5x102.5	332.5	0.10	0.50	1.0	10.00	62.35	3.20	0.59
A 2	28								61.62	3.16	0.56
A 3	28								60.88	3.12	0.48
A 4	28								57.66	2.96	0.52
A 5	28								63.96	3.28	0.56
A 6	28								73.03	3.75	0.51
A 7	28								69.10	3.54	0.53
A 8	28								67.05	3.44	0.57
A 9	28								69.25	3.55	0.50
A10	28								68.37	3.51	0.54
A11	28	590x665x102.5	133.0x102.5	332.5	0.20	0.50	1.0	5.00	29.19	1.50	0.50
A12	28	586x659x101.0							40.20	2.06	0.64
A13	29	590x665x101.0							34.48	1.77	0.47
A14	28	585x658x101.0							32.72	1.68	0.58
A15	28	590x660x102.0							39.61	2.03	0.56
A16	28	588x661x101.0							38.14	1.96	0.52
A17	29	592x660x100.0							42.11	2.16	0.64
A18	28	590x660x100.0							32.57	1.67	0.61
A19	28	590x661x101.0							35.58	1.82	0.64
A20	28	590x660x102.0							24.94	1.28	0.62
A21	28	559x664x100.0	199.5x102.5	332.5	0.30	0.50	1.0	3.33	24.94	1.28	0.59
A22	29	587x662x100.0							31.79	1.63	0.57
A23	29	585x660x102.0							34.23	1.76	0.53
A24	29	585x656x100.0							31.10	1.59	0.53
A25	29	585x658x101.0							29.24	1.50	0.55
A26	29	585x659x102.5							27.68	1.42	0.57
A27	29	585x657x101.5							21.03	1.08	0.48
A28	29	587x659x102.0							28.75	1.47	0.39
A29	28	590x665x103.5							28.12	1.44	0.33
A30	28	590x657x102.5							28.85	1.48	0.32
A31	28	590x662x101.0	266.0x102.5	332.5	0.40	0.50	1.0	2.50	24.50	1.26	0.55
A32	29	590x660x102.0							29.63	1.52	0.50
A33	29	590x657x102.0							25.38	1.30	0.43
A34	29	590x658x102.0							28.61	1.47	0.38
A35	29	590x657x102.0							26.04	1.34	0.47
A36	29	590x660x101.0							28.83	1.43	0.45
A37	29	588x662x102.0							29.86	1.53	0.57
A38	29	590x662x100.0							26.59	1.36	0.48
A39	29	588x659x102.5							29.49	1.51	0.47
A40	29	590x656x101.0							30.19	1.55	0.44

$$f_b = 90.04 \text{ Nmm}^{-2}$$

$$\text{Mortar mix by volume } 1:1/4:3; \quad f_m = 17.61 \text{ Nmm}^{-2}$$

$$f_k = 19.50 \text{ Nmm}^{-2}$$

$$\text{Loading rate} = 7.0 \text{ Nmm}^{-2} \text{min.}^{-1}$$

Table 5.9 - Test results of 102.5mm thick masonry under central strip concentrated loading for brickwork type A.

Wall No.	Age at test (days)	Wall dimens. h x l x t (mm)	Plate dimens. a x b (mm)	Edge dist. d (mm)	$A_r$	d/l	b/t	l/a	$f_{cb}$ (Nmm <sup>-2</sup> )	$\zeta$	$F_r$
B 1	28	585x664x101.0	66.5x102.5	332.5	0.10	0.50	1.0	10.00	49.88	2.68	0.59
B 2	28	589x663x102.0							40.34	2.17	0.36
B 3	28	587x667x102.5							56.04	3.01	0.39
B 4	28	582x661x101.0							40.34	2.17	0.69
B 5	28	583x664x101.0							55.75	3.00	0.70
B 6	28	585x668x103.0							54.28	2.92	0.65
B 7	28	583x665x103.0							50.02	2.69	0.45
B 8	28	579x662x101.0							39.61	2.13	0.48
B 9	28	587x662x103.0							55.75	3.00	0.34
B10	28	583x662x100.0							50.17	2.70	0.58
B11	28	576x665x102.0	133.0x102.5	332.5	0.20	0.50	1.0	5.00	41.81	2.25	0.46
B12	28	580x663x101.0							41.08	2.21	0.29
B13	28	575x663x102.0							32.28	1.74	0.41
B14	28	576x666x100.0							33.01	1.77	0.38
B15	28	576x662x102.0							30.81	1.66	0.54
B16	28	574x669x100.0							30.08	1.62	0.49
B17	28	581x667x102.0							27.87	1.50	0.41
B18	28	585x667x102.0							36.68	1.97	0.44
B19	28	586x660x101.0							33.38	1.79	0.44
B20	28	584x666x102.0							34.48	1.85	0.44
B21	28	584x664x101.0	199.5x102.5	332.5	0.30	0.50	1.0	3.33	27.63	1.49	0.82
B22	28	583x668x102.0							29.34	1.58	0.43
B23	28	582x667x102.0							26.90	1.45	0.47
B24	28	576x669x100.0							27.39	1.47	0.38
B25	28	575x665x101.0							28.85	1.55	0.19
B26	28	577x664x102.0							28.75	1.55	0.21
B27	28	577x665x103.0							26.90	1.45	0.17
B28	28	574x667x101.0							32.28	1.74	0.23
B29	28	570x662x101.0							29.59	1.59	0.24
B30	28	571x668x102.0							23.72	1.28	0.21
B31	29	575x665x100.0	266.0x102.5	332.5	0.40	0.50	1.0	2.50	26.41	1.42	0.19
B32	29	570x669x102.0							24.57	1.32	0.21
B33	28	583x664x101.0							25.67	1.38	0.46
B34	28	576x662x103.0							26.63	1.43	0.22
B35	28	585x663x101.0							28.97	1.56	0.29
B36	28	579x667x101.0							26.55	1.43	0.21
B37	28	586x665x103.0							25.86	1.39	0.18
B38	28	582x668x101.0							27.14	1.46	0.43
B39	28	584x666x101.0							20.91	1.12	0.32
B40	28	582x669x102.0							28.06	1.51	0.39

$$f_b = 82.55 \text{ Nmm}^{-2}$$

$$\text{Mortar mix by volume 1:1/4:3; } f_m = 17.61 \text{ Nmm}^{-2}$$

$$f_k = 18.60 \text{ Nmm}^{-2}$$

$$\text{Loading rate} = 7.0 \text{ Nmm}^{-2} \text{ min.}^{-1}$$

Table 5.10 - Test results of 102.5mm thick masonry under central strip concentrated loading for brickwork type B.

Wall No.	Age at test (days)	Wall dimens. h x l x t (mm)	Plate dimens. a x b (mm)	Edge dist. d (mm)	$A_r$	d/l	b/t	l/a	$f_{cb}$ (Nmm <sup>-2</sup> )	$\zeta$	$F_r$
C 1	28	585x670x101.0	66.5x102.5	332.5	0.10	0.50	1.0	10.00	63.38	3.96	0.46
C 2	28	578x668x101.0							64.55	4.03	0.55
C 3	28	584x668x102.0							60.15	3.76	0.44
C 4	28	582x667x101.0							52.08	3.26	0.54
C 5	28	584x669x103.0							61.32	3.83	0.36
C 6	28	585x668x103.0							53.55	3.35	0.54
C 7	28	589x669x102.0							55.40	3.35	0.34
C 8	28	580x670x102.5							55.02	3.44	0.27
C 9	28	580x670x101.0							64.55	4.03	0.58
C10	28	575x669x101.5							61.03	3.81	0.34
C11	28	580x665x101.0	133.0x102.5	332.5	0.20	0.50	1.0	5.00	39.90	2.49	0.44
C12	28	580x668x103.0							42.25	2.64	0.47
C13	28	583x670x102.0							36.31	2.27	0.57
C14	28	577x669x101.5							37.78	2.36	0.19
C15	28	579x662x102.0							36.24	2.27	0.28
C16	28	583x670x101.0							34.11	2.13	0.62
C17	28	582x668x102.0							38.88	2.43	0.25
C18	28	577x666x102.0							38.88	2.43	0.60
C19	28	577x662x101.0							32.72	2.05	0.34
C20	28	575x660x100.0							38.14	2.38	0.29
C21	28	575x662x101.0	199.5x102.5	332.5	0.30	0.50	1.0	3.33	33.65	2.10	0.55
C22	28	573x663x103.0							30.32	1.90	0.50
C23	28	578x662x102.0							31.79	1.99	0.59
C24	28	574x662x102.0							33.99	2.12	0.44
C25	28	575x666x101.0							31.79	1.99	0.29
C26	28	571x663x102.0							31.69	1.98	0.31
C27	28	568x663x102.0							27.39	1.71	0.23
C28	28	575x666x101.0							31.30	1.96	0.20
C29	28	570x660x100.0							27.87	1.74	0.23
C30	28	573x667x100.0							24.94	1.56	0.29
C31	28	570x665x100.0	266.0x102.5	332.5	0.40	0.50	1.0	2.50	33.01	2.06	0.13
C32	28	569x668x101.0							27.32	1.71	0.30
C33	28	575x666x101.0							26.22	1.64	0.39
C34	28	580x665x102.0							28.97	1.81	0.30
C35	28	578x662x102.0							32.09	2.01	0.29
C36	28	571x662x100.0							30.08	1.88	0.17
C37	28	575x662x100.0							27.87	1.74	0.20
C38	28	571x663x102.5							29.71	1.86	0.62
C39	28	576x665x102.5							30.63	1.91	0.40
C40	28	580x675x102.0							26.41	1.65	0.28

$$f_b = 62.45 \text{ Nmm}^{-2}$$

$$\text{Mortar mix by volume } 1:1/4:3; \quad f_m = 17.61 \text{ Nmm}^{-2}$$

$$f_k = 16.00 \text{ Nmm}^{-2}$$

$$\text{Loading rate} = 4.5 \text{ Nmm}^{-2} \text{ min.}^{-1}$$

Table 5.11 - Test results of 102.5mm thick masonry under central strip concentrated loading for brickwork type C.

Wall No.	Age at test (days)	Wall dimens. h x l x t (mm)	Plate dimens. a x b (mm)	Edge dist. d (mm)	$A_r$	d/l	b/t	l/a	$f_{cb}$ (Nmm <sup>-2</sup> )	$\zeta$	$F_r$
D 1	28	582x660x 99.0	66.5x102.5	332.5	0.10	0.50	1.0	10.00	34.48	3.25	0.60
D 2	28	590x664x100.0							29.34	2.77	0.35
D 3	28	590x663x101.0							22.30	2.10	
D 4	28	590x661x100.0							30.51	2.88	0.60
D 5	28	595x665x100.0							22.00	2.08	0.37
D 6	28	590x662x 98.0							20.54	1.94	0.61
D 7	28	597x664x100.0							23.77	2.24	0.25
D 8	28	593x664x 99.0							26.70	2.52	0.38
D 9	28	590x660x101.0							26.40	2.49	0.56
D10	28	587x666x 99.0							29.34	2.77	0.65
D11	28	591x662x100.0	133.0x102.5	332.5	0.20	0.50	1.0	5.00	23.03	2.17	0.41
D12	28	590x670x100.0							17.60	1.66	0.42
D13	28	593x665x102.0							21.49	2.03	0.24
D14	28	590x660x 98.0							15.55	1.47	0.45
D15	28	591x665x100.0							18.85	1.78	0.47
D16	28	590x660x 98.0							17.38	1.64	0.51
D17	28	588x668x100.0							18.27	1.72	0.44
D18	28	590x667x100.0							18.05	1.70	0.45
D19	28	591x660x 99.0							22.01	2.08	0.50
D20	28	590x660x100.0							16.87	1.59	0.30
D21	28	595x660x 9.00	199.5x102.5	332.5	0.30	0.50	1.0	3.33	18.29	1.73	0.45
D22	28	590x665x100.0							17.85	1.68	0.52
D23	28	588x668x100.0							16.14	1.52	0.39
D24	28	590x670x100.0							16.14	1.52	0.67
D25	28	585x664x100.0							13.94	1.32	0.35
D26	28	585x671x100.0							16.48	1.55	0.33
D27	28	591x669x 99.0							15.16	1.43	0.16
D28	28	590x668x100.0							18.88	1.78	0.27
D29	28	585x667x101.0							13.89	1.31	0.21
D30	28	592x670x101.0							11.98	1.13	0.16
D31	28	593x661x 99.0	266.0x102.5	332.5	0.40	0.50	1.0	2.50	18.16	1.71	0.30
D32	28	595x666x100.0							14.30	1.35	0.26
D33	28	592x666x101.0							15.40	1.45	0.25
D34	28	590x664x100.0							13.57	1.28	0.28
D35	28	588x660x100.0							17.97	1.70	0.37
D36	28	591x667x100.0							12.84	1.21	0.24
D37	28	590x665x100.0							17.31	1.63	0.38
D38	28	588x662x100.0							16.50	1.56	0.33
D39	28	585x660x100.0							19.15	1.81	0.55
D40	28	595x663x100.0							11.47	1.08	0.47

$$f_b = 28.80 \text{ Nmm}^{-2}$$

$$\text{Mortar mix by volume } 1:1/4:3; \quad f_m = 17.61 \text{ Nmm}^{-2}$$

$$f_k = 10.60 \text{ Nmm}^{-2}$$

$$\text{Loading rate} = 7.0 \text{ Nmm}^{-2} \text{min.}^{-1}$$

Table 5.12 - Test results of 102.5mm thick masonry under central strip concentrated loading for brickwork type D.

Wall No.	Age at test (days)	Wall dims. h x l x t (mm)	Plate dims. a x b (mm)	Edge dist. d (mm)	$A_r$	d/l	b/t	l/a	$f_{cb}$ (Nmm <sup>-2</sup> )	$\zeta$	$F_r$
E1c	28	590x665x102.5	66.5x102.5	332.5	0.05	0.50	1.0	20.00	76.82	3.90	0.77
E2c	28								76.28	3.87	0.38
E3c	28								78.92	4.01	0.48
E4c	28								72.47	3.68	0.74
E5c	28								57.51	2.92	0.99

Table 5.13 - Test results of 102.5mm thick masonry under central strip concentrated loading for brickwork type E.

Wall No.	Age at test (days)	Wall dims. h x l x t (mm)	Plate dims. a x b (mm)	Edge dist. d (mm)	$A_r$	d/l	b/t	l/a	$f_{cb}$ (Nmm <sup>-2</sup> )	$\zeta$	$F_r$
E27	28	600x675x103.0	33.2x102.5	169.0	0.05	0.25	1.0	20.00	58.68	2.98	0.95
E28	28	595x672x103.0							78.64	3.99	0.67
E29	28	604x675x102.5							69.83	3.54	0.99
E30	28	595x672x102.5							56.34	2.86	0.95
E31	28	601x665x102.5							61.32	3.11	0.99
E32	28	603x676x102.5	66.5x102.5	169.0	0.10	0.25	1.0	10.00	57.51	2.92	0.68
E33	28	606x670x103.0							57.95	2.94	0.72
E34	28	601x676x102.0							57.51	2.92	0.77
E35	28	608x676x103.0							55.90	2.84	0.77
E36	28	609x670x102.5							58.83	2.99	0.62
E37	28	605x670x102.5	99.7x102.5	167.0	0.15	0.25	1.0	6.66	39.12	1.99	0.74
E38	28	606x665x102.5							38.14	1.94	0.70
E39	28	589x668x100.0							41.27	2.09	0.76
E40	28	590x675x100.0							40.39	2.05	0.63
E41	28	598x670x101.0							38.44	1.95	0.78
E42	28	602x669x100.0	133.0x102.5	168.0	0.20	0.25	1.0	5.00	28.68	1.46	0.68
E43	28	594x675x100.0							33.30	1.69	0.56
E44	28	590x675x101.0							30.30	1.54	0.63
E45	28	587x672x101.0							28.31	1.44	0.73
E46	28	595x668x101.0							33.74	1.71	0.75
E47	28	590x675x102.5	199.5x102.5	168.0	0.30	0.25	1.0	3.33	26.41	1.34	0.64
E48	28	593x673x102.0							42.30	2.15	0.37
E49	28	590x667x101.0							32.76	1.66	0.67
E50	28	596x672x101.5							29.34	1.49	0.46
E51	28	597x675x101.0							38.63	1.96	0.33
E52	28	595x665x100.0	266.0x102.5	167.0	0.40	0.25	1.0	2.50	30.99	1.57	0.45
E53	28	601x670x101.0							32.68	1.66	0.67
E54	28	595x672x102.0							31.54	1.60	0.38
E55	28	595x662x100.0							36.68	1.86	0.72
E56	28	595x663x103.0							35.65	1.81	0.37

$$f_b = 92.41 \text{ Nmm}^{-2}$$

$$\text{Mortar mix by volume } 1:1/4:3; \quad f_m = 27.42 \text{ Nmm}^{-2}$$

$$f_k = 19.60 \text{ Nmm}^{-2}$$

$$\text{Loading rate} = 14.5 \text{ Nmm}^{-2} \text{ min.}^{-1}$$

Table 5.14 - Test results of 102.5mm thick masonry under intermediate strip concentrated loading for brickwork type E.



Wall No.	Age at test (days)	Wall dimens. h x l x t (mm)	Plate dimens. a x b (mm)	Edge dist. d (mm)	$A_r$	d/l	b/t	l/a	$f_{cb}$ (Nmm <sup>-2</sup> )	$\zeta$	$F_r$						
E 1a	28	590x665x102.5	33.2x102.5	16.63	0.05	0.025	1.0	20.00	55.16	2.80	0.82						
E 2a	28								44.89	2.28	0.78						
E 3a	28								63.96	3.25	0.78						
E 4a	28								63.67	3.23	0.78						
E 5a	28								49.58	2.52	0.75						
E 1b	28								68.95	3.50	0.65						
E 2b	28								57.21	2.90	0.38						
E 3b	28								52.81	2.68	0.97						
E 4b	28								51.34	2.61	0.34						
E 5b	28								65.13	3.31	0.72						
E 6a	28	589x667x100.0	66.5x102.5	33.25	0.10	0.050	1.0	10.00	46.07	2.34	0.68						
E 7a	28	590x664x100.0							37.70	1.91	0.82						
E 8a	28	595x665x100.0							46.07	2.34	0.64						
E 9a	28	590x665x100.0							46.07	2.34	0.64						
E10a	28	590x665x101.0							46.51	2.36	0.66						
E 6b	28								40.05	2.03	0.82						
E 7b	28								43.43	2.20	0.61						
E 8b	28								29.93	1.52	0.54						
E 9b	28								54.58	2.77	0.89						
E10b	28								37.12	1.88	0.83						
E11a	28	590x665x102.5	99.7x102.5	49.87	0.15	0.075	1.0	6.66	42.06	2.14	0.70						
E12a	28	590x665x102.5							45.48	2.31	0.37						
E13a	28	590x665x102.5							42.06	2.14	0.67						
E14a	28	585x665x101.0							37.75	1.92	0.61						
E15a	28	590x661x100.0							36.19	1.84	0.66						
E11b	28								26.21	1.33	0.82						
E13b	28								31.00	1.57	0.54						
E14b	28								39.12	1.99	0.59						
E15b	28								38.44	1.95	0.64						
E16a	28	595x665x101.0							133.0x102.5	66.50	0.20	0.100	1.0	5.00	36.24	1.84	0.65
E17a	28	592x665x102.0													37.78	1.92	0.58
E18a	28	592x662x100.0													36.60	1.86	0.80
E19a	28	590x668x101.0													26.92	1.37	0.74
E20a	28	595x663x102.0													34.48	1.75	0.85
E16b	28														28.46	1.44	0.64
E17b	28		30.88	1.57	0.71												
E18b	28		39.83	2.02	0.83												
E19b	28		32.42	1.65	0.79												
E20b	28		37.41	1.90	0.69												
E21	28	594x672x102.0	199.5x102.5	99.75	0.30	0.150	1.0	3.33	31.49	1.60	0.58						
E22	28	590x665x102.5							28.85	1.46	0.34						
E23	28	598x670x102.0							32.03	1.63	0.90						
E24	28	602x680x103.0							38.83	1.97	0.45						
E25	28	605x673x102.0							26.33	1.34	0.85						
E26	28	597x677x103.0	266.0x102.5	133.0	0.40	0.200	1.0	2.50	36.68	1.86	0.68						

$$f_b = 92.41 \text{ Nmm}^{-2}$$

$$\text{Mortar mix by volume } 1:1/4:3; \quad f_m = 27.42 \text{ Nmm}^{-2}$$

$$f_k = 19.60 \text{ Nmm}^{-2}$$

$$\text{Loading rate} = 14.5 \text{ Nmm}^{-2} \text{ min.}^{-1}$$

Table 5.15 - Test results of 102.5mm thick masonry under end strip concentrated loading for brickwork type E.

Wall No.	Age at test (days)	Wall dimens. h x l x t (mm)	Plate dimens. a x b (mm)	Edge dist. d (mm)	$A_r$	d/l	b/t	l/a	$f_{cb}$ (Nmm <sup>-2</sup> )	$\zeta$	$F_r$
F 1	7	612x665x102.5	33.2x102.5	332.5	0.05	0.500	1.0	20.00	34.33	2.35	0.77
F 2	7	600x669x101.0							41.68	2.85	0.71
F 3	7	600x667x101.0	66.5x102.5		0.10			10.00	23.97	1.64	0.68
F 4	7	600x668x101.0							36.92	2.53	0.60
F 5	7	605x667x100.0	99.7x102.5		0.15			6.66	19.25	1.32	0.31
F 6	7	610x665x101.0							25.31	1.73	0.70
F13	7	605x665x102.5	33.2x102.5	166.2	0.05	0.250	1.0	20.00	29.05	1.99	0.70
F14	7	604x670x100.0							45.11	3.09	0.73
F15	7	610x670x100.0	66.5x102.5		0.10			10.00	21.05	1.44	0.96
F16	7	603x672x102.0							22.99	1.57	0.80
F17	7	605x666x100.0	99.7x102.5		0.15			6.66	17.44	1.19	0.57
F18	7	600x660x103.0							15.37	1.05	0.63
F 7	7	600x665x102.0	33.2x102.5	16.6	0.05	0.025	1.0	20.00	40.98	2.81	0.93
F8a	7	600x666x102.0							45.99	3.15	1.00
F8b	7	600x666x102.0							40.39	2.77	0.87
F11	7	607x671x102.5	66.5x102.5	33.2	0.10	0.050		10.00	20.98	1.44	0.61
F12	7	608x666x101.0							24.56	1.68	0.48
F 9	7	600x671x101.0	99.7x102.5	50.0	0.15	0.075		6.66	16.87	1.16	0.88
F10	7	608x672x102.0							17.20	1.18	0.85
F19	7	600x670x212.0	33.2x215.0	332.5	0.05	0.500	1.0	20.00	23.41	2.41	0.89
F20	7	605x665x212.0							30.22	3.12	0.89
F21	7	605x666x213.0	66.5x215.0		0.10			10.00	24.71	2.55	0.71
F22	7	605x665x215.0							26.65	2.75	0.97
F23	7	600x675x215.0	99.7x215.0		0.15			6.66	20.98	2.16	0.54
F24	7	602x680x215.0							16.65	1.72	0.78
F31	7	590x665x218.0	33.2x215.0	166.2	0.05	0.250	1.0	20.00	39.73	4.10	0.97
F32	7	590x670x218.0							44.28	4.56	0.78
F33	7	595x665x217.0	66.5x215.0		0.10			10.00	21.76	2.24	0.95
F34	7	595x665x215.0							18.39	1.90	0.99
F35	7	595x665x217.0	99.7x215.0		0.15			6.66	16.17	1.67	0.83
F36	7	590x667x215.0							18.88	1.95	0.91
F25	7	600x675x217.0	33.2x215.0	16.6	0.05	0.025	1.0	20.00	26.61	2.74	0.95
F26	7	600x675x215.0							27.41	2.83	1.00
F27	7	600x670x217.0	66.5x215.0	33.2	0.10	0.050		10.00	18.05	1.86	0.65
F28	7	600x675x215.0							15.21	1.57	0.78
F29	7	600x675x218.0	99.7x215.0	50.0	0.15	0.075		6.66	17.24	1.78	0.69
F30	7	600x670x218.0							19.31	1.99	0.67

$$f_b = 81.83 \text{ Nmm}^{-2}$$

Mortar mix by volume 1:1:6;  $f_m = 4.21 \text{ Nmm}^{-2}$

$$t = 102.5\text{mm}; f_k = 14.6 \text{ Nmm}^{-2}$$

$$t = 215.0\text{mm}; f_k = 9.7 \text{ Nmm}^{-2}$$

$$\text{Loading rate} = 14.5 \text{ Nmm}^{-2}\text{min.}^{-1}$$

Table 5.16 - Test results of 102.5 and 215.0mm thick masonry under central, intermediate and end strip concentrated loading for brickwork type F.

Wall No.	Age at test (days)	Wall dimens. h x l x t (mm)	Plate dimens. a x b (mm)	Edge dist. d (mm)	$A_r$	d/l	b/t	l/a	$f_{cb}$ (Nmm <sup>-2</sup> )	$\zeta$	$F_r$
G19	7	597x666x100.0	33.2x102.5	332.5	0.05	0.500	1.0	20.00	6.32	3.76	1.00
G20	7	595x670x100.0							7.82	4.65	1.00
G21	7	600x670x100.0	66.5x102.5		0.10			10.00	5.04	3.00	0.95
G22	7	600x670x100.0							5.49	3.27	0.88
G23	7	600x670x100.0	99.7x102.5		0.15			6.66	5.91	3.52	0.83
G24	7	600x668x100.0							5.51	3.28	0.88
G31	7	600x670x100.0	33.2x102.5	166.2	0.05	0.250	1.0	20.00	3.61	2.15	1.00
G32	7	600x665x100.0							6.02	3.58	1.00
G33	7	600x670x100.0	66.5x102.5		0.10			10.00	4.06	2.42	0.85
G34	7	600x670x100.0							5.04	3.00	1.00
G35	7	600x670x100.0	99.7x102.5		0.15			6.66	3.96	2.36	1.00
G36	7	595x665x 99.0							4.15	2.47	1.00
G25	7	600x670x100.0	33.2x102.5	16.6	0.05	0.025	1.0	20.00	3.46	2.06	1.00
G26	7	605x670x100.0							3.46	2.06	1.00
G27	7	600x670x100.0	66.5x102.5	33.2	0.10	0.050		10.00	4.11	2.45	1.00
G28	7	600x670x100.0							3.83	2.28	1.00
G29	7	603x671x 99.0	99.7x102.5	50.0	0.15	0.075		6.66	4.15	2.47	1.00
G30	7	600x670x 99.0							4.00	2.38	1.00
G 1	7	605x666x210.0	33.2x215.0	332.5	0.05	0.500	1.0	20.00	8.45	4.88	0.98
G 2	7	607x670x210.0							6.16	3.56	1.00
G7a	7	600x671x210.0							9.23	5.34	0.99
G 3	7	605x665x216.0	66.5x215.0		0.10			10.00	6.56	3.79	1.00
G 4	7	600x665x215.0							5.35	3.09	0.96
G 5	7	606x665x215.0	99.7x215.0		0.15			6.66	5.90	3.41	1.00
G 6	7	600x667x214.0							5.11	2.95	0.82
G13	7	605x665x213.0	33.2x215.0	166.2	0.05	0.250	1.0	20.00	6.16	3.56	0.99
G14	7	599x666x215.0							8.06	4.66	1.00
G15	7	600x604x212.0	66.5x215.0		0.10			10.00	5.25	3.03	1.00
G16	7	595x665x215.0							5.46	3.16	1.00
G17	7	595x661x210.0	99.7x215.0		0.15			6.66	3.15	1.82	0.91
G18	7	605x675x213.0							4.82	2.79	0.98
G7a	7	600x671x213.0	33.2x215.0	16.6	0.05	0.025	1.0	20.00	6.07	3.51	0.93
G7b	7	600x671x213.0							4.94	2.86	0.86
G8a	7	600x670x215.0							6.52	3.77	1.00
G8b	7	600x670x215.0							5.94	3.43	1.00
G 9	7	600x666x214.0	66.5x215.0	33.2	0.10	0.050		10.00	4.01	2.32	1.00
G10a	7	604x666x210.0							3.60	2.08	1.00
G10b	7	604x666x210.0							4.69	2.71	1.00
G11	7	600x670x213.0	99.7x215.0	50.0	0.15	0.075		6.66	3.52	2.03	1.00
G12	7	600x670x213.0							4.09	2.36	1.00

$$f_b = 4.47 \text{ Nmm}^{-2}$$

$$\text{Mortar mix by volume 1:1:6; } f_m = 4.21 \text{ Nmm}^{-2}$$

$$t = 102.5\text{mm; } f_k = 1.68 \text{ Nmm}^{-2}$$

$$t = 215.0\text{mm; } f_k = 1.73 \text{ Nmm}^{-2}$$

$$\text{Loading rate} = 14.5 \text{ Nmm}^{-2} \text{ min.}^{-1}$$

Table 5.17 - Test results of 102.5 and 215.0mm thick masonry under central, intermediate and end strip concentrated loading for brickwork type G.

Wall No.	Age at test (days)	Wall dimens. h x l x t (mm)	Plate dimens. a x b (mm)	Edge dist. d (mm)	$A_r$	d/l	b/t	l/a	$f_{cb}$ (Nmm <sup>-2</sup> )	$\zeta$	$F_r$	
F50	7	612x 217x102.5	100x102.5	103.5	0.460	0.5	1.0	2.17	28.88	1.98	0.44	
F51	7	615x 445x102.5		222.5	0.225				17.65	1.21	0.94	
F52	7	615x 676x101.0		338.0	0.145				30.00	2.05	0.59	
F53	7	613x 893x102.0		446.5	0.112				33.43	2.29	0.65	
F54	7	605x1130x103.0		565.0	0.088				29.76	2.04	0.75	
F55	7	609x1353x102.0		678.0	0.074				33.24	2.28	0.74	
G50	7	600x 211x101.0	225x100.0	105.5	1.000	0.5	1.0	1.00	1.71	1.02	1.00	
G51	7	603x 446x100.0		223.0	0.505				3.19	1.90	0.56	
G52	7	600x 656x101.0		328.0	0.343				2.94	1.75	0.43	
G53	7	600x 910x 98.0		455.0	0.247				4.04	2.81	0.36	
G54	7	596x1125x100.0		562.5	0.200				5.00	2.29	1.36	0.78
G55	7	600x1355x 99.0		677.5	0.166				6.02	2.44	1.45	0.45

Brickwork type F

$$f_b = 81.83 \text{ Nmm}^{-2}$$

$$\text{Mortar mix by volume 1:1:6; } f_m = 4.21 \text{ Nmm}^{-2}$$

$$f_k = 14.6 \text{ Nmm}^{-2}$$

Brickwork type G

$$f_b = 4.47 \text{ Nmm}^{-2}$$

$$\text{Mortar mix by volume 1:1:6; } f_m = 4.21 \text{ Nmm}^{-2}$$

$$f_k = 1.68 \text{ Nmm}^{-2}$$

Table 5.18 - Results of test on 102.5mm thick brickwork types F and G under central strip concentrated load for varying length of specimens.

## Chapter 6

### EXPERIMENTAL STUDY: ANALYSIS OF RESULTS

#### 6.1. INTRODUCTION

In general compressive strength of brickwork masonry under the action of concentrated load is influenced by such parameters as mentioned earlier in chapter 1. However, in the present investigation concentrated load has been applied to masonry specimens through a rigid steel bearing plate and the variables which are thought to be of importance have been examined experimentally. These are:

- the properties of masonry and its constituent materials;
- the loading area ratio;
- the loading position and the effect of edge distance;
- the loading configuration;
- the thickness of the unit;
- the aspect ratio of the unit;
- the effective cross-sectional area of brickwork element;
- the type of brick unit.

This chapter contains the analysis of the experimental results reported in chapter 5 and Appendix B. The effect of parameters listed above on the bearing strength and the enhancement factor have been examined and expressions for the compressive strength of brickwork masonry under concentrated loads for four ratios of loaded area have been determined statistically. The mode of failure and crack pattern of specimens tested under various loading configurations have also been included.

#### 6.2. ENHANCEMENT FACTOR ( $\zeta$ )

The apparent compressive strength of brickwork masonry loaded partially is known to be greater than its uniaxial compressive strength because of the restraint provided by the surrounding lightly stressed material. This in turn has led to the term "enhancement factor" which is defined as the ratio of compressive strengths of brickwork masonry under concentrated and uniformly distributed loads or simply the increase in the capacity of brickwork masonry

under the applied concentrated load with respect to its uniaxial compressive strength.

BS 5628<sup>[1]</sup> expresses the local design strength under concentrated load as  $\leq \zeta f_k / \gamma_m$ , where  $\gamma_m$  is the material partial safety factor and states that at the height of  $0.4h$  beneath the loading the stress due to the design load should be checked and must not be greater than  $\beta f_k / \gamma_m$ , where  $\beta$  is the capacity reduction factor for the effect of slenderness. Values of 1.25, 1.50 and 2.0 have been given for the enhancement factor,  $\zeta$ , for the three types of bearings (refer to section 3.3 and Figs. 3.4 & 3.5). The origin of these values are not known to the author, but it is believed that the proposals<sup>[98]</sup> were based on research on concrete.

To establish an expression for the enhancement factor, the above definition suggests that for every specimen tested under concentrated load, an identical specimen should be tested under uniform axial load. This could prove uneconomical when considering the variables involved and the number of specimens needing to be tested, bearing in mind the variation in strengths of units and jointing mortar which ultimately influence the brickwork strength.

However, enhancement factor could be expressed as:

$$\zeta_1 = f_{cb} / f_{mm} \quad (6.1)$$

$$\text{or } \zeta_2 = f'_{cb} / f_k \quad (6.2)$$

where  $f_{cb}$  is the mean bearing strength of masonry partially loaded;  
 $f'_{cb}$  is the characteristic bearing strength of masonry partially loaded;  
 $f_{mm}$  is the mean masonry compressive strength under uniform load;  
 $f_k$  is the characteristic compressive strength of masonry.

Variation between the enhancement factors obtained by the two equations above have been examined by plotting the results obtained for brickwork types A, B, C, D, E, F, G (reported in chapter 5), H, and L (reported in Tables B2 & B3, Appendix B) under central strip and types E, F, G, H and L under intermediate and end strip loading configurations against the loaded area ratio and are as shown in Figs. 6.1 to 6.25. Also the results of tests on brickwork type M (reported in Table B1, Appendix B) under central, intermediate and end edge loading configurations against loaded area ratio are as shown in Figs. 6.26 to 6.28.

The mean bearing strength curves have been established by the method of least squares approximation. The characteristic bearing strength at 95% lower confidence limit has been determined statistically based on the standard deviation of the data points about the mean curve. The values for the mean masonry strength,  $f_{mm}$  obtained experimentally (refer to Table 5.8) and the characteristic compressive strength of masonry,  $f_k$  obtained from the tables in chapter 2 have been shown on the same plot in each case. Table 6.1 contains the equations of the curves obtained for the mean and characteristic bearing strength of masonry partially loaded in terms of loaded area ratio. The ratio of the enhancement factors based on Equations 6.1 and 6.2 have been calculated and are as shown in Table 6.1.

Inspecting the results for the ratio  $\zeta_1/\zeta_2$  in Table 6.1, it can be seen that for those sets of data where a sufficient number of samples was tested when loaded area ratio ( $A_r$ ) is one, the value for this ratio is very close to unity, suggesting that Equations 6.1 and 6.2 would yield same value for the enhancement factor as would be expected. Those with values less or greater than unity for the ratio  $\zeta_1/\zeta_2$  are due to inaccuracy of the apparent value for the mean masonry strength (or in other words results of tests) when  $A_r = 1.0$ , which in some cases is based on only two test results.

It can be shown that Equations 6.1 and 6.2 would give same value for the enhancement factor  $\zeta$ , provided that a reasonable number of specimens are tested when  $A_r = 1.0$  which would provide more accurate values for the mean and characteristic compressive strength of masonry under uniform loading. This has been demonstrated in the case of brickwork type G where ten samples were tested under uniform compressive load (i.e. when  $A_r=1.0$ ). The values for  $f_{mm}$  and  $f_k$  were based on these results. Cumulatively the mean of values for the ratio  $\zeta_1/\zeta_2$  shown in Table 6.1 is found to be 0.958 with standard deviation of 0.191 and coefficient of variation of 19.95%. However the values reported in Table 6.1 for  $f_{mm}$  are apparent values based on small numbers of test results of which the average of the strength is not the true mean. The enhancement factor obtained based on Equation 6.2 has been adopted in the foregoing analysis, because of the higher degree of certainty incorporated in the characteristic values with respect to failure.

Loading config.	Loading position	t (mm)	f <sub>b</sub> (Nmm <sup>-2</sup> )	f <sub>mm</sub> (Nmm <sup>-2</sup> )	f <sub>k</sub> (Nmm <sup>-2</sup> )	Equation of mean bearing strength	Equation of charact. bearing strength	ζ <sub>1</sub> /ζ <sub>2</sub>	
Strip	Central	102.5	90.04	31.42	19.50 <sup>1</sup>	$f_{cb}=18.075A_r^{-0.485}$	$f'_{cb}=12.827A_r^{-0.485}$	0.874	
		102.5	82.55	27.91	18.80 <sup>1</sup>	$f_{cb}=19.487A_r^{-0.365}$	$f'_{cb}=15.265A_r^{-0.365}$	0.849	
		102.5	62.45	17.50	16.00 <sup>1</sup>	$f_{cb}=17.061A_r^{-0.521}$	$f'_{cb}=14.605A_r^{-0.521}$	1.068	
		102.5	28.80	13.63	10.60 <sup>1</sup>	$f_{cb}=11.175A_r^{-0.344}$	$f'_{cb}=8.601A_r^{-0.344}$	1.011	
		102.5	92.41	31.90	19.60 <sup>1</sup>	$f_{cb}=31.895A_r^{-0.272}$	$f'_{cb}=26.384A_r^{-0.272}$	0.743	
		102.5	81.83	15.22	14.60 <sup>2</sup>	$f_{cb}=14.815A_r^{-0.289}$	$f'_{cb}=11.166A_r^{-0.289}$	1.272	
		215.0	81.83	12.26	9.70 <sup>2</sup>	$f_{cb}=12.205A_r^{-0.272}$	$f'_{cb}=9.956A_r^{-0.272}$	0.971	
		102.5	4.47	2.17	1.68 <sup>2</sup>	$f_{cb}=2.179A_r^{-0.412}$	$f'_{cb}=1.740A_r^{-0.412}$	0.968	
		215.0	4.47	2.04	1.73 <sup>2</sup>	$f_{cb}=2.039A_r^{-0.464}$	$f'_{cb}=1.678A_r^{-0.464}$	1.032	
		215.0	72.70	17.85	11.50 <sup>1</sup>	$f_{cb}=23.434A_r^{-0.026}$	$f'_{cb}=21.962A_r^{-0.026}$	0.687	
	102.5	33.02	14.25	9.00 <sup>1</sup>	$f_{cb}=12.320A_r^{-0.253}$	$f'_{cb}=8.987A_r^{-0.253}$	0.865		
	Interm.	102.5	92.41	31.90	19.60 <sup>1</sup>	$f_{cb}=24.297A_r^{-0.303}$	$f'_{cb}=18.100A_r^{-0.303}$	0.826	
		102.5	81.83	15.22	14.60 <sup>2</sup>	$f_{cb}=14.238A_r^{-0.227}$	$f'_{cb}=9.575A_r^{-0.227}$	1.425	
		215.0	81.83	12.26	9.70 <sup>2</sup>	$f_{cb}=11.485A_r^{-0.333}$	$f'_{cb}=7.880A_r^{-0.333}$	1.154	
		102.5	4.47	2.17	1.68 <sup>2</sup>	$f_{cb}=2.176A_r^{-0.288}$	$f'_{cb}=1.679A_r^{-0.288}$	1.001	
		215.0	4.47	2.04	1.73 <sup>2</sup>	$f_{cb}=2.011A_r^{-0.406}$	$f'_{cb}=1.639A_r^{-0.406}$	1.042	
		215.0	72.70	17.85	11.50 <sup>1</sup>	$f_{cb}=12.083A_r^{-0.413}$	$f'_{cb}=9.552A_r^{-0.413}$	0.815	
		102.5	33.02	14.25	9.00 <sup>2</sup>	$f_{cb}=7.247A_r^{-0.450}$	$f'_{cb}=6.223A_r^{-0.450}$	0.737	
	End	102.5	92.41	31.90	19.60 <sup>1</sup>	$f_{cb}=24.032A_r^{-0.257}$	$f'_{cb}=18.247A_r^{-0.257}$	0.809	
		102.5	81.83	15.22	14.60 <sup>2</sup>	$f_{cb}=13.932A_r^{-0.291}$	$f'_{cb}=9.223A_r^{-0.291}$	1.448	
		215.0	81.83	12.26	9.70 <sup>2</sup>	$f_{cb}=11.971A_r^{-0.223}$	$f'_{cb}=9.547A_r^{-0.223}$	0.992	
		102.5	4.47	2.17	1.68 <sup>2</sup>	$f_{cb}=2.198A_r^{-0.218}$	$f'_{cb}=1.705A_r^{-0.218}$	0.997	
		215.0	4.47	2.04	1.73 <sup>2</sup>	$f_{cb}=2.011A_r^{-0.340}$	$f'_{cb}=1.702A_r^{-0.340}$	1.003	
		215.0	72.70	17.85	11.50 <sup>1</sup>	$f_{cb}=10.021A_r^{-0.442}$	$f'_{cb}=7.812A_r^{-0.442}$	0.826	
		102.5	33.02	14.25	9.00 <sup>2</sup>	$f_{cb}=7.708A_r^{-0.316}$	$f'_{cb}=6.296A_r^{-0.316}$	0.773	
	Edge	Central	215.0	72.70	17.85	11.50 <sup>1</sup>	$f_{cb}=8.076A_r^{-0.562}$	$f'_{cb}=5.536A_r^{-0.562}$	0.940
		Interm.	215.0	72.70	17.85	11.50 <sup>1</sup>	$f_{cb}=10.570A_r^{-0.456}$	$f'_{cb}=9.441A_r^{-0.456}$	0.736
		End	215.0	72.70	17.85	11.50 <sup>1</sup>	$f_{cb}=9.818A_r^{-0.444}$	$f'_{cb}=6.537A_r^{-0.444}$	0.968

1 Mortar designation M(i)

2 Mortar designation M(iii)

Table 6.1 - Equations of the mean and characteristic bearing strength of masonry and the ratios of enhancement factors for different loading positions.



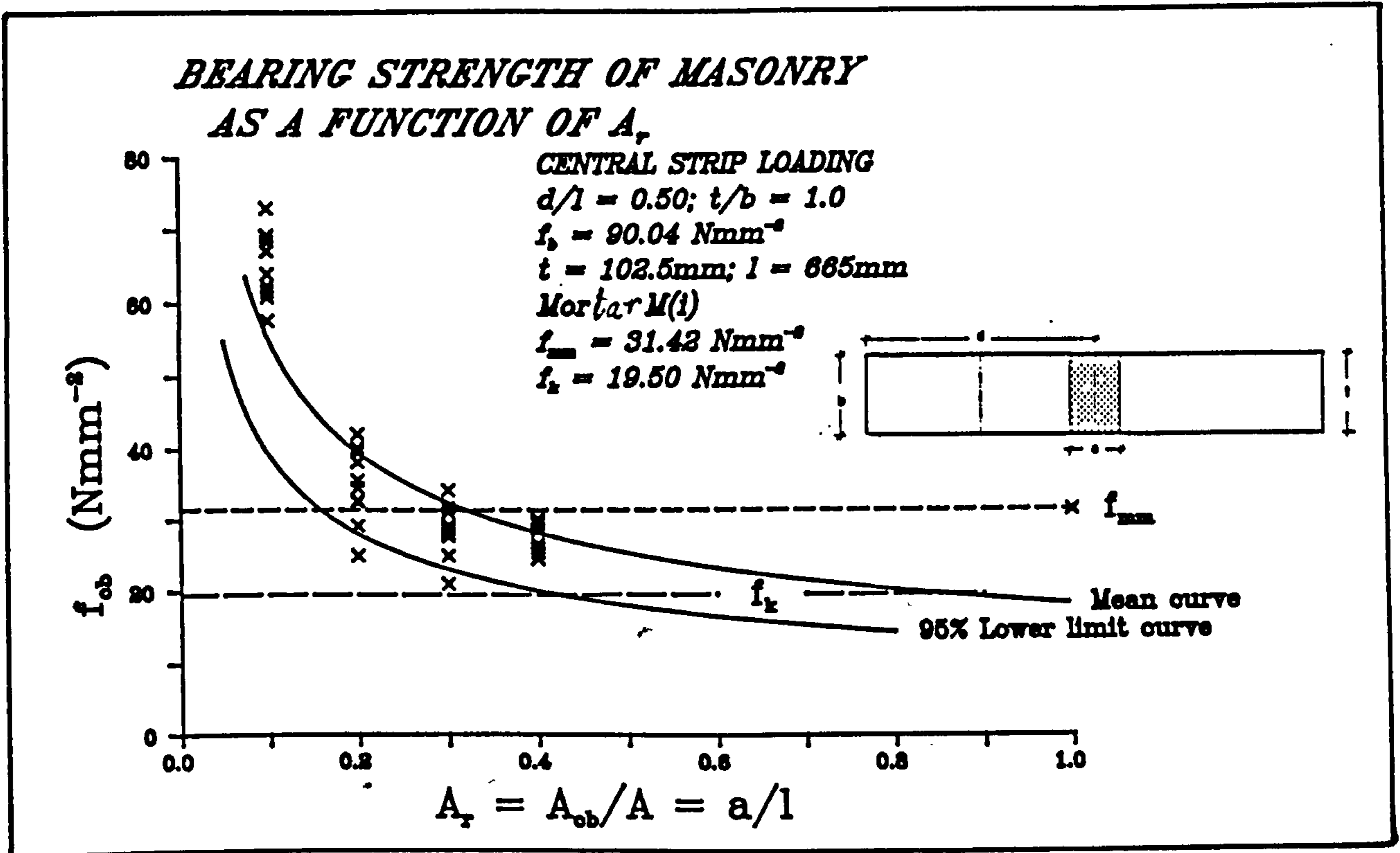


Fig. 6.1 - Bearing strength of masonry type A as a function of loaded area ratio under central strip loading ( $t=102.5\text{mm}$ ).

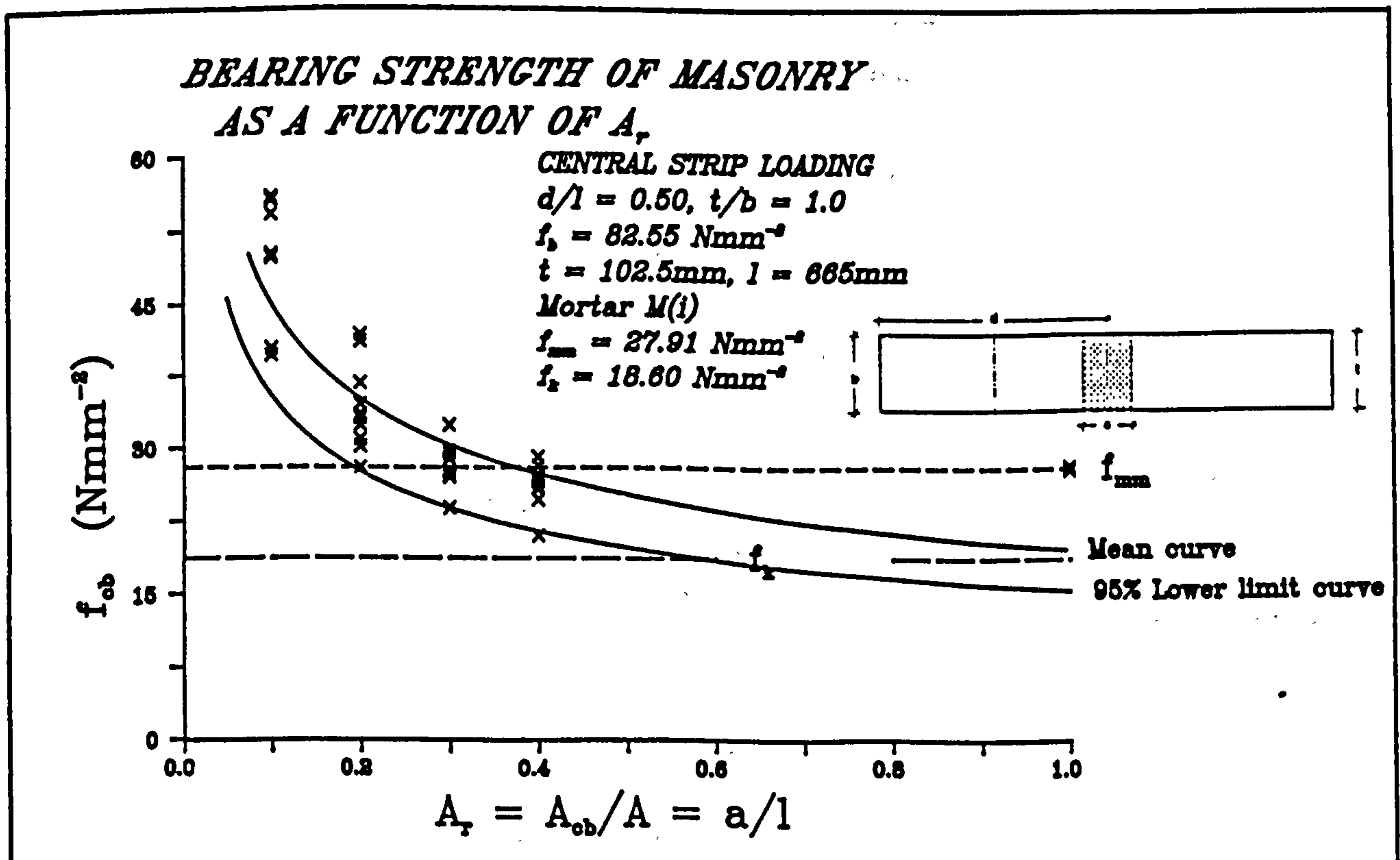


Fig. 6.2 - Bearing strength of masonry type B as a function of loaded area ratio under central strip loading ( $t=102.5\text{mm}$ ).

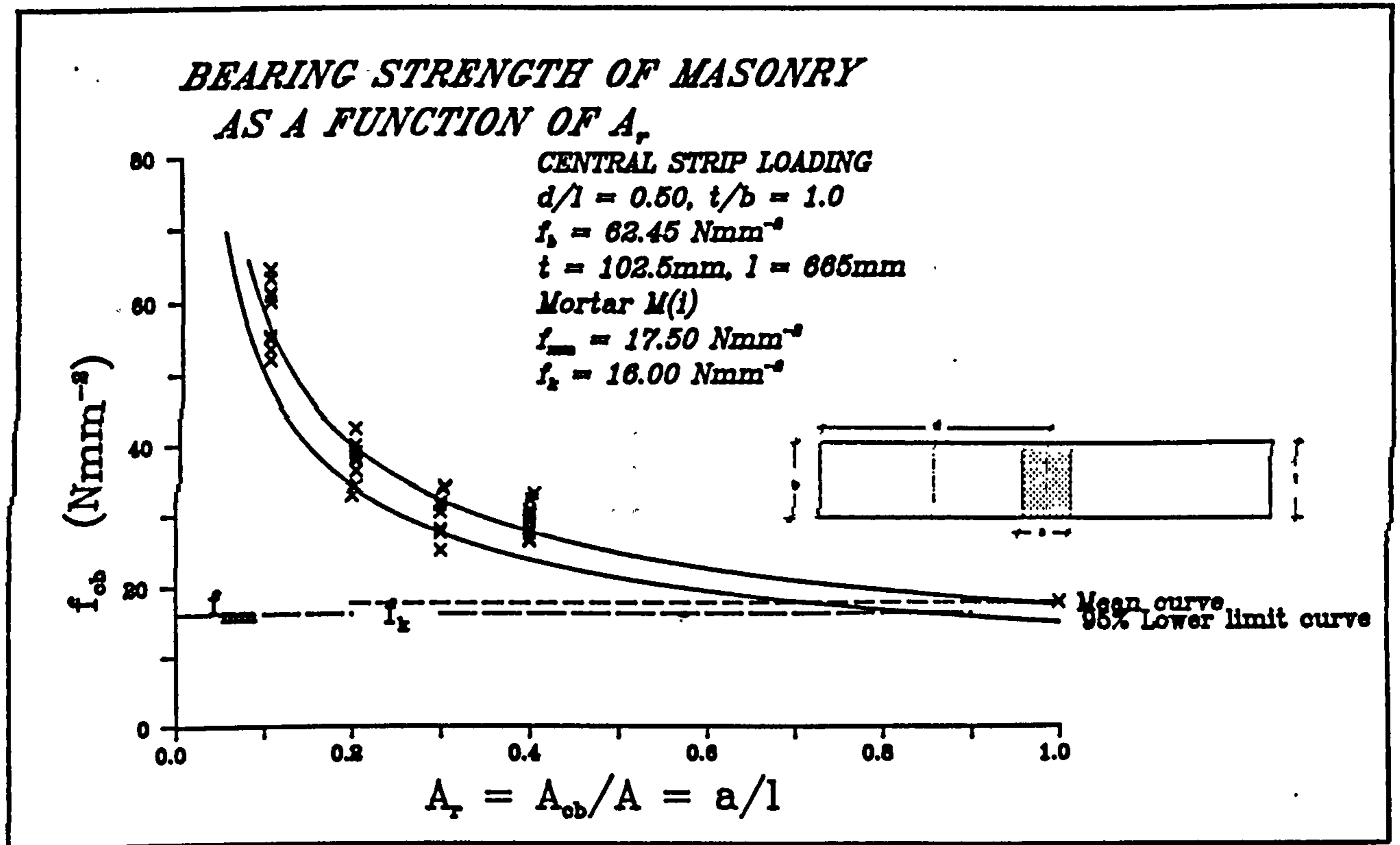


Fig. 6.3 - Bearing strength of masonry type C as a function of loaded area ratio under central strip loading ( $t=102.5\text{mm}$ ).

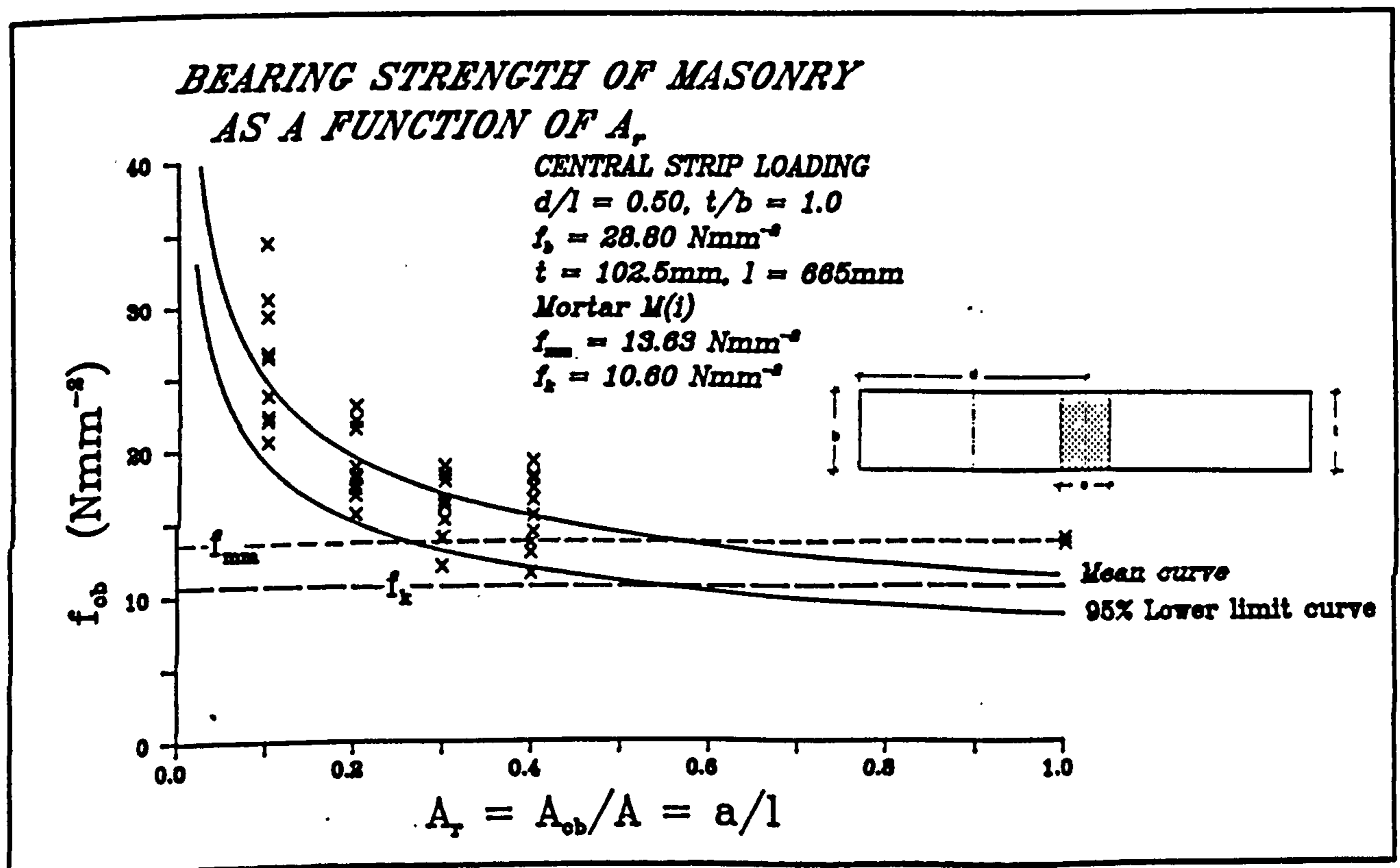


Fig. 6.4 - Bearing strength of masonry type D as a function of loaded area ratio under central strip loading ( $t=102.5\text{mm}$ ).

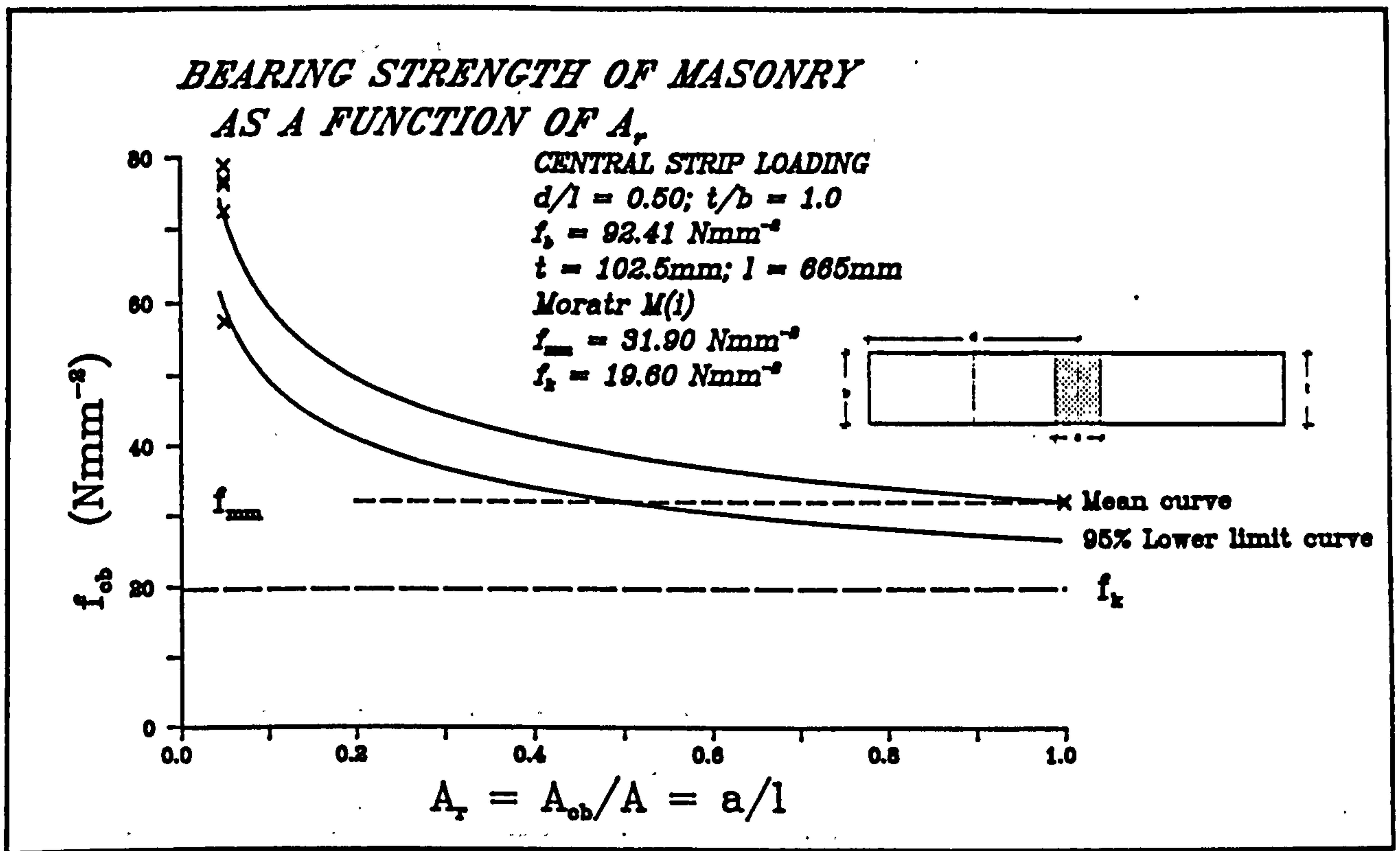


Fig. 6.5 - Bearing strength of masonry type E as a function of loaded area ratio under central strip loading ( $t=102.5\text{mm}$ ).

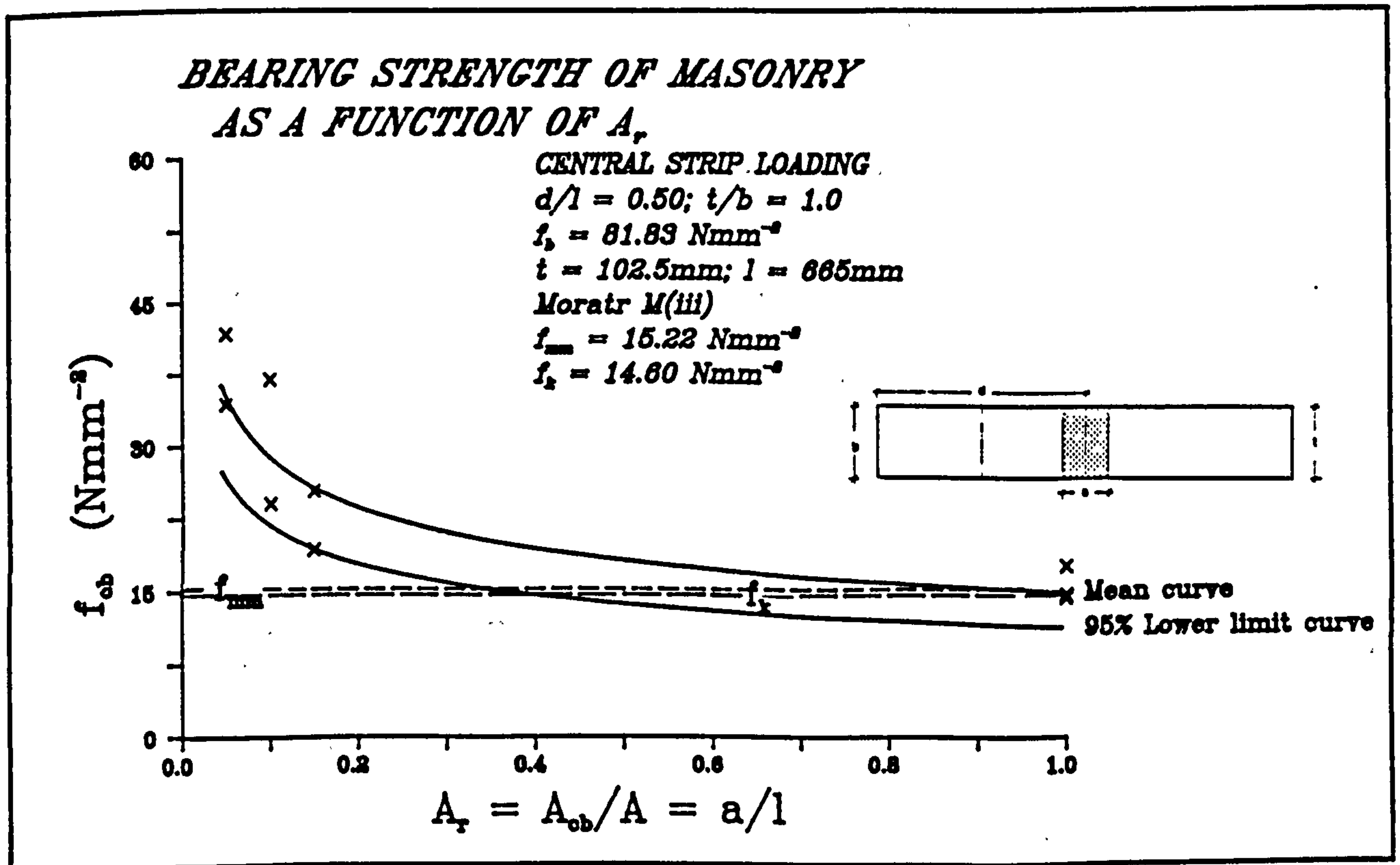


Fig. 6.6 - Bearing strength of masonry type F as a function of loaded area ratio under central strip loading ( $t=102.5\text{mm}$ ).

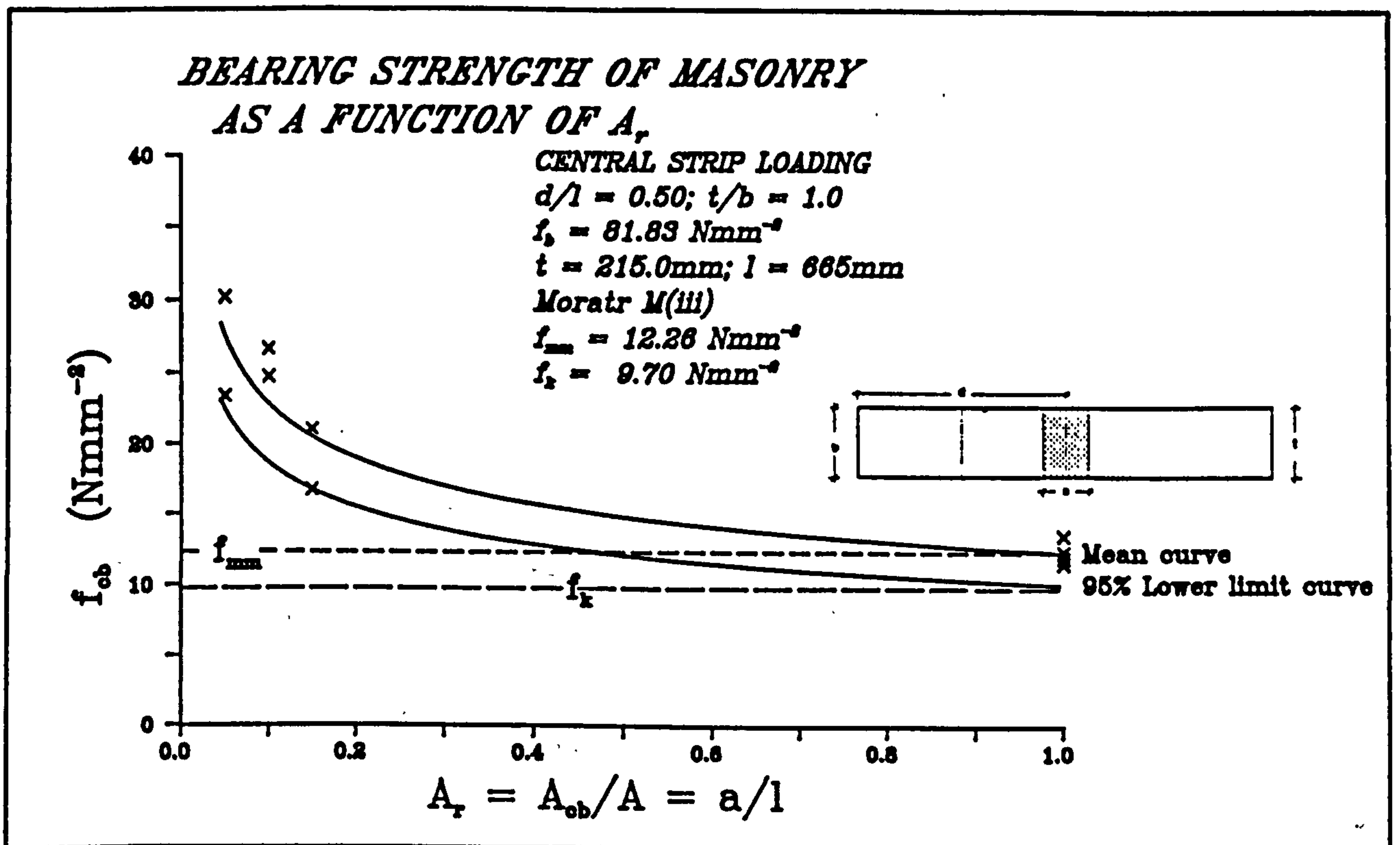


Fig. 6.7 - Bearing strength of masonry type F as a function of loaded area ratio under central strip loading ( $t=215.0\text{mm}$ ).

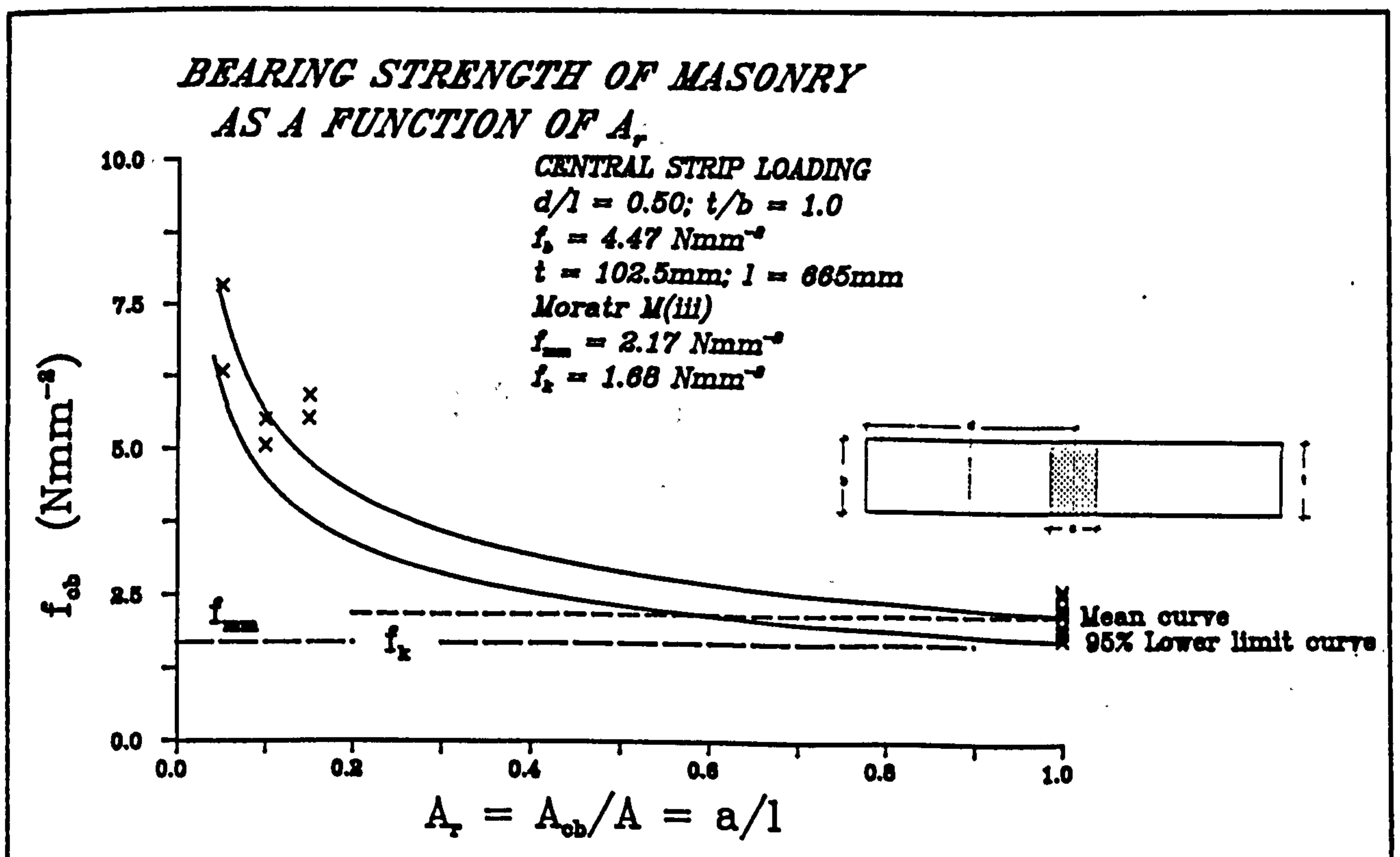


Fig. 6.8 - Bearing strength of masonry type G as a function of loaded area ratio under central strip loading ( $t=102.5\text{mm}$ ).

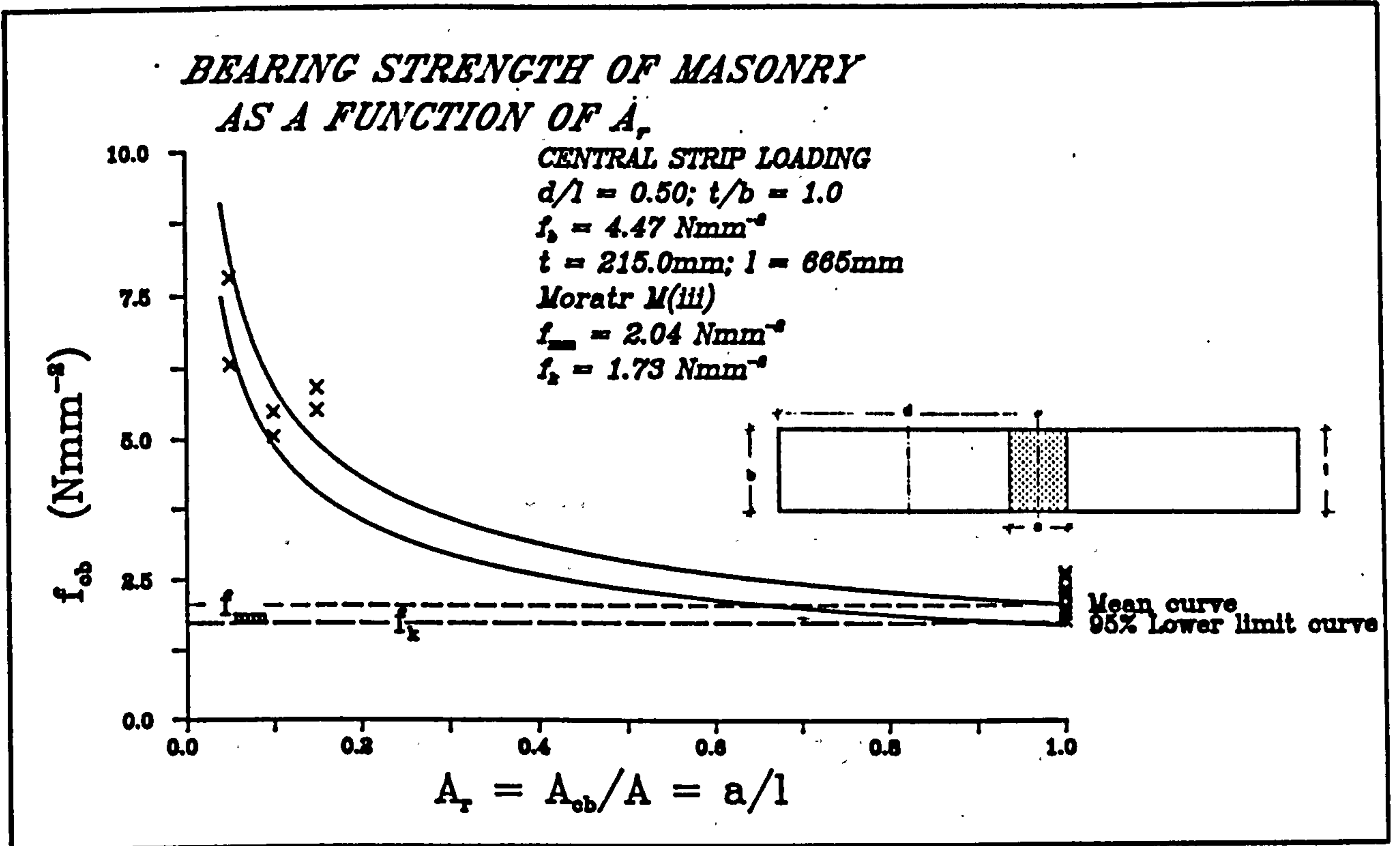


Fig. 6.9 - Bearing strength of masonry type G as a function of loaded area ratio under central strip loading ( $t=215.0\text{mm}$ ).

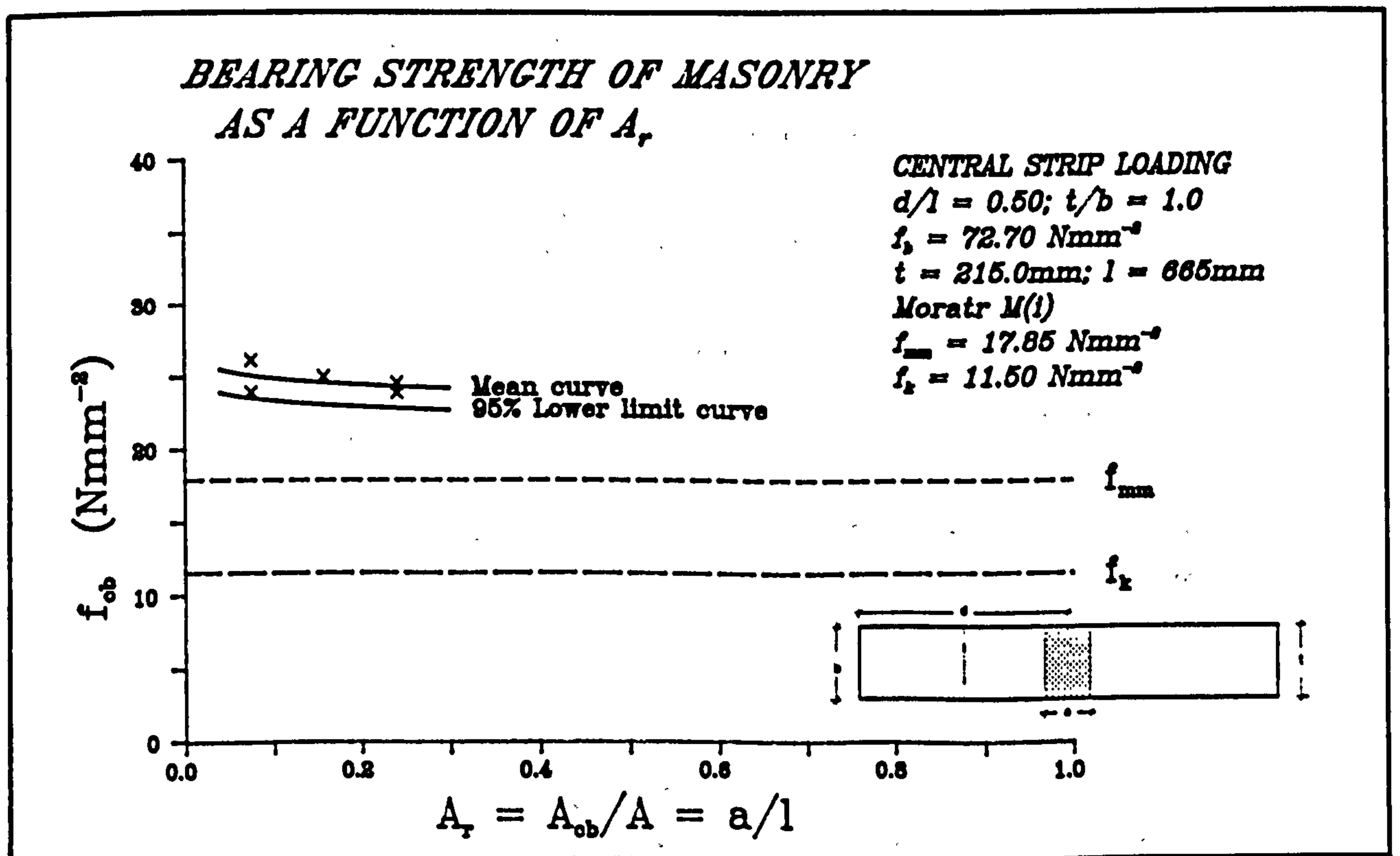


Fig. 6.10 - Bearing strength of masonry type H as a function of loaded area ratio under central strip loading ( $t=215.0\text{mm}$ ).

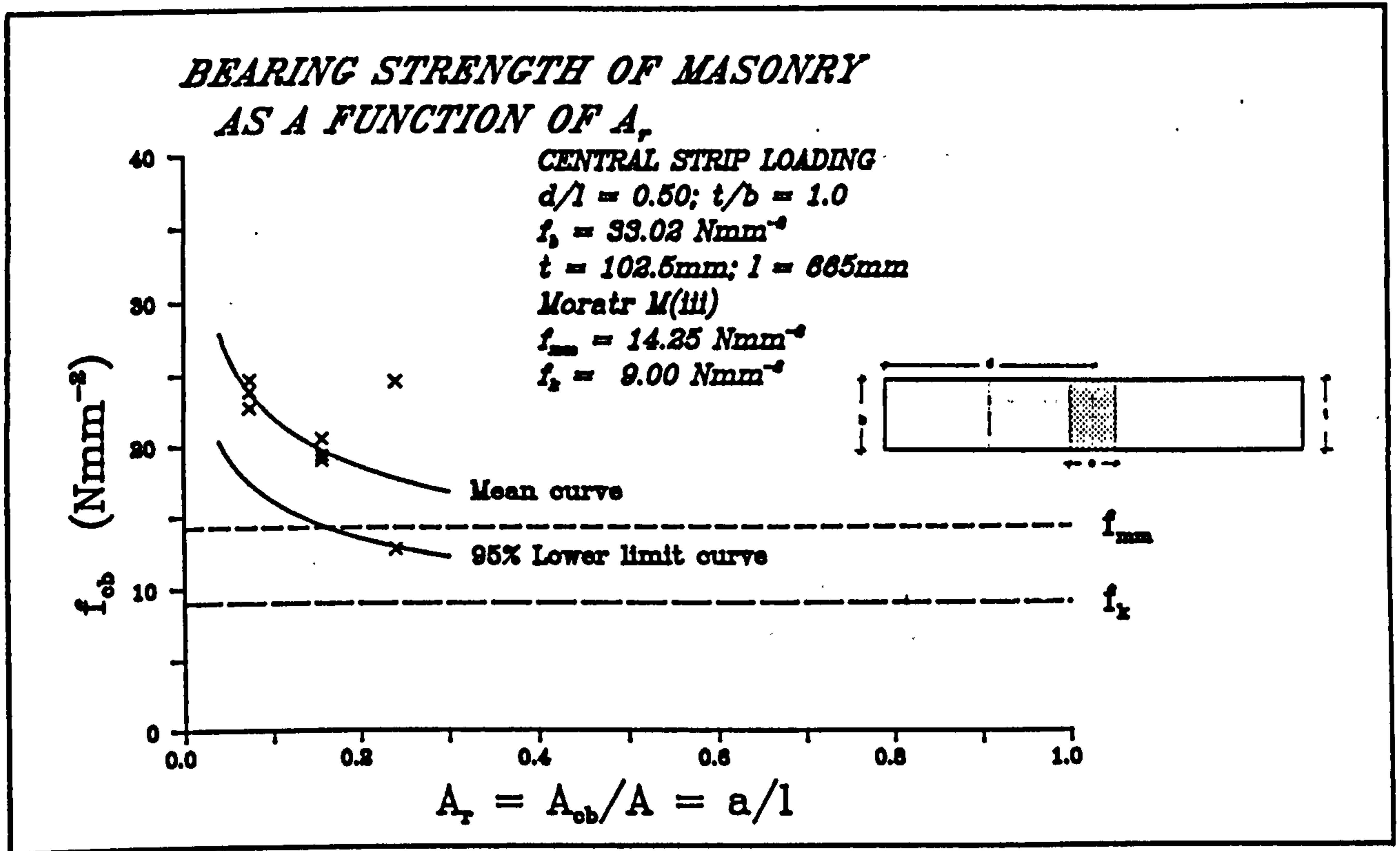


Fig. 6.11 - Bearing strength of masonry type L as a function of loaded area ratio under central strip loading ( $t=102.5\text{mm}$ ).

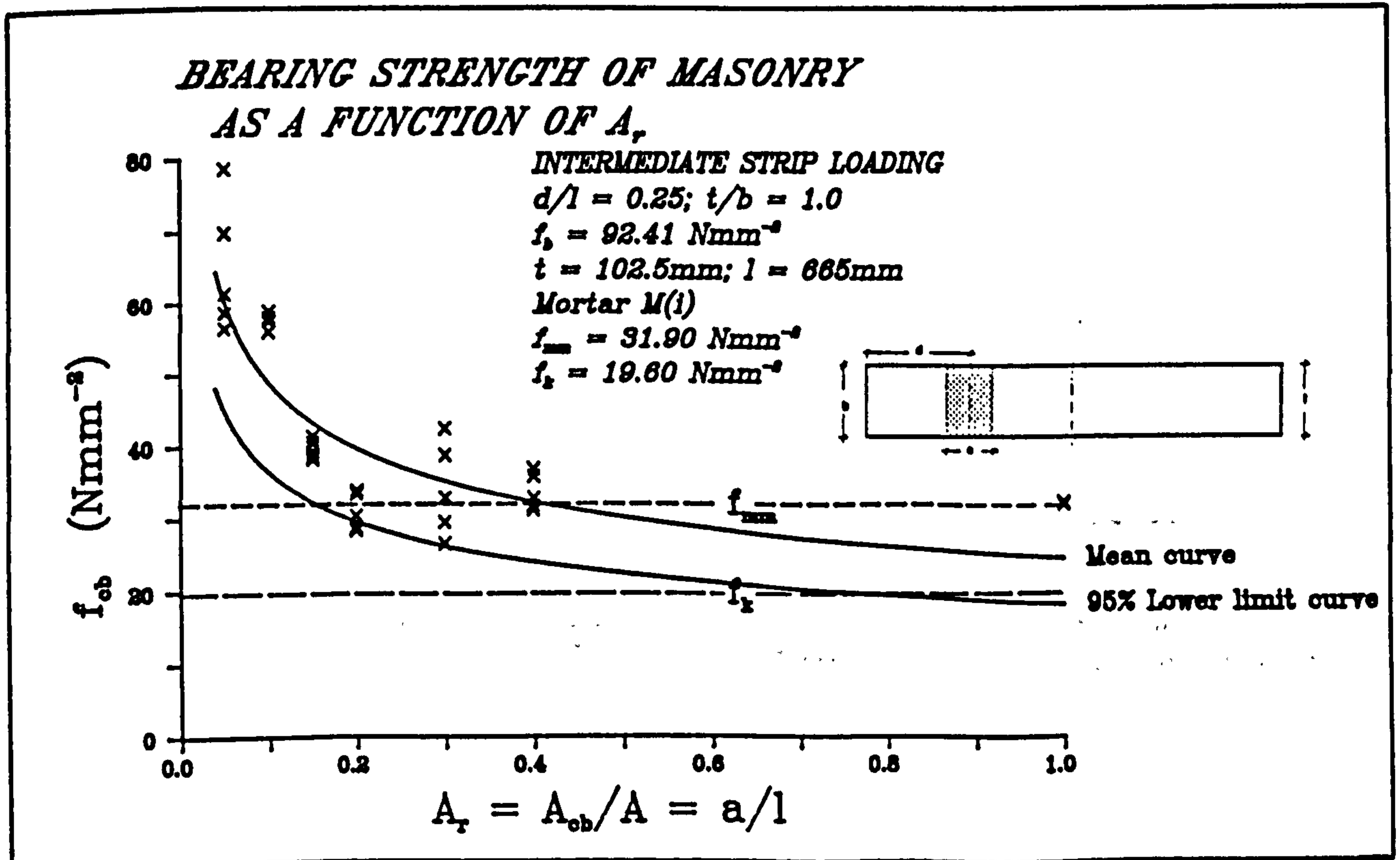


Fig. 6.12 - Bearing strength of masonry type E as a function of loaded area ratio under intermediate strip loading ( $t=102.5\text{mm}$ ).

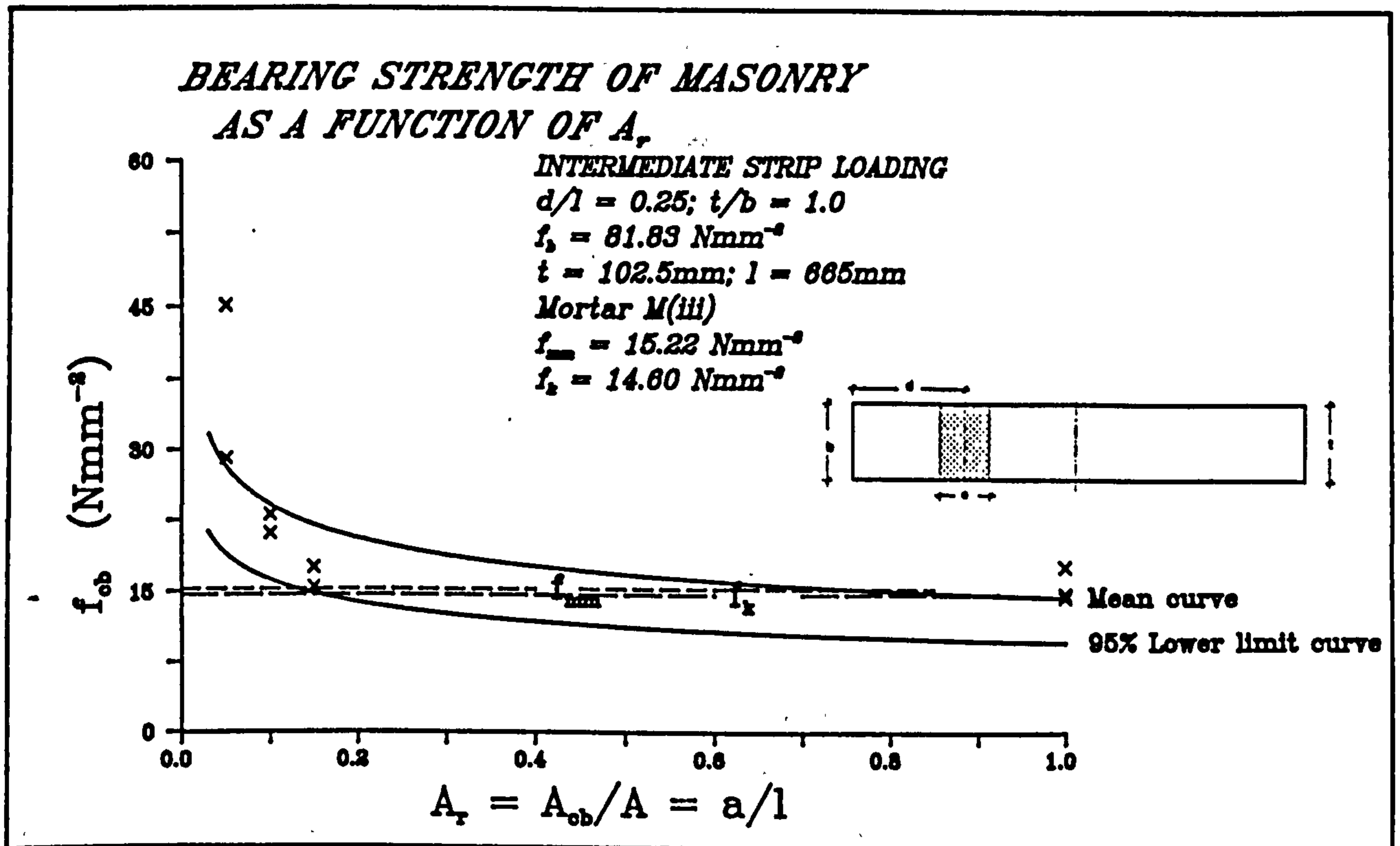


Fig. 6.13 - Bearing strength of masonry type F as a function of loaded area ratio under intermediate strip loading ( $t=102.5\text{mm}$ ).

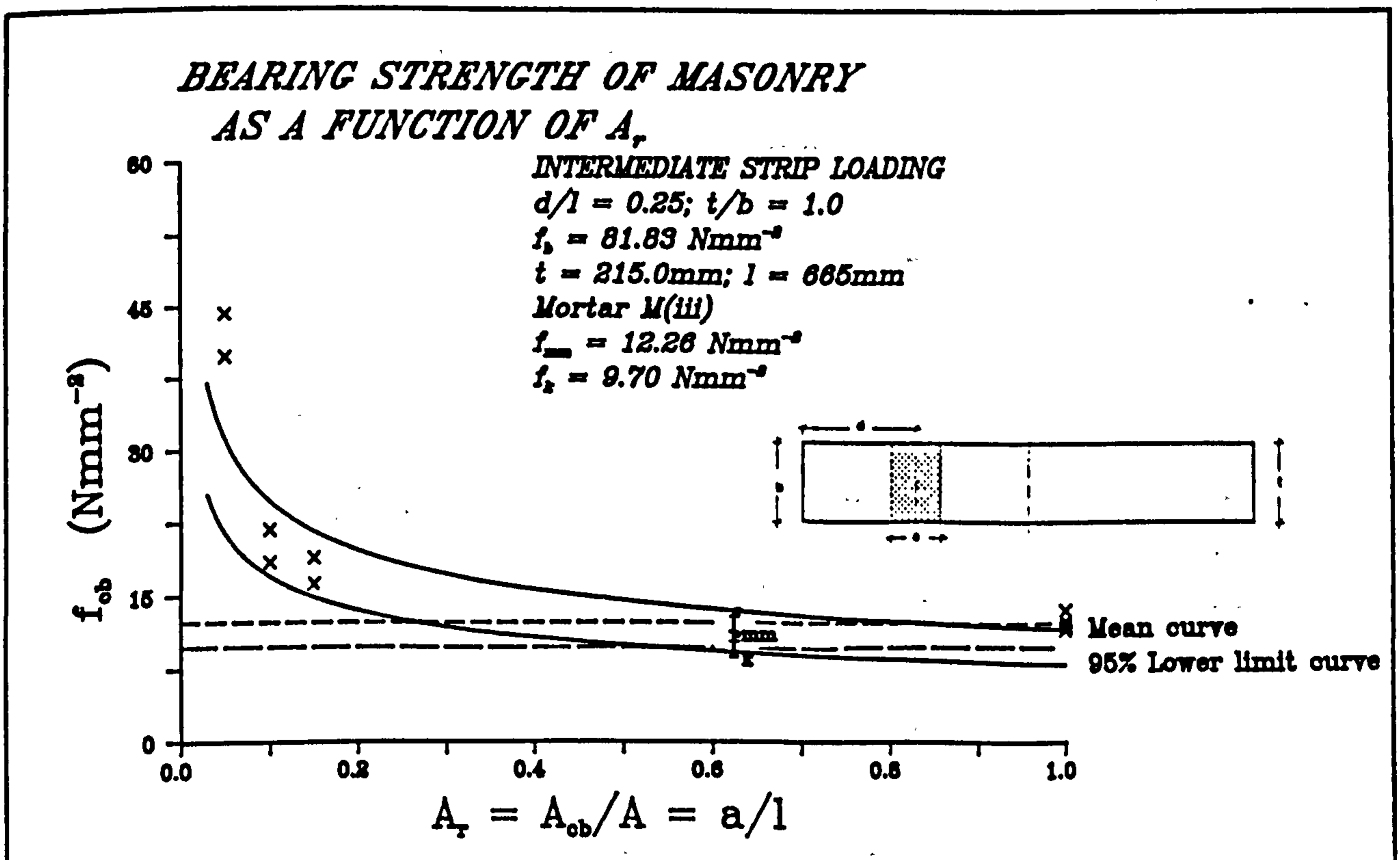


Fig. 6.14 - Bearing strength of masonry type F as a function of loaded area ratio under intermediate strip loading ( $t=215.0\text{mm}$ ).

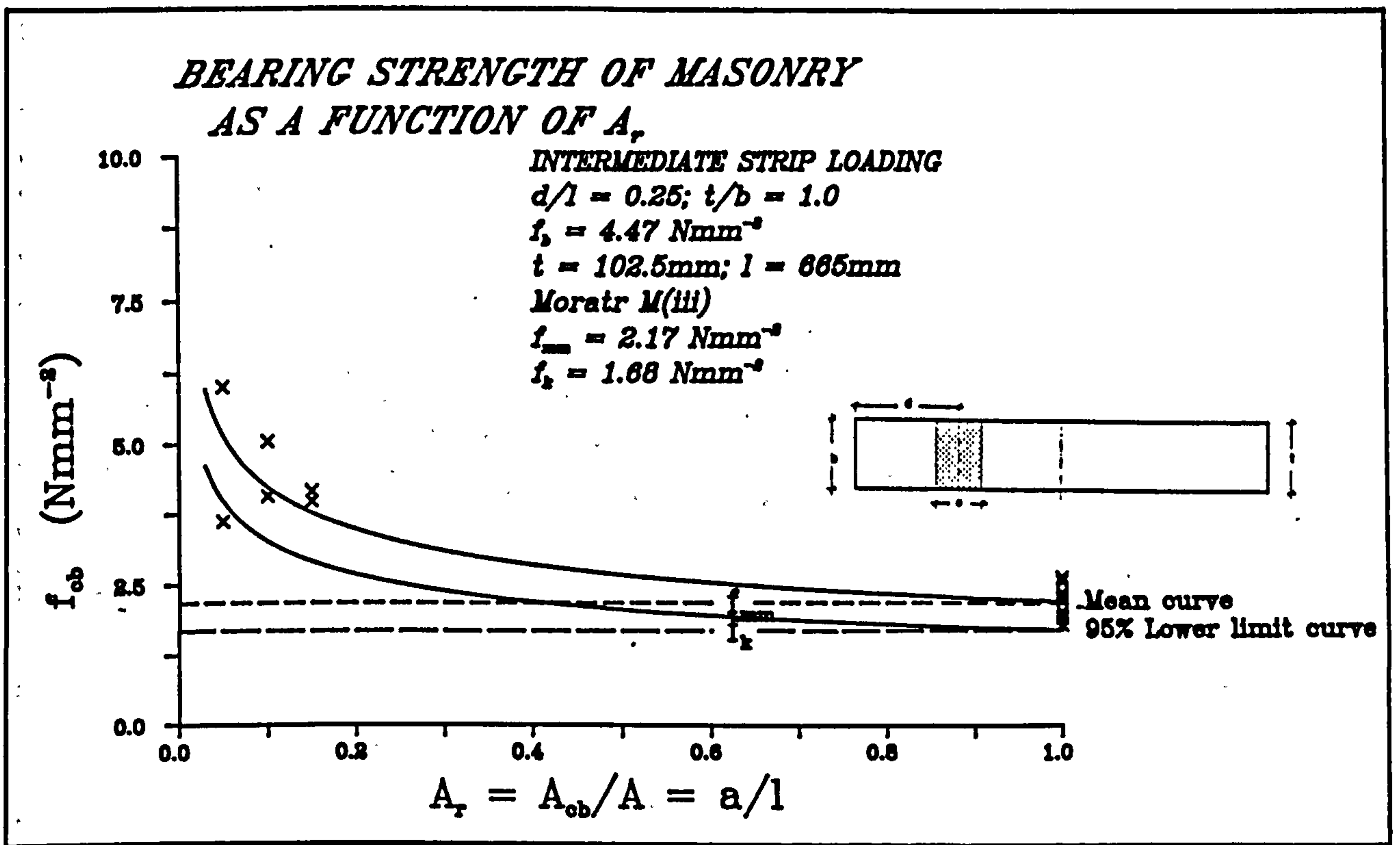


Fig. 6.15 - Bearing strength of masonry type G as a function of loaded area ratio under intermediate strip loading ( $t=102.5\text{mm}$ ).

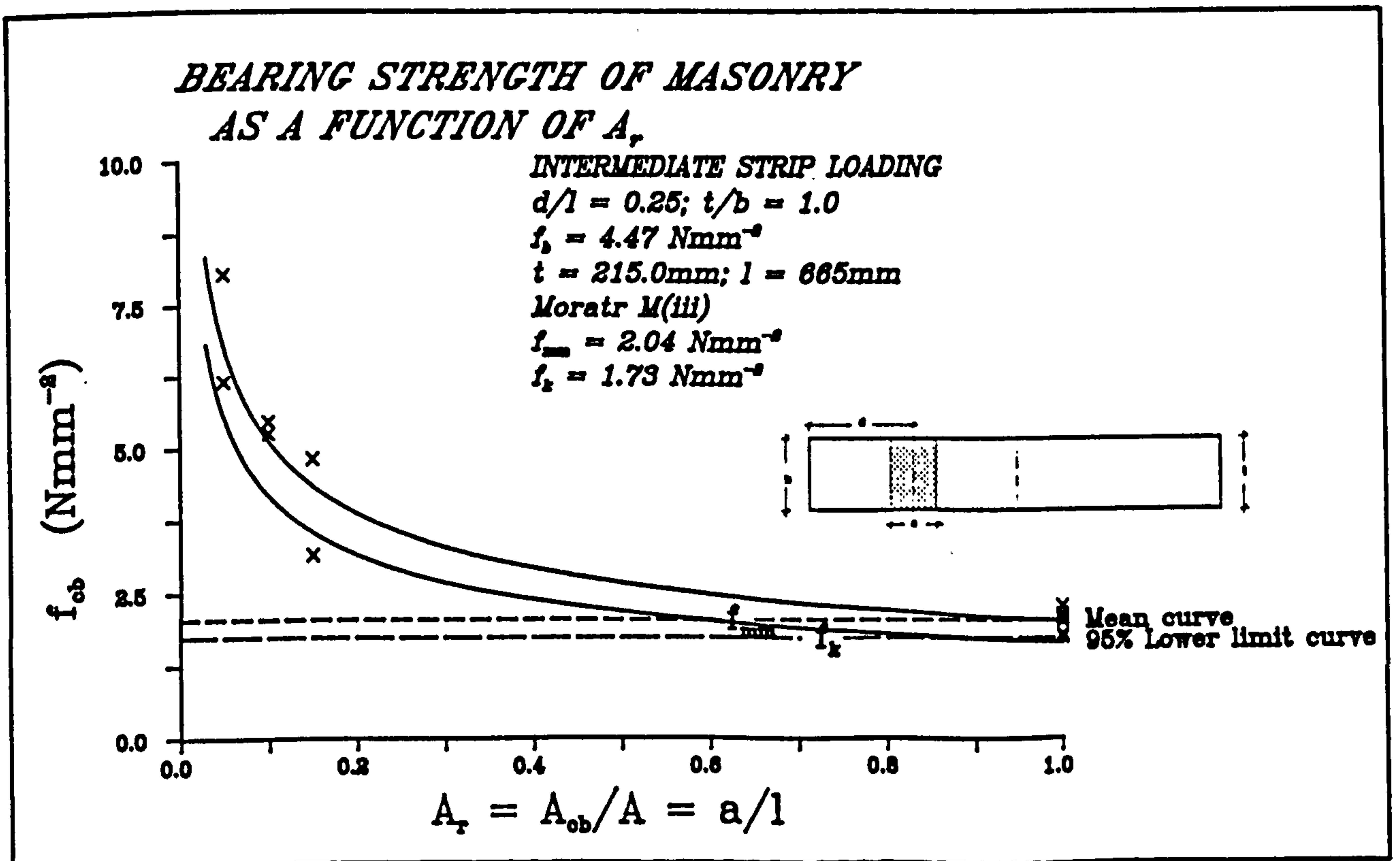


Fig. 6.16 - Bearing strength of masonry type G as a function of loaded area ratio under intermediate strip loading ( $t=215.0\text{mm}$ ).



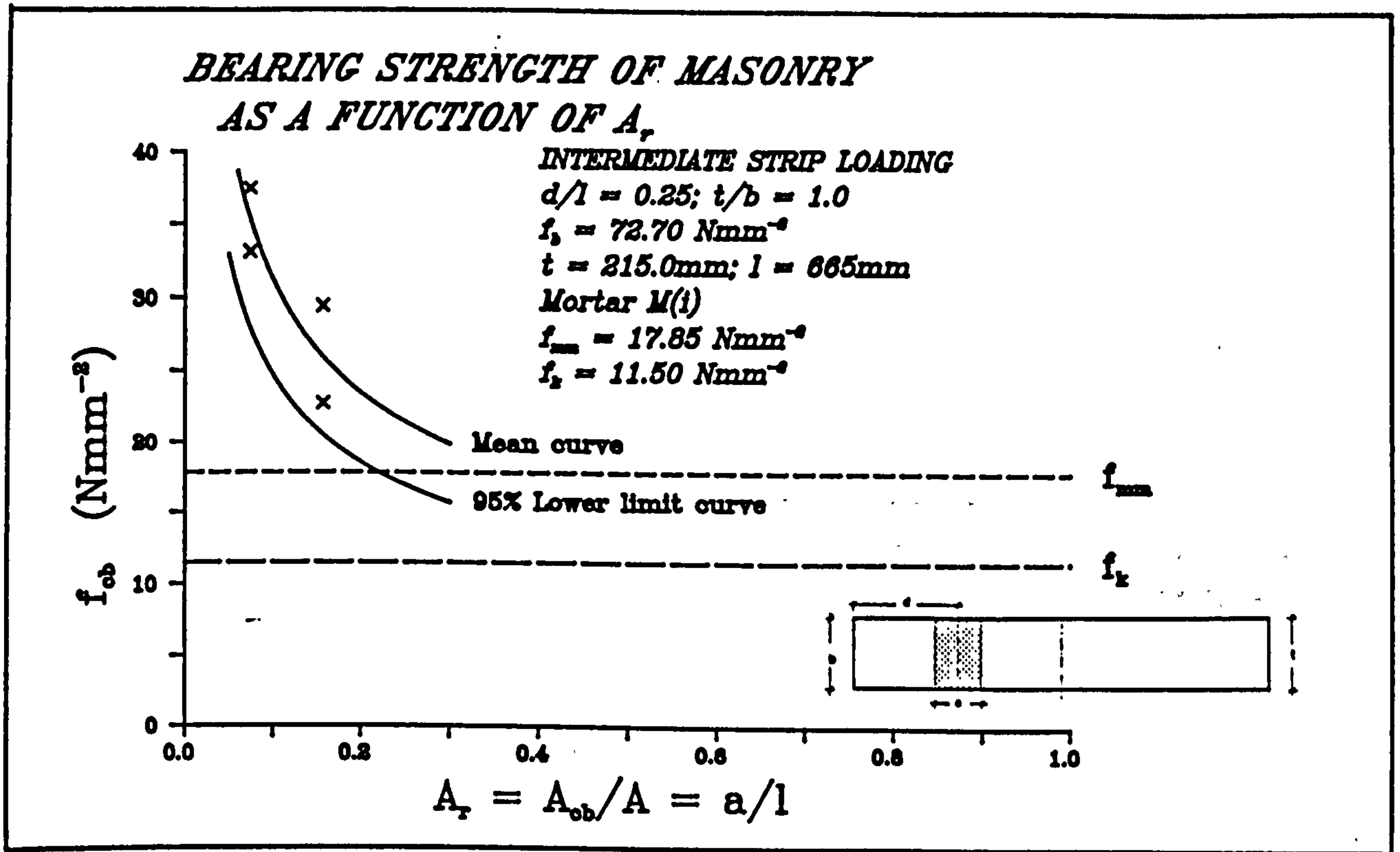


Fig. 6.17 - Bearing strength of masonry type H as a function of loaded area ratio under intermediate strip loading ( $t=215.0\text{mm}$ ).

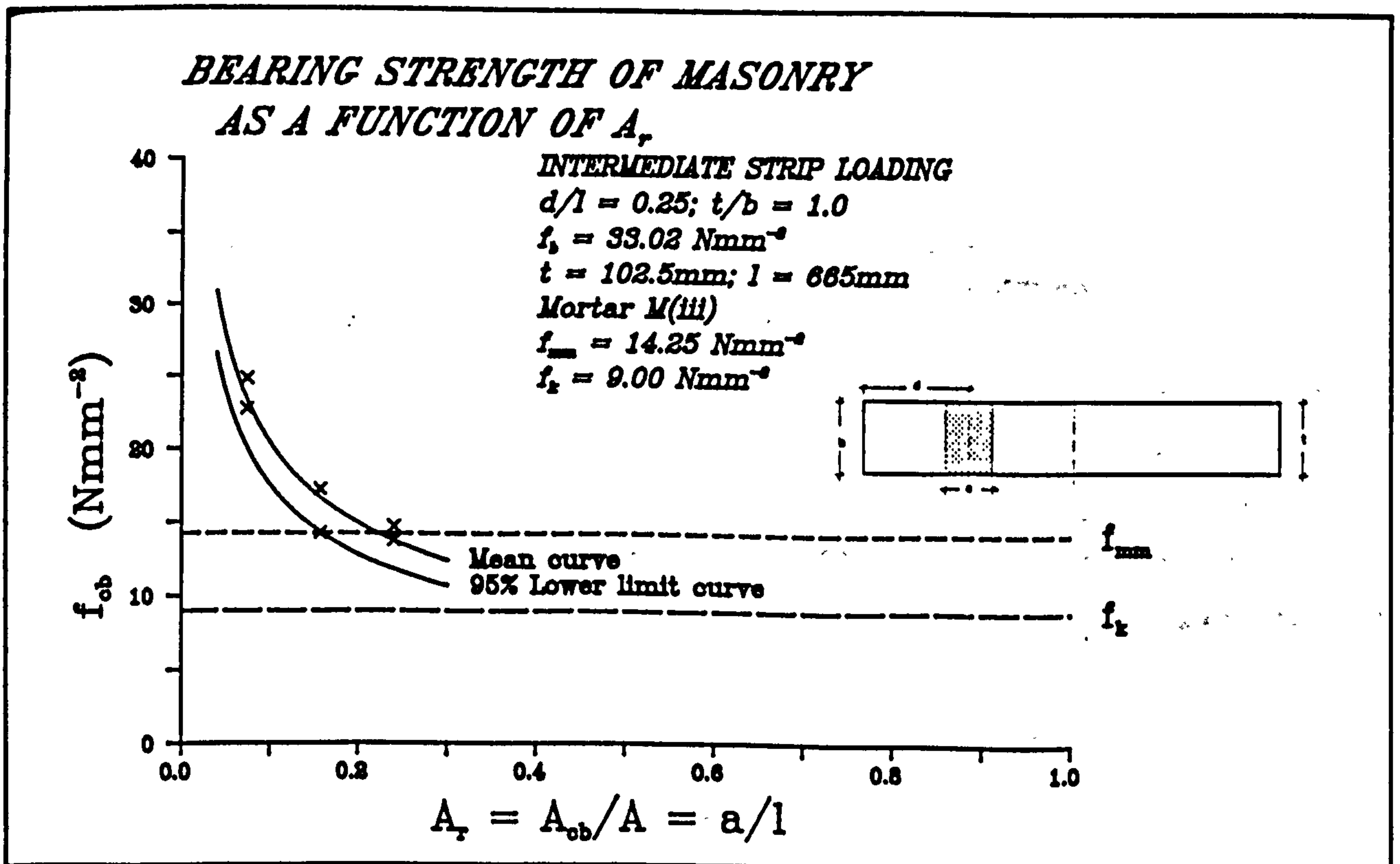


Fig. 6.18 - Bearing strength of masonry type L as a function of loaded area ratio under intermediate strip loading ( $t=102.5\text{mm}$ ).

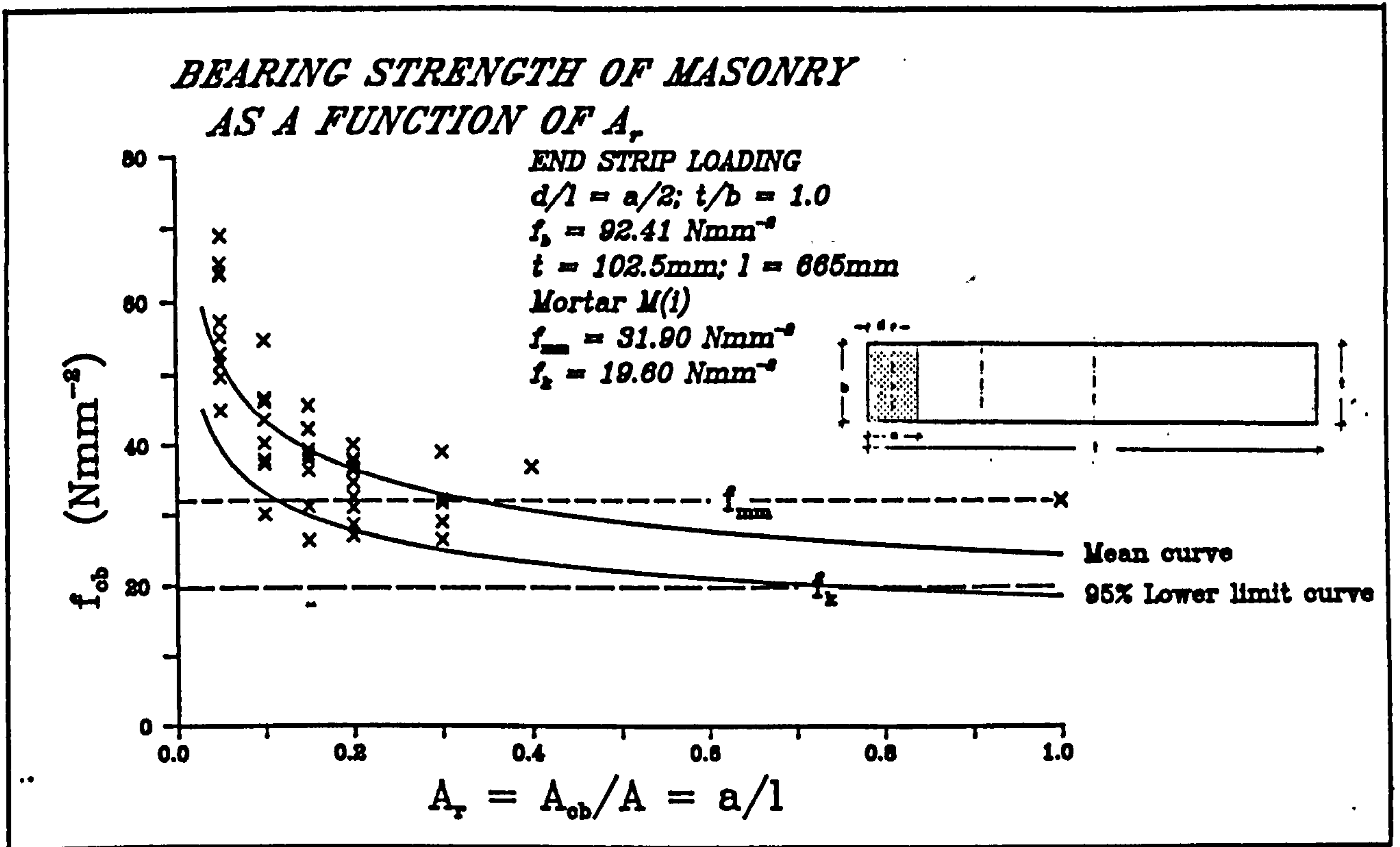


Fig. 6.19 - Bearing strength of masonry type E as a function of loaded area ratio under end strip loading ( $t=102.5\text{mm}$ ).

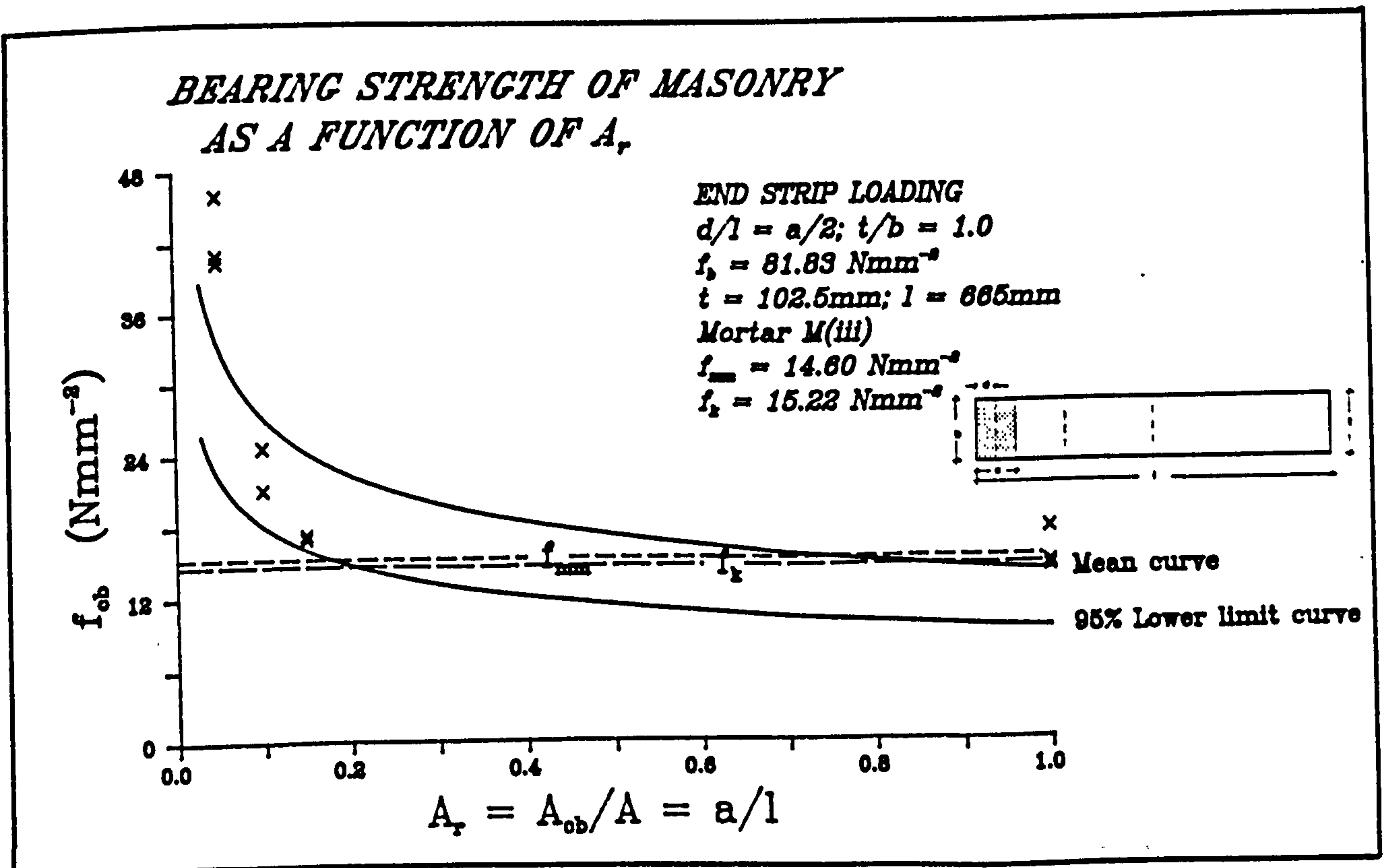


Fig. 6.20 - Bearing strength of masonry type F as a function of loaded area ratio under end strip loading ( $t=102.5\text{mm}$ ).

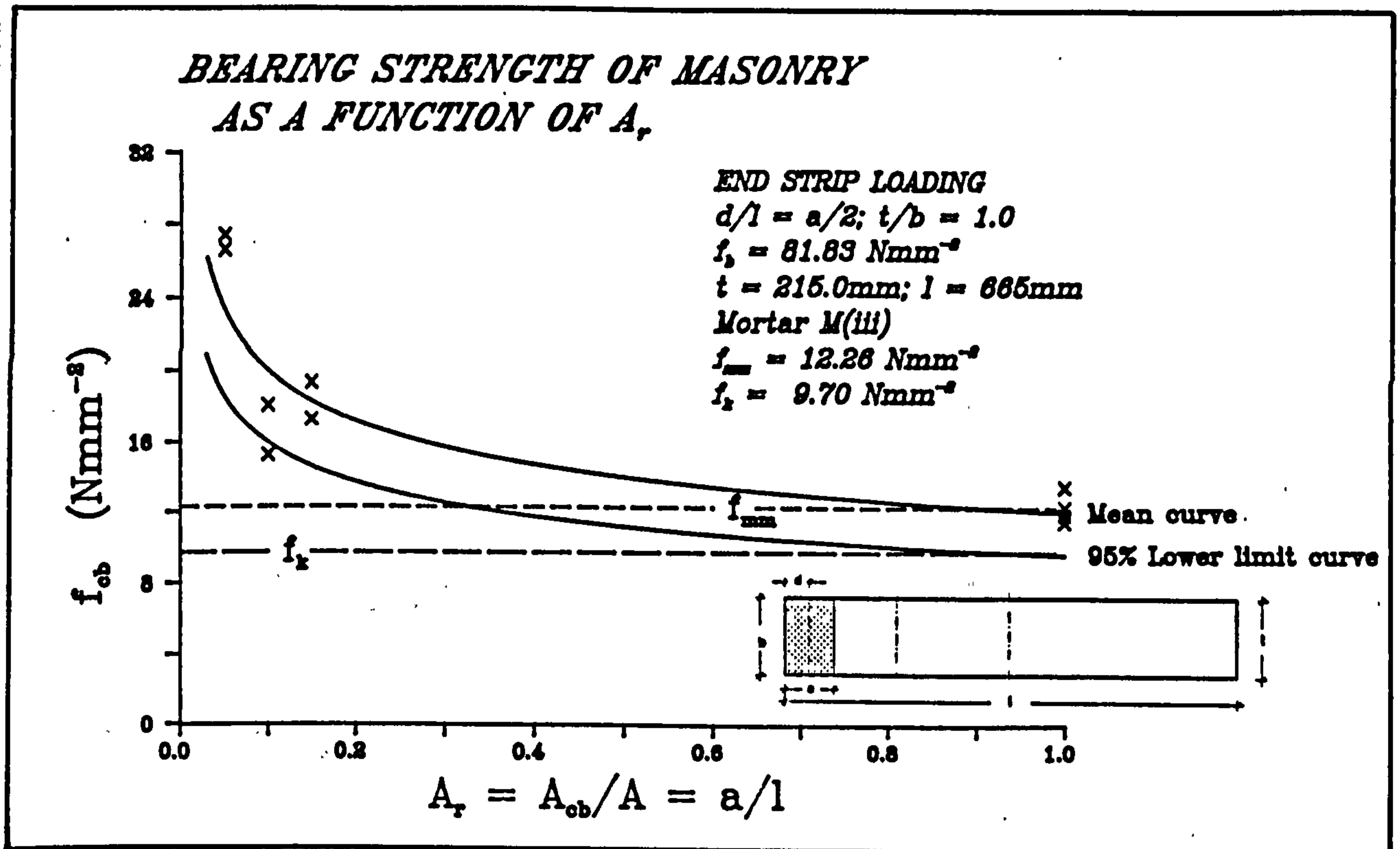


Fig. 6.21 - Bearing strength of masonry type F as a function of loaded area ratio under end strip loading ( $t=215.0\text{mm}$ ).

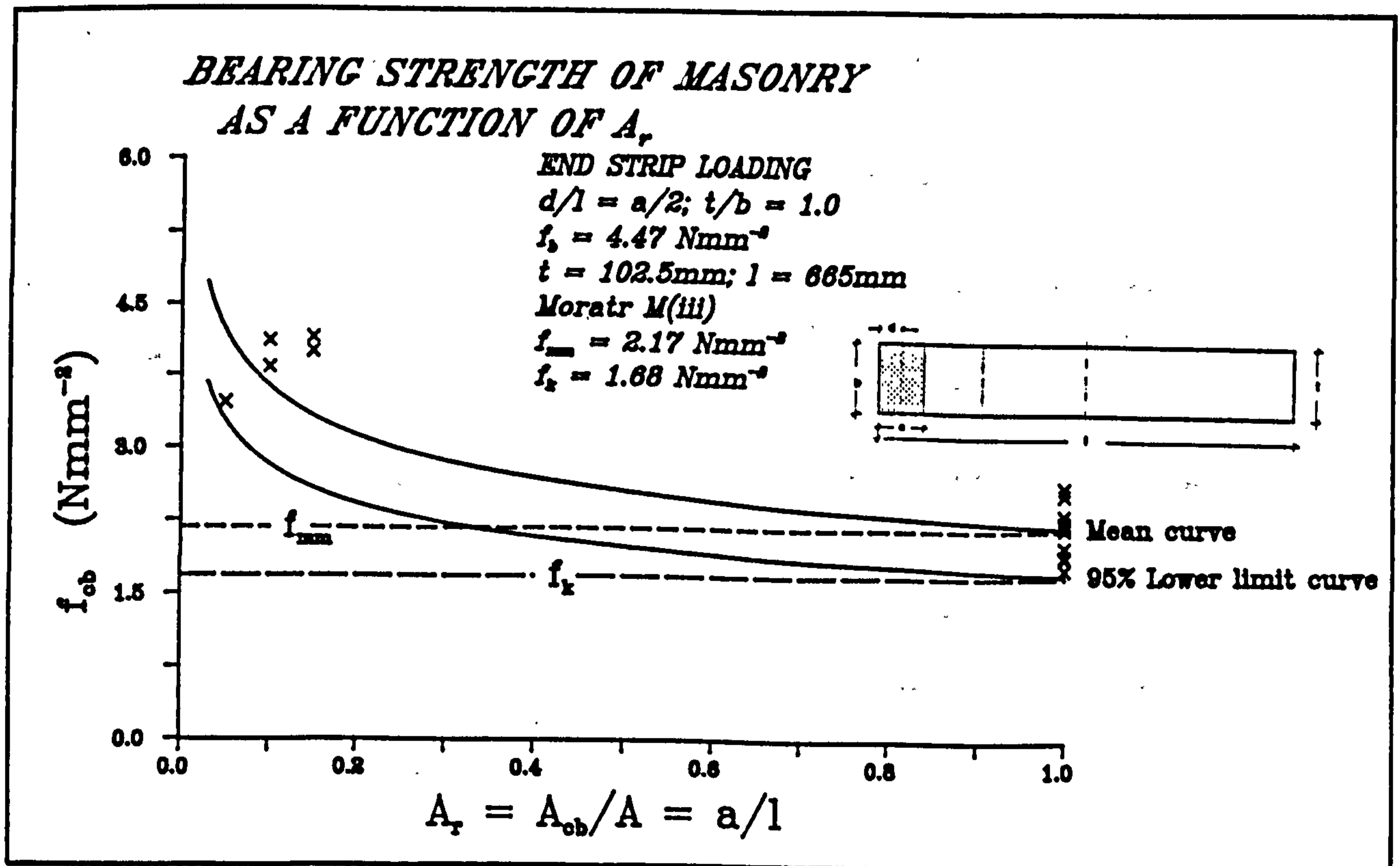


Fig. 6.22 - Bearing strength of masonry type G as a function of loaded area ratio under end strip loading ( $t=102.5\text{mm}$ ).

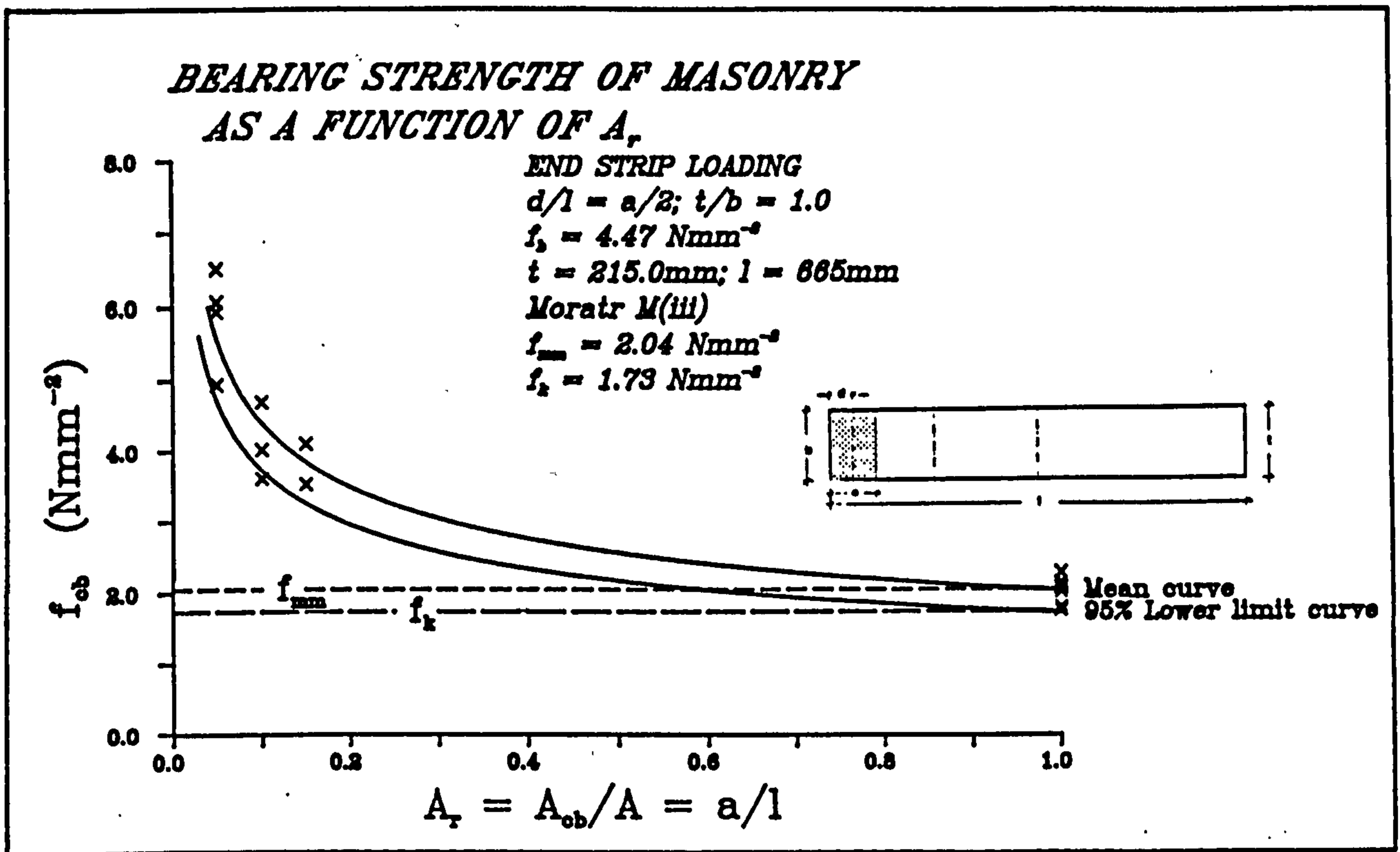


Fig. 6.23 - Bearing strength of masonry type G as a function of loaded area ratio under end strip loading ( $t=215.0\text{mm}$ ).

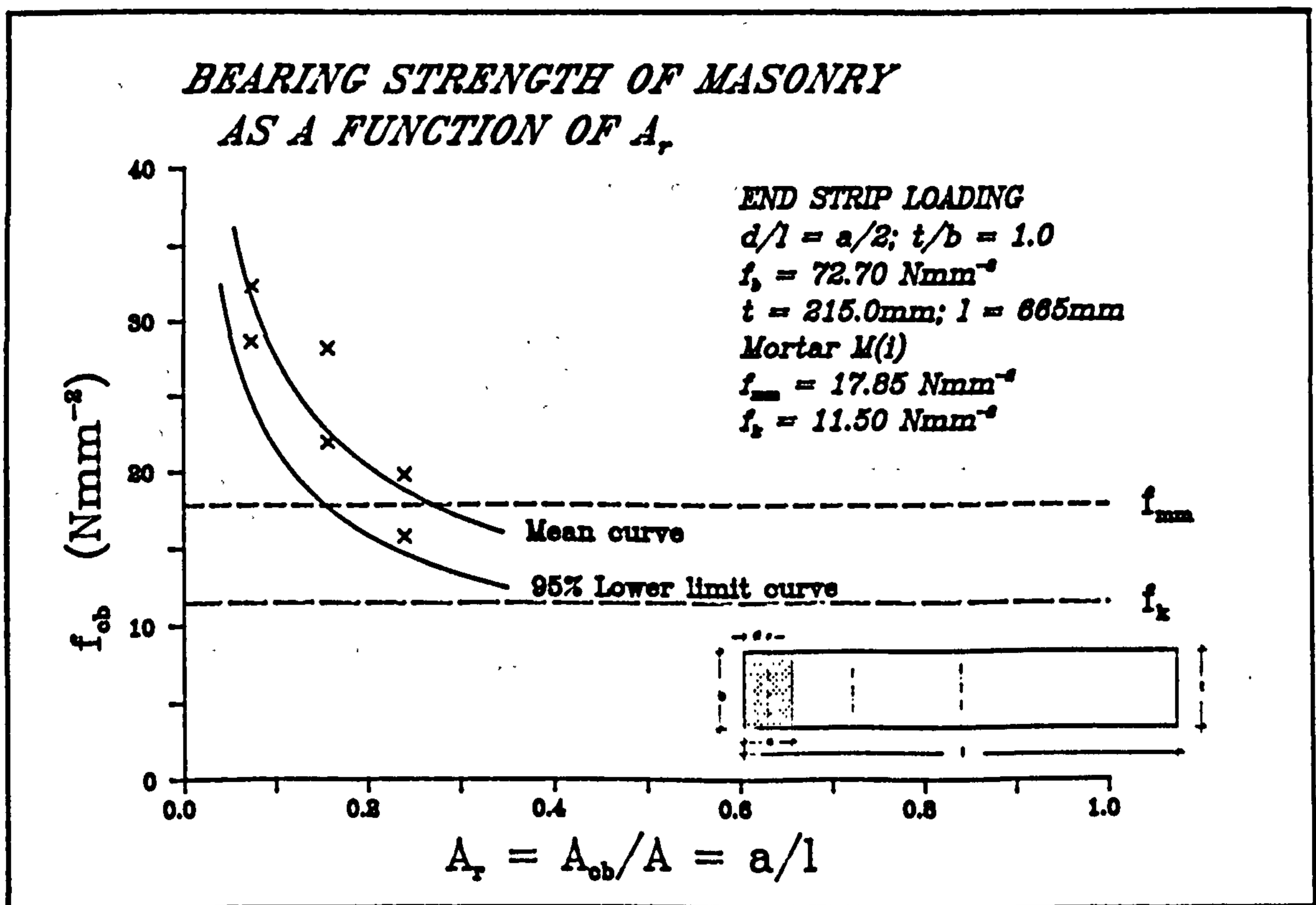


Fig. 6.24 - Bearing strength of masonry type H as a function of loaded area ratio under end strip loading ( $t=215.0\text{mm}$ ).

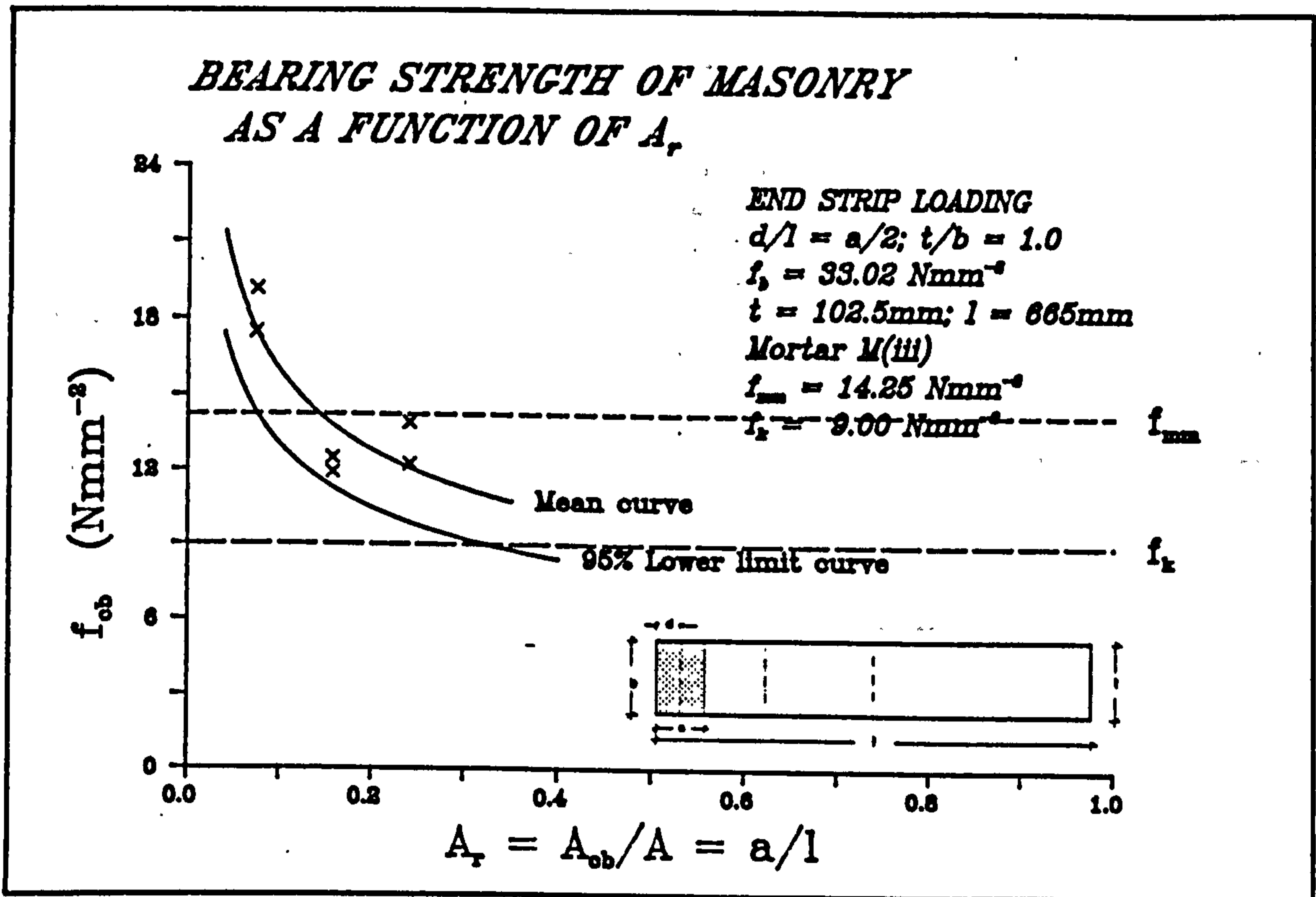


Fig. 6.25 - Bearing strength of masonry type L as a function of loaded area ratio under end strip loading ( $t=102.5\text{mm}$ ).

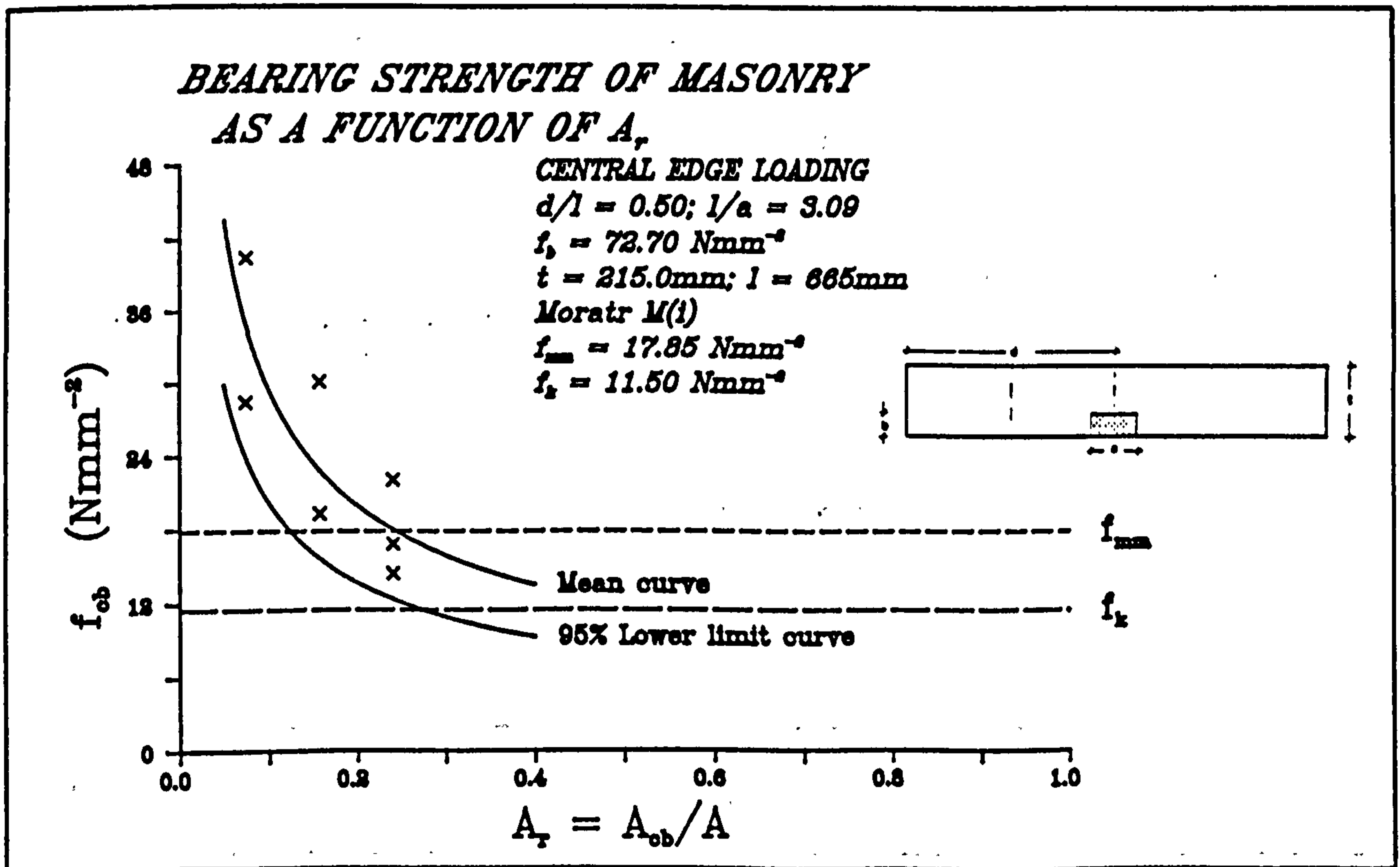


Fig. 6.26 - Bearing strength of masonry type M as a function of loaded area ratio under central edge loading ( $t=215.0\text{mm}$ ).

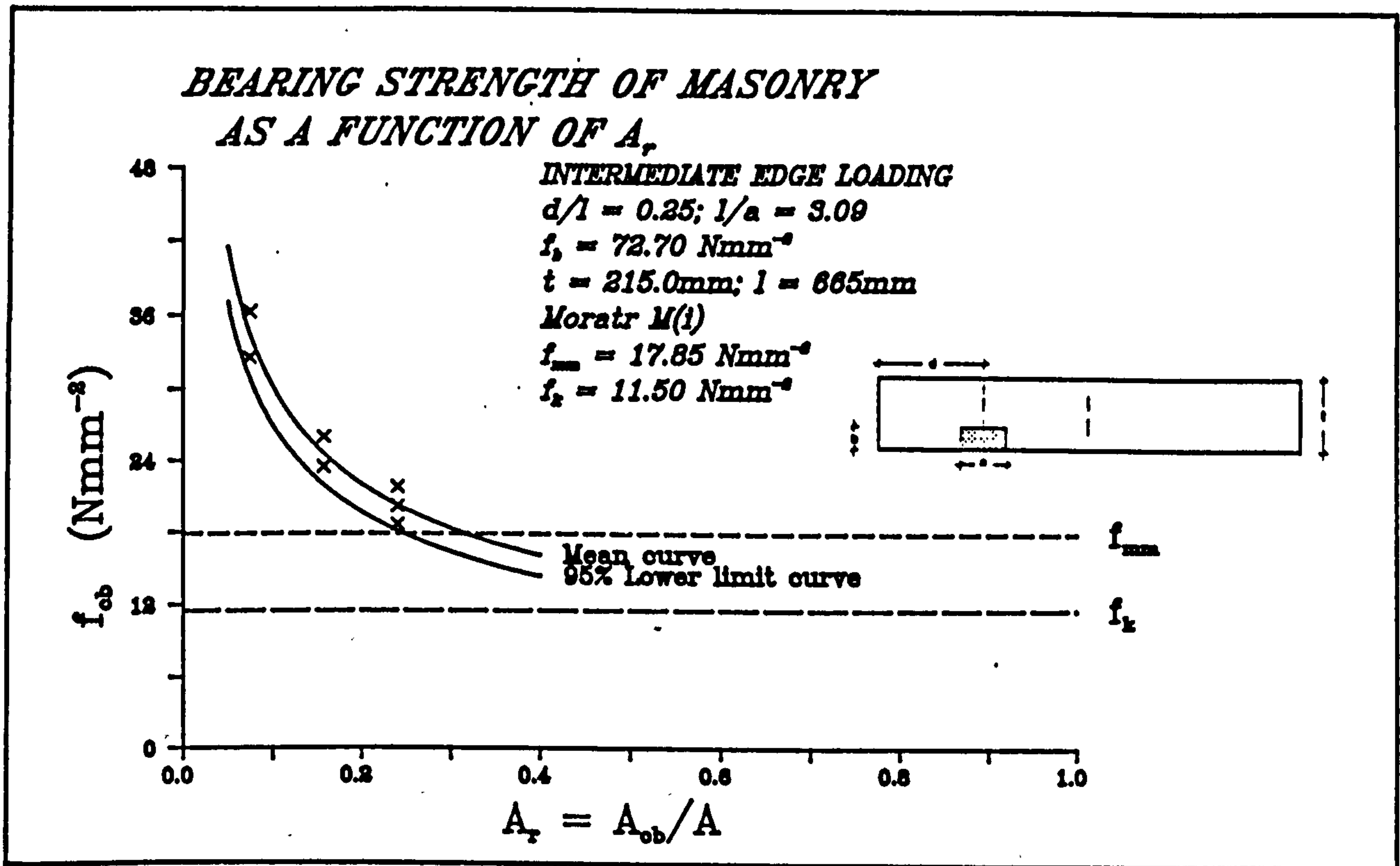


Fig. 6.27 - Bearing strength of masonry type M as a function of loaded area ratio under intermediate edge loading ( $t=215.0\text{mm}$ ).

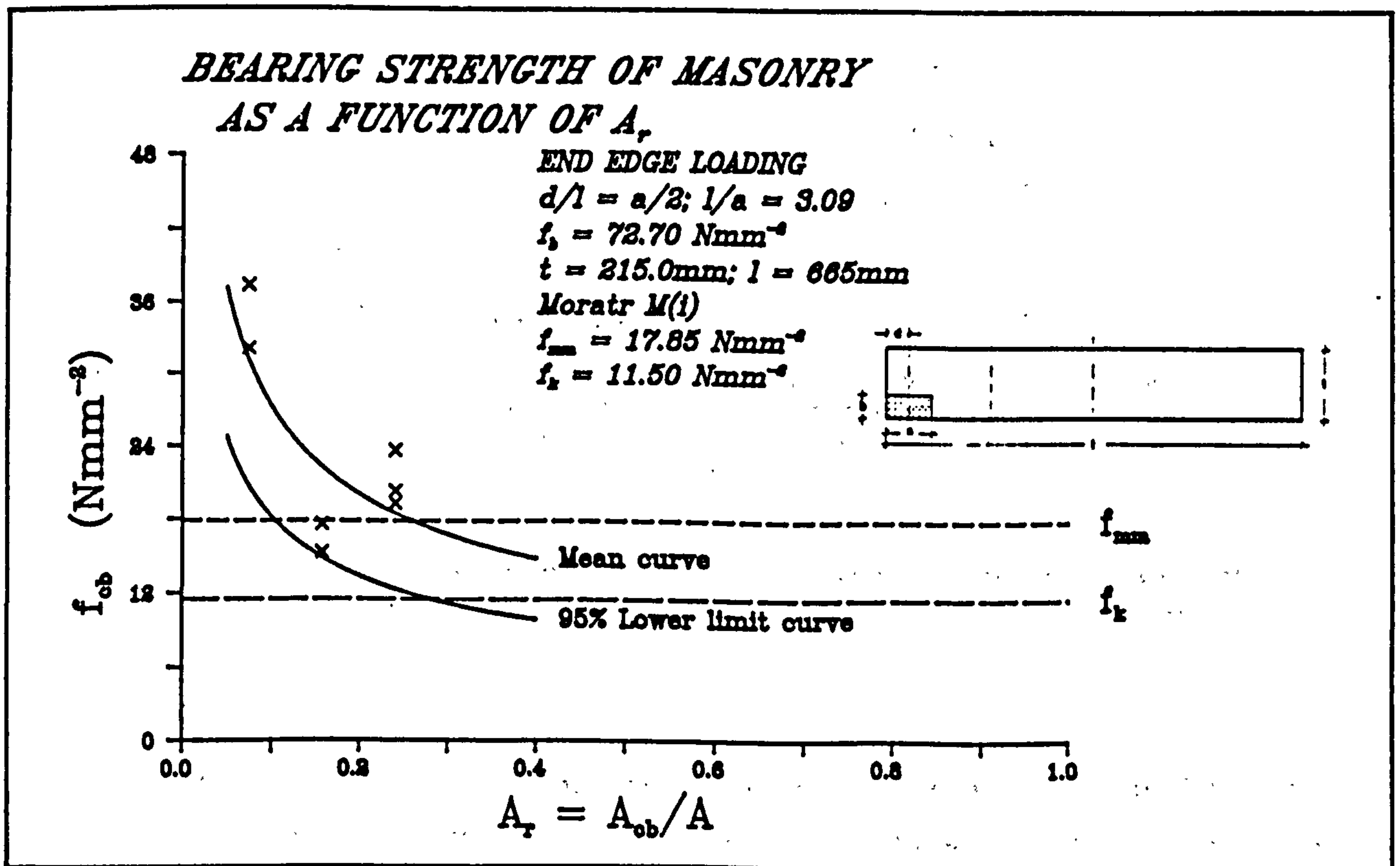


Fig. 6.28 - Bearing strength of masonry type M as a function of loaded area ratio under end edge loading ( $t=215.0\text{mm}$ ).

### 6.3. CHARACTERISTIC BEARING STRENGTH OF MASONRY ( $f'_{cb}$ )

The relationship between compressive strength of masonry under concentrated load in terms of unit brick strength,  $f_b$ , for a given loaded area ratio,  $A_r$ , has been represented by an expression of the form:

$$f_{cb} = k.f_b^n \quad (6.3)$$

The results obtained from tests on brickwork types A, B, C and D have been analysed statistically and the mean bearing strength curves determined assuming an expression as above. The standard deviation of the mean curve is calculated and hence the characteristic bearing strength  $f'_{cb}$  curve at 95% confidence limit assuming normal distribution.

The results for 102.5mm thick specimens constructed using mortar grade M(i) tested under central strip concentrated load for loaded area ratios of 0.1, 0.2, 0.3 and 0.4 are shown graphically in Figs. 6.29 to 6.32 respectively. The equations obtained for the mean and characteristic curves are presented in Table 6.2 together with the equations for the mean and characteristic compressive strengths of masonry corresponding to  $A_r = 1.0$  for comparison.

$A_r$	Equation of the mean bearing strength	Equation of characteristic bearing strength
0.1	$f_{cb}=2.400f_b^{0.725}$	$f'_{cb}=1.770f_b^{0.725}$
0.2	$f_{cb}=2.900f_b^{0.570}$	$f'_{cb}=2.190f_b^{0.570}$
0.3	$f_{cb}=2.710f_b^{0.540}$	$f'_{cb}=2.090f_b^{0.540}$
0.4	$f_{cb}=2.880f_b^{0.515}$	$f'_{cb}=2.240f_b^{0.515}$
1.0	$f_{mm}=1.216f_b^{0.699*}$	$f_k=1.779f_b^{0.532}$
*	This equation has been derived based on the experimental results of crushing tests of brickwork masonry control specimens under uniform compressive load applied over the whole cross-sectional area.	

Table 6.2 - Equations for mean and characteristic bearing strength of brickwork in terms of brick strength for different loaded area ratios.

The results show that the characteristic bearing strength is 75% of the mean bearing strength. Figs. 6.33 and 6.34 have been included which show that as the bearing area decreases, the bearing strength increases. This increase is quite significant when the loaded area ratio is less than 0.25, and when this ratio reaches a value of 0.5 (i.e. when half of the cross-sectional area is

loaded) the characteristic bearing strength,  $f'_{cb}$  approaches the characteristic compressive strength of masonry,  $f_k$ . The increase in bearing strength from  $A_r=0.4$  to  $A_r=0.3$ ,  $0.2$  and  $0.1$  is 4%, 25% and 90% respectively at  $f_b=50 \text{ Nmm}^{-2}$  and this enhancement in strength increases to 5.5%, 30% and 120% respectively for  $f_b=100 \text{ Nmm}^{-2}$ . This increase may be shown to be function of unit brick strength,  $f_b$ , when the loaded area is small as shown in Fig. 6.35.

#### 6.4. FACTORS AFFECTING THE BEARING STRENGTH

The parameters which have an effect on the bearing strength of masonry and their influence on the enhancement factor under concentrated load which have been studied experimentally will be examined in this section.

##### 6.4.1. Loaded area ratio, $A_r$

The importance of this parameter has become obvious from the figures already presented in this chapter. To establish a relationship between loaded area ratio ( $A_r$ ) and enhancement factor ( $\zeta$ ), the results of tests carried out under the action of concentrated strip loading have been sorted into three categories depending on the position of loading. No differentiation has been made between the strength of units, mortar mix or thickness of the specimens, but the length and the height of the specimens were kept constant. An expression in the form:

$$\zeta = k.A_r^n \quad (6.4)$$

have been considered. The data have been analysed statistically and the equations for the mean curve ( $\zeta$ ) and the 95% lower limit curve ( $\zeta'$ ) are presented in Table 6.3 and in graphical form in Figs. 6.36 to 6.38 for central, intermediate and end strip loading respectively, ( $A_r \leq 0.5$ ).

Loading type	Equation of mean curve	Equation of 95% lower confidence level	No. of specimens tested
Central Strip	$\zeta = 1.126 A_r^{-0.371}$	$\zeta' = 0.806 A_r^{-0.371}$	241
Interm. Strip	$\zeta = 1.187 A_r^{-0.309}$	$\zeta' = 0.837 A_r^{-0.309}$	94
End Strip	$\zeta = 1.182 A_r^{-0.264}$	$\zeta' = 0.876 A_r^{-0.264}$	115

Table 6.3 - Relationships for enhancement factor in terms of loaded area ratio.



**BEARING STRENGTH OF MASONRY AS A FUNCTION  
OF BRICK STRENGTH, LOADED AREA RATIO = 0.1**

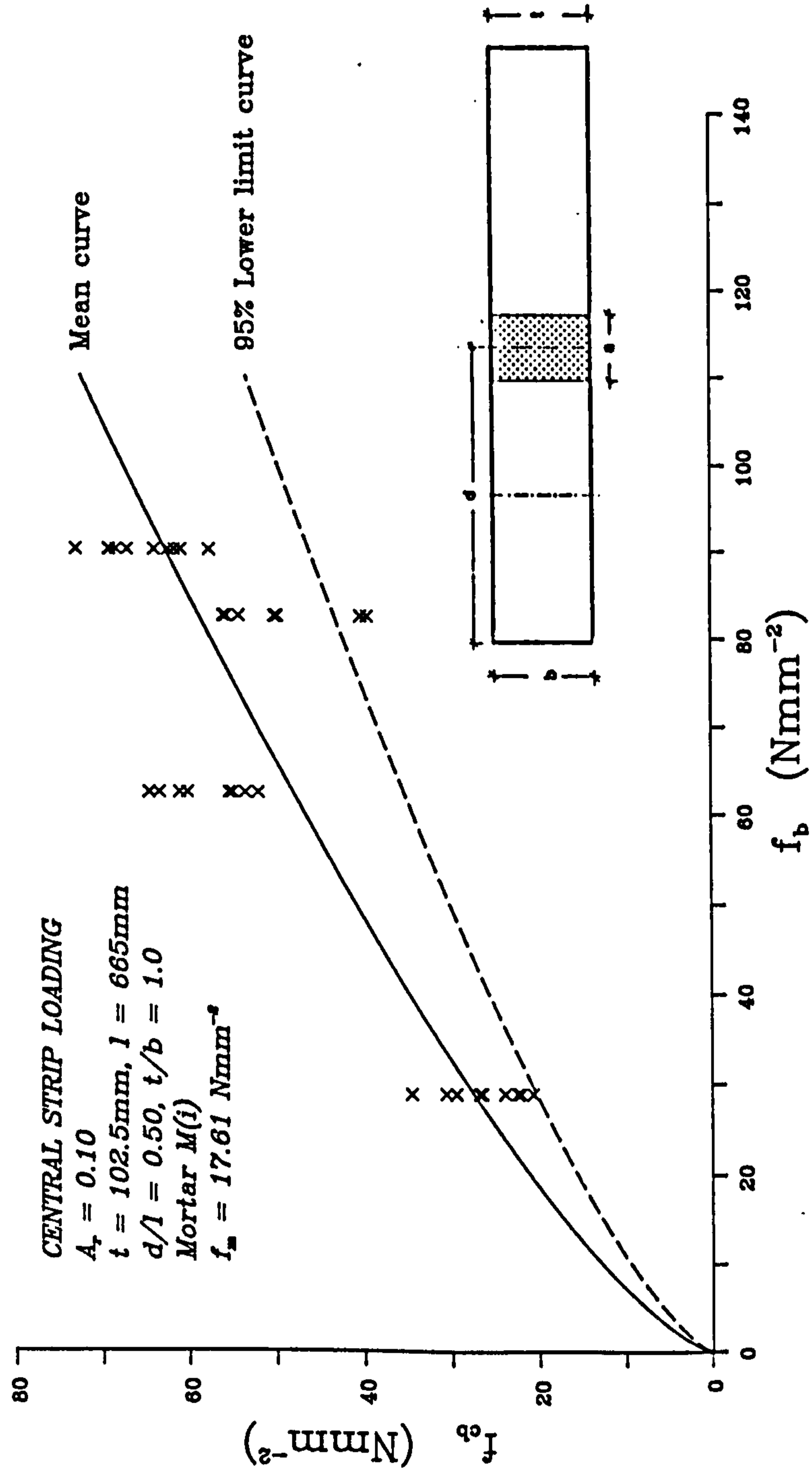


Fig. 6.29 - Bearing strength of brickwork masonry in terms of brick strength under central strip loading ( $A_r=0.10$ ).

**BEARING STRENGTH OF MASONRY AS A FUNCTION  
OF BRICK STRENGTH, LOADED AREA RATIO 0.2**

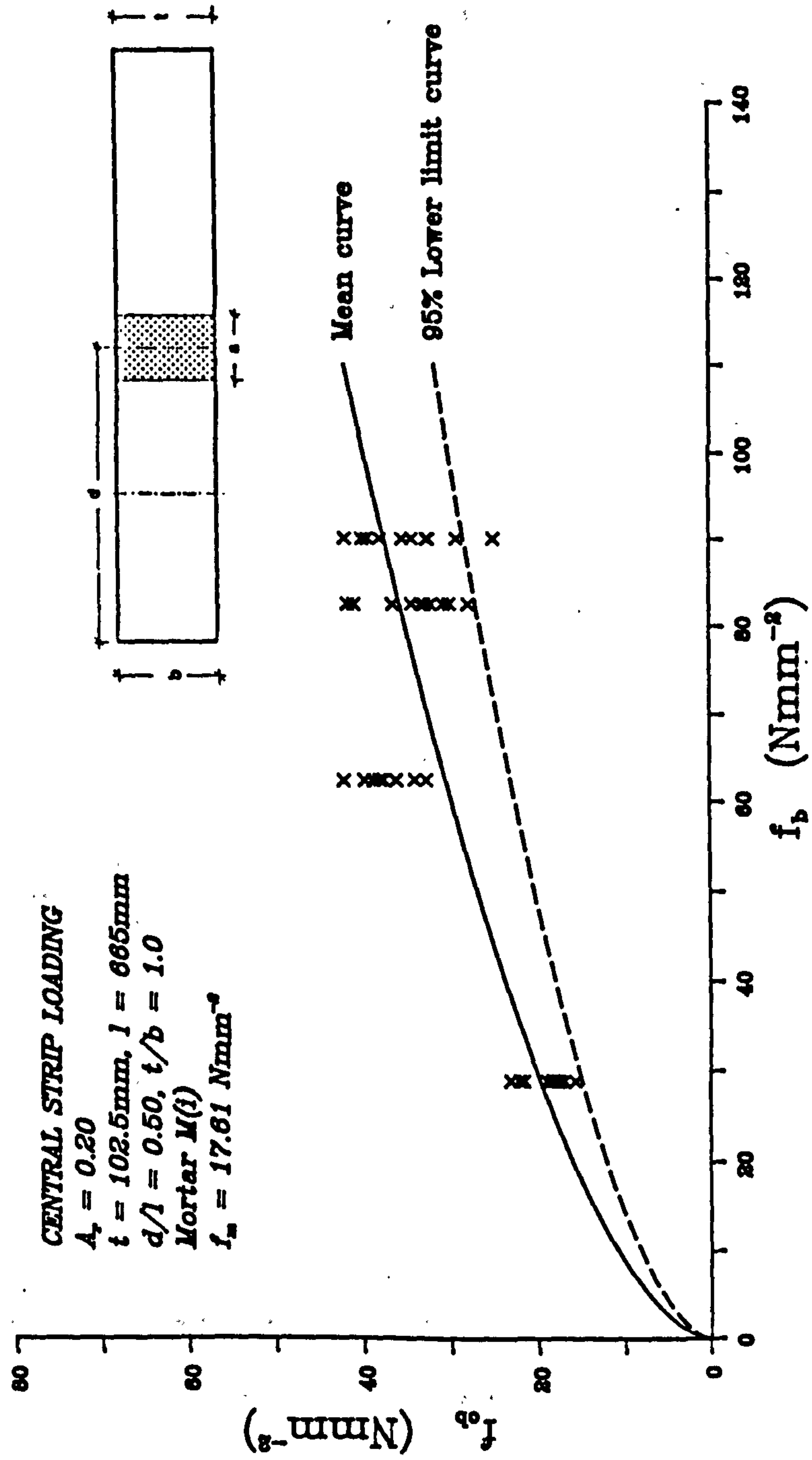


Fig. 6.30 - Bearing strength of brickwork masonry in terms of brick strength under central strip loading ( $A_r=0.20$ ).

**BEARING STRENGTH OF MASONRY AS A FUNCTION OF BRICK STRENGTH, LOADED AREA RATIO=0.3**

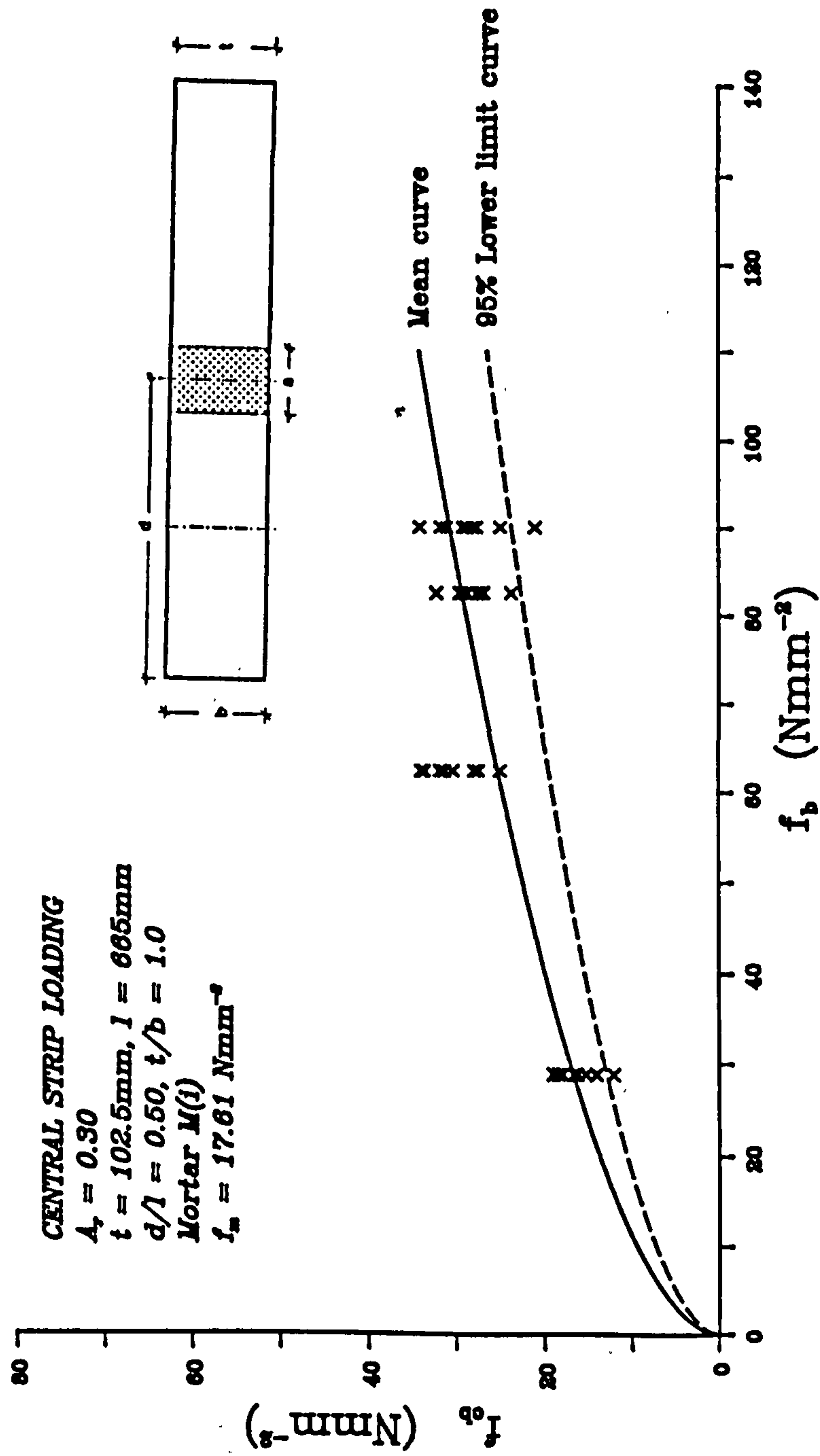


Fig. 6.31 - Bearing strength of brickwork masonry in terms of brick strength under central strip loading ( $A_r=0.30$ ).

**BEARING STRENGTH OF MASONRY AS A FUNCTION  
OF BRICK STRENGTH, LOADED AREA RATIO = 0.4**

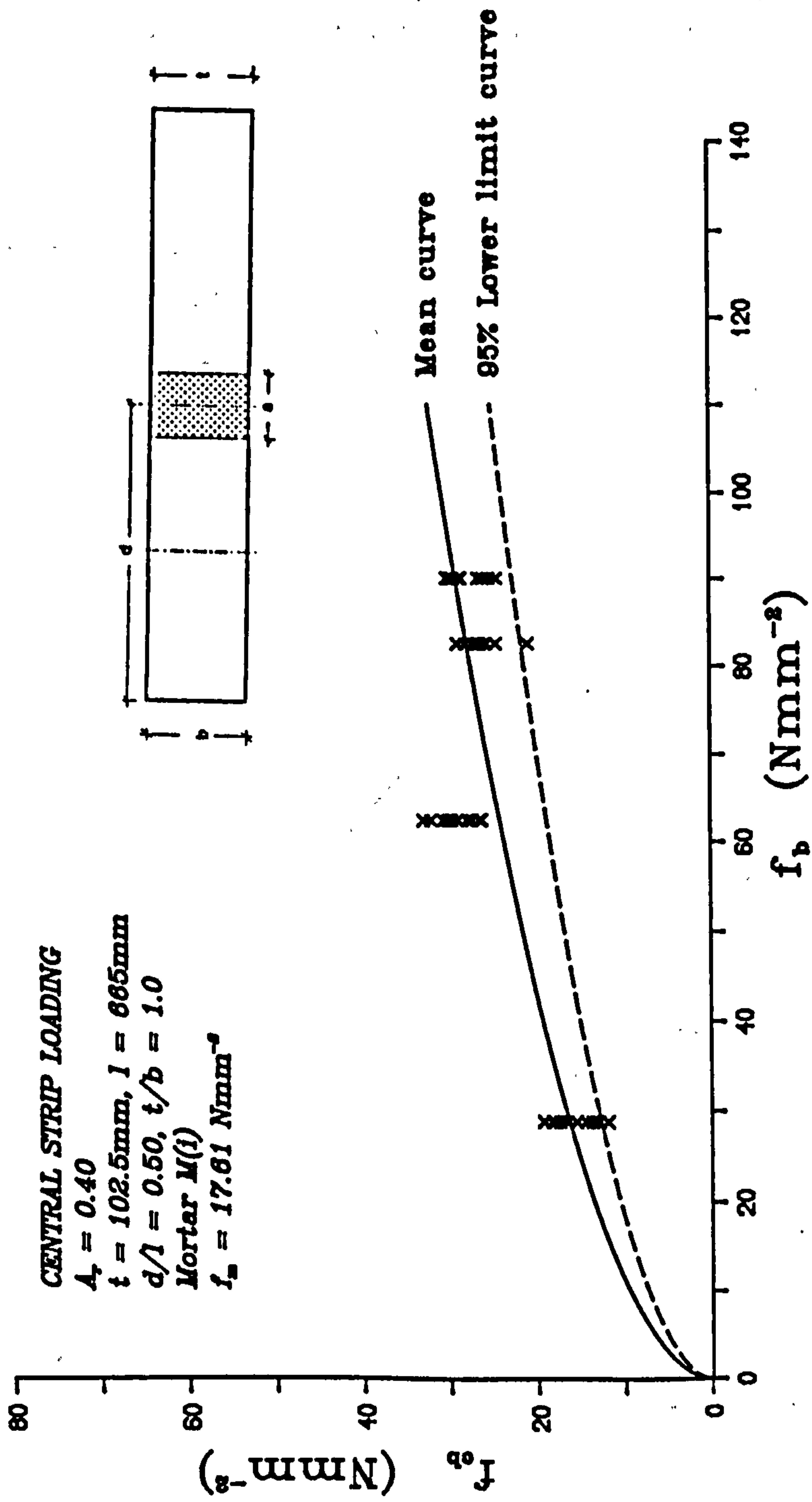


Fig. 6.32 - Bearing strength of brickwork masonry in terms of brick strength under central strip loading ( $A_r=0.40$ ).

**BEARING STRENGTH OF MASONRY AS A FUNCTION  
OF BRICK STRENGTH AND LOADED AREA RATIO**

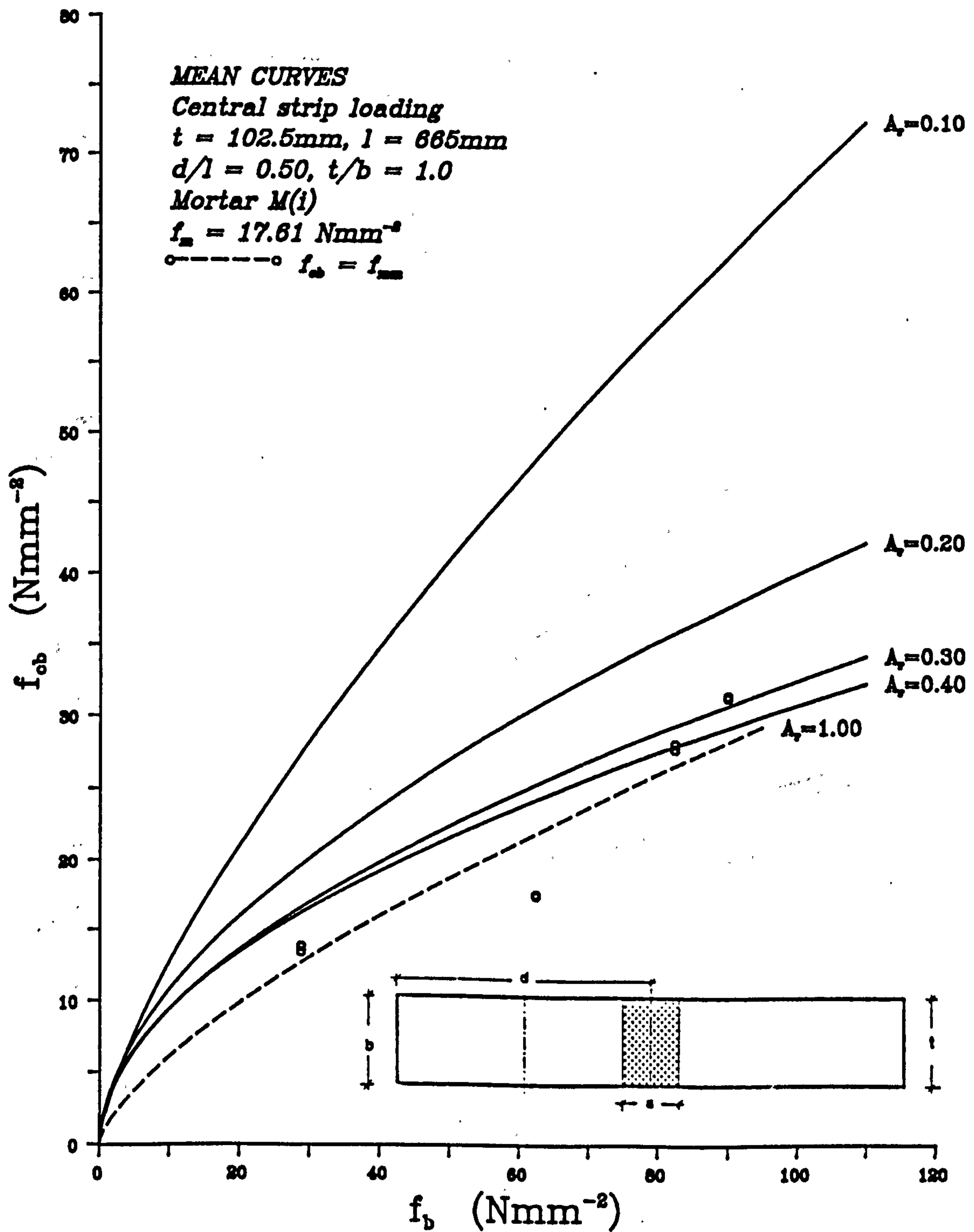


Fig. 6.33 - Mean bearing strength of brickwork masonry in terms of brick strength and loaded area ratios under central strip loading.

**BEARING STRENGTH OF MASONRY AS A FUNCTION  
OF BRICK STRENGTH AND LOADED AREA RATIO**

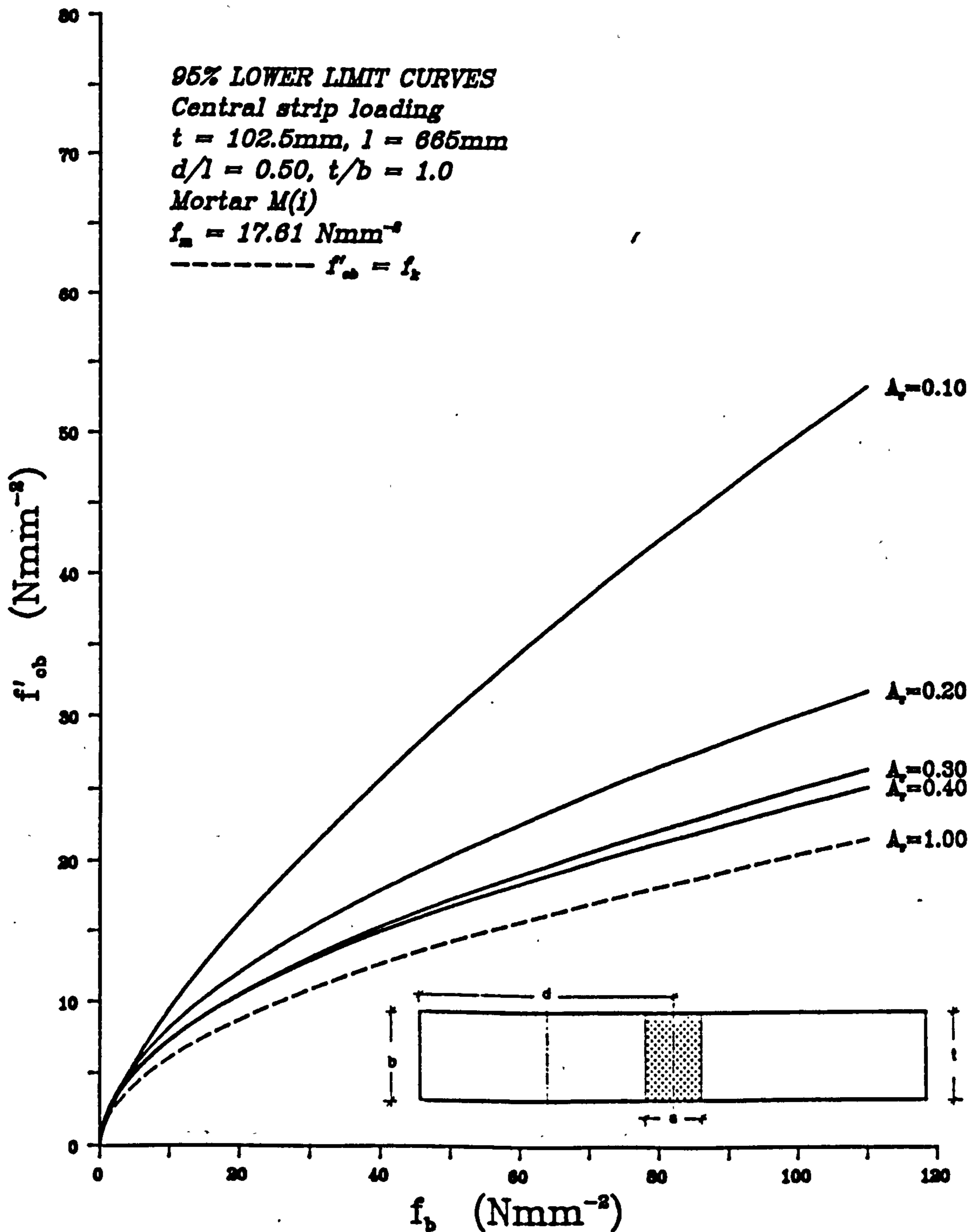


Fig. 6.34 - Characteristic bearing strength of masonry in terms of brick strength and loaded area ratios under central strip loading.

**ENHANCEMENT FACTOR AS A FUNCTION OF UNIT  
BRICK STRENGTH AND LOADED AREA RATIO**

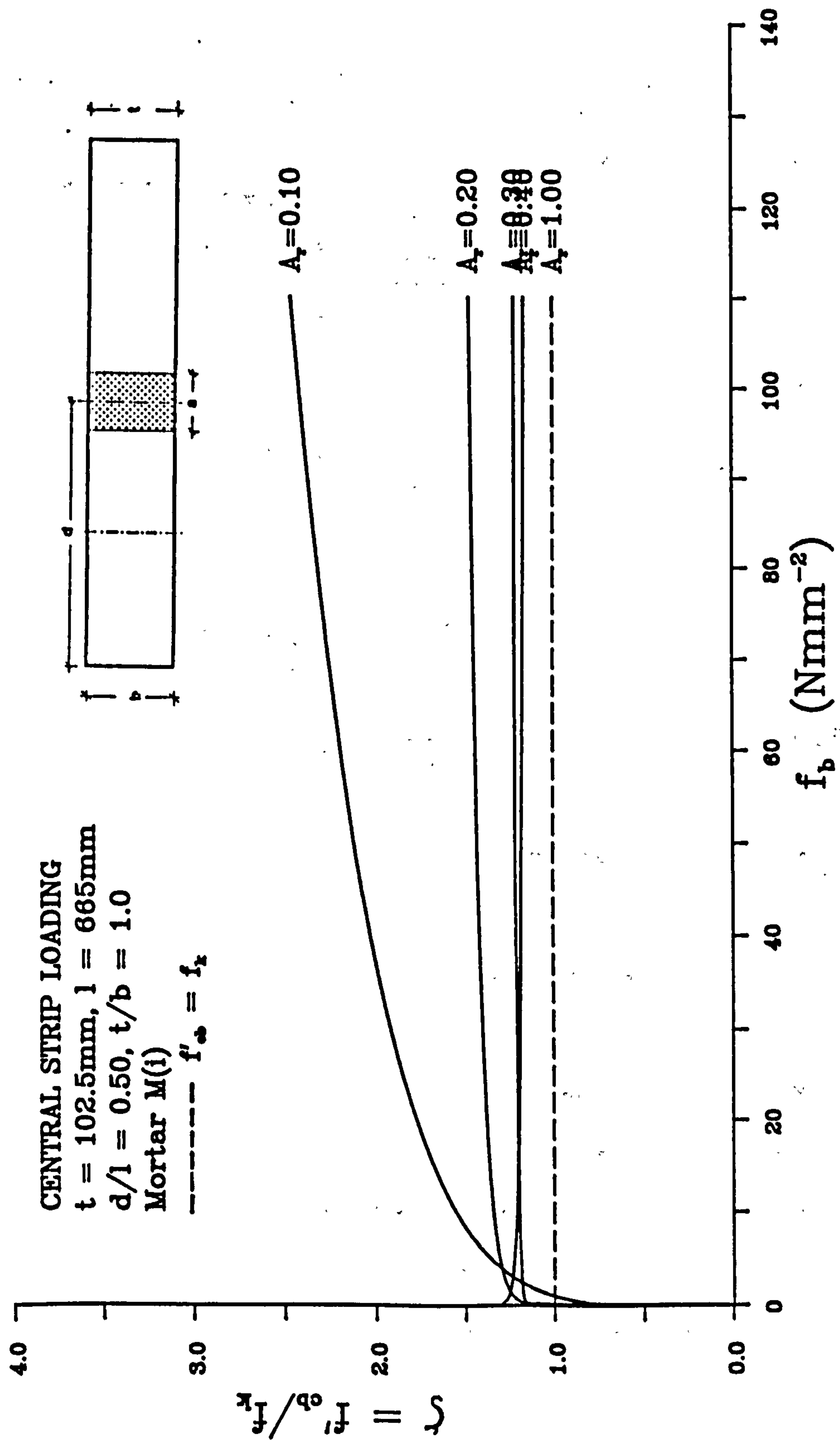


Fig. 6.35 - Enhancement factor in terms of brick strength and loaded area ratios under central strip loading.

**EFFECT OF LOADED AREA RATIO ON ENHANCEMENT FACTOR**

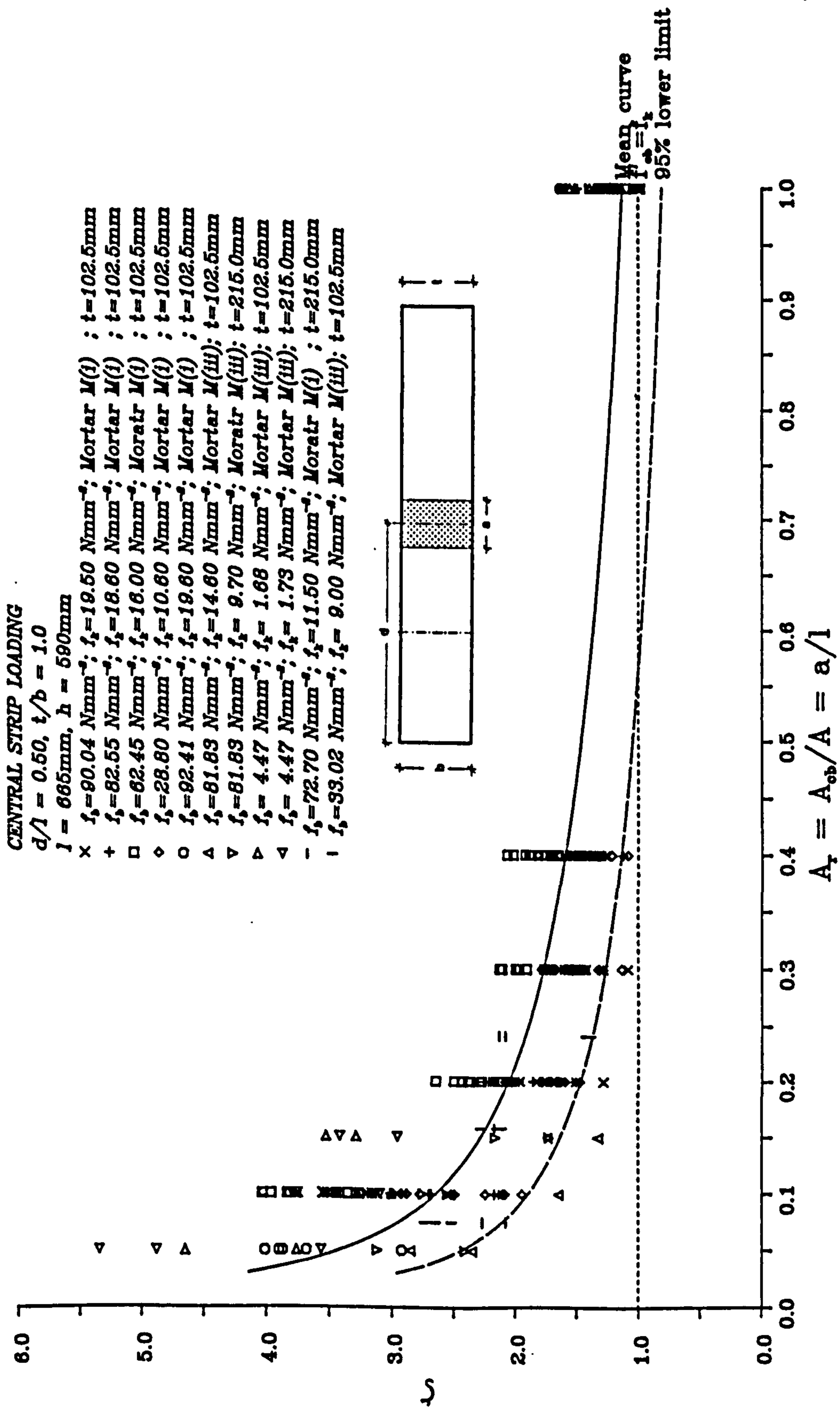


Fig. 6.36 - Influence of loaded area ratio on enhancement factor under central strip loading.



### EFFECT OF LOADED AREA RATIO ON ENHANCEMENT RATIO

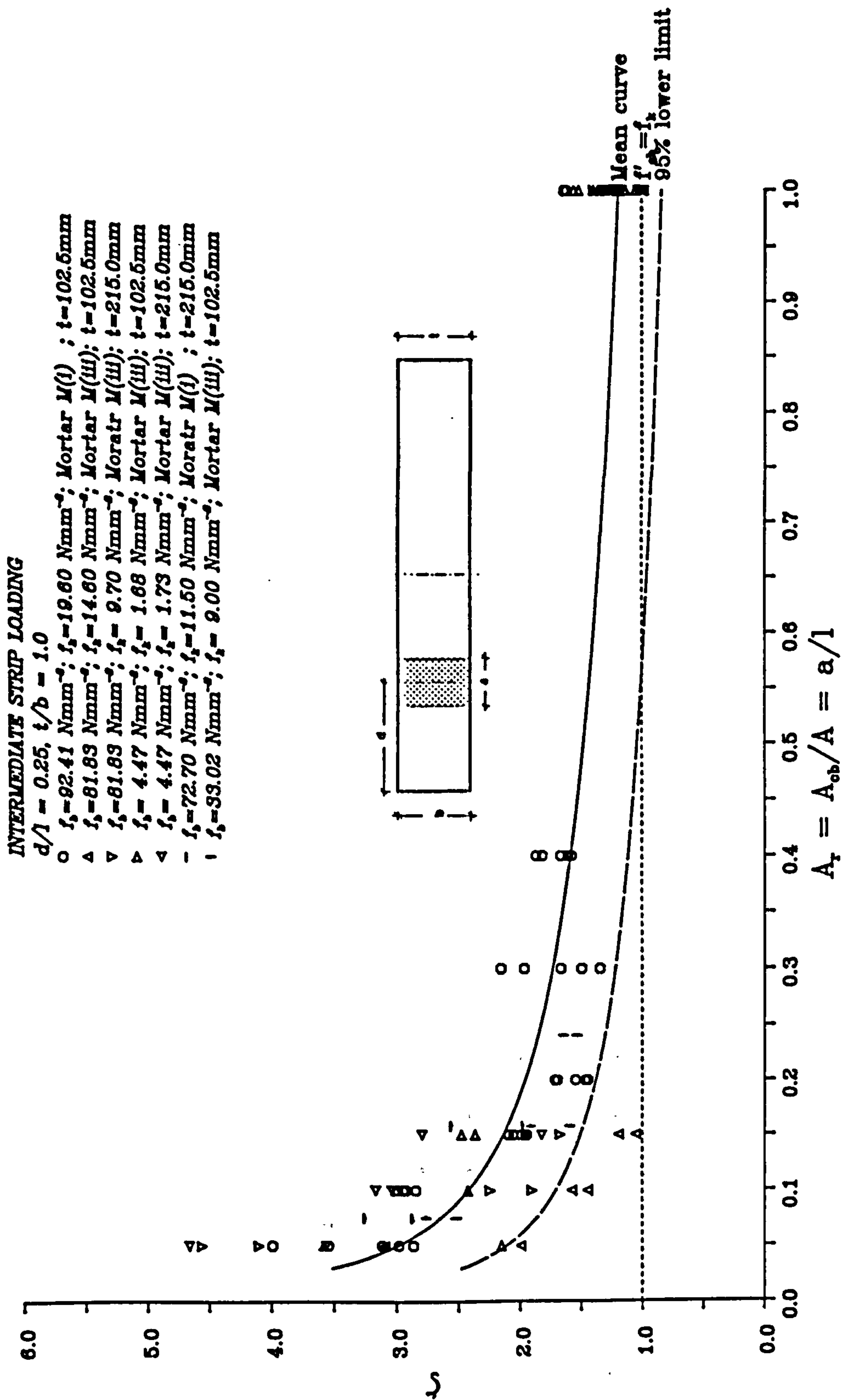


Fig. 6.37 - Influence of loaded area ratio on enhancement factor under intermediate strip loading.

**EFFECT OF LOADED AREA RATIO ON ENHANCEMENT FACTOR**

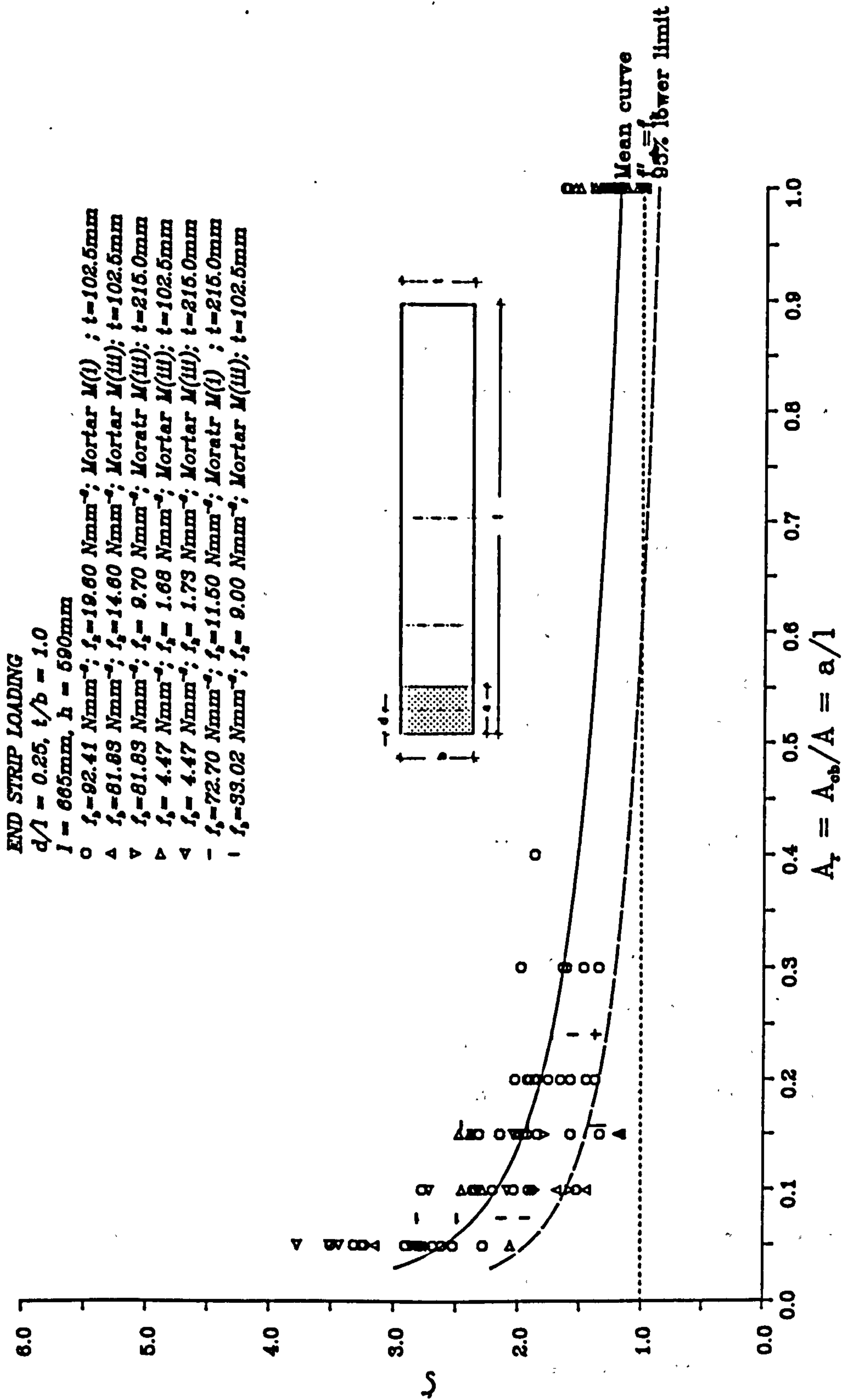


Fig. 6.38 - Influence of loaded area ratio on enhancement factor under end strip loading.

It is conclusive from Figs. 6.36 and 6.38 that no increase in bearing strength is justified when  $A_r \geq 0.5$ , and when  $A_r \leq 0.5$  increase in bearing strength is warranted depending on the loading position.

#### 6.4.2. Masonry and its constituent materials strengths

The effect of brick strength on the bearing strength of masonry has already been covered in section 6.3, Figs. 6.29 to 6.35. These figures show that as the unit strength increases, the bearing strength increases. This increase in strength is however dependent on the loaded area ratio ( $A_r$ ). As loaded area ratio decreases, the bearing strength increases. Fig. 6.34 could be used as a design chart for masonry constructed with mortar designation M(i), 102.5mm in thickness under central strip loading configuration.

As brick and mortar strength ultimately influence the brickwork strength, therefore any increase in the strengths of brick and/or mortar would give rise to higher bearing strength under concentrated load. This has been indicated in Figs. 6.39 to 6.41 which show bearing strength of masonry in terms of loaded area ratio  $A_r$ , and the characteristic compressive strength  $f_k$ , under central, intermediate and end strip loading positions. It is evident from these plots that higher  $f_k$  values give higher bearing strength.

However, the increase in  $f_k$  value is not so clearly pronounced in Figs. 6.42 to 6.44 which shows the influence of  $f_k$  on the enhancement factor.

It would appear that higher  $f_k$  values will result in the higher enhancement factor ( $\zeta$ ). This may be seen from Figs. 6.42 to 6.44 in the region where  $A_r$  is small. The lower tails of the curves do not show this trend consistently which could be explained by the fact that only few specimens were tested for  $A_r=1.0$ .

#### 6.4.3. Masonry thickness

The effect of masonry thickness has been studied from the results of tests on brickwork types F and G. Two thicknesses, single leaf 102.5mm and bonded masonry 215.0mm have been investigated under the action of central, intermediate and end strip loading. The results have been plotted and are as shown in Figs. 6.45 to 6.47 for clay brickwork type F and Figs. 6.48 to 6.50 for AAC brickwork type G under central, intermediate and end strip concentrated loads respectively.

**BEARING STRENGTH OF MASONRY AS A FUNCTION OF  $A_r$  AND  $f_b$**

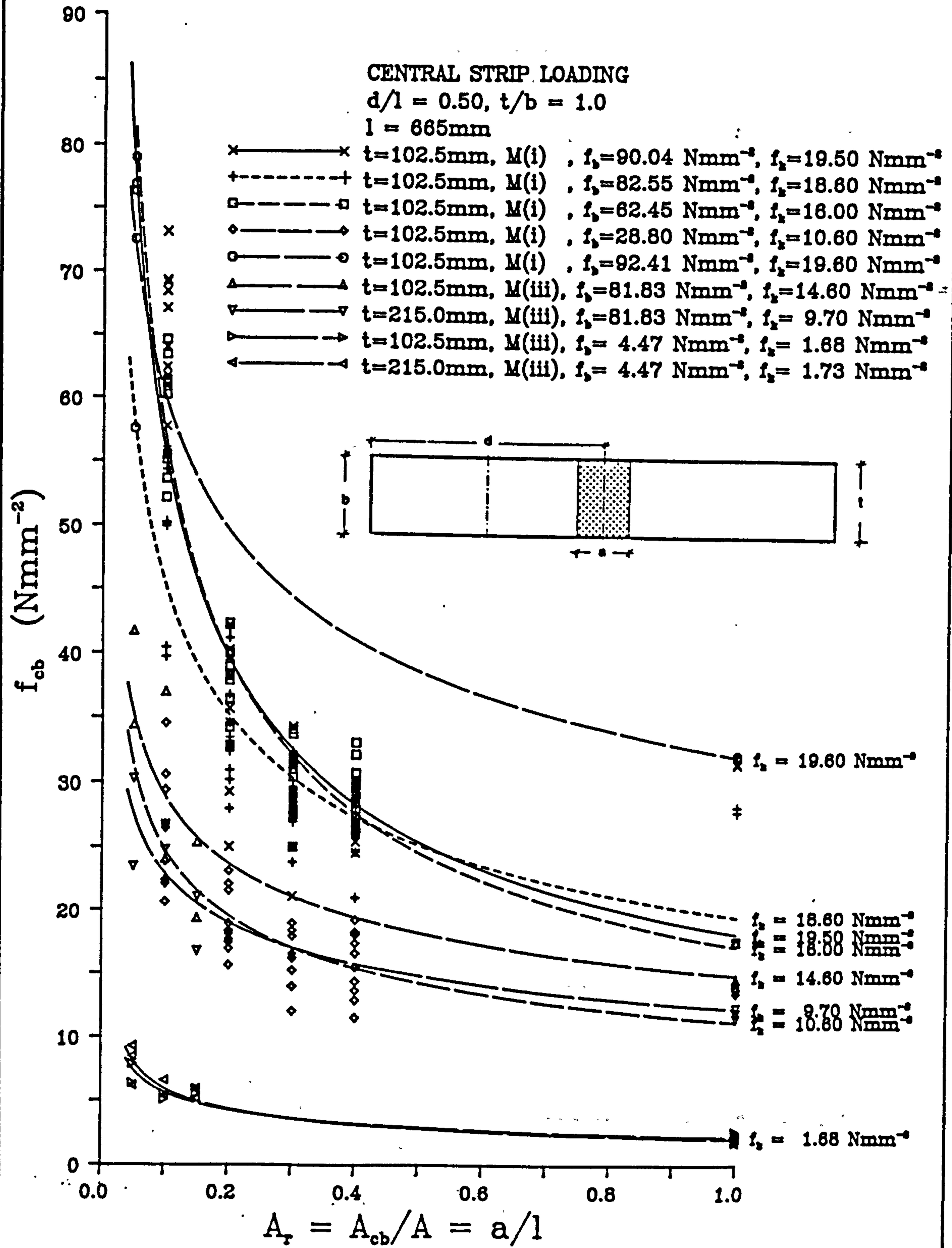


Fig. 6.39 - Influence of characteristic compressive strength of masonry on the bearing strength under central strip loading.

**BEARING STRENGTH OF MASONRY AS A FUNCTION  
OF  $A_T$  AND  $f_b$**

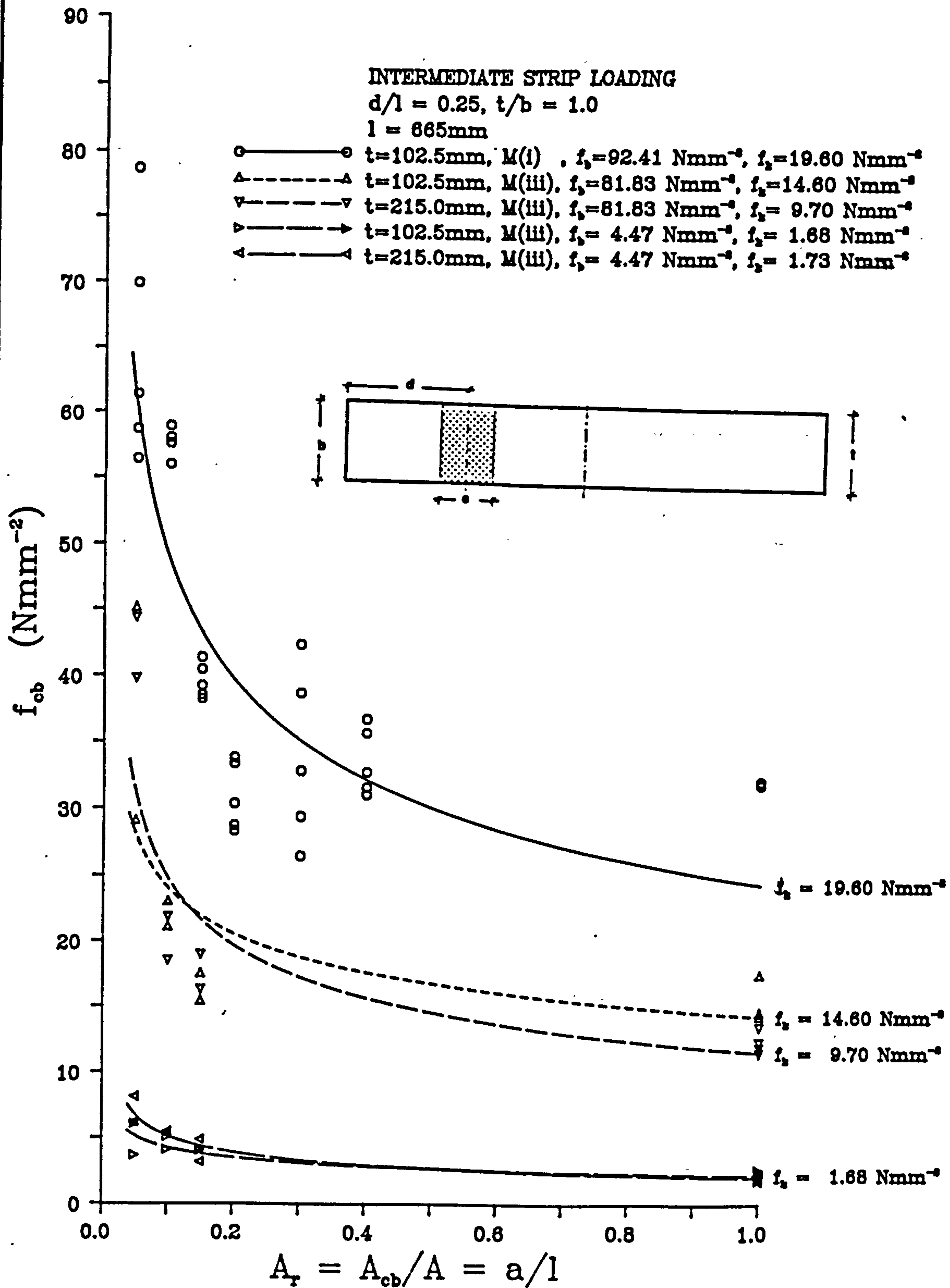


Fig. 6.40 - Influence of characteristic compressive strength of masonry on the bearing strength under intermediate strip loading.

**BEARING STRENGTH OF MASONRY AS A FUNCTION  
OF  $A_r$  AND  $f_b$**

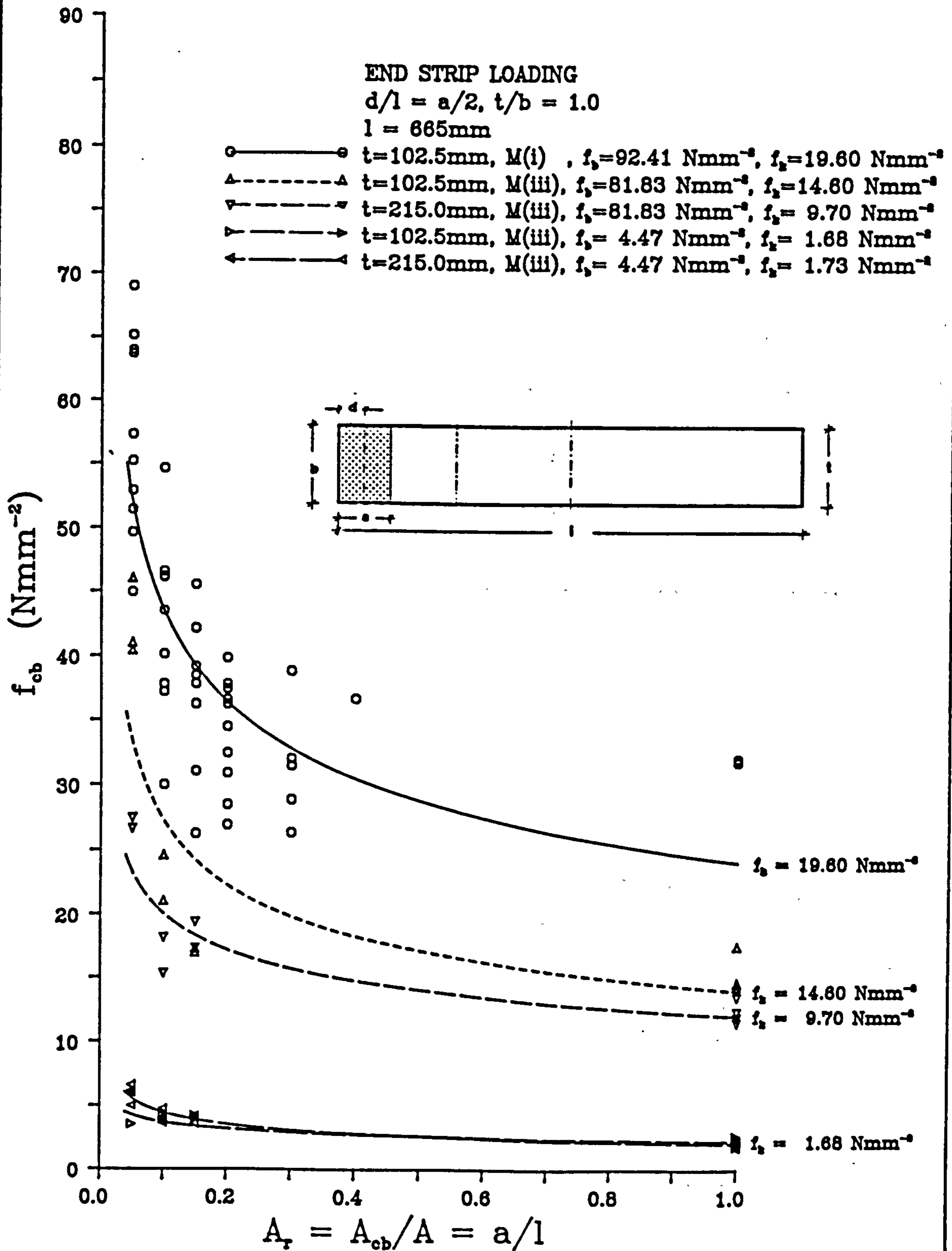


Fig. 6.41 - Influence of characteristic compressive strength of masonry on the bearing strength under end strip loading.

### ENHANCEMENT FACTOR AS A FUNCTION OF $A_r$ AND $f_c$

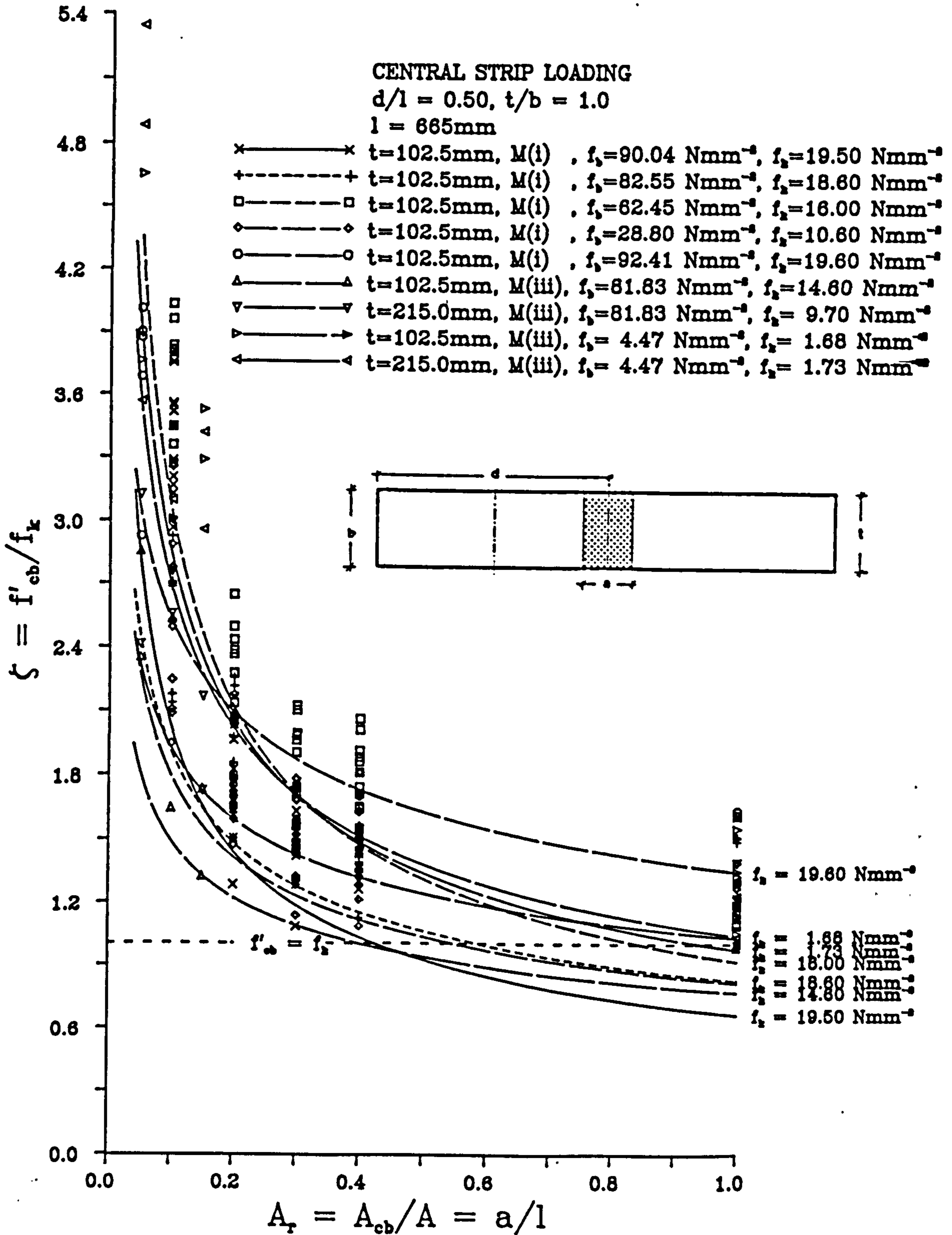


Fig. 6.42 - Influence of characteristic compressive strength of masonry on the enhancement factor under central strip loading.

### ENHANCEMENT FACTOR AS A FUNCTION OF $A_r$ AND $f_c$

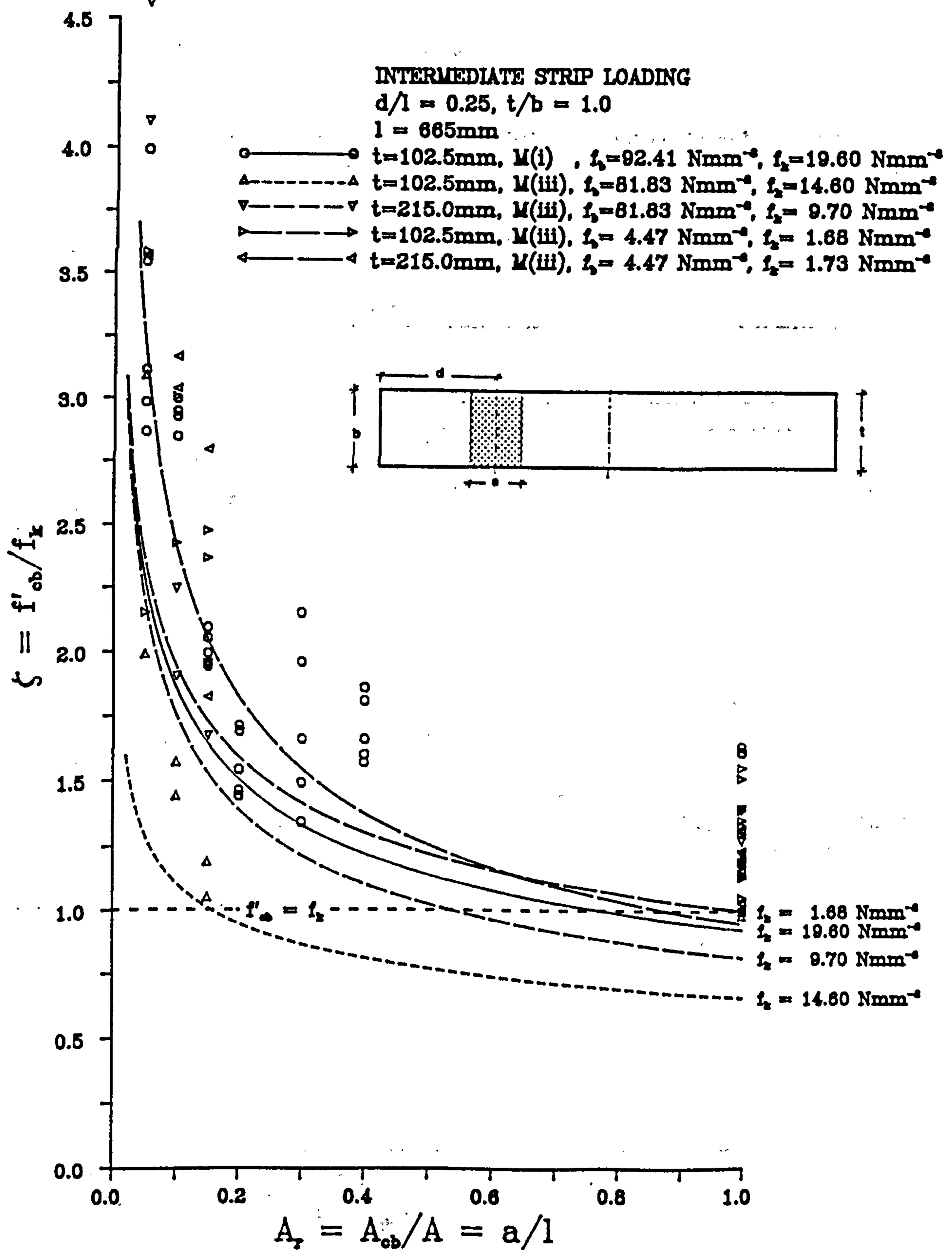


Fig. 6.43 - Influence of characteristic compressive strength of masonry on the enhancement factor under intermediate strip loading.



### ENHANCEMENT FACTOR AS A FUNCTION OF $A_r$ AND $f_c$

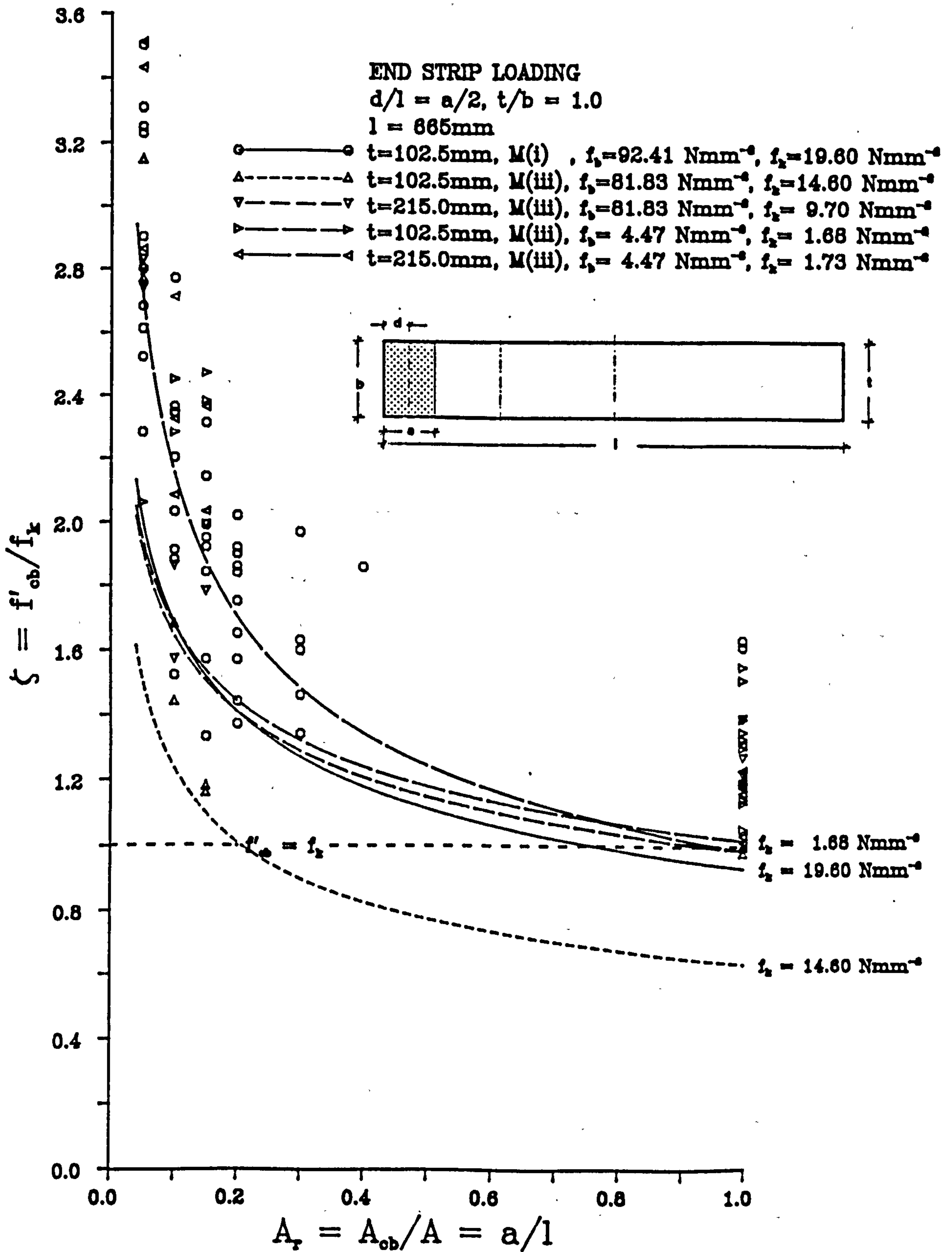


Fig. 6.44 - Influence of characteristic compressive strength of masonry on the enhancement factor under end strip loading.

**EFFECT OF MASONRY THICKNESS ON ITS BEARING STRENGTH**

**CENTRAL STRIP LOADING**

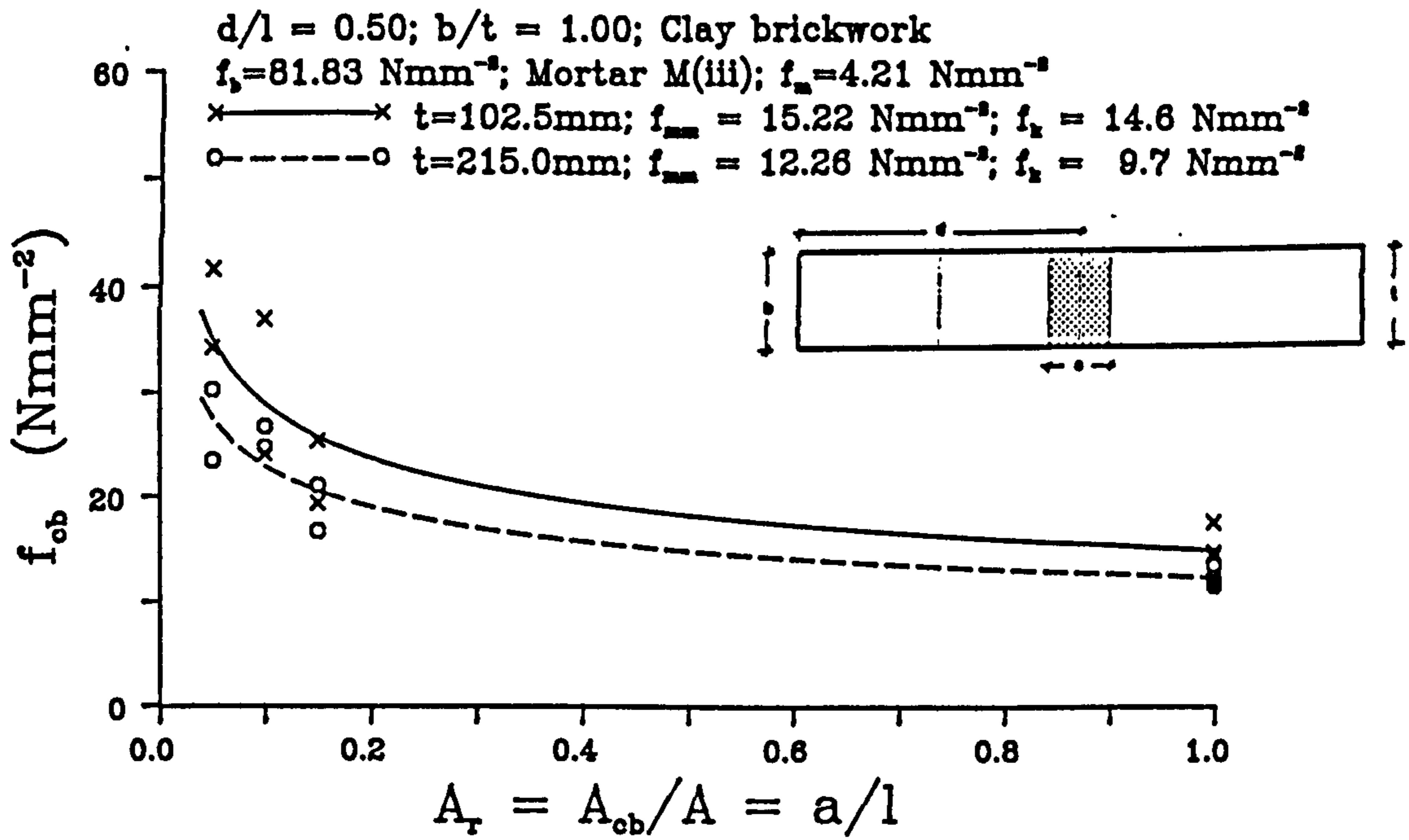


Fig. 6.45 - Effect of specimen thickness on the bearing strength of brickwork type F under central strip loading.

**EFFECT OF MASONRY THICKNESS ON ITS BEARING STRENGTH**

**INTERMEDIATE STRIP LOADING**

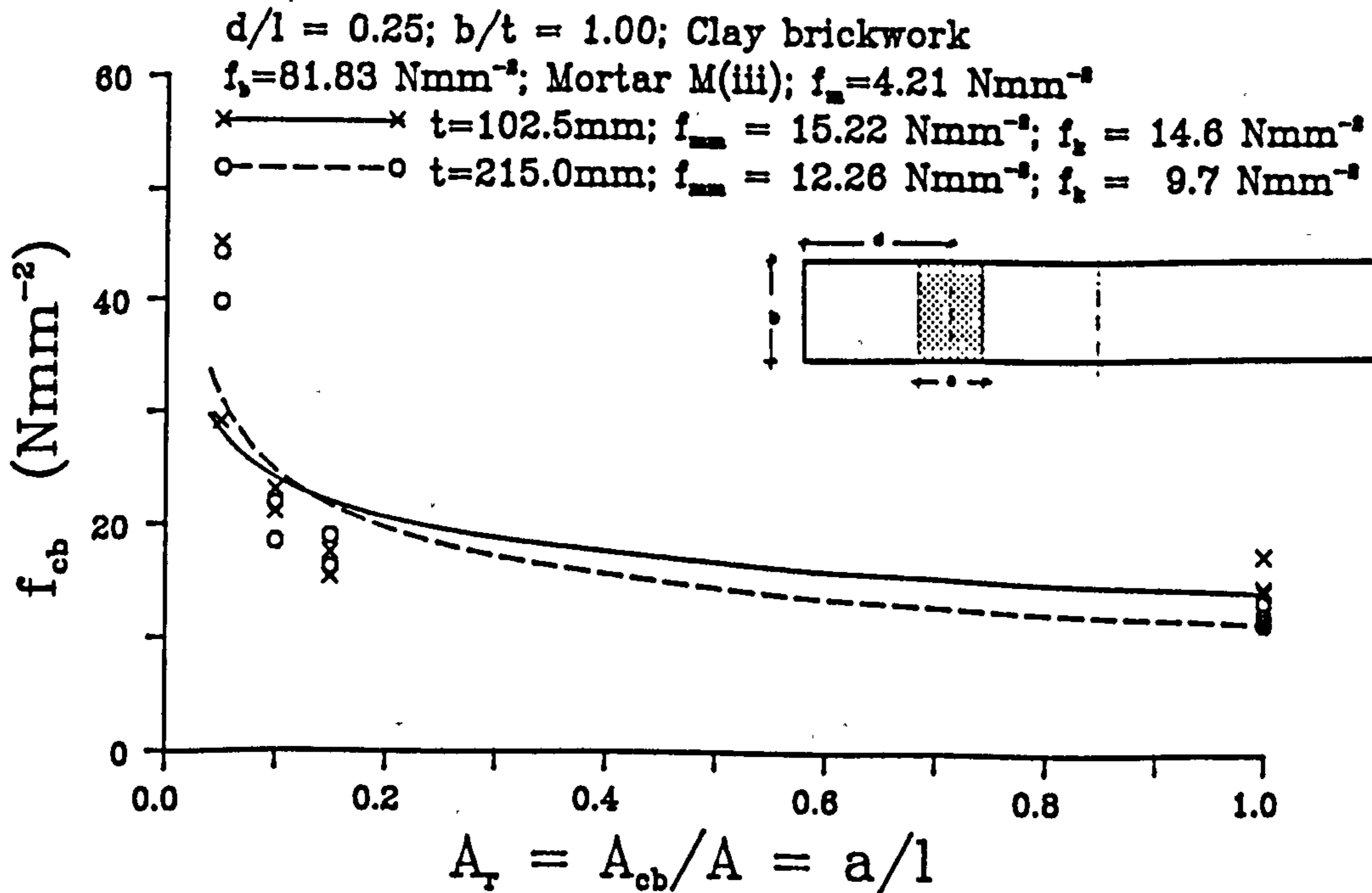


Fig. 6.46 - Effect of specimen thickness on the bearing strength of brickwork type F under intermediate strip loading.

**EFFECT OF MASONRY THICKNESS ON ITS BEARING STRENGTH**

**END STRIP LOADING**

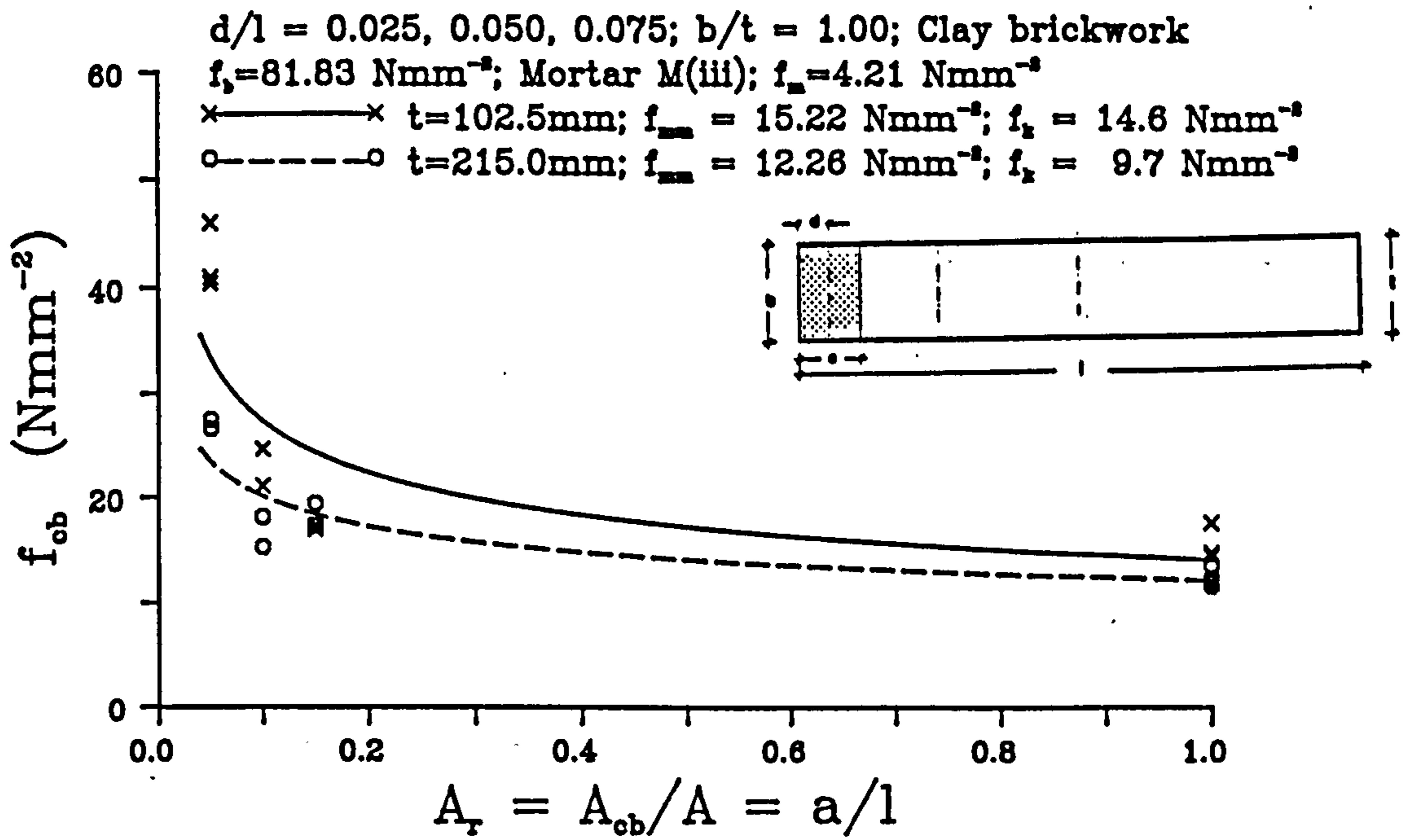


Fig. 6.47 - Effect of specimen thickness on the bearing strength of brickwork type F under end strip loading.

**EFFECT OF MASONRY THICKNESS ON ITS BEARING STRENGTH**

**CENTRAL STRIP LOADING**

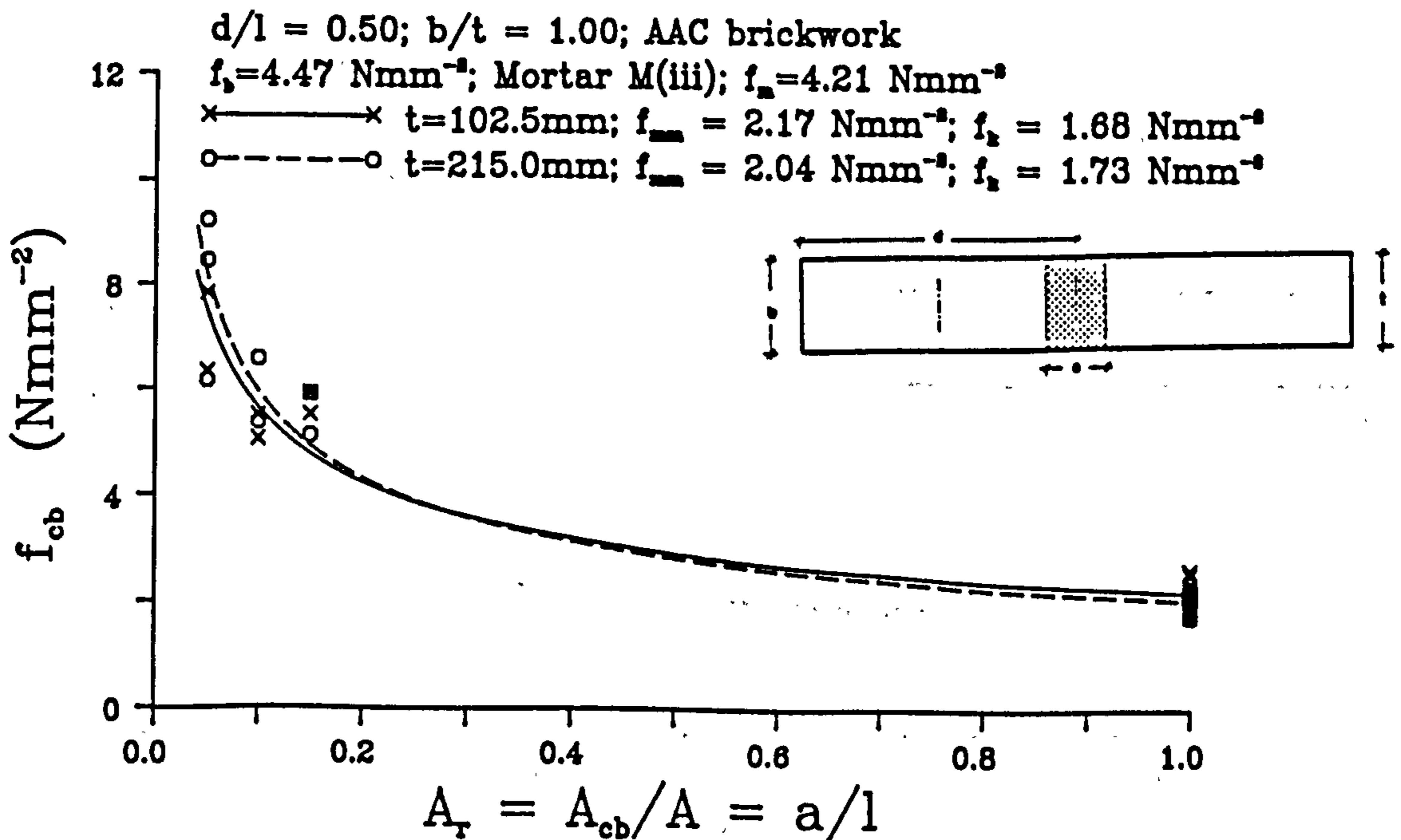


Fig. 6.48 - Effect of specimen thickness on the bearing strength of brickwork type G under central strip loading.

**EFFECT OF MASONRY THICKNESS ON ITS BEARING STRENGTH**

**INTERMEDIATE STRIP LOADING**

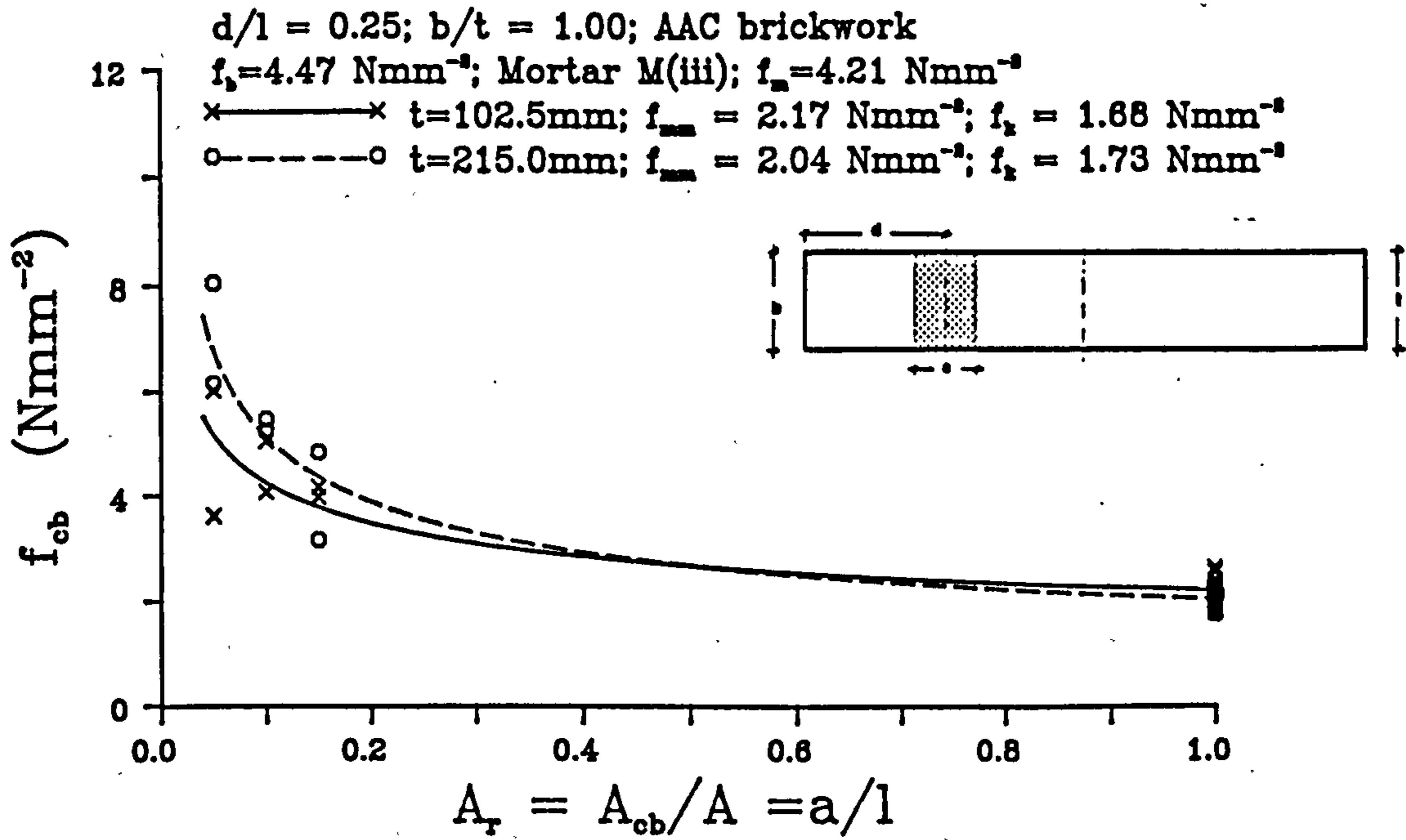


Fig. 6.49 - Effect of specimen thickness on the bearing strength of brickwork type G under intermediate strip loading.

**EFFECT OF MASONRY THICKNESS ON ITS BEARING STRENGTH**

**END STRIP LOADING**

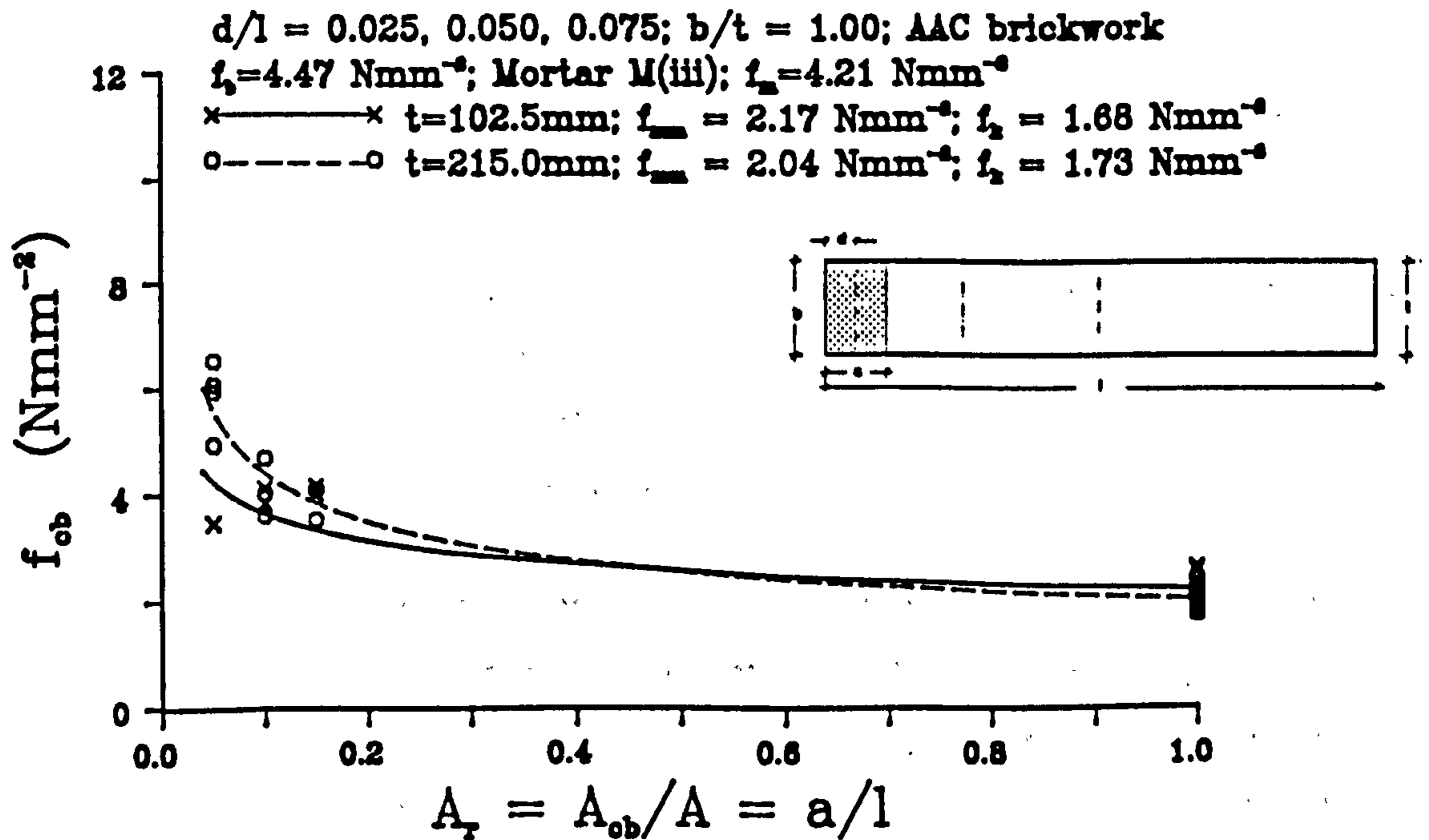


Fig. 6.50 - Effect of specimen thickness on the bearing strength of brickwork type G under end strip loading.

It is apparent from Figs. 6.45 to 6.47 that 102.5mm thick clay brickwork yields higher bearing strength in comparison to 215.0mm thick brickwork. This increase is approximately about 15-25% when  $A_r \leq 0.25$  under central and end strip loading. However, in the case of AAC brickwork the 215.0mm thick masonry gives higher bearing strength at low values of loaded area ratio ( $A_r \leq 0.25$ ). This increase in strength is not significant under central strip loading, but could be about 15-25% in the case of intermediate and end strip loading as shown in Figs. 6.48 to 6.50.

The effect of masonry thickness on the enhancement factor under central, intermediate and end strip loading for the two types of brickwork are presented in Figs. 6.51 to 6.56 respectively. These figures clearly show that 215.0mm thick specimens show higher values for the enhancement factor, even though the effect of specimen thickness has been taken into account in choosing a suitable value for  $f_k$ . Decrease of up to 30% in the value of enhancement factor has been observed in some cases when the specimen thickness has been decreased from 215.0mm to 102.5mm

#### 6.4.4. Aspect ratio

Effect of masonry aspect ratio ( $l/h$ ) for clay and AAC brickwork have been studied by keeping the height of specimens constant and varying the length. A bearing plate with cross-sectional area ( $a \times b$ ) of  $100 \times 102.5 \text{ mm}^2$  was used for clay brickwork and the effect of aspect ratio on the bearing strength and enhancement factor are as shown in Figs. 6.57 and 6.58 respectively. In the case of AAC brickwork, bearing plate with cross-sectional area ( $a \times b$ ) of  $225 \times 100 \text{ mm}^2$  was used and the results are presented in Figs. 6.59 and 6.60.

The results are not very decisive, but the inference is that the limiting value for aspect ratio (i.e. the  $l/h$  ratio beyond which this effect is not significant) is about 1.0 for clay and AAC brickwork. Ali and Page<sup>[70, 71]</sup> used value of 1.25 for  $l/h$  in their linear finite element analysis.

However, it should be mentioned that in this investigation only one specimen was tested under central strip concentrated load for a particular value of  $l/h$  for a given bearing plate dimension. Further work is needed to study the effect of bearing plate dimension on the bearing strength using fewer test specimens for a particular case.

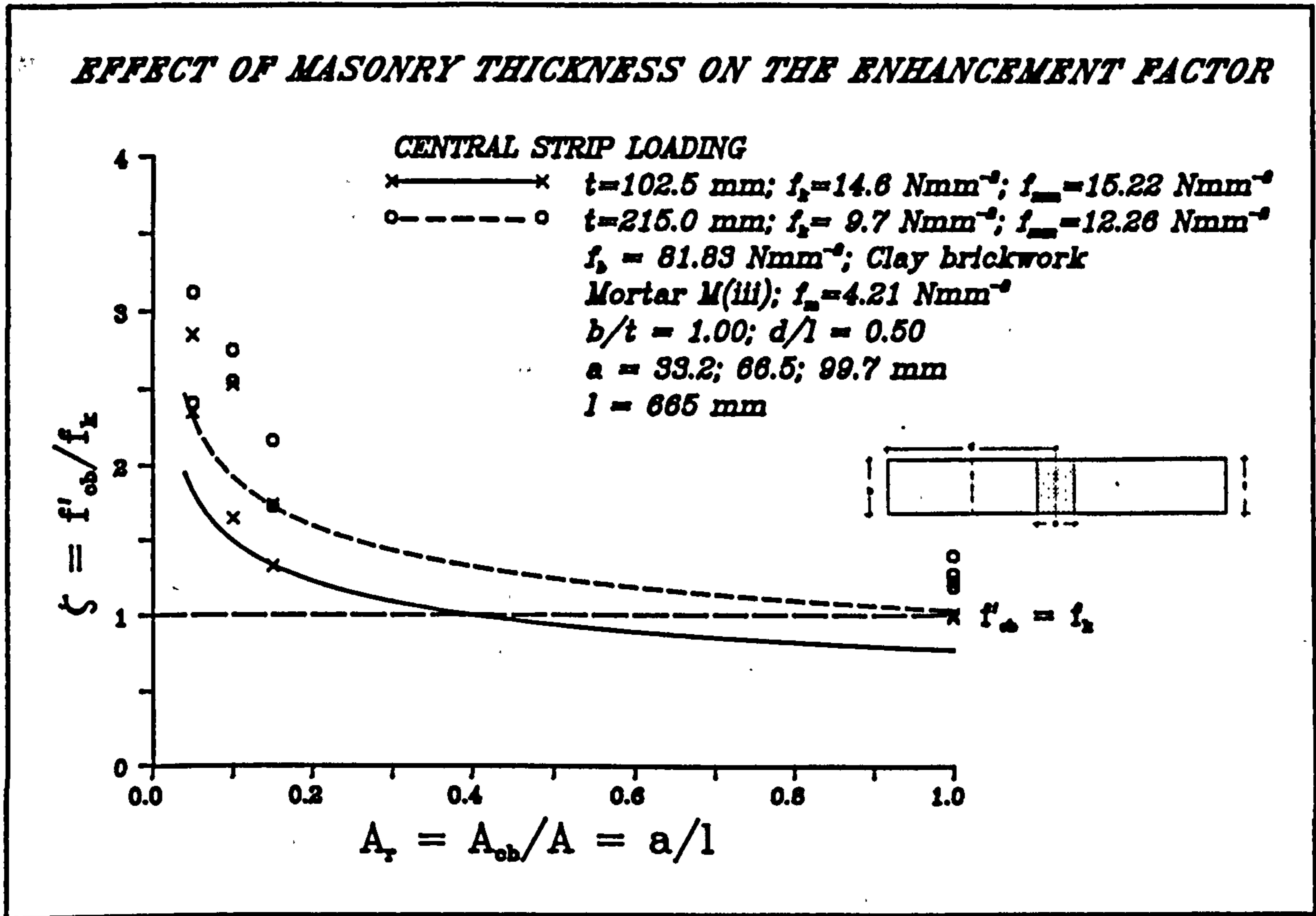


Fig. 6.51 - Effect of specimen thickness on the enhancement factor for brickwork type F under central strip loading.

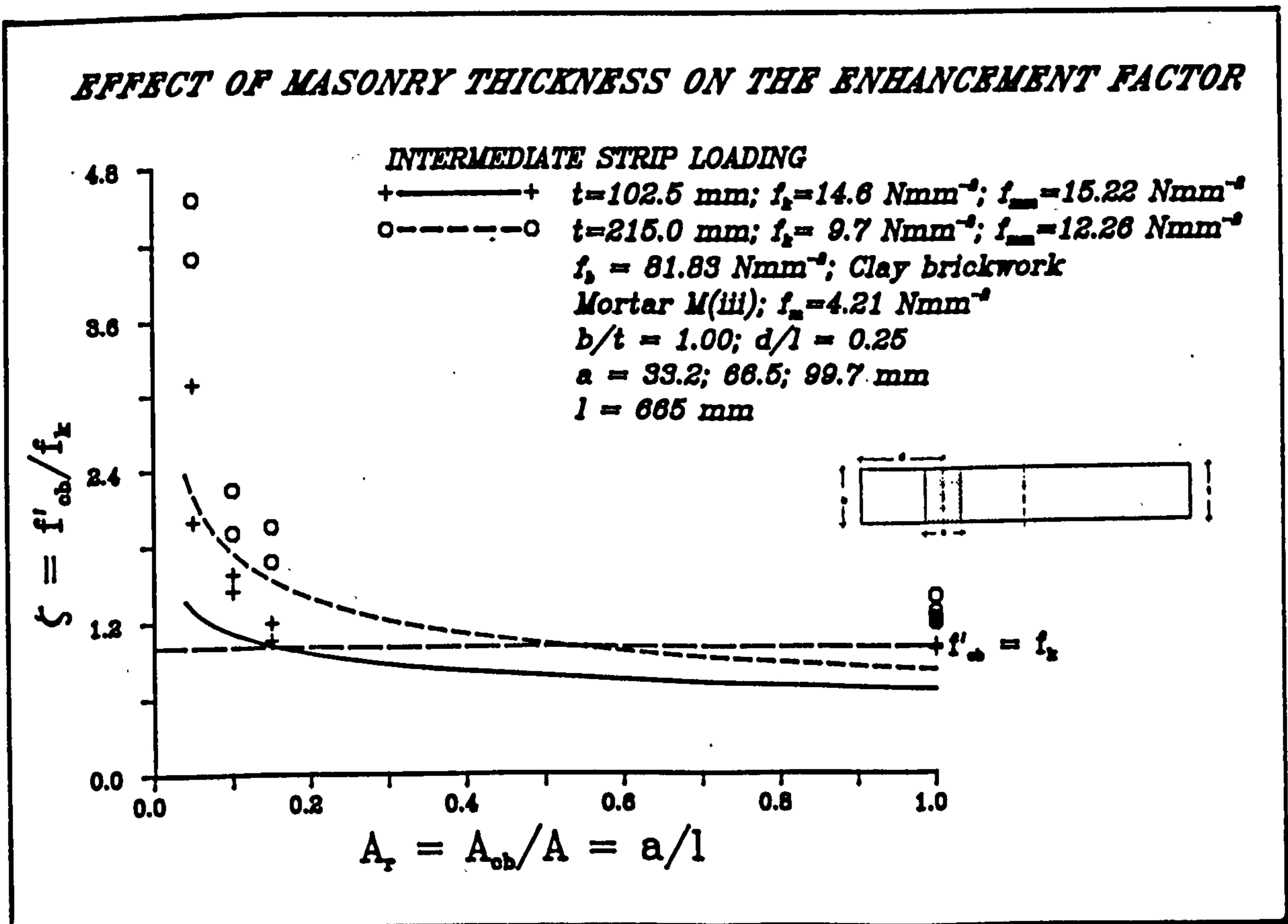


Fig. 6.52 - Effect of specimen thickness on the enhancement factor for brickwork type F under intermediate strip loading.

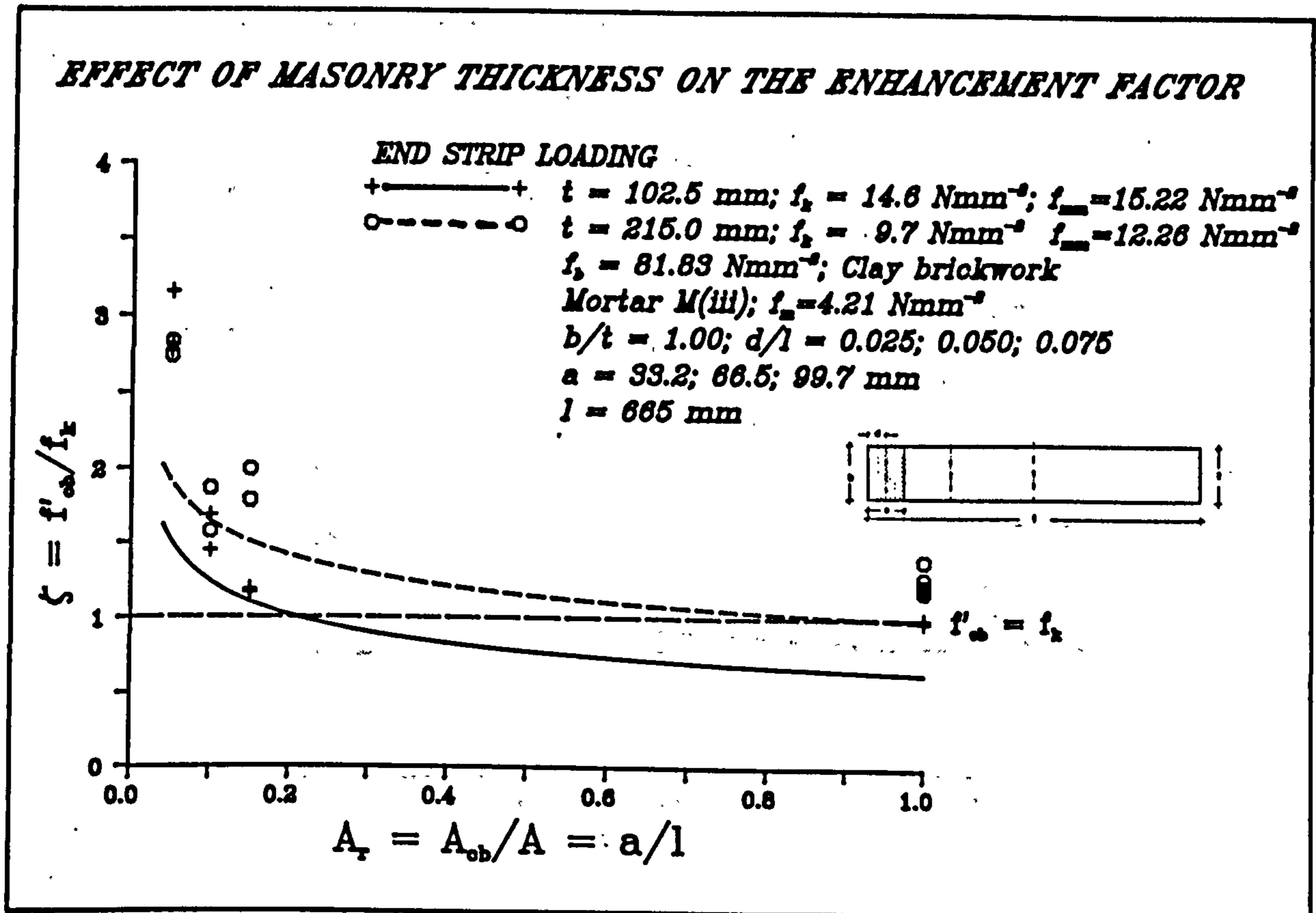


Fig. 6.53 - Effect of specimen thickness on the enhancement factor for brickwork type F under end strip loading.

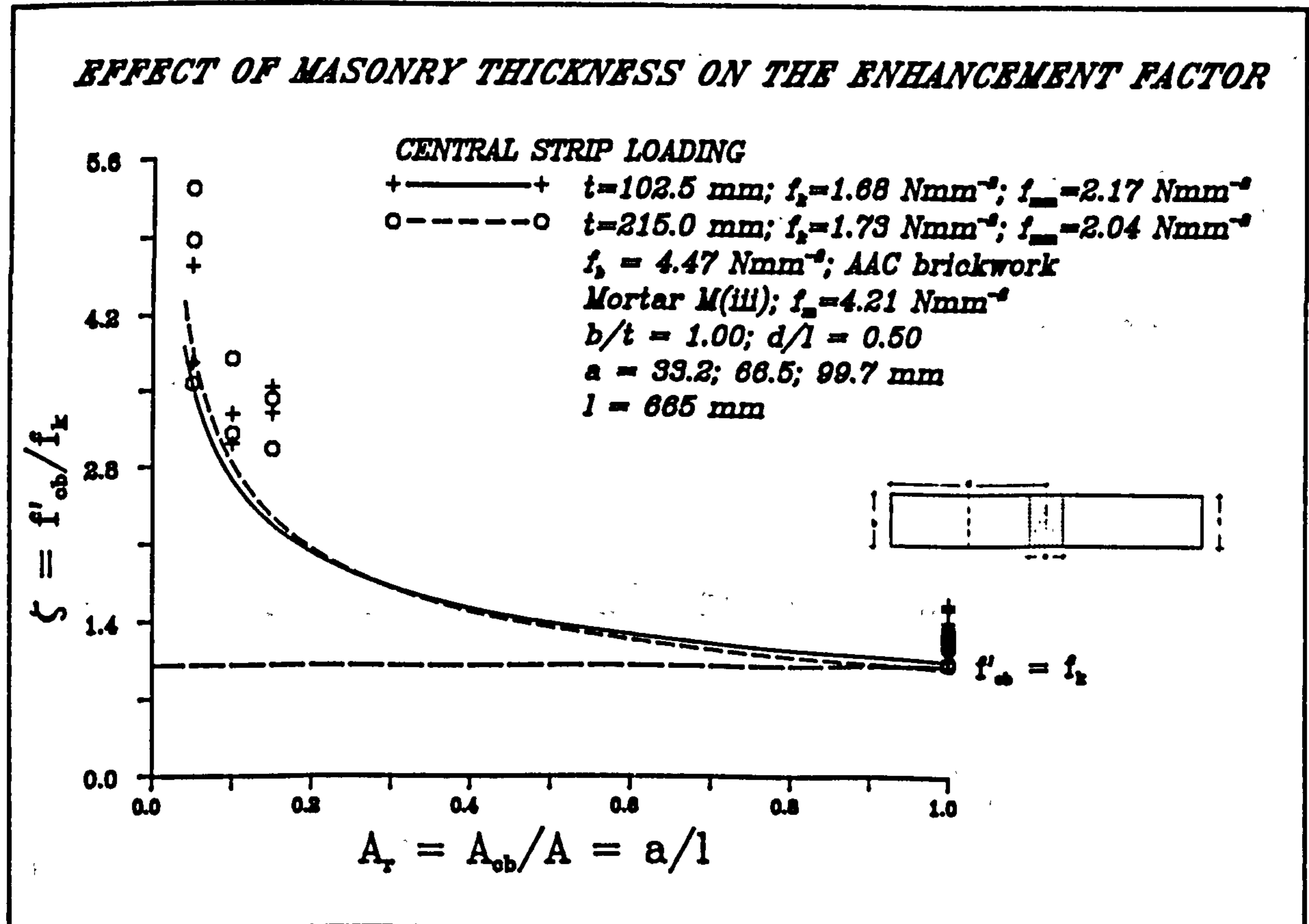


Fig. 6.54 - Effect of specimen thickness on the enhancement factor for brickwork type G under central strip loading.

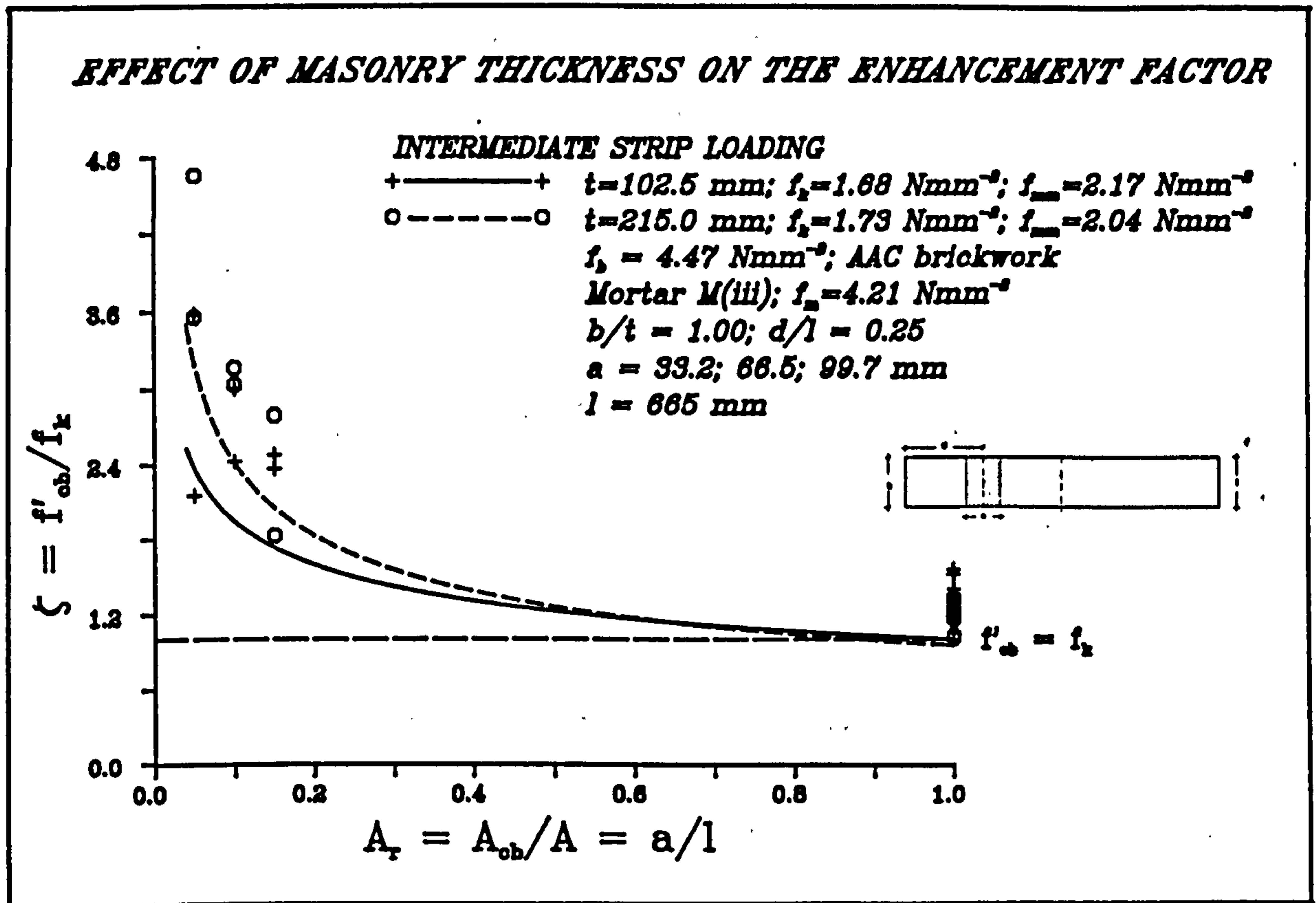


Fig. 6.55 - Effect of specimen thickness on the enhancement factor for brickwork type G under intermediate strip loading.

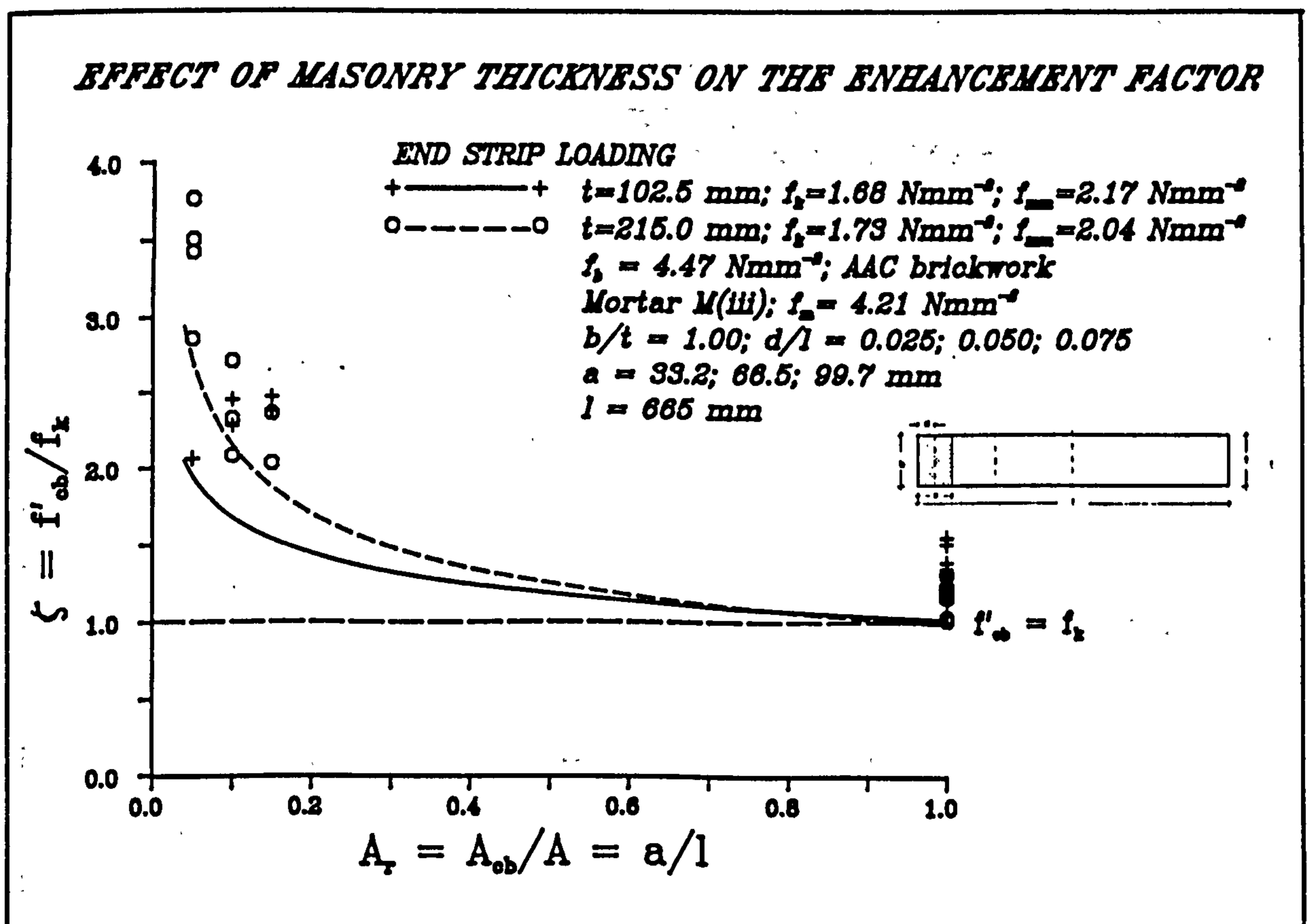


Fig. 6.56 - Effect of specimen thickness on the enhancement factor for brickwork type G under end strip loading.



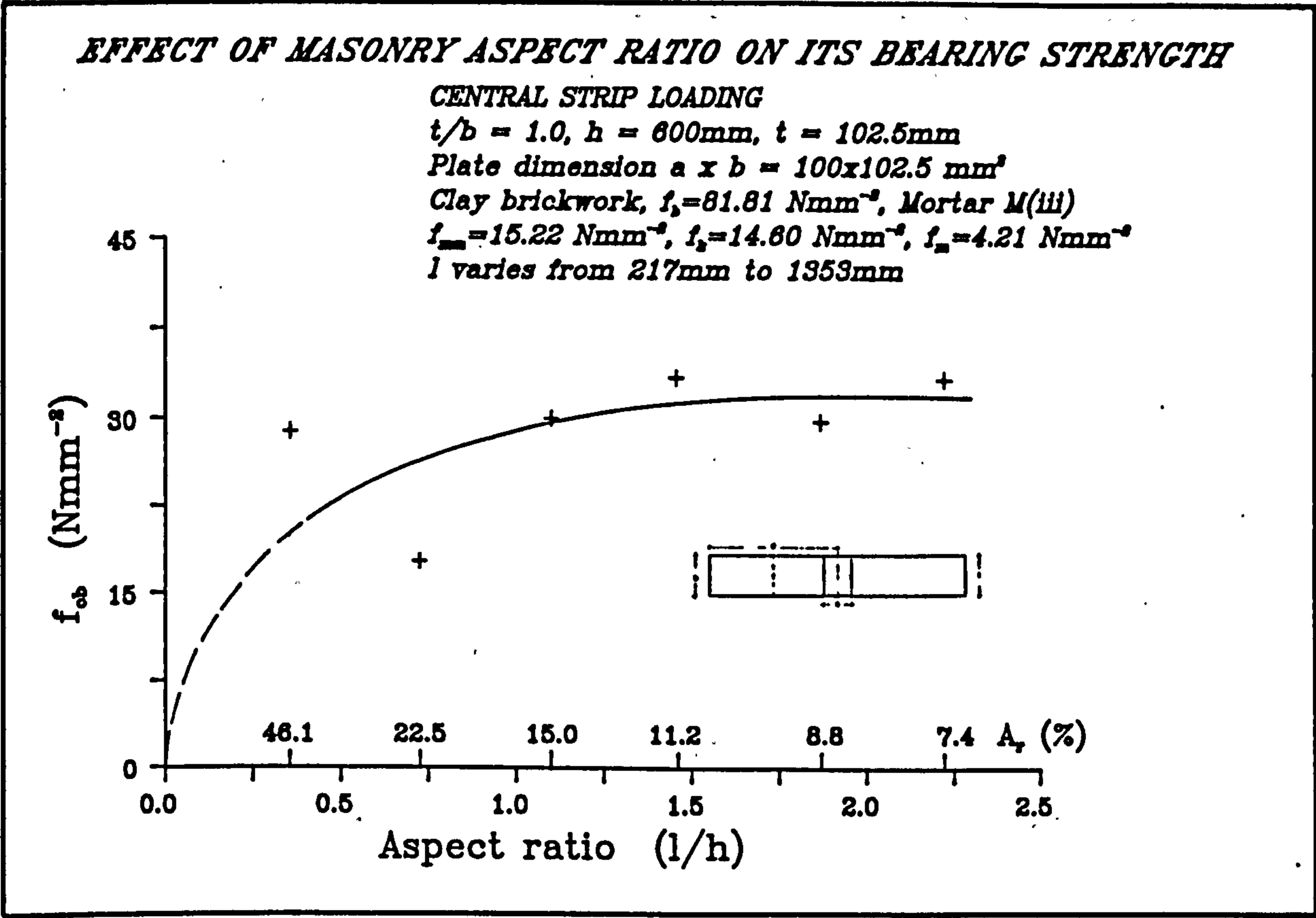


Fig. 6.57 - Influence of aspect ratio on the bearing strength of clay brickwork masonry.

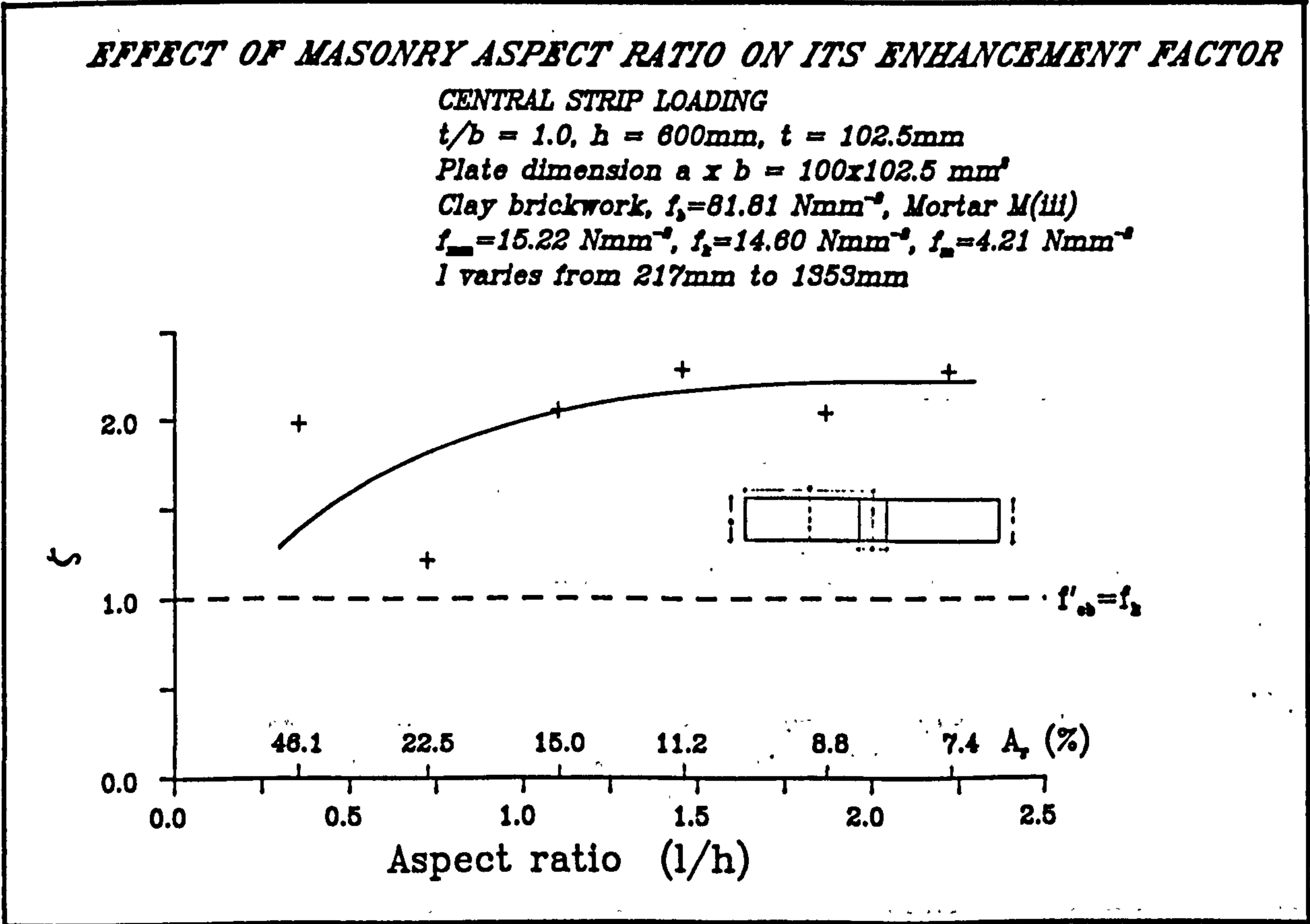


Fig. 6.58 - Influence of aspect ratio on the enhancement factor for clay brickwork masonry.

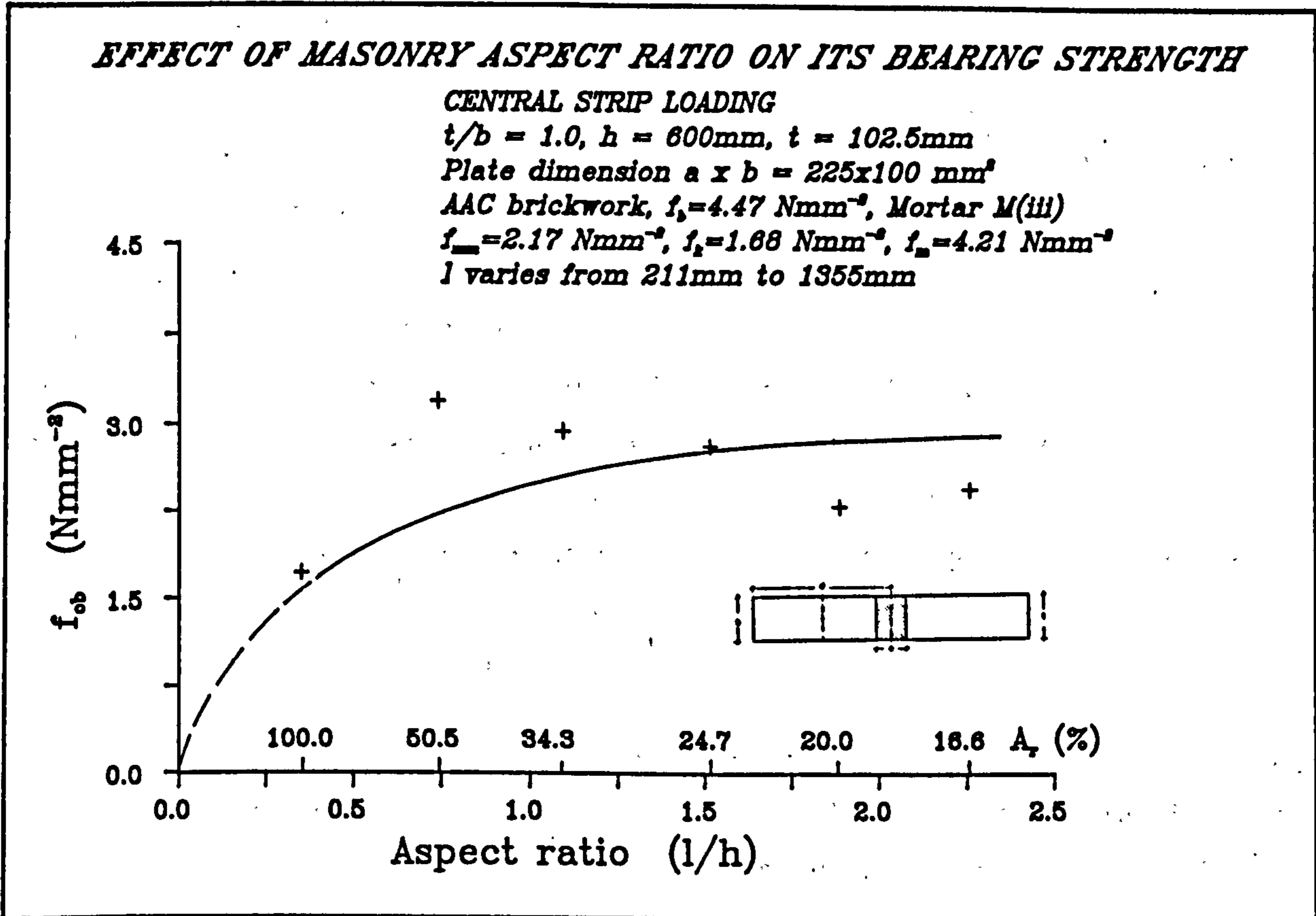


Fig. 6.59 - Influence of aspect ratio on the bearing strength of AAC brickwork masonry.

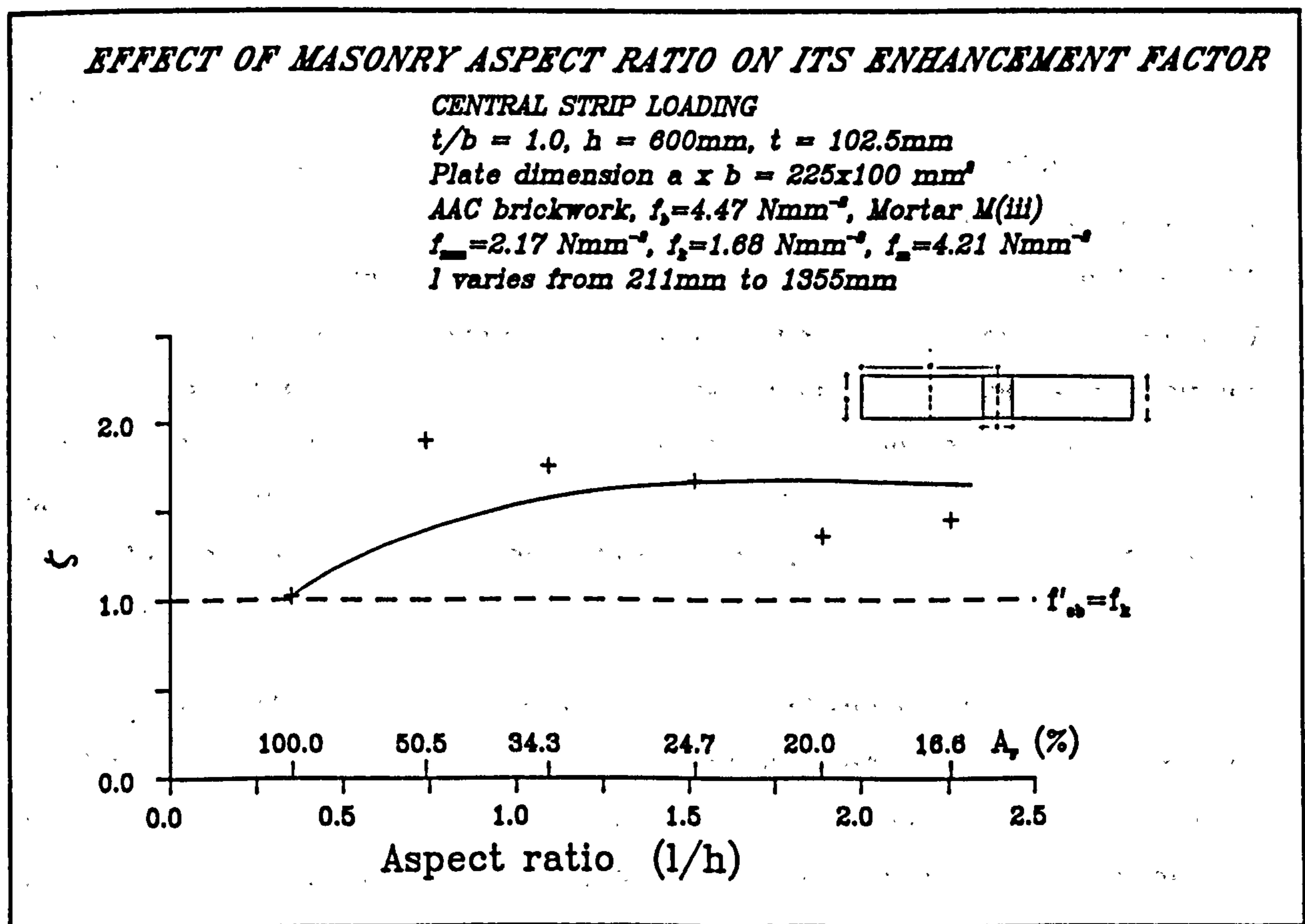


Fig. 6.60 - Influence of aspect ratio on the enhancement factor for AAC brickwork masonry.

#### **6.4.5. Loading position**

To study the effect of loading position, the location of applied concentrated load was varied across the top of the specimens. Three positions namely central, intermediate and end loading were investigated (refer to Figs. 5.1 & 5.2). Brickwork types E, F (for two thicknesses), G (for two thicknesses), H and L were tested under strip loading and brickwork type M tested under edge loading. The results are presented in Figs. 6.61 to 6.67 for strip and Fig. 6.68 for edge loadings. These figures show the effect of loading position on the bearing strength of brickwork masonry in terms of loaded area ratio. It can be concluded from the results that as the loading moves away from the centre of the specimen (i.e. as the eccentricity is increased in the longitudinal direction) the bearing strength decreases.

The effect of loading position on the enhancement factor for brickwork in terms of loaded area ratio is shown in Figs. 6.69 to 6.76. These results also confirm that as the edge distance decreases the enhancement factor decreases. The decrease in the strength is thought to be caused by the increase in the transverse tensile stress which increase as the edge distance decreases and reaches its ultimate value when the load is applied at the end of the specimen.

#### **6.4.6. Loading configuration**

Two loading configurations, strip and edge (or patch) loading have been investigated by employing the same specimens constructed of the same brick strength and mortar mix of which the results have been reported in Tables B2 and B1 in Appendix B respectively. The results have been plotted in Figs. 6.77 to 6.79 for three loading positions; central, intermediate and end positions respectively, which shows the variation of bearing strength in terms of loaded area ratio for the two loading configurations. It can be seen from Figs. 6.78 and 6.79 that there is hardly any difference between the two types of loading for the same loading position.

The influence of loading configuration on the enhancement factor are shown in Figs. 6.80 to 6.82 for central, intermediate and end loading positions respectively. The plots show strip loading yields higher enhancement factor but not to a significant value considering that the characteristic bearing strength is dependent on the standard deviation of the data points.

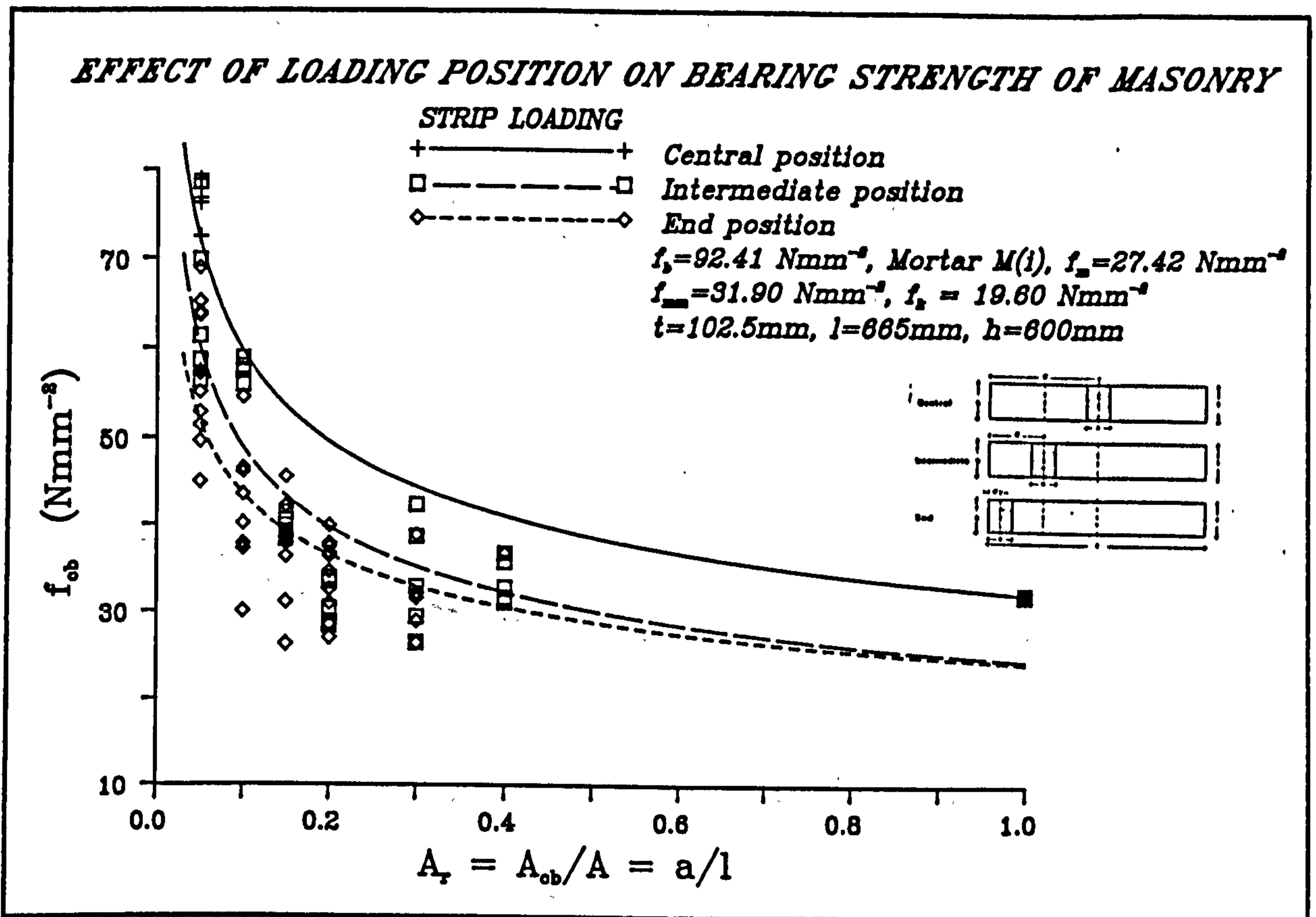


Fig. 6.61 - Effect of loading position on bearing strength of brickwork type E under strip loading ( $t=102.5\text{mm}$ ).

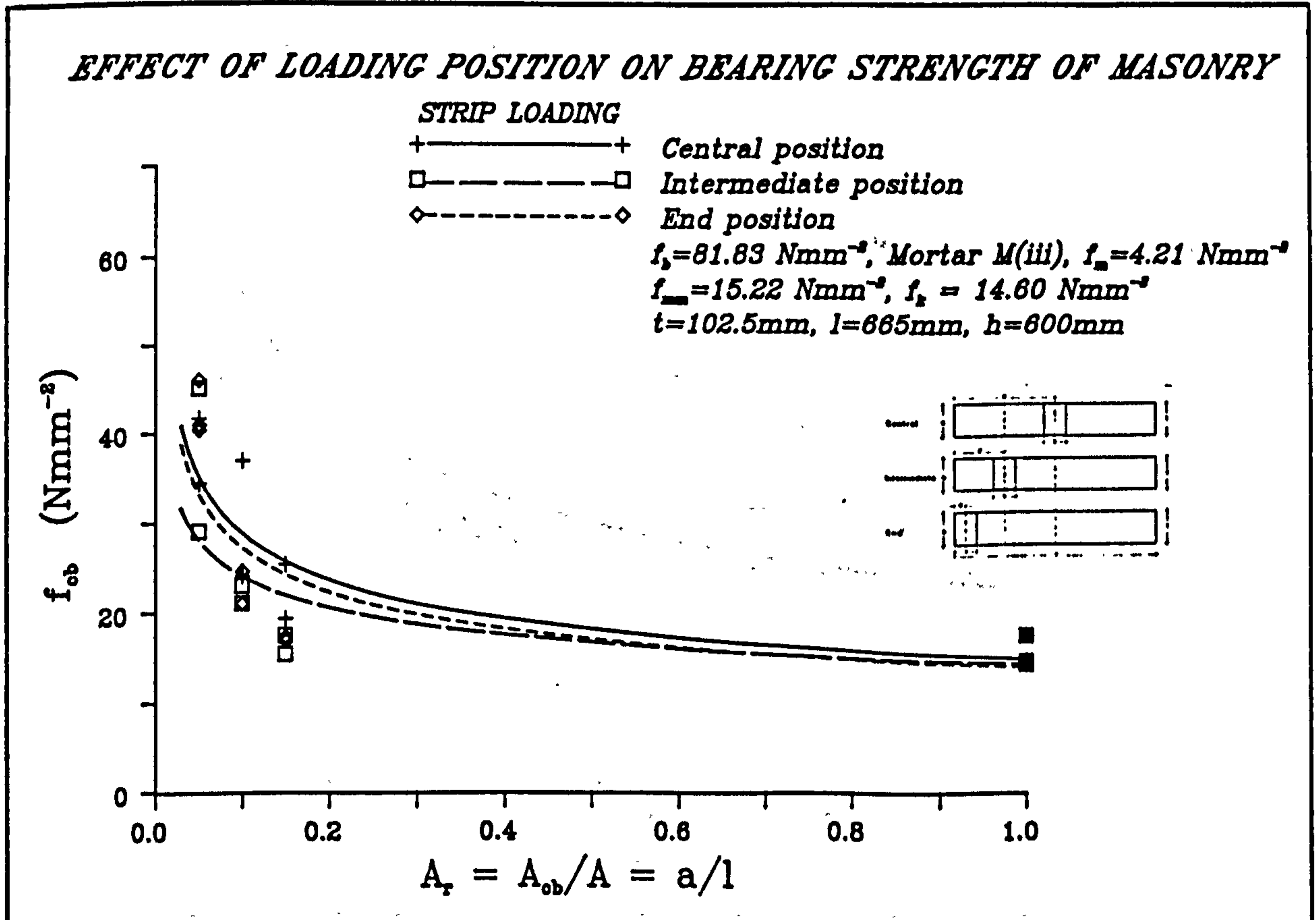


Fig. 6.62 - Effect of loading position on bearing strength of brickwork type F under strip loading ( $t=102.5\text{mm}$ ).

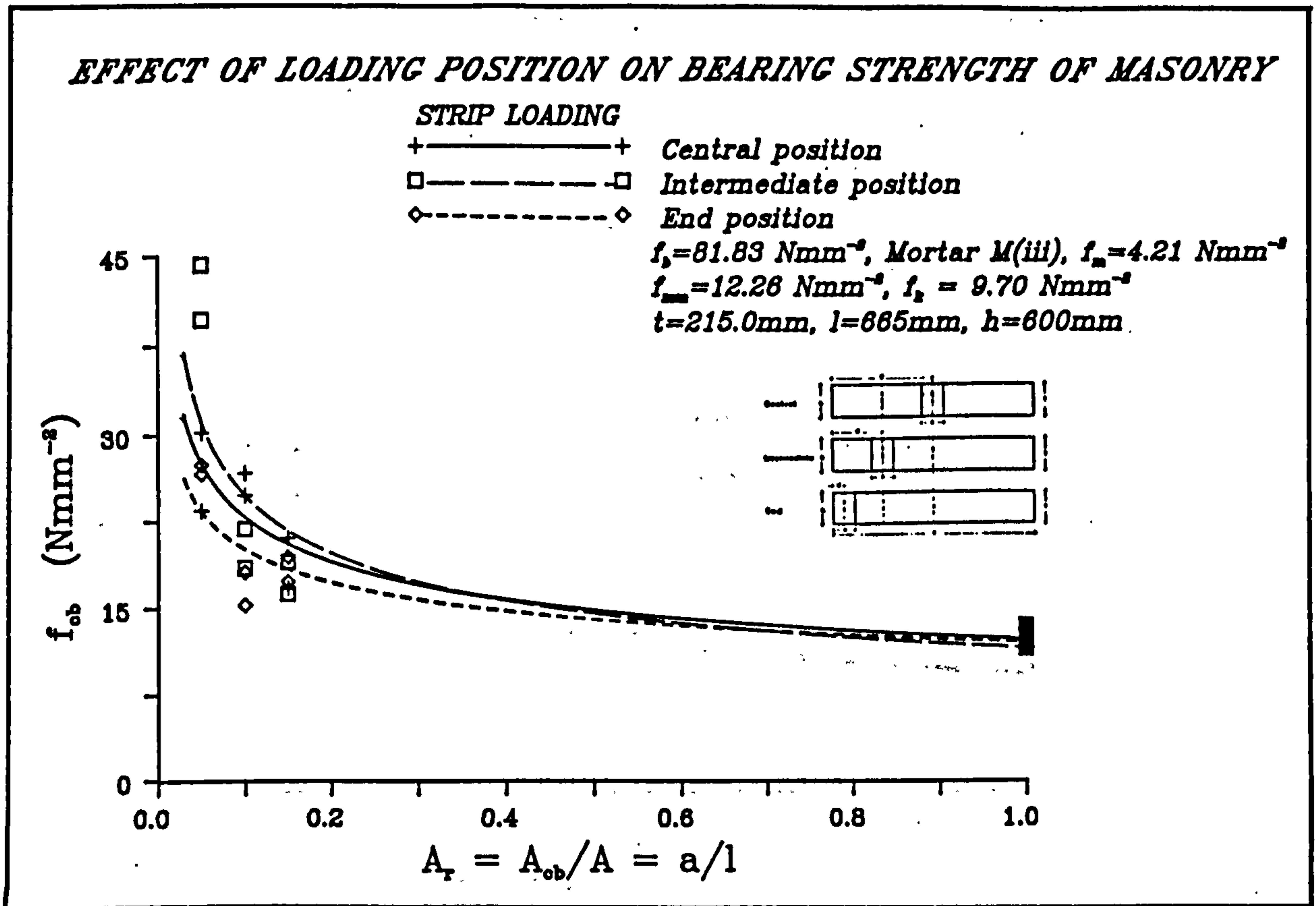


Fig. 6.63 - Effect of loading position on bearing strength of brickwork type F under strip loading ( $t=215.0\text{mm}$ ).

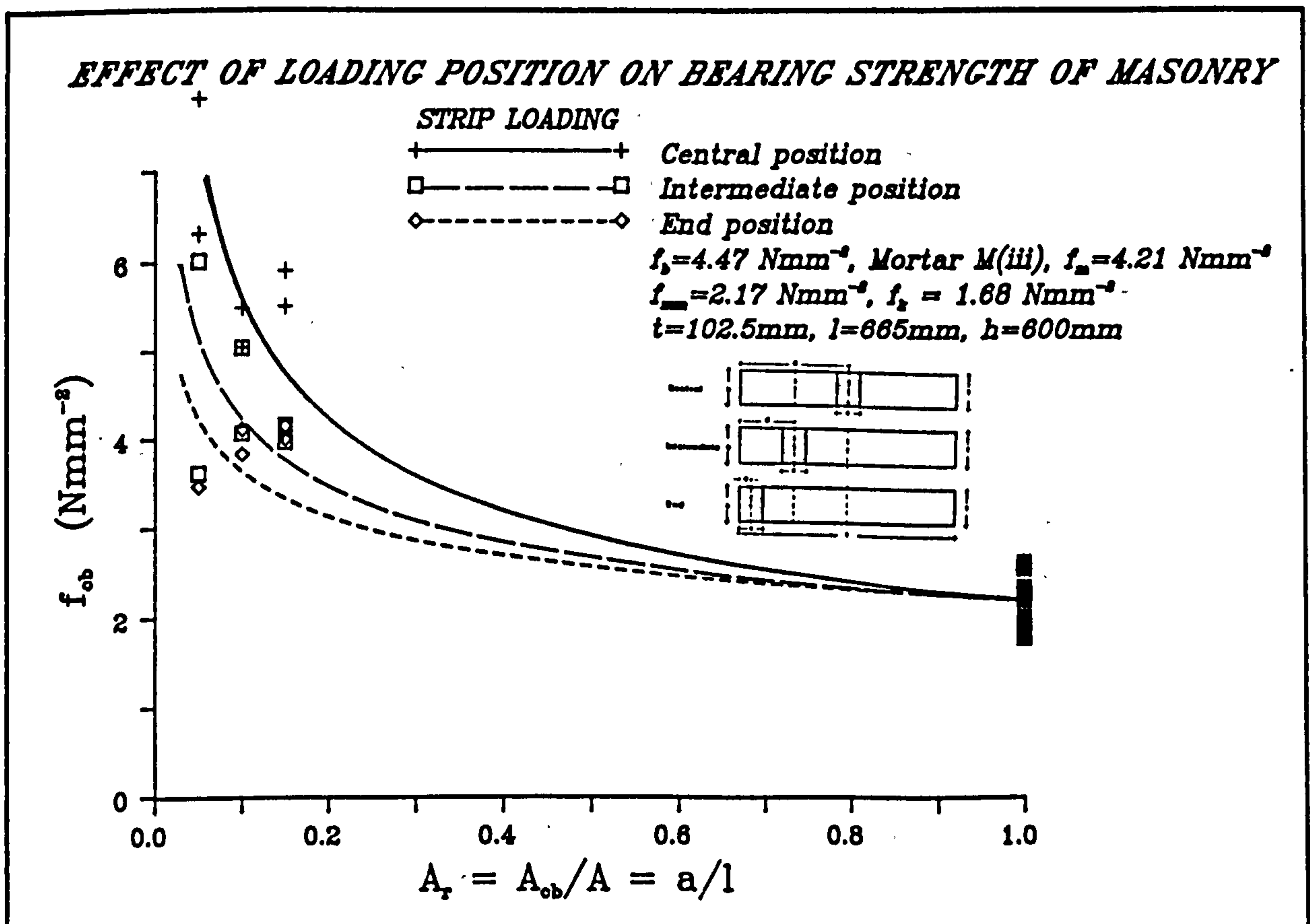


Fig. 6.64 - Effect of loading position on bearing strength of brickwork type G under strip loading ( $t=102.5\text{mm}$ ).

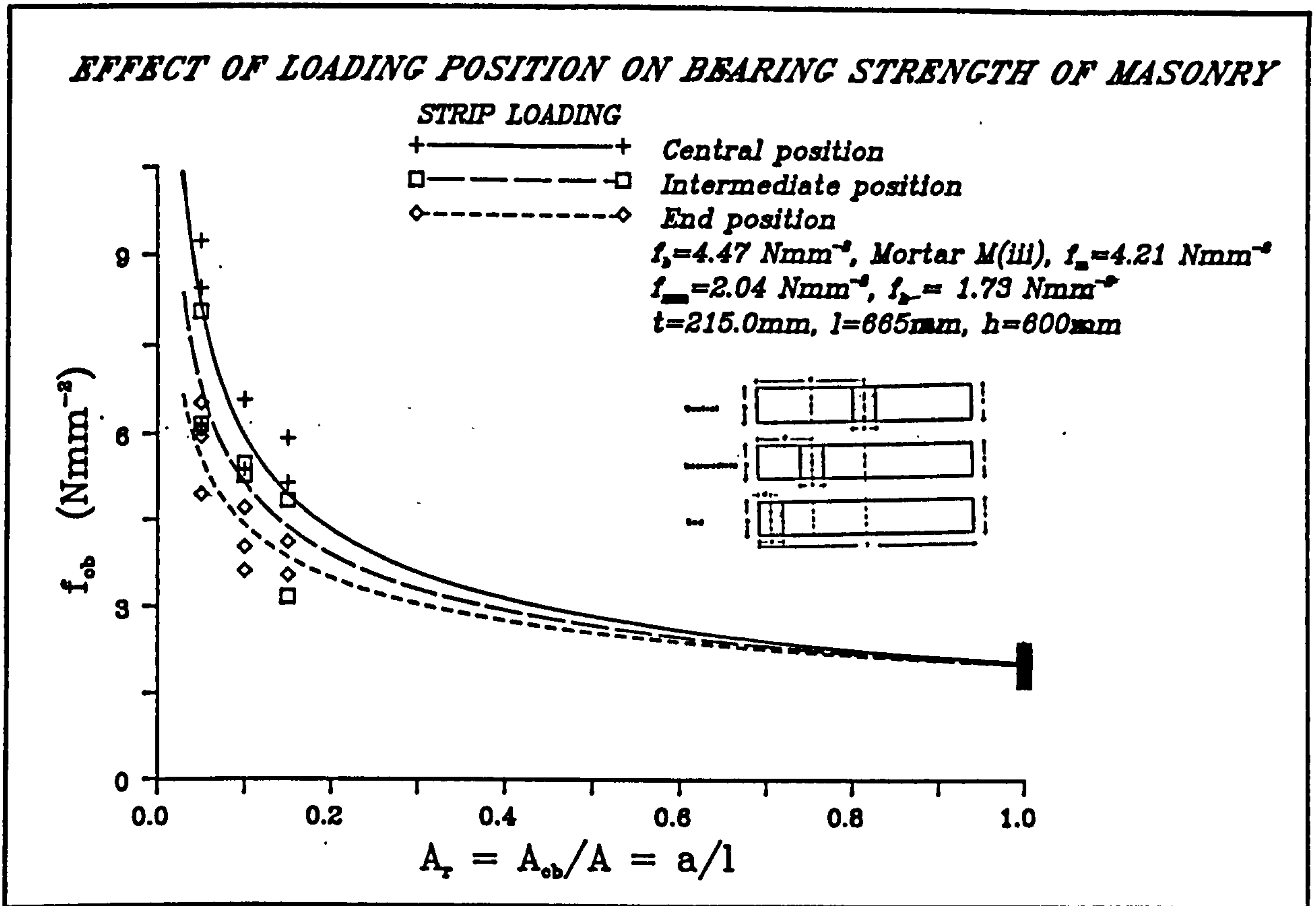


Fig. 6.65 - Effect of loading position on bearing strength of brickwork type G under strip loading ( $t=215.0\text{mm}$ ).

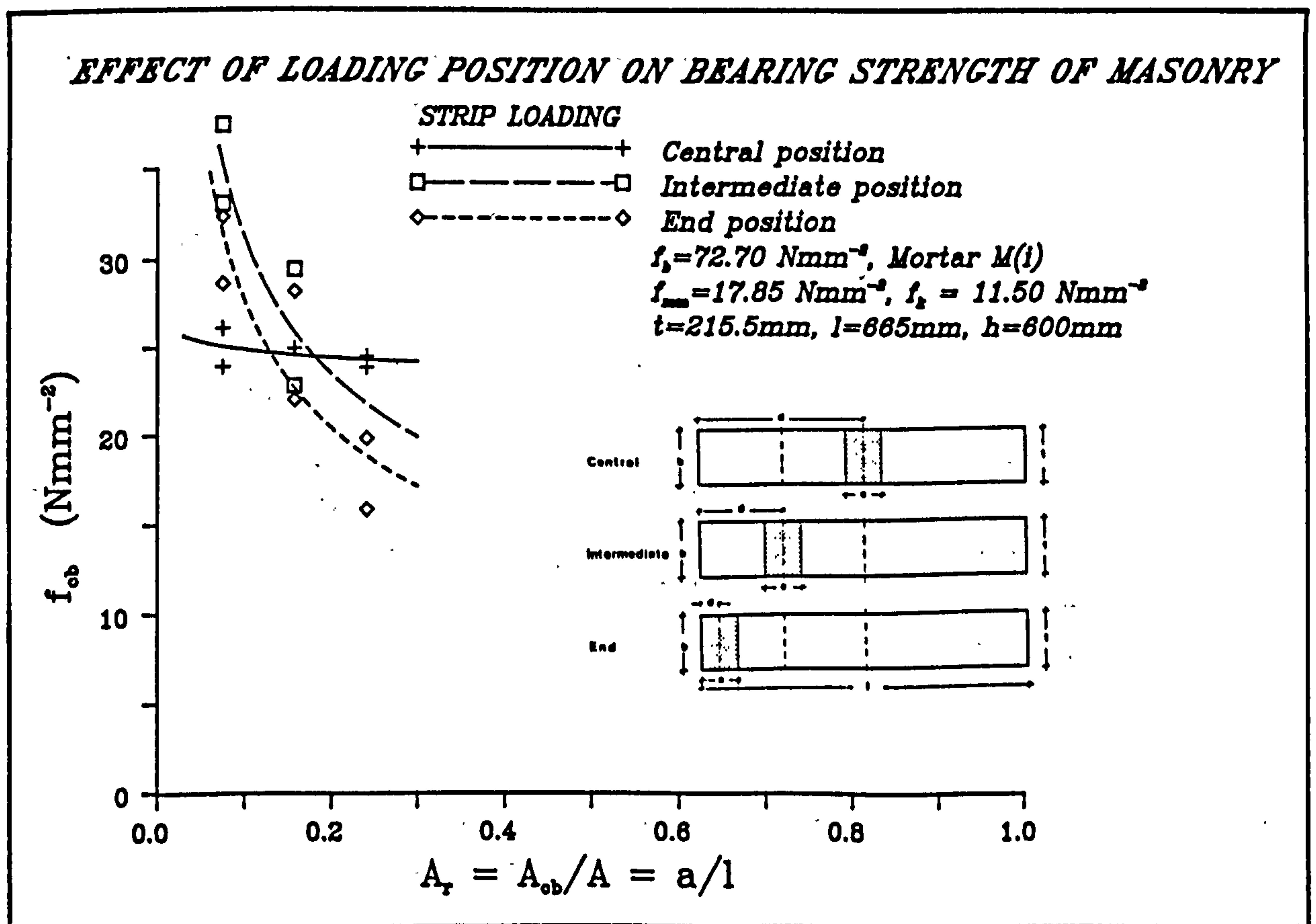


Fig. 6.66 - Effect of loading position on bearing strength of brickwork type H under strip loading ( $t=215.0\text{mm}$ ).

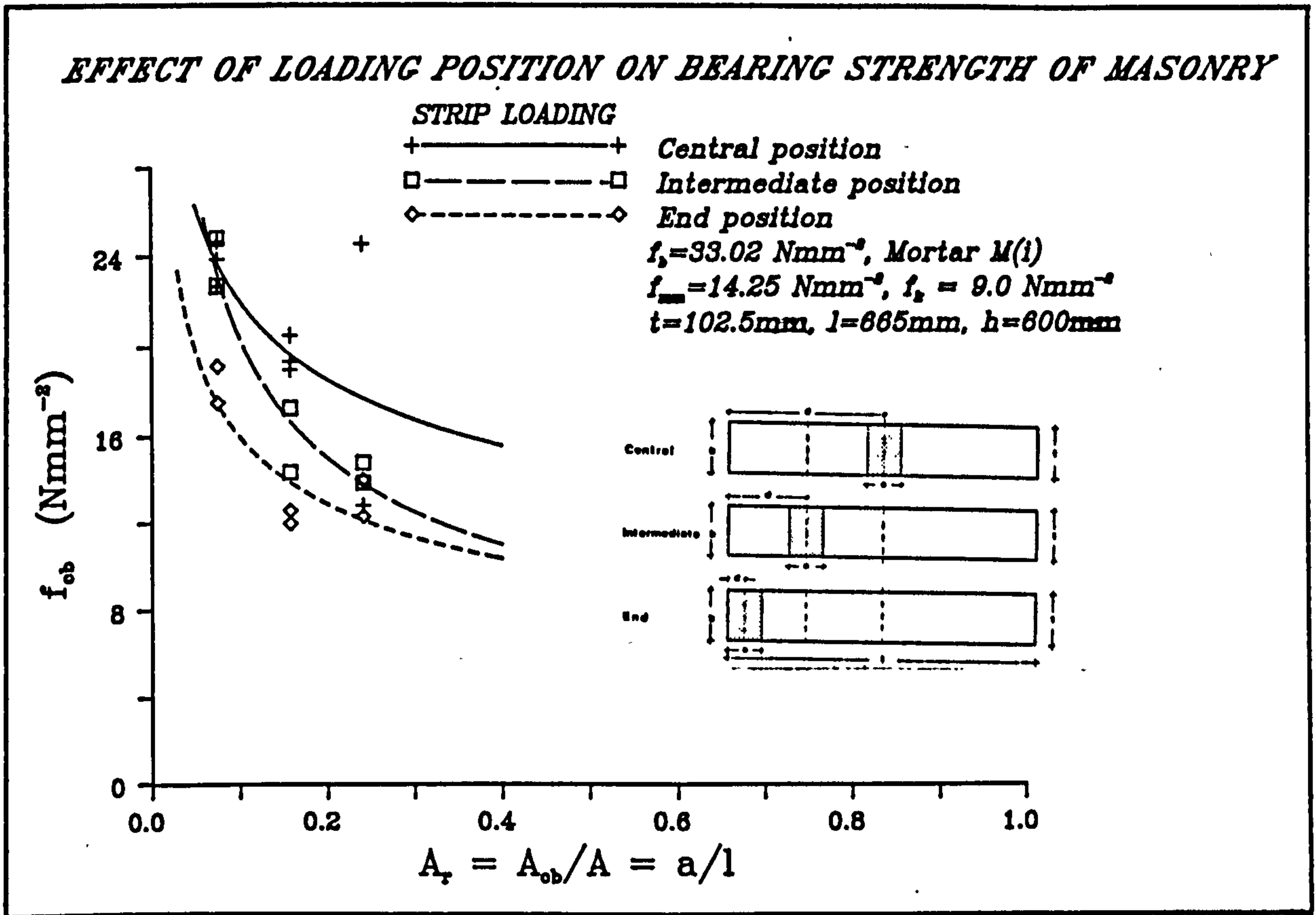


Fig. 6.67 - Effect of loading position on bearing strength of brickwork type L under strip loading ( $t=102.5\text{mm}$ ).

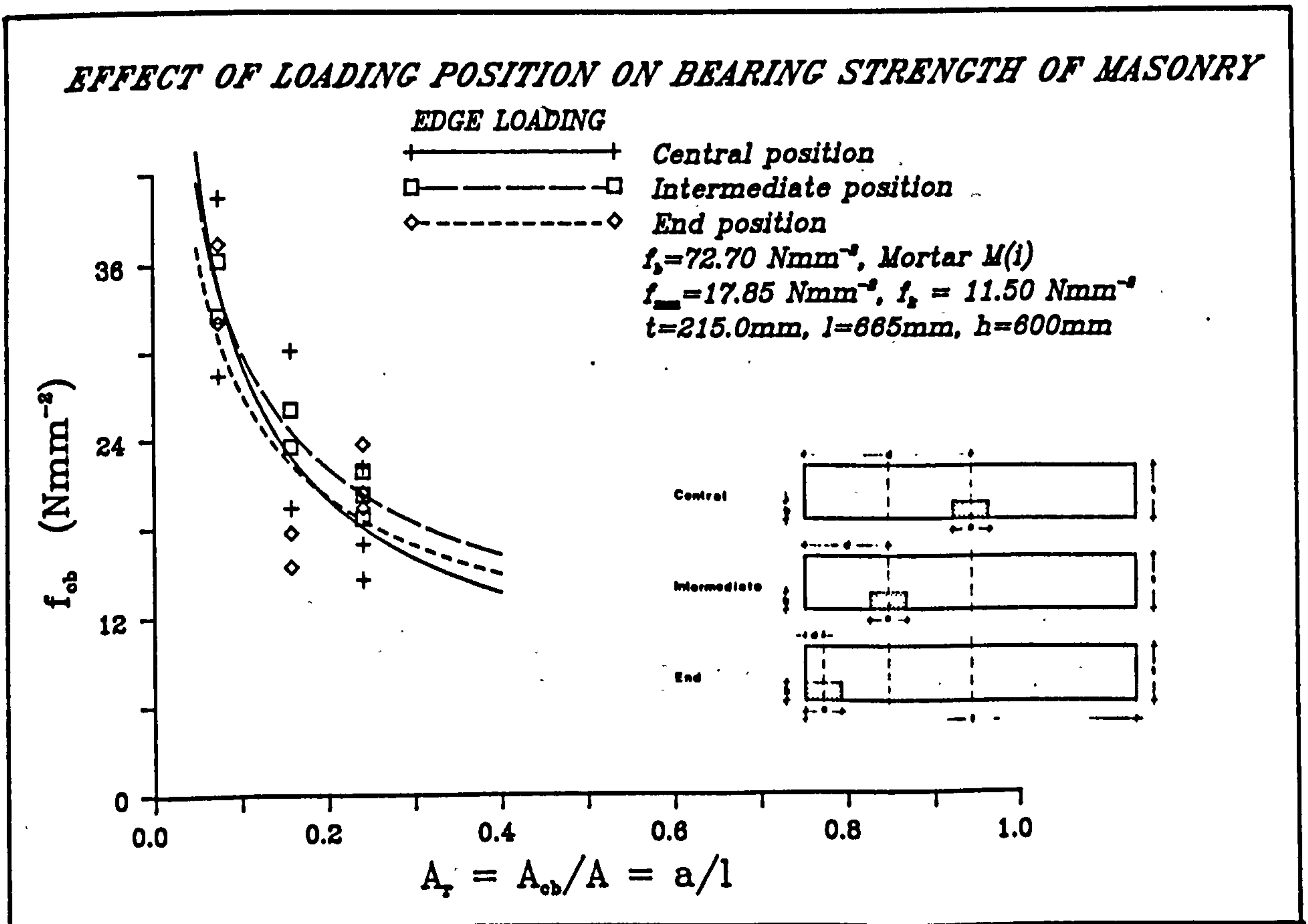


Fig. 6.68 - Effect of loading position on bearing strength of brickwork type M under edge loading ( $t=215.0\text{mm}$ ).

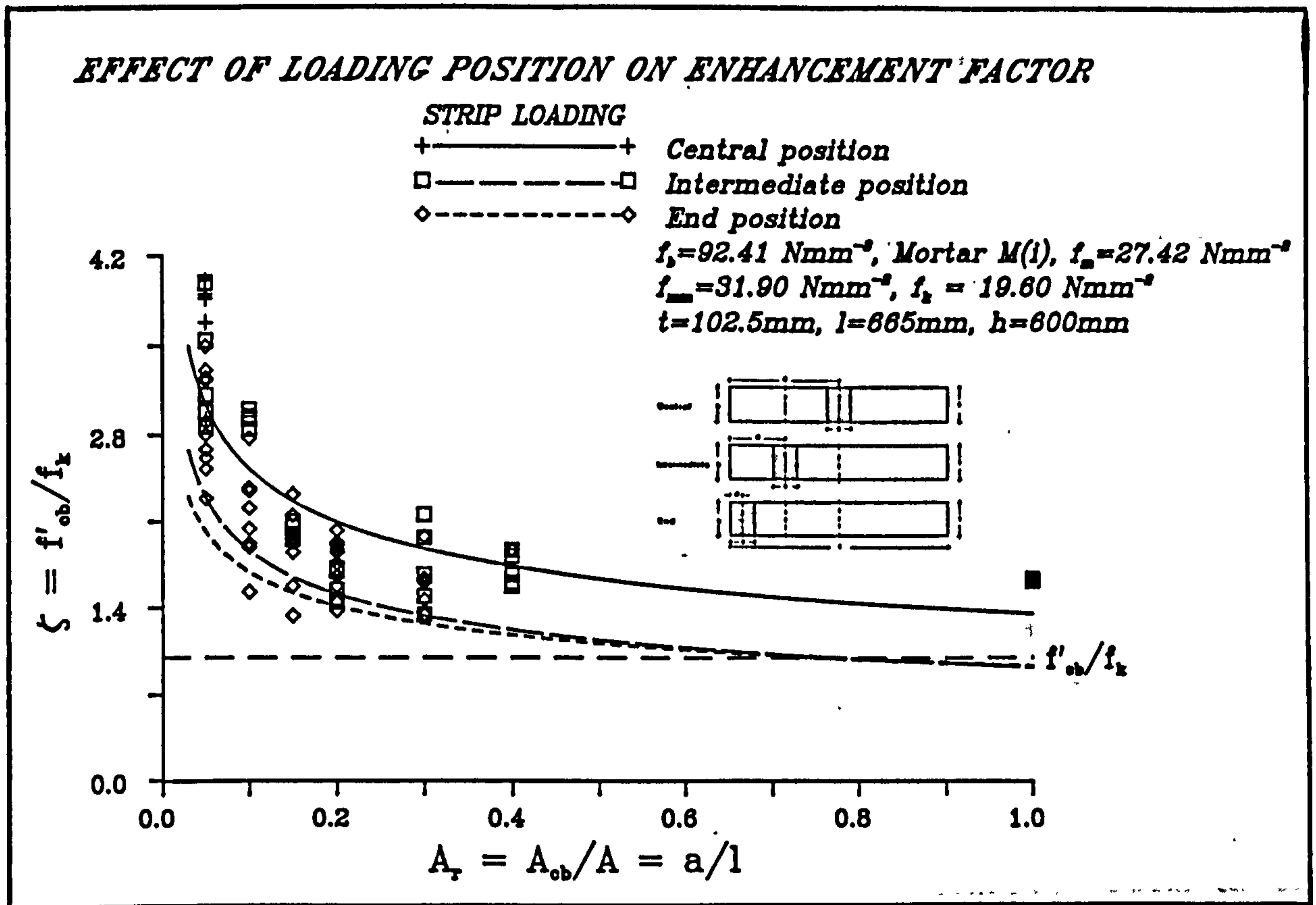


Fig. 6.69 - Effect of loading position on enhancement factor for brickwork type E under strip loading ( $t=102.5\text{mm}$ ).

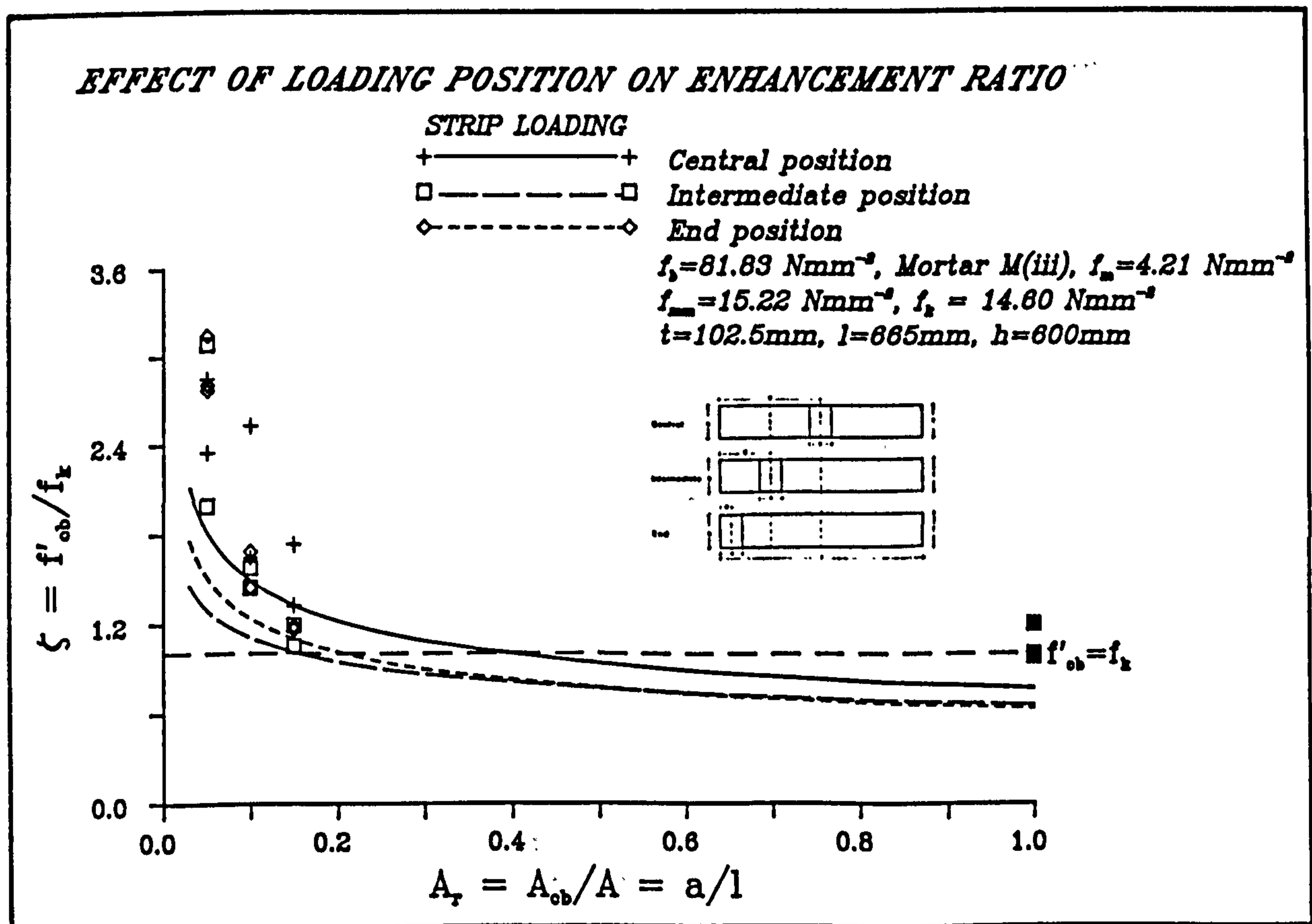


Fig. 6.70 - Effect of loading position on enhancement factor for brickwork type F under strip loading ( $t=102.5\text{mm}$ ).



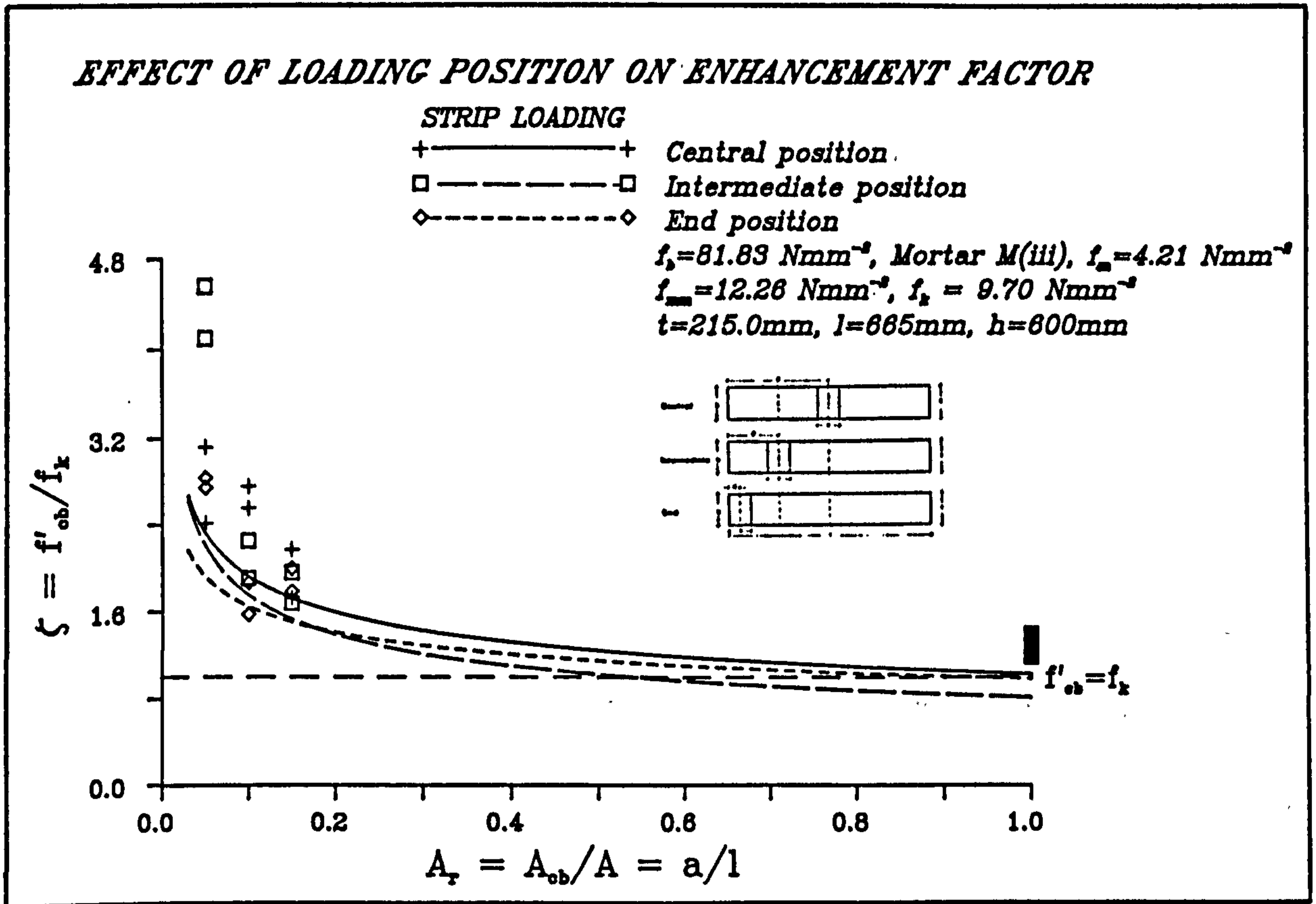


Fig. 6.71 - Effect of loading position on enhancement factor for brickwork type F under strip loading ( $t=215.0\text{mm}$ ).

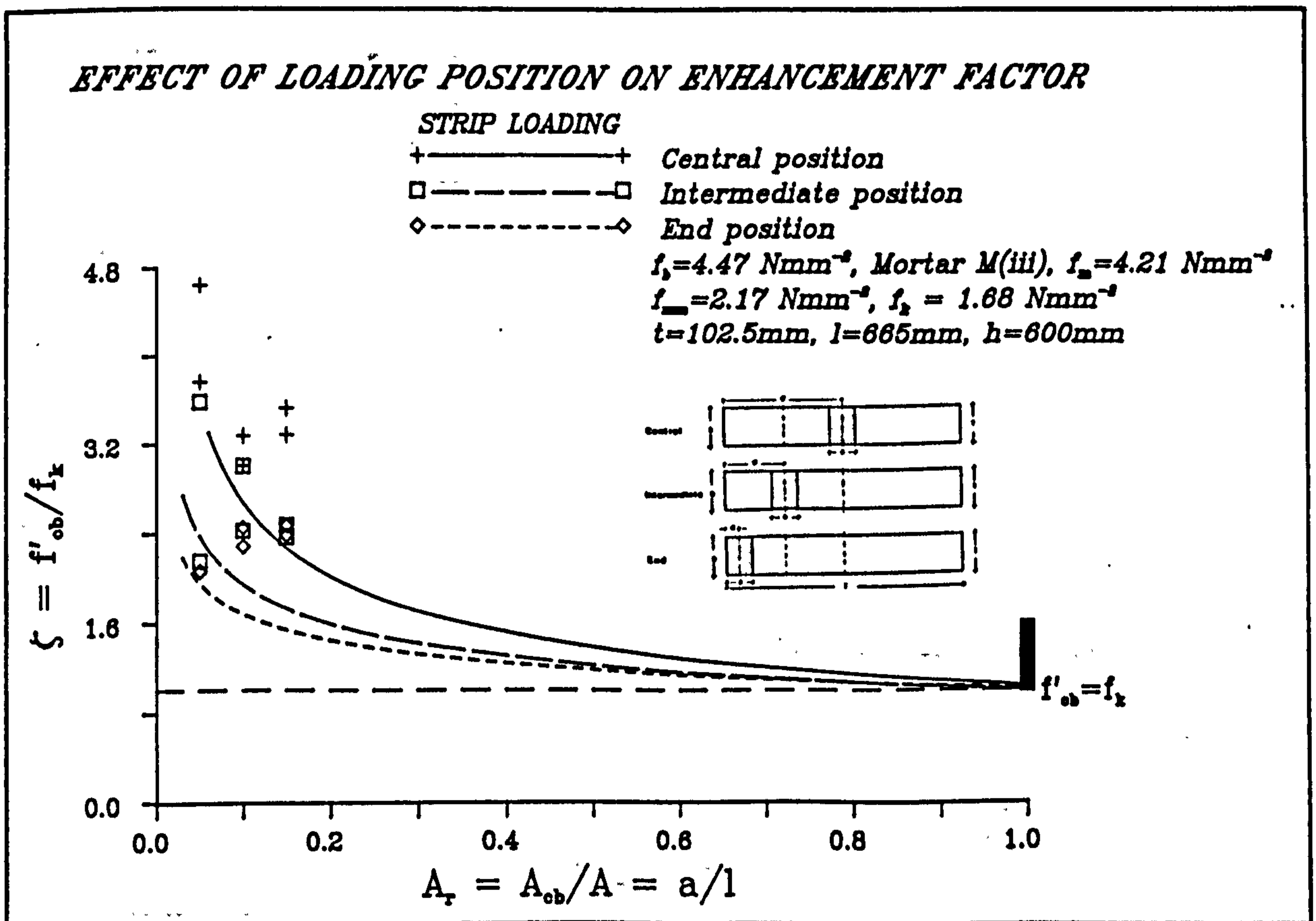


Fig. 6.72 - Effect of loading position on enhancement factor for brickwork type G under strip loading ( $t=102.5\text{mm}$ ).

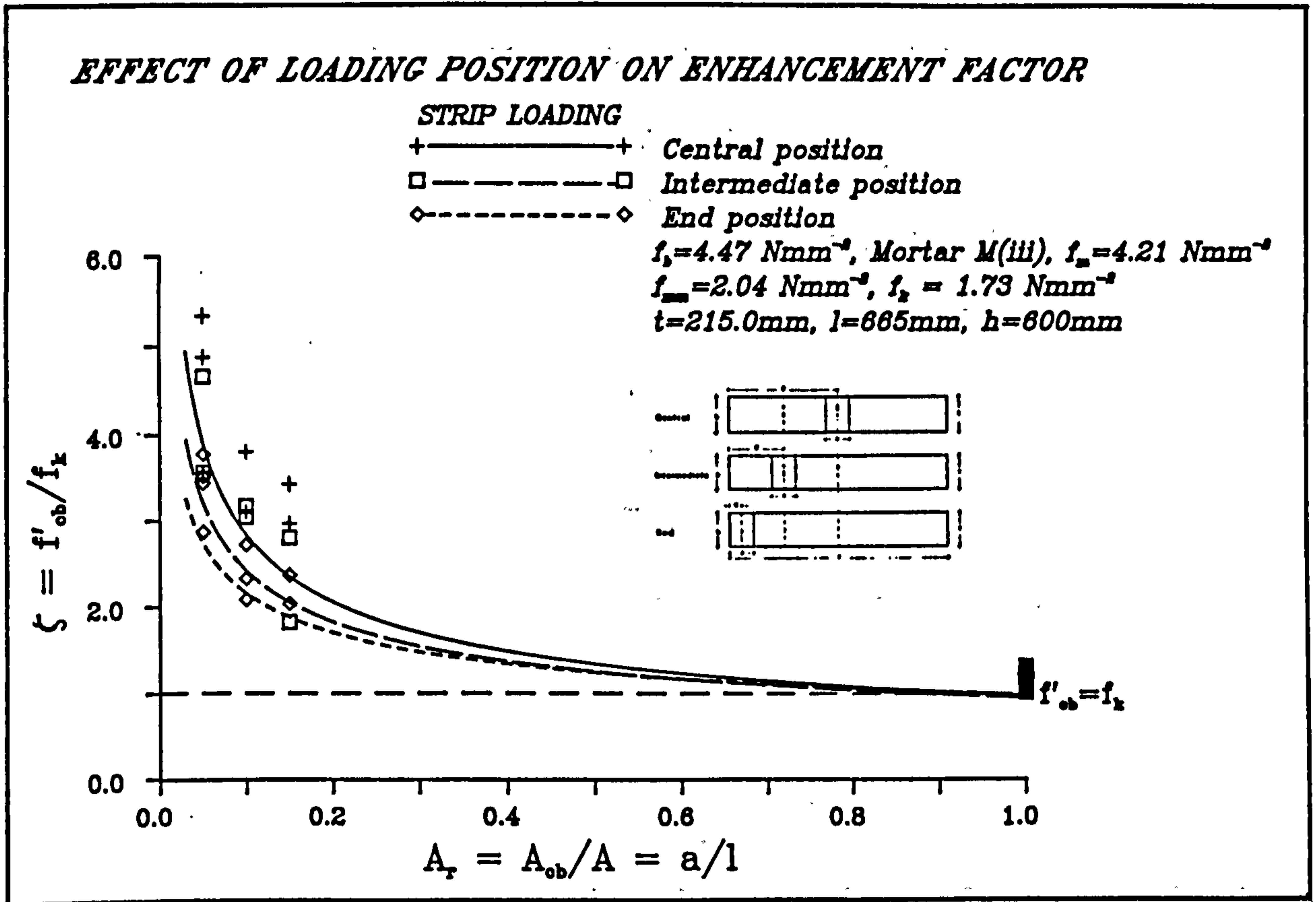


Fig. 6.73 - Effect of loading position on enhancement factor for brickwork type G under strip loading ( $t=215.0\text{mm}$ ).

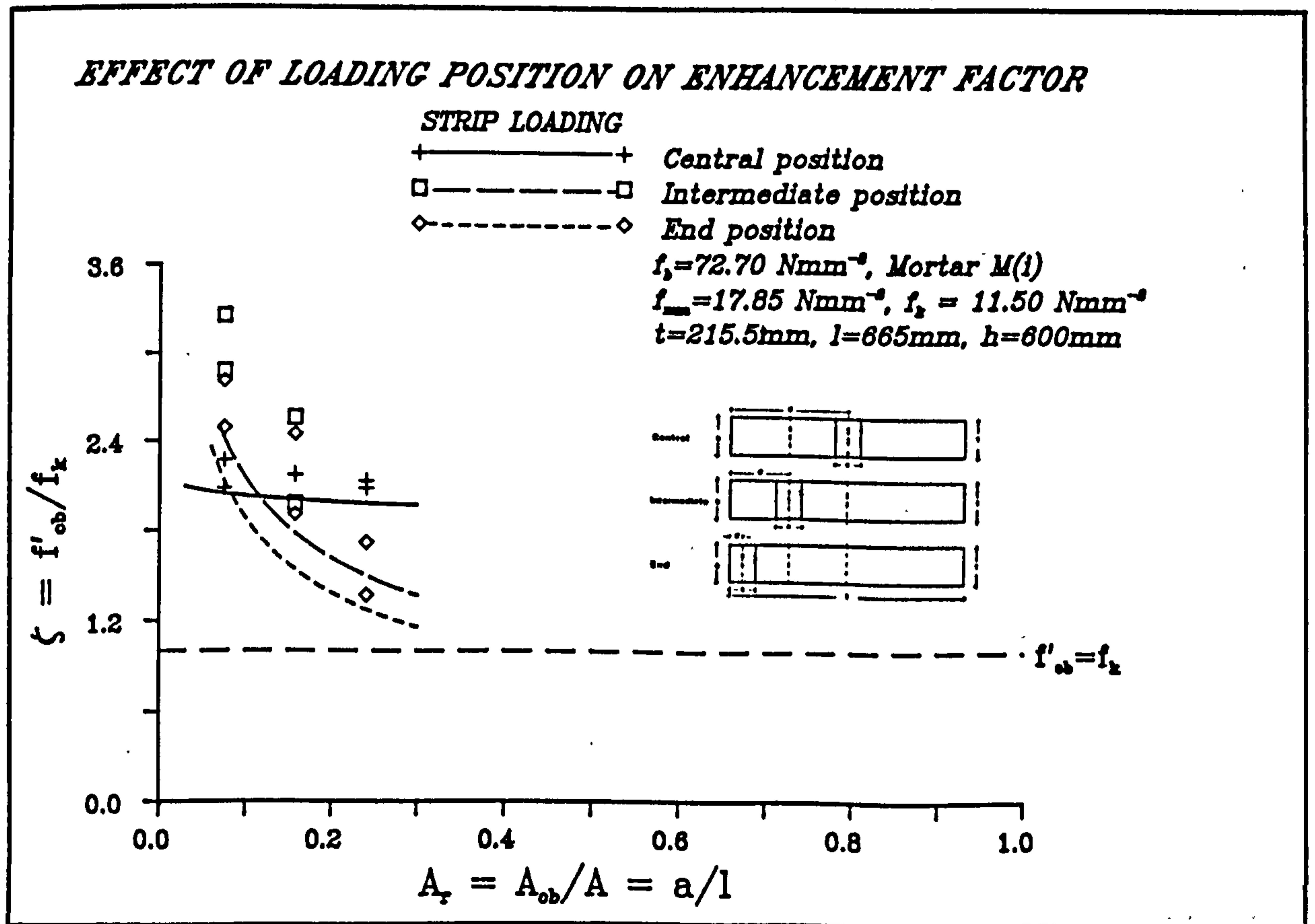


Fig. 6.74 - Effect of loading position on enhancement factor for brickwork type H under strip loading ( $t=215.0\text{mm}$ ).

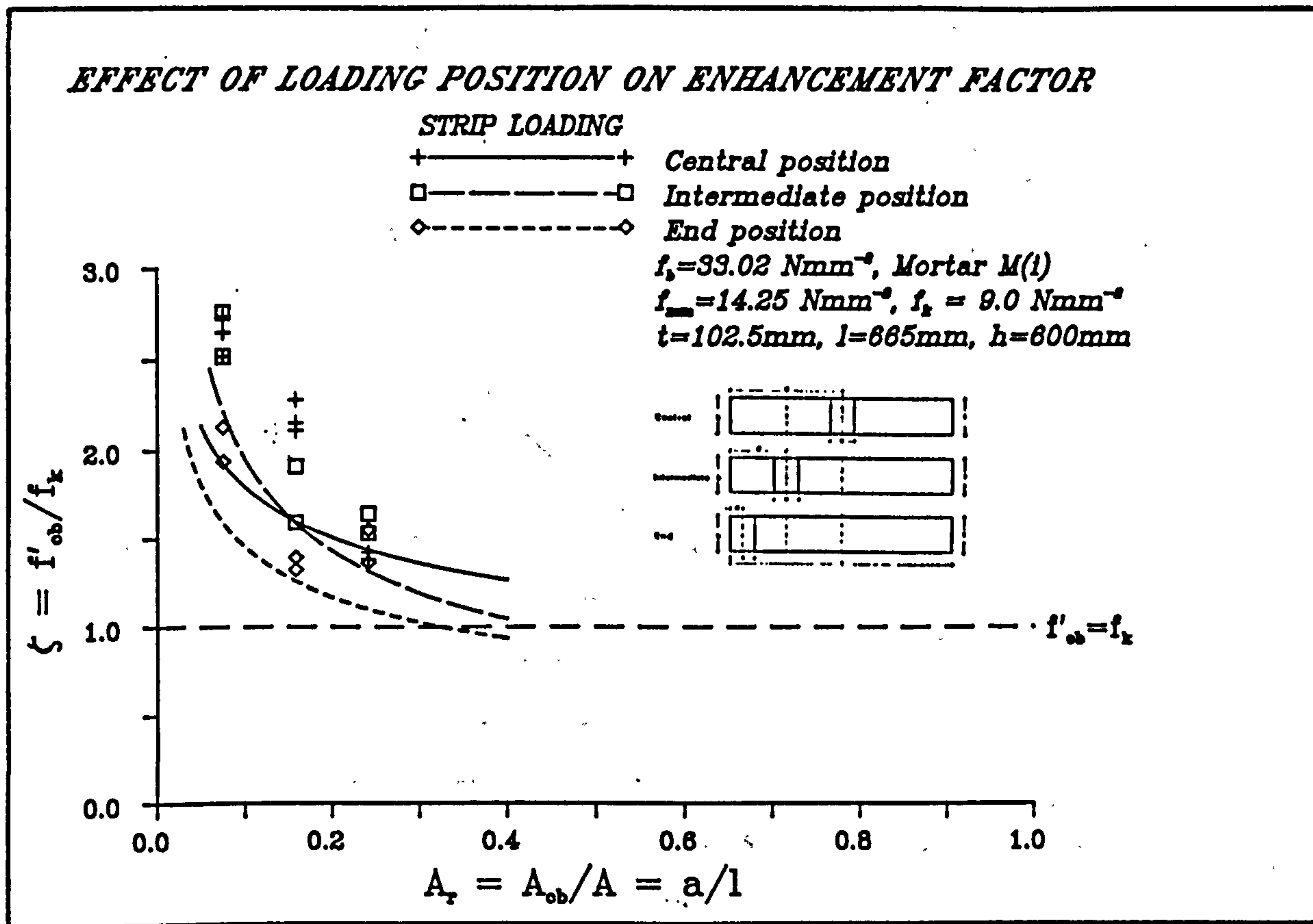


Fig. 6.75 - Effect of loading position on enhancement factor for brickwork type L under strip loading ( $t=102.5\text{mm}$ ).

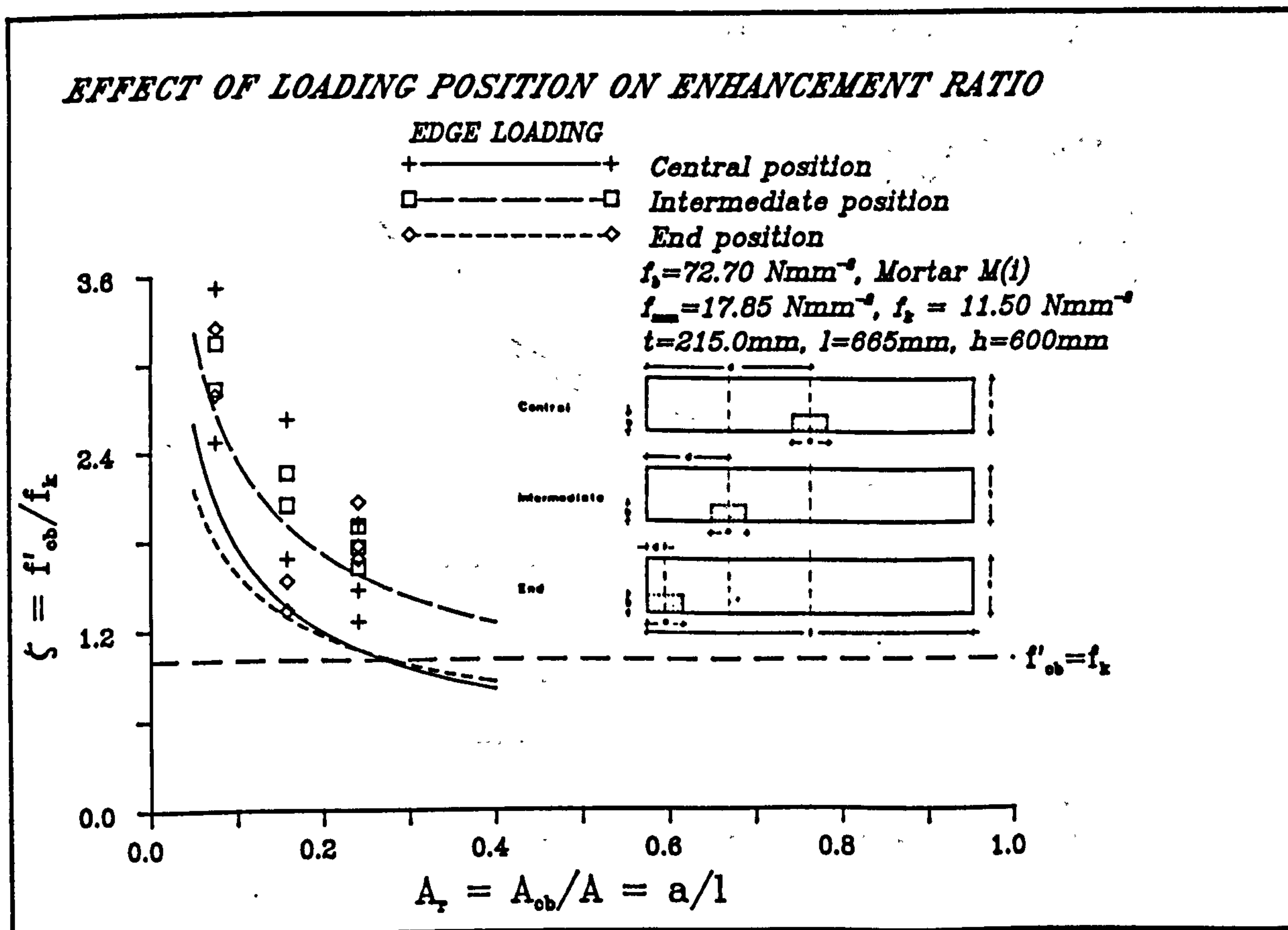


Fig. 6.76 - Effect of loading position on enhancement factor for brickwork type M under edge loading ( $t=215.0\text{mm}$ ).

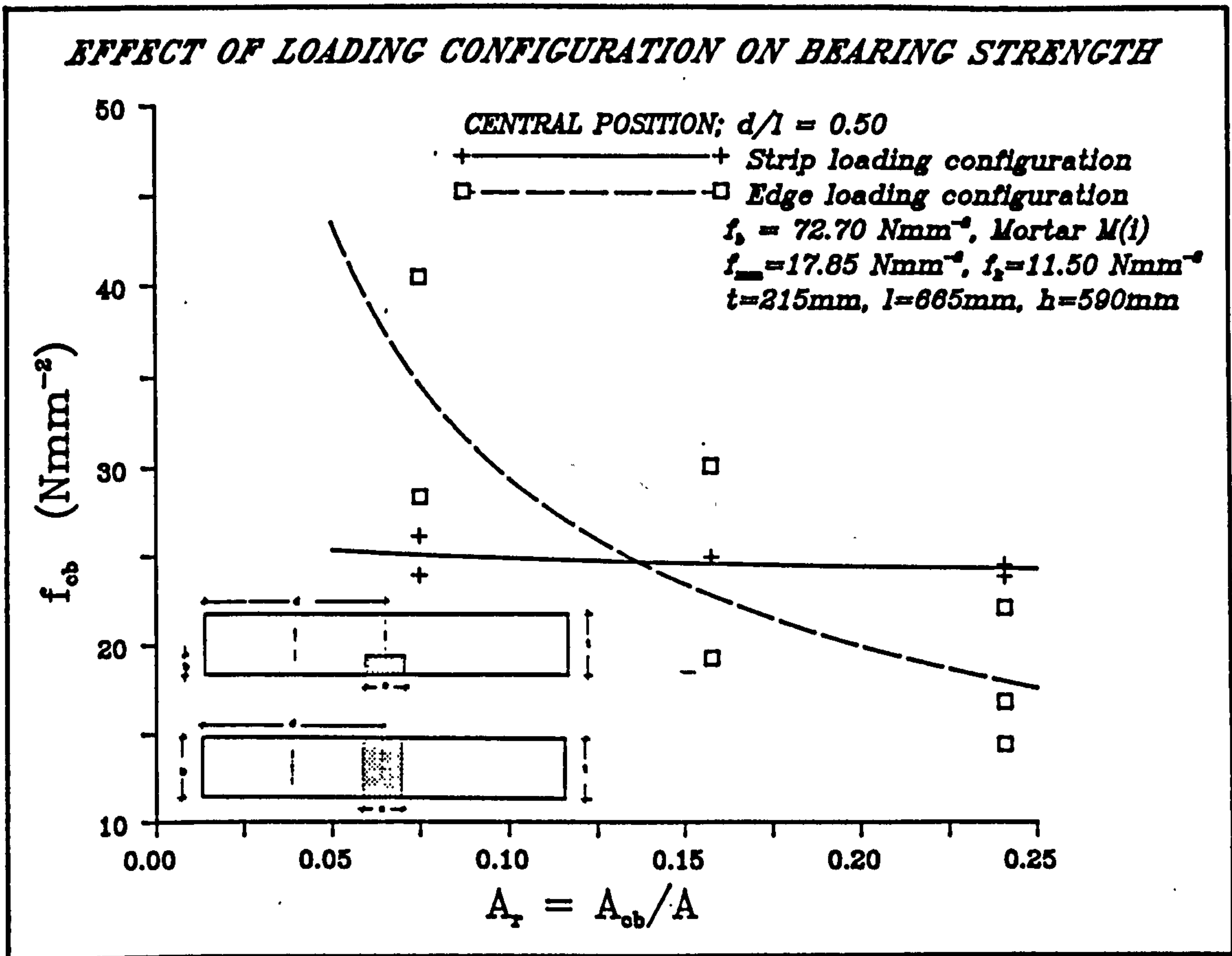


Fig. 6.77 - Effect of loading configuration on the bearing strength of masonry under central loading position.

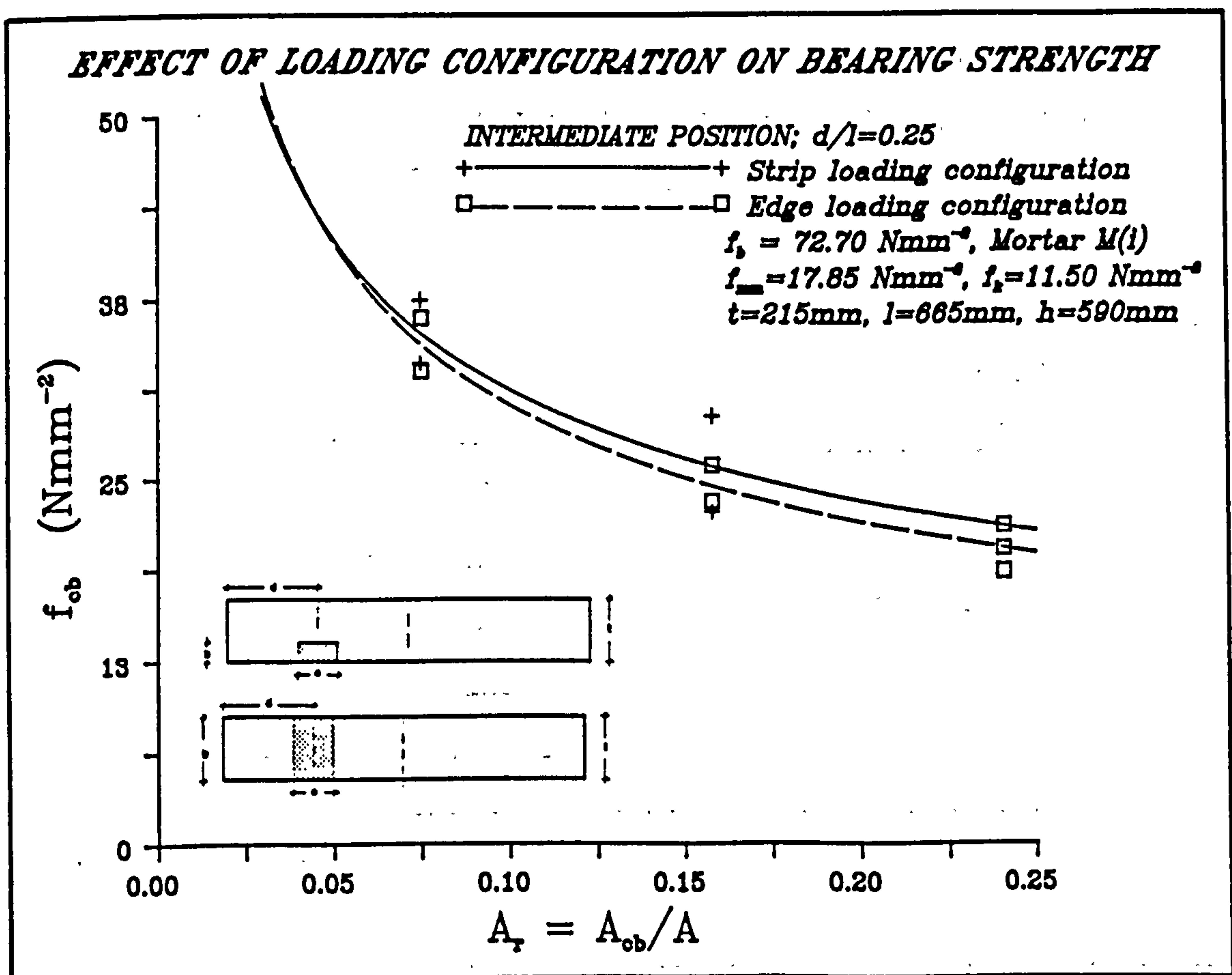


Fig. 6.78 - Effect of loading configuration on the bearing strength of masonry under intermediate loading position.

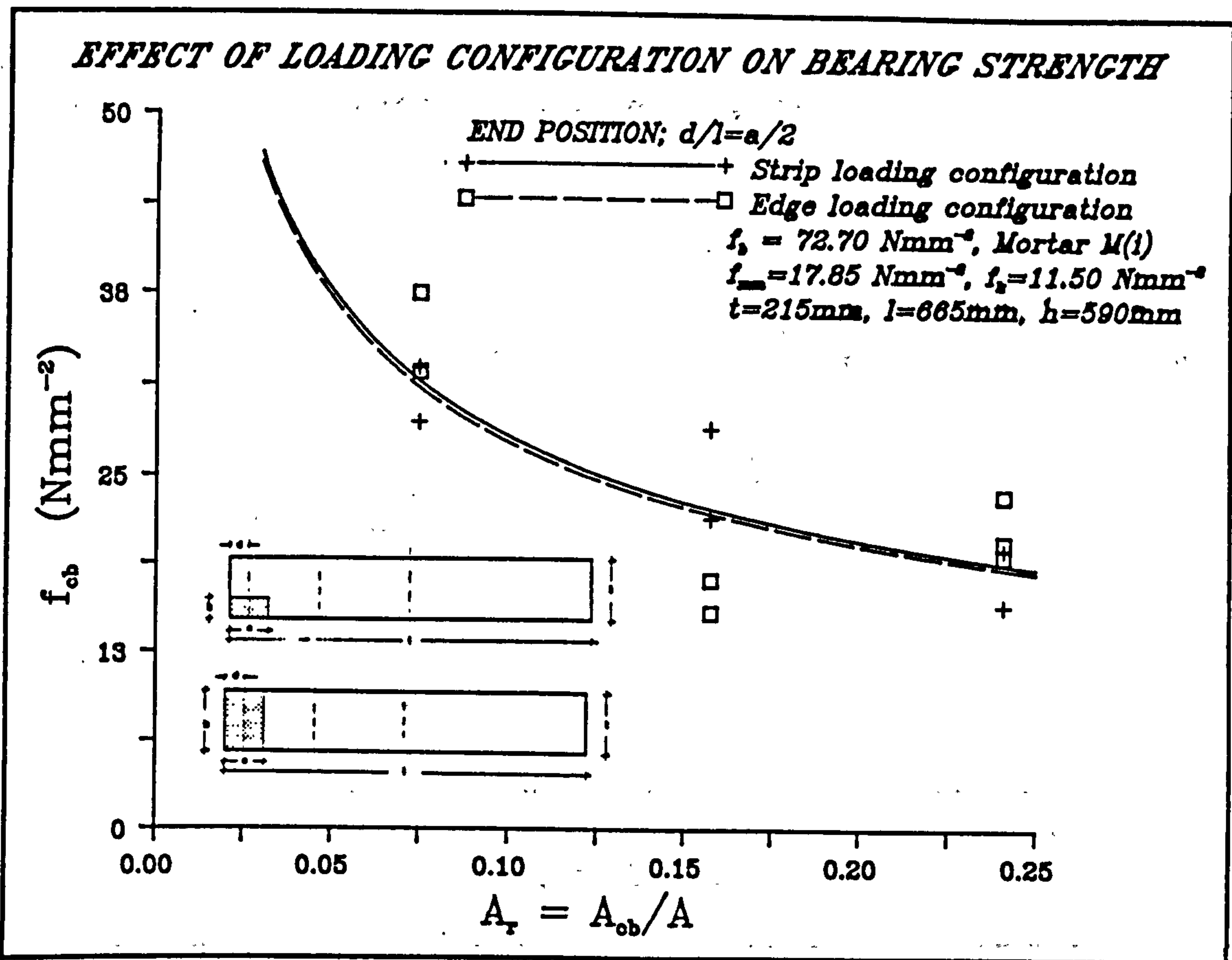


Fig. 6.79 - Effect of loading configuration on the bearing strength of masonry under end loading position.

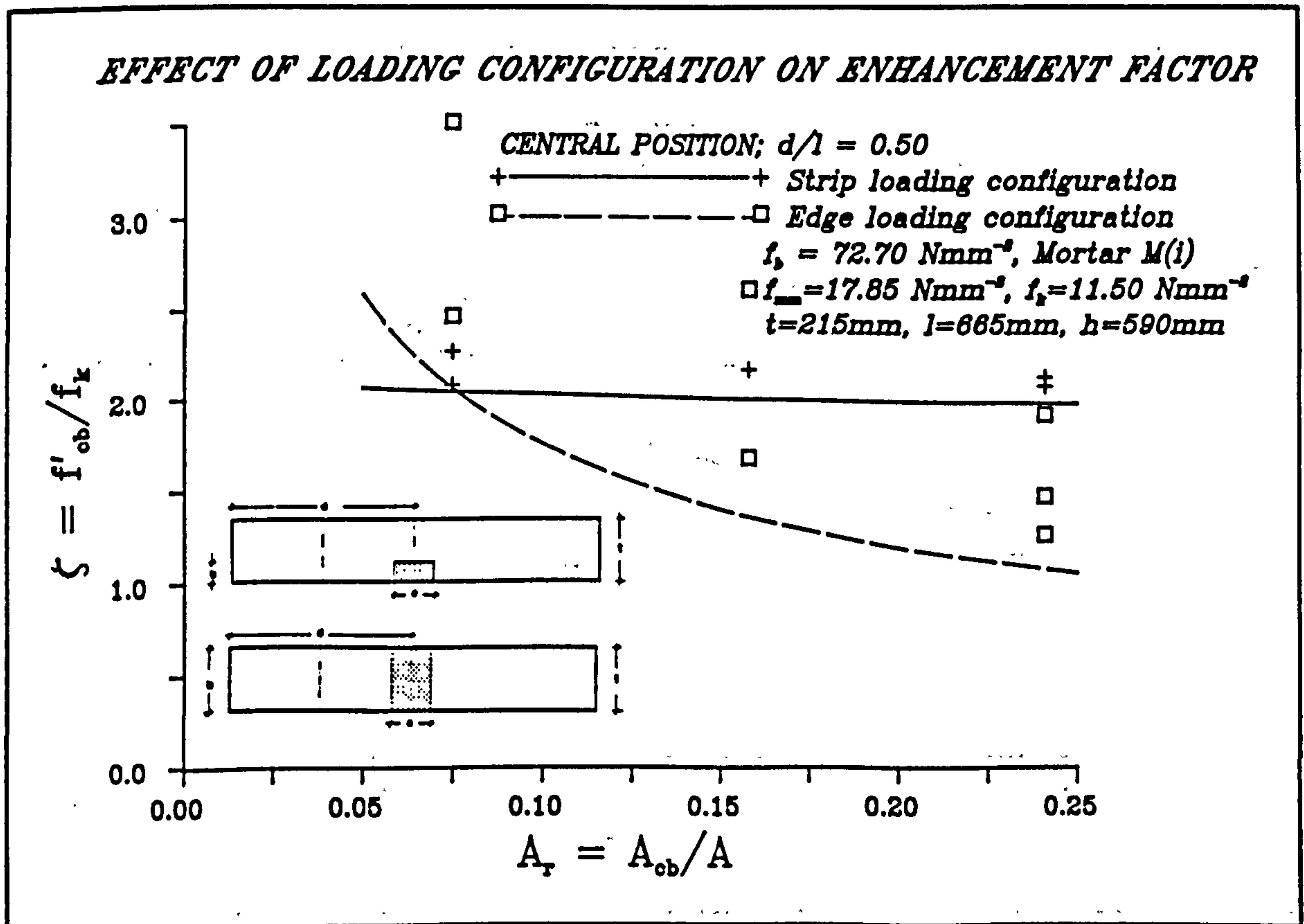


Fig. 6.80 - Effect of loading configuration on enhancement factor under central loading position.

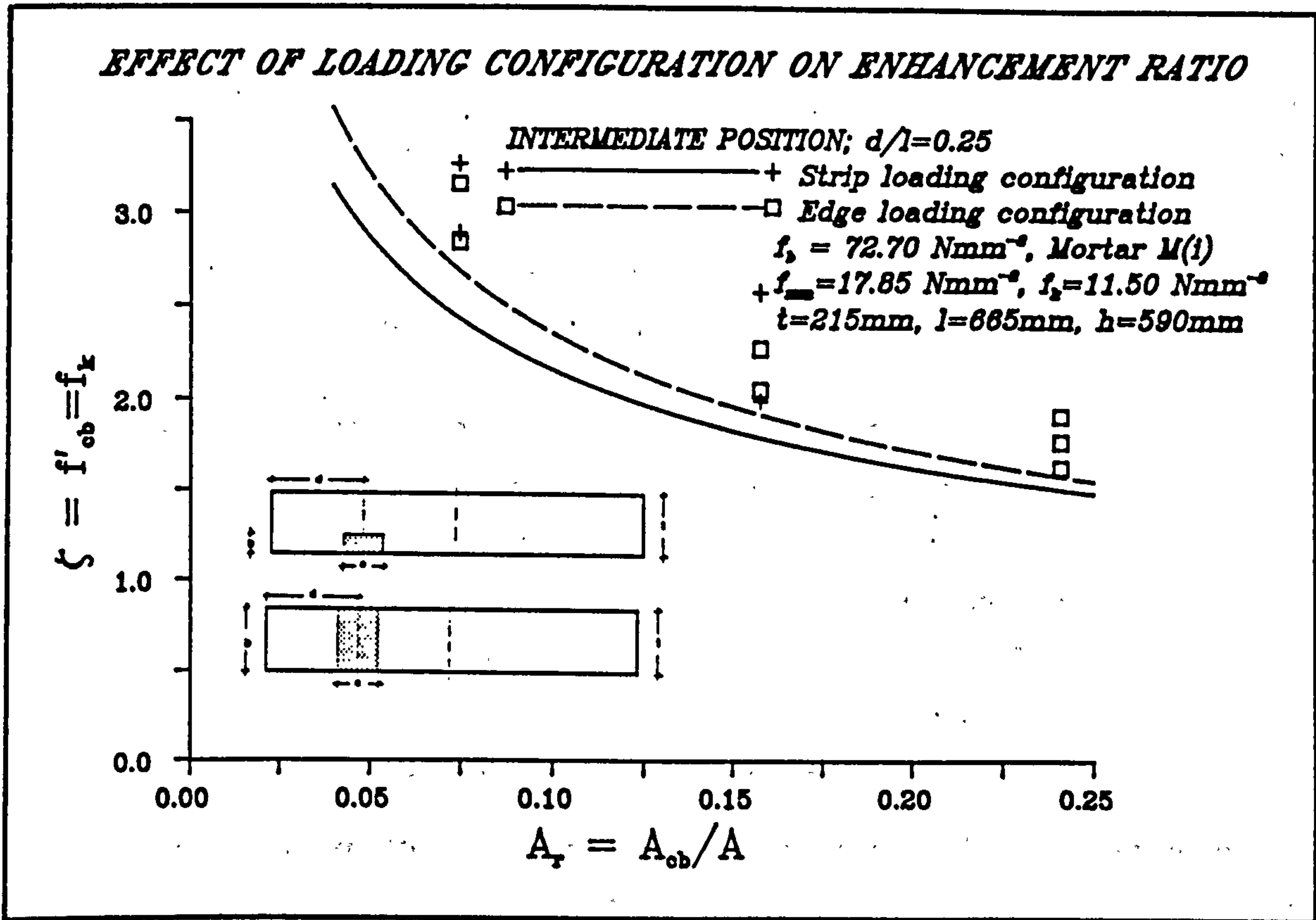


Fig. 6.81 - Effect of loading configuration on enhancement factor under intermediate loading position.

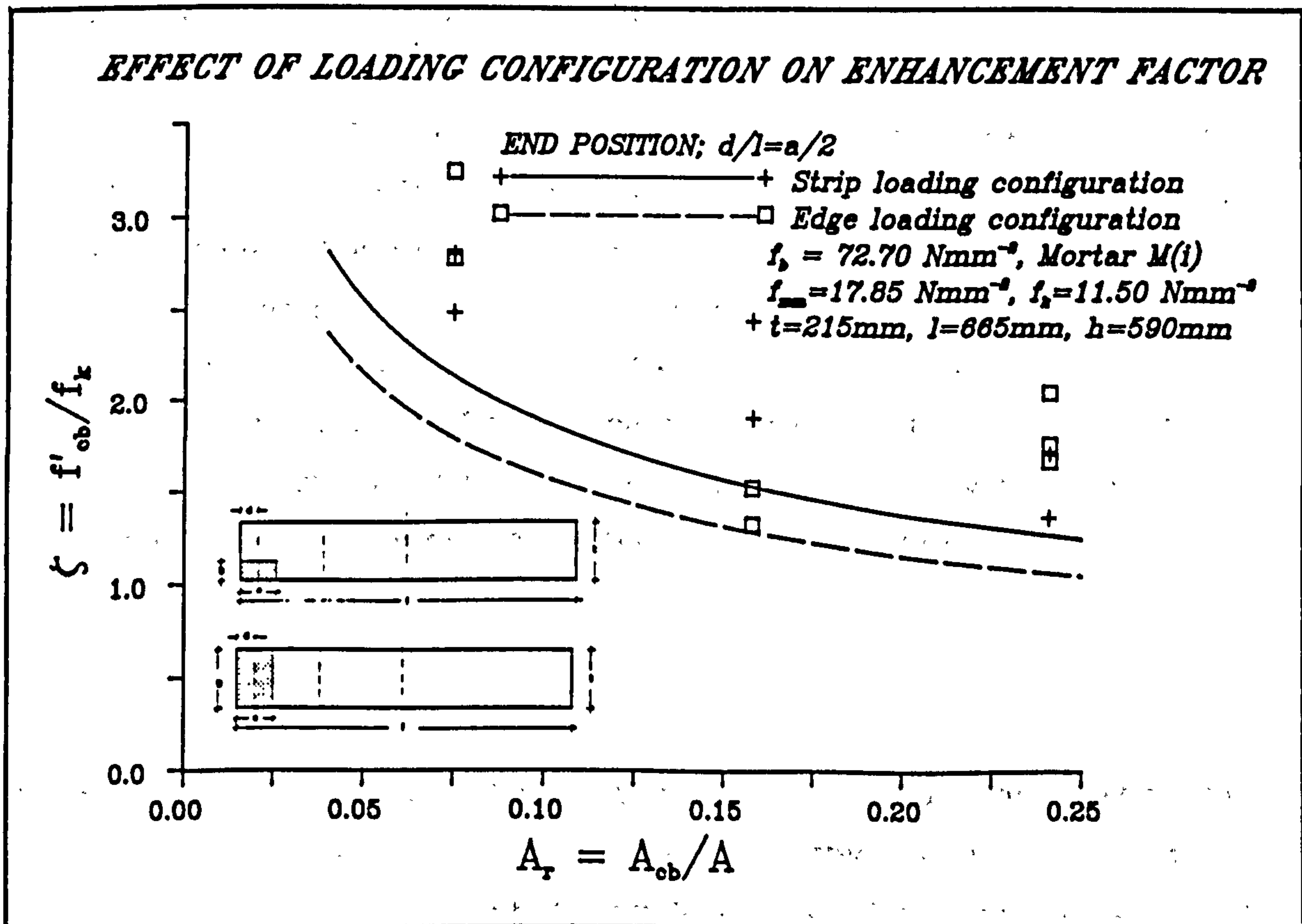


Fig. 6.82 - Effect of loading configuration on enhancement factor under end loading position.

#### 6.4.7. Type of brick unit

Influence of brick unit on the enhancement factor has been investigated by comparing the results of tests on brickwork types F (clay) and G (AAC) for three loading positions and two thicknesses of masonry constructed using the same mortar mix. The results are presented in Figs. 6.83 to 6.85 for central, intermediate and end strip concentrated loads respectively.

It is shown the bonded masonry yields higher enhancement factor and also the type of unit affects the bearing strength considerably. From the plots it could be concluded that AAC brickwork gives higher values of enhancement factor than clay brickwork. Depending on the position of loading, this increase is quite significant at low values of loaded area ratios (i.e.  $A_r \leq 0.25$ ).

### 6.5. EFFECTIVE AREA CONTRIBUTING TO THE BEARING CAPACITY

When a concentrated load is applied partially to a surface of an element having an area  $A$ , only a portion of its cross-sectional area is stressed by the dispersed load. The area beyond this stressed zone is not influenced by the concentrated load and the bearing strength under partial load is not affected to any significant degree beyond the effective area,  $A_e$ .

Some codes of practice relate the loaded area in relation to effective area in the calculation of the enhancement factor. In the case of concrete, the effective area given by the CEB<sup>[99]</sup> and German<sup>[100]</sup> codes are reproduced and are shown in Figs. 6.86 and 6.87 respectively. In the case of brickwork masonry, some of the codes<sup>[1, 85]</sup> assume dispersion of the concentrated load to be at an angle of  $45^\circ$ , and some<sup>[76]</sup> give limiting value for the loaded area. Chinese code<sup>[69]</sup> adopts expressions for effective area in terms of length of loading and the thickness of the element under concentrated load as shown in Fig. 3.2. To determine the effective area the limiting values for effective length and thickness contributing to the bearing capacity of brickwork masonry have to be investigated.

#### 6.5.1. Effective length

To determine the effective length contributing to the bearing strength of brickwork masonry a series of tests was conducted using brickwork types F (clay) and G (AAC) under central strip loading configuration by keeping the length of loading plate constant and varying the length of specimen. In the case of clay brickwork the length of bearing plate,  $a$ , was chosen as 100mm

(roughly same as the thickness of the specimens) and the result is as shown in Fig. 6.88. It can be observed that the limiting value for the effective length,  $l_e$ , could be about six times the loaded length or in this particular case, six times the thickness of the specimen. In the case of AAC brickwork the length of bearing plate,  $a$ , was chosen to be twice the thickness of the specimens (i.e. 225.0mm). The result is presented in Fig. 6.89, which shows the limiting value is about three times the loading length or again six times the thickness of the specimen.

No research work in this respect has been carried out on brickwork masonry, but it has been shown<sup>[60]</sup> that the limiting value for the effective length of concrete contributing to the bearing capacity of the specimen can be as high as eight times the actual loaded length.

### 6.5.2. Effective thickness

To determine the limiting value of the effective thickness,  $t_e$ , contributing to the bearing strength of masonry the result of tests on brickwork type M under central, intermediate and end edge (patch) loading configuration is considered. The length of the loading plate was kept constant and the width was varied. The results are presented in Fig. 6.90, which shows as the ratio  $t/b$  increases, the bearing strength increases. This is true for all three loading positions. However, this increase in the bearing strength could be due to the decrease in loaded area ratio,  $A_r$  and since it has been shown previously (ref. to Fig. 6.78 and 6.79) that there is hardly any difference between strip and edge loading configurations, therefore it could be concluded from Fig. 6.90 that the limiting value for  $t/b$  is one (i.e. when patch loading becomes strip loading).

### 6.5.3. Effective area

From the experimental investigations reported in the two previous subsections, it is possible to deduce that the effective area,  $A_e$  contributing to the bearing capacity of brickwork masonry under concentrated load is  $6t^2$ . However, when the cross-sectional area of an element under partial load is greater than  $6t^2$ , it is recommended that the bearing strength be expressed in terms of its effective loaded area ratio,  $A_{re}$ , (where  $A_{re}=A_{cb}/A_e$ ), which would put all available data into perspective and reduce the scatter commonly encountered. It should be mentioned that the results analysed in this chapter have not been modified for the effect of this parameter because  $A_{re}$  and  $A_r$  are the same for the specimens tested.



**EFFECT OF TYPE OF UNIT ON ENHANCEMENT FACTOR**

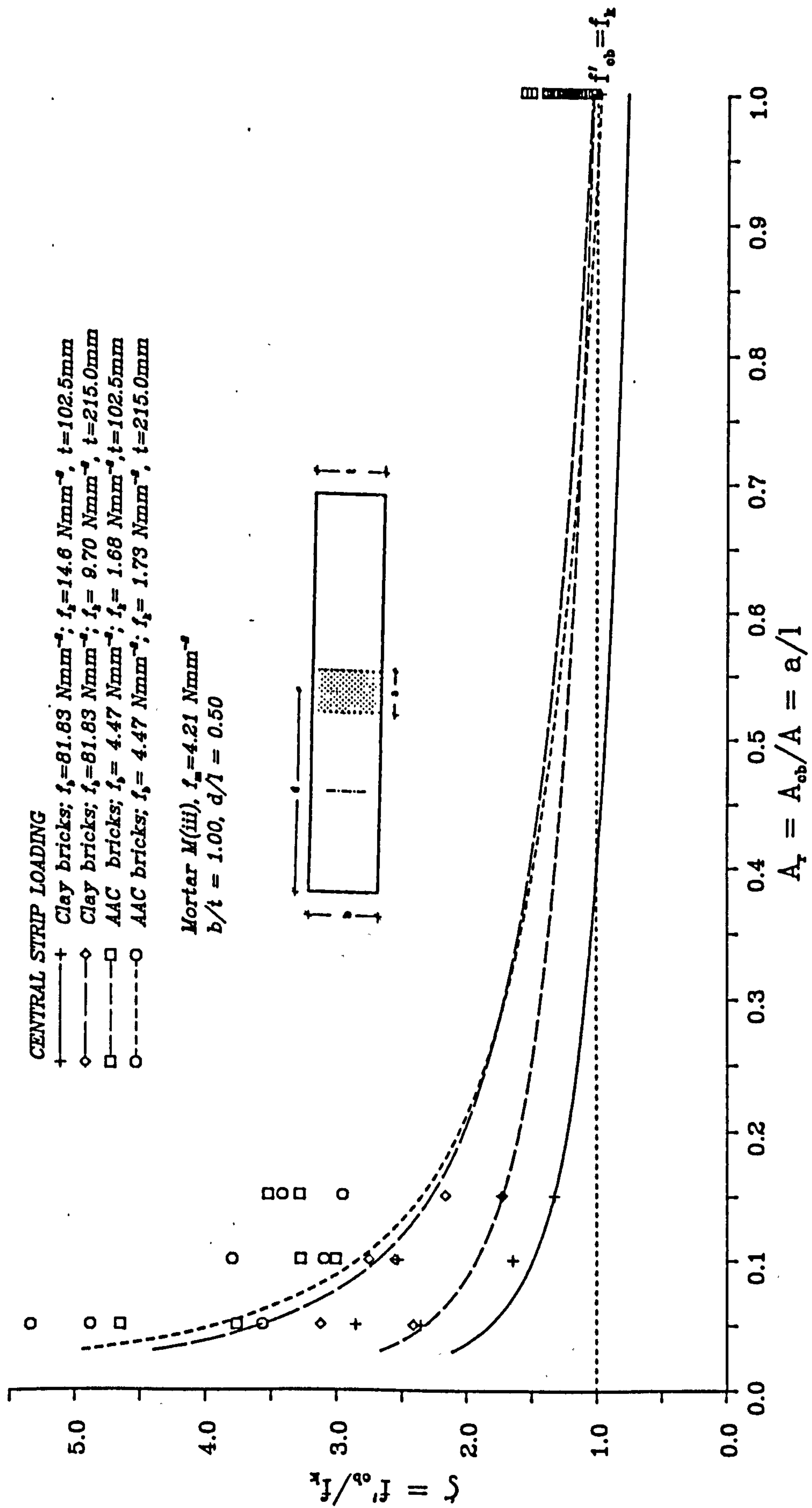


Fig. 6.83 - Influence of unit brick type on enhancement factor under central strip loading.

**EFFECT OF TYPE OF UNIT ON ENHANCEMENT FACTOR**

**INTERMEDIATE STRIP LOADING**

- + Clay bricks;  $f_s = 81.83 \text{ Nmm}^{-2}$ ;  $f_c = 14.6 \text{ Nmm}^{-2}$ ;  $t = 102.5 \text{ mm}$
- ◇ Clay bricks;  $f_s = 81.83 \text{ Nmm}^{-2}$ ;  $f_c = 9.70 \text{ Nmm}^{-2}$ ;  $t = 215.0 \text{ mm}$
- AAC bricks;  $f_s = 4.47 \text{ Nmm}^{-2}$ ;  $f_c = 1.68 \text{ Nmm}^{-2}$ ;  $t = 102.5 \text{ mm}$
- AAC bricks;  $f_s = 4.47 \text{ Nmm}^{-2}$ ;  $f_c = 1.73 \text{ Nmm}^{-2}$ ;  $t = 215.0 \text{ mm}$

Mortar M(III),  $f_m = 4.21 \text{ Nmm}^{-2}$   
 $b/t = 1.00$ ,  $d/l = 0.25$

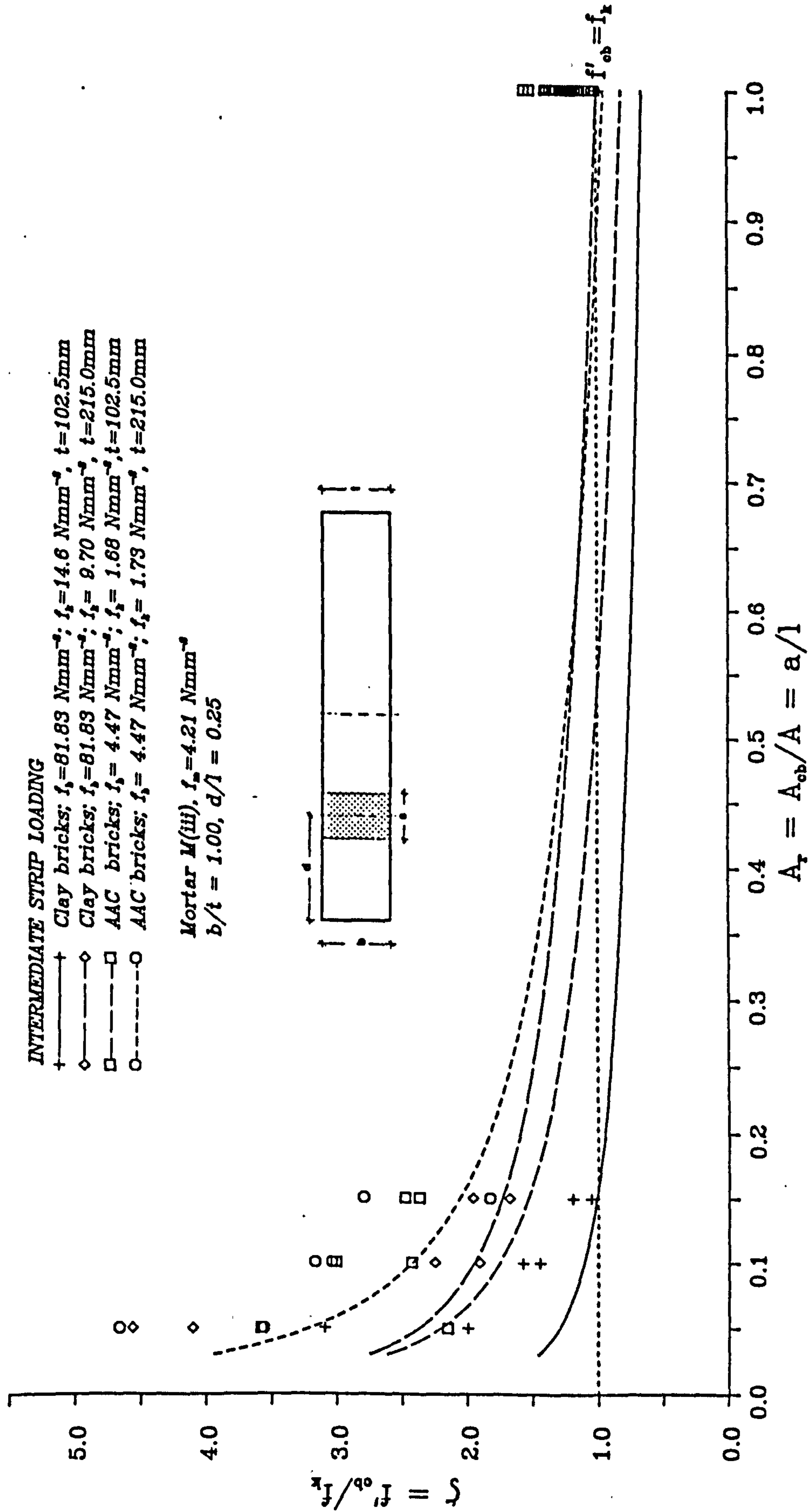
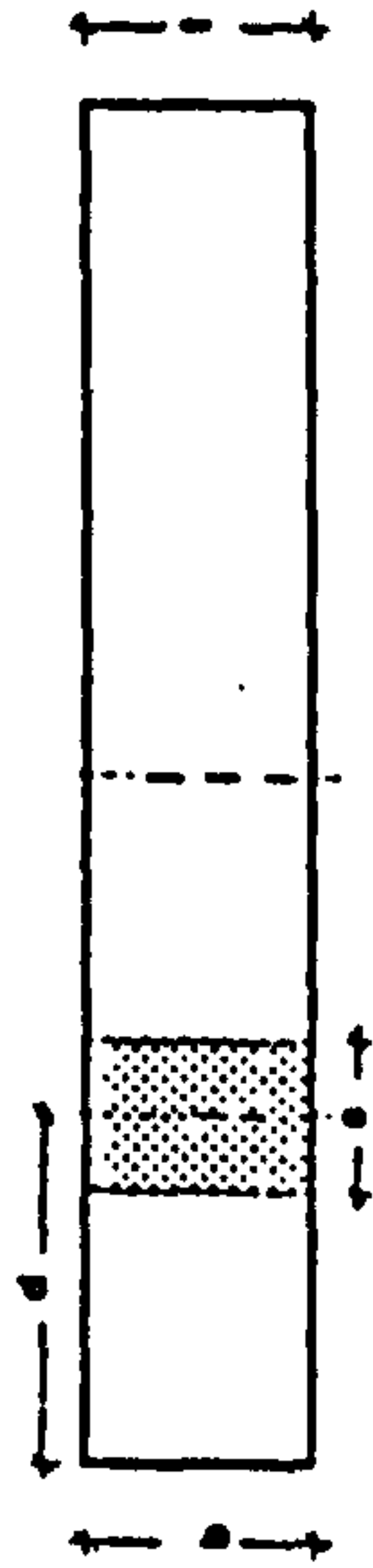


Fig. 6.84 - Influence of unit brick type on enhancement factor under intermediate strip loading.

**EFFECT OF TYPE OF UNIT ON ENHANCEMENT FACTOR**

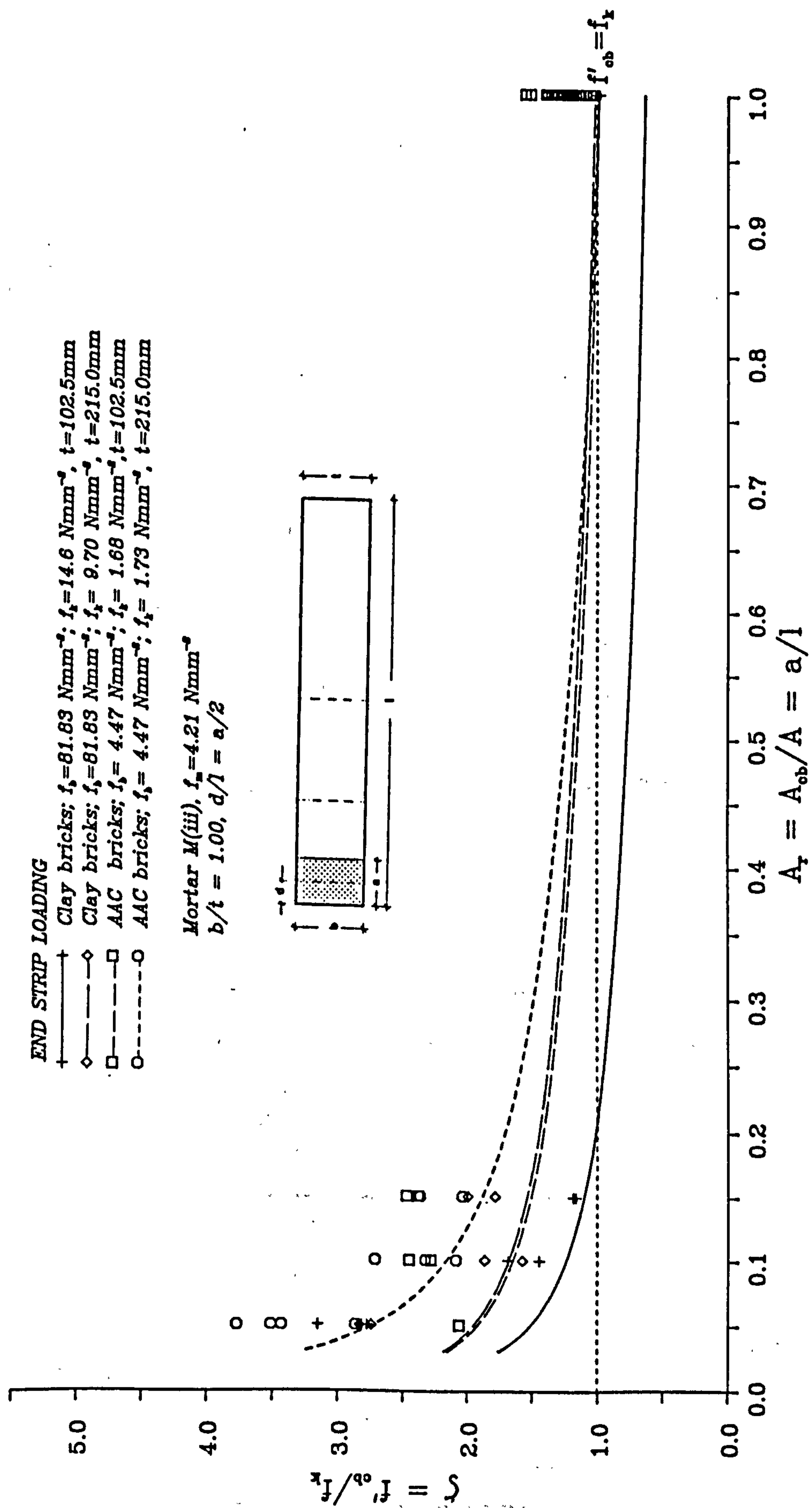


Fig. 6.85 - Influence of unit brick type on enhancement factor under end strip loading.

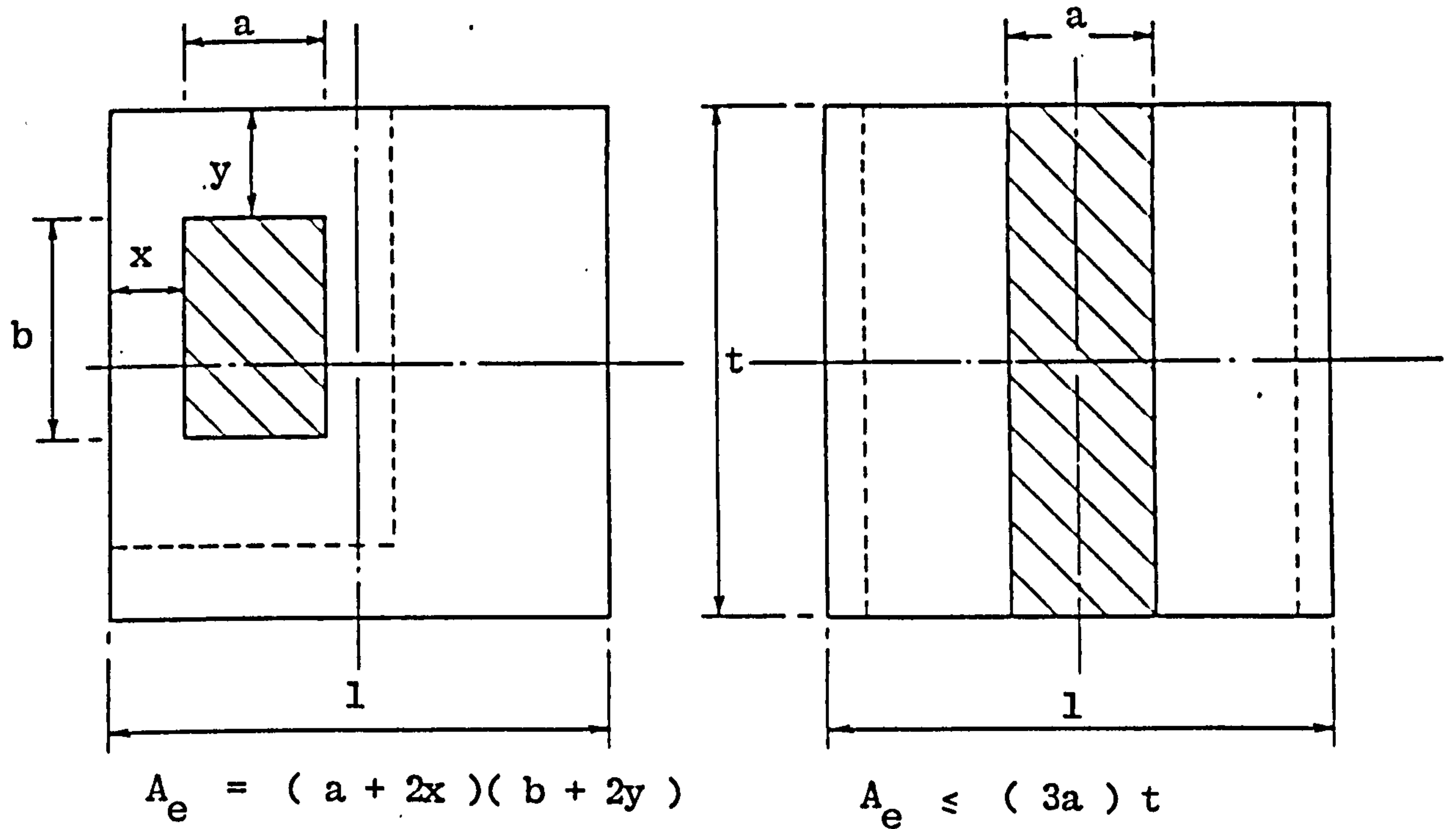


Fig. 6.86 - Effective areas according to CEB<sup>[99]</sup>.

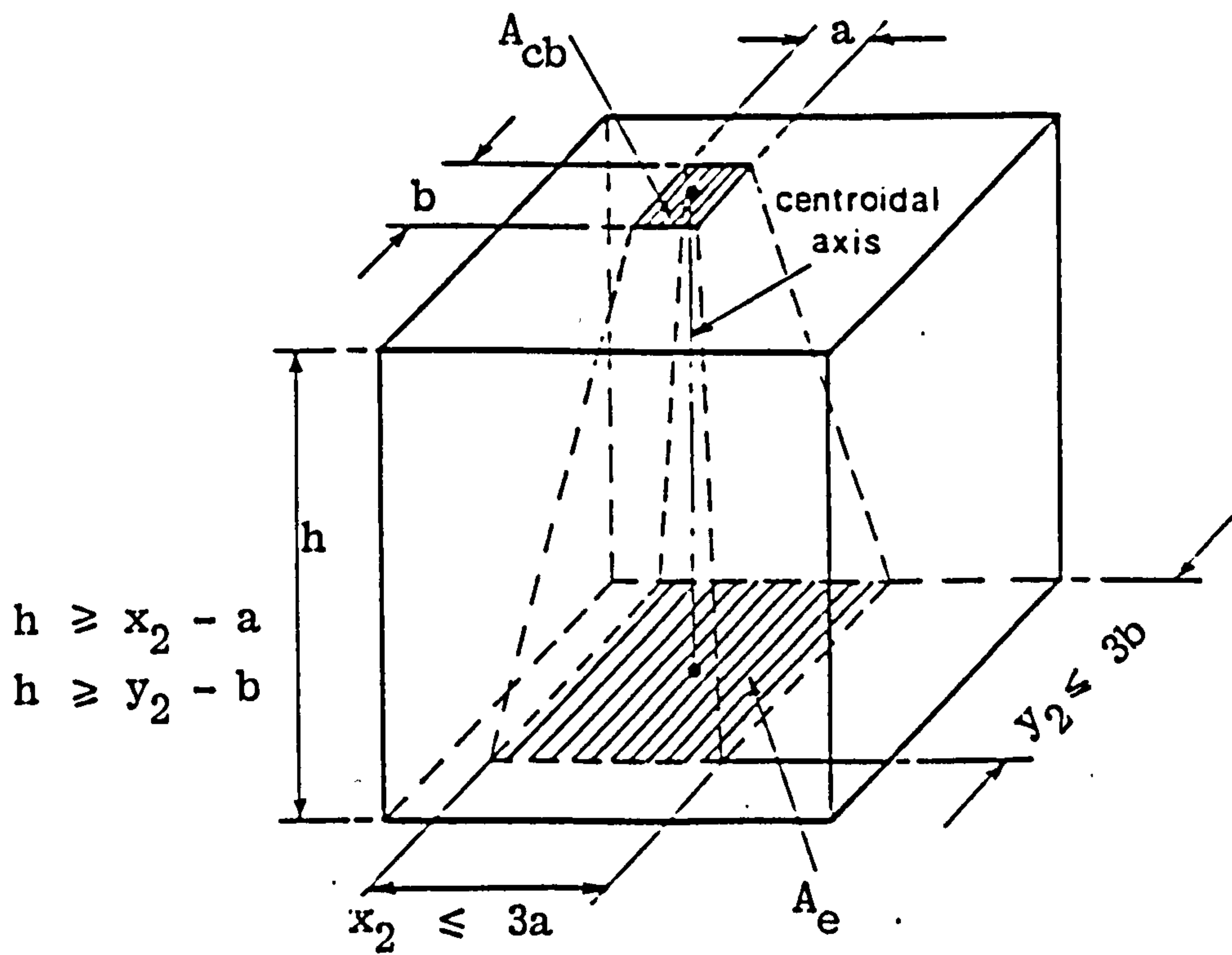


Fig. 6.87 - Effective area according to DIN 1045<sup>[100]</sup>.

**DETERMINATION OF THE LIMITING VALUE OF THE "EFFECTIVE LENGTH"  
CONTRIBUTING TO THE BEARING STRENGTH OF MASONRY**

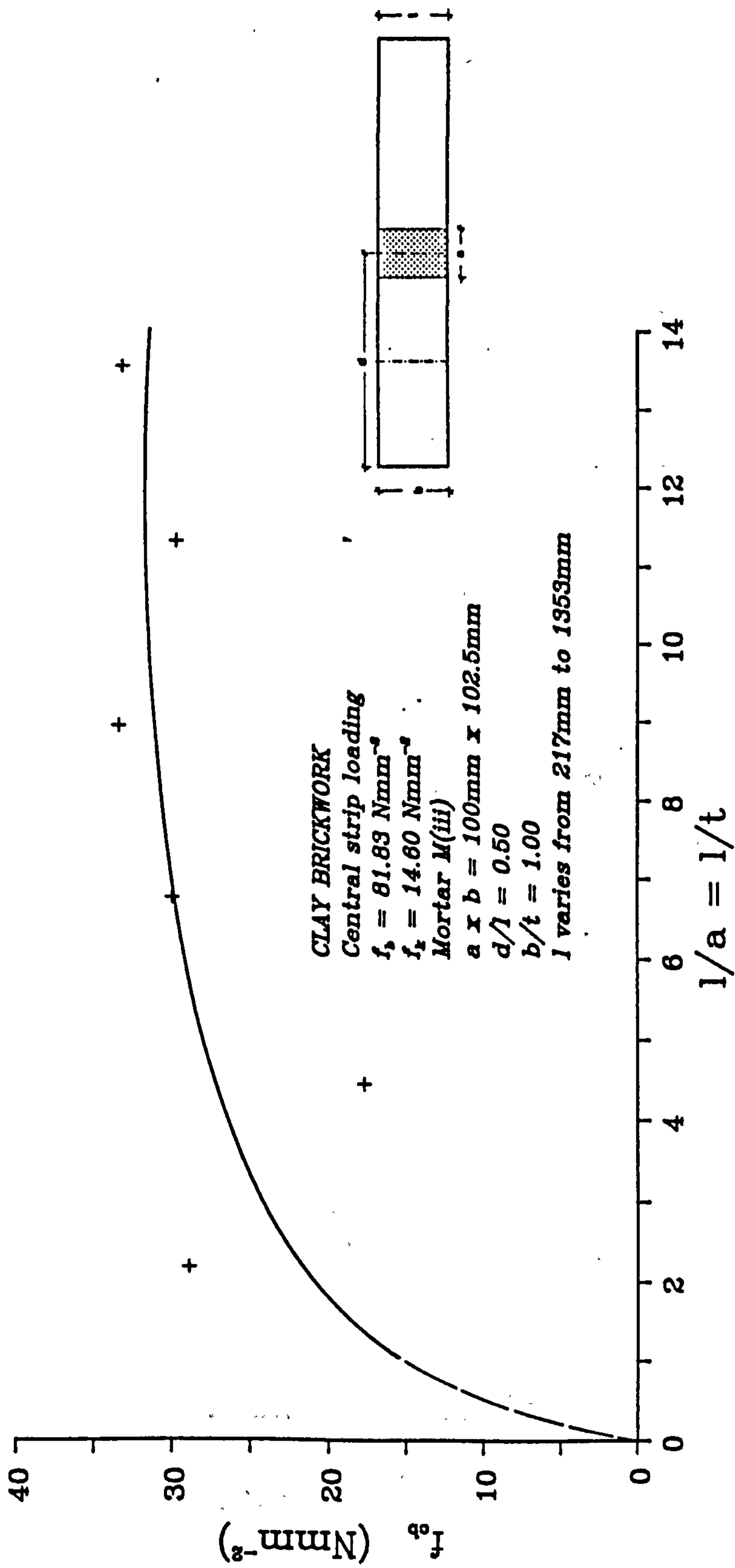


Fig. 6.88 - Determination of the limiting value of the effective length contributing to the bearing strength of clay masonry under central strip load.

**DETERMINATION OF THE LIMITING VALUE OF THE "EFFECTIVE LENGTH"  
CONTRIBUTING TO THE BEARING STRENGTH OF MASONRY**

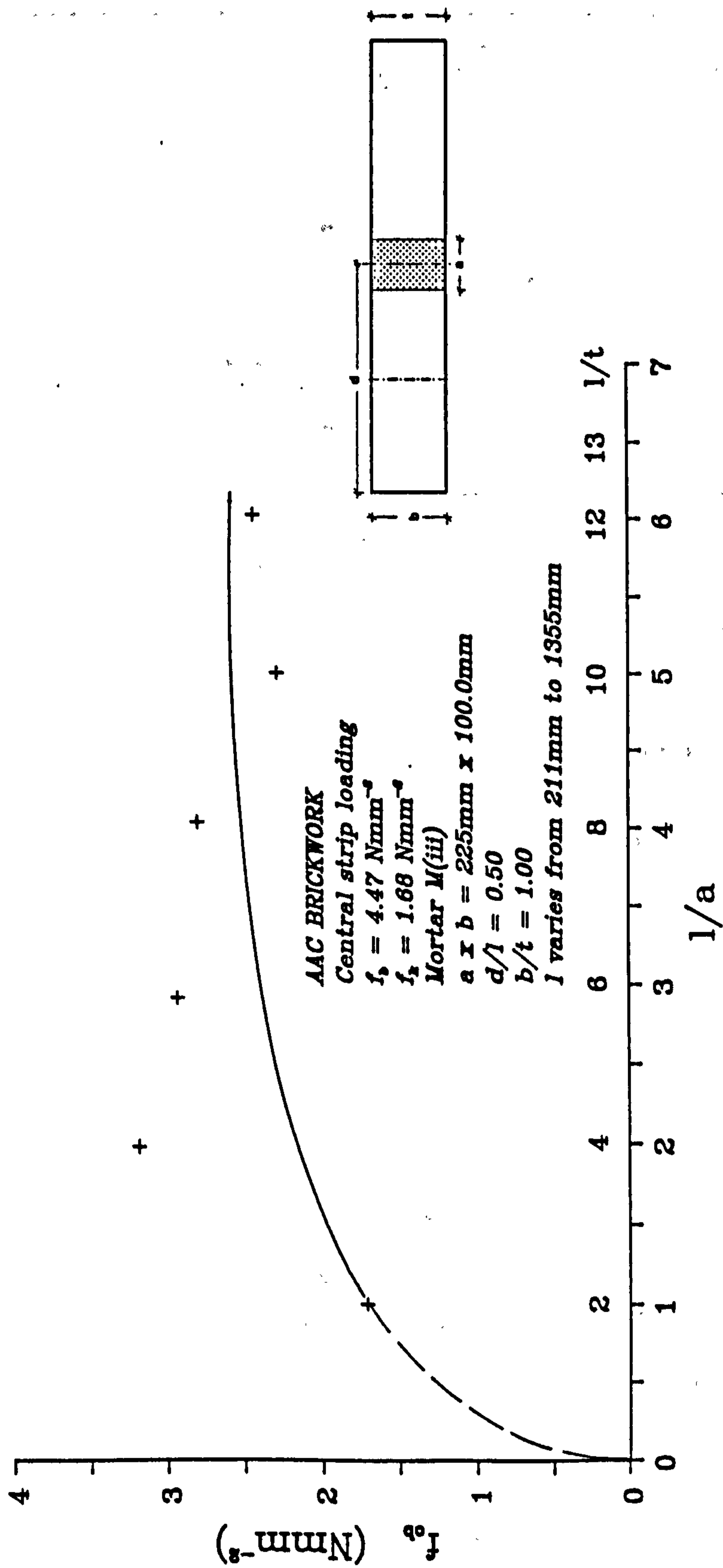


Fig. 6.89 - Determination of the limiting value of the effective length contributing to the bearing strength of AAC masonry under central strip load.

**DETERMINATION OF THE LIMITING VALUE OF THE "EFFECTIVE THICKNESS"  
CONTRIBUTING TO THE BEARING STRENGTH OF MASONRY**

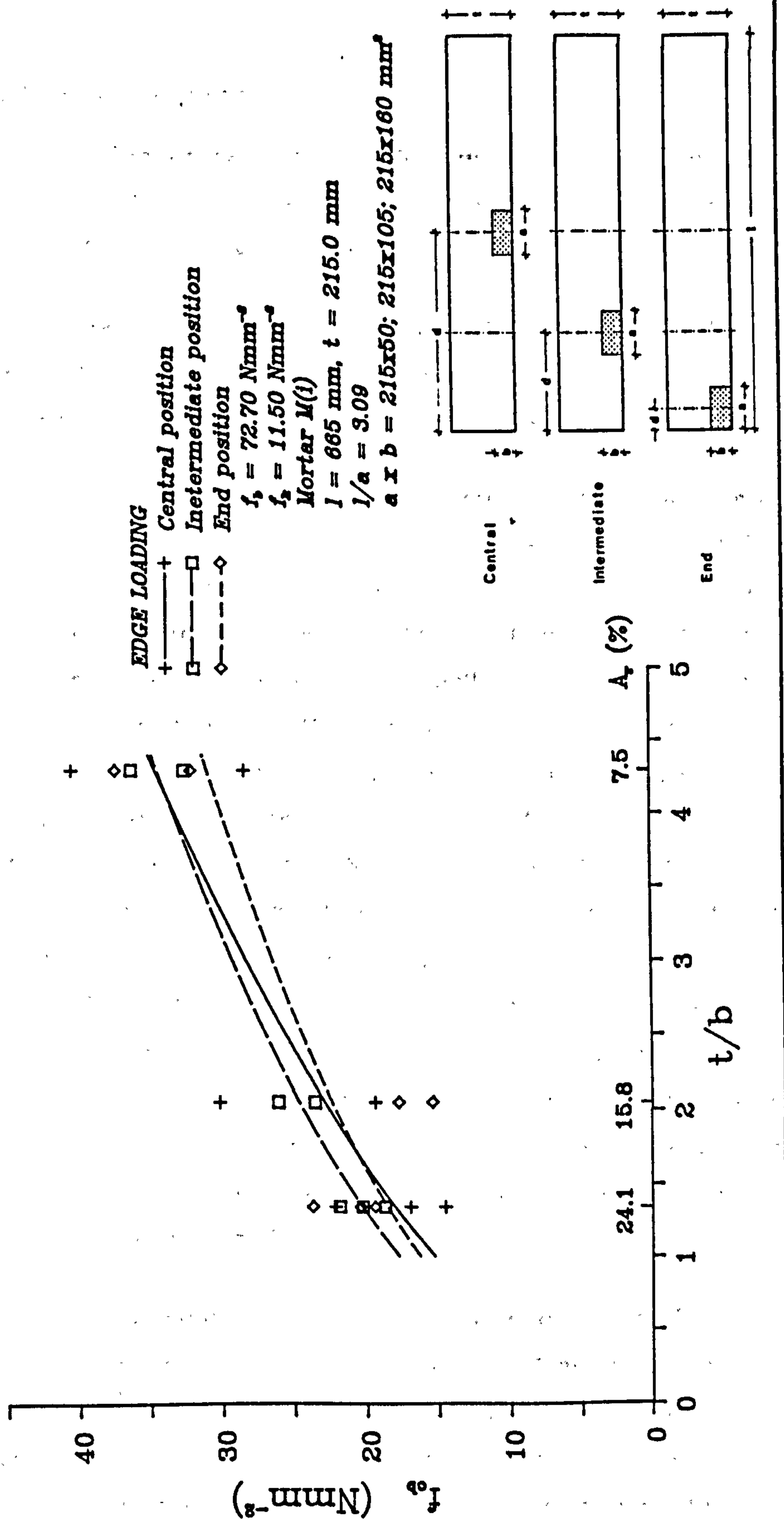


Fig. 6.90 - Determination of the limiting value of the effective thickness contributing to the bearing strength of clay masonry under central, intermediate and end strip loads.

## **6.6. MODE OF FAILURE**

### **6.6.1. Strip Loading Configuration**

Typical failure mode and crack pattern under central strip concentrated load for brickwork types A, B, C, D, E, F, and G for various loaded area ratios are presented in Figs. 6.91 to 6.99 respectively.

The appearance of cracks in relation to failure of the specimen depends on the loaded area ratio,  $A_r$ , the type of brick unit used in the construction and the position of applied load along the length of the specimen.

For clay brickwork under central strip loading, a vertical crack under the centre of the applied concentrated load is observed first (at about 30-70% of the ultimate load depending on the loaded area ratio) followed by diagonal cracks under the edges of the bearing plate confined within a fan of  $30^\circ$  before failure. This is sometimes accompanied by spalling and local failure of the brickwork under the bearing plate within the bearing zone. The primary vertical crack is initiated below the middle half of the specimen and propagating up and down the height of the specimen as the load is increased. This will eventually split the specimen into two halves at failure. As loaded area ratio,  $A_r$ , increases the formation of vertical cracks increases and also the ratio of cracking load to ultimate load at failure ( $F_r = F_c / F_u$ ) decreases. The results show when  $A_r = 0.05$ ,  $F_r = 0.70$  and decreases to  $F_r = 0.35$  at  $A_r = 0.40$ . The effect of thickness on the failure pattern is also pronounced in a way that the primary vertical crack is no longer the dominant crack in a 215.0mm thick specimen compared to 102.5mm thick specimen. In this case the failure is caused by the formation of diagonal cracks and local crushing under the bearing plate as it is clearly shown by comparing Figs. 6.96 and 6.97.

AAC brickwork specimens subjected to this form of loading, (see Figs. 6.98 and 6.99), it exhibits tensile cracking parallel to the line of action of the imposed load and also the formation of a wedge or a cone, immediately under the loaded face which moves downwards, splitting the specimen apart (see Fig. 6.110). In some cases diagonal cracks have been observed under the edges of the bearing plate or local crushing of the unit within the bearing zone.

In the case of intermediate strip concentrated load of which typical failure mode and crack pattern for brickwork types E, F and G for various loaded area ratios are shown in Figs. 6.100 to 6.104, the failure mode of clay and AAC



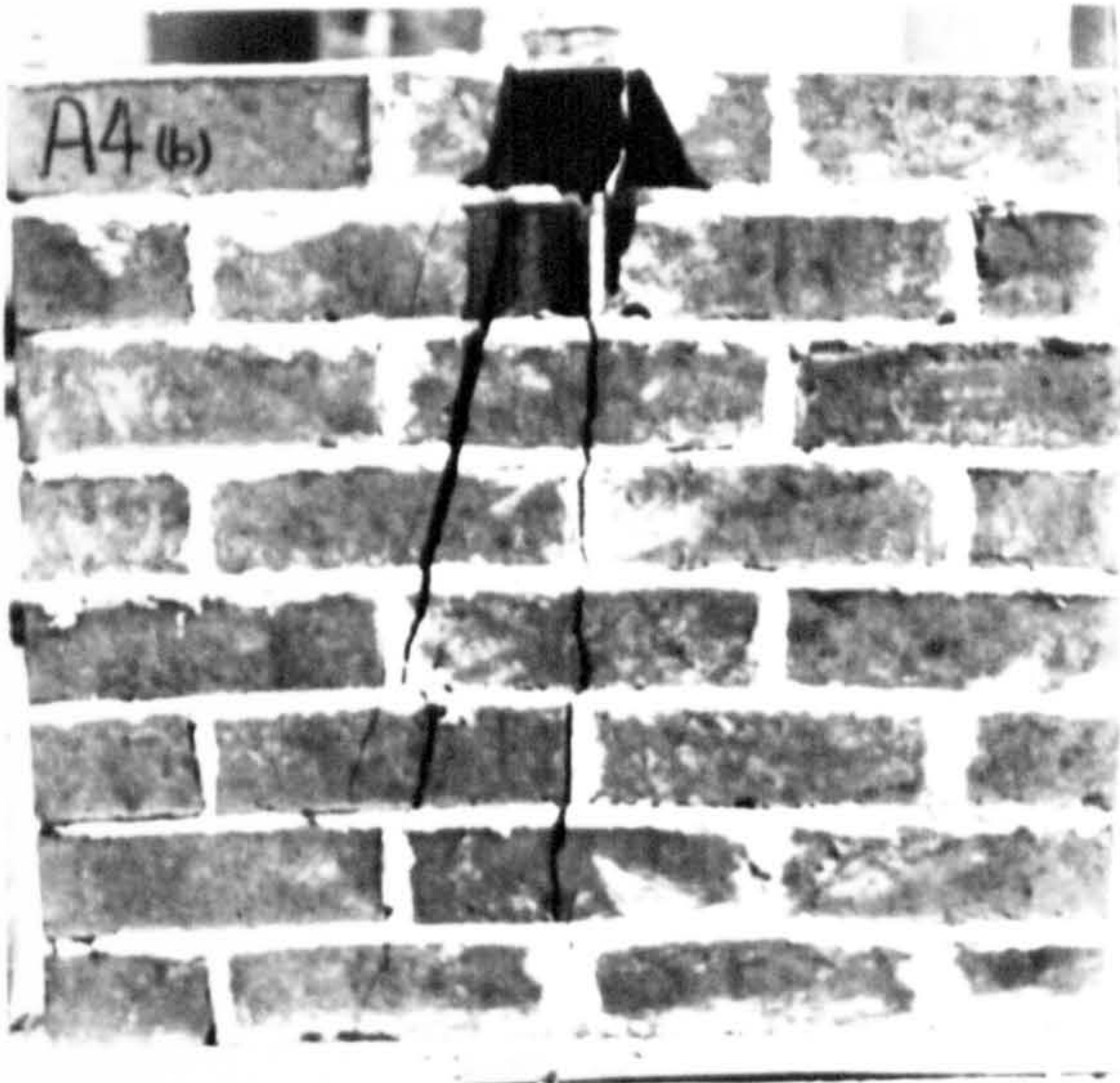
brickwork are the same as their respective central position, except that the ratio of cracking load to the ultimate load at failure is greater than in the former case. Again in this case as loaded area ratio increases, the ratio  $F_r$  decreases. The results show for  $A_r=0.05$ ,  $F_r=0.87$  and decreases to  $F_r=0.50$  at  $A_r=0.40$ . The formation of vertical crack under the centre line of the bearing plate or sometimes in the a plane of perpend (plane of weakness) and diagonal cracks under the edges of the plate are accompanied sometimes by spalling of the brickwork and local crushing.

Typical failure mode and crack pattern under end strip concentrated load for brickwork types E, F and G for various loaded area ratios are presented in Figs. 6.105 to 6.109 respectively. Vertical and diagonal cracks are observed under the edge of the bearing plate sometimes running down the whole height of the specimen. These sometimes are accompanied by spalling of the brickwork and local crushing especially under small bearing plate. It is worth mentioning that, from the experimental results, the ratio of cracking load to the ultimate load at failure,  $F_r$ , for this type of loading configuration is approximately 0.68 and remains unchanged for varying area ratio,  $A_r$ .

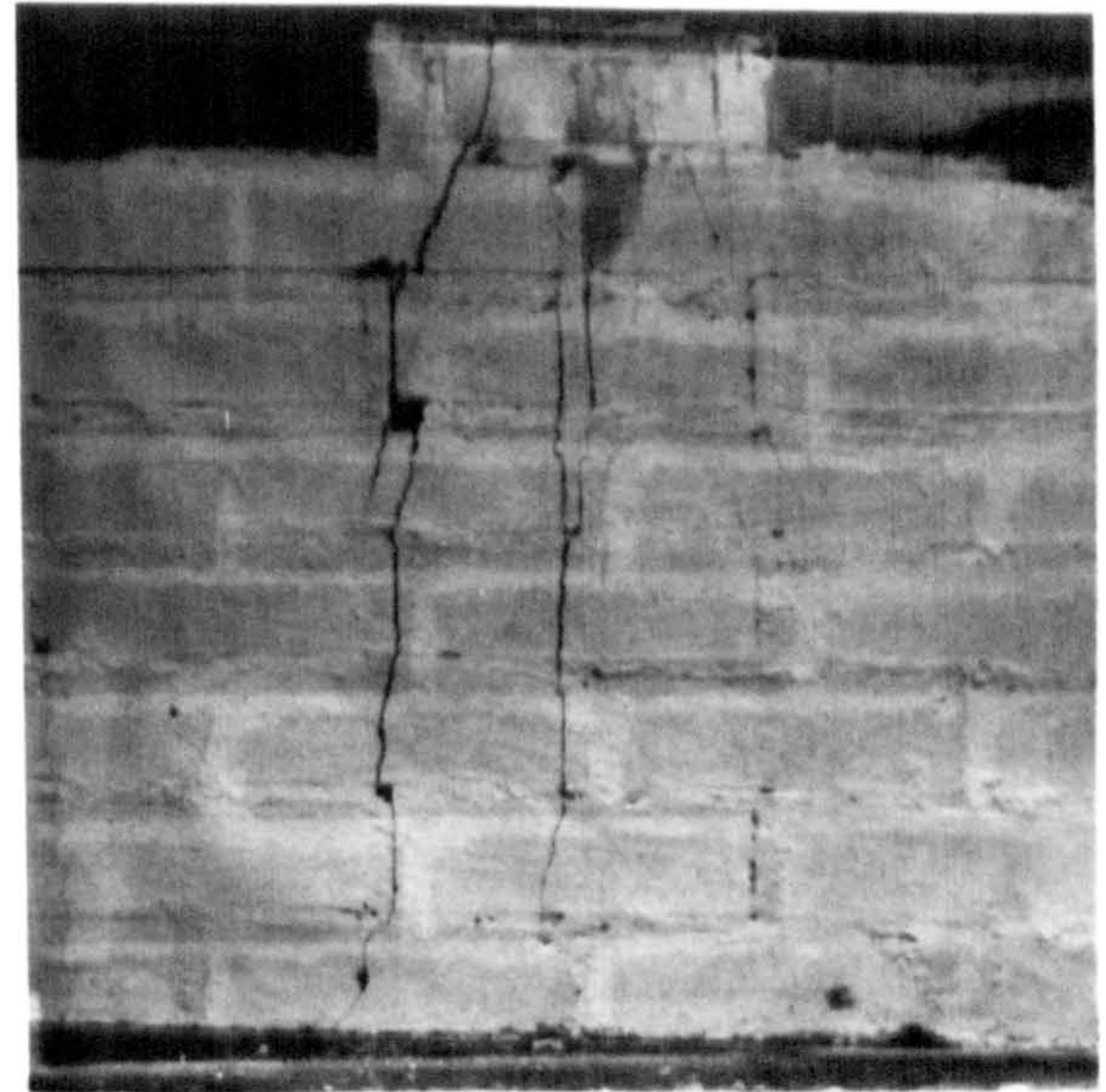
#### **6.6.2. Edge Loading Configuration**

Typical failure mode and crack pattern under central, intermediate and end edge concentrated load for brickwork type M (results reported in Table B1 in Appendix B) for various loaded area ratios are presented in Figs. 6.111 to 6.113 respectively.

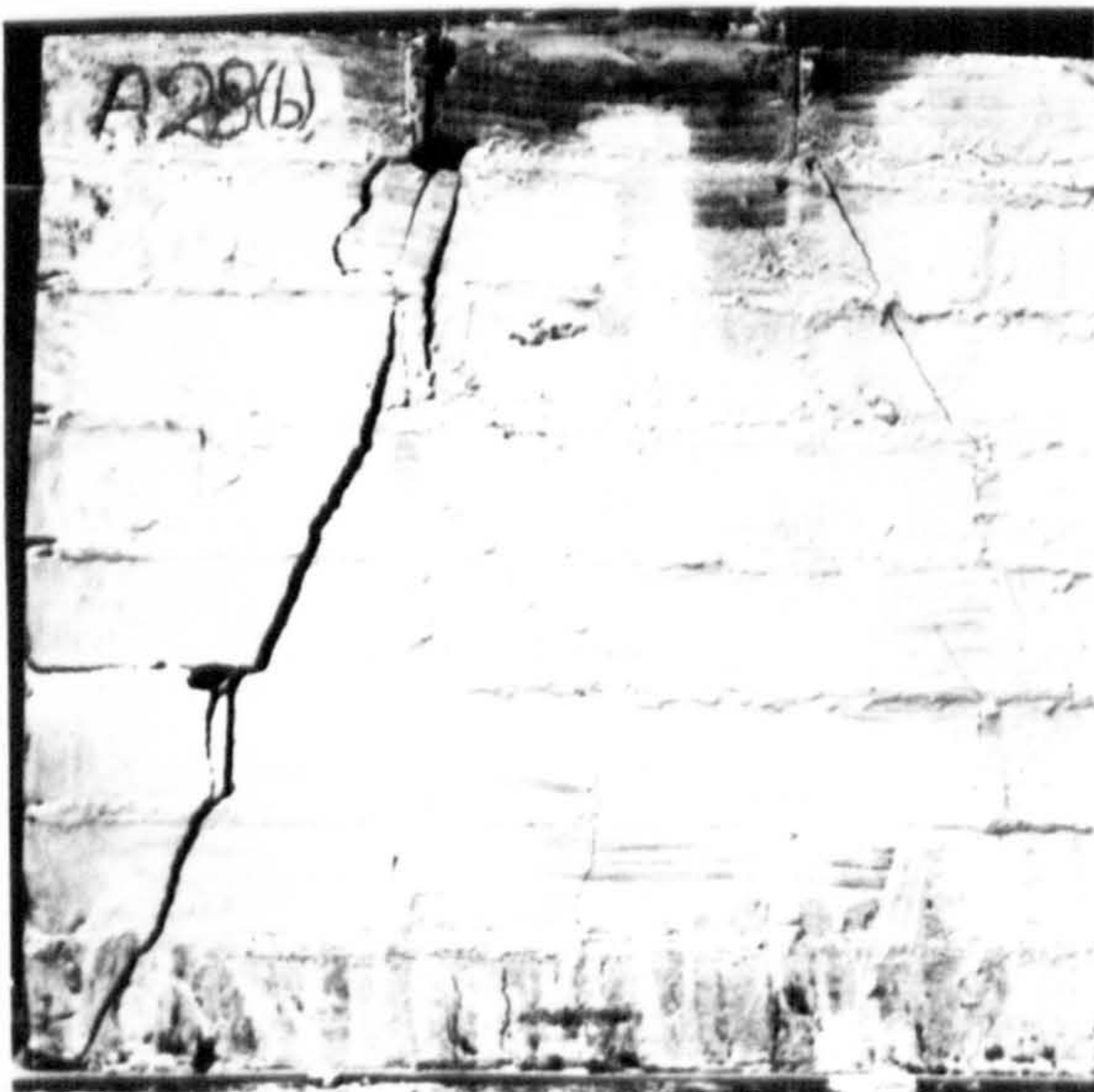
Spalling was frequently observed to be the first sign, usually followed by vertical cracks on one or more faces, often initiating at the mid-height under the edge and at the centre of the plate. Diagonal cracks were formed under the edge/s of the bearing plate, sometimes running down the whole height of the specimen contained within  $30^\circ$  fan to the vertical. In some cases local crushing and collapse of brickwork under the bearing was observed at failure.



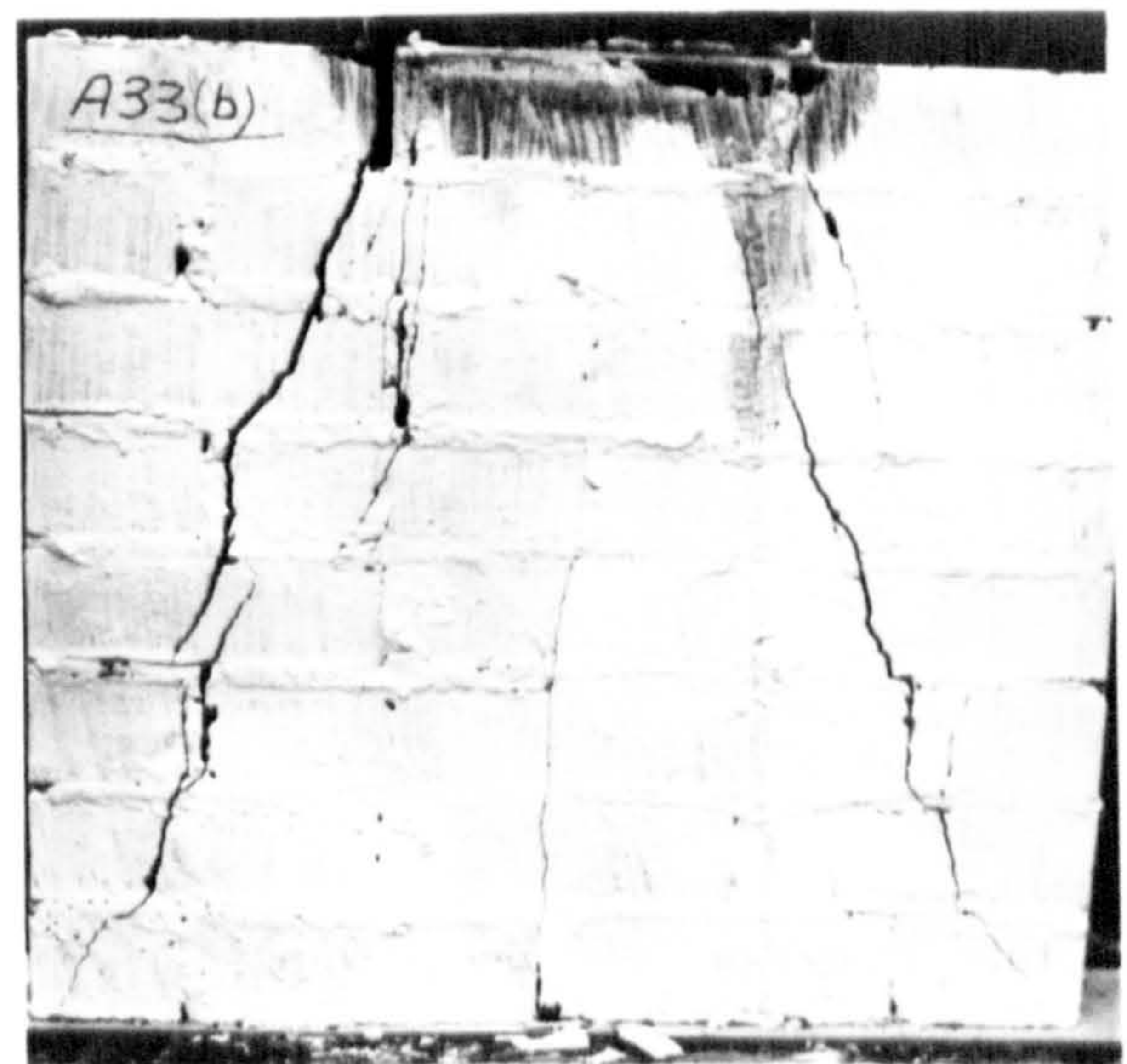
(a)-  $A_r = 0.10$



(b)-  $A_r = 0.20$

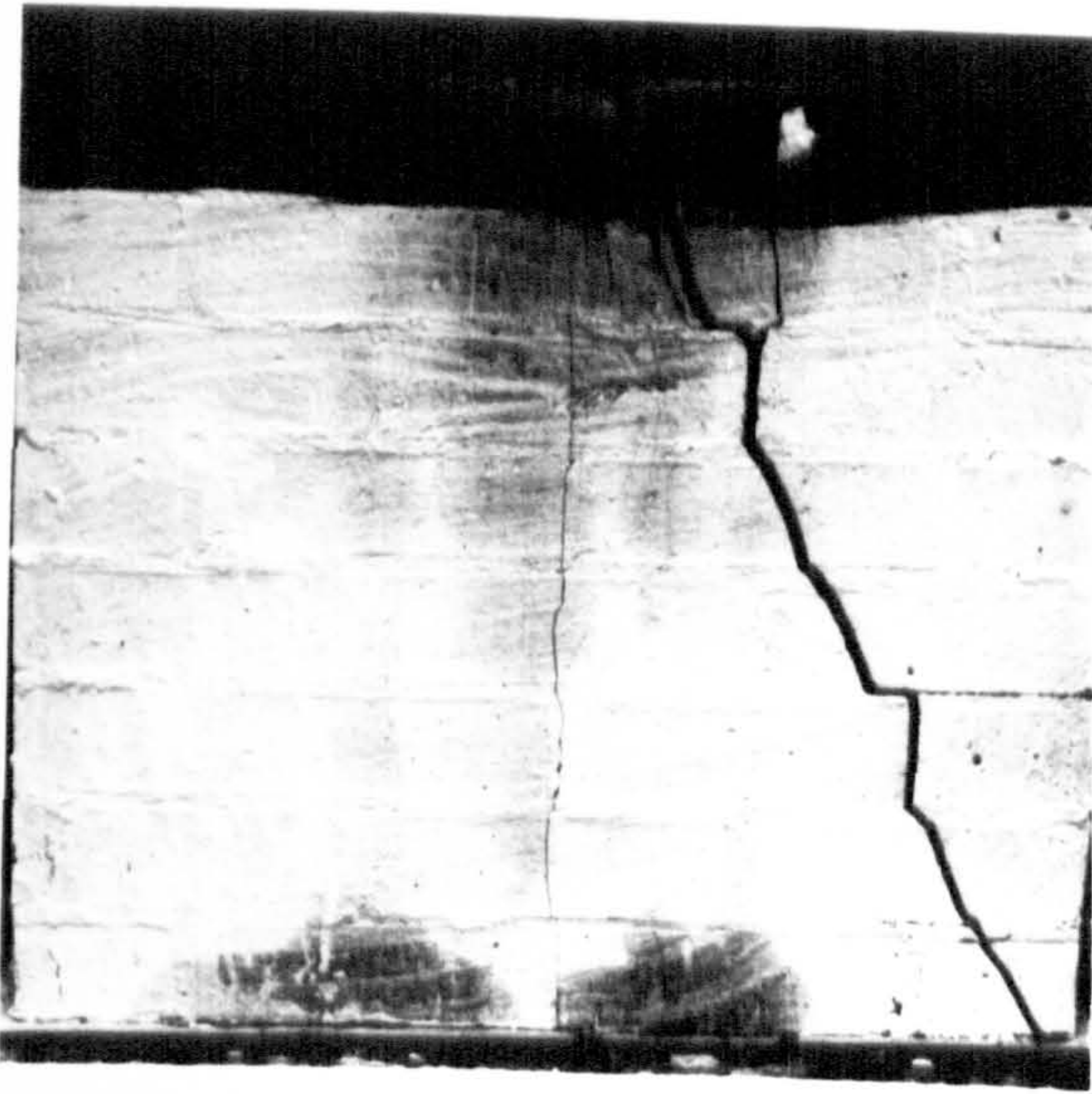


(c)-  $A_r = 0.20$

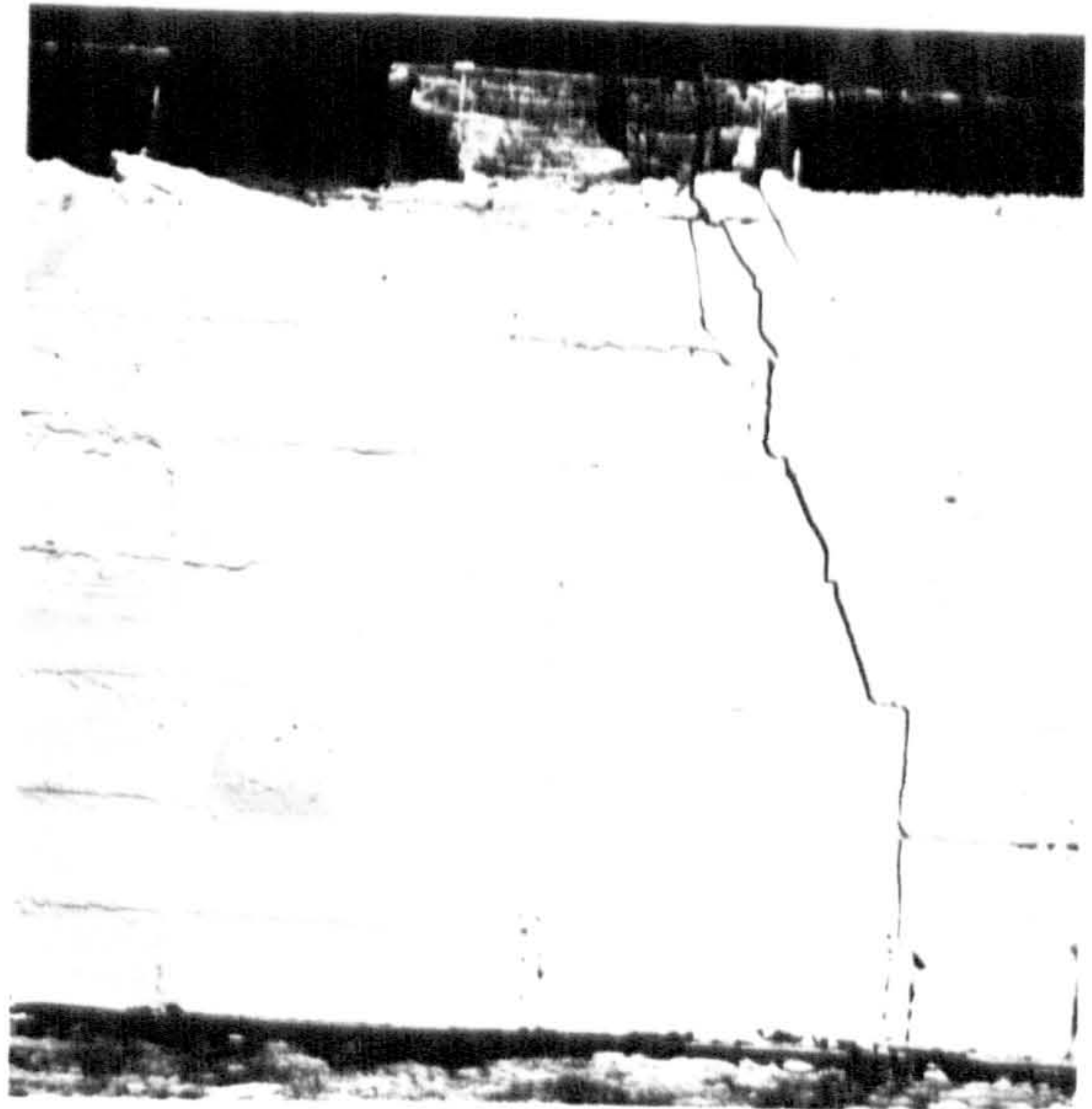


(d)-  $A_r = 0.40$

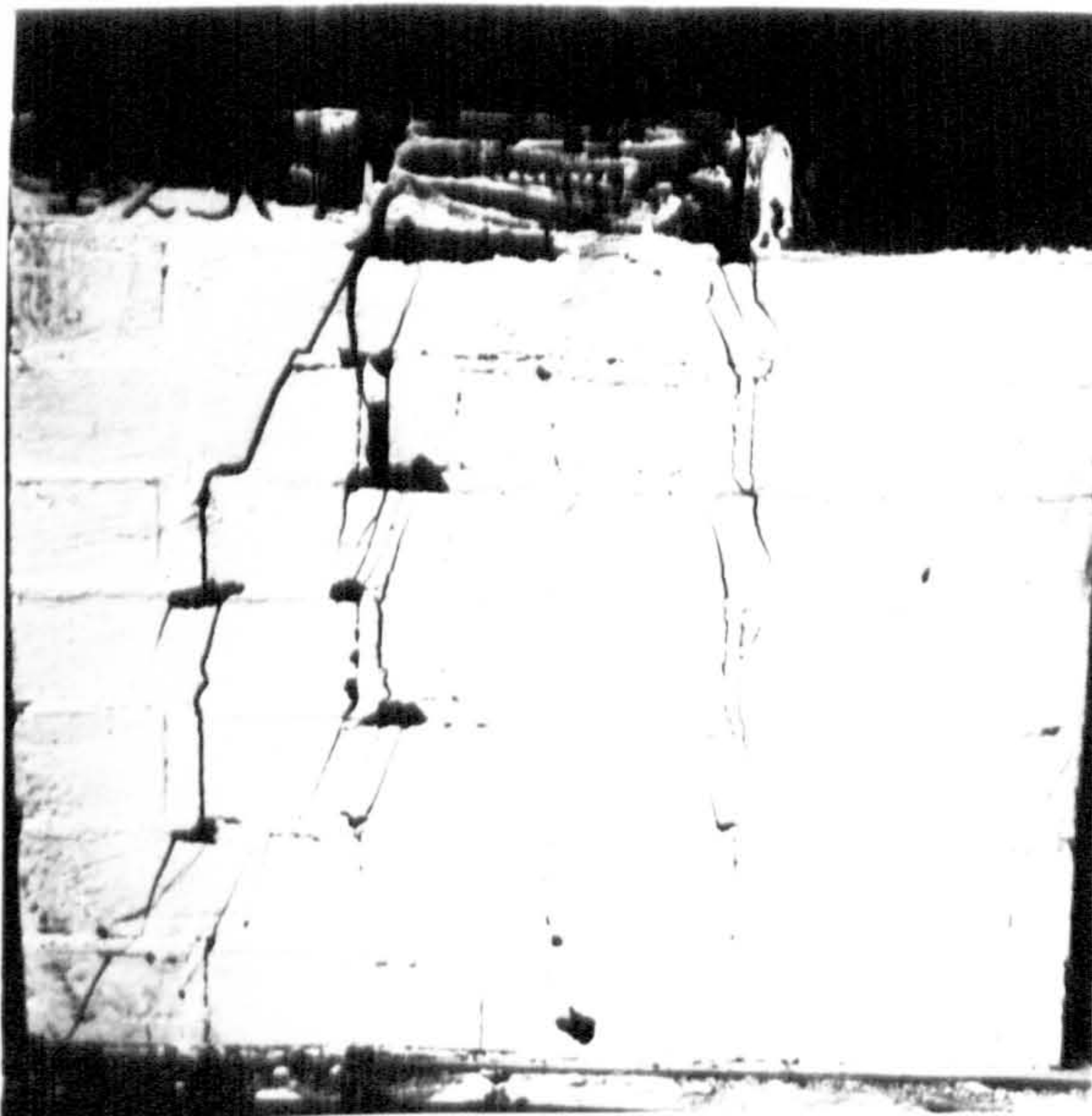
Fig. 6.91 - Typical failure mode and crack pattern for brickwork type A under central strip loading ( $t=10.5\text{mm}$ ).



(a)-  $A_r = 0.10$



(b)-  $A_r = 0.20$

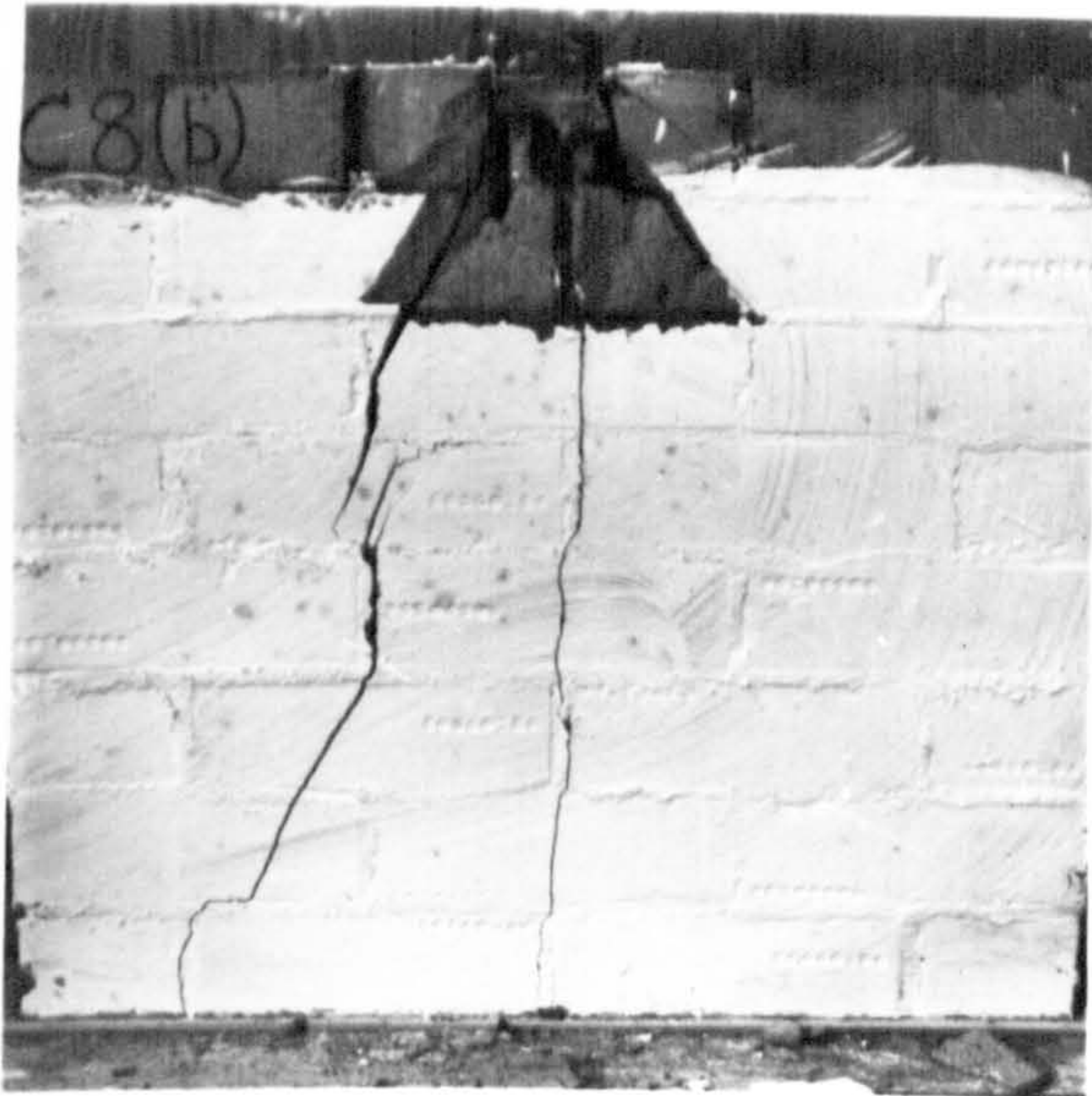


(c)-  $A_r = 0.30$



(d)-  $A_r = 0.40$

Fig. 6.92 - Typical failure mode and crack pattern for brickwork type B under central strip loading ( $t=102.5\text{mm}$ ).



(a)-  $A_r = 0.10$



(b)-  $A_r = 0.20$

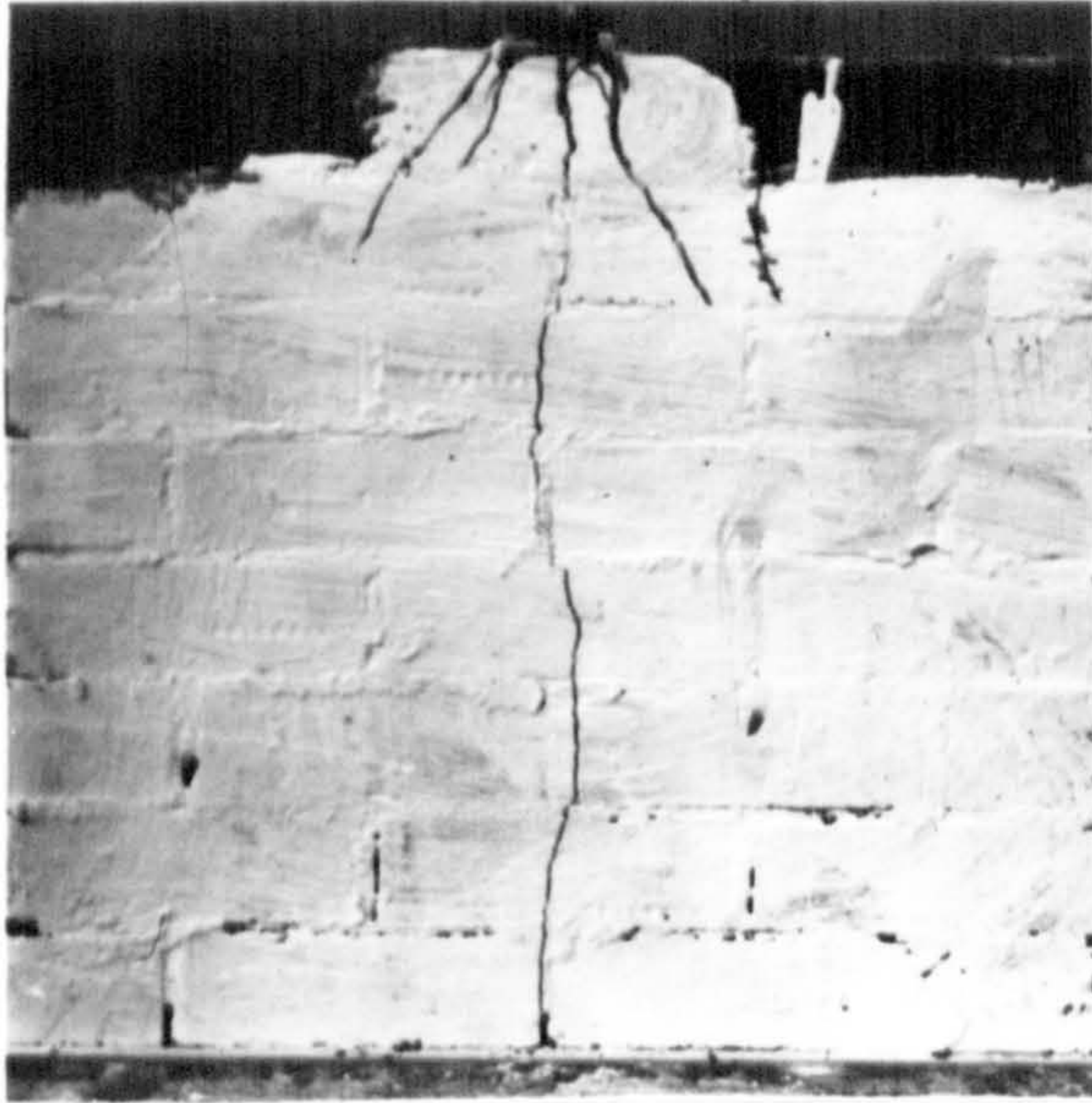


(c)-  $A_r = 0.30$

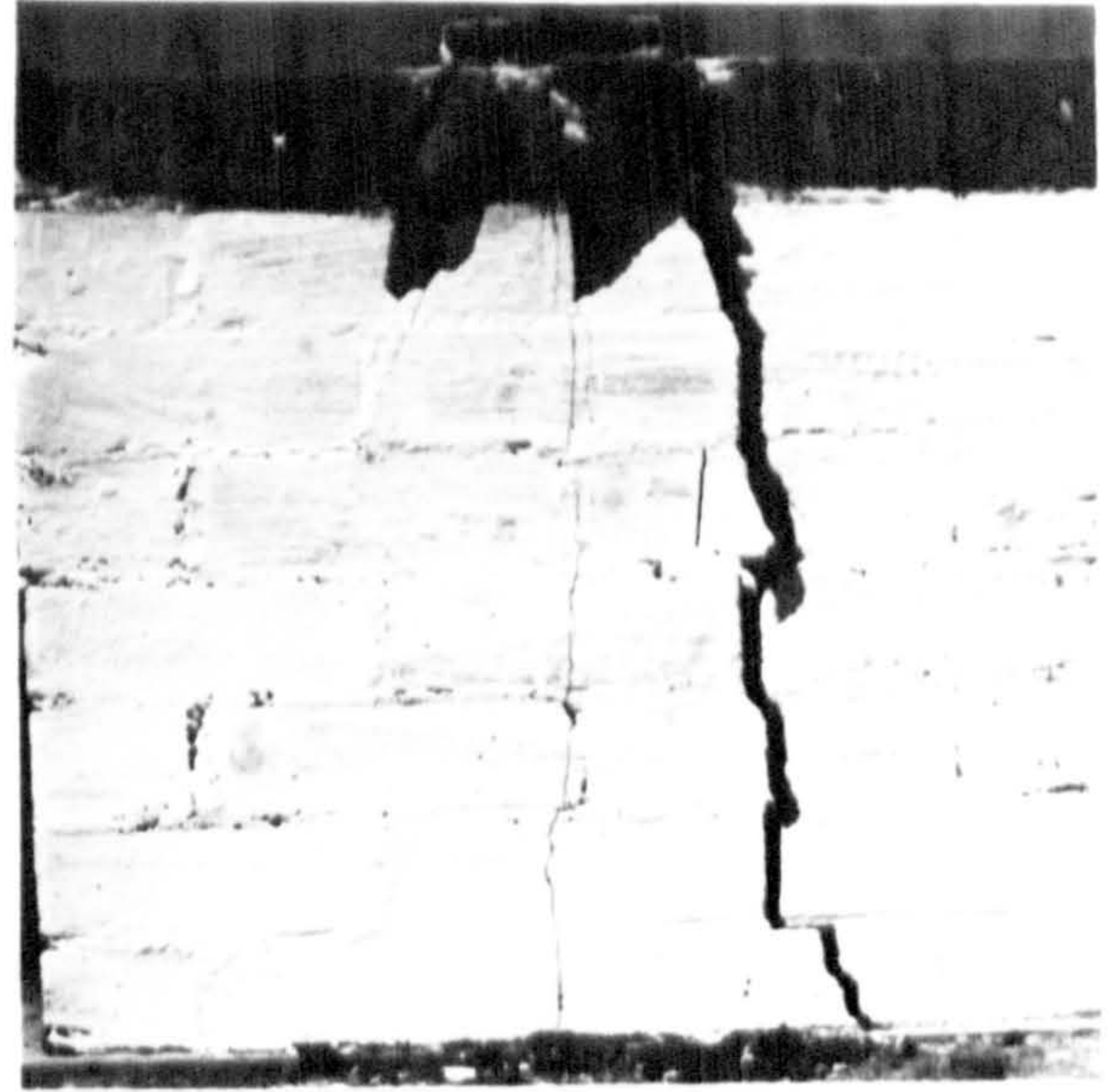


(d)-  $A_r = 0.40$

Fig. 6.93 - Typical failure mode and crack pattern for brickwork type C under central strip loading ( $t=102.5\text{mm}$ ).



(a)  $A_r = 0.10$



(b)  $A_r = 0.20$

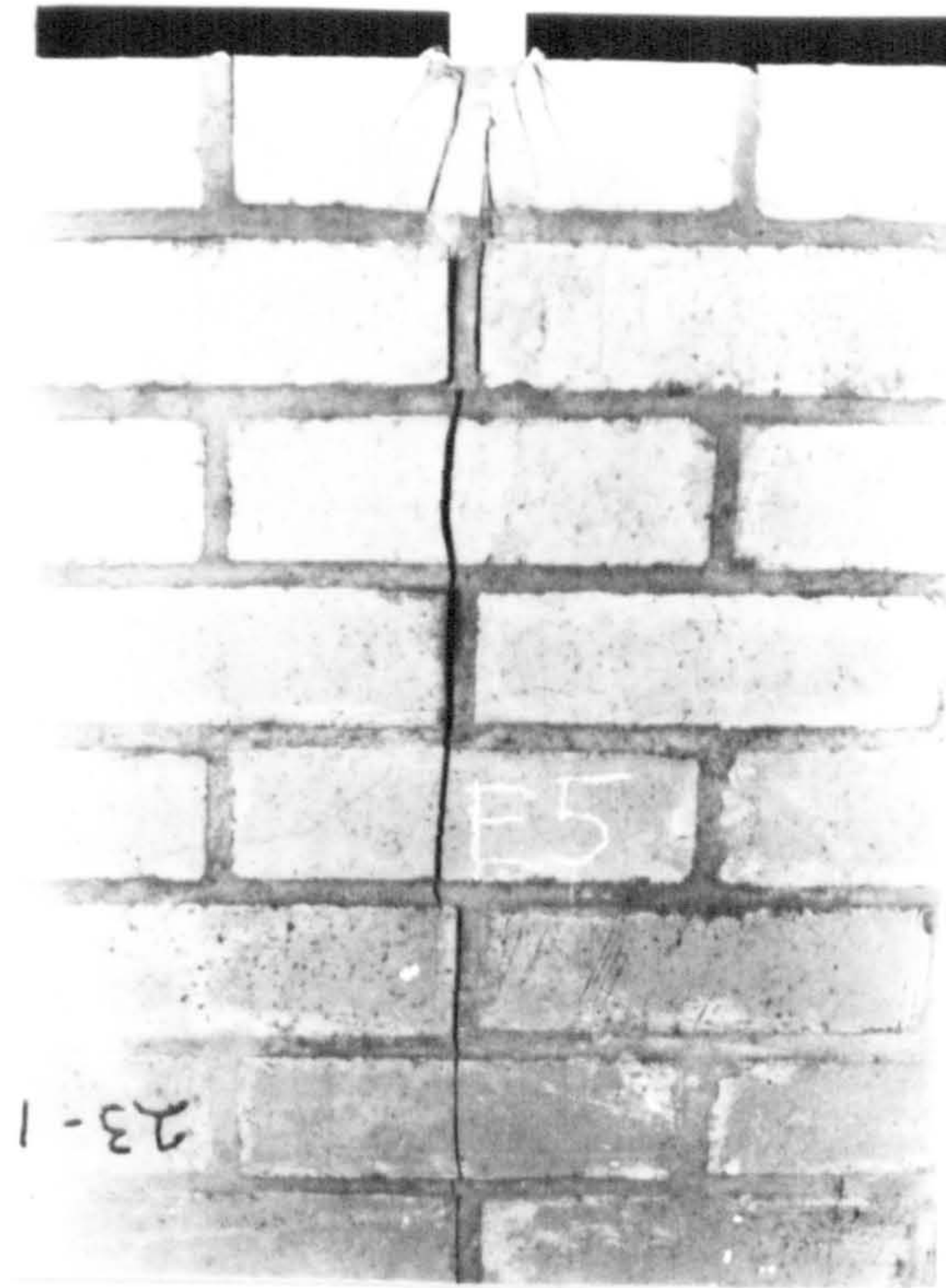


(c)  $A_r = 0.30$

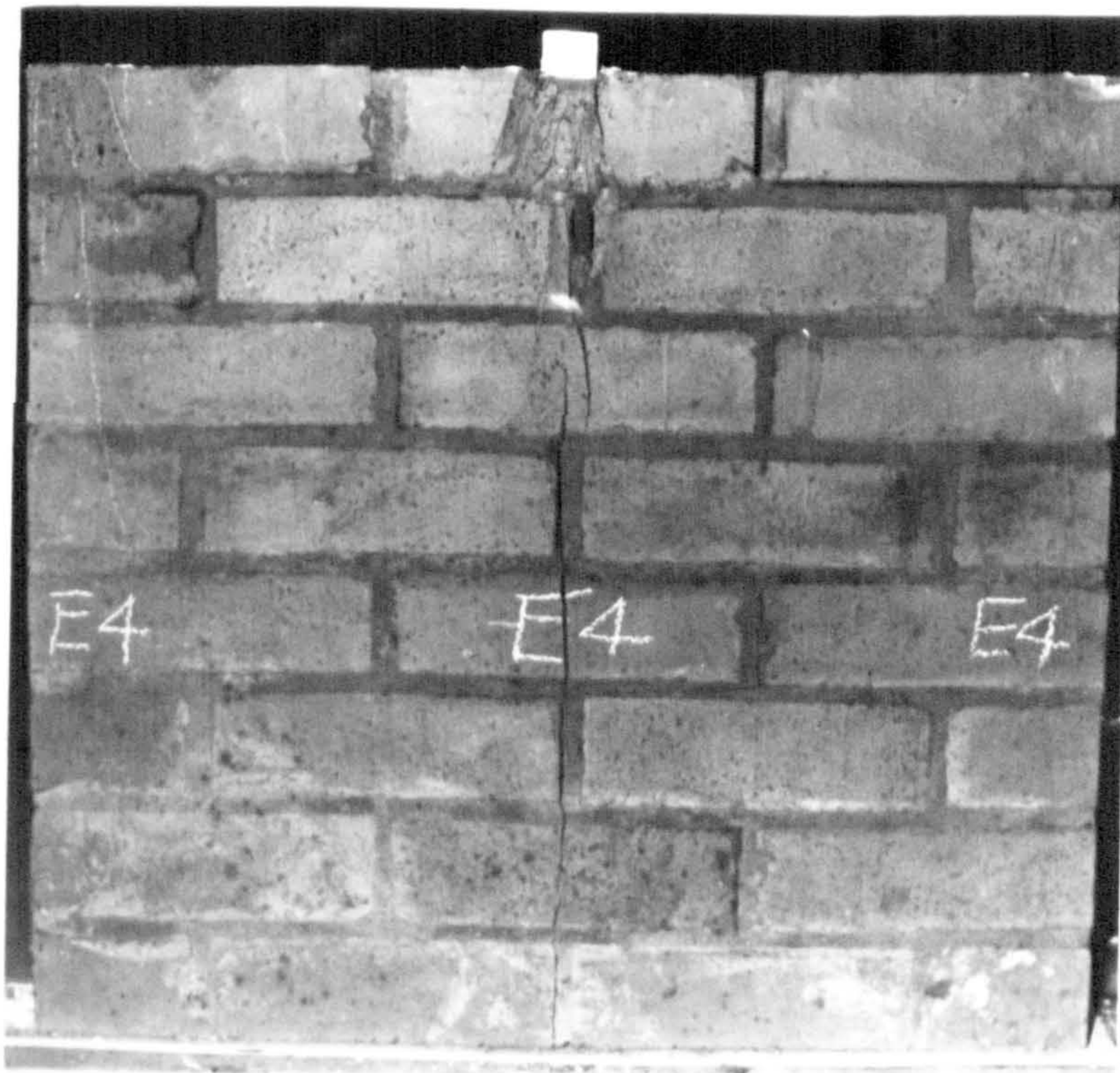


(d)  $A_r = 0.40$

Fig. 6.94 - Typical failure mode and crack pattern for brickwork type D under central strip loading ( $t=10.5\text{mm}$ ).

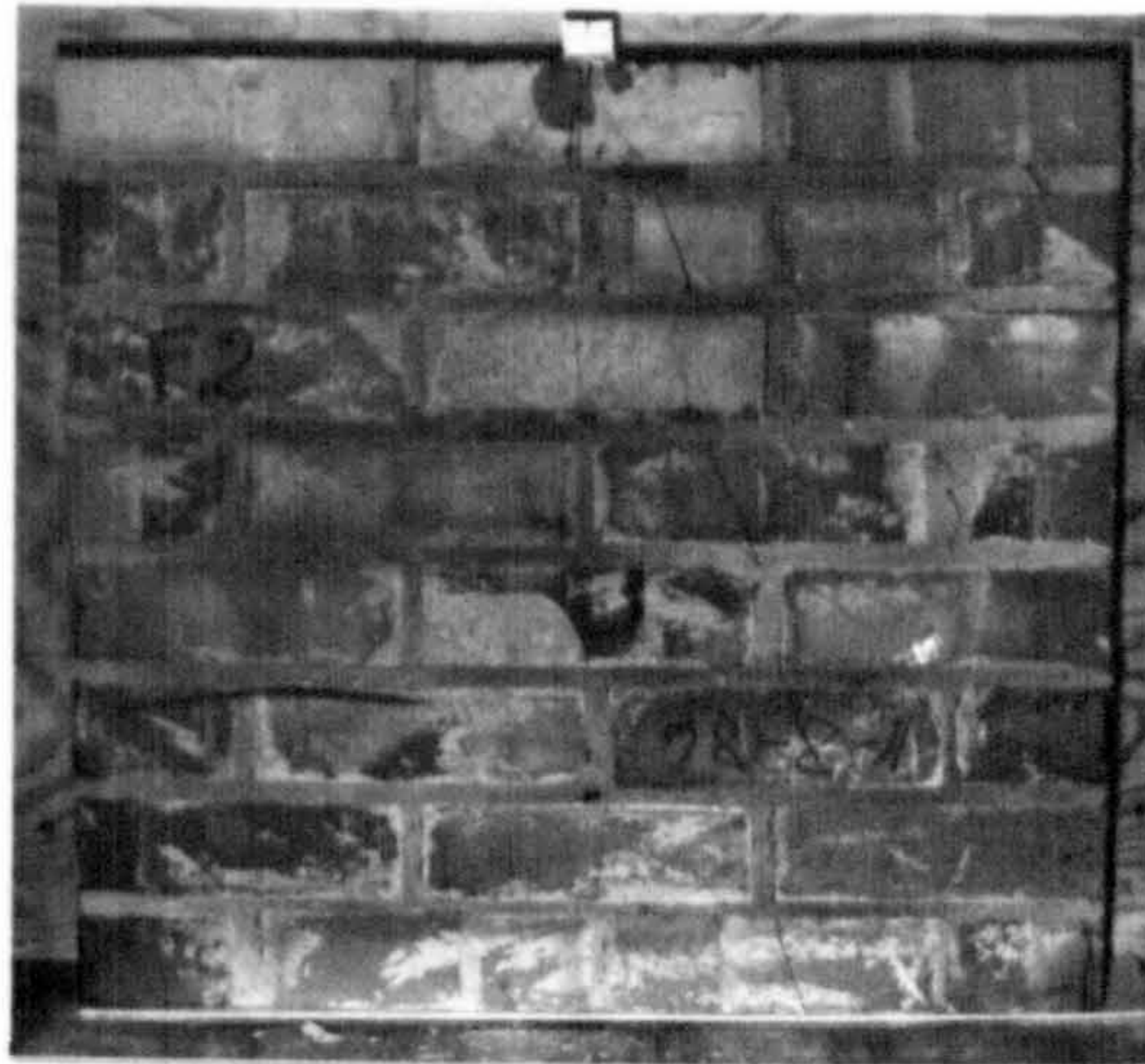


(a)-  $A_r = 0.05$

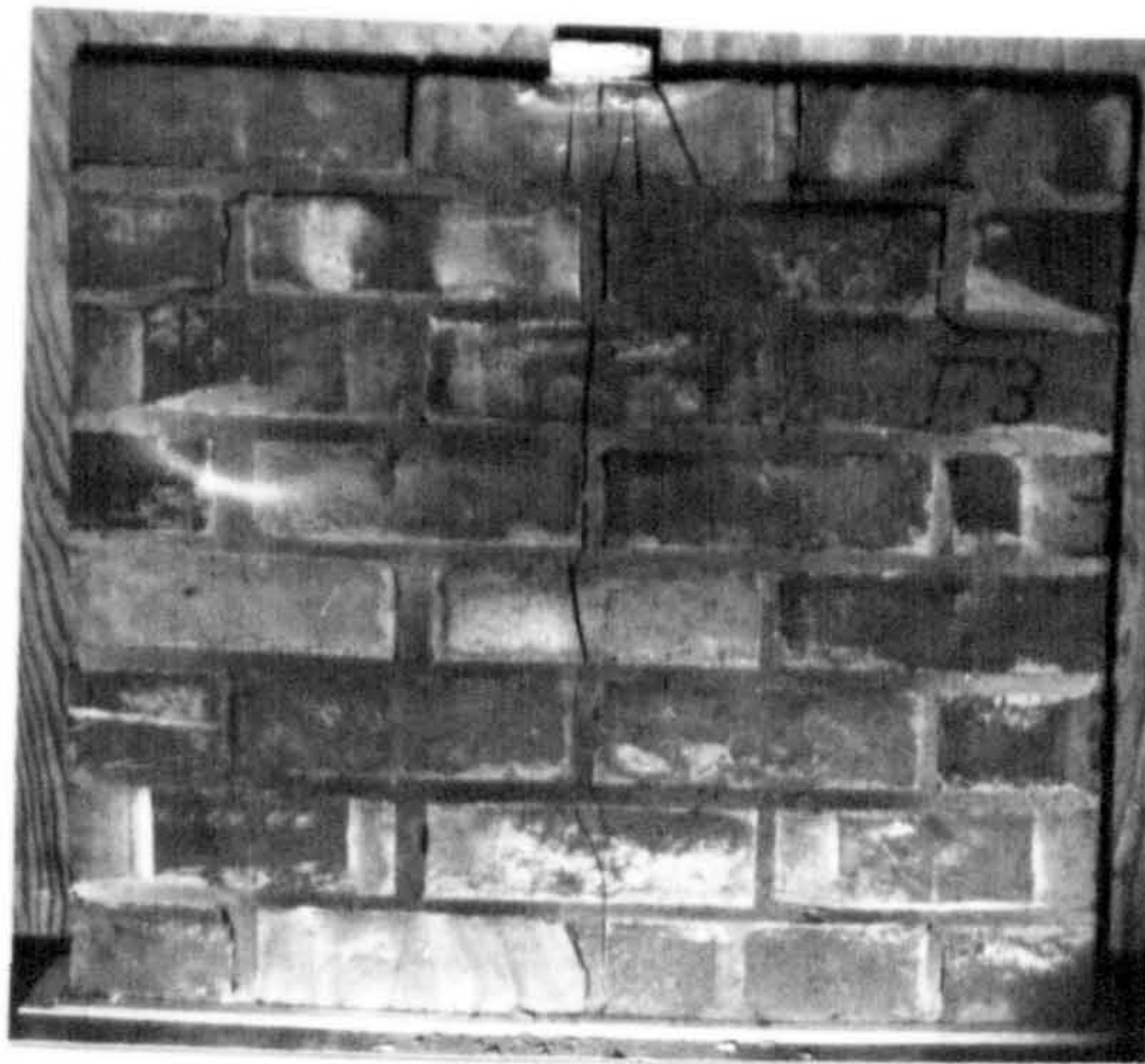


(b)-  $A_r = 0.05$

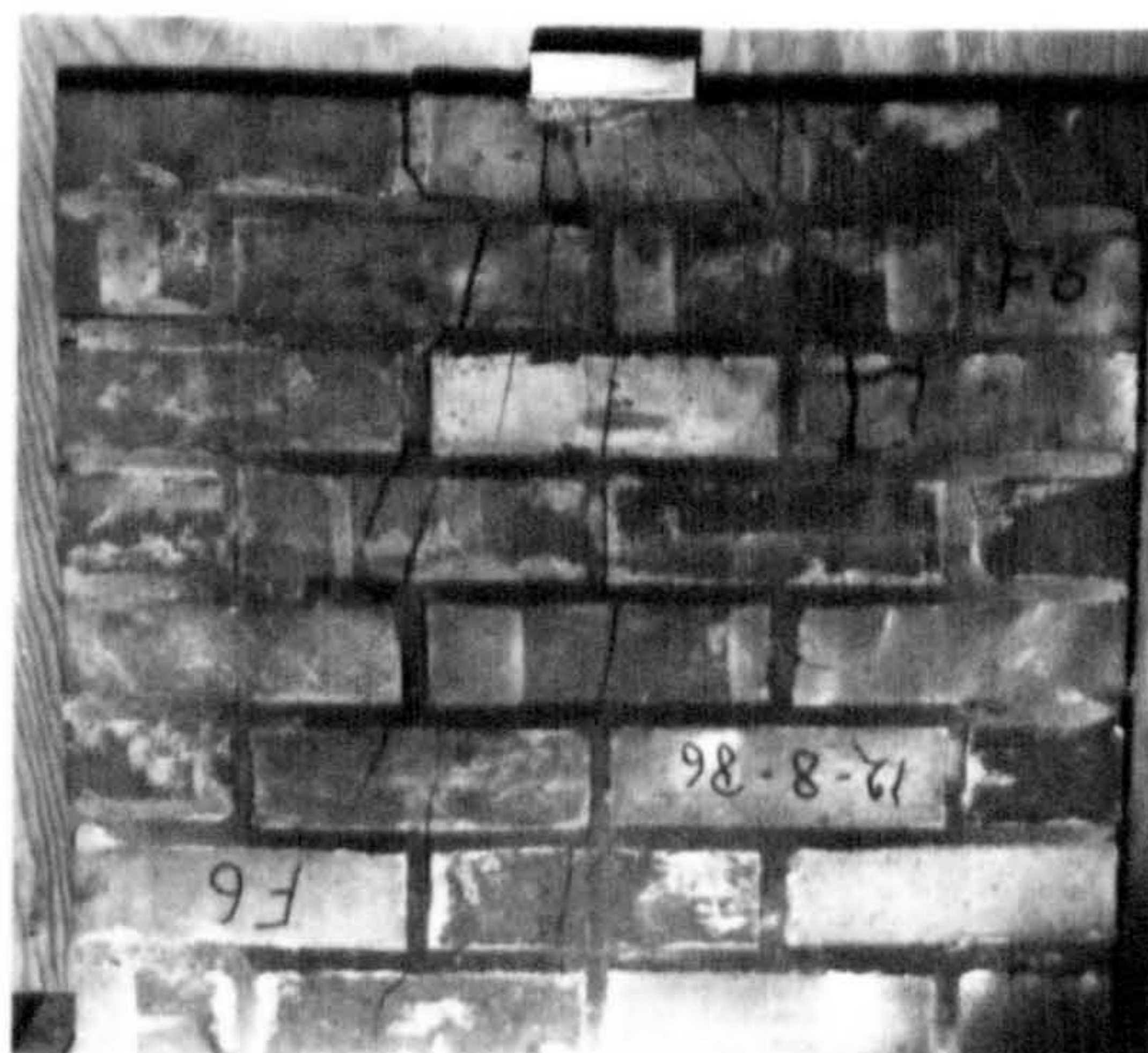
Fig. 6.95 - Typical failure mode and crack pattern for brickwork type E under central strip loading ( $t=102.5\text{mm}$ ).



(a)-  $A_r = 0.05$



(b)-  $A_r = 0.10$



(c)-  $A_r = 0.15$

Fig. 6.96 - Typical failure mode and crack pattern for brickwork type F under central strip loading ( $t=102.5\text{mm}$ ).



(a)-  $A_r = 0.05$



(b)-  $A_r = 0.10$



(c)-  $A_r = 0.15$

Fig. 6.97 - Typical failure mode and crack pattern for brickwork type F under central strip loading ( $t=215.0\text{mm}$ ).





(a)-  $A_r = 0.05$

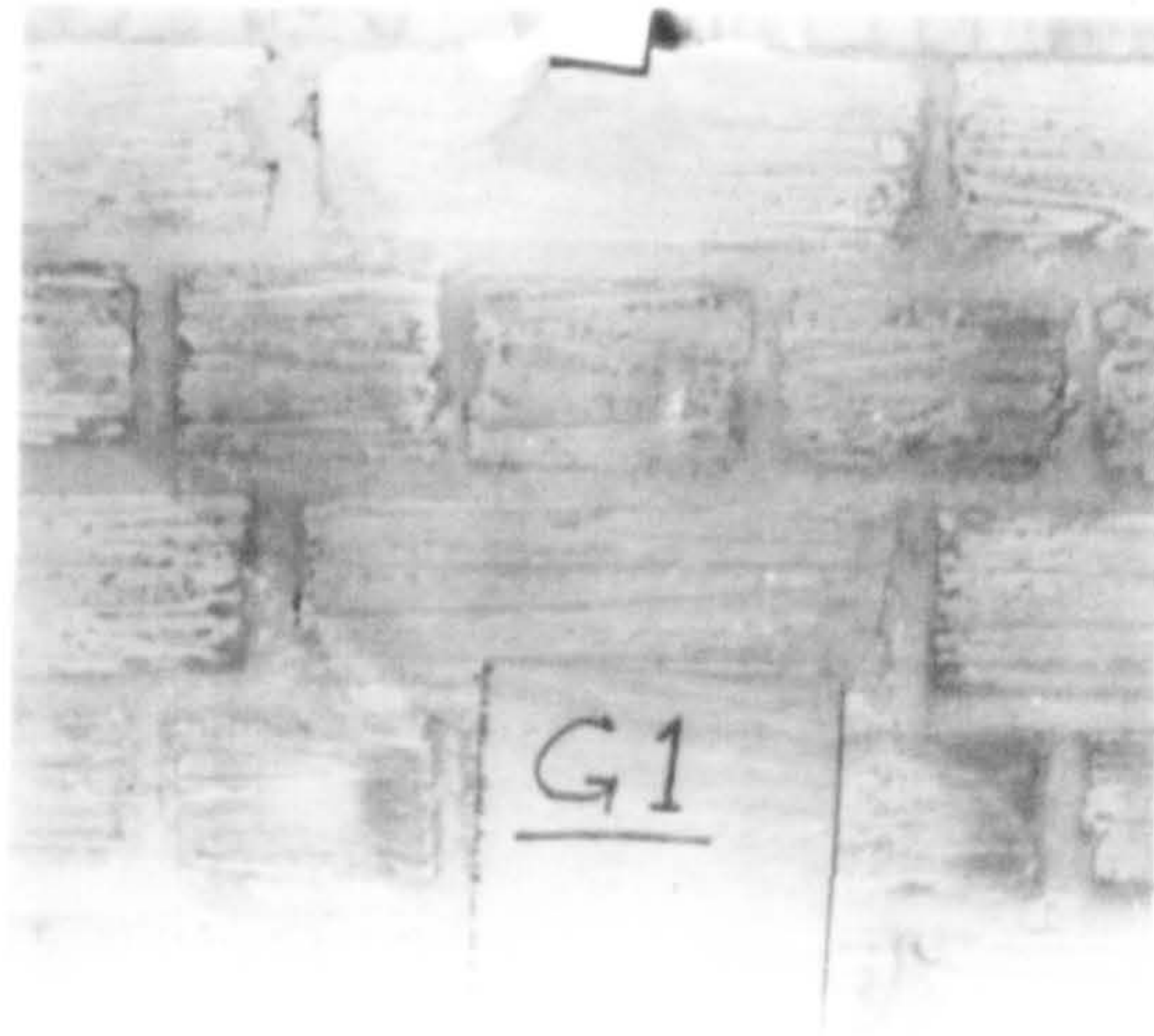


(b)-  $A_r = 0.10$

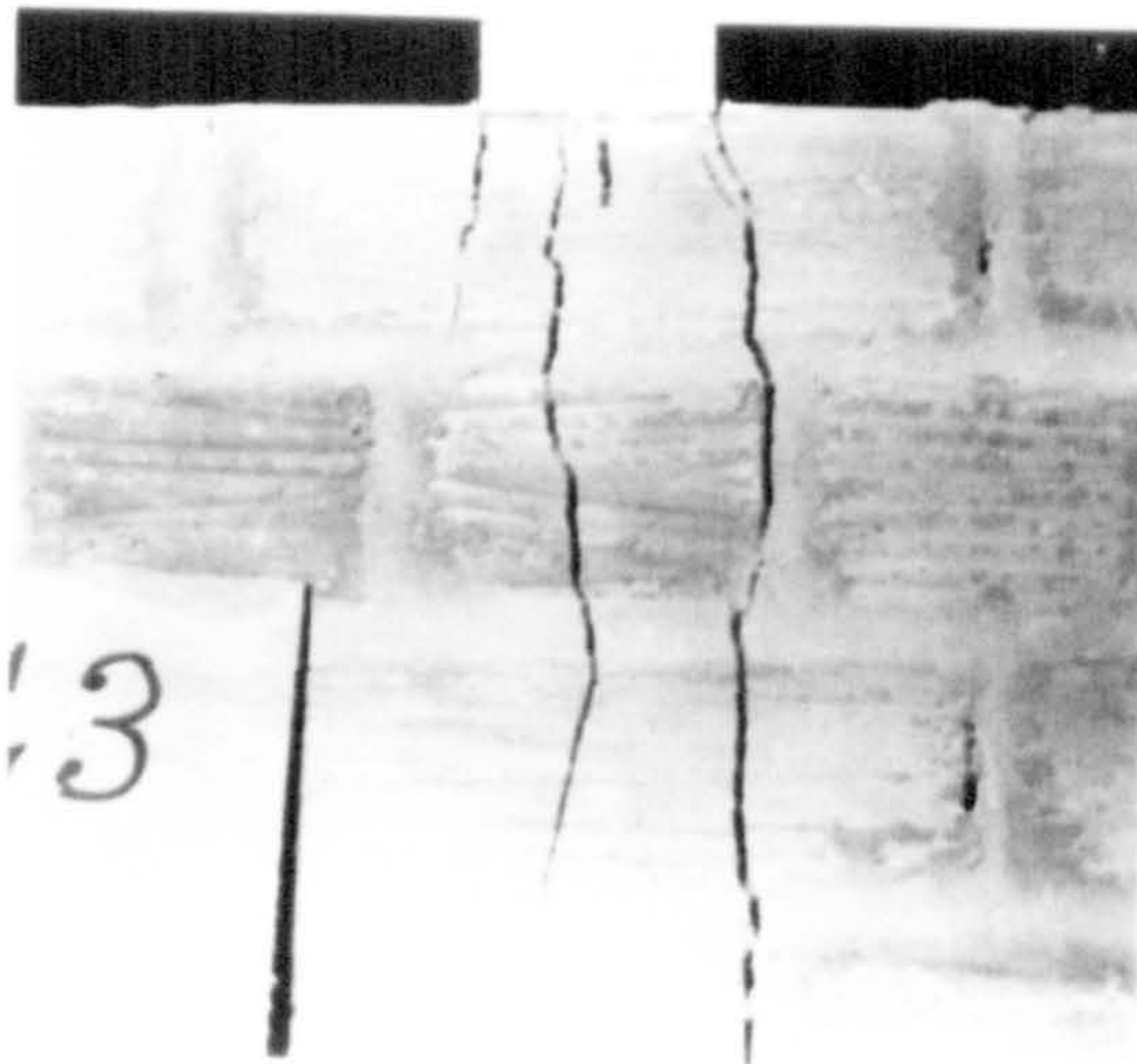


(c)-  $A_r = 0.15$

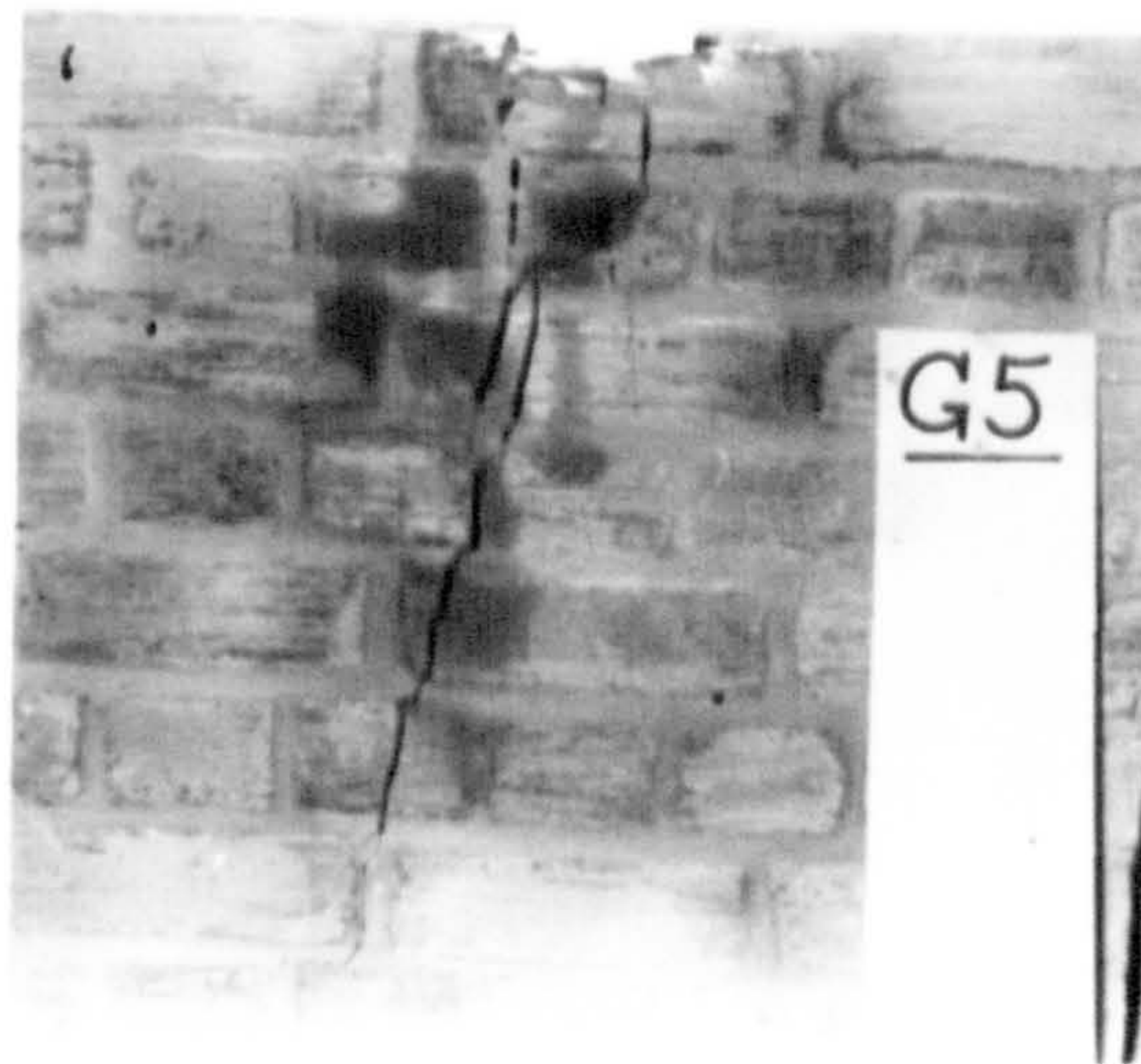
Fig. 6.98 - Typical failure mode and crack pattern for brickwork type G under central strip loading ( $t=102.5\text{mm}$ ).



(a)-  $A_r = 0.05$

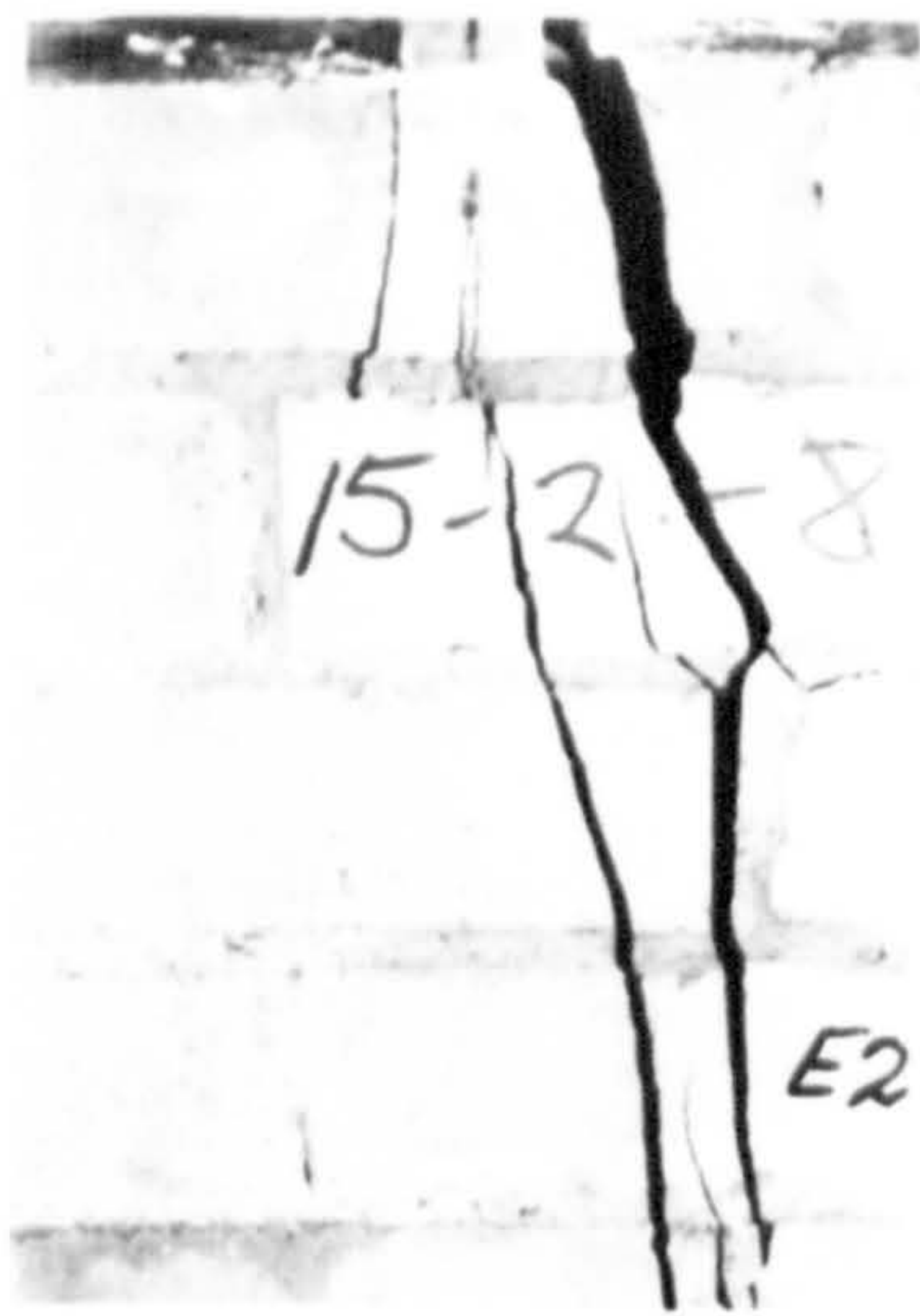


(b)-  $A_r = 0.10$

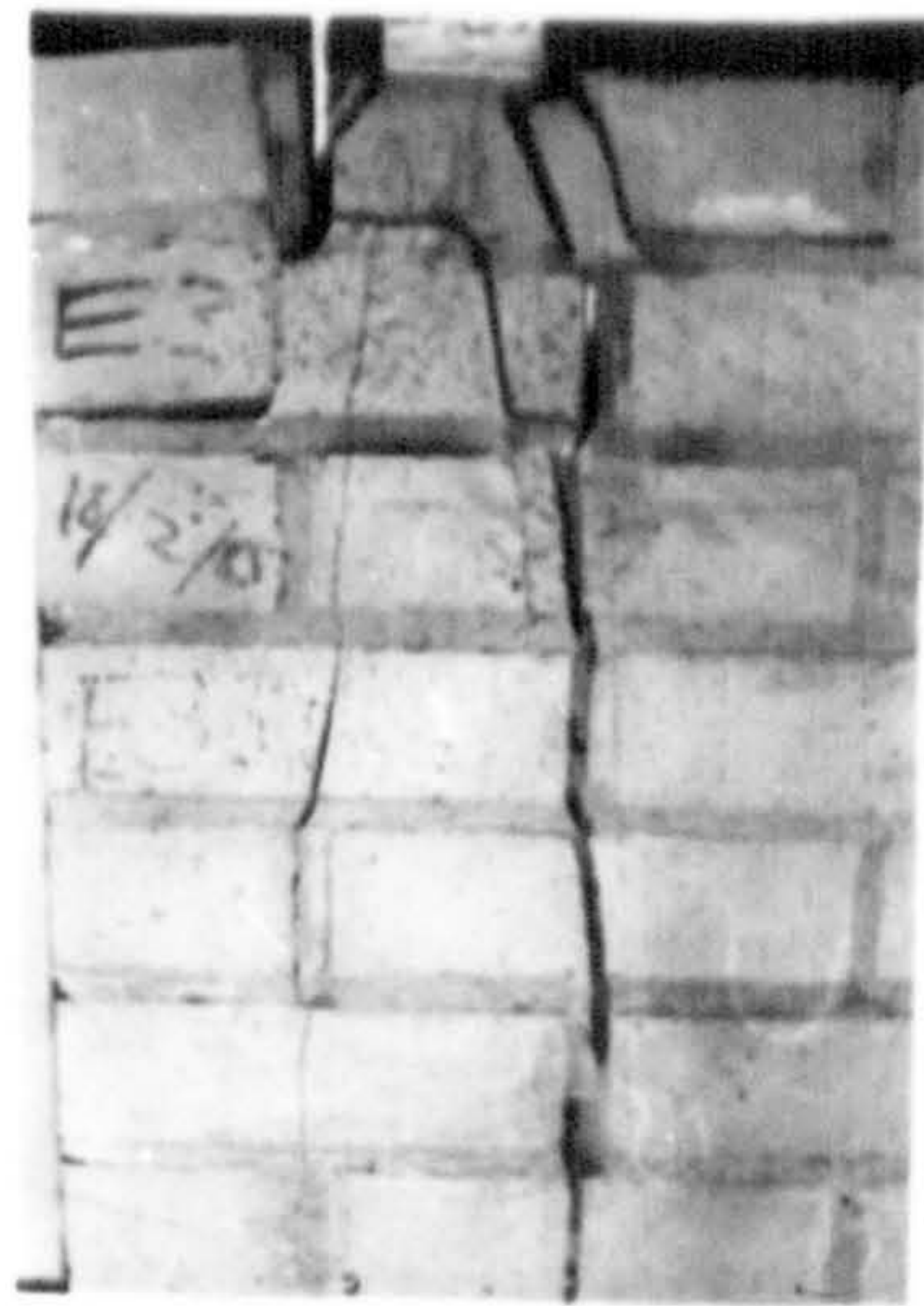


(c)-  $A_r = 0.15$

Fig. 6.99 - Typical failure mode and crack pattern for brickwork type G under central strip loading ( $t=215.0\text{mm}$ ).



(a)-  $A_r = 0.05$



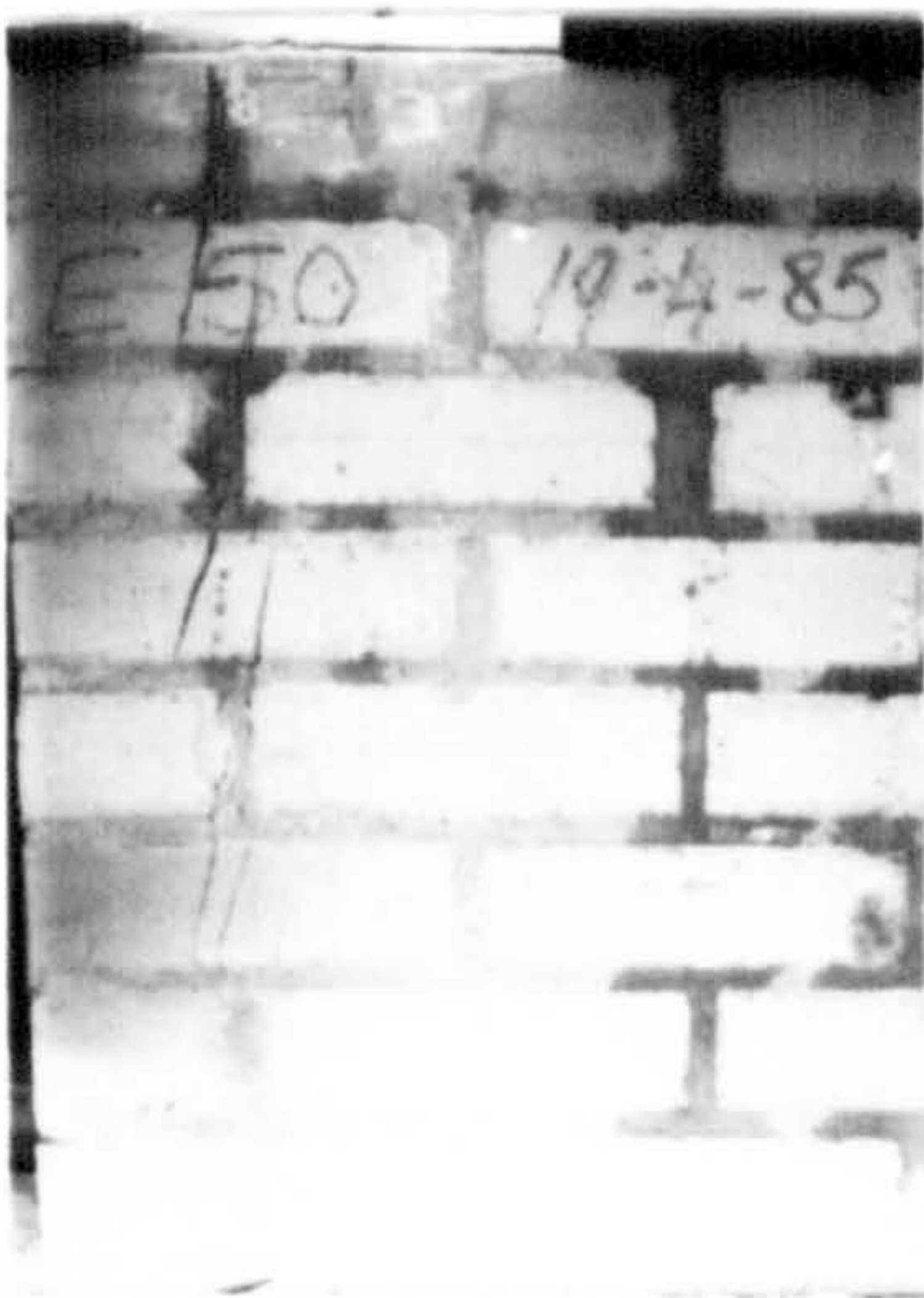
(b)-  $A_r = 0.10$



(c)-  $A_r = 0.15$



(d)-  $A_r = 0.20$

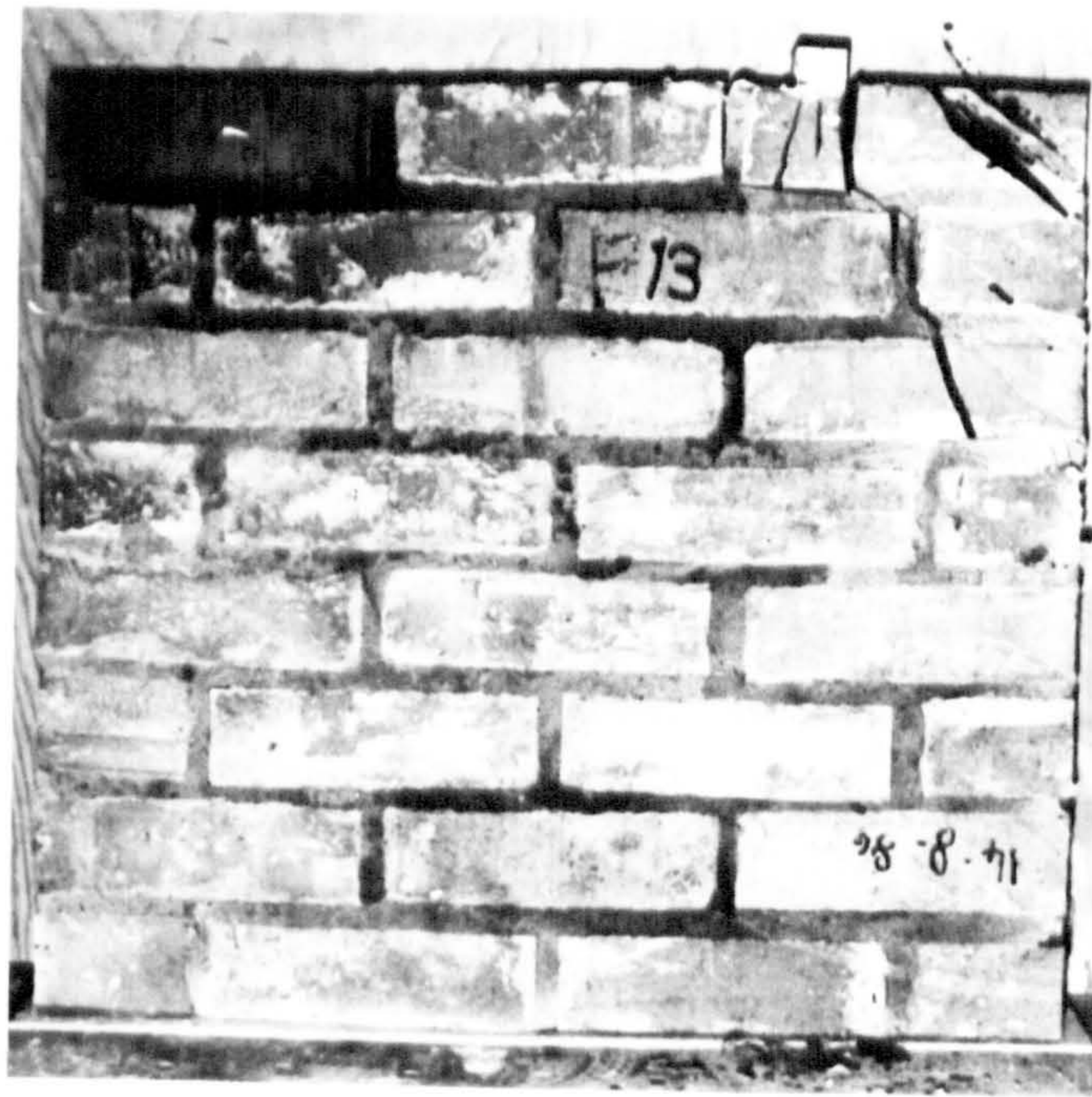


(e)-  $A_r = 0.30$



(f)-  $A_r = 0.40$

Fig. 6.100 - Typical failure mode and crack pattern for brickwork type E under intermediate strip loading ( $t=102.5\text{mm}$ ).



(a)-  $A_r = 0.05$

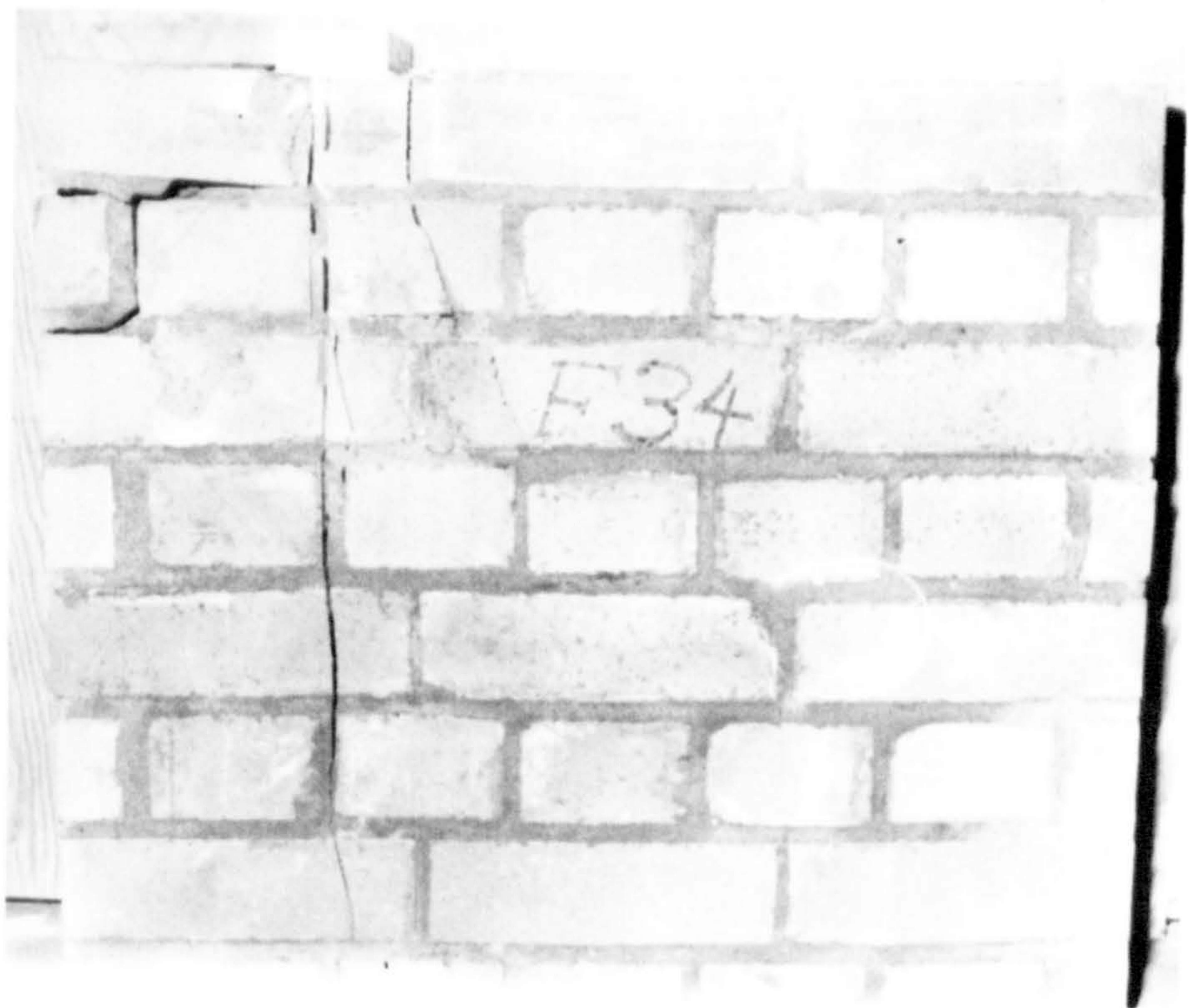


(b)-  $A_r = 0.15$

Fig. 6.101 - Typical failure mode and crack pattern for brickwork type F under intermediate strip loading ( $t=102.5\text{mm}$ ).



(a)-  $A_r = 0.05$

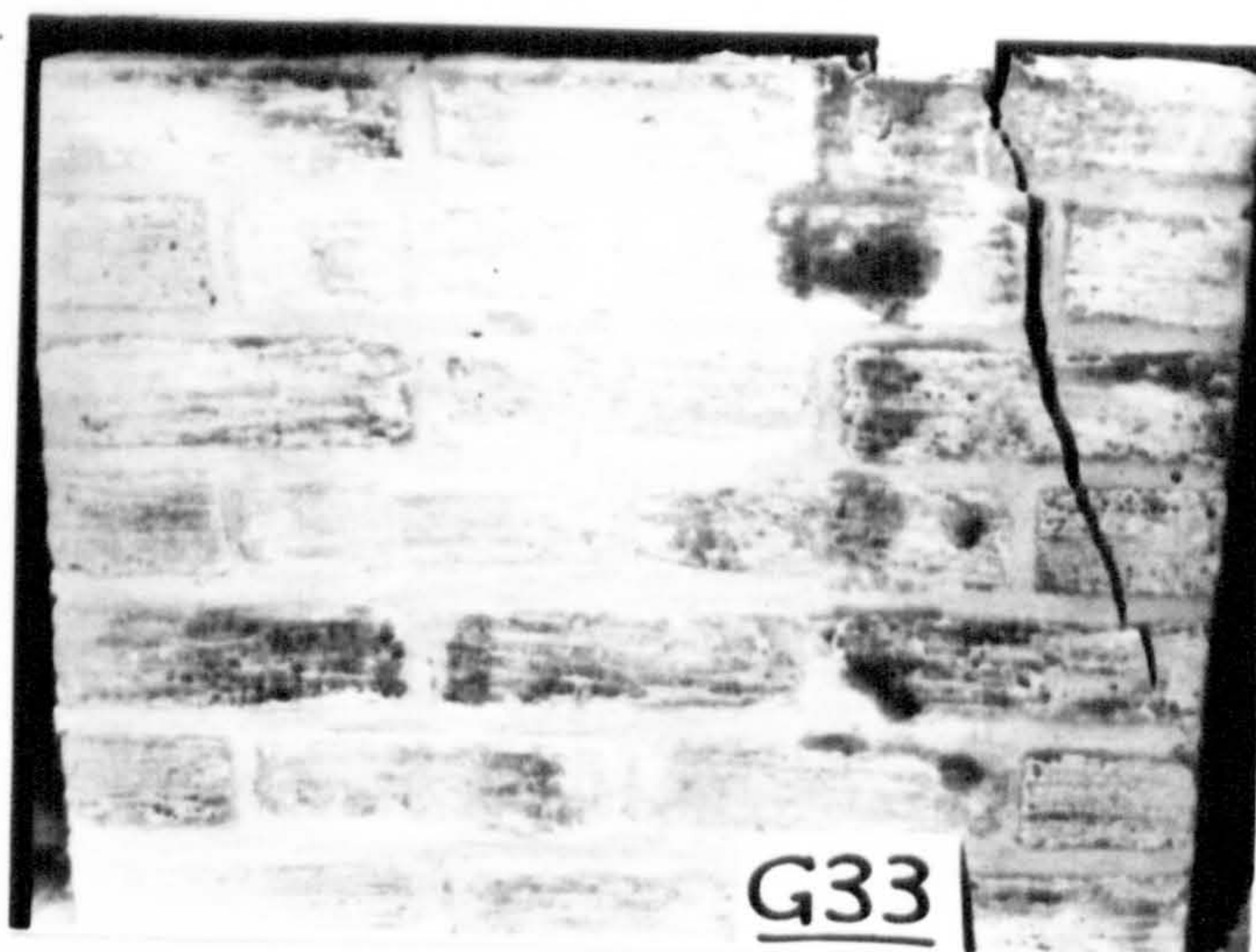


(b)-  $A_r = 0.10$

Fig. 6.102 - Typical failure mode and crack pattern for brickwork type F under intermediate strip loading ( $t=215.0\text{mm}$ ).



(a)-  $A_r = 0.05$



(b)-  $A_r = 0.10$



(c)-  $A_r = 0.15$

Fig. 6.103 - Typical failure mode and crack pattern for brickwork type G under intermediate strip loading ( $t=102.5\text{mm}$ ).



(a)-  $A_r = 0.05$

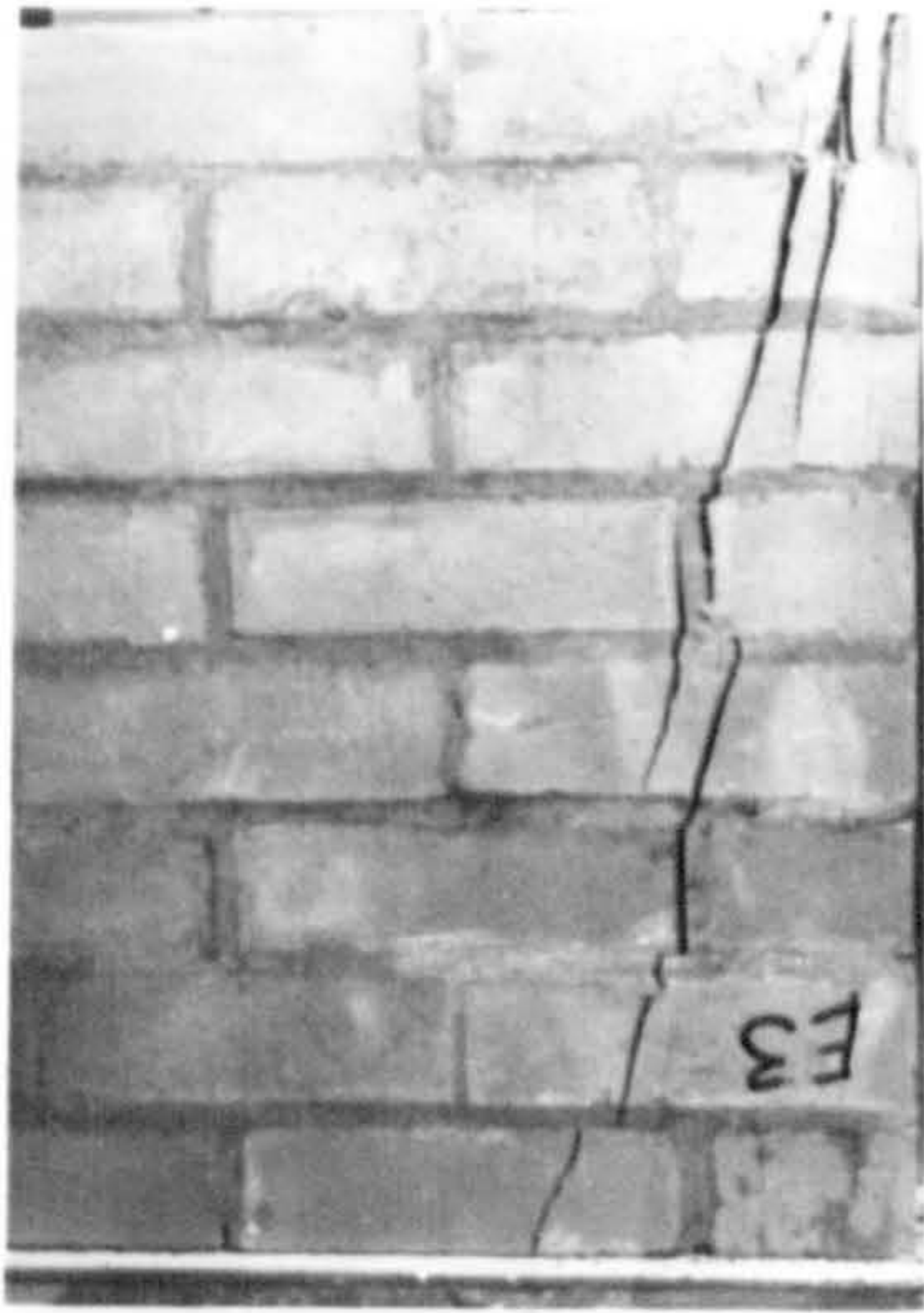


(b)-  $A_r = 0.10$



(c)-  $A_r = 0.15$

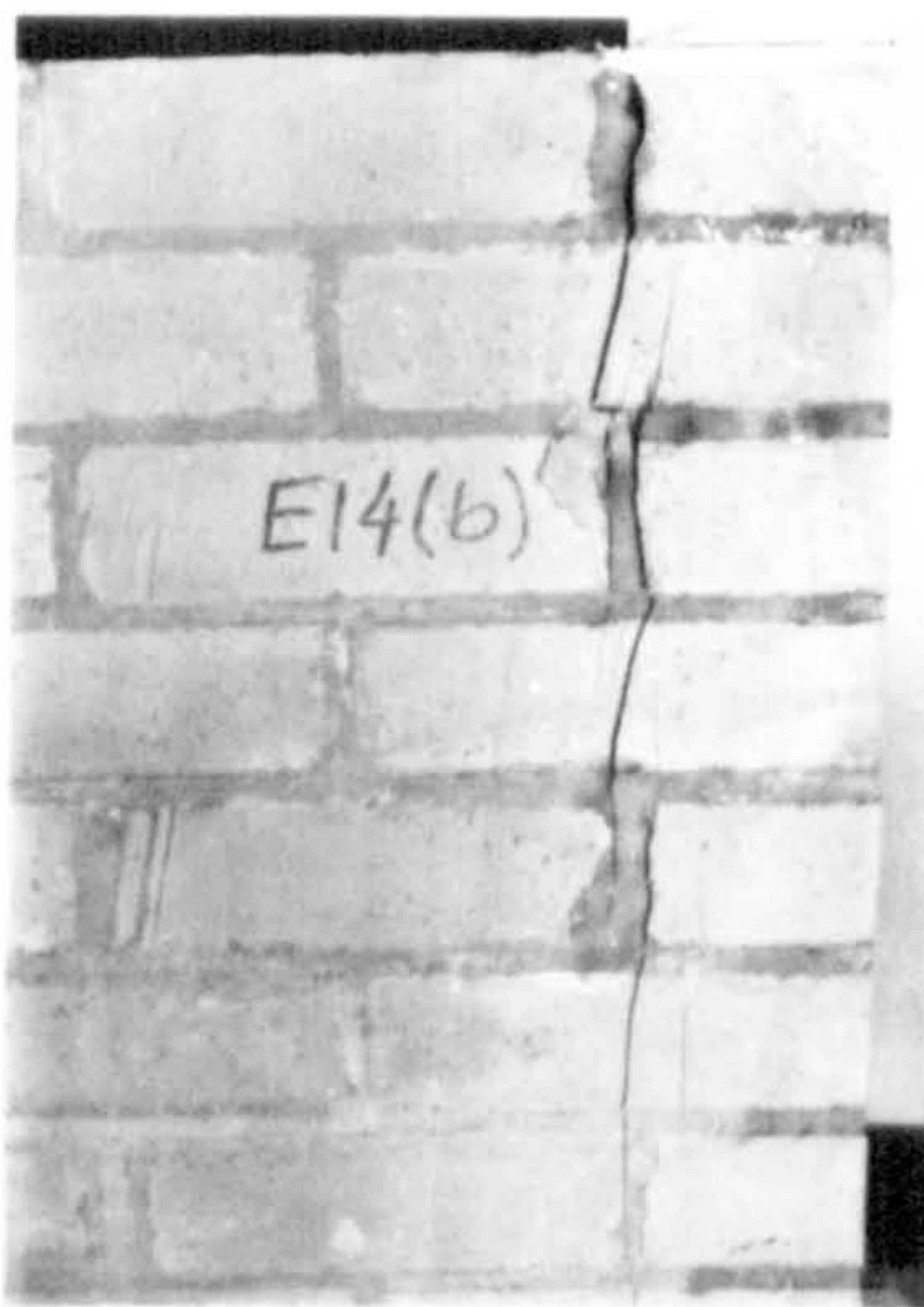
Fig. 6.104 - Typical failure mode and crack pattern for brickwork type G under intermediate strip loading ( $t=215.0\text{mm}$ ).



(a)-  $A_r = 0.05$



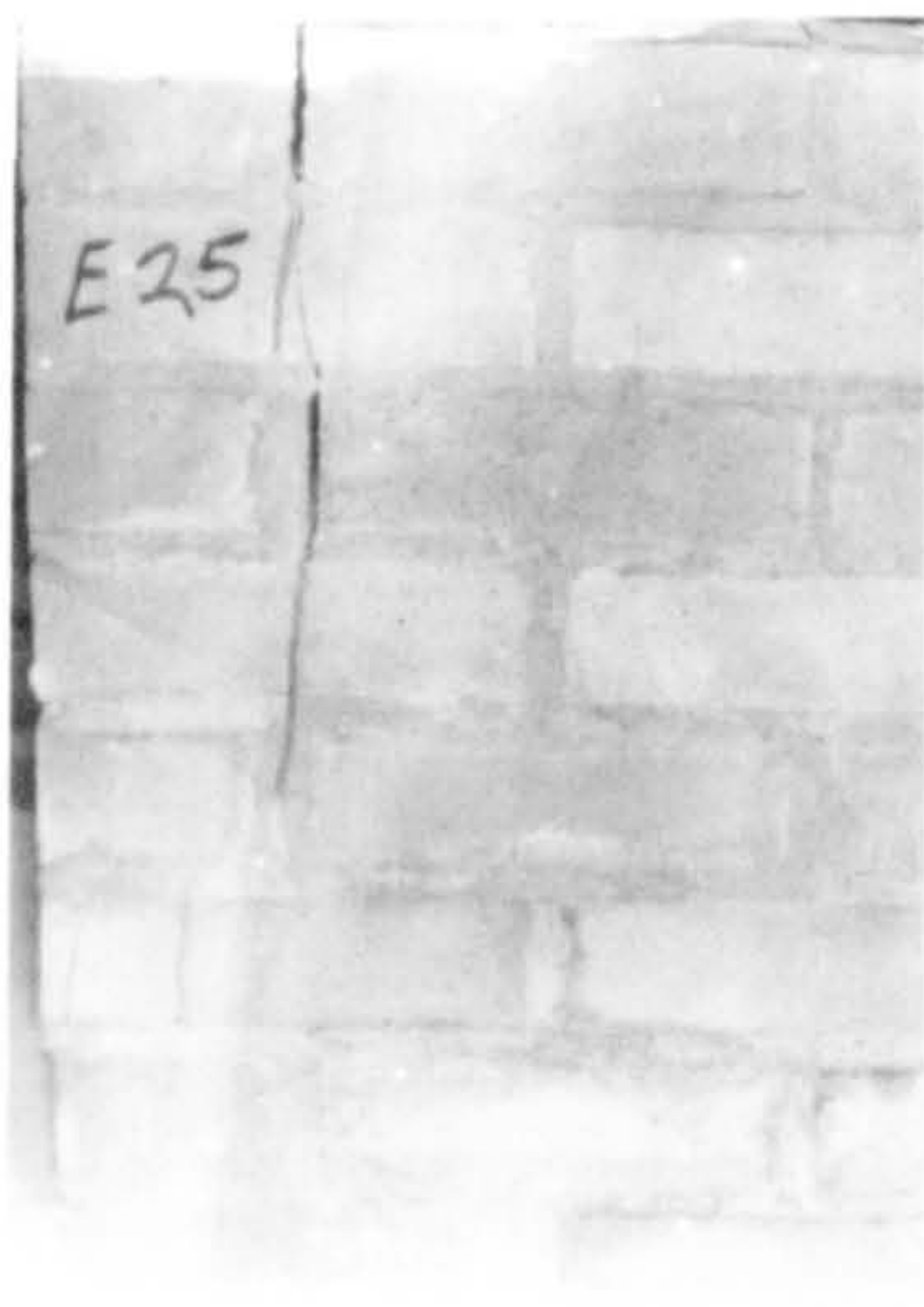
(b)-  $A_r = 0.10$



(c)-  $A_r = 0.15$



(d)-  $A_r = 0.20$



(e)-  $A_r = 0.30$



(f)-  $A_r = 0.40$

Fig 6.105 - Typical failure mode and crack pattern for brickwork type E under end strip loading ( $t=102.5\text{mm}$ ).





(a)-  $A_r = 0.05$



(b)-  $A_r = 0.10$



(c)-  $A_r = 0.15$

Fig. 6.106 - Typical failure mode and crack pattern for brickwork type F under end strip loading ( $t=102.5\text{mm}$ ).



(a)-  $A_r = 0.05$



(b)-  $A_r = 0.10$



(c)-  $A_r = 0.15$

Fig. 6.107 - Typical failure mode and crack pattern for brickwork type F under end strip loading ( $t=215.0\text{mm}$ ).



(a)-  $A_r = 0.05$



(b)-  $A_r = 0.10$



(c)-  $A_r = 0.15$

Fig. 6.108 - Typical failure mode and crack pattern for brickwork type G under end strip loading ( $t=102.5\text{mm}$ ).



(a)-  $A_r = 0.05$



(b)-  $A_r = 0.10$

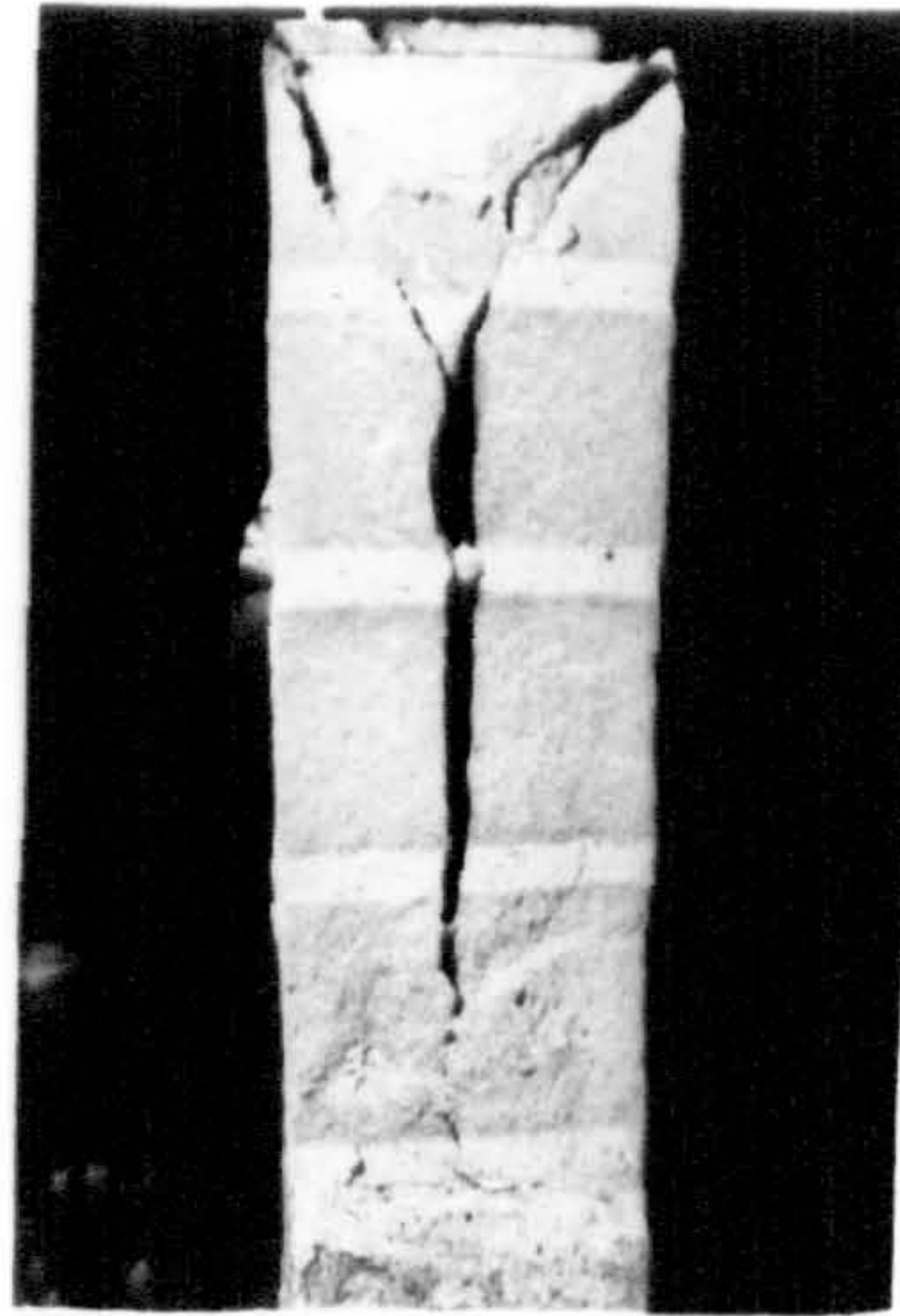


(c)-  $A_r = 0.15$

Fig. 6.109 - Typical failure mode and crack pattern for brickwork type G under end strip loading ( $t=215.0\text{mm}$ ).



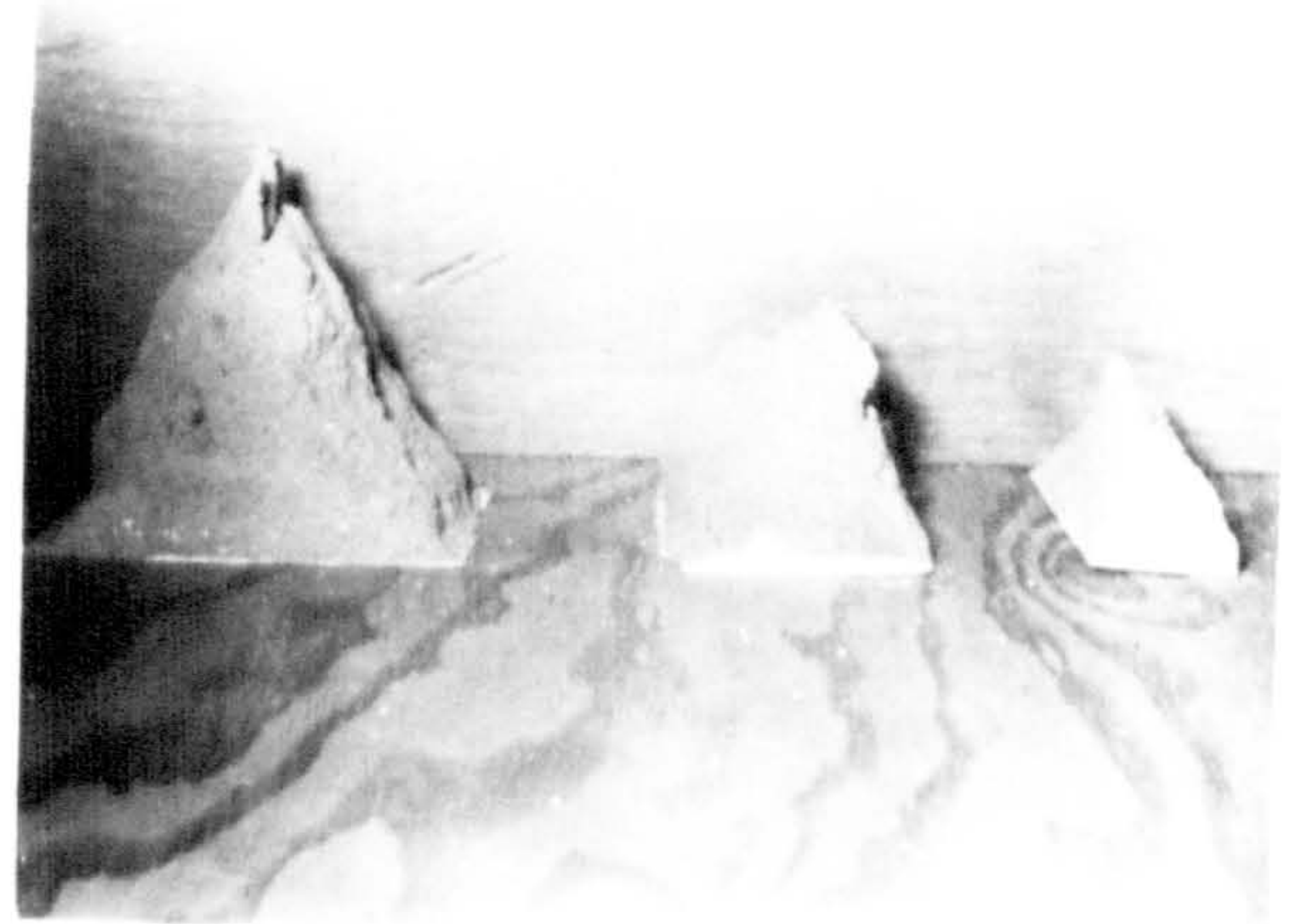
(a)



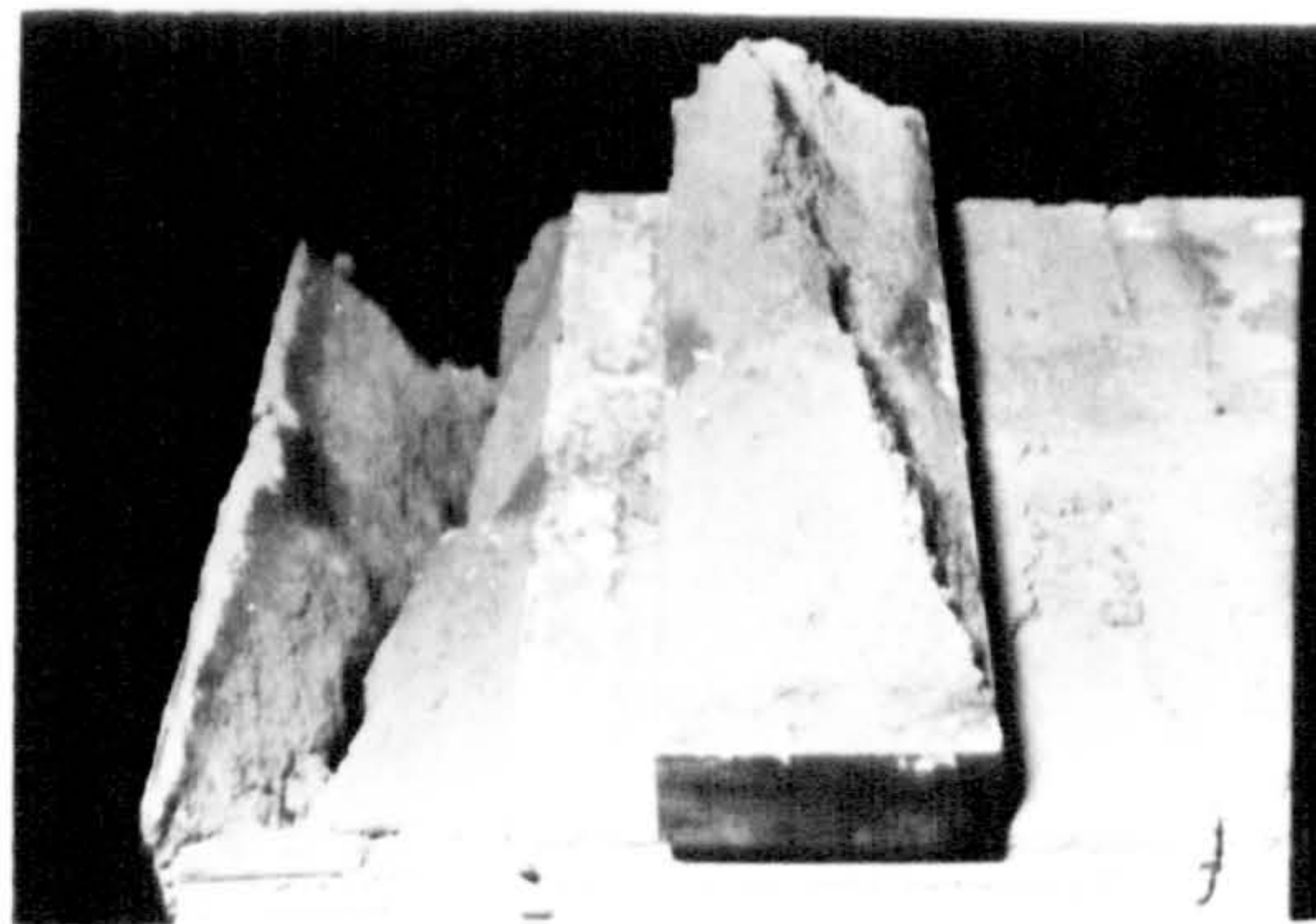
(b)



(c)

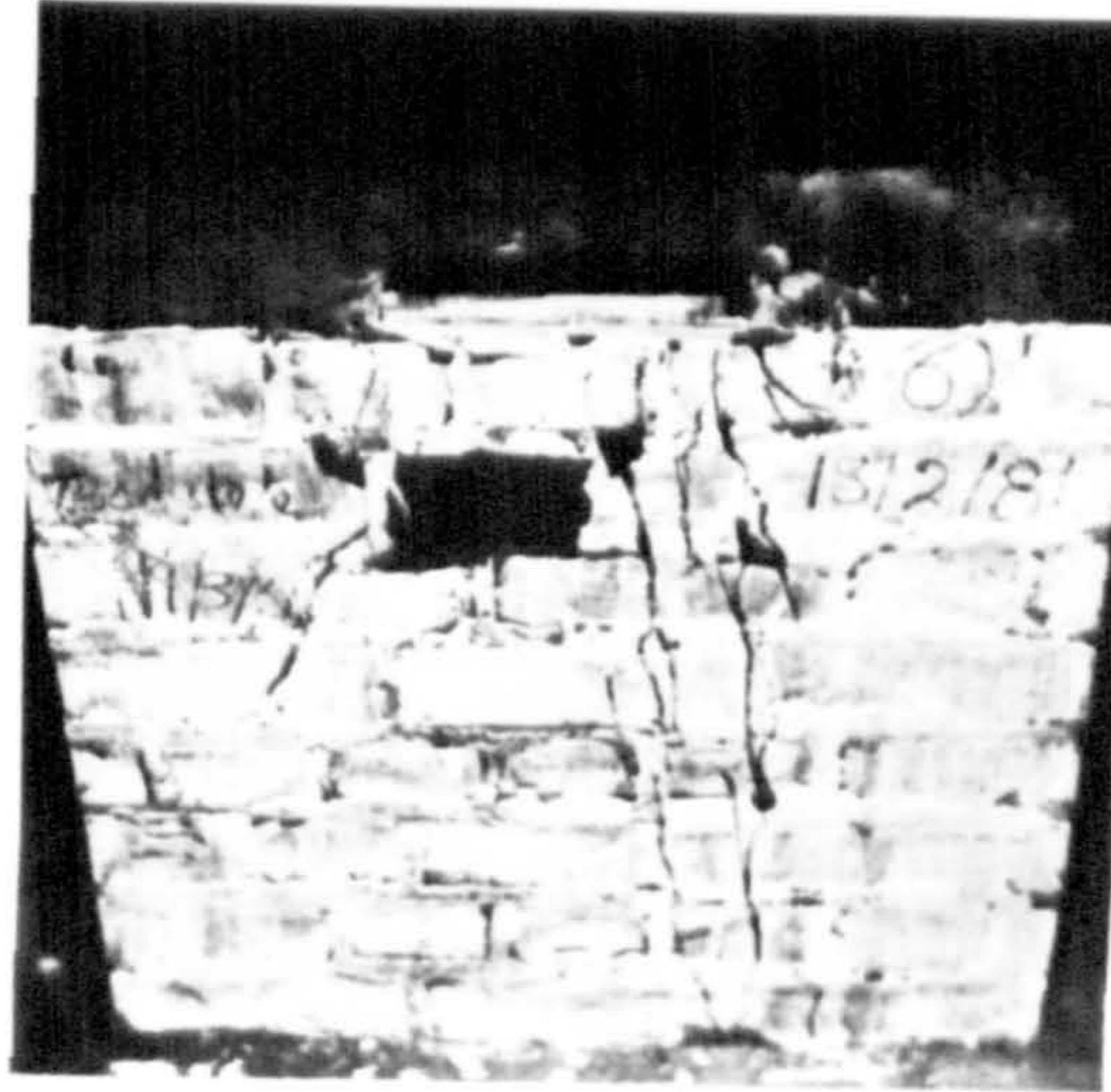


(d)



(e)

Fig. 6.110 - Formation of wedge or cone under strip loading for AAC brickwork masonry



(a)-  $A_r = 0.08$



(b)-  $A_r = 0.16$

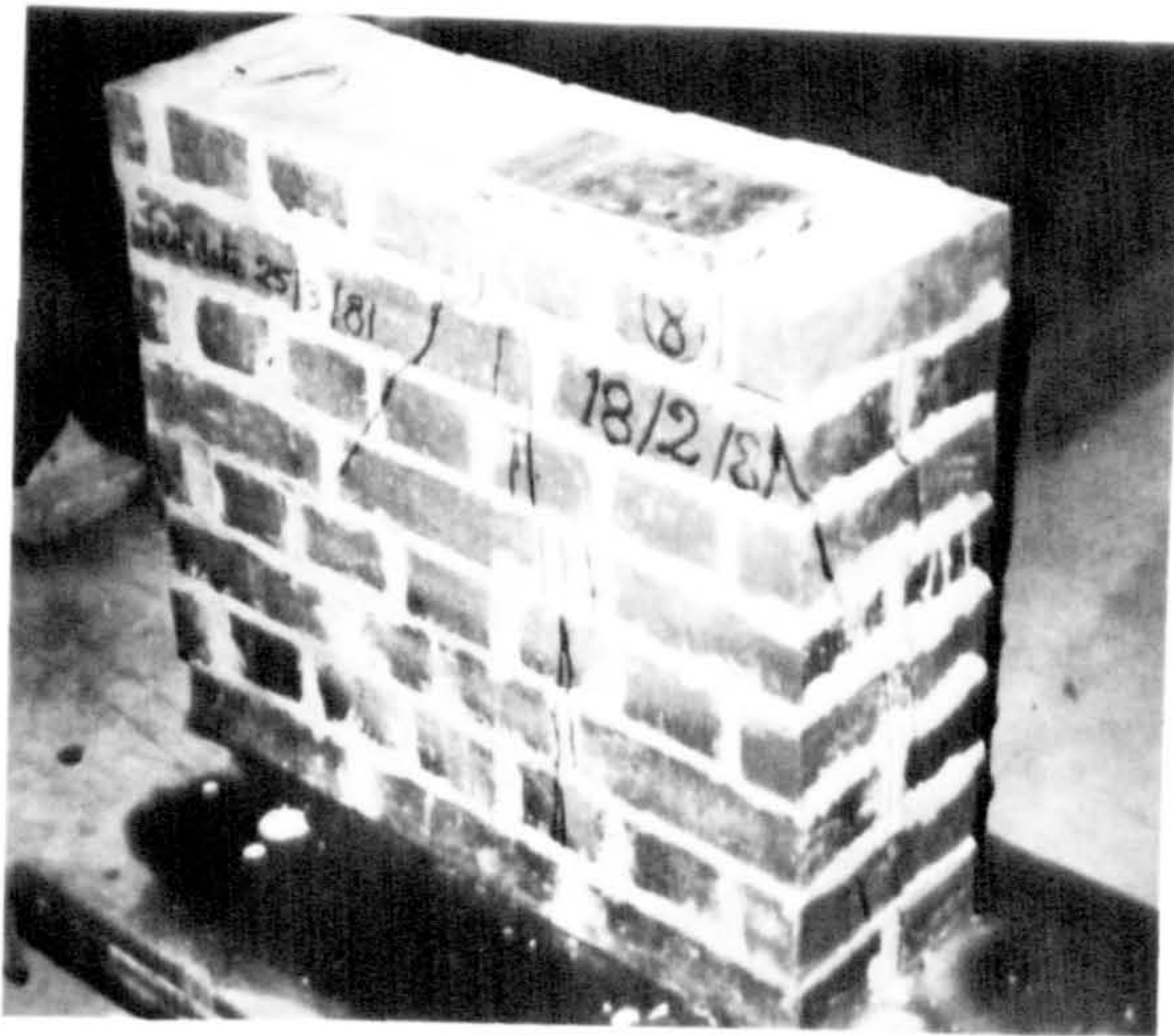


(c)-  $A_r = 0.24$

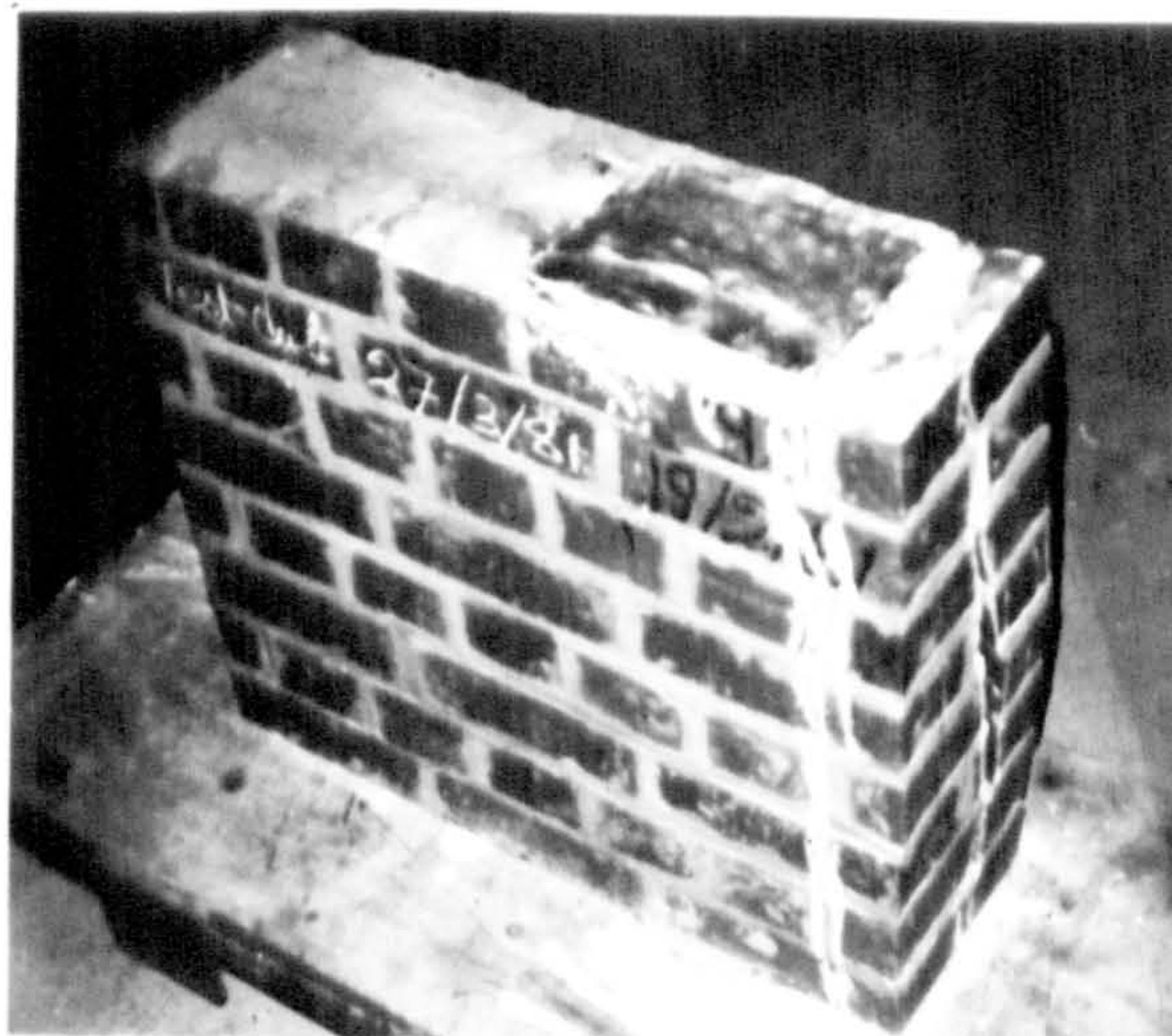
Fig. 6.111 - Typical failure mode and crack pattern for brickwork type M under central edge loading ( $t=215.0\text{mm}$ ).



(a)-  $A_r = 0.08$

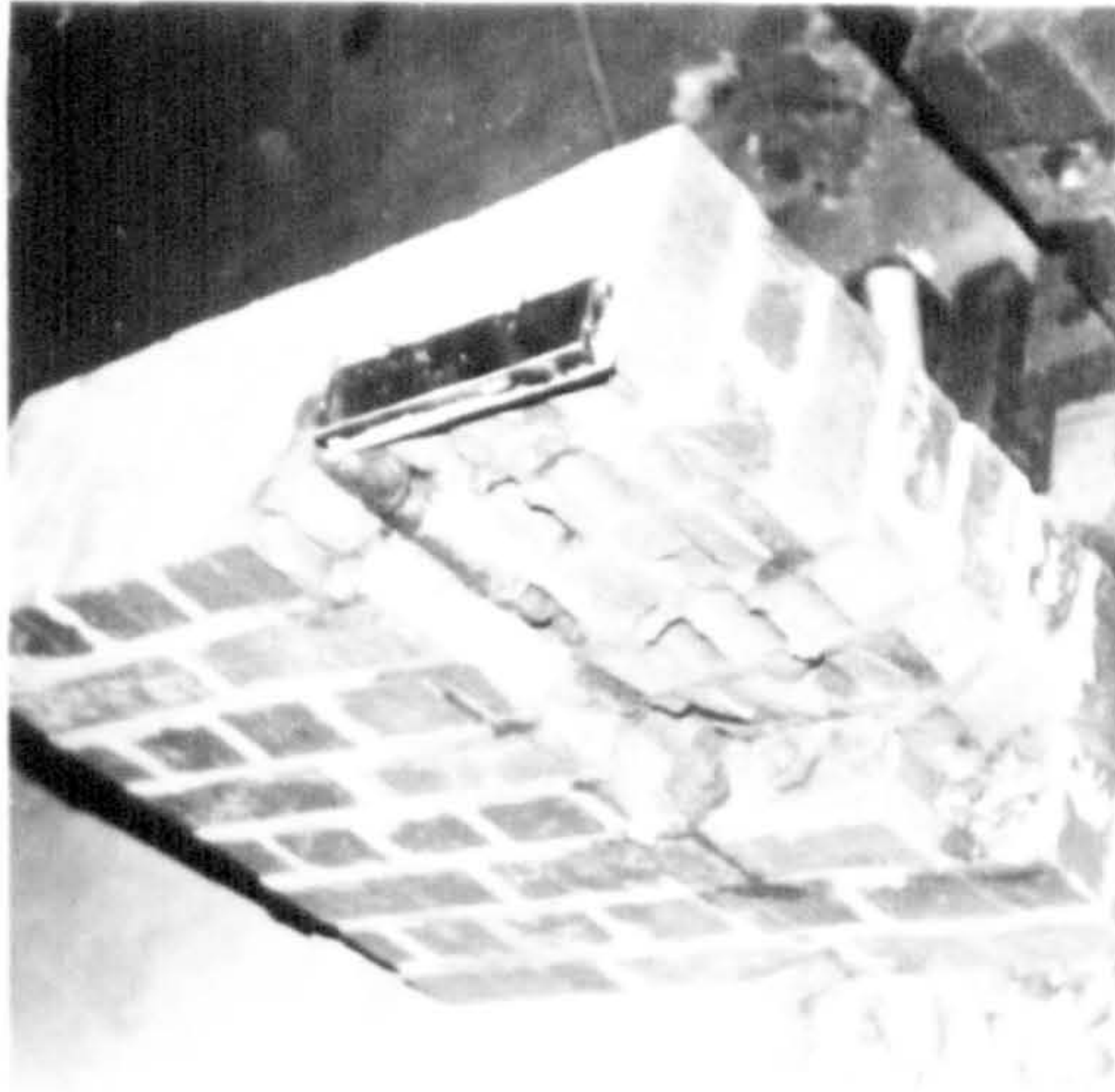


(b)-  $A_r = 0.16$



(c)-  $A_r = 0.24$

Fig. 6.112 - Typical failure mode and crack pattern for brickwork type M1 under intermediate edge loading ( $t=215.0\text{mm}$ ).



(a)-  $A_r = 0.08$



(b)-  $A_r = 0.16$



(c)-  $A_r = 0.24$

Fig. 6.113 - Typical failure mode and crack pattern for brickwork type M under end edge loading ( $t=215.0\text{mm}$ ).



## 6.7. SUMMARY AND CONCLUSIONS

Enhancement factor could be expressed either as a ratio of mean bearing to mean masonry strengths or the ratio of characteristic bearing strength to characteristic compressive strength of masonry. However, it has been shown that the two definitions yield same value for the enhancement factor provided that a reasonable number of samples have been tested under uniform load for the determination of the mean and characteristic compressive strengths of masonry.

Expressions for the mean and characteristic bearing strength of masonry in terms of unit brick strength for loaded area ratios of 0.1, 0.2, 0.3 and 0.4 for 102.5mm thick specimen constructed with mortar grade M(i) have been given.

Characteristic bearing strength is found to be 75% of the mean bearing strength.

Enhancement factor is a function of loaded area ratio and unit strength. It has been shown that when the loaded area ratio decreases the enhancement factor increases with increase in unit strength.

Increase in the strength of unit would increase the bearing capacity under partial loading. As brick and mortar strengths influence the masonry strength, it has been shown that as characteristic compressive strength of masonry increases, the bearing strength increases.

Decrease in loaded area ratio leads to increase in bearing strength. The influence of this parameter is found to be significant and is considered as a primary variable. The enhanced strength for drop in loaded area ratio of 0.4 to 0.3, 0.2 and 0.1 could be as high as 5, 30 and 120% respectively.

Depending on the type of brick unit used, masonry thickness influences the bearing strength. It has been shown that 102.5mm thick clay brickwork yields higher bearing strength in comparison to 215.0mm thick brickwork, and vice versa in the case of AAC brickwork at low values of loaded area ratios ( $A_r \leq 0.25$ ). This parameter shows the same effect on the enhancement factor. Also the AAC brickwork gives higher values for enhancement factor in comparison to clay brickwork.

The limiting value for aspect ratio for clay and AAC brickwork is found to be about one.

The effect of loading configuration (strip and edge) on the bearing strength and enhancement factor is found to be insignificant.

Position of applied concentrated load is found to be an important parameter and it has been shown that as the edge distance increases the bearing strength increases and conversely as edge distance decreases, the bearing strength decreases.

The effective area contributing to the bearing capacity of brickwork masonry is found to be equal to  $6t^2$ .

The appearance of cracks in relation to failure of brickwork under concentrated load depends on the loaded area ratio, the position of applied load along the length of the element, the thickness of the element and the type of units used in its construction. For single leaf, 102.5mm thick elements constructed with high strength units (in relation to the mortar cube strength), the mode of failure is by vertical splitting under the centre of applied load accompanied by diagonal cracks under the edge/s of bearing contained within a fan of  $30^\circ$  to the vertical, followed by local crushing at ultimate load. For bonded masonry, 215.0mm thick element, the diagonal cracks dominate the failure mode. For elements constructed with low strength units (i.e. brick strength approximately same as mortar cube strength) the failure is more or less localized. Sometimes the failure is by crushing of the unit under the bearing and other-times a wedge or cone is formed which ultimately splits the element. It has been observed that as the loaded area increases the diagonal cracks tend to become more vertical or in otherwords the angle of inclination to the vertical decreases. The effect of load position, i.e. where the load is applied at the end of the element in contrast to the central position, vertical and diagonal cracks form under the inner edge of the bearing sometimes running down the whole height. In most cases the final failure is caused by the crushing of brickwork in the bearing zone.

**STRESS DISTRIBUTION IN MASONRY UNDER CONCENTRATED LOAD**

**7.1. INTRODUCTION**

The main object of this chapter is to analyse brickwork masonry panels subjected to concentrated load by the method of finite element and to study the nature of stress distributions set up under this type of loading rather than to predict failure of the masonry panels.

As mentioned previously in chapter 3, most analytical investigations on brickwork masonry structures have been concerned with stress distributions subjected to uniform vertical compression. The work reported by Ali *et al*<sup>[70, 71]</sup> which has been reviewed in section 3.2 seems to be only published material on concentrated load on masonry. However, it was pointed out in section 3.4 that work carried out by Ali was to develop a nonlinear finite element program based on nonlinear fracture model of masonry for the analysis of the in-plane behaviour of masonry subjected to concentrated load. This work has now been completed<sup>[101]</sup> and contains a comprehensive material model which is incorporated into nonlinear finite element computer models capable of simulating the behaviour of masonry at all levels of applied load up to failure. It models brickwork masonry as a composite of nonlinear bricks set in a nonlinear mortar matrix. The nonlinear response of masonry has been produced by a combination of a nonlinear deformation characteristics and progressive failure of the constituent components. The material properties for the model were determined from various simple tests on samples of bricks, mortar and small masonry specimens. A series of failure criteria were adopted to model the different modes of failure in masonry constituents and due to the crack sensitive nature of the problem, emphasis was given to the modelling of crack and post-cracking behaviour of the materials.

Predicted failure load and mode obtained by the finite element analyses were verified by conducting tests on solid concrete brick panels, 1022mm (12-courses) high, 710mm (3-stretchers) long and 110mm thick set in mortar 1:5 cement:sand mix by volume. Twenty four panels were tested under concentric and eccentric strip concentrated load for various loaded area ratios. In general, good agreement was shown between theory and experiments. Sensivity analyses were also carried out for various parameters defining the material model and the finite element analysis. The modulus of elasticity and

the strength parameters, particularly the joint bond strength were found to be the most significant properties.

The finite element program was utilized to conduct a comprehensive parametric study of the behaviour of storey-height walls subjected to concentrated loads with the aid of substructuring and mesh-refinement schemes. The conclusions drawn from this study (apart from those mentioned in section 3.2) reveal that aspect ratio (ratio of length to height of specimen) of the panels is an important parameter. The ultimate bearing strength of the walls analysed were shown to be a function of the loaded area ratio, loading position and the length of the wall. The capacity decreased with increase of the loaded area ratio, eccentricity of the load and the length of the wall. These three parameters also influence the mode of failure which changes from splitting to the more gradual development of vertical cracks depending on the position of the loading plate in relation to the nearest plane of weakness (perpend joint) of the wall.

A standard finite element package available at the Department of Civil Engineering and Building Science at Edinburgh University has been used to carry out limited number of analyses in order to establish whether the stress distribution within brickwork masonry subjected to concentrated load could be obtained by use of such a package. The analyses carried out are two dimensional plane stress linear elastic, assuming masonry as a homogeneous continuum subjected to concentric and eccentric strip partial load. This is extended to treat masonry as an assemblage of separate elastic bricks and mortar joints. A nonlinear analysis under central strip partial load on the basis of a continuum has also been carried out.

## **7.2. METHOD OF FINITE ELEMENT ANALYSIS**

Standard finite element software called PAFEC<sup>[102]</sup> (Program for Automatic Finite Element Calculations) which is a general purpose package developed in Nottingham have been used to analyse brickwork masonry panels under concentrated load. It includes an extensive number of facilities, performs several types of analysis and contains large selection of elements.

The element used throughout the study is a flat eight noded isoparametric curvilinear quadrilateral (element No. 36210), normally used in plane stress mode for finding stresses and displacements in thin structures. The size of

panels were chosen to be 665mm (3-stretchers) in length, 590mm (8-courses) high and 102.5mm in thickness. Due to the large number of elements and limitation of the file space only two dimensional analysis have been carried out assuming plane stress. The panels were restrained at the bottom in the horizontal and vertical direction and the concentrated load has been applied by means of uniform pressure ( $\sigma_{cb}=50 \text{ Nmm}^{-2}$ ) applied over partial surface of the panel simulating strip loading configuration either concentric or eccentric with respect to the longitudinal direction. For the linear elastic analyses the material constants were set to: elastic modulus,  $E=7 \text{ kNmm}^{-2}$  and Poisson's ratio,  $\nu=0.20$  for the case of homogeneous continuum and  $E_b=80 \text{ kNmm}^{-2}$ ,  $E_m=44 \text{ kNmm}^{-2}$  with  $\nu_b=0.15$  and  $\nu_m=0.25$  for non-homogeneous model. For non-linear analysis the stress-strain relationship obtained for brickwork type F were idealized into elastic and plastic ranges. The yielding stress of  $8.8 \text{ Nmm}^{-2}$  were obtained with the initial elastic tangent modulus of  $22 \text{ kNmm}^{-2}$  and plastic modulus of  $3.3 \text{ kNmm}^{-2}$ .

### 7.3. RESULTS OF FINITE ELEMENT ANALYSES

#### 7.3.1. Concentric Position

Three types of analyses have been conducted under concentrated load applied at the centre of the panels. Linear elastic analysis modelling brickwork as homogeneous (assuming masonry as a single material), non-homogeneous (assuming masonry as a two-phase material, brick units and mortar joints) and non-linear analysis.

##### 7.3.1.1. Homogeneous

The results are presented in Fig. 7.1. Only half of the structure is considered since the panel is symmetrical about its centre (see Fig. 7.1(a)). The distribution of vertical stress,  $\sigma_y$ , as a ratio of applied concentrated pressure,  $\sigma_{cb}$ , which is an indication of the nature of the load dispersion is shown in Fig. 7.1(b). The vertical stress is compressive except for a small area at the top corners of the panel. The distribution of vertical stress becomes uniform at a depth below the top of the panel approximately equal to  $0.6h$ . Most codes suggest that the concentrated load can be assumed to disperse at an angle of  $45^\circ$  beneath the loaded area. This has been shown in Fig. 7.1(b) and can be seen that the influence of concentrated load extends beyond this dispersion line particularly in the region immediately beneath the load and is approximately contained within a fan of  $30^\circ$  to the horizontal.

The distribution of transverse stress at different sections down the height of the panel is presented in Fig. 7.1-(c) with its magnitude in terms of applied stress,  $\sigma_{cb}$ . The transverse stress is compressive immediately underneath the loaded area and becomes tensile at a height approximately equal to  $0.15h$  under the centre of the load. The transverse tensile stress is maximum under the centre of the plate and decreases at various sections away from the loaded region. The location of maximum transverse tensile stress changes ( $y/h$  increases) as the distribution is taken away from the loading point. The graphical output obtained from the package for finite element mesh, displaced shape, inplane stress vectors, largest absolute, maximum and minimum principal stress contours are presented in Fig. 7.2 (a)-(f) respectively.

### 7.3.1.2. Non-homogeneous

The finite element mesh for this analysis is as shown in Fig. 7.3-(a) with the shaded area representing the mortar joints. Again only half the structure is considered with the vertical plane under the concentrated load being restraint in the horizontal direction to simulate the appropriate boundary condition. Concentrated pressure of  $50 \text{ Nmm}^{-2}$  is applied over 5% of the surface. The non-dimensional vertical stress distribution is shown in Fig. 7.3(b) at various levels. The magnitude of vertical stress distribution is approximately the same as the homogeneous case. The distribution of transverse stress down the height of two sections (section I: across bricks and bed joints, section II: across bricks, vertical perpend and bed joints) are as shown in Fig. 7.3(c). The transverse stress at section I is compressive immediately under the applied concentrated load and tensile which is maximum at a height of  $0.11h$  beneath the loaded area in the brick unit. It can be seen that the transverse stress in the joints are always compressive. The transverse stress at section II is again compressive immediately under the applied concentrated pressure and tensile which is maximum at the same height as in section I. The distribution of the stress is compressive in the first perpend joint with subsequent ones in tension. The stress in the perpend exceeds the stress in the joints suggesting that the splitting of the brickwork could be initiated in the vertical perpend due to the bond failure. Comparing the transverse tensile stress in the cases of homogeneous and non-homogeneous, it can be seen that the peak stress is markedly greater in the latter case (compare Figs. 7.1(c) & 7.3(c)).

### 7.3.1.3. Nonlinear analysis

The results of nonlinear analysis subjected to concentrated pressure applied over 10% of the top surface of brickwork masonry are presented in Figs. 7.4 and 7.5. The vertical stress distribution (see Fig. 7.4(b)) shown in a non-dimensional scale is compressive except for a small area at the top corners of the panel and becomes uniform at a depth below the loaded area approximately equal to  $0.6h$  contained within a fan of  $30^\circ$ . The distribution of transverse stress down the height in a non-dimensional scale for various sections is as shown in Fig. 7.4(c). Transverse stresses at these sections are compressive below the loaded area and become tensile below this region. Under the centre of loaded area the transverse tensile stress is maximum at a height of  $0.35h$  with a magnitude of  $0.05\sigma_{cb}$ . For a distribution at a section away from the centre of the load the magnitude of transverse tensile stress decreases and the location of the peak changes (i.e.  $y/h$  increases).

### 7.3.2. Eccentric Position

The finite element mesh for the linear elastic analysis assuming brickwork as homogeneous continuum under end strip concentrated load is shown in Fig. 7.5(a). The distribution of vertical stress is as shown in Fig. 7.6(b). Vertical compressive stresses are a maximum under the loaded area whereas vertical tensile stresses are a maximum near the base of the panel and do develop at the other unloaded end of the panel. The distribution of transverse stress for different sections are shown in Fig. 7.5(c). Immediately underneath the loaded area the stress is compressive and becomes tensile at the depth equal to  $0.05h$  with the peak occurring under the inner edge of the applied load. The distribution of transverse stress at other sections away from the loaded area is tensile within the top region of the panel and compressive below this region. The graphical output obtained from PAFEC are presented in Fig. 7.7.

Comparing the results obtained for the cases of concentric and eccentric loading it can be seen that as the eccentricity of load is increased (i.e. decreasing the edge distance from central to end loading position) the magnitude of the tensile transverse stress increases. For the loaded area ratio of 0.05 the maximum transverse tensile stress under eccentric concentrated load is approximately twice its respective value under concentric load.

#### **7.4. SUMMARY AND CONCLUSION**

Two dimensional plane stress finite element analyses have been used to study the nature of stress distributions under concentric and eccentric concentrated load using a standard package. For the concentric loading two types of analyses namely linear elastic and nonlinear analysis were performed, with the former case modelling brickwork masonry as homogeneous continuum and as an assemblage of separate bricks and mortar joints. The following conclusions can be drawn from this study:

- Standard package (PAFEC) could be used successfully to simulate brickwork masonry panels under concentrated load. In general the accuracy of the results depend on the type of analysis and the size of elements.
- A finite element model which treats units and joints separately is more effective, since it reflects the effect of varying stiffness of its constituent materials. This is particularly important in the study of transverse tensile stress where peak stress has been shown to be greater than that obtained in the homogeneous model.
- A nonlinear analysis is also more effective since it reflects the effect of material/s nonlinearity and its influence on the transverse stress distribution which shows higher peak stress. However, it can be uneconomical especially when masonry is modelled as an assemblage of separate bricks and joints.
- The distribution of vertical stress is compressive with its peak under the loaded area and tensile at the top corners of the panel. It is best contained within a fan of  $30^\circ$  to the horizontal.
- The distribution of transverse stress is compressive immediately below the loaded area and tensile below this region. The study of transverse stress in the non-homogeneous case shows that bricks and vertical perpend exhibit transverse tensile stress which causes the splitting of the specimen due to bond failure in the perpend

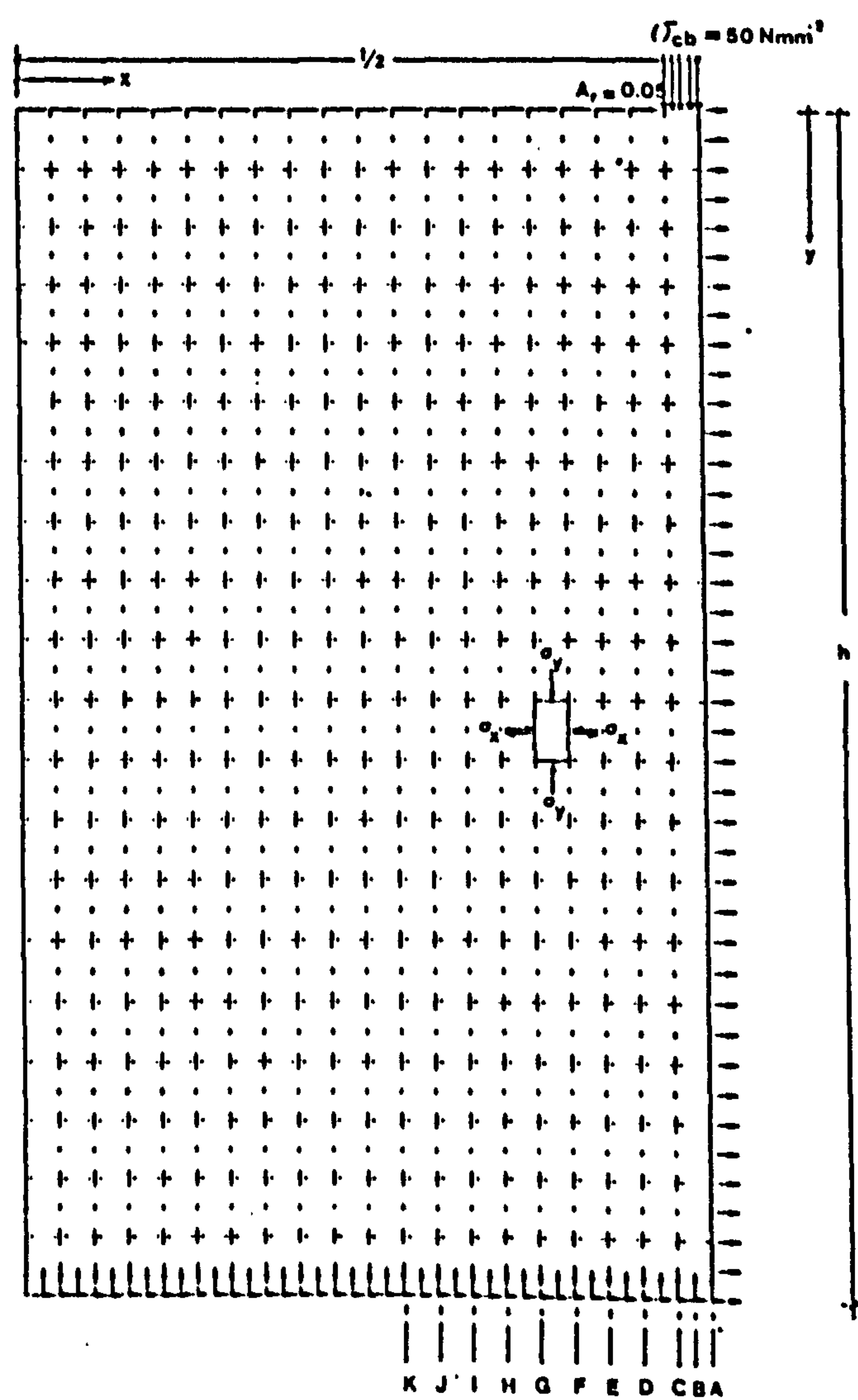


and tensile crack in the units.

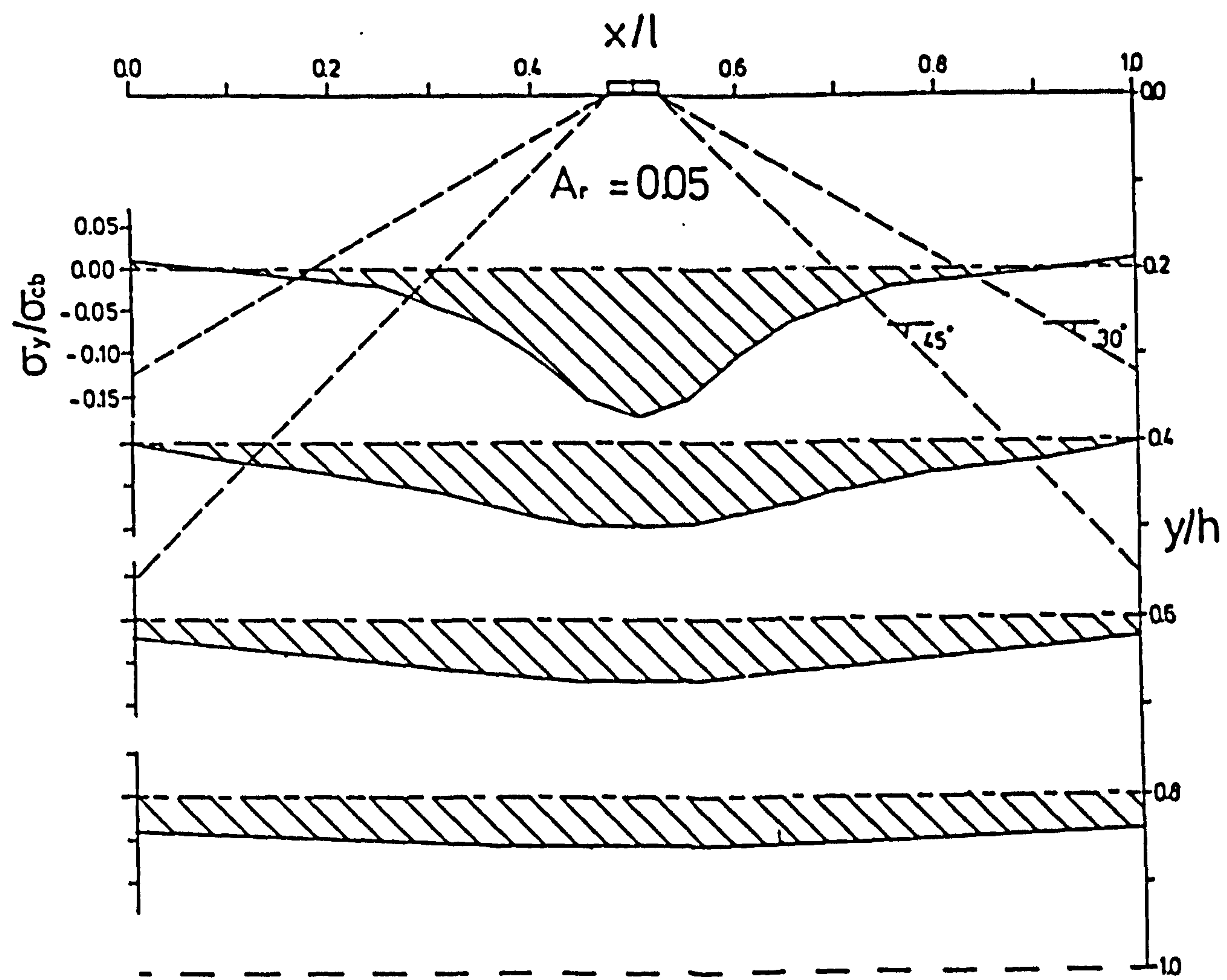
- As concentrated load is applied to the end of the panel (eccentric in contrast to concentric loading), the transverse tensile stress markedly increase. This increase is as high as 200% for loaded area ratio of 0.05.

Unfortunately a non-homogeneous nonlinear analysis was not performed due to the limitation of file size and excessive number of elements involved. However, the results reported in this chapter are in good agreement with existing results<sup>[101]</sup>.

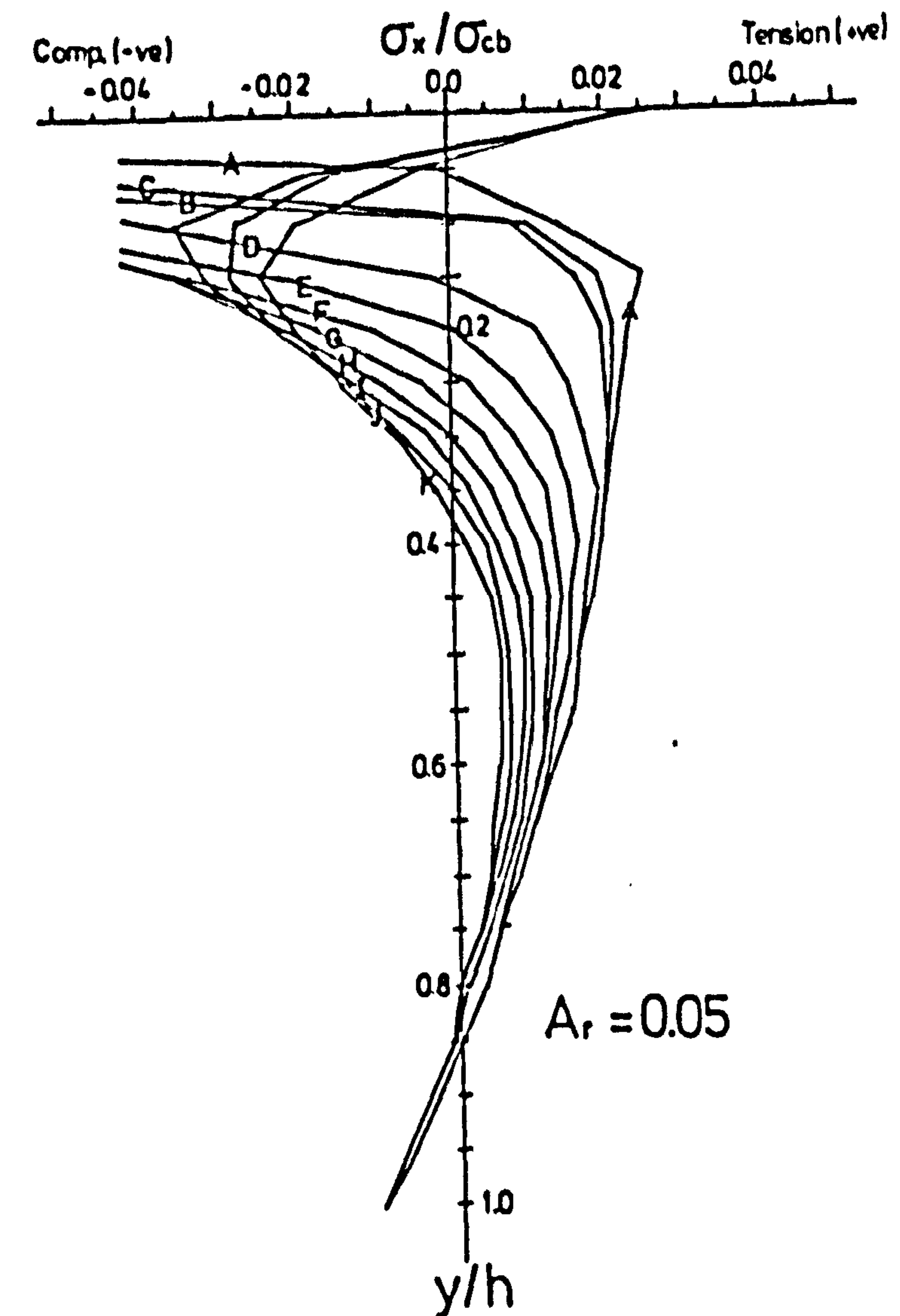
**CONTAINS  
PULLOUTS**



(a) - Finite element mesh.

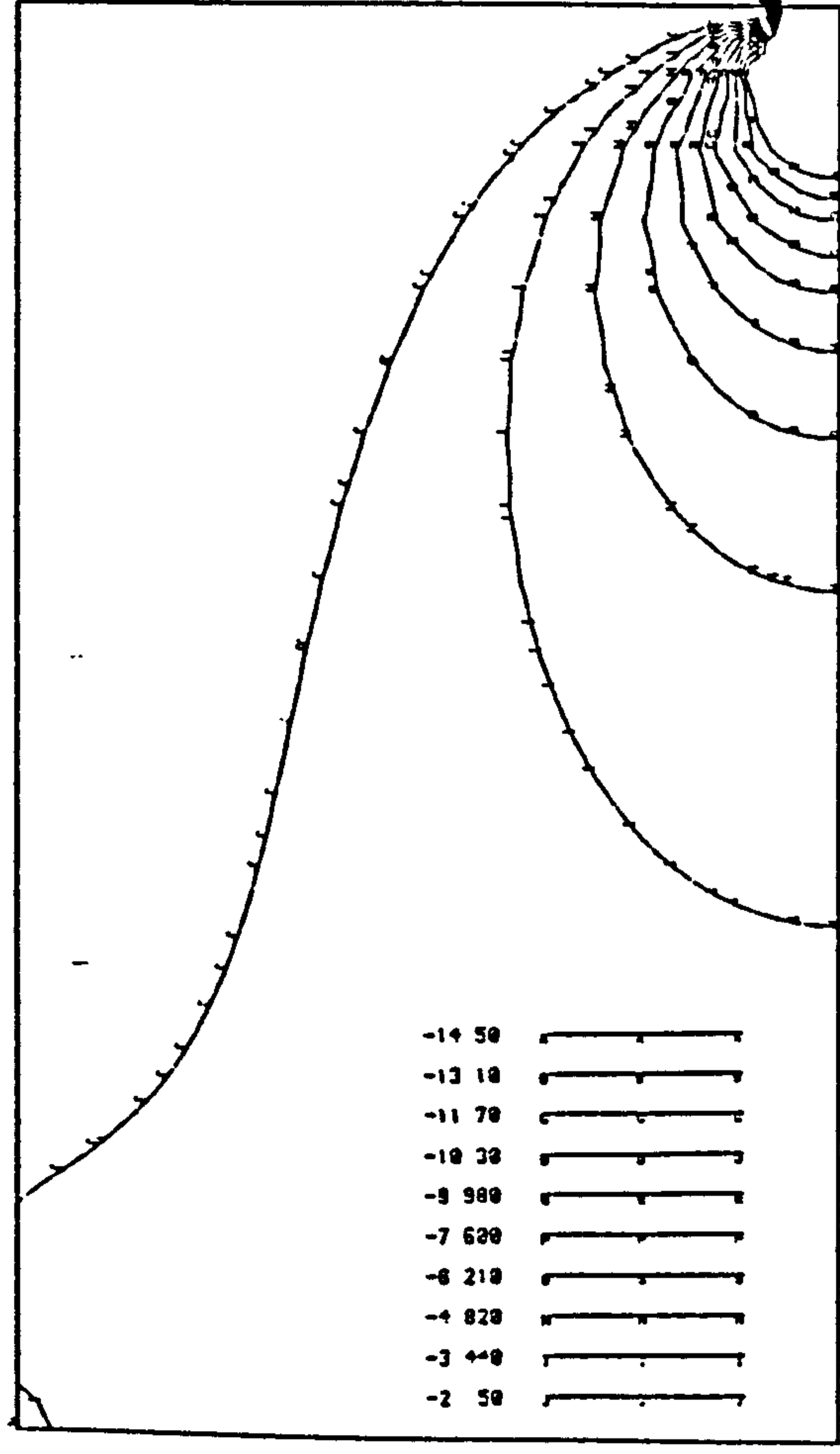


(b) - Vertical stress distribution.

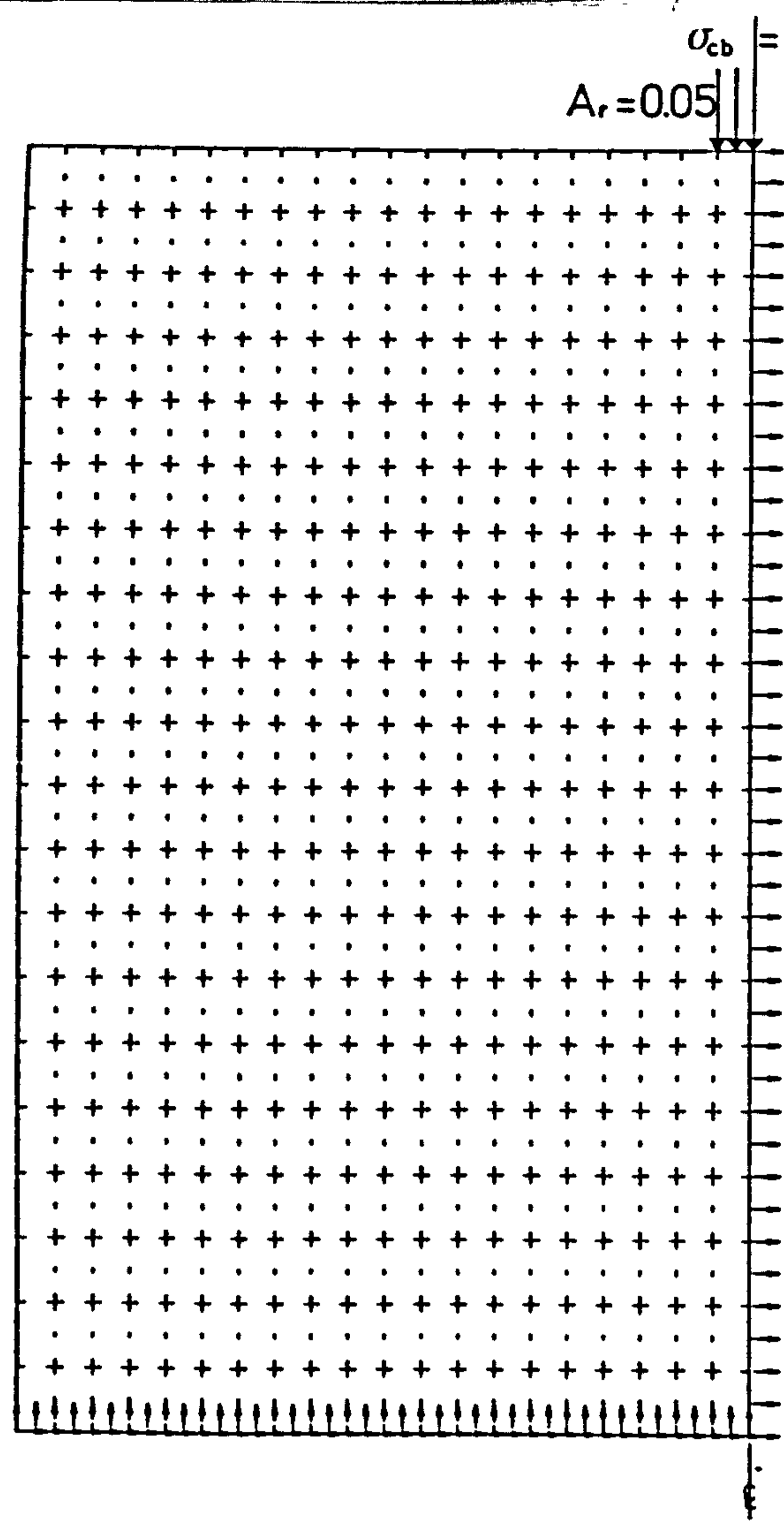


(c) - Transverse stress distribution.

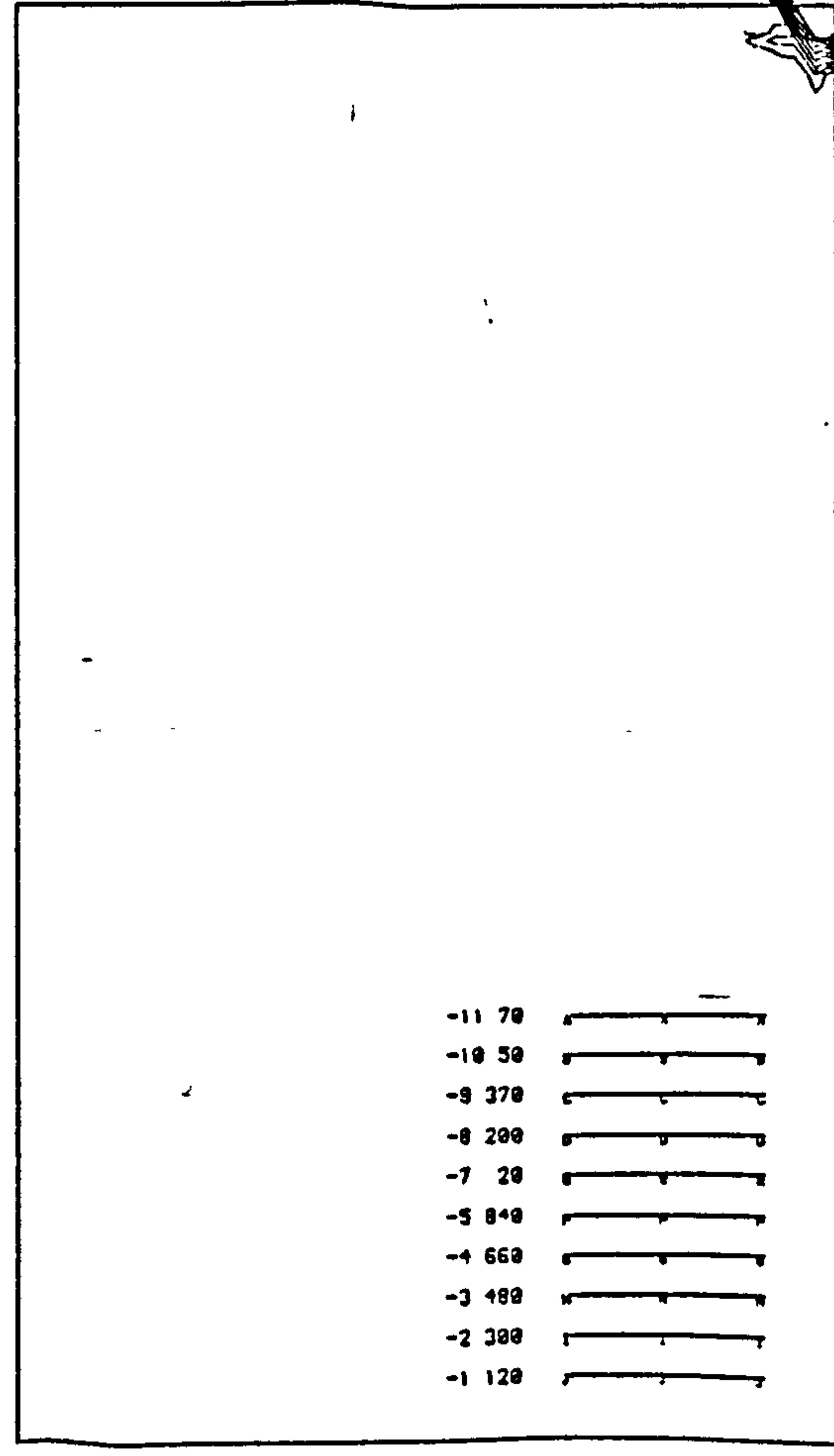
Fig. 7.1 - Results of linear finite element analysis under concentric concentrated load modelling brickwork as homogeneous material.



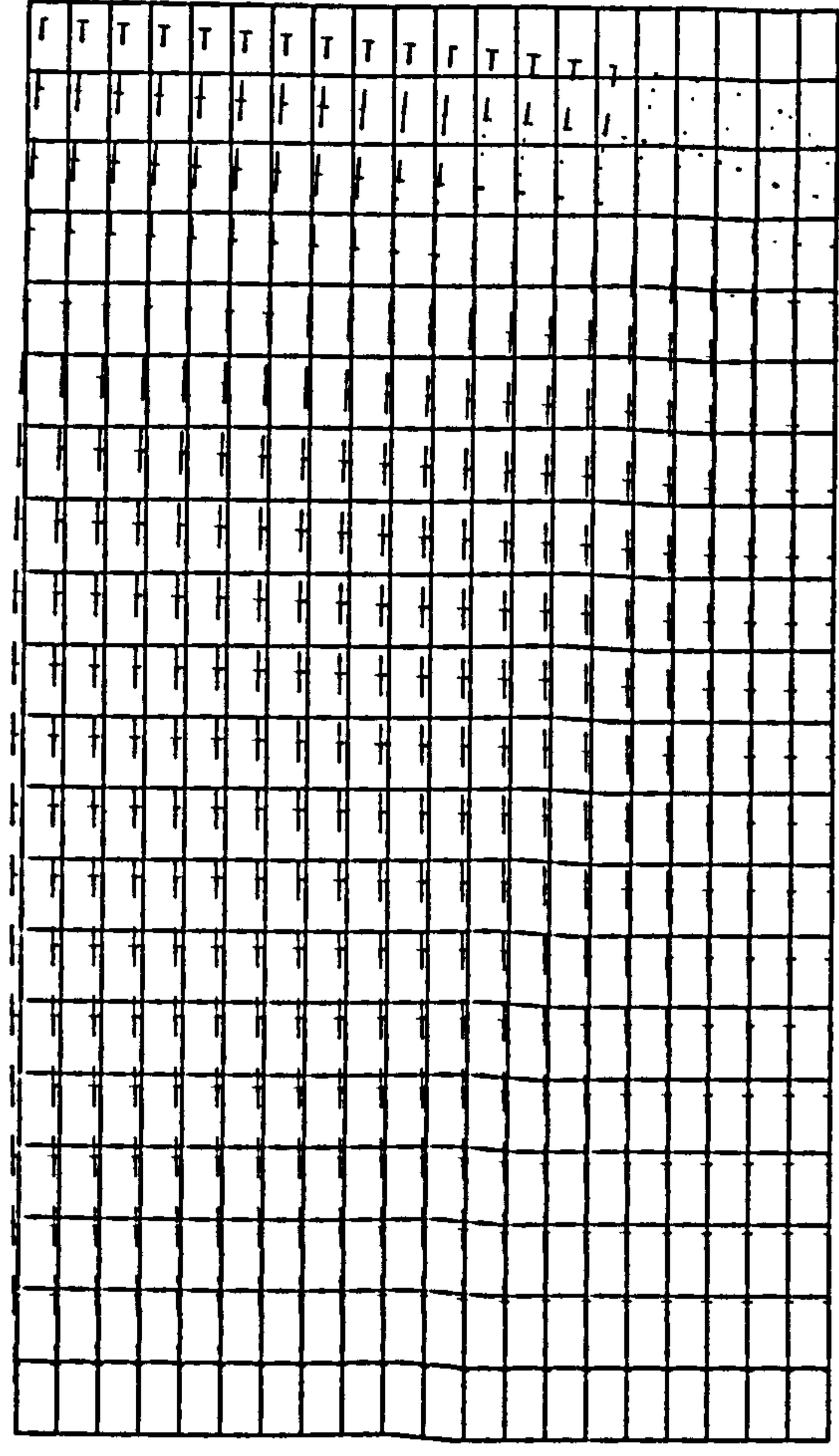
(d) - Largest absolute principal stress contours.



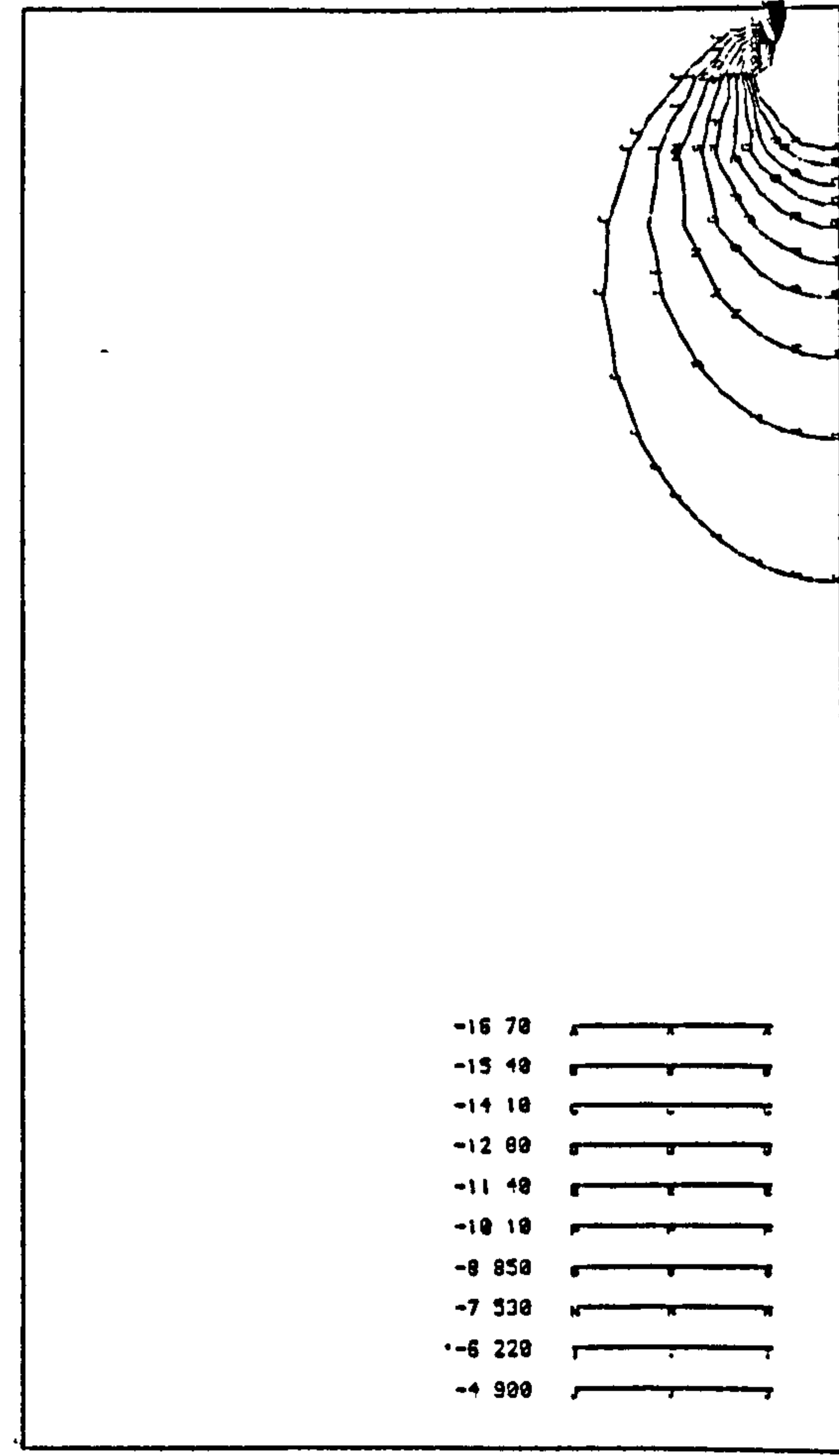
(a) - Finite element Mesh.



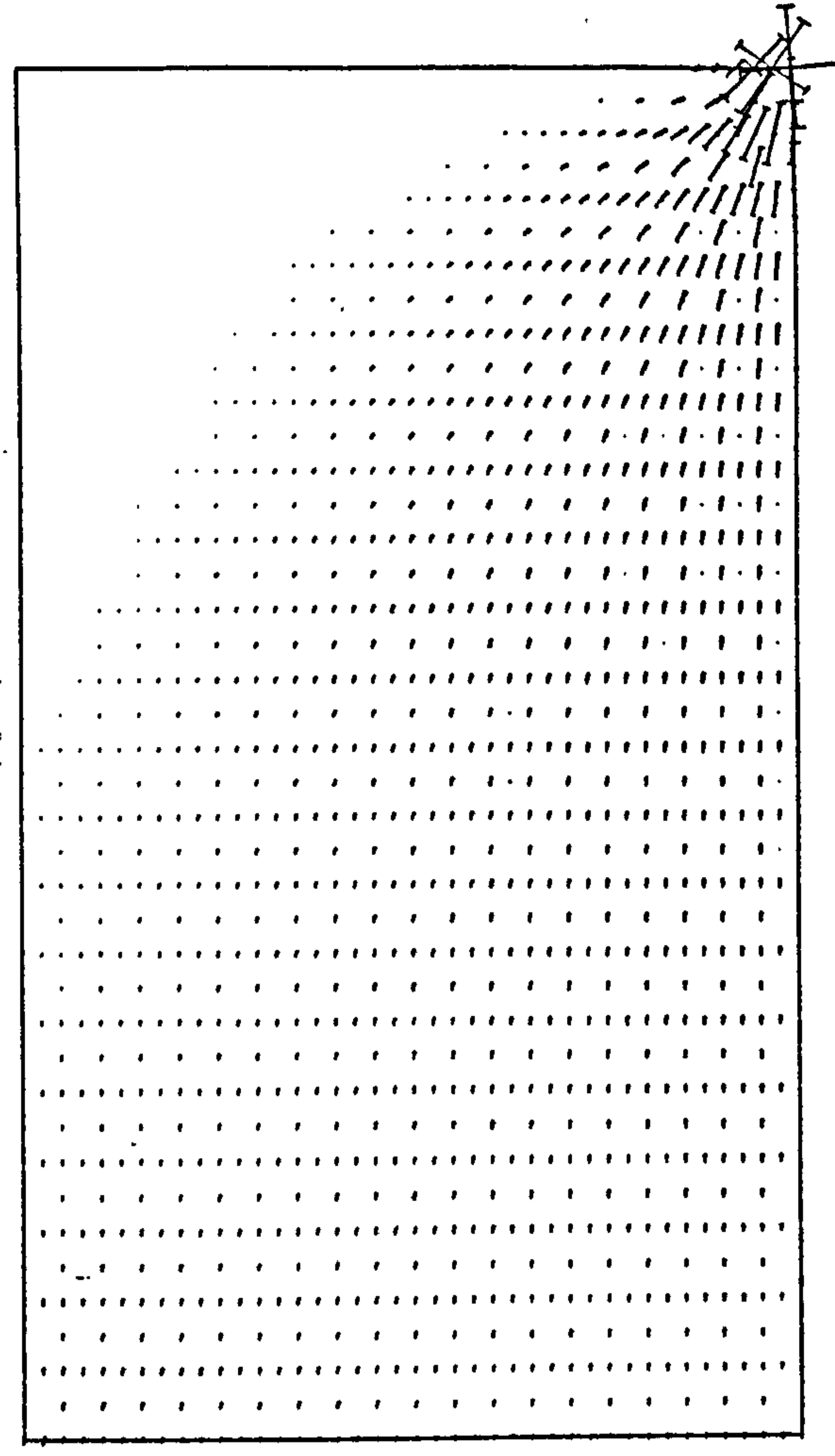
(e) - Maximum principal stress contours.



(b) - Displaced shape.

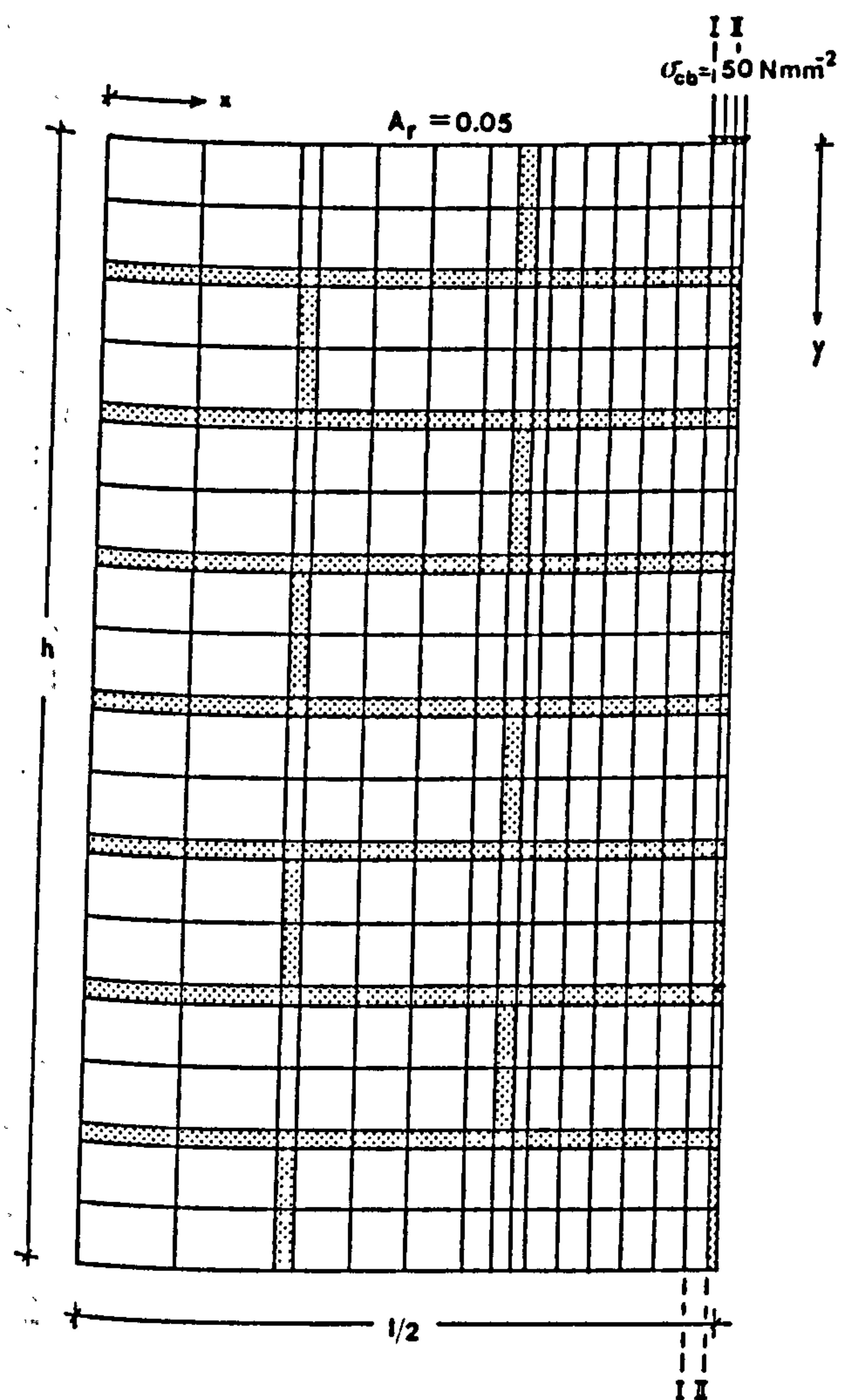


(f) - Minimum principal stress contours.

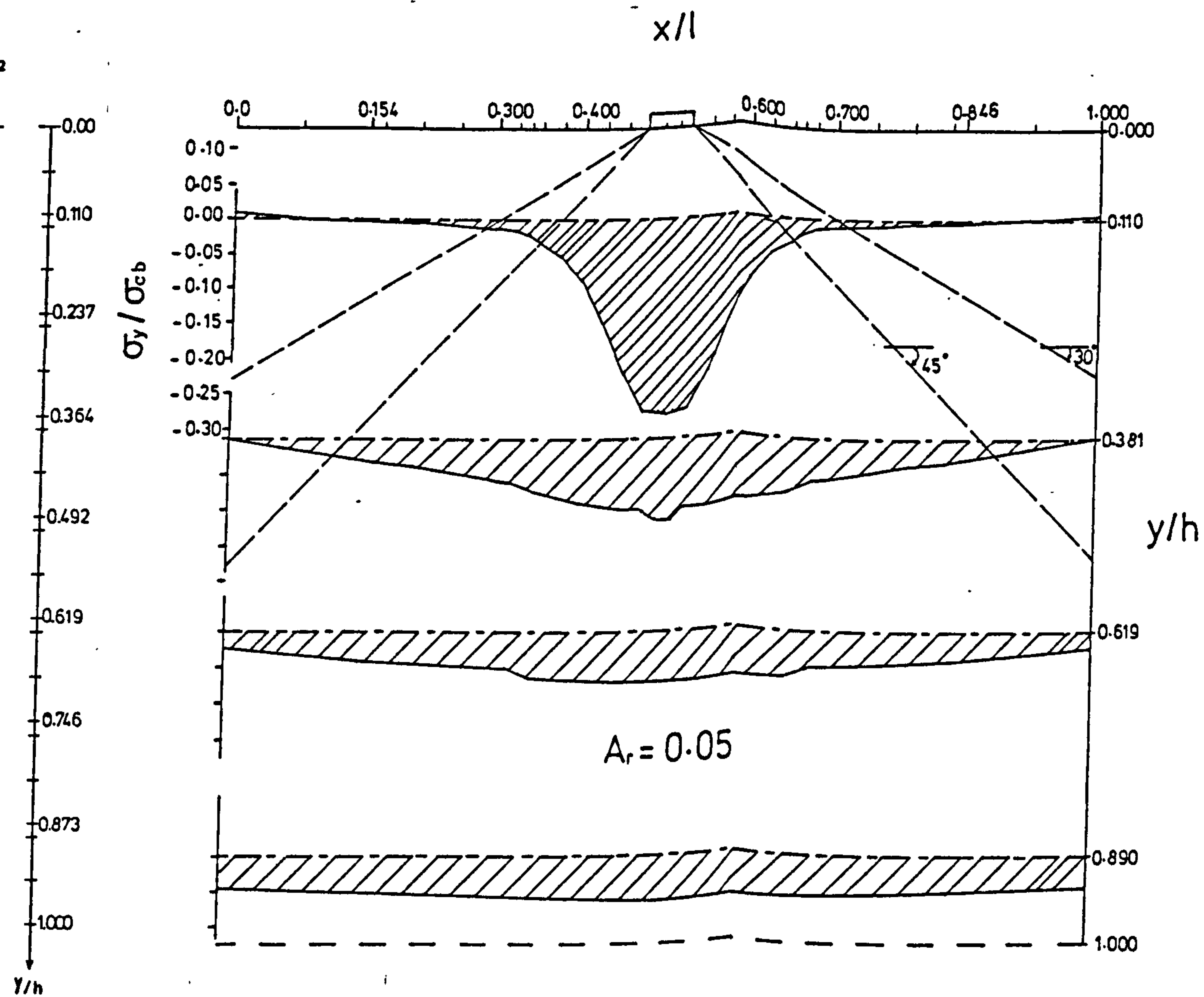


(c) - In-plane stress vectors.

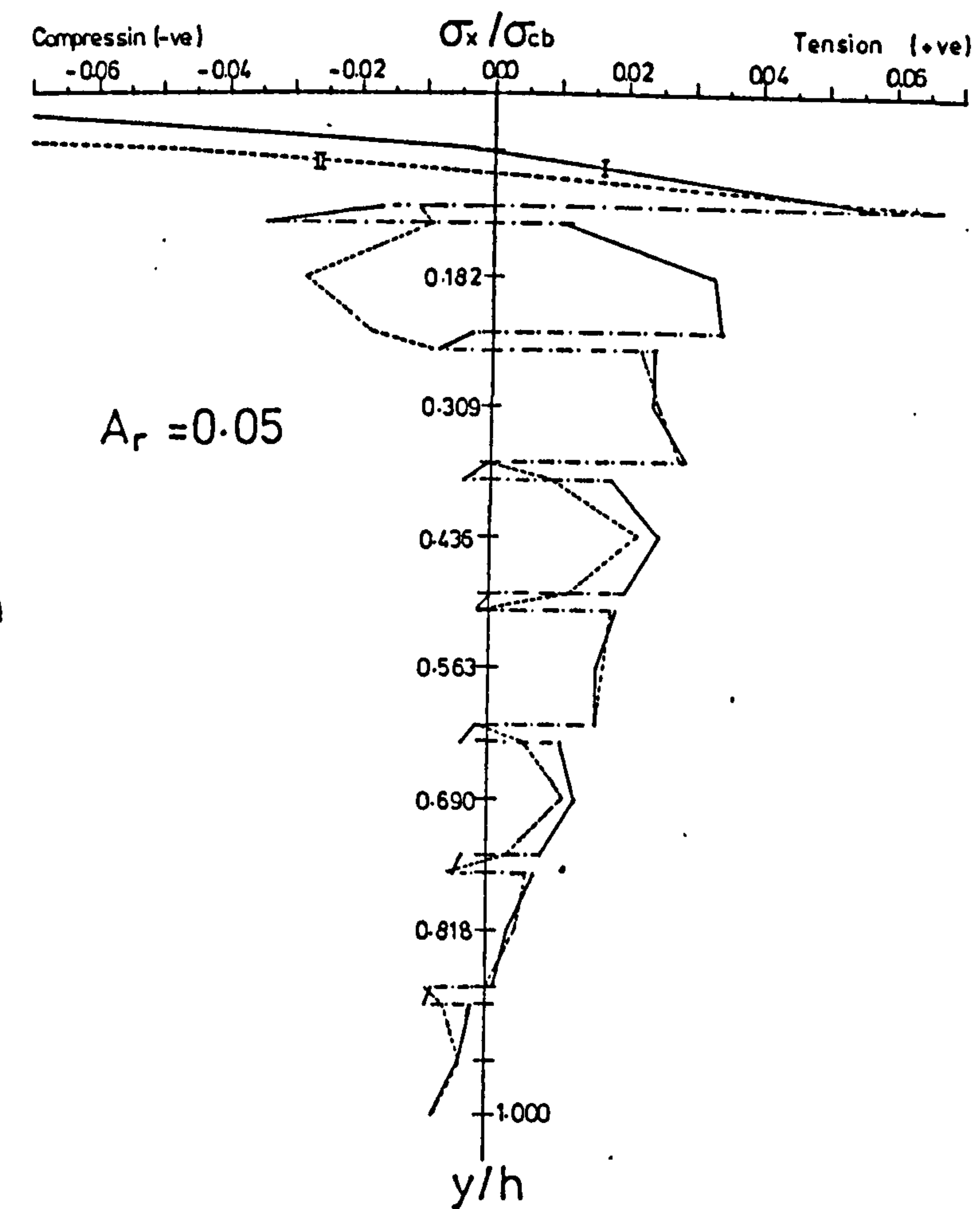
Fig. 7.2 - Linear homogeneous finite element analysis of brickwork under concentric concentrated load ( $A_r=0.05$ ).



(a) - Finite element mesh.

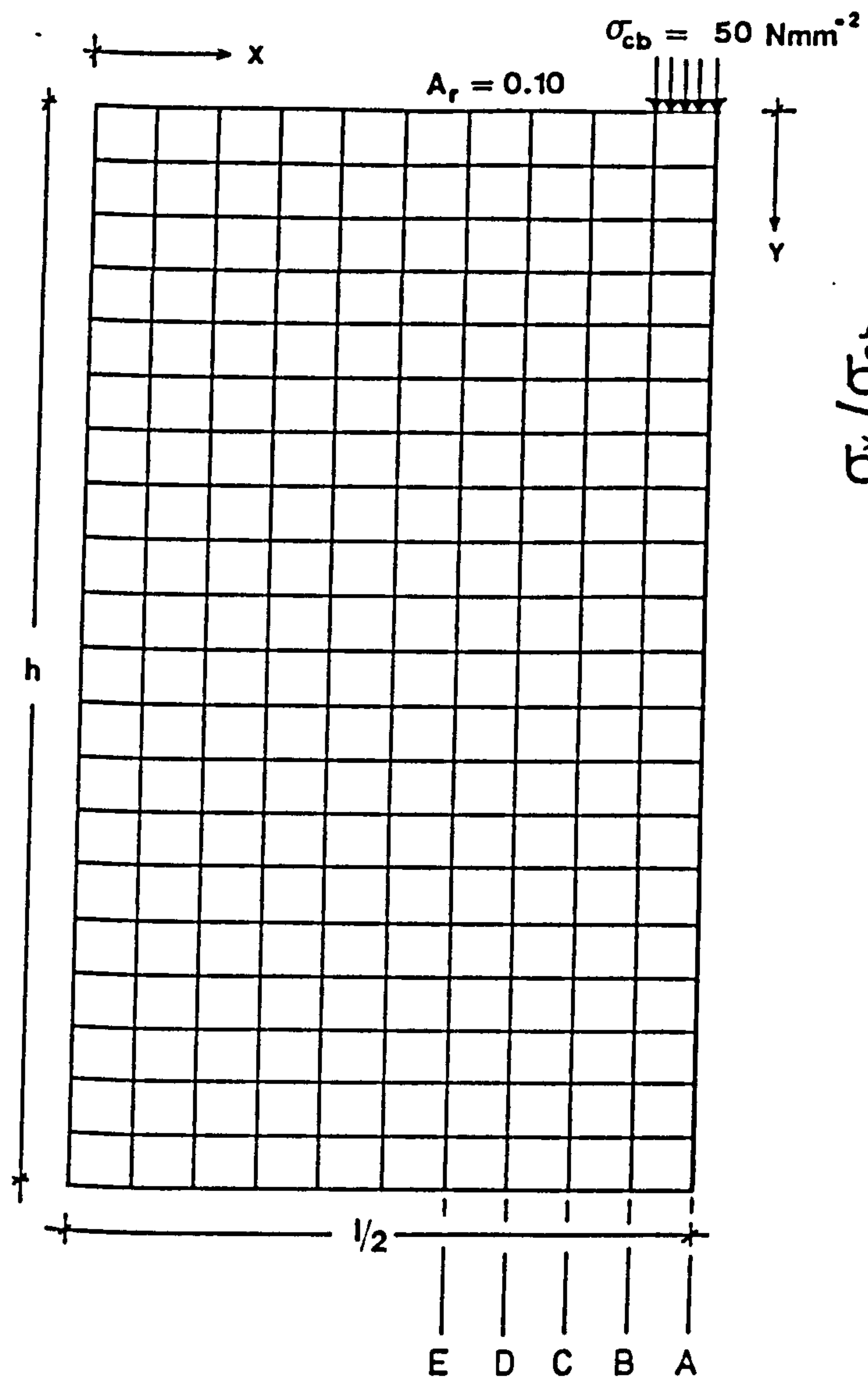


(b) - Vertical stress distribution.

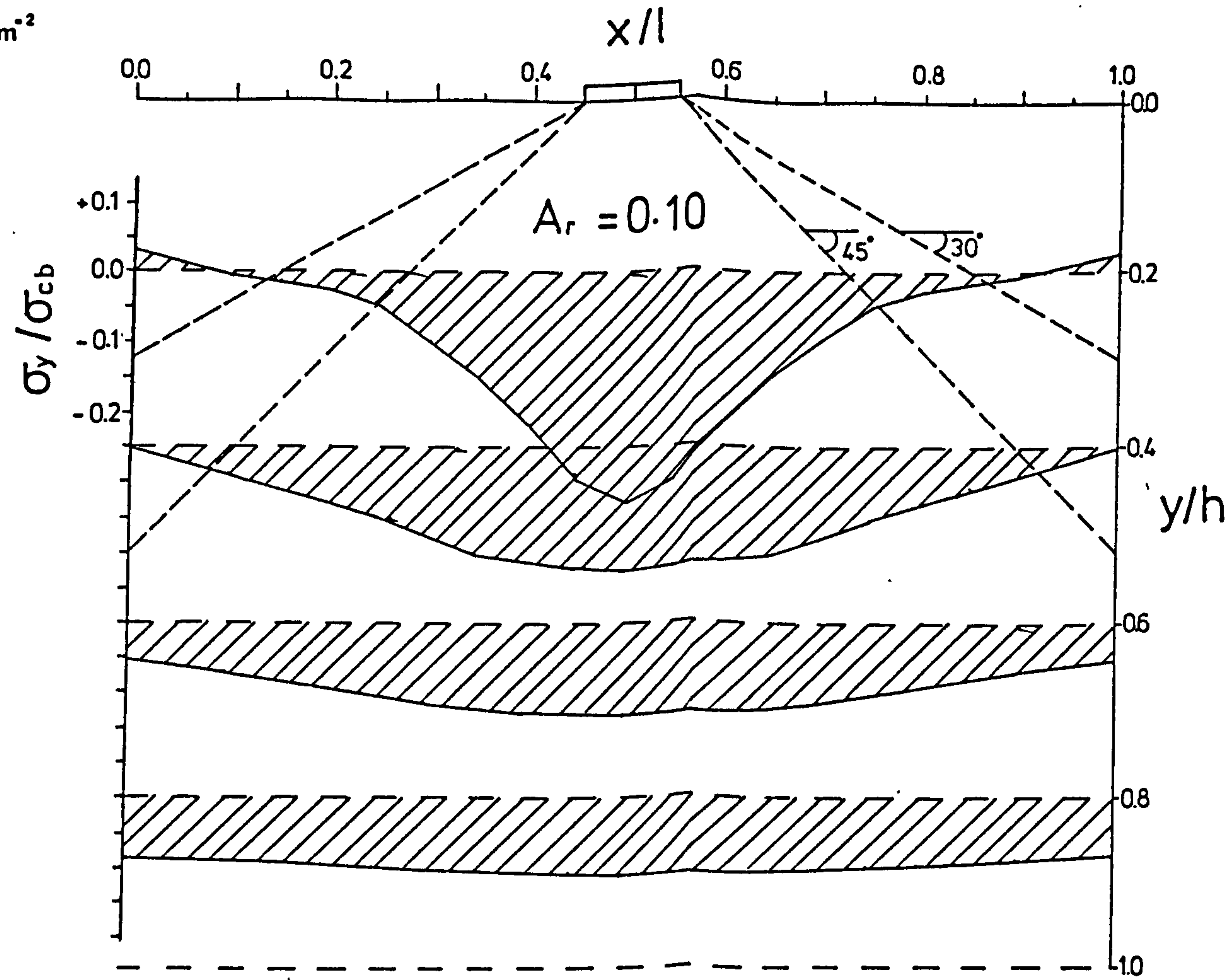


(c) - Transverse stress distribution.

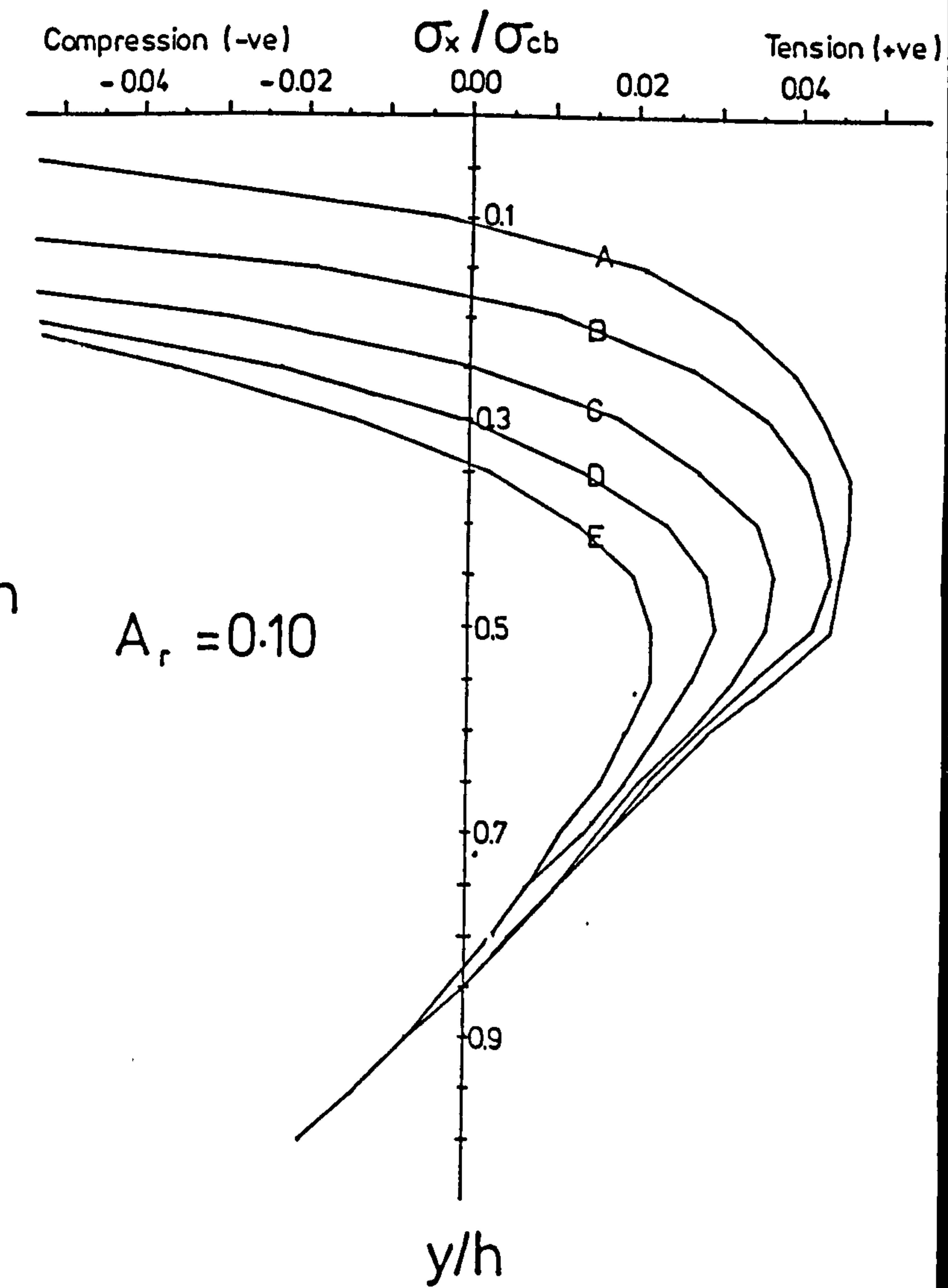
Fig. 7.3 - Results of linear finite element analysis under concentric concentrated load modelling brickwork as non-homogeneous material.



(a) - Finite element mesh.

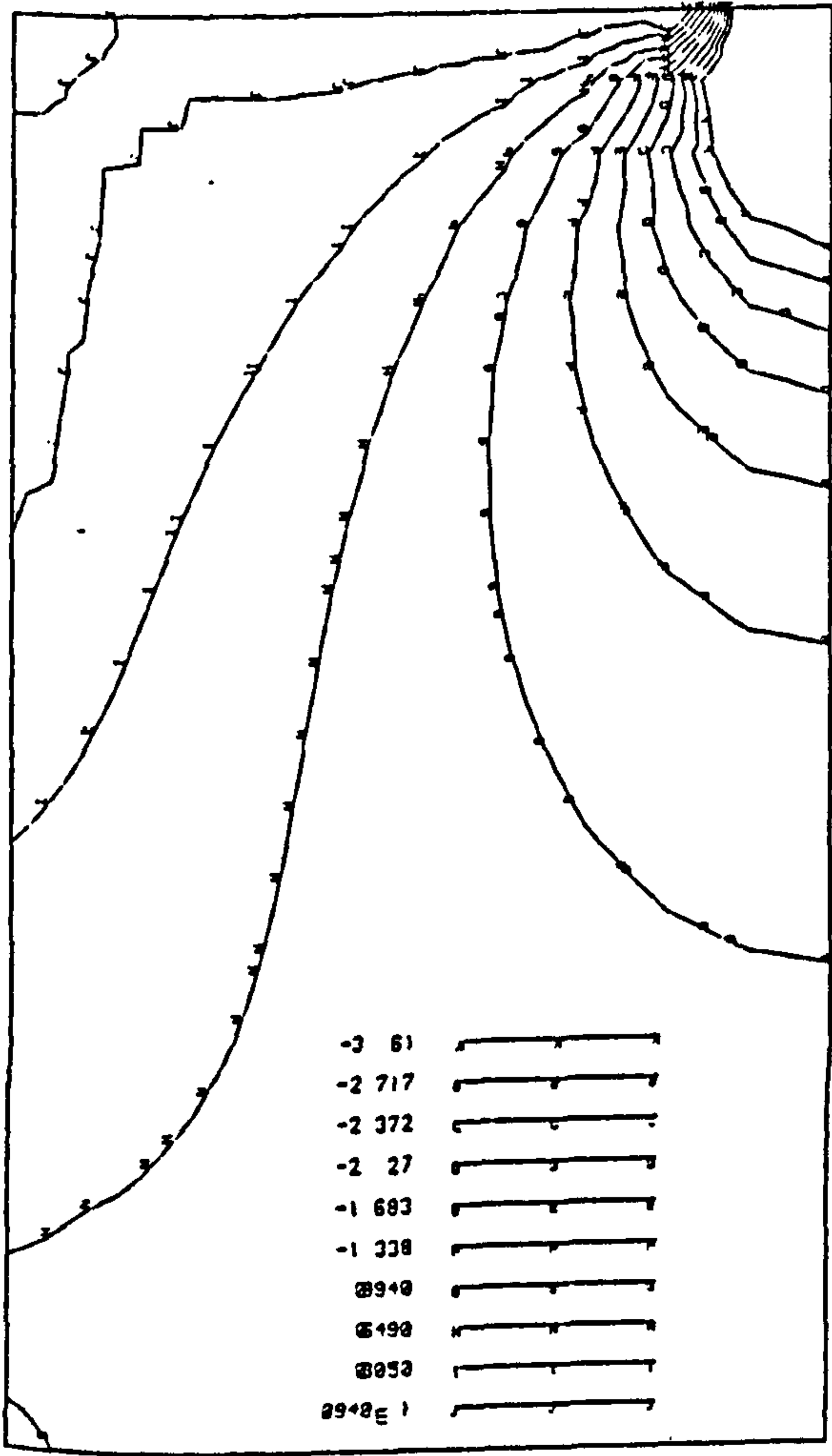


(b) - Vertical stress distribution.

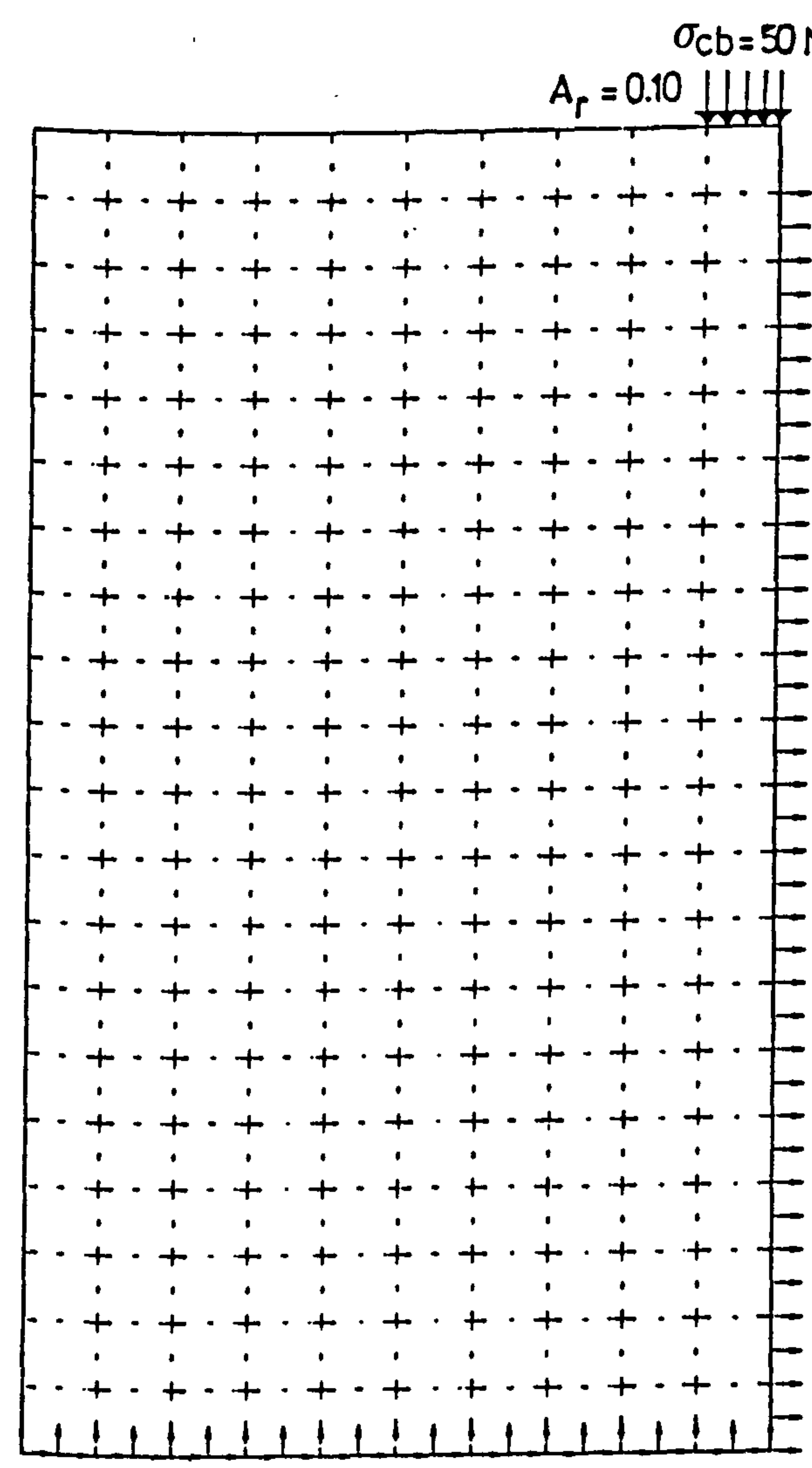


(c) - Transverse stress distribution.

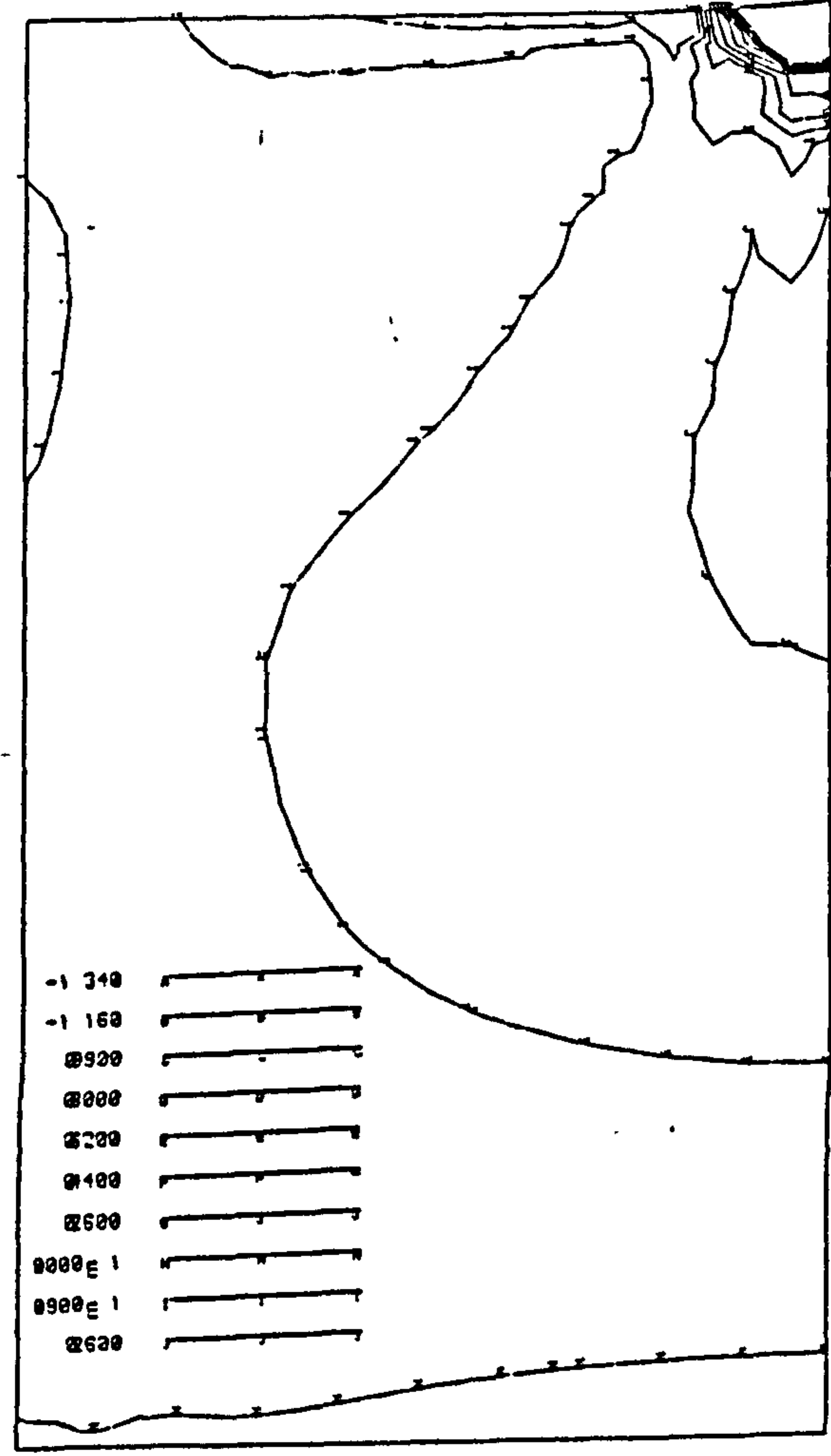
Fig. 7.4 - Results of non-linear finite element analysis under concentric concentrated load modelling masonry as homogeneous material.



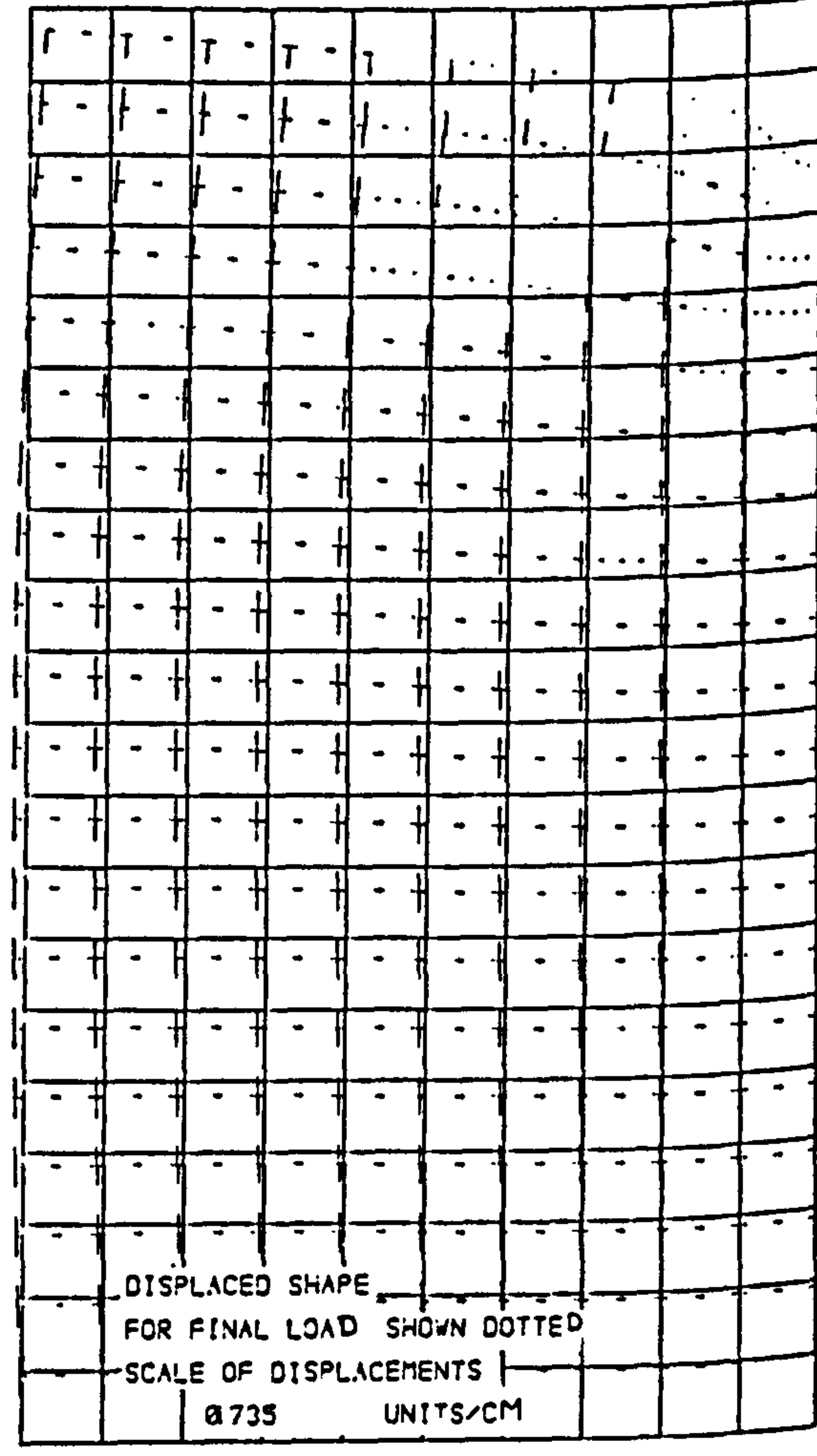
(d) - Largest absolute principal stress contours.



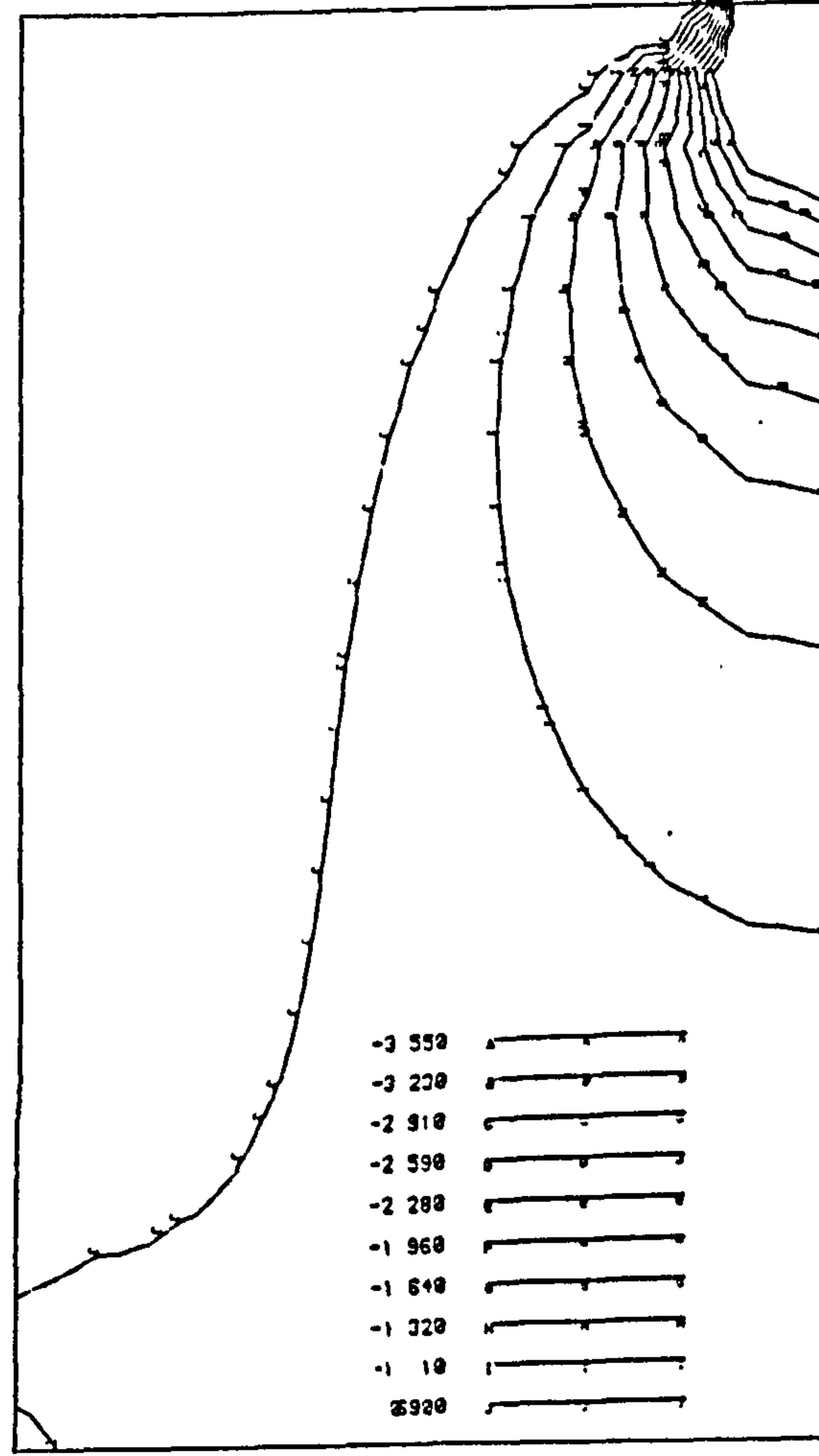
(a) - Finite element Mesh.



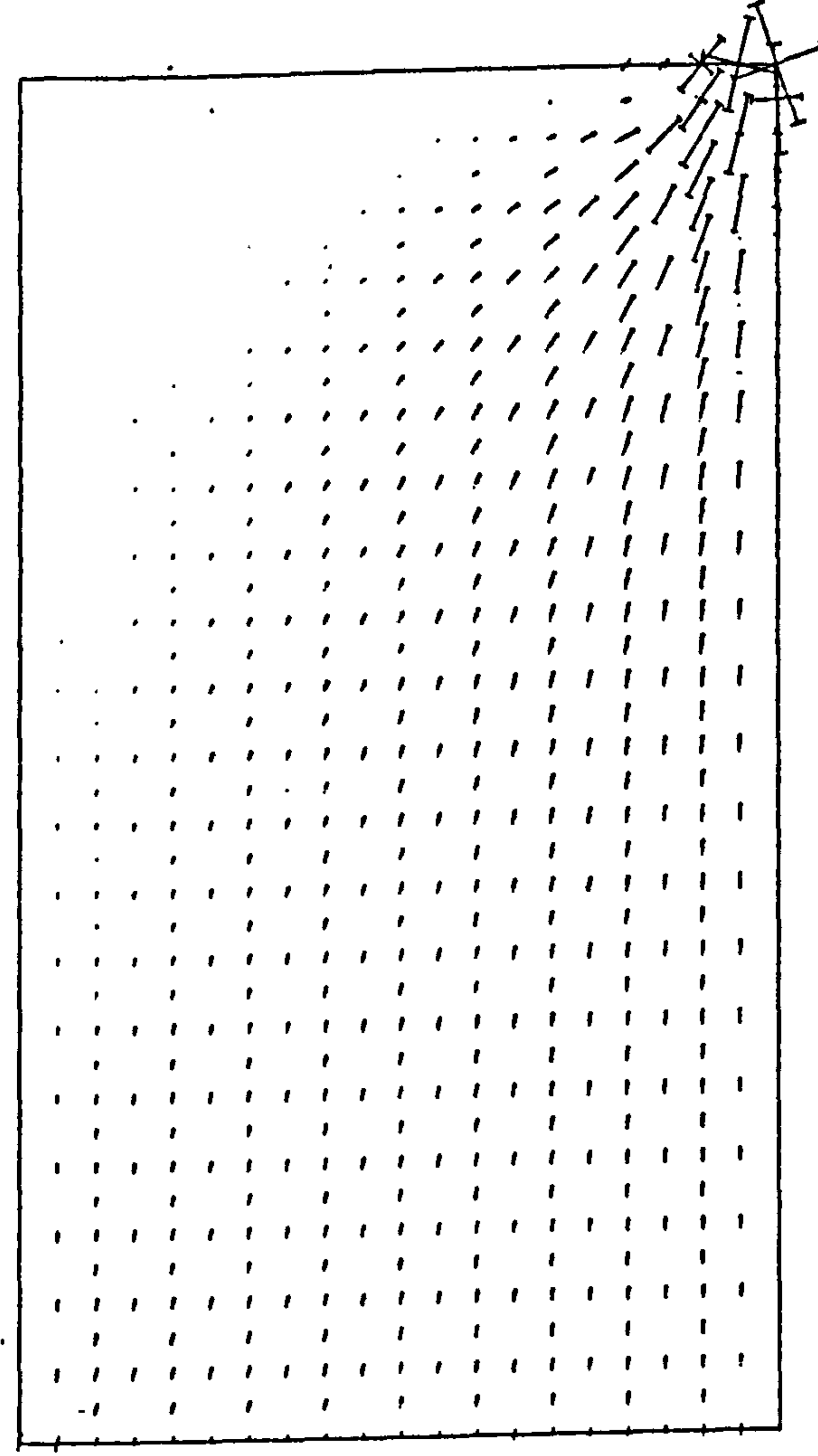
(e) - Maximum principal stress contours.



(b) - Displaced shape.

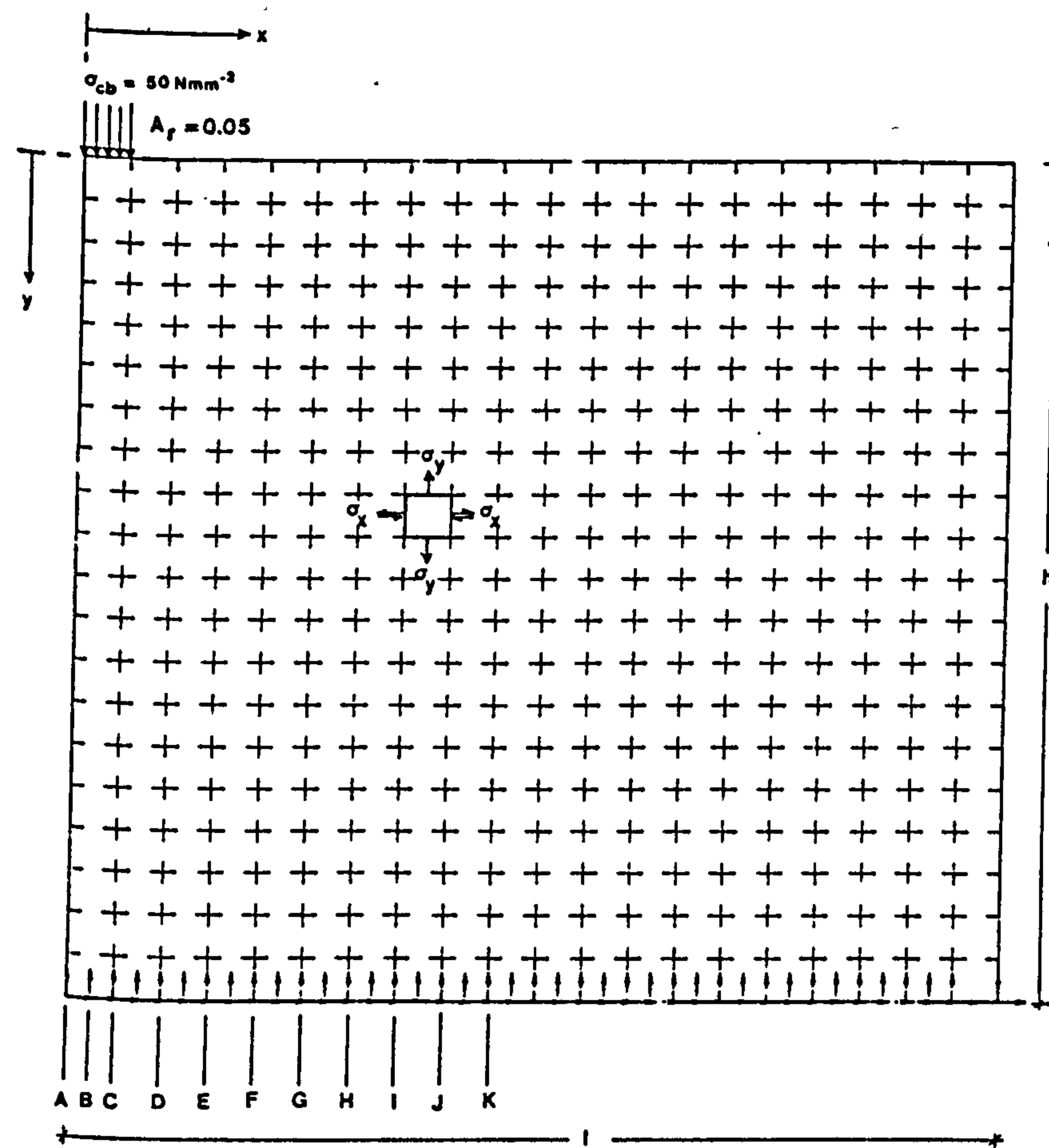


(f) - Minimum principal stress contours.

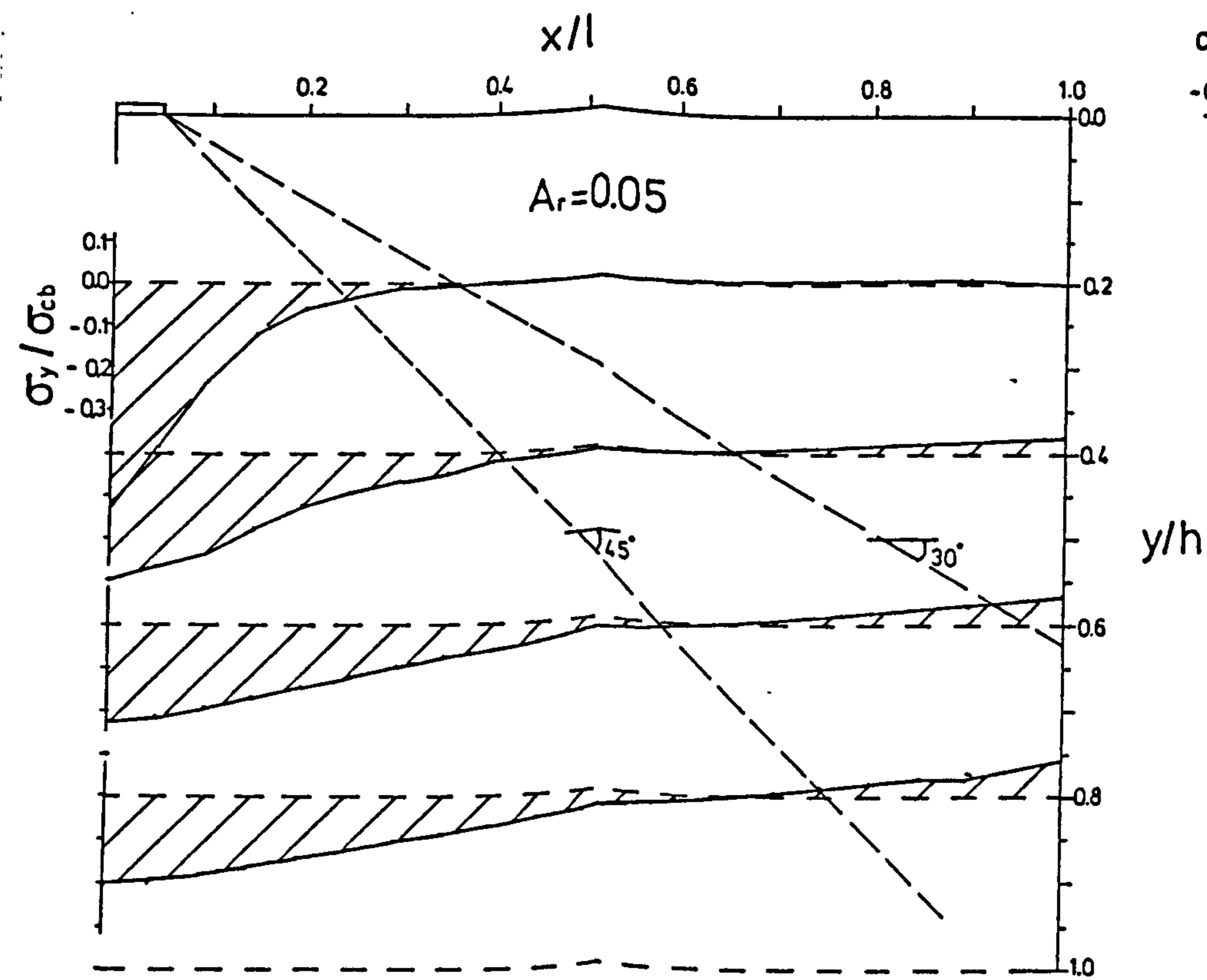


(c) - In-plane stress vectors.

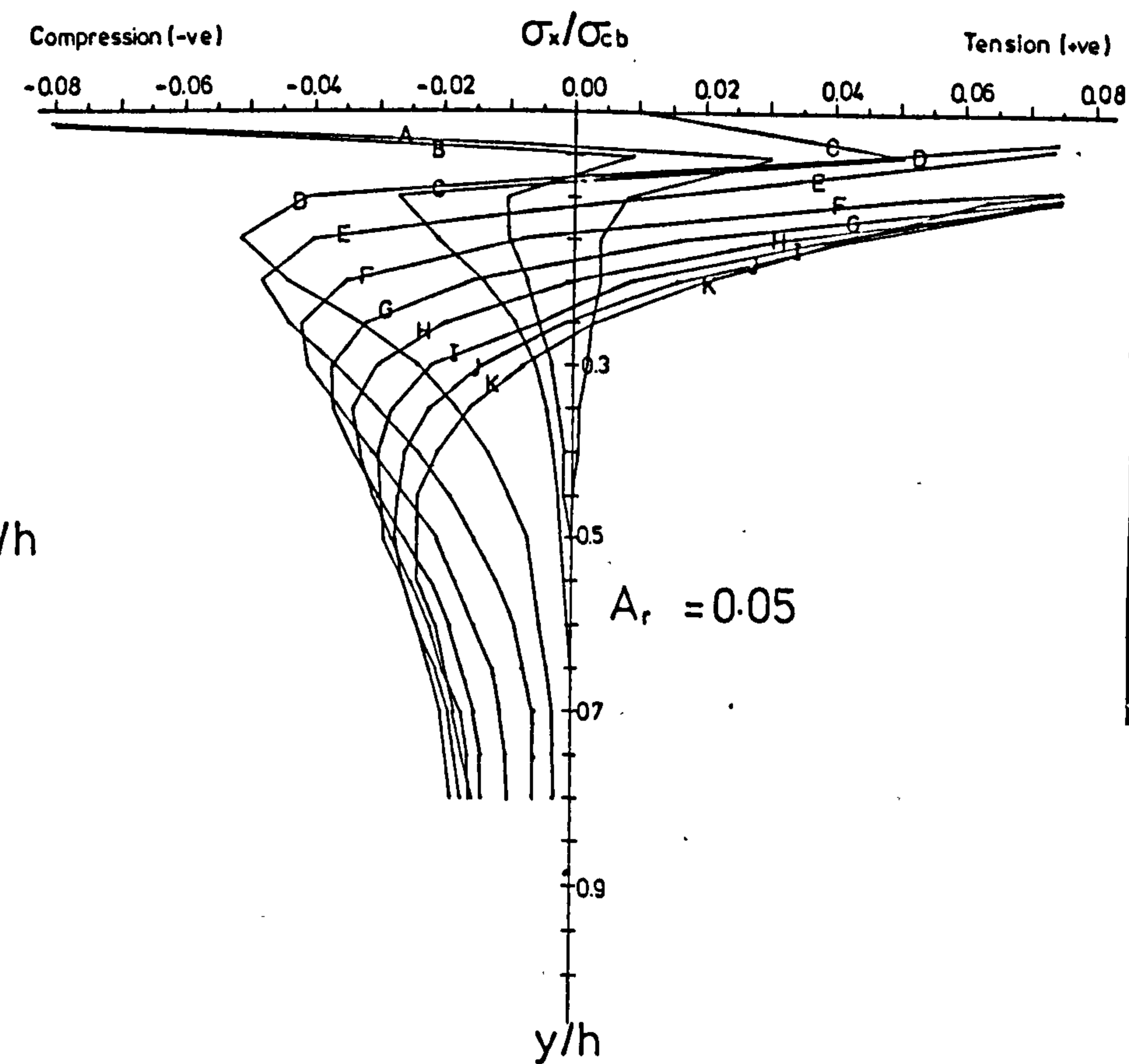
Fig. 7.5 - Non-linear finite element analysis of brickwork under concentric concentrated load ( $A_r=0.10$ ).



(a) - Finite element Mesh.



(b) - Vertical stress distribution.

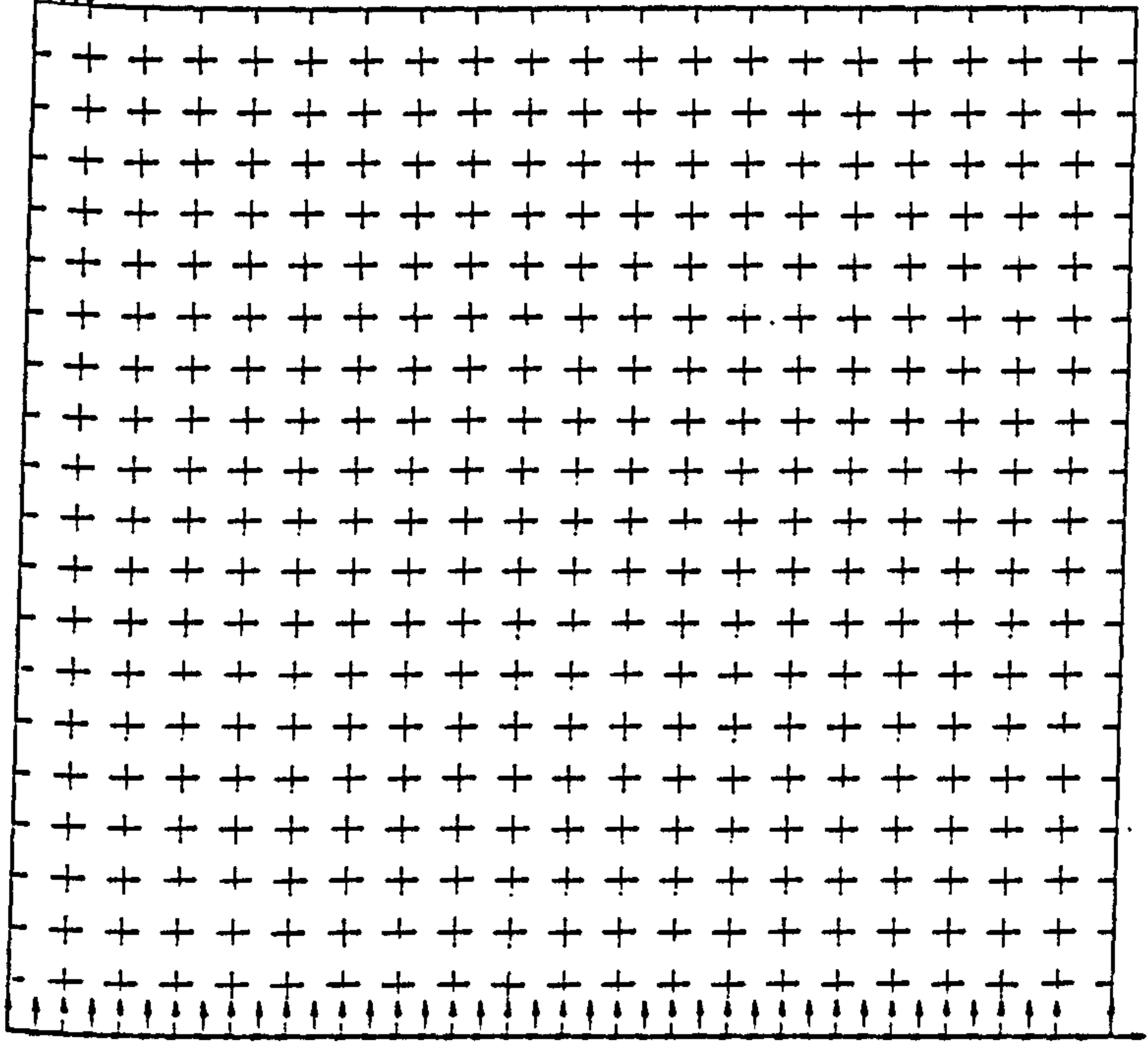


(c) - Transverse stress distribution.

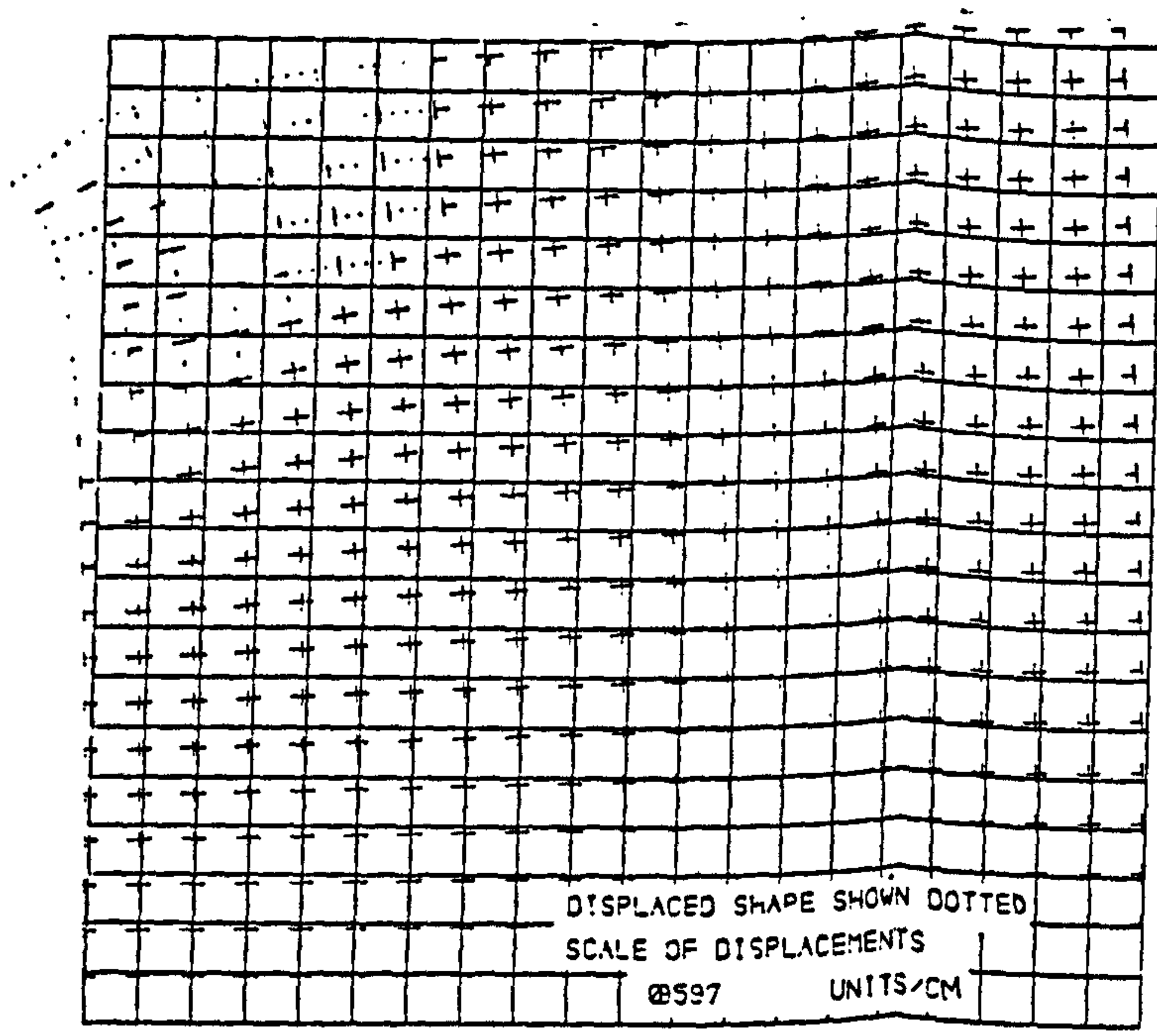
Fig. 7.6 - Results of linear finite element analysis of brickwork under eccentric concentrated load modelling masonry as homogeneous material.



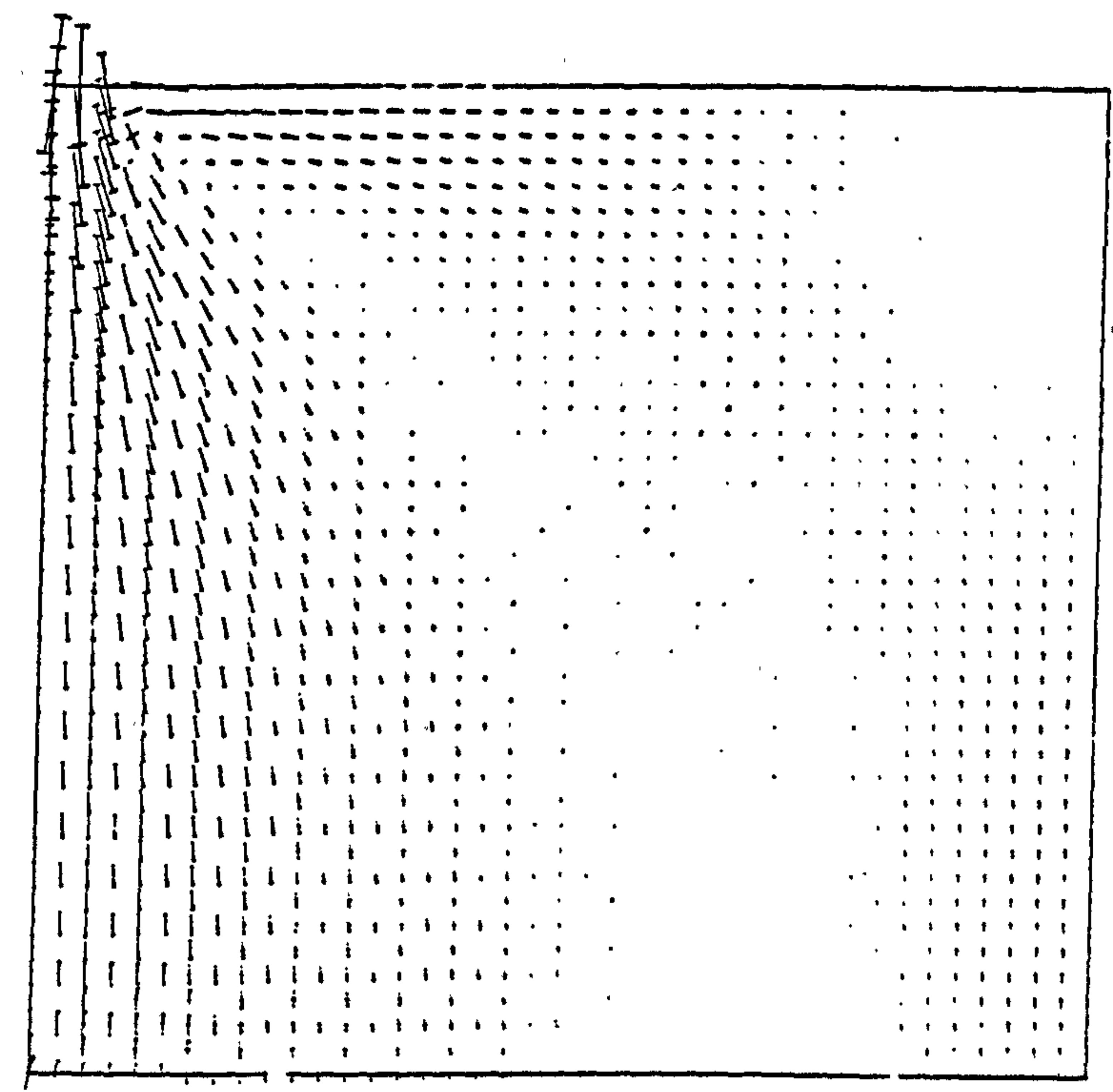
$\sigma_{33} = 50 \text{ N/mm}^2$   
 $A_r = 0.05$



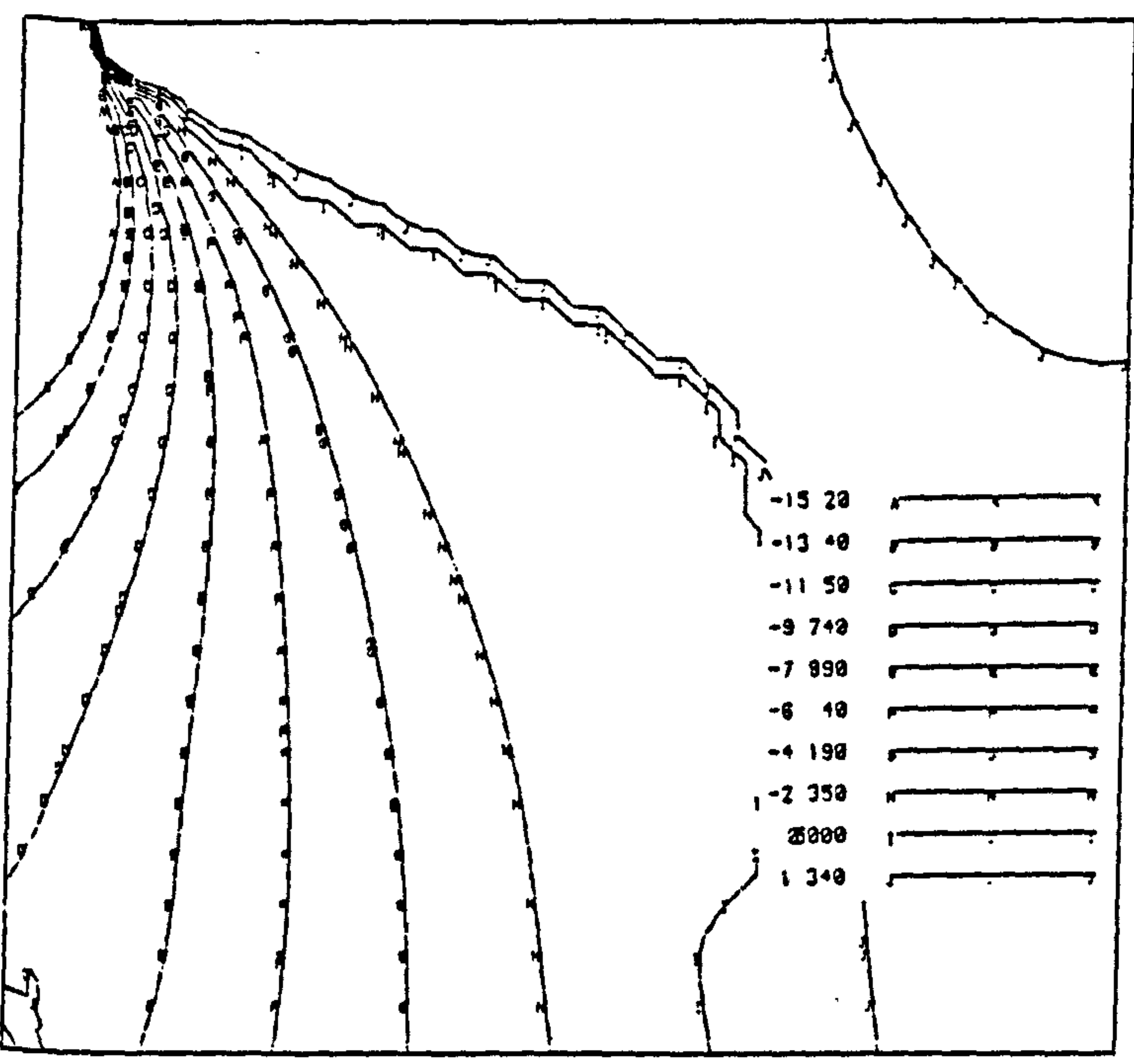
(a) - Finite element Mesh.



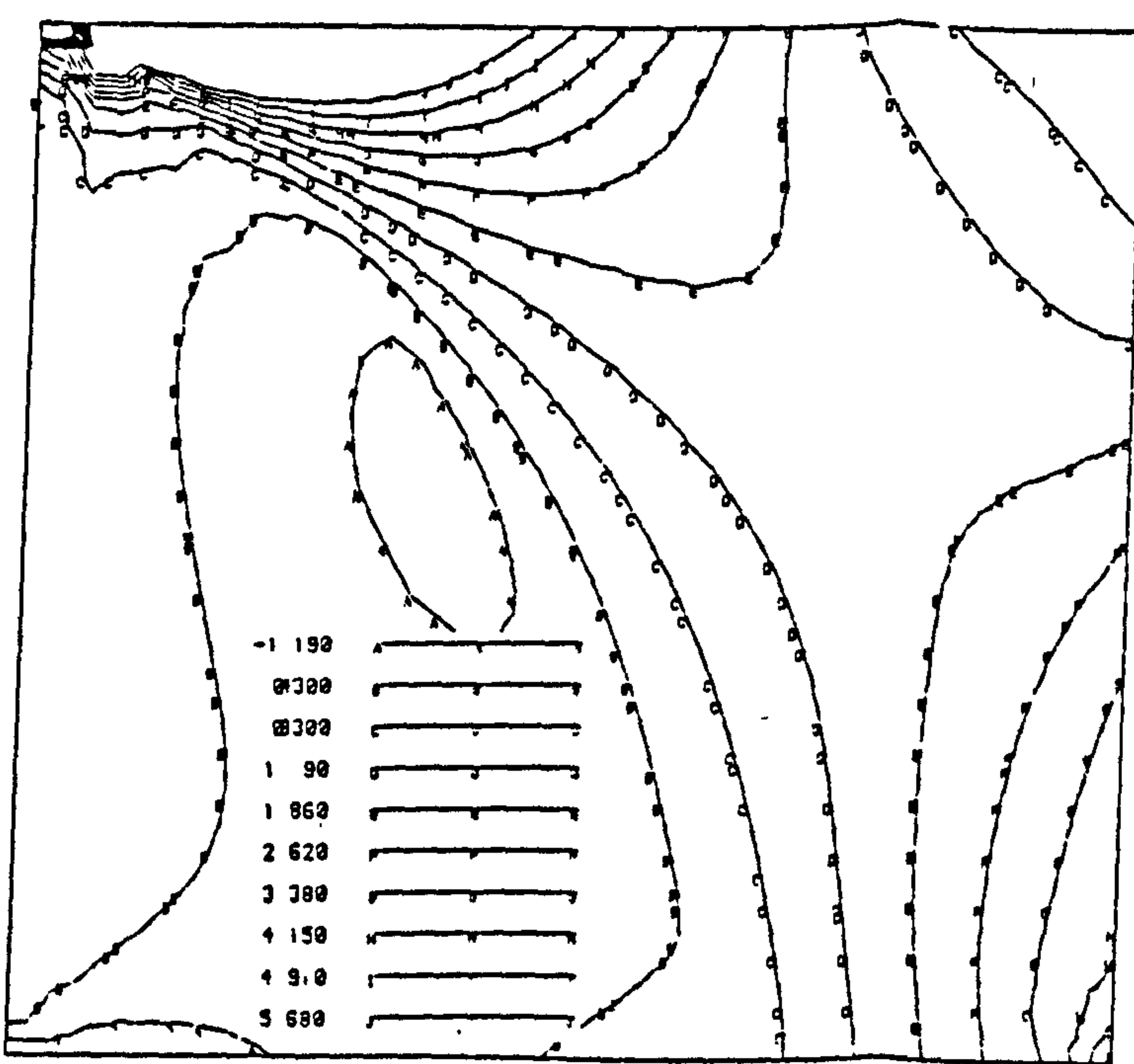
(b) - Displaced shape.



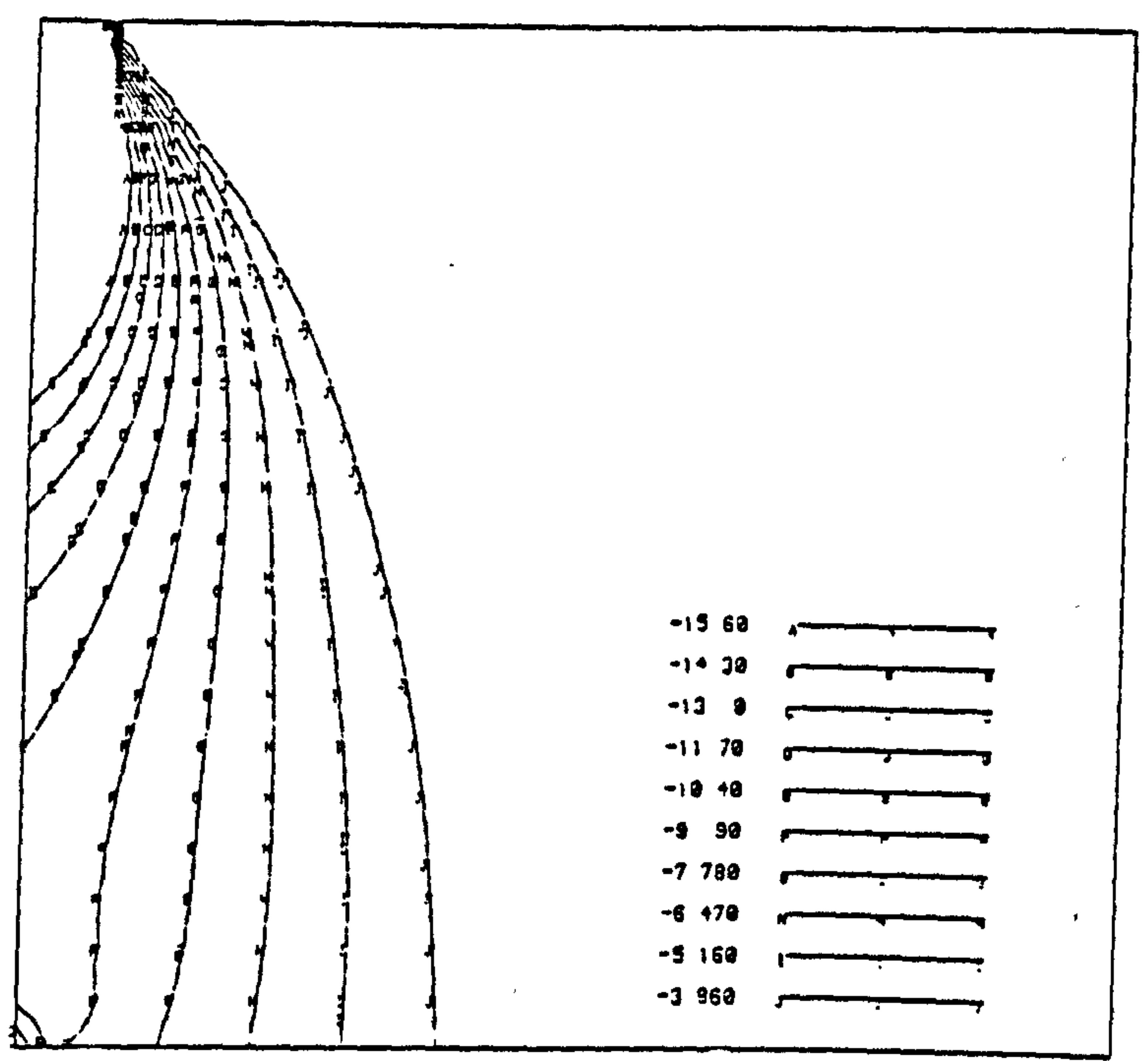
(c) - In-plane stress vectors.



(d) - Largest absolute principal stress contours.



(e) - Maximum principal stress contours.



(f) - Minimum principal stress contours.

Fig. 7.7 - Linear homogeneous finite element analysis of brickwork under eccentric concentrated load ( $A_r=0.05$ ).

## Chapter 8

### FAILURE MECHANISM, ENVELOPE AND DESIGN RECOMMENDATION

#### 8.1. FAILURE MECHANISM OF MASONRY UNDER CONCENTRATED LOAD

Brickwork masonry fails under a uniformly distributed compressive load by vertical splitting due to the development of lateral tension. Failure mechanism based on stack-bonded prisms (see Fig. 8.1(a)) has been derived by various researchers<sup>[13,25,26,31,47-49,103]</sup> and suggests that failure is by vertical splitting due to horizontal tension induced in the bricks. The state of stress in a brick within the prism under uniform vertical load is a combination of axial compression and bi-lateral tension (see Fig. 8.1(b)). Bi-lateral tension is the result of the differential strain between mortar and the brick. The mortar is consequently in a state of tri-axial compression (see Fig. 8.1(c)). The lateral tension produced which is sometimes referred to as '*bursting stress*', will eventually cause failure in the brittle brick: Based on this theory, failure envelopes have been derived theoretically and experimentally and are well documented elsewhere<sup>[4]</sup>.

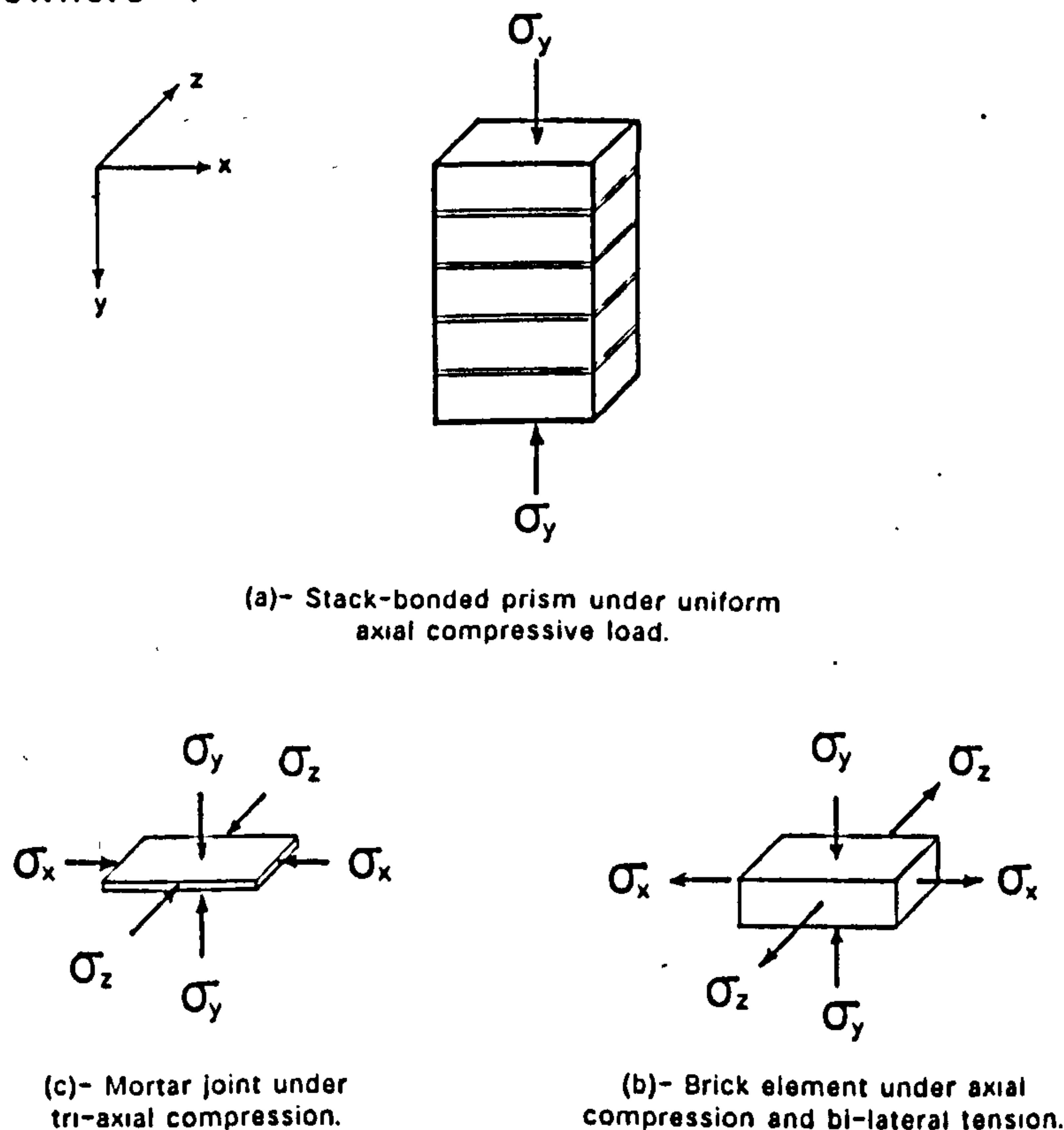
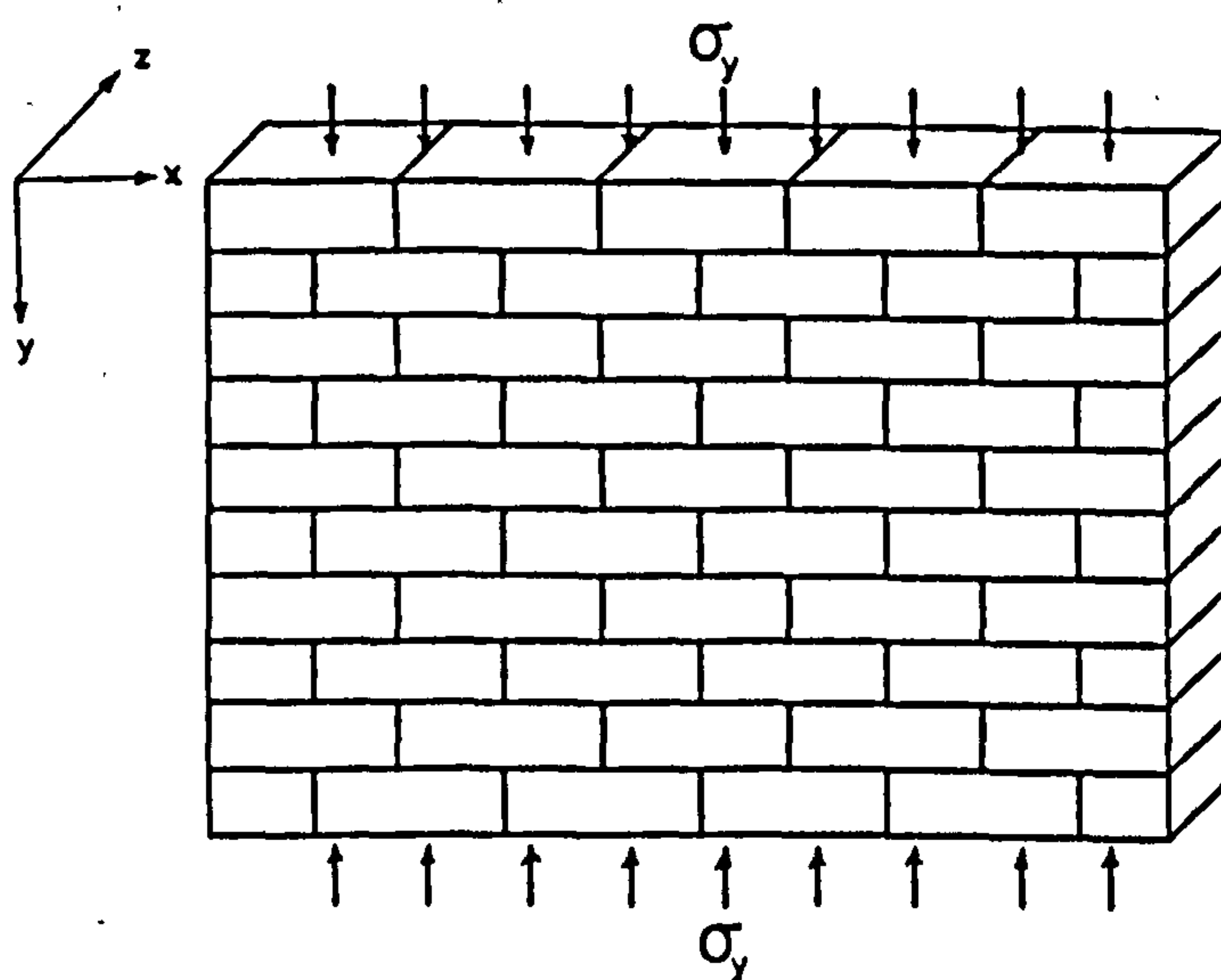


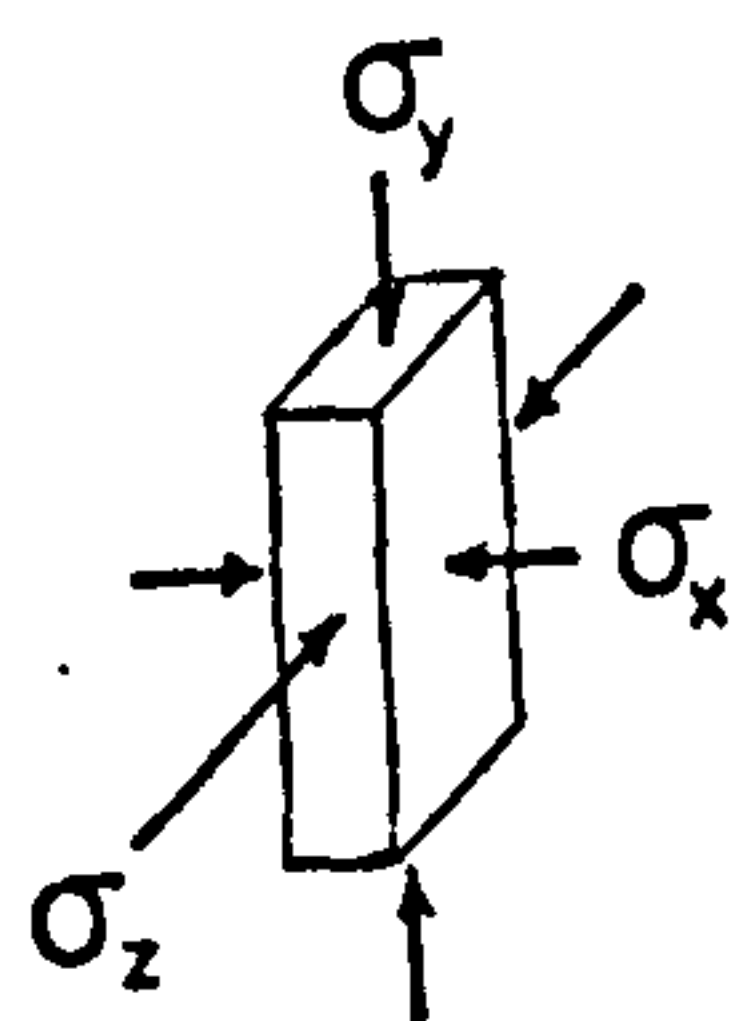
Fig. 8.1 - State of stress in a brick and mortar joint within a stack bonded brickwork prism under uniform axial compressive load.

However, for a brickwork panel (as shown in Fig. 8.2(a)), the above explanation is not sufficient since it ignores the presence of the perpendicular joints. In the

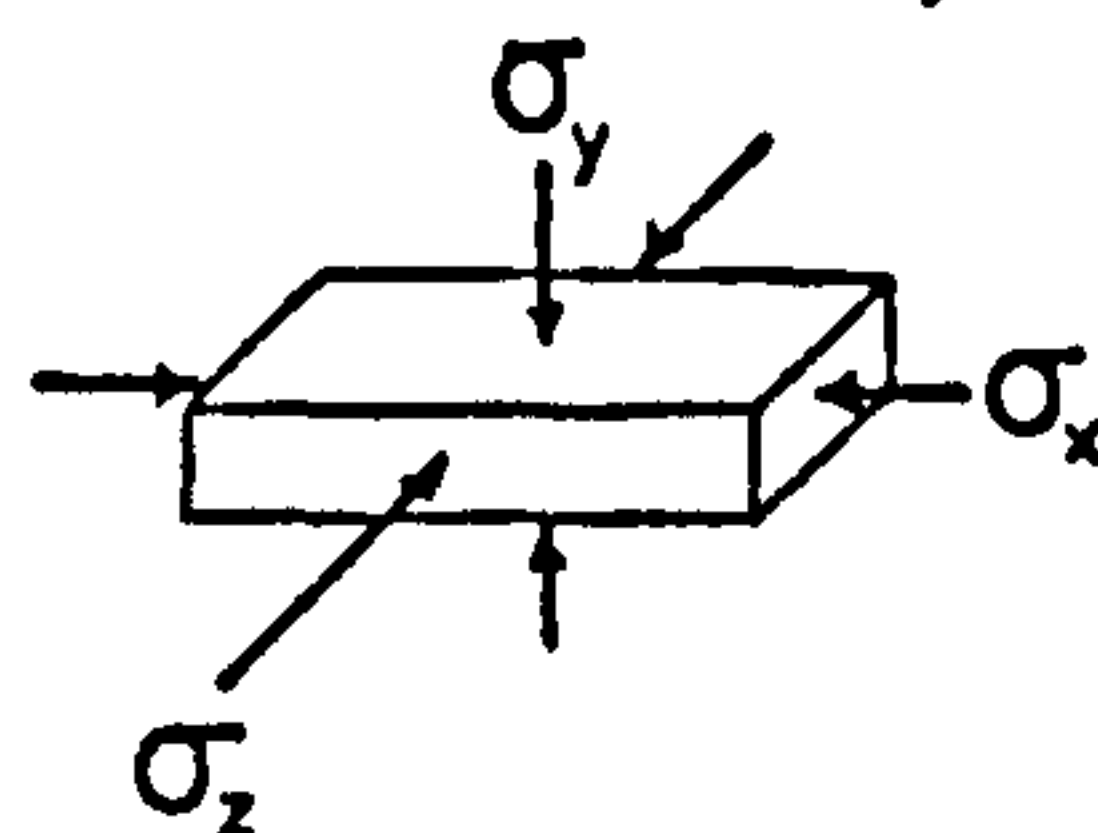
previous chapter the analytical study revealed that perpends exhibit lateral compressive or tensile stresses (Figs. 7.3(c) & 8.2(b) & (e)) which were greater than the stress in the bed joints. The transverse tensile stress set up within the brickwork would cause tensile bond failure between the perpend and the adjacent brick/s. Meantime, the bed joints above and below the perpend are in a state of triaxial compression (Fig. 8.2(c)) and the bricks in a state of axial compression and bi-lateral tension (Fig. 8.2(d)). Since the tensile bond strength of brickwork is small in relation to the tri-axial compressive strength of mortar and lateral tensile strength of brick, a crack is formed in the perpend. As the load increases the crack propagates up and down and when the transverse tensile stress reaches the tensile strength of the bricks the crack would pass through the joints and bricks which eventually cause failure in the brickwork.



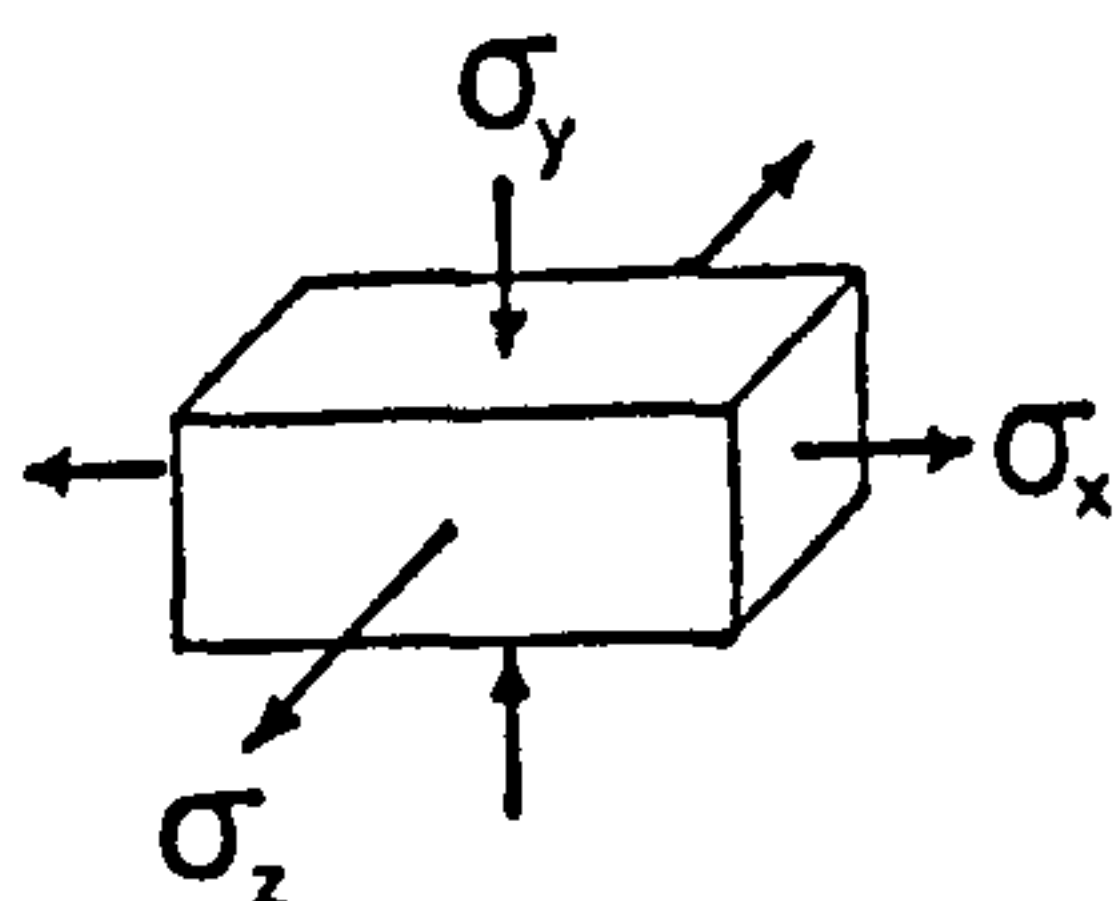
(a)- Brickwork panel under uniform axial compressive load.



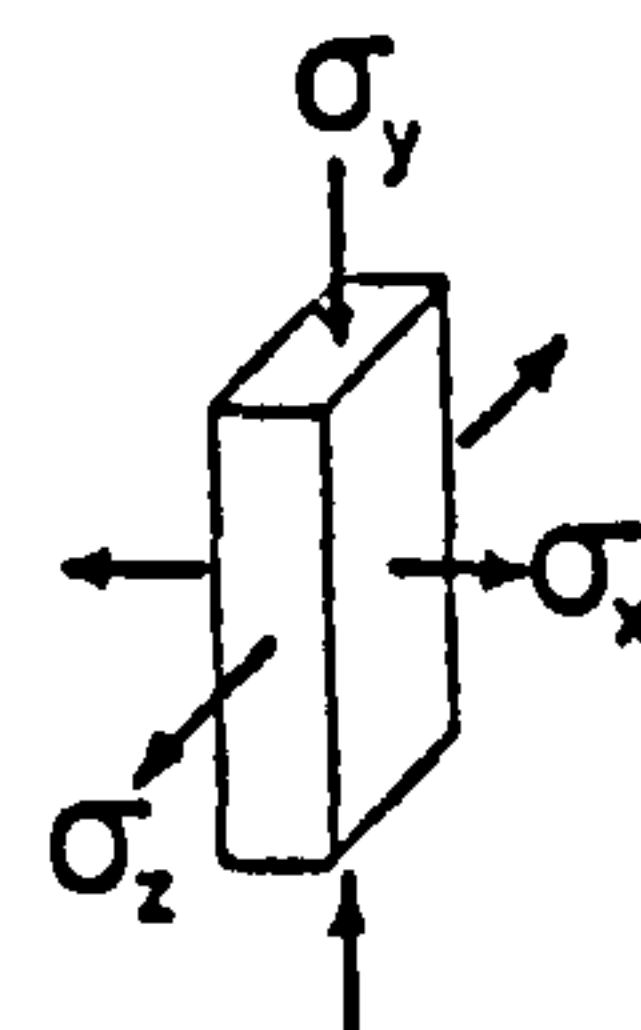
(b)- Perpend joint under tri-axial compression near the ends of the panel.



(c)- Mortar bed joint under tri-axial compression.



(d)- Brick unit under axial compression and bi-lateral tension.

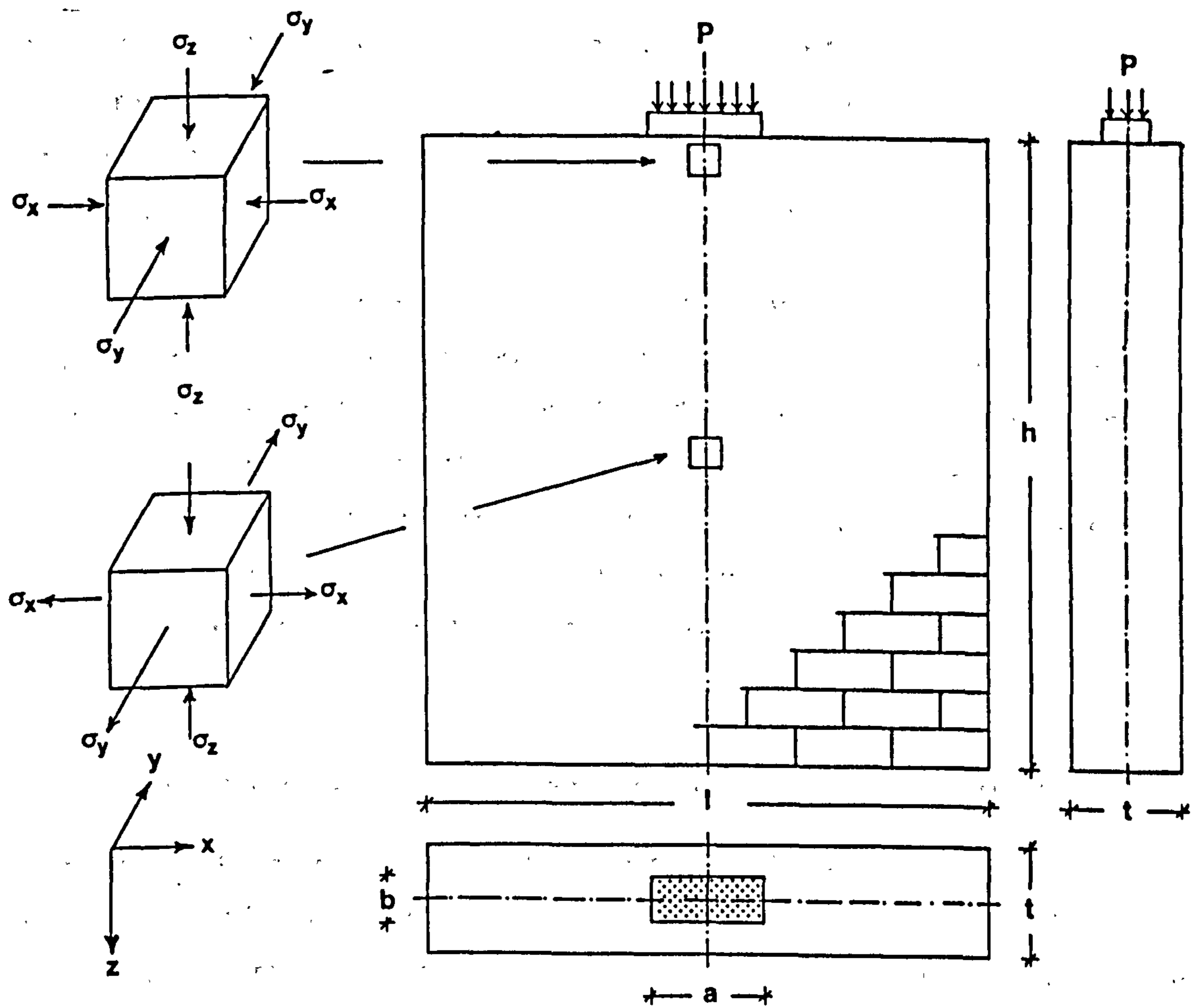


(e)- Perpend joint under axial compression and bi-lateral tension within the panel.

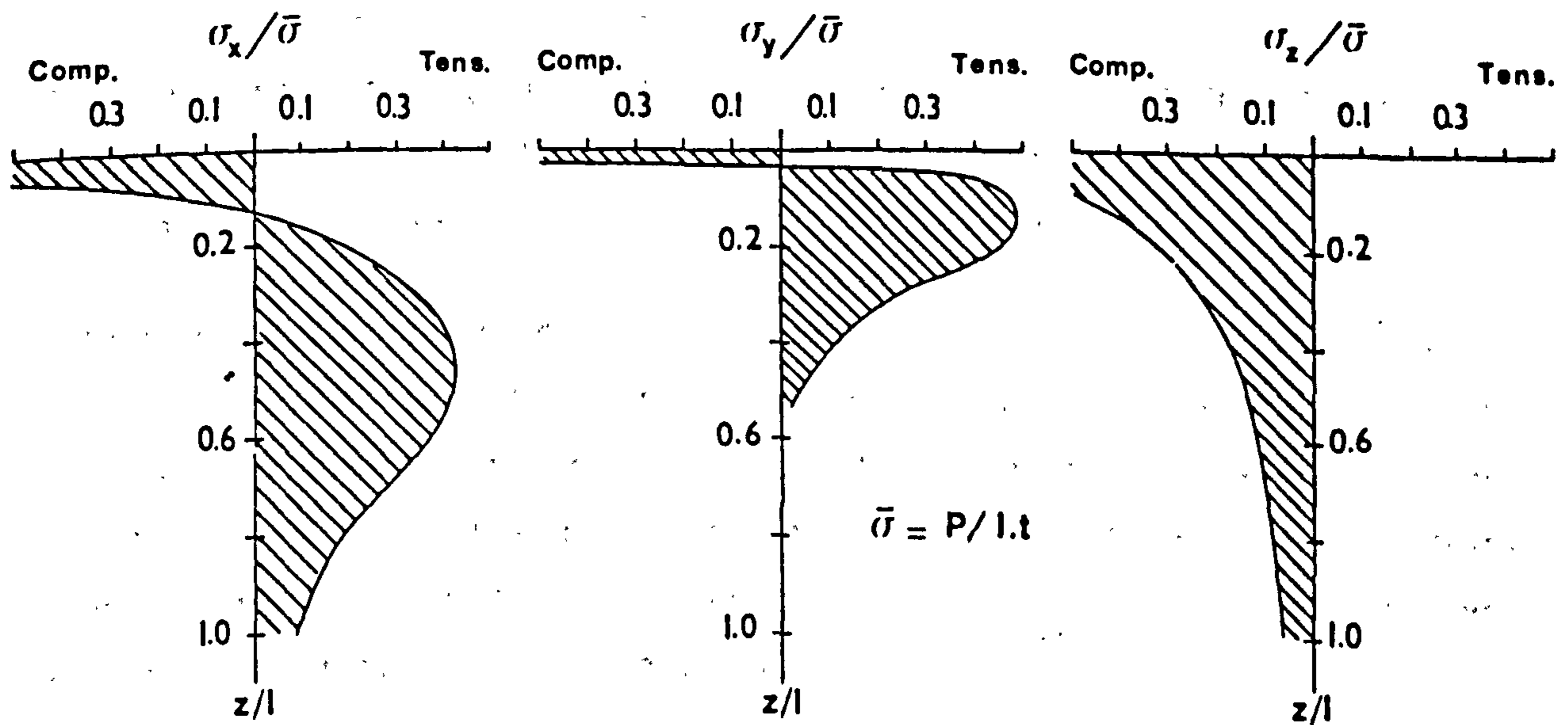
Fig. 8.2 - State of stress in a brick, mortar bed joint and perpend within a brickwork panel under uniform axial compressive load.

Considering a brickwork specimen (Fig. 8.3(a)) partially loaded concentrically at its centroid, an element immediately under the applied load is in a state of tri-axial compression. The effective compressive strength of brickwork within the local bearing area is increased, hence the enhancement of the bearing stress at failure. Further down the centre line of the specimen, as the concentrated load disperses, the state of stress in an element is one of axial compression ( $\sigma_z$ ) and bi-lateral tension ( $\sigma_x$  and  $\sigma_y$ ), as indicated in Fig. 8.3(b). When the transverse tensile stress in the perpendicular joint reaches the tensile bond strength and/or the transverse tensile stress is greater than the tensile strength of the brick in this stress condition, a vertical crack appears. The crack is usually observed near the region where the horizontal tensile stress ( $\sigma_x$ ) is a maximum. With load increasing, the crack develops up and down the height of the specimen. Meanwhile, other vertical and diagonal cracks appear and the state of stress in the brick masonry will change. Thus the tri-axial stress may become uniaxial stress along a strip between the vertical cracks. In some cases the local compressive stress may reach the compressive strength of the unit, and the specimen will be crushed.

In general, the mode of failure under concentrated load applied through a rigid bearing plate is governed by three parameters. These are the loaded area ratio, the position of load and the strength characteristics of units. The appearance of the primary crack in relation to failure of the specimen depends on the loaded area ratio,  $A_r$ . For small values of loaded area ratio ( $A_r \leq 0.20$ ) the vertical crack appears suddenly followed sometimes by diagonal cracks under the edges of bearing plate and sometimes accompanied by spalling of brickwork shortly before failure. In this case the failure is caused by a vertical tensile crack, splitting the specimen into two halves. As the loaded area increases ( $A_r \geq 0.20$ ), the ratio of cracking load to ultimate load at failure ( $F_r = F_c / F_u$ ) decreases, resulting in progressive failure. Conversely, as  $A_r$  decreases,  $F_r$  increases. In this case failure is gradual and is caused by the development of vertical cracks followed by diagonal cracks under the edges of bearing accompanied sometimes by spalling and local failure within the bearing zone. This has been shown in Figs. 6.91-99 for various loaded area ratios for the central strip loading configuration. It is worth noting that for higher loaded area ratios (i.e.  $A_r \geq 0.30$ ) sometimes vertical cracks have been observed under the edges of the bearing plate. It is believed that these vertical cracks are caused by the shear bond failure in the perpendicular under the edges of the loading plate.



(a)



(b)

Fig. 8.3 - State of stress in an element and stress distributions on the centre line of brickwork masonry subjected to concentrated load.

The effect of the load position on the mode of failure is not so different for intermediate loading position in contrast to the central loading position. However, for the end loading position, vertical and diagonal cracks form under

the edge of the bearing sometimes running down the whole height of the specimen. In this case the failure is due to the development of the vertical and/or diagonal crack/s under the inner edge of the plate sometimes accompanied by local failure within the bearing zone (see Figs. 6.105-109).

The influence of low strength units (as in the case of AAC units) on the failure under central strip load is seen as the formation of a wedge or a cone, immediately under the loaded face (see Fig. 6.110) which moves downwards, splitting the specimen apart (see Fig. 6.98(b) & (c)). As the loaded area ratio decreases ( $A_r=0.05$ ) the failure is of the form of local crushing of the unit (see Figs. 6.98(a), 6.99(a) & 6.103(a)). As the position of the loading becomes eccentric diagonal crack/s dominate the mode of failure (see Figs. 6.103, 6.104, 6.108 and 6.109).

## 8.2. FAILURE ENVELOPE FOR MASONRY UNDER CONCENTRATED LOAD

The analyses of results reported in chapter 6 have shown that the major parameters influencing the bearing strength of brickwork masonry are the constituents strength characteristics which are incorporated into characteristic compressive strength of masonry  $f_k$ ; the loaded area ratio  $A_r$  and the position of the loading (i.e. the effect of edge distance) for a given element thickness. Already design charts for the characteristic compressive bearing strength of brickwork masonry,  $f'_{cb}$ , in terms of unit brick strength  $f_b$  for mortar grade M(l), element thickness  $t=102.5\text{mm}$  and loaded area ratios of 0.1, 0.2, 0.3 and 0.4 have been derived and presented in Table 6.2 and Fig. 6.34.

However, an attempt is made in this section to derive failure envelopes for masonry 102.5mm and 215.0mm in thickness on a non-dimensional scale for enhancement factor (as a ratio of  $f_{cb}$  and  $f_k$ ) in terms of loaded area ratio ( $A_r=A_{cb}/A$ ) and ratio of edge distance to the total length,  $d/l$  (i.e. for central loading position  $d/l=0.50$ , intermediate loading position  $d/l=0.25$  and end loading position  $d/l$  is approximately zero).

All the results reported in this thesis have been sorted according to the specimen thickness and loading positions. The ratio  $\zeta=f_{cb}/f_k$  have been plotted against loaded area ratio  $A_r$ . As before the best fit to the data points representing the mean curve and hence the 95% lower confidence limits have been determined. The results obtained are shown in Table 8.1 and graphically in Figs. 8.4 and 8.5 for central, intermediate and end loading positions for 102.5mm and 215.0mm masonry thicknesses respectively. Figs. 8.6 and 8.7

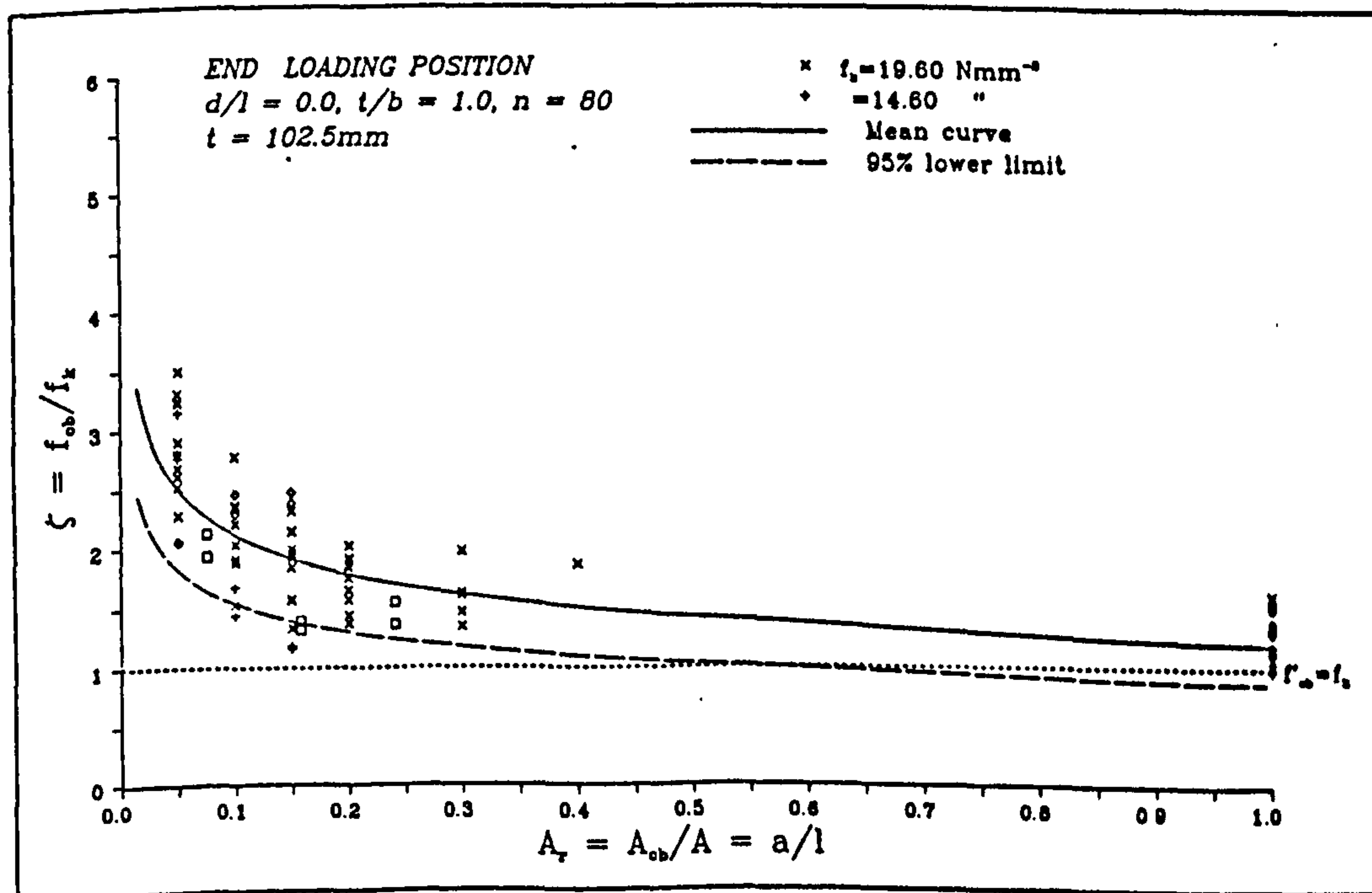
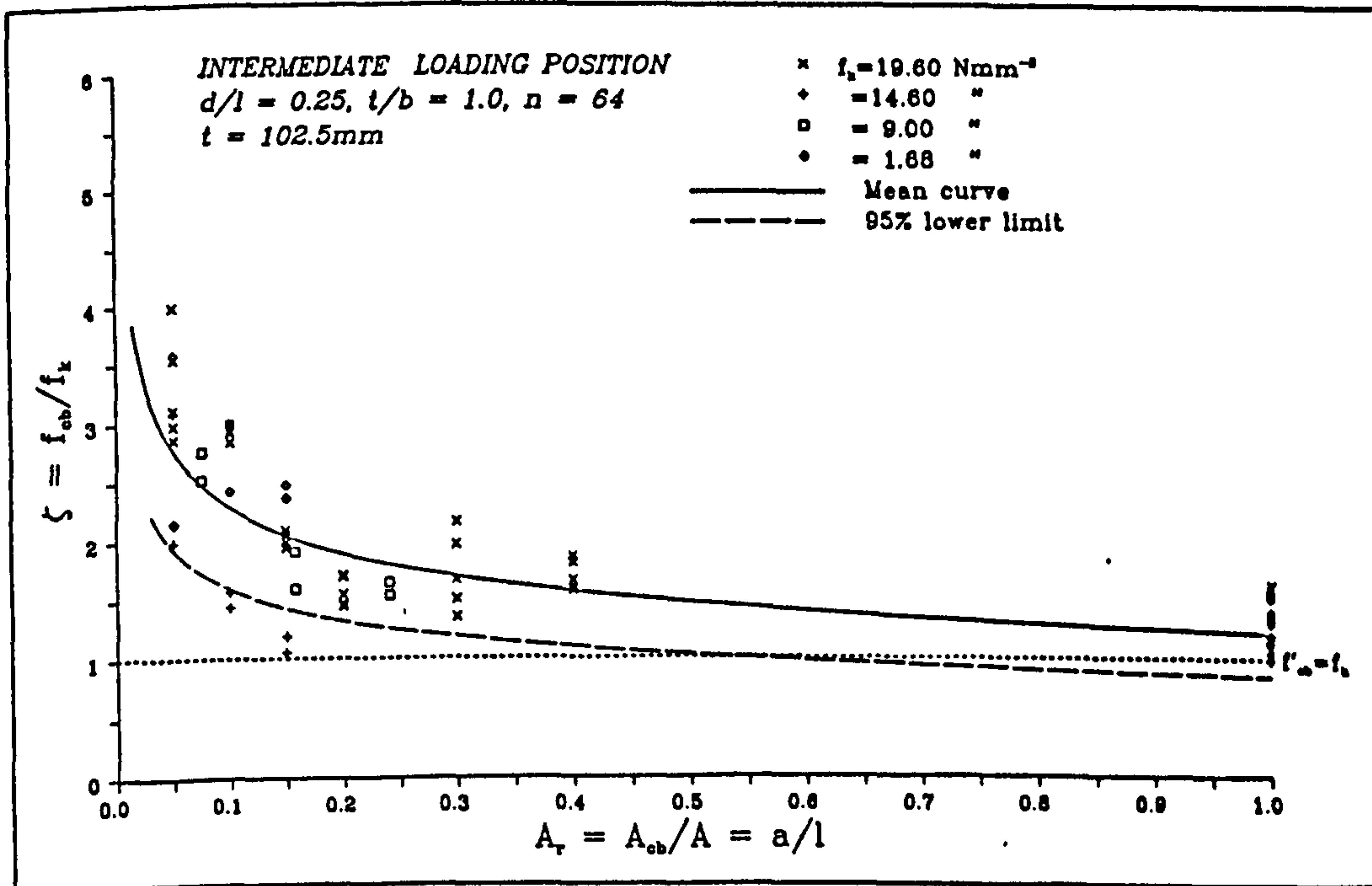
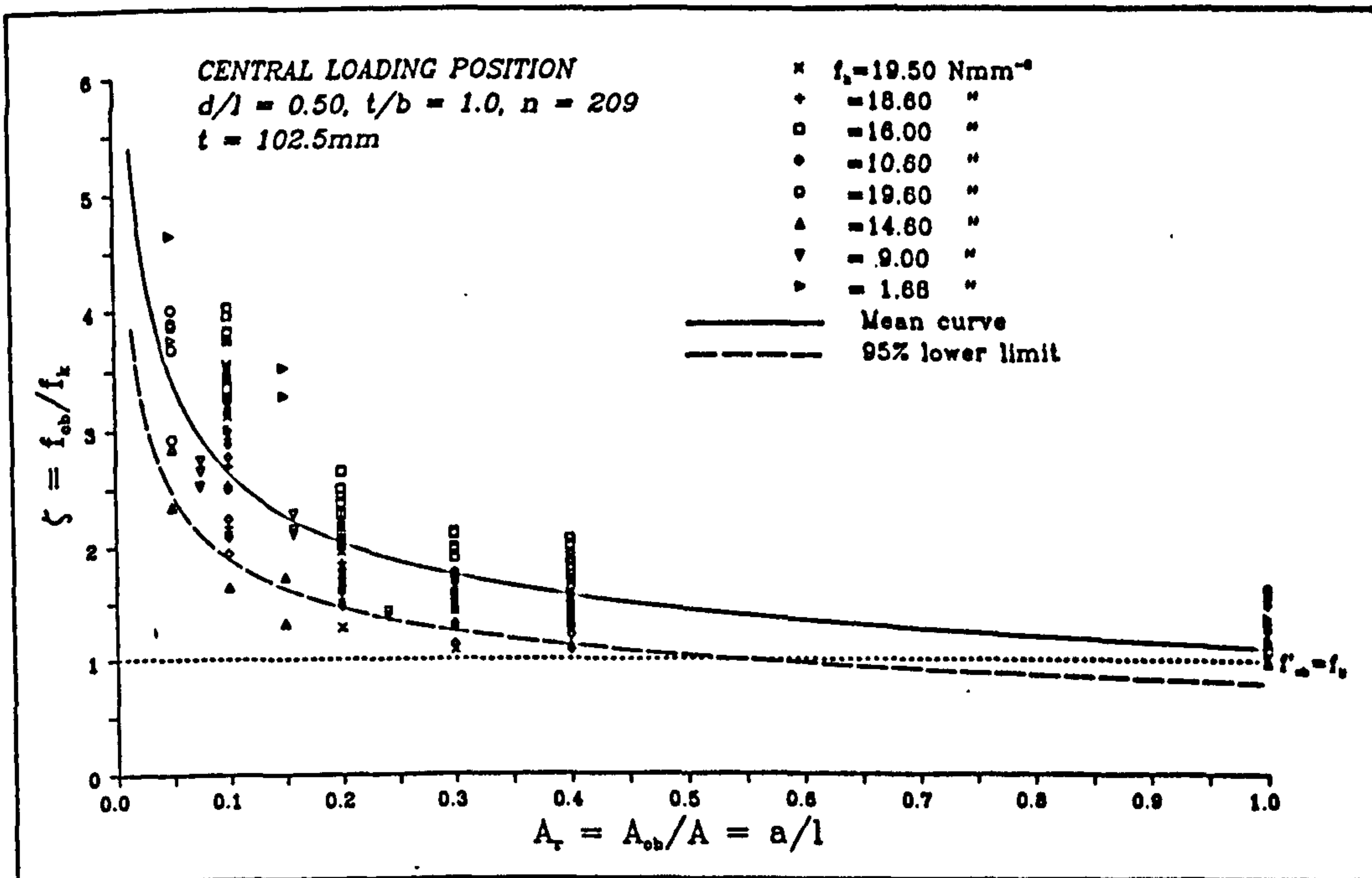


Fig. 8.4 - Mean and characteristic curves for enhancement factor of 102.5mm thick masonry as a function of loaded area ratio for central, intermediate and end loading positions respectively.

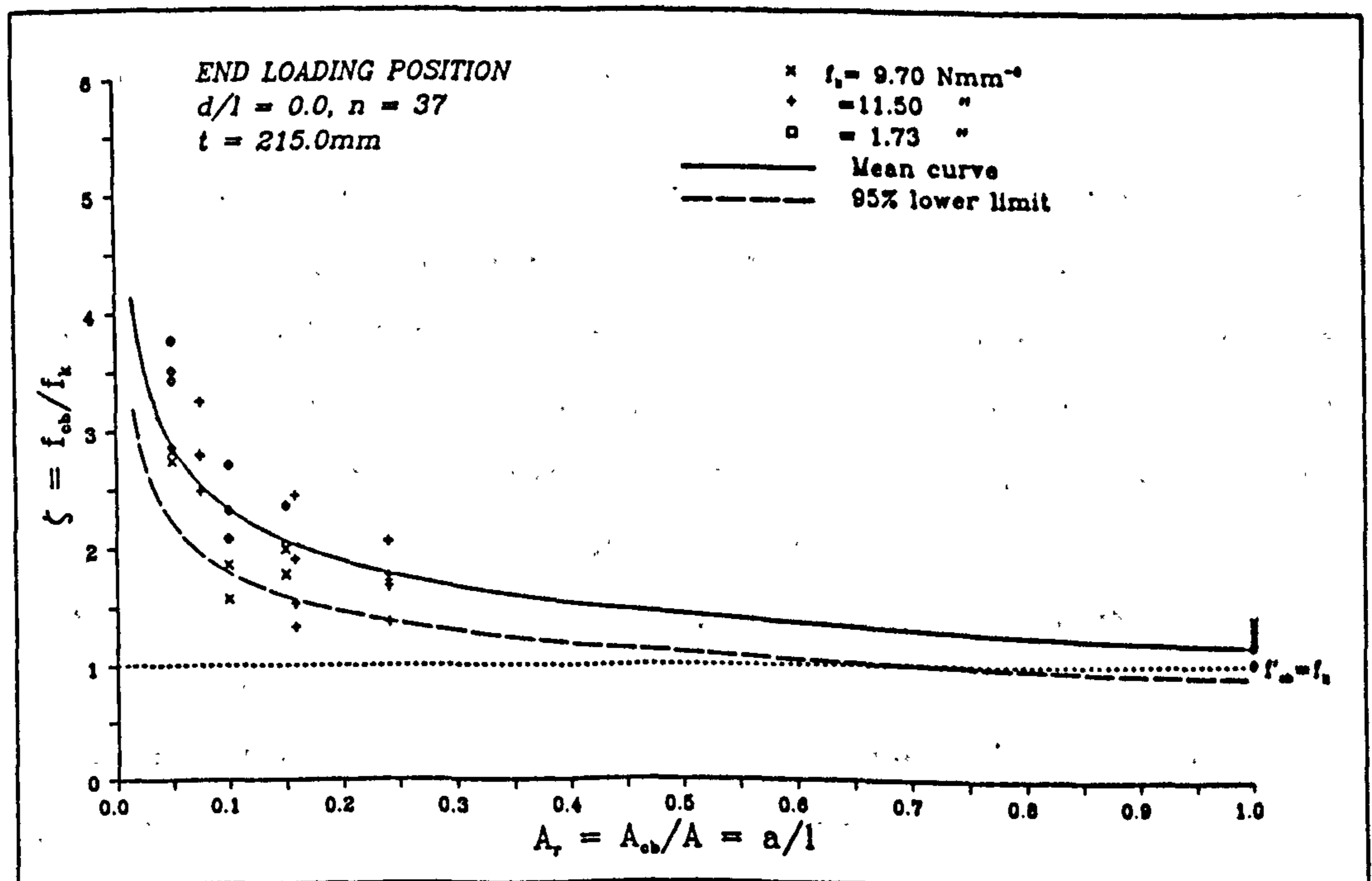
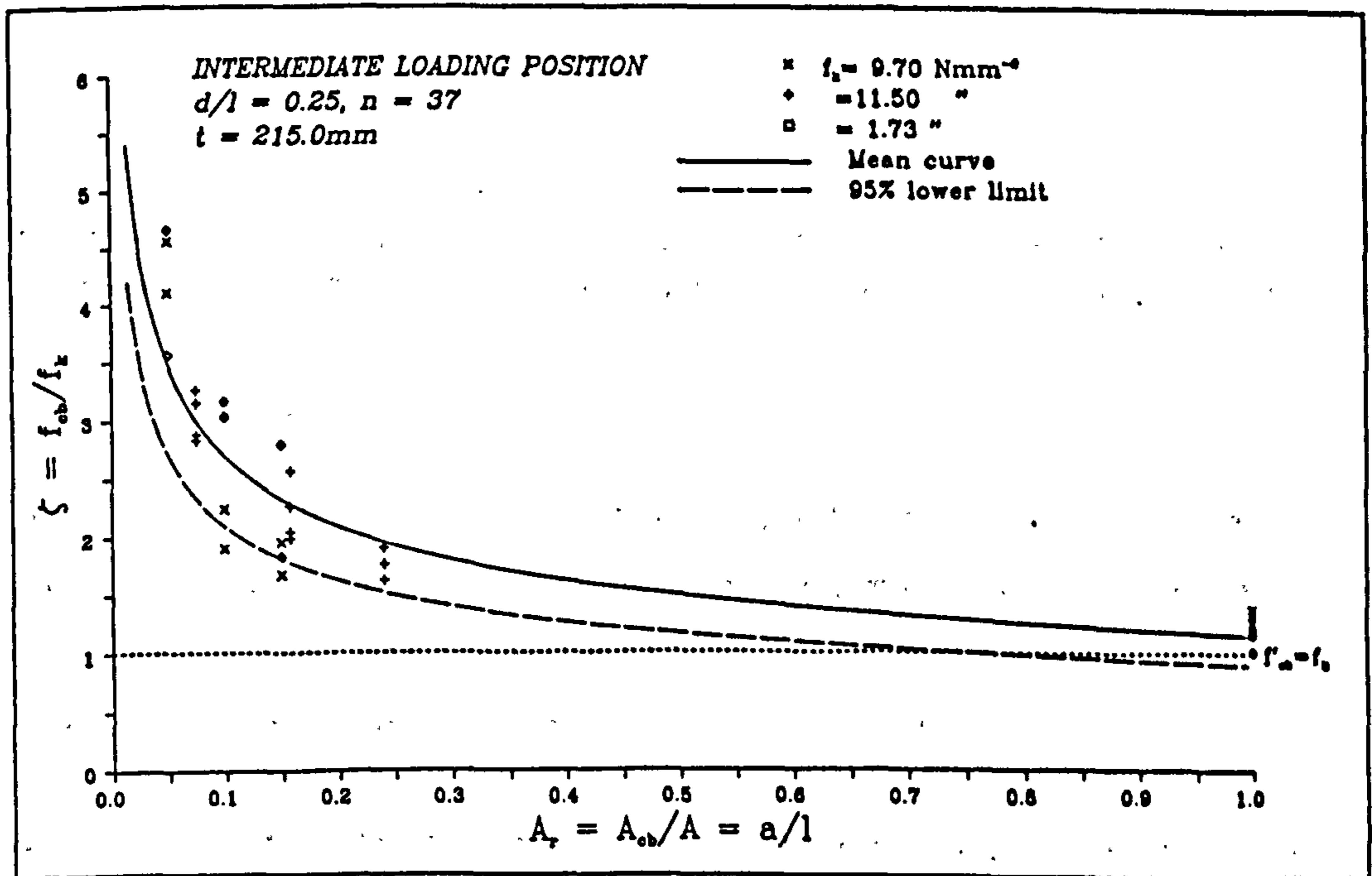
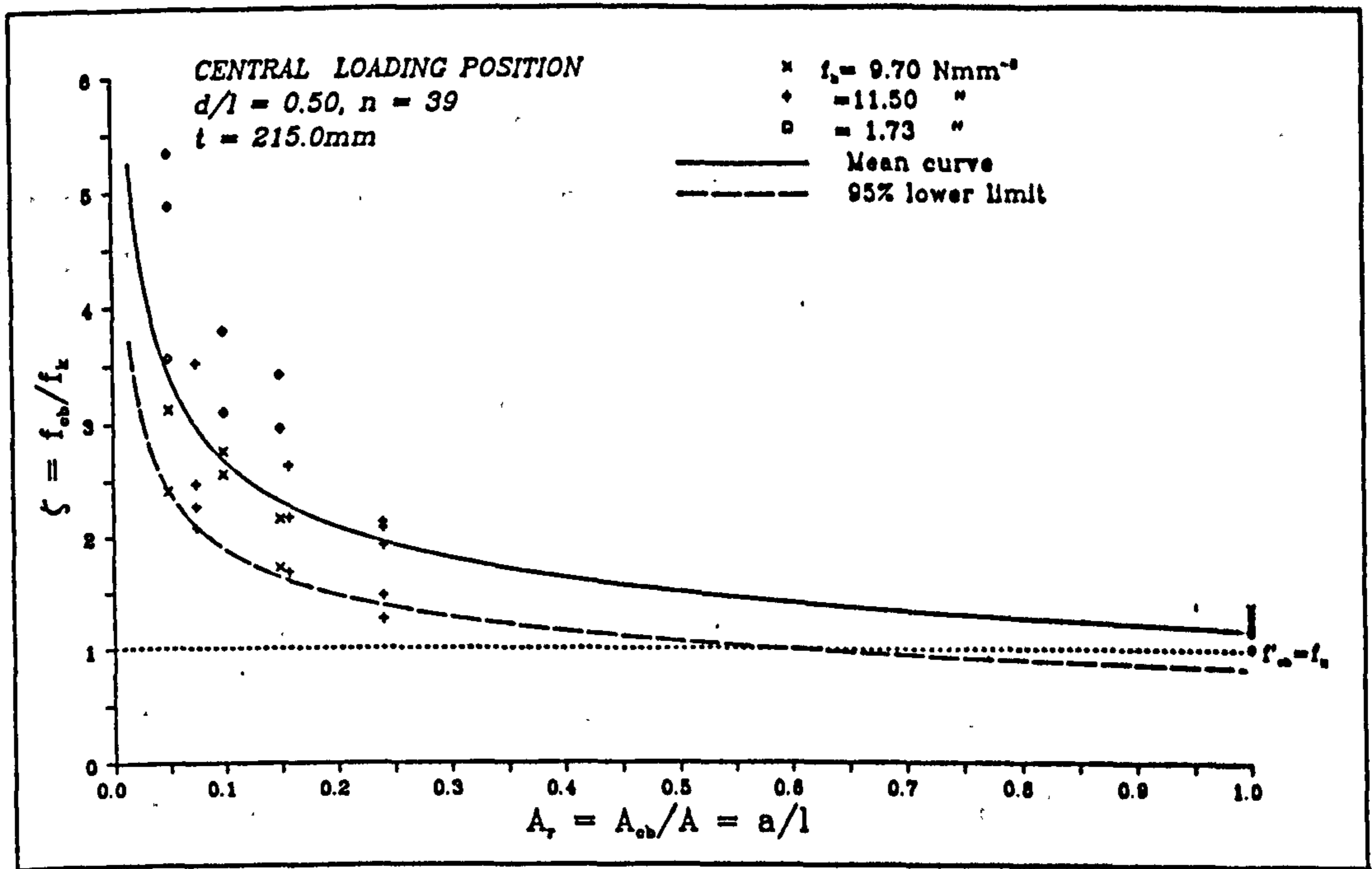


Fig. 8.5 - Mean and characteristic curves for enhancement factor of 215.0mm thick masonry as a function of loaded area ratio for central, intermediate and end loading positions respectively.



represent the three dimensional failure envelopes for brickwork masonry 102.5mm and 215.0mm in thickness. The curves are the 95% lower confidence limit, (for  $A_r < 1.0$ ).

t (mm)	Loading position	Mean curve equation	95% lower limit equation	n
102.5	Central	$\zeta = 1.107A_r^{-0.377}$	$\zeta' = 0.792A_r^{-0.377}$	209
	Intermediate	$\zeta = 1.212A_r^{-0.275}$	$\zeta' = 0.845A_r^{-0.275}$	64
	End	$\zeta = 1.195A_r^{-0.247}$	$\zeta' = 0.869A_r^{-0.247}$	80
215.0	Central	$\zeta = 1.174A_r^{-0.357}$	$\zeta' = 0.829A_r^{-0.357}$	39
	Intermediate	$\zeta = 1.156A_r^{-0.367}$	$\zeta' = 0.898A_r^{-0.367}$	37
	End	$\zeta = 1.159A_r^{-0.303}$	$\zeta' = 0.893A_r^{-0.303}$	42

Table 8.1 - Equations of the mean and 95% lower confidence limit curves for failure envelopes under various loading position and masonry thickness.

### 8.3. DESIGN RECOMMENDATION

Current design guides for predicting the capacity of brickwork masonry subjected to concentrated load are at best approximate and, depending on their country of origin, they vary considerably. A complete review of provisions adopted by various codes of practice has been covered in section 3.3.

To formulate a realistic design guide it is essential to consider major parameters which have an effect on the bearing strength of brickwork masonry and in doing so produce an easy and reliable formula.

The idea is to obtain an expression for the enhancement factor for brick masonry taking into account the primarily variables. These have found to be the bearing area, position of loading along the length of the element and the effective length contributing to the bearing strength. However, the former and the latter parameters could be presented as a single variable by "effective area ratio,  $A_{re}$ " which is the ratio of loaded area to the effective area contributing to the strength enhancement. Effective area,  $A_e$  is the product of the effective length,  $l_e$  and the effective thickness,  $t_e$ . It has already been shown that the effective thickness is the same as the thickness of the element or, in other words, the worst type of loading is one where the concentrated load is applied over the whole thickness (see Figs. 6.78, 6.79 and 6.90). Also it was shown

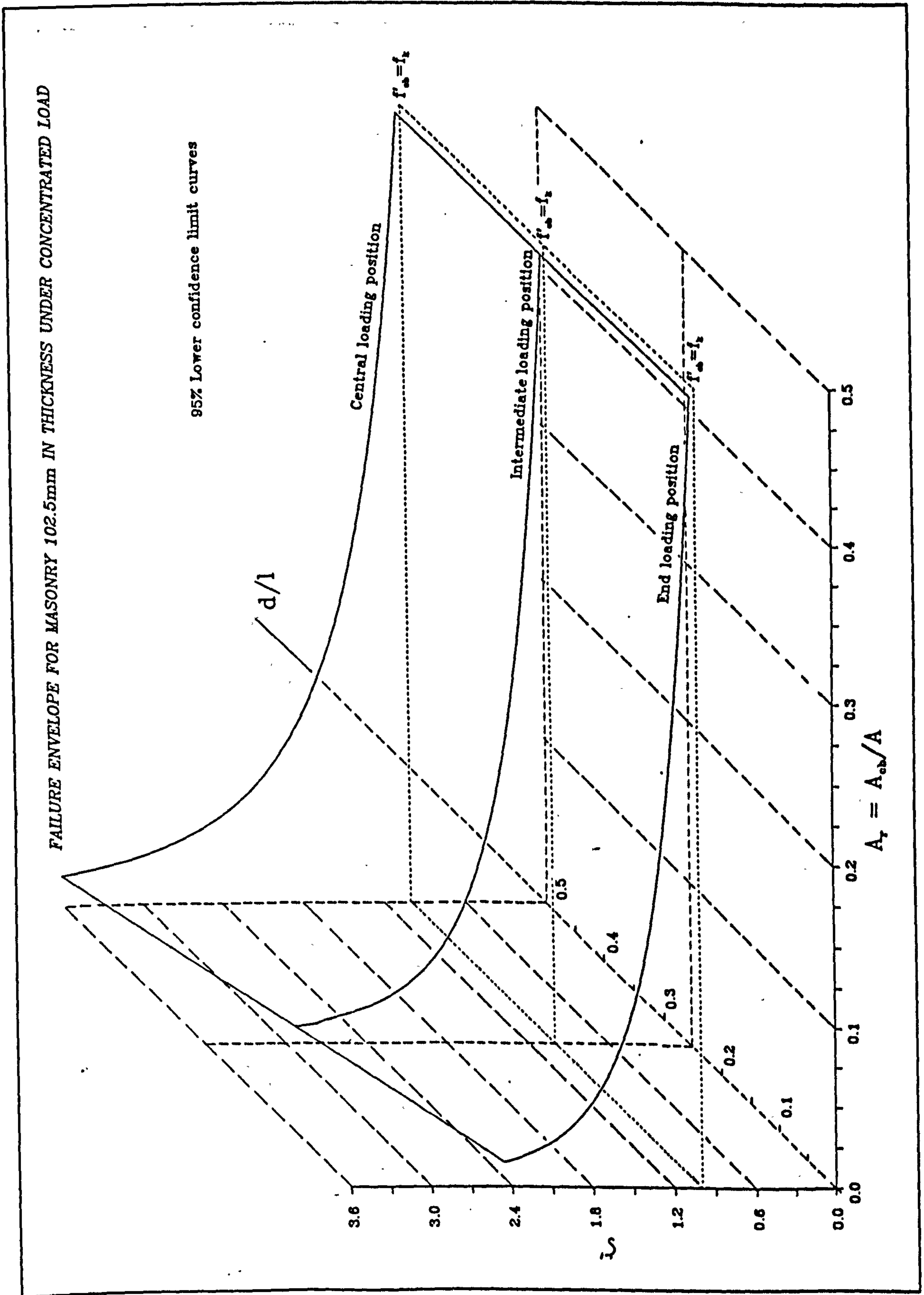


Fig. 8.6 - Failure envelope for brick masonry 102.5mm in thickness.

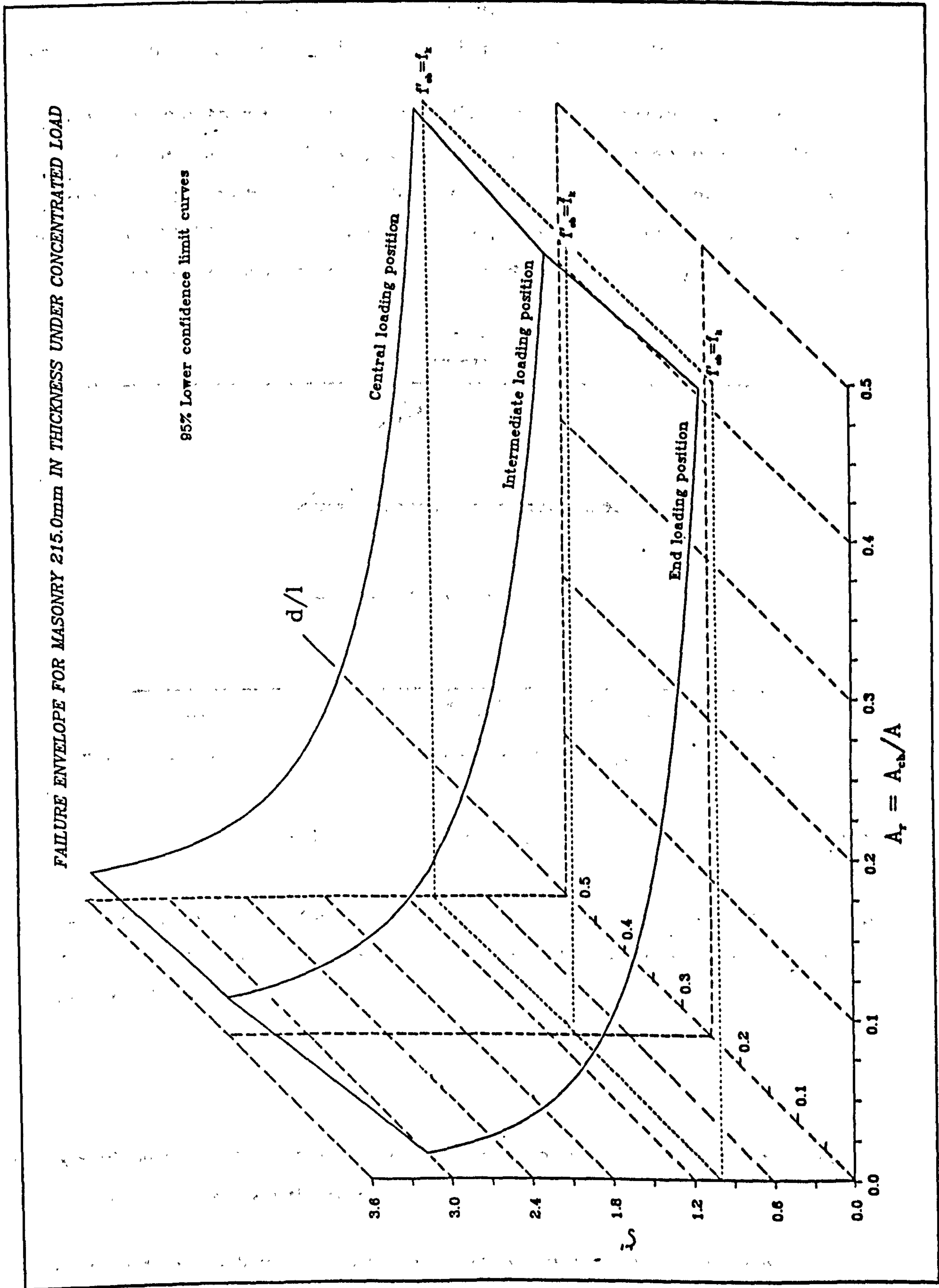


Fig. 8.7 - Failure envelope for brick masonry 215.0mm in thickness.

that the effective length is about three times the loading length,  $a$ , or six times the thickness of the specimen (see Figs. 6.88 and 6.89).

It is also possible to arrive at the effective length theoretically by assuming that the concentrated load disperses through brickwork at an angle of  $45^\circ$  and the stress at a height of  $0.4h$  below the bearing becomes uniform as postulated in BS 5628<sup>[1]</sup>. Hence the effective length at this level where the stress is assumed to be uniform (refer to Fig. 8.8) is shown by expression 8.1.

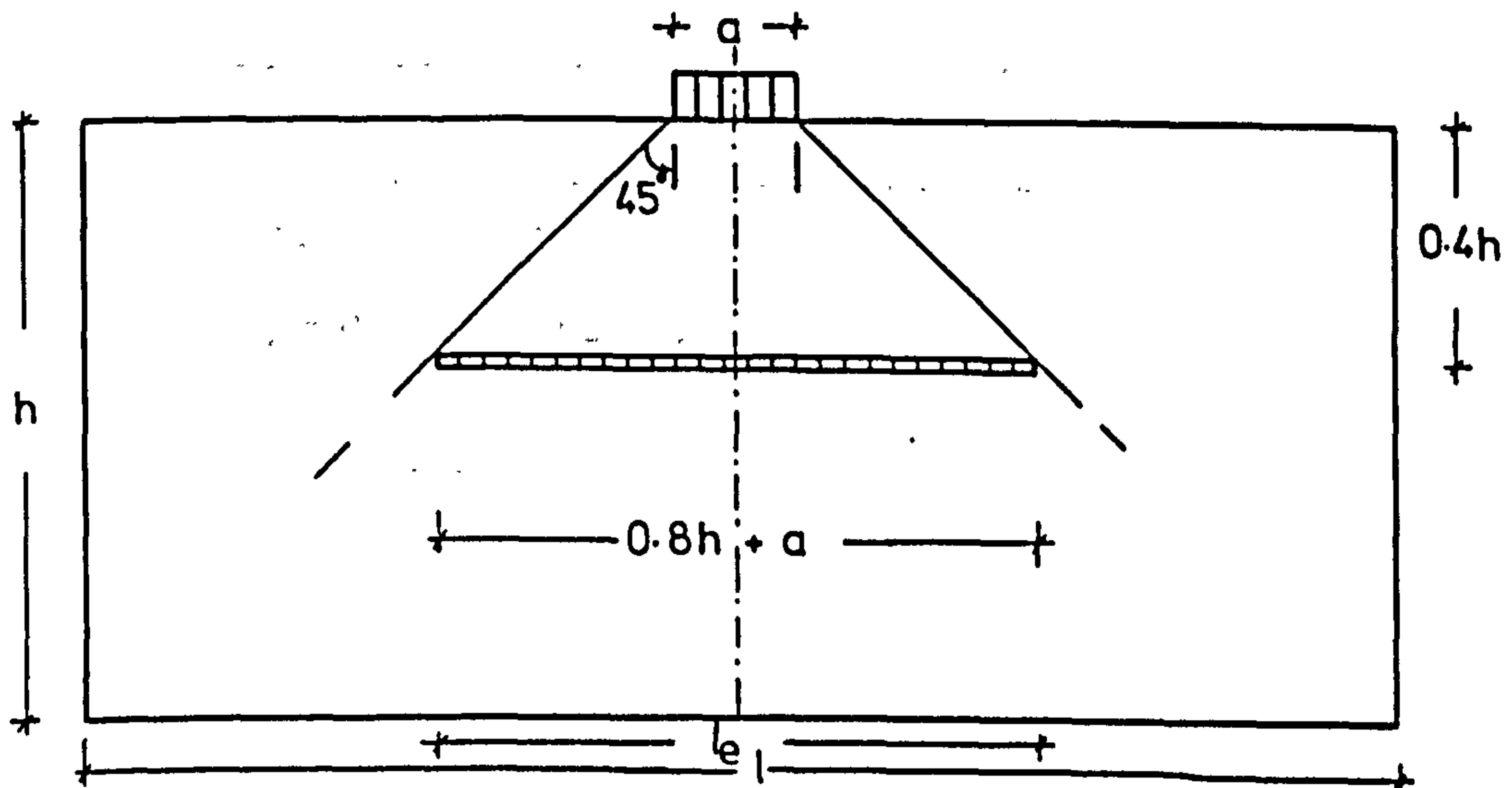


Fig. 8.8 - Dispersion of concentrated load in brickwork masonry.

$$l_e = 2 ( 0.4h ) + a = 0.8h + a \quad (8.1)$$

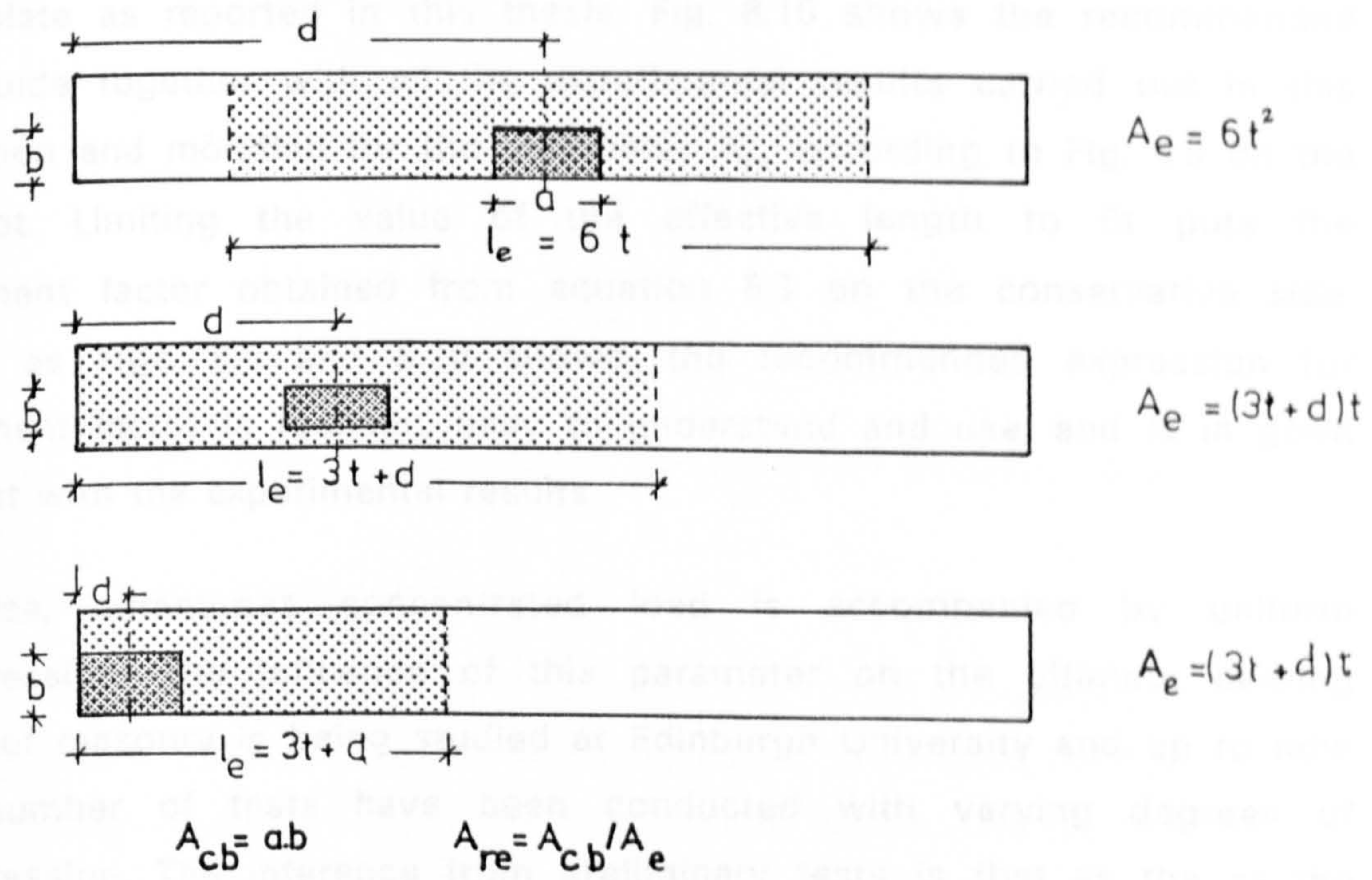
For masonry where the effect of slenderness is negligible, BS 5628<sup>[1]</sup> gives  $h/t=8.0$  for  $\beta=1.00$ . Hence expression 8.1 could be written in terms of the element's thickness such that;

$$l_e = 6.4t + a \quad (8.2)$$

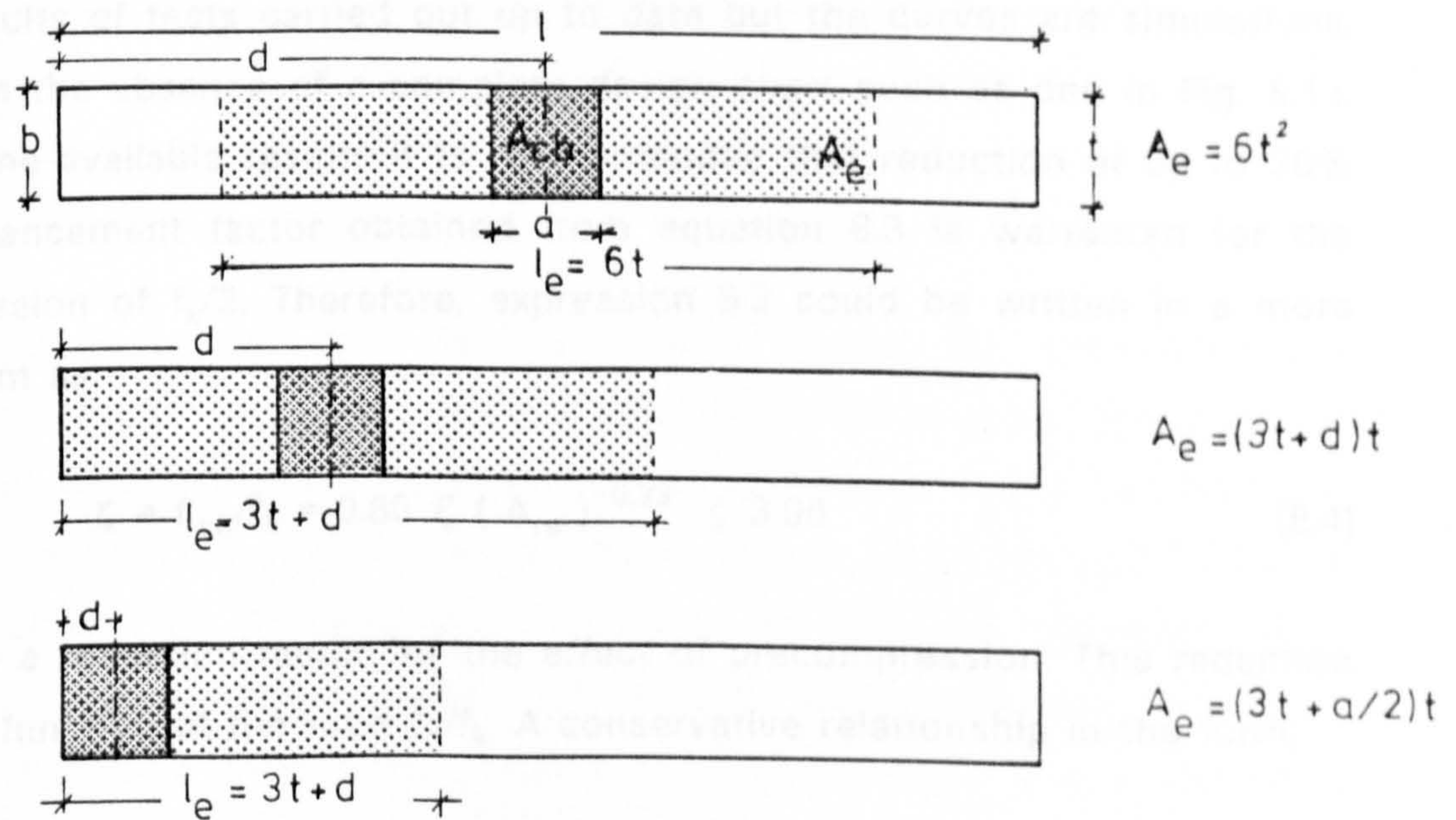
This would lend some support to the assumption of  $6t$  as the effective length although it has no known theoretical basis.

An expression in the form of equation 8.3 is recommended for determining the enhancement factor for masonry under rigid bearing where  $A_{re}=A_{cb}/A_e$  and  $A_e$  is calculated in accordance to the proposals shown in Fig. 8.9.

$$\zeta = 0.80 ( A_{re} )^{-0.33} \leq 3.00 \quad (8.3)$$



(a)- Strip loading configuration.



(b)- Edge and concentric loading configurations.

Fig. 8.9 - Effective area under bearing.

The above recommended design guide not only is a function of loaded area, but it also takes account of loading position in relation to the edge of the brickwork panel and the effective length. It is based on the experimental results for concentrated loads on masonry panels applied through a rigid

bearing plate as reported in this thesis. Fig. 8.10 shows the recommended design guide together with all the experimental results carried out in this investigation and modified for the parameter  $A_{re}$  according to Fig. 8.9 on the same plot. Limiting the value of the effective length to  $6t$  puts the enhancement factor obtained from equation 8.3 on the conservative side. However, as Figs. 8.9 and 8.10 shows, the recommended expression for enhancement factor is realistic, easy to understand and use, and is in good agreement with the experimental results.

In practice, sometimes concentrated load is accompanied by uniform precompression. The influence of this parameter on the ultimate bearing strength of masonry is being studied at Edinburgh University and up to now limited number of tests have been conducted with varying degrees of precompression. The inference from preliminary tests is that as the precompression increases, the ultimate bearing strength under concentrated load decreases, hence decrease in the enhancement factor. The aim is to achieve a sufficient number of test results so that a design chart similar to that shown in Fig. 8.11 could be produced. The data points shown in Fig. 8.11 are the results of tests carried out up to date but the curves are simulations. However, in the absence of a complete design chart such as one in Fig. 8.11, based on the available results it is recommended that reduction of up to 30% in the enhancement factor obtained from equation 8.3 is warranted for the precompression of  $f_c/2$ . Therefore, expression 8.3 could be written in a more general form as:

$$\zeta = f'_{cb}/f_k = 0.80 \xi (A_{re})^{-0.33} \leq 3.00 \quad (8.4)$$

where  $\xi$  is a reduction factor for the effect of precompression. This reduction factor is a function of the ratio  $f_c/f_k$ . A conservative relationship in the form;

$$\xi = 1.0 - 0.6 f_c/f_k \quad (8.5)$$

is proposed with some typical values shown in Table 8.2.

$f_c/f_k$	$\xi$
0.0	1.00
0.1	0.94
0.2	0.88
0.3	0.82
0.4	0.76
0.5	0.70

Table 8.2 – Proposed reduction factor for the effect of precompression.

#### 8.4. SUMMARY AND CONCLUSION

The failure mechanism of brickwork masonry subjected to concentrated load applied through a rigid bearing has been examined. In general, the failure is by vertical splitting caused by the transverse tensile stress. The primary vertical crack is initiated either in the brick due to the tensile failure and/or in the vertical perpend due to the tensile bond failure. The influence of parameters such as loaded area ratio, unit brick strength and the loading position on the ultimate failure and crack pattern of brickwork has been discussed.

Three dimensional failure envelopes for 102.5mm and 215.0mm thick masonry on a non-dimensional scales for enhancement factor,  $\zeta'$  ( $=f_{cb}/f_k$ ), in terms of loaded area ratio,  $A_r$  ( $=A_{cb}/A$ ), and the loading position,  $d/l$ , based on the experimental test results carried out in this investigation are presented.

From the experimental test results, design guide for predicting the enhancement factor (and hence the characteristic bearing strength) of brickwork masonry subjected to concentrated loads under rigid bearing have been recommended. Expression in the form of  $\zeta=f'_{cb}/f_k=0.80(A_{re})^{-0.33}\leq 3.0$ , is proposed where  $A_{re}$  is calculated according to Fig. 8.9. However when concentrated load is accompanied with uniform precompression the above expression could be written as  $\zeta=0.8\xi(A_{re})^{-0.33}\leq 3.0$ , where  $\xi$  is a reduction factor for the effect of precompression defined by  $\xi = 1.0 - 0.6 f_c/f_k$  (see Table 8.2).

Fig. 8.10 - Recommended design guide and its comparison with the experimental test results.

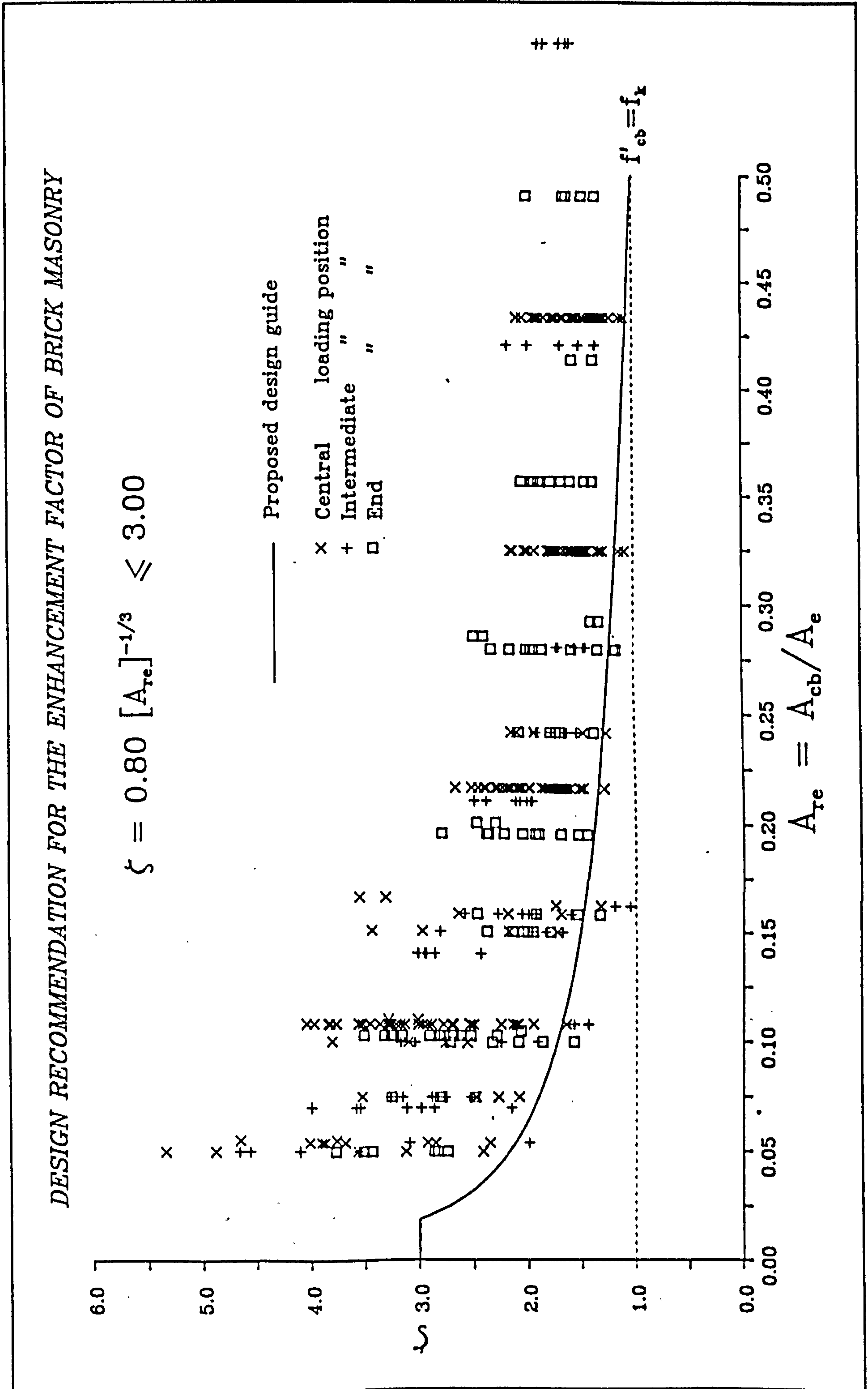
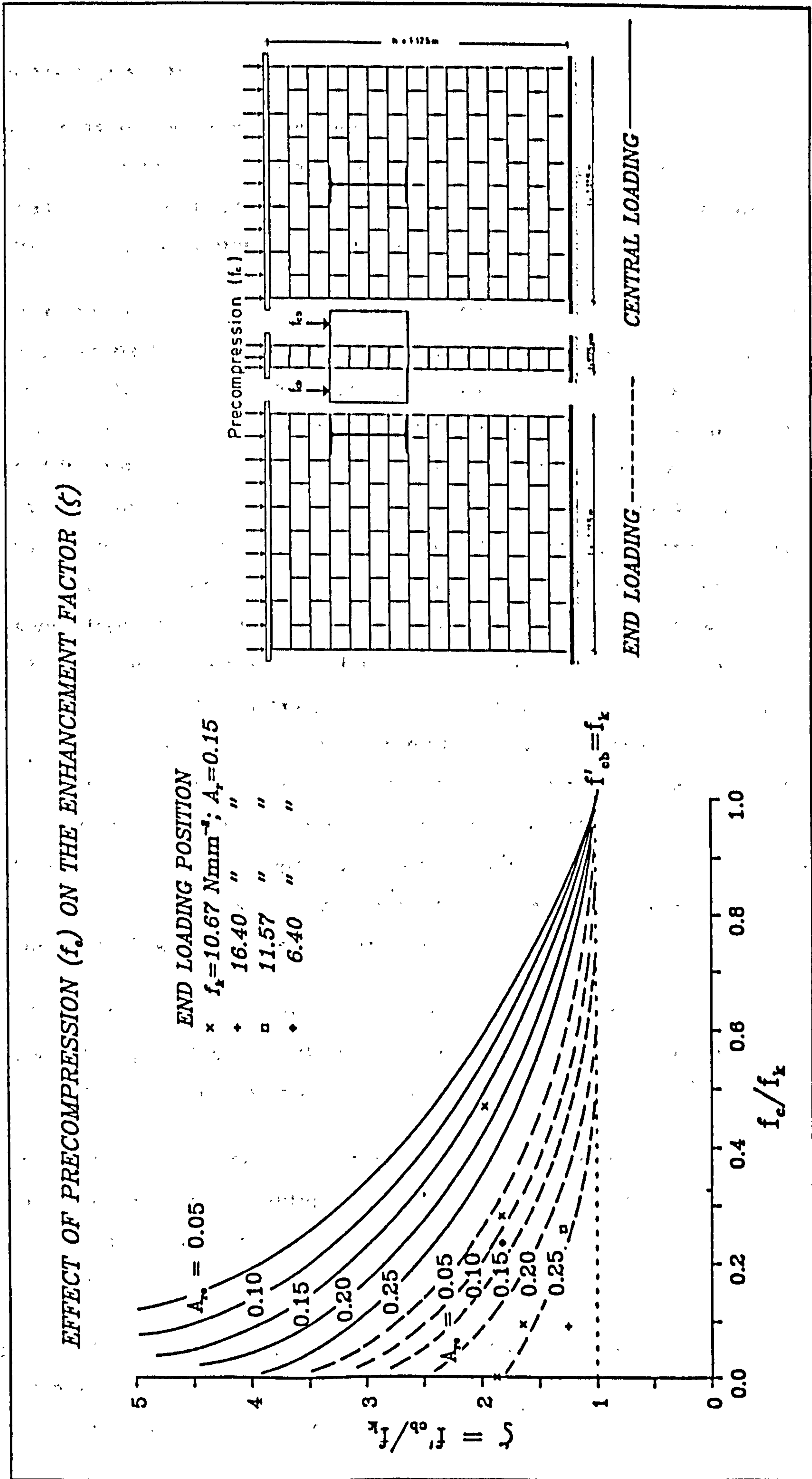




Fig. 8.11 - Simulated design chart showing the effect of precompression on the enhancement factor of brickwork masonry under concentrated load.



## Chapter 9

### GENERAL SUMMARY AND CONCLUSIONS

#### 9.1. GENERAL SUMMARY

This thesis presents a comprehensive study of the behaviour of brickwork masonry subjected to concentrated load applied through a rigid bearing plate. The increase in strength under this type of load has been investigated in relation to its uni-axial compressive strength.

An introduction to the problem of stress concentration in brickwork, its behaviour under partial load and the parameters which have an influence on the bearing strength in general have been described in chapter 1. As the compressive strength of brickwork masonry under partial load must be represented in terms of its strength under uni-axial load, a complete literature survey on the compressive strength of axially loaded brickwork has been carried out. In total 646 wall test results have been collected and analysed statistically for the determination of accurate values for characteristic compressive strength of brickwork masonry based on limit state theory. Chapter 2 has been devoted to this study. Relationships for mean and characteristic strengths for brickwork wall and brickwork masonry have been derived in terms of unit brick crushing strength for two mortar mixes and wall thicknesses. This is also given in terms of unit brick and mortar cube strengths for two brick masonry thicknesses. Based on the collected results, graphical and tabular design charts have been obtained for brickwork wall and masonry strengths. A method for calculating the characteristic strength based on small number of test samples has been proposed.

Chapter 3 described the previous investigations carried out on the compressive strength of brickwork masonry subjected to concentrated loads and reviewed the existing rules given in various codes.

Experimental study of properties of materials used in this investigation have been reported in chapter 4. Chapter 5 contains a description of construction of brickwork specimens, testing equipment, method of testing, the test program and the complete results.

The analyses of the results have been given in chapter 6. Statistical analysis were performed to relate the bearing strength of brickwork in terms of loaded area ratio for different unit strengths. Mean and characteristic curves were

determined in each case. The definition for enhancement factor has been given as the ratio of mean bearing to mean compressive strengths of masonry or as a ratio of characteristic bearing to characteristic compressive strengths of masonry. Based on the crushing strength of unit, design charts have been produced for the mean and characteristic bearing strengths of masonry for various loaded area ratios. Factors affecting the bearing strength such as the properties of masonry and its constituent materials, the loaded area ratio, the loading position and the effect of edge distance, the loading configuration, the thickness of the element, the type of brick unit, the aspect ratio and the effective cross sectional area of the brickwork element and their influences on the enhancement factor have been examined. The mode of failure and the crack pattern under various loading configurations and positions were discussed.

A theoretical study based on stress distributions in masonry under concentrated load by finite element method has been described in chapter 7. Two dimensional plane stress linear elastic analysis, assuming masonry as a homogeneous continuum subjected to concentric and eccentric strip partial loads have been carried out. This study was extended to treat masonry as an assemblage of separate elastic bricks and mortar joints. A nonlinear analysis under central strip partial load on the basis of a continuum has also been performed.

Based on the observation of the mode of failure and crack patterns, a mechanism of failure has been proposed in chapter 8. The results have been utilized to establish three dimensional failure envelopes for masonry under concentrated load. From the outcome of the investigation design guides were recommended.

## 9.2. GENERAL CONCLUSIONS

The following conclusions have been reached as a result of the investigations presented in this thesis:

Relationships of the form  $K.f_b^n$  and  $K.f_m^l.f_b^n$  have been established for mean and characteristic brickwork wall strengths for specific mortar grades and strengths and two wall thicknesses by statistical analysis of wall test results. The constant and indices in the above formulae depend on the mortar mix and also on the type of wall, i.e. whether the wall thickness is equal to the unit thickness or is of bonded construction. In broad terms, the wall strength is

proportional to the square root of the unit strength and to the fifth root of the mortar cube strength.

The test results were found to be consistent with normal distribution in statistical terms.

The characteristic compressive strength of various types of masonry ( $f_k$ ) has been derived from the wall strength relationships by applying a correction to allow for the effect of slenderness ratio on the basis of the reduction factors given in BS 5628:Pt.1.

A limited comparison between characteristic compressive strengths derived from wall tests and from prism tests indicates that the latter gives a high value of  $f_k$ . This may be due to discrepancies in correcting for slenderness effects.

The apparent enhancement of compressive strength of brickwork masonry under concentrated loading is confirmed for all load cases and material types. The principal variable affecting this strength enhancement is loaded area ratio. The enhancement factor is also dependent on load position and brick strength.

Enhancement factor could be expressed either as a ratio of mean bearing to mean masonry strengths or the ratio of characteristic bearing strength to characteristic compressive strength of masonry. However, it has been shown that the two definitions yield same value for the enhancement factor provided that a reasonable number of samples have been tested under uniform load for the determination of the mean and characteristic compressive strengths of masonry.

Expressions for the mean and characteristic bearing strengths of masonry in terms of unit brick strength for loaded area ratios of 0.1, 0.2, 0.3 and 0.4 for 102.5mm thick specimen constructed with mortar grade M(i) have been given.

Characteristic bearing strength is found to be 75% of the mean bearing strength.

Increase in the strength of unit would increase the bearing capacity under partial loading. As brick and mortar strengths influence the masonry strength, it has been shown that as characteristic compressive strength of masonry increases, the bearing strength increases.

Decrease in loaded area ratio leads to increase in bearing strength. The influence of this parameter is found to be significant and is considered as a primary variable. The enhanced strength for drop in loaded area ratio of 0.4 to 0.3, 0.2 and 0.1 could be as high as 5, 30 and 120% respectively.

Depending on the type of brick unit used, masonry thickness influences the bearing strength. It has been shown that 102.5mm thick clay brickwork yields higher bearing strength in comparison to 215.0mm thick brickwork, and vice versa in the case of AAC brickwork at low values of loaded area ratios ( $A_r \leq 0.25$ ). This parameter shows the same effect on the enhancement factor. Also the AAC brickwork gives higher values for enhancement factor in comparison to clay brickwork.

The effect of loading configuration (strip and edge) on the bearing strength and enhancement factor is found to be insignificant.

Position of applied concentrated load is found to be an important parameter and it has been shown that as the edge distance increases the bearing strength increases and conversely as edge distance decreases, the bearing strength decreases.

The failure mechanism of brickwork masonry subjected to concentrated load in general is by vertical splitting caused by the transverse tensile stress. The primary vertical crack is initiated either in the brick due to the tensile failure and/or in the vertical perpend due to the tensile bond failure.

Three dimensional failure envelopes for two masonry thicknesses on a non-dimensional scales for enhancement factor,  $\zeta'$  ( $=f'_{cb}/f_k$ ), in terms of loaded area ratio,  $A_r$  ( $=A_{cb}/A$ ), and the loading position,  $d/l$ , based on the experimental test results carried out in this investigation are presented.

From the experimental test results, design guide for predicting the enhancement factor (and hence the characteristic bearing strength) of brickwork masonry subjected to concentrated loads under rigid bearing have been recommended. Expression in the form of  $\zeta = f'_{cb}/f_k = 0.80(A_{re})^{-0.33} \leq 3.0$ , is proposed where  $A_{re}$  is calculated according to Fig. 8.9. However, when concentrated load is accompanied with uniform precompression the above expression could be written as  $\zeta = 0.80\xi(A_{re})^{-0.33} \leq 3.0$ , where  $\xi$  is a reduction factor for the effect of precompression defined by  $\xi = 0.7 + 0.6f_c/f_k \leq 1.0$ .

### **9.3. SUGGESTIONS FOR FURTHER RESEARCH**

The failure criterion of brickwork masonry subjected to concentrated load established in this thesis applies only to the particular case where the load is transmitted through a rigid steel bearing plate. A logical extension to this study would be to determine the influence of other parameters such as the characteristics of the element by which the load is applied, the support conditions of the masonry, the degree of precompression, the rotation of the end of the element applying the concentrated load, the effect of spreader under the bearing, the presence of horizontal component of load and/or lateral restraint, the angle of dispersion of concentrated load, the height at which the vertical stress becomes uniform and the aspect ratio of brickwork panel for the same loaded area ratio. As perpend are thought to be a plane of weakness, the presence of a perpend under the bearing needs to be examined. Reinforcing the brickwork would improve the bearing capacity but to what extent is not known, therefore, the amount and positioning of reinforcement needs to be investigated.

To recommend a realistic general design rule the major variables must be identified and should be incorporated into the proposal. For example, a valid design chart showing the effect of precompression on the enhancement factor (see the simulated chart shown in Fig.8.11) is required to modify or correct the value of enhancement factor.

## REFERENCES

1. BRITISH STANDARD INSTITUTION, *Recommendations for the Structural Use of Unreinforced Masonry*. BS 5628:Part 1:1978. (1985), pp.40.
2. THOMAS, F.G. *Basic Parameters and Terminology in the Consideration of Structural Safety*. Conseil International du Batiment, CIB Bulletin, V 3, Pt. 4. (1964), pp.4-12.
3. INTERNATIONAL STANDARD, *General Principles for the Verification of the Safety of Structures*. ISO 2394, (1973).
4. HENDRY, A.W. *Structural Brickwork*. MacMillan Press, London, (1983).
5. BEECH, D.G. *The Concept of Characteristic Strength*. Proc. 6th Int. Sympos. on Loadbearing Brickwork. BCS, London. (1977), pp.277-88.
6. FISHER, R.A. *The Fiducial Argument in Statistical Inference*. *Amm Eugen.*, V 6, (1935), pp.391.
7. MORSY, E.H. *An Investigation of Mortar Properties Influencing Brickwork Strength*. Ph.D. Thesis, Dept. Civil Engineering & Building Science, Univ. of Edinburgh. (1968).
8. MONK, C.B., Jr. *An Historical Survey and Analysis of the Compressive Strength of Clay Masonry*. Structural Clay Products Research Foundation, Research Report No.12, Geneva, Illinois. (1967).
9. DAVEY, N. and THOMAS, F.G. *The Structural Uses of Brickwork*. Inst. of Civil Eng., Structural and Buildings, Paper No.24. (1950).
10. THOMAS, F.G. *The Strength of Brickwork*. *Structural Engineer*, V 31, No.2, (1953), pp.35-46.
11. BRITISH STANDARDS INSTITUTE *Structural Recommendations for Loadbearing Walls*. CP 111, London. (1936), (1948), (1964), (1970).
12. FOSTER, D. *Results of Full Storey-Height Walls Tested in U.K. Till 1960's*. Structural Clay Products Ltd.
13. HALLER, P. *The Physics of the Fired Brick: Part One: Strength Properties*. Library Commun. 929, Building Research Station, [Translated by G.L. Cairne]. (1960).
14. STRUCTURAL CLAY PRODUCTS RESEARCH FOUNDATION *Small Scale Specimen Testing*. Progress Report No.1, SCPI, Geneva, Ill. (1964), pp.80.

15. STRUCTURAL CLAY PRODUCTS RESEARCH FOUNDATION  
*"Compressive and Transverse Tests of Five-inch Brick Walls"*. Research Report No.8, SCPI, Geneva, Ill., (1965), pp.9.
16. STRUCTURAL CLAY PRODUCTS RESEARCH FOUNDATION  
*"Compressive, Transverse and Racking Strength Tests of Four-inch Brick Walls"*. Research Report No.9, SCPI, Geneva, Ill. (1965). pp.23.
17. STRUCTURAL CLAY PRODUCTS RESEARCH FOUNDATION  
*"Compressive and Transverse Strength Tests of Eight-inch Brick Walls"*. Research Report No.10, SCPI, Geneva, Ill., (1966). pp.23.
18. STRUCTURAL CLAY PRODUCTS RESEARCH FOUNDATION  
*"Compressive, Transverse and Shear Strength Tests of Six and Eight-inch Single-Wythe Walls Built with Solid and Heavy-Duty Hollow Clay Masonry Units"*. Research Report No.16, SCPI, McLean, Virginia. (1969). pp.22.
19. PRASAN, S. *"Crushing Tests on Storey-height Walls 4.5-in Thick"*. Proc. of British Ceramic Society, No.4. (1965), pp.67-80.
20. BRADSHAW, R.E. and HENDRY, A.W. *"Further Crushing-Tests on Storey-Height Walls 4.5in. Thick"*. Proc. of British Ceramic Society, No.11. (1968). pp.25-53.
21. BRADSHAW, R.E. and HENDRY, A.W. *"Preliminary Crushing Tests on Storey-height Cavity Walls"*. in *Designing, Engineering and Construction With Masonry Products*, ed. F.B. Johnson. Gulf, Houston, Tex. (1969), pp.101-9.
22. SIMMS, L.G. *"The Strength of Walls Built in the Laboratory With Some Types of Clay Bricks and Blocks"*. Proc. of British Ceramic Society, No.4. (1965), pp.81-92.
23. McDOWALL, I.C., McNEILLY, T.H. and RYAN, W.G. *"The Strength of Brick Walls and Wallettes"*. Special Report No.1, Brick Development Research Institute, Univ. of Malbourne, Victoria, Australia. (1966), pp.42.
24. STEDHAM, M.E.C. *"Quality Control for Load-bearing Brickwork. III. Wall Tests"*. Proc. of the British Ceramic Society, No.11. (1968), pp.83-99.
25. SINHA, B.P. and HENDRY, A.W. *"Splitting Failure of Brickwork as a Function of the Deformation Properties of Bricks and Mortar"*. The British Ceramic Research Association, Tech. Note No.86, (1966), pp.15.
26. HILSDORF, H.K. *"Investigation into the Failure Mechanism of Brick Masonry Loaded in Axial Compression"*. in *Designing, Engineering and Construction with Masonry Products*. ed. F.B. Johnson, Gulf, Houston, Texas. (1969), pp.34-41.



27. SINHA, B.P. *"Further Crushing Tests on Model Storey-height Brick Walls"*. British Ceramic Research Association, Heavey Clay Division, Tech. Note No.130. (1968).
28. SINHA, B.P. *"The Influence of Number of Courses and the Effect of Brick Strength on Brickwork Strength"*. British Ceramic Research Association, Heavey Clay Division, Tech. Note No.131. (1968).
29. SINHA, B.P. and HENDRY, A.W. *"The Effect of Brickwork Bond on the Load-bearing Capacity of Model-Brick Walls"*. British Ceramic Research Association, Heavey Clay Division, Tech. Note No.81. (1966).
30. WEST, H.W.H., HODGKINSON, H.R. and DAVENPORT, S.T.E. *"The Performance of Walls Built of Wire-Cut Bricks With and Without Perforations"*. British Ceramic Research Association, Special Pub. No.60. (1968).
31. FRANCIS, A.J., HORMAN, C.B. and JERREMS, L.E. *"The Effect of Joint Thickness and Other Factors on the Compressive Strength of Brickwork"*. Proc. of the Second International Brick Masonry Conferance, BCRA, Stoke-on-Trent. (1970), pp.31-7.
32. ASTBURY, N.F. and WEST, H.W.H. *"Tests on Storey-height brickwork Panels and Development of Site Control Tests for Brickwork"*. in *Designing, Engineering and Construction With Masonry Products*. ed. F.B. Johnson, Gulf, Houston, Texas. (1969), pp.216-24.
33. WEST, H.W.H., HODGKINSON, H.R., BEECH, D.G. and DAVENPORT, S.T.E. *"The Comparative Strengths of Walls Built of Standard and Modular Bricks"*. Proc. 2nd. IBMaC, BCRA, Stoke-on-Trent. (1970), pp.172-6.
34. WEST, H.W.H., HODGKINSON, H.R., BEECH, D.G. and GOODWIN, J.F. *"The Compressive Strength of Calcium Silicate Brick Walls Under Axial Loading"*. Proc. 6th Int. Sympos. on Load Bearing Brickwork, BCS, London. (1978), pp.19-43.
35. ANDERSON, G.W. *"Stack-bonded Small Specimens as Design and Construction Criteria"*. Proc. 2nd. IBMaC, BCRA, Stoke-on Trent. (1970), pp.38-43.
36. BASE, D.G. *"Compression Tests on Six Single-leaf Brick Walls"*. Dept. Civil Eng., Univ. of Melbourne, Report of Investigation No. ST78/66. (1968).
37. STANDARD ASSOCIATION OF AUSTRALIA. *"Rules for Brickwork in Buildings"*. AS CA47, Sydney. (1969).

38. JAMES, J.A. *"The Performance of Walls and Small Brickwork Specimens Built With Two Types of Western Australian Loadbearing Bricks"*. Building Development Laboratories Pty. Ltd., Morley, Western Australia. Report No. W/2. (1970).
39. JAMES, J.A. *"The Performance of Walls and Small Brickwork Specimens Built With Two Types of Western Australian Loadbearing Bricks"*. Building Development Laboratories Pty. Ltd., Morley, Western Australia. Report No. W/2/Add. (1972), pp.4.
40. JAMES, J.A. *"The Performance of Walls and Small Brickwork Specimens Built With Cardup 9"x6" Bricks"*. Building Development Laboratories Pty. Ltd., Morley, Western Australia. Report No. W/4. (1970), pp.11.
41. JAMES, J.A. *"The Performance of Walls and Small Brickwork Specimens Built With Midland Red Loadbearing Bricks"*. Building Development Laboratories Pty. Ltd., Morley, Western Australia. Report No. W/M/3. (1971), pp.9.
42. JAMES, J.A. *"The Performance of Walls and Small Brickwork Specimens Built With Cardup Modulated 11 5/8"x3 5/8"x3" Bricks"*. Building Development Laboratories Pty. Ltd., Morley, Western Australia. Report No. W/C/2. (1971), pp.9.
43. JAMES, J.A. *"Review of the Methods of the S.A.A. Brickwork Code - ASCA 47-1969 For Determining the Permissible Compressive Force of Axially-Loaded Brickwork"*. Building Development Laboratories Pty. Ltd., Morley, Western Australia. Report No. S/CA47-1969/2. (1972), pp.11.
44. JAMES, J.A. *"Investigation of the Effect of Workmanship and Curing Conditions on the Strength of Brickwork"*. Building Development Laboratories Pty. Ltd., Morley, Western Australia. Report No. W/WORK/1. (1971), pp.30.
45. JAMES, J.A. *"Investigation of the Behaviour of Single Leaf, 9" and 11" Cavity Height Walls Under Axial Load"*. Building Development Laboratories Pty. Ltd., Morley, Western Australia. Report No. W/3/A. (1972), pp.37.
46. JAMES, J.A. *"Investigation of the Behaviour of Storey-Height Single-Leaf Walls, 9" Walls and 11" Cavity Walls Under Eccentric Compressive Load"*. Building Development Laboratories Pty. Ltd., Morley, Western Australia. Report No. W/4/A. (1973), pp.21.
47. KHOO, C.L. and HENDRY, A.W. *"A Failure Criterion for Brickwork in Axial Compression"*. British Ceramic Research Association, Heavy Clay Division, Tech. Note 179. (1972), pp.30.
48. KHOO, C.L. and HENDRY, A.W. *"Strength Tests on Brickwork and Mortar Under Complex Stresses for the Development of a Failure Criterion for Brickwork in Compression"*. Proc. British Ceramic Society, No. 21, Stoke-on-Trent. (1973),

pp.57-66.

49. KHOO, C.L. *"A Failure Criterion for Brickwork In Axial Compression"*. Ph.D. Thesis, Dept. Civil Engineering & Building Science, Univ. of Edinburgh. (1972).
50. RYAN, T.A.Jr., BRIAN, L.Jr. and RYAN, B.F. *"Minitab Reference Manual"*. Minitab Project, Statistical Dept., The Pennsylvania Univ., P.A. 16892. (180).
51. WEST, H.W.H., EVERILL, J.B. and BEECH, D.G. *"Experiments in the Use of the 9-inch Brickwork Cube for Site Control Testing"*. Proc. British Ceramic Society, No.11, BCRA. (1968). pp.135-41.
52. WEST, H.W.H., EVERILL, J.B. and BEECH, D.G. *"Development of a Standard 9-in. Cube Test for Brickwork"*. Trans. British Ceramic Society, Vol. 65. (1966), pp.111-28.
53. STEDHAM, M.E.C. *"Quality Control for Load Bearing Brickwork. I: 9-in. Cube Tests- preliminary Results"*. Trans. British Ceramic Society, Vol. 64. (1965), pp.1-17.
54. STEDHAM, M.E.C. *"Quality Control for Load Bearing Brickwork. II: 9-in. Cubes Tests- Further Results"*. Proc. British Ceramic Society, No. 4. (1965), pp.9-23.
55. BRADSHAW, R.E. *"The Brick in Slender Crosswall Construction"*. Clay Products Technical Bureau, Tech. Note. 1, Vol. 7. (1965), pp.9-12.
56. SINHA, B.P., and HENDRY, A.W. *"Further Tests on Model Brick Walls and Piers"*. Proc. British Ceramic Society, Vol. 17, Pt.3. (1970), pp.83-95.
57. MAURENBRECHER, A.H.P. *"Use of the Prism Test to Determine Compressive Strength of Masonry"*. Proc. North American Masonry Conference, The Masonry Society, Boulder, Colorado. (1978), pp.91.1-10.
58. BINGHAU, X. and YILIANG, Q. *"The Relation Between the Coefficients of Variation of the Compressive Strengths of Units, Mortars and Brickwork"*. Proc. 7th IBMaC, Vol.1, BDRI, Melbourne, Australia. (1985), pp.557-64.
59. RUTHERFORD, D.J. *"Stress Concentrations in Load Bearing Brickwork Details"*. Ph.D. Thesis, Dept. Civil Engineering & Building Science, Univ. of Edinburgh. (1968).
60. WILLIAMS, A. *"The Bearing Capacity of Concrete Loaded Over a Limited Area"*. Cement and Concrete Association, Tech. Report 526. (1979), pp.70.
61. INSTITUTION OF STRUCTURAL ENGINEERS *"Report on Bearing Girders"*. The Structural Engineer, Vol. X, No.2 , London. (1932), pp.84.

62. INSTITUTION OF STRUCTURAL ENGINEERS *"Interim Report on Bearing Pressures on Brickwork"*. The Structural Engineer, Vol.XI, No.9 & 10. London. (1933), pp.379.
63. INSTITUTION OF STRUCTURAL ENGINEERS *"Report on Bearing Pressures on Brick Walls"*. The Structural Engineer. London. (1938), pp.242-68.
64. BUILDING RESEARCH STATION *"Brick Piers and Some Slender Brick Walls Under Uniform and Concentrated Loading"*. Dept. of Scientific and Industrial Research, Structural Aspects of Housing, Note No. D470, Interim Note No. 15. (1956), pp.9
65. HENDRY, A.W., BRADSHAW, R.E. and RUTHERFORD, D.J. *"Tests on Cavity walls and the Effect of Concentrated Loads and Joint Thickness on the Strength of Brickwork"*. Clay Products Technical Bureau, Research Note, Vol.1, No.2. (1968), pp.12.
66. KIRTSCHIG, K. and KASTEN, D. *"Partial Surface Load of Masonry"*. Proc. 5th IBMaC, BIA, Session IV, paper 26, Washington D.C. (1979).
67. MALEK, M.H. *"Concentrated Loads on Brickwork"*. B.Sc. Hons. Dissertation, Dept. Civil Engineering & Building Science, Univ. of Edinburgh. (1981).
68. DAI-XIN, T. *"Testing and Analysis of the Bearing Strength of Brick Masonry"*. Proc. 7th IBMaC, BDRI, Vol.1. Melbourne. (1985), pp.747-55.
69. CHINESE CODE OF PRACTICE *"The Design Code of Brick Masonry"*. GBJ-3-73.
70. ALI, S. and PAGE, A.W. *"Concentrated Loads on Brickwork - A Preliminary Study"*. Proc. 7th IBMaC, BDRI, Vol.1. Melbourne. (1985), pp.711-21.
71. ALI, S. and PAGE, A.W. *"An Elastic Analysis of Concentrated Loads on Brickwork"*. Masonry International, No. 6. (1985), pp.9-21.
72. MANN, W. and PFEIFER, M. *"Investigations on the Stresses in Masonry Walls Subjected to Concentrated Loads"*. Proc. 7th IBMaC, BDRI, Vol.1. Melbourne. (1985), pp.735-46.
73. DEUTSCHE NORMEN *"Masonry: Engineer-Designed Buildings Calculation and Construction"*. DIN 1053, Part 2, Berlin. (1981).
74. LIND, V. *"Edge Strength of Masonry"*. Ziegelindustrie International, No.3. (1985), pp.199-204.
75. ARORA, S.K. *"Tests on Masonry Walls Subjected to Concentrated Load"*. Building Research Station, Note No. N138/85. (1985), pp.42.

76. CONSEIL INTERNATIONAL DU BATIMENT *"International Recommendations for Masonry Structures"*. International Council for Building, W23A. Rotherdam. (1980).
77. GOSUDARSTRENNYI KOMITEL SOVETA MINISTROV SSSR PO DELAM STROITEL'STVA (GOSSTROI SSSR). [State Committee for Construction, Council of Ministers of the USSR (Gosstroi USSR)]. *"Building Standards and Regulations, Part II, Sect.V, Chapter 2. Plain and Reinforced Masonry Structures"*. Design Standards SNiP II-V.2-71. Moscow. (1972). Translated by D.E. Allen, Canada Institute for Scientific & Technical Information, National Research Council of Canada. Technical Translation 1884, Ottawa, Canada.
78. STRUCTURAL CLAY PRODUCTS INSTITUTE *"Recommended Building Code Requirements for Engineered Brick Masonry"*. Washington D.C. (1966).
79. COLORADO MASONRY INSTITUTE *"Building Code Requirements for Masonry Construction"*. CMI 301-76. (1976).
80. THE MASONRY SOCIETY *"Standard Building Code Requirements for Masonry Construction"*. TMS Doc. No. 401-81. (1981).
81. UNIFORM BUILDING CODE *"Part V: Engineering Regulations - Quality and Design of the Materials of Costruction"*. Chapter 24, Masonry. (1985).
82. AMERICAN CONCRETE INSTITUTE *"Building Code Requirements for Concrete Masonry Structures"*. ACI 531-79. Detroit. (1979).
83. CANADIAN STANDARDS ASSOCIATION *"Masonry Design and Construction for Buildings"*. CAN3-S304-M78.
84. LATTBETONG Ab. *"Lattbetong Handboken"*. Stockholm. (1974).
85. STANDARD ASSOCIATION OF AUSTRALIA *"S.A.A. Brickwork Code"*. AS1640:1974.
86. STANDARD ASSOCIATION OF AUSTRALIA *"S.A.A. Blockwork Code"*. AS 1475:1977.
87. STANDARD ASSOCIATION OF AUSTRALIA *"S.A.A. Masonry Code"*. Draft. (1986).
88. BRITISH STANDARDS INSTITUTION *"Clay Bricks and Blocks"*. BS 3921. London. (1974).
89. BRITISH STANDARDS INSTITUTION *"Sands for Mortar for Plain and Reinforced Brickwork, Blockwalling and Masonry"*. BS 1200. London. (1985).

90. BRITISH STANDARDS INSTITUTION *"Specification for Ordinary and Rapid-hardening Portland Cement"*. BS 12. London. (1983).
91. BRITISH STANDARDS INSTITUTION *"Building Limes"*. BS 890. London. (1972).
92. BRITISH STANDARDS INSTITUTION *"Methods of Testing Mortars, Screeds and Plasters"*. BS 4551. London. (1983).
93. POWELL, B. and HODGKINSON, H.R. *"The Determination of Stress/Strain Relationship of Brickwork"*. Proc. 4th IBMaC, Paper 2.a.5. Brugge. (1976).
94. TURNSEK, V. and CACOVIC, *"Some Experimental Results on the Strength of Brick Masonry Walls"*. Proc. 2nd IBMaC, BCRA, Stoke-on-Trent. (1970), pp.149-56.
95. SINHA, B.P. and PEDRESCHI, R. *"Compressive Strength and Some Elastic Properties of Brickwork"*. The Int. Journal of Masonry Construction, Vol.3, No.1. (1983), pp.19-25.
96. WARREN, D. and LENCZNER, D. *"A Creep-Time Function for Single-Leaf Brickwork Walls"*. Int. Journal of Masonry Construction, Vol.2, No.1. (1981).
97. AMENY, P. LOOV, R.E. and SHRIVE, N.G. *"Prediction of Elastic Behaviour of Masonry"*. The Int. Journal of Masonry Construction, Vol.3, No.1. (1983), pp.1-9.
98. CRANSTON, W.B. *"Bearing Stresses on Masonry"*. Cement and Concrete Association. (1977).
99. COMITE EURO-INTERNATIONAL DU BETON AND FEDERATION INTERNATIONALE DE LA PRECONTRAINTTE *"CEB-FIP Model Code for Concrete Structures"*. Comite Euro-International du Beton, Paris. (1978), pp.348.
100. GERMAN COMMITTEE FOR REINFORCED CONCRETE *"Concrete and Reinforced Concrete Structures: Design and Construction"*. DIN 1045. Koln. (1972). Translated and Published by British Standards Institution.
101. ALI, SK. S. *"Concentrated Loads on Solid Masonry"*. Ph.D. Thesis, Univ. of Newcastle, Australia. (1987).
102. PAFEC, *"Data Preparation User Manual 6.1"*. PAFEC Ltd., Strelley, Nottigham. (1985).
103. LENCZNER, D. *"Elements of Loadbearing Brickwork"*. Pergamon, Oxford. (1972).

## I. APPENDIX A

### II. METHOD OF CALCULATING CHARACTERISTIC COMPRESSIVE STRENGTH OF BRICKWORK MASONRY FROM SMALL NUMBER OF TEST RESULTS

In practice only a small number of samples would be tested experimentally and assuming a normal distribution based on a small sample size would lead to unacceptable values for characteristic strength. The reason for this may be explained by the fact that the variation in strength of masonry is high. This tends to give rise to a high standard deviation of the sample. Also, the calculated mean based on a small sample would not represent the true mean.

However, assuming lognormal distribution and provided that the number of test results is small, say a minimum of ten, it would be possible to calculate the characteristic value by the method below. The value obtained for the characteristic strength using this method would be the closest that could be calculated compared to the actual true characteristic value if it was determined using normal distribution based on a much larger number of test samples.

If the strengths obtained on n number of test specimens is  $x_i$ , for  $i=1$  to n, then;

$$x_k = x_m - k.S_d \quad (1)$$

$$\text{where } k = t_{\alpha} \cdot \{(n+1)/n\}^{0.5} \quad (2)$$

where;  $x_k$  = characteristic strength of the sample,

$S_d$  = standard deviation of the sample,

$t_{\alpha}$  = Student's t with unilateral probability  $\alpha\%$  and  
(n-1) degrees of freedom.

Using lognormal distribution;

let  $y_i = \log(x_i)$ , for  $i = 1$  to n, then calculating  $y_m$  and  $S_y$  from:

$$y_m = 1/n \{ \sum(y_i) \} \quad (3)$$

$$S_y = \{ 1/(n-1) [ \sum(y_i^2) - 1/n(\sum y_i)^2 ] \}^{0.5} \quad (4)$$

$$\text{Then } y_k = y_m - k.S_y \quad (5)$$

where  $k$  is a function of  $n$  and is obtained from Table A1. Then;

$$x_k = \text{antilog}(y_k) \quad (6)$$

No. of samples	Student's t	k
2	6.314	7.7320
3	2.920	3.3717
4	2.353	2.6307
5	2.132	2.3354
6	2.015	2.1764
7	1.943	2.0771
8	1.895	2.0100
9	1.860	1.9606
10	1.833	1.9225
11	1.812	1.8926
12	1.796	1.8693
13	1.782	1.8493
16	1.753	1.8070
17	1.746	1.7966
18	1.740	1.7877
19	1.734	1.7790
20	1.729	1.7717
31	1.697	1.7242
41	1.684	1.7044
51	1.678	1.6944
101	1.660	1.6682
201	1.650	1.6541
$\infty$	1.645	1.6450

Table A1 - Value of  $k$  at 95% confidence interval.



### I.II. COLLECTED DATA

Dimensions in (mm)		Mortar mix	Strength (Nmm <sup>-2</sup> )				Age (days)	h/t ratio	
Wall (h x l x t)	Brick (h x l x t)		Brick	Mortar	Cube	Wall			
2515x1367x105	Buthington LB75	1:1:6	80.74	9.14	28.41	21.58	28	24.0	
				7.61	23.51	18.08			
				8.36	27.03	18.41			
2515x1359x105	Kirton Brick		39.58	4.47	11.03	7.65			
				5.78	14.96	8.65			
2515x1378x105	Elm commons 2-holes		33.92	7.01	10.69	10.34			
				6.34	17.79	11.93			
				5.55	20.34	13.65			
Crossleys 115	H. Williamson		22.20	6.74	10.27	10.76	28	24.0	
				6.96	10.20	10.76			
				6.52	9.86	10.55			
	F.R.Sand/Lime			17.65	8.07	4.19	4.48		
					8.00	5.01	4.62		
					7.45	4.94	4.79		
	Hurworth	1:25:3	39.85	19.51	23.30	20.75			
					18.62	21.58			
					16.03	19.51			
	Coatham Stob		33.30	12.31	17.34	12.34			
					14.51	14.27			
					13.16	12.96			
	Kibbleworth		67.15	12.65	12.58	19.31			
					11.79	22.61			
					15.62	21.37			

Table A2 - Strength of single leaf walls with mortar designation M(i) & M(iii).  
(after Foster<sup>[12]</sup>)

Dimensions in (mm)		Mortar mix	Strength (Nmm <sup>-2</sup> )				Age (days)	h/t ratio
Wall (h x l x t)	Brick (h x l x t)		Brick	Mortar	Cube	Wall		
2762x1372x115	67 Blue Rustic 14-holes	1:25:3	73.50	19.03 19.48	37.23 37.92	21.44 24.20	28	24.0
2531x1372x115	67 Smooth Red 7-slots		61.71	19.93	29.65	25.58		22.0
				18.55	26.06	22.82		
				16.06	18.55	22.13		
2531x1372x115	67 Smooth Red 14-holes		56.47	18.68	27.17	20.75		
				19.24	27.85	20.75		
				18.03	26.20	20.06		
2531x1372x115	67 Smooth Red 7-slots		61.71	13.20	24.96	17.31		
				13.55	27.58	22.13		
				12.00	22.75	18.68		
2515x1362x105	Jacobean mixed darks Solid		56.12	21.10	23.03	23.72		24.0
				11.93	21.72	15.79		
				14.27	21.72	17.65		
2515x1338x103	Coernarvon common 3-holes		47.99	21.03	18.75	19.17		24.4
				19.65	19.24	18.27		
				19.99	20.68	14.34		
2515x1375x105	Jacobean Blue/Brown Solid		68.88	15.96	33.09	28.68		24.0
				17.62	32.03	27.99		
				15.00	35.37	26.68		
2515x1375x105	Chesterton Buff 14-holes		64.19	17.58	21.48	18.06		
				16.31	27.30	19.44		
				19.31	33.23	19.86		
2515x1375x105	Chesterton Tudor 14-holes		63.98	21.48	32.96	19.10		
				19.31	33.23	19.86		
				21.48	32.96	19.10		
2515x1359x105	Common		46.95	17.03	17.62	17.24		
				12.62	25.79	17.37		
				15.89	19.62	15.24		
2515x1359x105	Spade facing		47.37	20.27	19.51	17.03		
				15.49	24.96	17.72		
				16.22	20.06	17.86		
2616x905x102	Kirton Brick		39.58	--	--	12.48		25.6
				--	--	8.69		
				--	--			
2515x1375x105	Hooton Common		44.26	14.38	12.80	10.74		24.0
				15.86	13.18	10.10		
				17.35	12.13	11.86		
2515x1375x105	Buttington LB75		80.74	26.65	32.13	29.85		
				27.92	25.99	28.41		
				27.03	30.27	28.54		
2515x1394x102	Catherall multi Blue/Brown		52.19	13.38	25.79	22.27		24.7
				15.17	29.96	19.06		
				14.23	33.09	22.89		
2515x1341x103	Caernarvon LB50		48.54	23.65	15.79	18.27		24.4
				21.72	20.52	14.69		
				22.72	25.65	20.89		
2515x1356x103	Catherall Buff Rustic with stain		53.92	20.72	22.61	15.72		
				15.25	25.79	14.65		
				18.24	17.93	15.58		
2515x1351x105	Buckley Old Wks Red Multi Rustics		50.33	16.79	21.41	19.82		24.0
				19.51	20.28	17.48		
				15.55	19.13	17.03		
2515x1359x105	Buckley Old Wks Mixed Buff		43.71	16.24	20.82	17.51		
				16.93	18.20	16.06		
				16.10	18.48	16.41		

Table A3 - Strength of single leaf walls with mortar designation M(i).  
(after Foster<sup>[12]</sup>).

Dimensions in (mm)		Mortar mix	Strength (Nmm <sup>-2</sup> )				Age (days)	h/t ratio	
Wall (h x l x t)	Brick (h x l x t)		Brick	Mortar	Cube	Wall			
2515x1353x219	Steerpoint W/C 14-holes	1:1:6	47.02	3.77 3.79 3.11	13.41 13.17 10.07	7.93 8.27 7.72	28	11.5	
	Pinhoe W/C 10-holes		41.85	4.35 5.92 2.42	14.58 14.89 14.00	8.69 8.55 7.86			
2515x1359x219	Kirton Brick		39.85	5.35 5.20	12.48 12.20	5.77 7.24			
	Keele Red 7-slots		68.53	4.68 4.33	21.65 19.86	9.96 8.27			
	Brownhill Buff 7-slots		60.07	3.21 3.85	19.31 19.68	7.79 9.79			
	Apedale Red Solid		91.42	3.88 4.54	47.64 34.54	14.27 14.27			
2515x1384x225	Elm Common 2-holes		33.92	7.33 6.63 8.83	10.89 16.06 14.96	7.52 9.58 9.31		11.2	
	H.Williamson		22.20	5.85 8.14 7.86	13.03 9.45 11.65	9.79 9.72 10.34			
	F.R. Sand/Lime		17.65	5.89 7.79 6.74	8.00 8.07 6.16	5.65 4.09 3.55			
2531x1350x229	Exmouth S/D		42.82	5.86 4.02	13.51 14.48	7.96 8.14		11.1	
	Ottery S/D		37.85	4.68 4.56	9.31 7.65	5.00 5.00			
	Rougemont W/C facing 7-slots		76.19	4.55 4.87 6.12 6.40 3.08 2.83 3.63 3.40 3.39	24.82 19.44 22.96 19.86 18.75 21.58 18.62 17.79 18.89	12.62 11.79 8.17 8.27 9.65 8.27 9.45 8.96 10.62	7 28 7 28	12.6	
	67 Buff S/F 7-slots		60.74	3.21 3.85 4.65	19.31 19.68 19.86	7.79 9.79 11.10			
				60.74	3.34 3.45 3.53	18.89 18.82 18.68	9.14 10.62 9.79		11.6
2762x1350x219	67 Red Solids		91.42 83.77	3.88 4.54	47.64 34.54	13.93 14.27	21	12.6 12.6	
2531x1350x229	Pinhoe W/C		48.68	5.50 5.57	21.65 18.48	9.79 9.31	28	11.1	
	Rougemont S/D		35.09	3.87 5.67	6.03 6.04	6.14 6.14			
	Pinhoe S/D		39.23	4.12 5.10	10.00 6.79	6.14 5.48			
2762x1350x229	Western S/D		20.62	3.32 3.83	6.64 7.72	5.31 5.65		12.1	
	Western W/C		31.58	3.70 4.02	20.48 20.48	10.62 11.62		12.1	
	Honickowle Lower S/P		33.58	3.23 3.66	10.41 10.41	7.65 7.31			
2531x1350x229			26.34	3.72 3.13	9.65 --	5.15 5.48		11.1	
			33.09	3.33 3.66	10.27 10.27	6.96 7.48			

Table A4 - Strength of bonded walls with mortar designation M(iii).  
(after Foster<sup>[12]</sup>).

Dimensions in (mm)		Mortar mix	Strength (Nmm <sup>-2</sup> )				Age (days)	h/t ratio		
Wall (h x l x t)	Brick (h x l x t)		Brick	Mortar	Cube	Wall				
2515x1378x219	Jacobean Blue/Brown Solid	1:25:3	68.88	16.00	31.78	20.48	28	11.5		
				14.34	27.03	19.03				
				12.00	27.48	19.44				
				15.72	34.68	19.79				
2515x1359x219	Common		48.95	15.48	16.41	10.96				
				13.17	19.82	9.24				
				13.03	21.06	11.45				
				17.27	21.55	13.34				
2515x1372x225	Hooton Common		44.26	18.53	20.34	11.36		11.2		
				15.62	11.38	10.00				
				16.62	16.38	9.00				
				20.82	26.48	24.06				
2515x1348x216	Caernarvon LB50		48.54	18.41	23.58	18.27		11.8		
				18.52	19.58	16.96				
				19.58	22.44	18.96				
				20.82	26.48	24.06				
2515x1394x219	Cutheral Multi Blue/Brown		52.19	21.27	27.03	19.31		11.5		
				20.13	27.35	19.86				
				23.72	23.65	16.55				
				18.31	19.94	12.67				
2515x1364x219	Catheral Buff Rustics with Stain		53.92	16.51	22.48	14.00				
				15.42	25.18	14.00				
				19.48	16.10	12.89				
				22.73	19.11	10.62				
2515x1391x219	Buckley Old Wks Red Multi Rustic		50.33	19.97	22.34	12.96				
				17.58	14.10	10.82				
				17.27	17.51	12.10				
				18.24	12.86	12.13				
2515x1384x219	Buckley Old Wks Mixed Buff		43.71	17.58	14.10	10.82				
				12.86	12.13	12.10				
				10.41	17.93	12.27				
				12.82	18.48	11.86				
				13.44	19.17	11.03				
				12.07	18.75	12.41				
				10.96	19.99	10.82				
				14.41	20.55	13.86				
				10.41	20.68	12.27				
				68.74	11.58	23.72			12.24	27
				11.03	23.99	12.41			28	29
				10.76	25.86	10.17			120	28
				10.41	23.24	13.03			28	28
				11.45	22.34	12.82			28	120
				13.86	25.92	14.75			28	120
				14.20	26.27	16.62			28	120
12.13	25.23	13.27	28	120						
--	--	18.62	330	330						
--	--	14.96	330	330						
2518x1436x219	Standard		61.02	12.76	21.86	12.89				
				13.24	17.86	13.27				
				13.58	21.79	11.40				
				12.34	21.79	12.96				
				12.62	20.89	11.27				

Table A5 - Strength of bonded walls with mortar designation M(i).  
(after Foster<sup>[12]</sup>).

Dimensions in (mm)		Mortar mix	Strength (Nmm <sup>-2</sup> )				Age (days)	h/t ratio	
Wall (h x l x t)	Brick (h x l x t)		Brick	Mortar	Cube	Wall			
2762x775x219	67 smooth Red 7-slots	1:25:3	61.57	21.37	25.86	14.41	28	12.6	
				18.48	23.72	14.96			
				21.99	28.13	17.31			
				13.44	27.44	12.62			
				14.89	28.13	15.86			
				12.76	21.24	14.07			
2762x667x219				10.34	21.72	13.65			
				12.27	26.13	16.41			
				9.65	24.96	16.06			
				9.41	24.75	14.34			
				9.45	21.65	14.69			
				12.48	24.82	14.34			
2762x565x219				10.96	22.89	16.89			
				13.48	27.92	16.89			
				14.93	28.54	17.31			
				14.00	27.30	13.27			
				11.65	27.10	17.31			
				9.10	20.89	14.07			
2762x457x219				9.55	21.86	14.96			
				15.86	28.13	15.44			
				13.65	24.82	15.93			
				15.86	27.37	16.48			
				11.24	22.75	14.96			
				11.55	24.06	14.96			
2762x1350x219	67 Blue Solid 67 Blue Rustic 14-holes		84.81	17.29	47.85	24.55		12.1	
			73.50	15.20	34.13	19.93			
				15.72	34.68	19.79			
2531x1350x229	67 Smooth Red 7-slots		61.71	15.03	26.41	16.62		11.1	
				15.93	23.10	12.27			
				15.51	27.03	18.62			
	67 Smooth Red 14-holes			56.47	17.79	25.99	14.00		
					16.96	25.65	12.96		
					20.48	27.23	14.00		
	67 Smooth Red 7-slots			61.71	15.03	21.58	14.89		
					13.24	25.23	15.31		
					14.55	22.41	14.89		
	Rougemont W/C Class A			86.74	12.89	42.89	16.27		
					12.41	42.89	15.93		
					13.58	33.78	21.58		
Rougemont W/C Class B			89.22	10.82	40.61	19.24			
				10.82	40.61	19.24			
Steerpoint S/P			48.61	10.89	17.79	11.10			
				8.27	17.44	10.27			
2762x1350x229	Steerpoint W/C		57.36	9.86	25.51	13.27		12.1	
				10.14	25.58	13.10			
	Hurworth			39.85	18.55	20.82	16.00		
					19.86	25.72	17.17		
					22.34	22.27	15.24		
	Kibbleworth			67.15	12.48	27.96	18.55		
					13.51	28.58	17.58		
					14.62	22.37	12.55		
	Coatham Stob			33.30	14.41	22.82	14.34		
					17.65	16.55	14.89		
					15.38	13.38	12.48		
	2515x1381x222	Jacobean Mixed Darks Solids		56.12	16.48	19.86	16.89		11.3
19.37					17.10	18.20			
14.62					26.48	16.96			
2515x1350x216	Caornarvon Common 3-holes		47.99	19.44	21.51	16.41		11.6	
				19.03	18.48	17.37			
				16.41	22.48	16.96			

Table A6 - Strength of bonded walls with mortar designation M(i).  
(after Foster<sup>[12]</sup>).

Dimensions in (mm)		Mortar mix	Strength (Nmm <sup>-2</sup> )				Age (days)	h/t ratio
Wall (h x l x t)	Brick (h x l x t)		Brick	Mortar	Prism	Wall		
2440x610x112.5	69x238x112.5	1:5:4.5	91.84	8.33 8.33 7.08 7.08 11.39		26.26 24.58 26.06 25.99 25.72	28	19.2
400x238x112.5 5-brick high running bond	69x238x112.5	1:5:4.5	91.85	8.80	31.75 <sup>*</sup> 32.67 30.14 31.47 30.70		28	3.2
400x238x112.5 5-brick high stack bonded	69x238x112.5	1:5:4.5	91.84	8.80	32.87 <sup>**</sup> 30.96 33.17 29.89 31.01		28	3.2

\* 5-brick high running bond prism

\*\* 5-brick high stack bond prism

Table A7 - Results of wall columns and 5-brick high prisms.  
(after SCPRF<sup>(15)</sup>).

Dimensions in (mm)		Mortar mix	Strength (Nmm <sup>-2</sup> )				Age (days)	h/t ratio
Wall (h x l x t)	Brick (h x l x t)		Brick	Mortar	Prism	Wall		
2375x600x100	55x206x92	1:5:4.5	110.96	11.69 11.69 9.20 9.20 9.20		35.18 37.54 38.14 39.69 39.91	28	26.1
985x600x100	57x200x89		73.85	7.94 7.94 7.94 7.94		35.78 31.10 33.93 29.90 34.57		10.9
1550x600x100	57x200x89		73.85	8.36 8.36 8.36 8.36 9.22		-- 33.17 28.52 33.16 29.98		17.4
2375x600x100	57x200x89		73.85	8.82		32.40 30.96 30.63 27.64 27.02		26.8
3025x600x100	57x200x89		73.85	8.98 8.98 9.71 9.71 10.47		31.56 31.49 26.77 26.98 29.94		34.1
3675x600x100	57x200x89		73.85	8.85 7.66 8.14 10.16 8.74		28.00 24.04 20.96 23.87 25.27		41.3
4550x600x100	57x200x89		73.85	9.51 7.80 7.59 7.12 11.65		19.04 15.80 17.78 21.74 21.07		51.3
2375x600x100	55.5x194x90.5		43.48	10.50 10.50 10.50 11.67 10.78		19.66 25.92 24.84 23.19 20.88		26.3
400x200x100 6-brick high running bond	57x200x89		73.85		43.04* 37.72 43.77 40.54 39.51**			4.0
400x200x100 6-brick high stack bond	57x200x89		73.85		45.76** 40.97 42.37 42.98 35.75***			4.0
400x600x100 6-brick high 3-stretchers long pier	57x200x89		73.85		37.67 42.72 36.12 40.91 45.96			4.0

\* 6-brick high running bonded prism

\*\* 6-brick high stack bonded prism

\*\*\* 6-brick high 3-stretchers long pier

Table A8 - Results of Wall columns, piers and prisms.  
(after SCPRF<sup>(16)</sup>).

Dimensions in (mm)		Mortar mix	Strength (Nmm <sup>-2</sup> )				Age (days)	h/t ratio
Wall (h x l x t)	Brick (h x l x t)		Brick	Mortar	Prism	Wall		
966x600x200* 15-courses high	55x200x89	1:5:4.5	81.81	13.47 11.40 11.40 11.32 11.32		29.72 36.07 33.81 -- 31.74	28	5.0
1866x600x200* 29-courses high				11.01 9.65 10.65 11.87 10.95		33.00 29.81 33.29 33.83 31.28		9.6
2447x600x200* 38-courses high				9.36 13.27 9.81 17.14 10.67		30.51 30.61 29.85 31.87 31.86		12.8
3025x600x200* 47-courses high				11.91 12.82 11.14 11.42 10.84		32.56 32.42 31.90 32.78 33.94		15.6
3990x600x200* 62-courses high				11.20 9.46 8.54 8.94 10.60		29.34 31.36 30.80 33.01 30.96		20.6
4572x600x200* 71-courses high				8.86 10.07 7.50 9.80 6.44		29.19 29.67 27.74 28.79 27.08		23.6
3990x600x200** 62-courses high				10.24 10.32 9.44		29.85 30.64 26.95		20.6
2222x610x92.2 <sup>+</sup>	57x203x92		85.50	11.50	30.20 <sup>#</sup> 28.06 29.51	20.62 21.17 23.79		24.1

\* metal ties every 6 courses

\*\* header at every 6 courses

# 6-brick high stack bonded prisms at h/t=4.32

+ results from Reference 65D

Table A9 - Results of wall columns and prisms.  
(after SCPRF<sup>[17,18]</sup>).



Dimensions in (mm)		Mortar mix	Strength (Nmm <sup>-2</sup> )				Age (days)	h/t ratio
Wall (h x l x t)	Brick (h x l x t)		Brick	Mortar	Prism <sup>*</sup>	Wall		
533x400x200 metal ties at 6-courses	55.5x194x90.5	1:5:4.5	43.48	10.83	24.76	28	2.7	
				10.83	25.87			
				10.31	26.89			
				10.31	26.27			
				10.31	26.55			
brick header at 7-courses				10.31	27.88			
				10.87	30.79			
				10.87	27.33			
				10.87	28.74			
				10.87	24.75			
metal ties at 6-courses	55x200x89		81.81	8.76	33.31			
				8.76	31.03			
				10.56	32.22			
				10.56	32.19			
				10.56	32.16			
brick header at 7-courses				10.56	30.50			
				8.76	36.24			
				8.76	34.74			
				8.76	33.95			
				8.76	33.02			
metal ties at 6-courses	57x206x92		110.96	6.97	38.58			
				6.97	38.25			
				6.97	34.04			
				6.97	33.02			
				8.31	40.52			
brick header at 7-courses				8.31	38.16			
				8.31	36.50			
				8.31	38.42			
				8.76	37.14			
				8.76	34.18			
533x400x100	55.5x194x90.5	1:5:4.5	43.48	11.17	31.63 <sup>#</sup>			
					31.32			
					28.85			
					32.83			
					30.85			
	55x200x89			81.81	8.76	34.08		
						37.10		
						36.73		
	57x206x92			110.96	10.83	33.68		
						33.75		
						38.40		
						43.67		
					40.18			
					34.66			
					43.93			

\* bonded double wythe, 2-stretchers in length and 8-courses high prism

# single leaf, 2-stretchers in length and 8-courses high prism

Table A10 - Results of single and double wythe bonded prisms.  
(after SCPRF<sup>[18]</sup>).

Dimensions in (mm)		Mortar mix	Strength (Nmm <sup>-2</sup> )				Age (days)	h/t ratio
Wall (h x l x t)	Brick (h x l x t)		Brick	Mortar	Prism	Wall		
2450x900x112.5	72x225x112.5	1:1:6	38.89	8.04		6.31	28	21.8
				6.52		14.07		
				0.55		4.55		
			51.71	13.51		14.34		
				6.52		17.79		
				4.34		14.82		
(1)		1:1:6	38.89	8.28		15.20	28	21.8
(2)		1:0:3	38.89	14.07		13.42		
(3)		1:0:3	38.89	9.31		>21.37	28	21.8
(4)		1:0:2	33.94	16.41		20.06		
(5)		1:0:1	33.94	15.44		14.74		
(6)		1:0:3	33.94	6.76		10.89		

- (1) vertical chase 1050x19x12.5 deep, axial loading + 0.21 Nmm<sup>-2</sup> superimposed.  
(1) vertical chase 1050x19x12.5 deep, axial loading + 0.55 Nmm<sup>-2</sup> superimposed.  
(3) reinforced 1-course every 1-course  
(4) reinforced 1-course every 3-courses  
(5) reinforced 1-course every 4-courses  
(6) reinforced 1-course every 5-courses

Table A11 - Results of single leaf walls.  
(after Prasan<sup>[19]</sup>).

Dimensions in (mm)		Mortar mix	Strength (Nmm <sup>-2</sup> )				Age (days)	h/t ratio
Wall (h x l x t)	Brick (h x l x t)		Brick	Mortar	Prism	Wall		
(2)	2450x900x112.5 standard	1:1:6	33.27	4.55		5.76	38	21.8
		1:0:3	42.99	13.89		11.24	46	
		1:0:3	42.99	10.93		12.34	18	
		1:0:3	42.99	10.62		14.55	18	
		1:0:3	42.99	16.89		16.89	78	
		1:0:3	42.99	5.96		16.06	2	
		1:0:3	42.99	16.10		18.41	18	
(1)		1:0:3	42.99	4.83		16.00	7	
		1:0:3	42.27	15.41		21.37	148	
(3)		1:0:3	42.99	5.27		11.24	7	
		1:0:3	42.27	4.79		14.03	8	
		1:0:3	25.58	5.55		8.72	19	
		1:0:3	25.58	5.31		7.48	7	
		1:0:3	25.58	6.48		7.17	13	

- (1) reinforced every second course  
(2) joint thickness = 5mm  
(3) 19mm off plumb

Table A12 - Results of single leaf walls.  
(after Bradshaw & Hendry<sup>[20]</sup>)

Dimensions in (mm)		Mortar mix	Strength (Nmm <sup>-2</sup> )				Age (days)	h/t ratio
Wall (h x l x t)	Brick (h x l x t)		Brick	Mortar	Prism	Wall		
2490x900x225	66x225x102.5	1:1:6	25.58	3.41		5.00	28	11.0
			29.37	7.86		6.38		
			32.96	7.55		6.14		
2490x900x267*			25.58	2.31		5.31		9.3
			25.58	4.62		5.90		
			47.26	16.27		11.96		
			29.96	8.38		8.48		
			29.96	7.58		5.21		
			29.96	7.58		4.45		

\* cavity walls 267mm thickness.

Table A13 - Strengths of bonded and cavity walls.  
(after Bradshaw & Hendry<sup>[21]</sup>).

Dimensions in (mm)		Mortar mix	Strength (Nmm <sup>-2</sup> )				Age (days)	h/t ratio
Wall (h x l x t)	Brick (h x l x t)		Brick	Mortar	Prism	Wall		
2400x1200x112.5	Solid bricks of standard shape (with & without frogs)	1:0:3	12.82	18.62		8.84	30	21.3
			20.68	16.55		8.62		
			24.13	15.17		9.31		
			32.41	--		9.31		
			30.68	12.41		9.31		
		1:25:3	21.10	16.27		5.9	30	
				15.44		7.31		
			21.37	17.65		8.55		
			22.06	13.79		7.45		
1:1:6			24.13	6.89			10.00	
							8.55	
							9.58	
							9.38	
							9.86	
2400x1200x225		1:0:3	12.82	24.13		6.76		10.7
			24.13	--		9.93		
			24.13	--		9.72		
			26.20	22.06		8.89		
			31.51	15.86		9.38		
			29.72	13.79		9.65		
			84.12	14.00		20.55		
		1:25:3	54.12	19.99		17.58	21	
			54.12	19.99		18.96		
			84.12	14.00		24.13		
			84.12	14.00		24.13		
			84.12	14.00		24.27		
			84.12	14.00		24.27		
			84.12	14.00		24.27		
2400x1200x103	Solid bricks with (vertical perfs. not more than 25%)	1:0:3	9.86	15.65		8.27	7	23.3
			19.17	15.86		9.72		
		1:1:3	29.51	14.20		11.10	30	
			29.51			10.34		
			40.95			9.24		
			40.95			12.82		
			46.82			12.20		
		1:1:6	46.82			14.07		
			29.51	4.41		10.82		
			29.51			8.34		
			40.95			10.34		
			40.95			7.58		
			46.82			9.72		
			46.82			9.79		
2400x1200x225		1:0:3	19.17	12.07		10.55	7	10.7
			12.07			10.55		
		1:25:3	60.12	13.38		17.72	21	
			60.12	14.82		20.27		
			60.12	13.51		19.37		
			87.56	14.96		22.61		
			87.56	12.82		25.72		
			87.56	12.82		25.30		

Table A14 - Results of single leaf and bonded walls.  
(after Simms<sup>[22]</sup>).

Dimensions in (mm)		Mortar mix	Strength (Nmm <sup>-2</sup> )				Age (days)	h/t ratio
Wall (h x l x t)	Brick (h x l x t)		Brick	Mortar	Prism	Wall		
2625x1387x112.5	75x225x108	1:5:4.5	65.50	12.19		13.79	41	23.3
			65.50	12.19		11.03	37	
			58.50	16.17		11.03	36	
			58.50	16.17		19.31	40	

Table A15 - Results of single leaf walls with mortar designation M(II).  
(after McDowall<sup>[23]</sup>).

Dimensions in (mm)		Mortar mix	Strength (Nmm <sup>-2</sup> )				Age (days)	h/t ratio
Wall (h x l x t)	Brick (h x l x t)		Brick	Mortar	Cube	Wall		
2515x1372x225	65x215x102.5	1:1:6	20.62	5.24	6.62	5.31	28	11.2
			20.62	5.24	7.72	5.65		
			26.34	7.79	9.65	5.17		
			26.34	7.79	--	5.45		
			31.58	4.96	20.48	10.62		
			31.58	4.96	--	11.58		
			33.09	7.58	10.27	6.96		
			33.09	7.58	--	7.45		
			33.58	6.96	10.41	7.65		
			33.58	6.96	--	7.24		
			35.09	5.52	6.05	6.14		
			35.09	5.52	6.04	6.14		
			37.85	7.52	9.31	4.96		
			37.85	7.52	7.65	4.96		
			39.23	6.76	10.00	6.14		
			39.23	6.76	6.79	4.76		
			42.82	6.96	13.51	7.24		
			42.82	6.96	14.48	8.14		
			48.68	6.55	21.65	9.79		
			48.68	6.55	18.48	9.31		
			76.19	3.72	24.82	12.55		
			76.19	3.72	19.44	11.72		
		1:25:3	57.36	17.31	24.13	13.24		
			57.36	17.31	25.58	13.03		
			86.74	19.31	42.89	16.20		
			86.74	19.31	--	15.86		
			89.22	18.13	33.79	21.51		
			89.22	18.13	40.61	19.17		
			48.61	19.72	17.79	11.10		
			48.61	19.72	17.44	10.27		

Table A16 - Strengths of bonded walls and 9-in. cubes.  
(after Stedham<sup>[24]</sup>).

Dimensions in (mm)		Mortar mix	Strength (Nmm <sup>-2</sup> )				Age (days)	h/t ratio
Wall (h x l x t)	Brick (h x l x t)		Brick	Mortar	Cube	Wall		
2540x1372x105	65x215x102.5 Solid brick	1:25:3	104.25	11.10	50.50	23.86	14	24.0
				11.24	49.50	26.06		
				17.93	46.26	30.20		
	3-holes		82.05	11.62	31.44	19.99		
				13.08	31.78	22.55		
				12.48	32.54	21.37		
	11-holes		80.53	16.55	30.47	18.82		
				16.79	29.92	18.13		
				14.89	33.37	19.37		
	Solid brick		82.60	13.82	45.78	21.37		
				14.62	39.58	21.79		
				13.38	38.89	23.51		
	3-holes		97.22	12.82	31.54	19.03		
				14.89	31.03	19.58		
				16.55	43.89	21.37		
	11-holes		79.57	17.80	24.98	17.44		
				22.10	27.83	16.48		
				26.41	29.43	17.31		
	Solid brick		90.05	14.41	40.89	24.27		
				13.17	44.20	23.51		
16.41		40.06		22.48				
3-holes	89.70	8.14	35.23	23.65				
		12.20	36.75	24.41				
		14.89	42.75	27.10				
7-slots	55.85	14.69	27.03	18.00				
		17.03	22.48	16.62				
		16.96	23.79	19.03				
16-holes	70.81	8.89	27.79	18.82				
		13.38	20.89	16.69				
		14.41	25.03	17.31				
3-holes	80.53	12.96	40.27	21.65				
		9.83	37.23	20.62				
		10.96	39.51	21.99				
7-slots	62.47	15.17	23.86	21.37				
		11.93	27.23	21.99				
		14.20	22.89	19.37				
14-holes	65.57	11.27	26.82	18.68				
		10.41	23.58	20.13				
		10.00	24.41	17.65				
Solid brick	41.78	14.20	24.34	19.03				
		10.62	23.92	20.06				
		10.20	18.20	18.20				
3-holes	48.13	12.96	19.72	16.20				
		13.79	22.61	15.93				
		12.55	16.27	16.27				
16-holes	44.33	11.89	25.86	17.65				
		10.62	23.99	14.20				
		10.89	22.20	13.93				

Table A17 - Results of single leaf walls with mortar designation M(I).  
(after West *et al* <sup>[30]</sup>).

Dimensions in (mm)		Mortar mix	Strength (Nmm <sup>-2</sup> )				Age (days)	h/t ratio
Wall (h x l x t)	Brick (h x l x t)		Brick	Mortar	Cube	Wall		
2540x1372x105	65x215x102.5 Solid brick	1:25:3	45.78	15.44 14.34 16.06	24.96 20.27 24.34	19.44 17.72 14.13	14	24.0
	3-holes		52.26	17.72 19.44 18.55	20.34 22.06 18.41	15.36 13.93 17.86		
	5-slots		40.20	13.03 12.13 16.48	20.68 15.24 15.51	15.79 16.34 14.96		
	Solid brick		31.58	12.03 19.00 13.13	10.51 16.75 17.41	13.17 12.96 12.34		
	3-holes		51.43	18.62 10.89 13.65	20.86 14.27 12.89	13.65 9.86 9.79		
	14-holes		30.20	18.13 16.27 15.79	14.89 9.58 13.76	13.79 13.10 12.72		
	Solid brick		85.84	10.79 12.89 16.13	42.75 45.85 47.30	34.13 34.47 27.30		
	16-holes		60.26	14.00 10.93 9.00	24.89 22.48 27.48	20.06 19.03 20.41		
	Solid brick	1:1:6	104.25	5.16 4.07 5.24	46.88 44.61 41.58	19.03 17.31 20.06		
	3-holes		82.05	4.94 4.87 6.23	27.23 31.44 33.16	16.41 15.03 15.31		
	Solid brick		82.60	4.72 6.72 5.24	35.51 37.09 32.54	18.96 18.89 18.55		
	3-holes		97.22	3.90 4.14 6.62	29.20 34.96 27.68	12.82 12.76 16.89		
	11-holes		79.57	6.81 3.72 7.04	22.59 23.39 25.79	12.58 11.50 12.86		
	11-holes		80.53	5.24 5.30 4.74	23.10 26.41 29.65	8.76 10.96 8.07		
	Solid brick		90.05	5.15 4.39 4.14	42.26 40.95 41.51	15.38 13.24 15.79		
	3-holes		89.70	4.69 3.63 3.34	42.33 37.30 36.03	16.82 16.62 18.00		

Table A18 - Results of single leaf walls with mortar designation M(i) & M(iii).  
(after West *et al* <sup>[30]</sup>).

Dimensions in (mm)		Mortar mix	Strength (Nmm <sup>-2</sup> )				Age (days)	h/t ratio
Wall (h x l x t)	Brick (h x l x t)		Brick	Mortar	Cube	Wall		
2540x1372x105	65x215x102.5 7-slots	1:1:6	55.85	5.40	19.62	13.10	14	24.0
				3.99	15.10	10.96		
				4.46	19.86	12.34		
	16-holes		70.81	3.79	17.86	10.14		
				5.25	17.58	11.93		
				5.83	19.72	10.82		
	3-holes		80.53	3.76	34.68	14.00		
				4.59	39.09	15.86		
				4.23	39.16	14.48		
	7-slots		62.47	6.33	20.13	14.89		
				5.11	22.06	15.24		
				5.39	20.62	16.34		
	14-holes		65.57	3.46	19.03	12.00		
				3.11	20.89	11.65		
				2.90	22.48	13.24		
	Solid brick		41.78	5.62	20.82	16.06		
				4.80	22.68	16.00		
				4.52	21.79	14.62		
	3-holes		48.13	5.45	16.41	10.55		
				4.99	18.48	10.96		
5.78		18.55		11.24				
16-holes	44.33	4.60	20.13	9.51				
		5.32	20.86	9.17				
		5.09	19.68	10.51				
Solid brick	45.78	6.87	24.34	18.48				
		5.81	19.93	16.06				
		7.58	21.41	17.10				
3-holes	52.26	4.08	13.93	11.45				
		7.08	12.13	11.10				
		6.21	17.79	10.62				
5-slots	40.20	5.86	11.10	11.31				
		4.42	12.55	12.89				
		6.34	13.86	12.27				
Solid brick	31.58	5.16	12.38	10.07				
		6.48	17.10	10.41				
		7.36	15.31	10.27				
3-holes	51.43	7.14	20.17	10.20				
		3.76	18.89	10.89				
		5.53	18.89	11.62				
14-holes	30.20	4.80	9.45	8.48				
		4.56	10.89	8.41				
		12.43	9.69	9.86				
Solid brick	85.84	7.32	38.82	25.92				
		6.31	43.30	24.55				
		4.01	43.16	22.48				
16-holes	60.26	3.00	20.82	16.34				
		5.39	21.75	16.00				
		5.62	22.06	15.31				

Table A19 - Results of single leaf walls with mortar designation M(iii).  
(after West *et al* <sup>[30]</sup>).



Dimensions in (mm)		Mortar mix	Strength (Nmm <sup>-2</sup> )				Age (days)	h/t ratio				
Wall (h x l x t)	Brick (h x l x t)		Brick	Mortar	Cube	Wall						
2540x1372x225	Wire cut perforated standard bricks	1:25:3	61.23	12.76	21.86	12.89	28	11.1				
				13.24	17.86	13.27						
				13.58	21.79	11.40						
				12.34	21.79	12.96						
				12.62	20.89	11.27						
				11.58	19.24	10.83						
				12.07	20.00	11.38						
				12.82	19.79	11.96						
				11.65	20.13	13.10						
				16.69	16.62	11.55						
				11.58	19.17	12.24						
				11.03	19.93	12.41						
				10.76	20.20	10.17						
				10.41	19.65	13.03						
				11.45	20.34	12.82						
			12.48	20.34	12.27							
			12.82	17.72	11.86							
			12.07	19.44	12.41							
			10.96	23.79	10.83							
			10.41	21.51	12.27							
			61.50				21.03	20.53	12.14			
							16.00	18.75	12.96			
							19.65	25.17	16.20			
							18.82	24.82	14.55			
							9.83	21.05	14.27			
							9.72	20.06	12.96			
			41.09				13.47	14.25	11.12			
							15.58	12.73	10.27			
			23.44				14.98	11.54	8.83			
							32.48	12.41	12.14			8.27
							33.58	13.93	12.82			11.96
							33.51	16.34	14.73			11.10
							33.37	16.87	13.24			10.69
31.44	15.72	13.12					10.83	46				
30.48	6.38	12.07					8.55	41				
31.17	7.10	9.60					7.58	28				

Table A20 - Results of bonded wall with mortar designation M(i).  
(reported by Astbury & West <sup>[32]</sup>).

Dimensions in (mm)		Mortar mix	Strength (Nmm <sup>-2</sup> )				Age (days)	h/t ratio			
Wall (h x l x t)	Brick (h x l x t)		Brick	Mortar	Cube	Wall					
2540x1372x105	65x215x102.5	1:25:3	122.80	2.12	44.75	23.79	14	24.0			
				11.72	29.51	19.24					
				11.20	41.99	20.20					
			80.53				16.55	30.47	18.82		
							16.79	29.92	18.13		
							14.89	33.37	19.37		

Table A21 - Results of single leaf walls with mortar designation M(i).  
(after West *et al* <sup>[33]</sup>).

Dimensions in (mm)		Mortar mix	Strength (Nmm <sup>-2</sup> )				Age (days)	h/t ratio
Wall (h x l x t)	Brick (h x l x t)		Brick	Mortar	Prism*	Wall		
2600x1370x103	65x215x102.5	1:25:3	33.50	18.08	19.0	22.4	28	25.0
				17.16	18.8	20.7		
				15.12	22.0	23.7		
			44.80	14.35	18.6	23.0		
				12.00	16.3	23.3		
				15.30	18.3	21.5		
			22.60	14.72	12.2	16.2		
				15.41	12.3	15.5		
				16.38	12.1	15.8		
		28.80	16.41	16.5	20.0			
			17.60	18.3	21.5			
			18.81	16.6	20.3			
		1:1:6	16.30	4.73	7.6	9.9		
				4.85	7.9	10.4		
				5.78	7.4	9.7		
			32.80	3.33	11.5	11.4		
				3.37	10.2	9.9		
				3.41	10.3	10.6		
			27.00	3.53	11.8	12.6		
				3.25	12.4	11.6		
				3.93	13.4	12.5		
			38.30	3.99	10.4	12.5		
				3.91	11.3	14.7		
				3.44	9.5	14.3		
			33.50	4.58	18.4	13.1		
				4.42	13.7	12.7		
				4.07	16.1	14.3		
44.80	4.05		11.4	14.3				
	3.23		12.7	15.5				
	3.36		12.2	14.9				
58.3	4.68	14.0	12.5					
	4.67	14.6	12.1					
	4.66	14.5	13.8					
22.60	3.92	11.7	11.0					
	4.00	11.6	11.8					
	3.89	10.4	11.5					
28.80	4.58	12.7	13.1					
	5.11	12.1	13.4					
	4.35	11.8	12.9					
1:2:9	33.50	2.74	12.9	10.9				
		1.94	14.0	10.1				
		1.72	14.1	10.8				
	44.80	1.66	11.0	12.0				
		1.59	9.8	12.3				
		1.72	11.8	12.2				
22.60	1.79	7.6	9.1					
	1.46	7.4	8.7					
	1.50	8.0	8.2					

\* 5-brick high stack bond prism.

Table A22 - Results of the strength of Calcium Silicate Brick walls.  
(after West *et al* <sup>[34]</sup>).

Dimensions in (mm)		Mortar mix	Strength (Nmm <sup>-2</sup> )				Age (days)	h/t ratio	
Wall (h x l x t)	Brick (h x l x t)		Brick	Mortar	Prism*	Wall			
2600x1370x103	65x215x102.5	1:25:3	31.80	14.3	14.6	14.9	14	25.0	
				11.6	11.7	15.8			
				10.9	11.5	17.4			
				14.0	12.7	14.6			
				13.1	13.4	15.8			
				12.6	13.8	15.0			
		1:1:6	31.80	31.80	3.4	10.5	10.0	14	
					3.5	9.1	9.3		
					2.9	9.6	8.5		
					3.1	11.2	12.1		
					3.5	10.6	11.8		
					3.6	10.2	13.3		
					5.1	13.0	15.8		
					3.7	13.6	16.6		
					4.2	12.9	15.8		
4.3	13.9	17.4							
1:2:9	31.80	31.80	1.2	8.3	8.8	14			
			1.3	7.5	8.4				
			1.5	8.4	9.9				
			1.6	8.1	8.1				
			2.3	7.6	9.9				
			1.3	7.1	9.0				

\* 5-brick high stack bond prism.

Table A23 - Results of the strength of Calcium Silicate Brick walls.  
(after West *et al* <sup>[34]</sup>).

Dimensions in (mm)		Mortar mix	Strength (Nmm <sup>-2</sup> )				Age (days)	h/t ratio
Wall (h x l x t)	Brick (h x l x t)		Brick	Mortar	Prism <sup>*</sup>	Wall		
2667x1388x115	standard	1:1:6	91.70	4.00	33.16	18.48	28	23.2
			88.25		32.47			
			68.26		21.51			
			57.92		23.17			
			108.94		34.61			
			132.38		38.82			
		1:1:6	91.70	4.21	38.47	28		
			88.25	4.07	28.61			
			68.26	4.27	24.61			
			58.61	4.34	19.92			
			57.92	3.59	22.55			
			108.94	3.86	42.75			
			132.38	4.55	40.82			
			41.02	3.93	23.85			
			39.44	3.79	21.37			
			68.95	4.27	31.03			
			43.71	3.72	28.20			
			77.91	3.79	27.72			
			72.39	4.41	32.75			
			21.10	3.72	14.55			
44.13	4.21	27.65						
75.15	4.21	28.48						
60.40	5.58	27.79						
33.92	3.31	22.68						
32.54	4.14	20.89						
96.53	3.93	36.54						
99.28	4.21	32.85						
55.71	3.93	30.75						
54.40	3.38	31.16						
46.95	4.34	25.51						
34.34	3.86	16.34						

\* 4-brick high stack bond prism.

Table A24 - Results of single leaf walls and stack bond prisms.  
(after Anderson<sup>[35]</sup>).

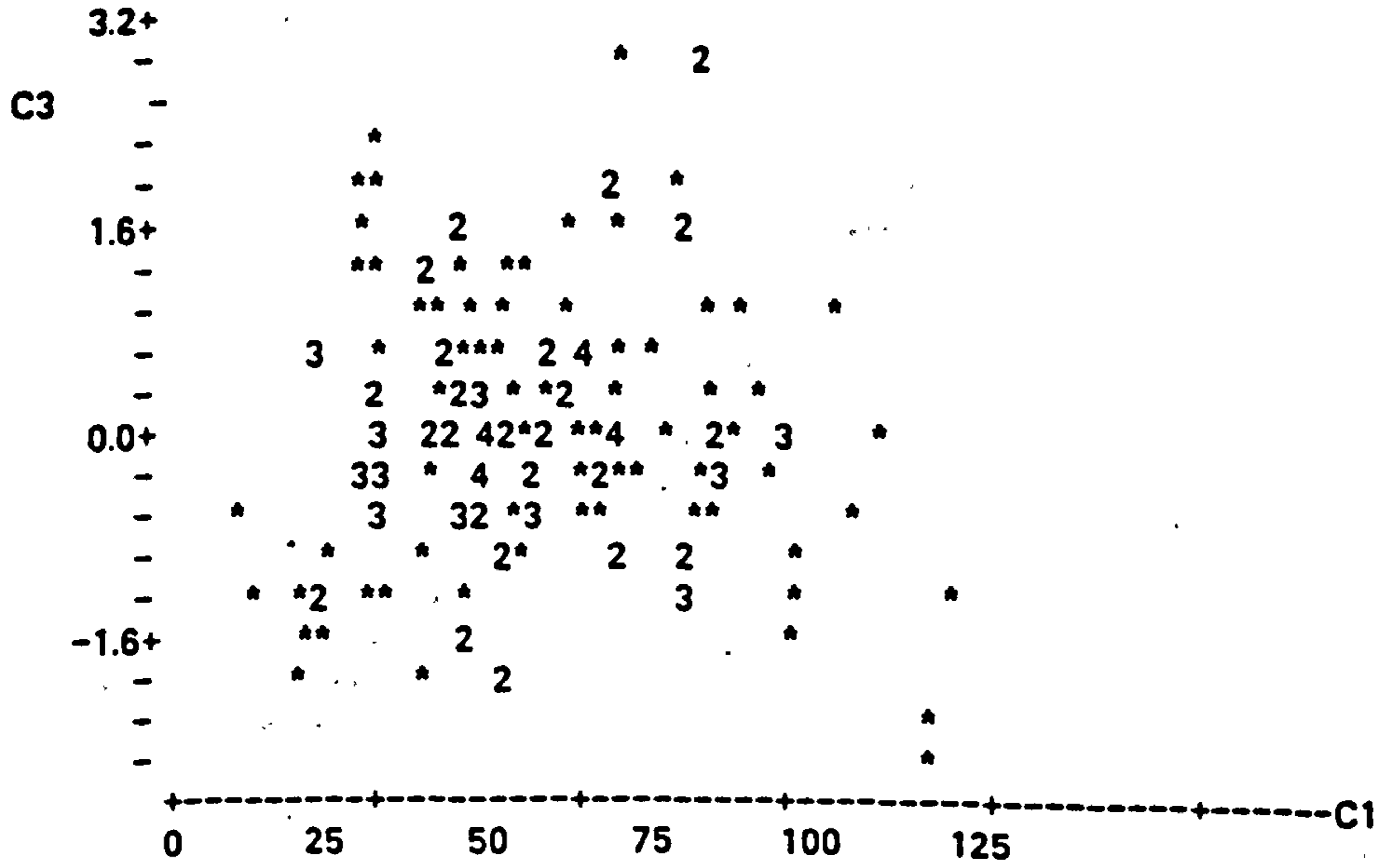
Dimensions in (mm)		Mortar mix	Strength (Nmm <sup>-2</sup> )				Age (days)	h/t ratio				
Wall (h x l x t)	Brick (h x l x t)		Brick	Mortar	Prism <sup>a</sup>	Wall						
2400x1400x105	75x225x106	1:1:6	68.60	4.10	25.51	15.17	28	22.9				
				5.14	23.24	15.88						
				4.10	23.06	18.55						
				3.76	26.30	18.06						
				64.84	5.96	28.17			15.10			
		0:1:5	68.60	0.48	11.45	6.62						
										4.96	28.54	17.86
										4.27	30.13	18.06
										3.93	27.48	18.48
2400x1400x150	75x228x150	1:1:6	47.16	3.90	18.20	15.44	28	16.0				
				47.16	3.62	22.89			14.96			
				50.06	3.93	20.55			17.31			
		2400x1400x105	75x225x108	1:1:6	66.12	3.59	26.92	22.55	28	22.9		
						3.65	26.23	20.82				
						3.83	28.61	22.75				
						82.05	4.10	26.58			21.17	
						3.96	28.06	21.51				
						4.00	20.00	19.03				
						3.96	24.79	20.75				
65.50	2.76	30.92	22.00	23.17								
								2.41	30.20	23.17		
2400x1400x225	75x225x108	1:1:6	65.50	2.69	31.51	21.44	28	10.7				
				2.83	31.30	21.31						
				3.03	30.54	19.03						
				2.76	32.10	18.48						
				3.03	32.03	19.03						
				3.31	35.72	18.89						
				3.03	32.13	19.44						
				2.76	33.20	20.27						
				2.69	32.86	19.10						
				2.90	33.03	20.55						
2400x1400x105	75x225x108	1:1:6	71.84	25.03	20.13	28	22.9					
				71.43	31.99			22.61				
				33.51	17.17			12.89				
				25.65	11.79			9.65				
		1:25:3	71.48	39.30	32.75							
		1:1:6	55.16	23.72								
										40.47	18.89	
										28.20	14.41	
										66.12	28.48	
55.92	27.58											
31.37	14.96											
1:25:3	66.12	44.88										
								66.12	38.82			
								64.81	40.95			
								55.92	34.47			

\* 4-brick high stack bond prism.

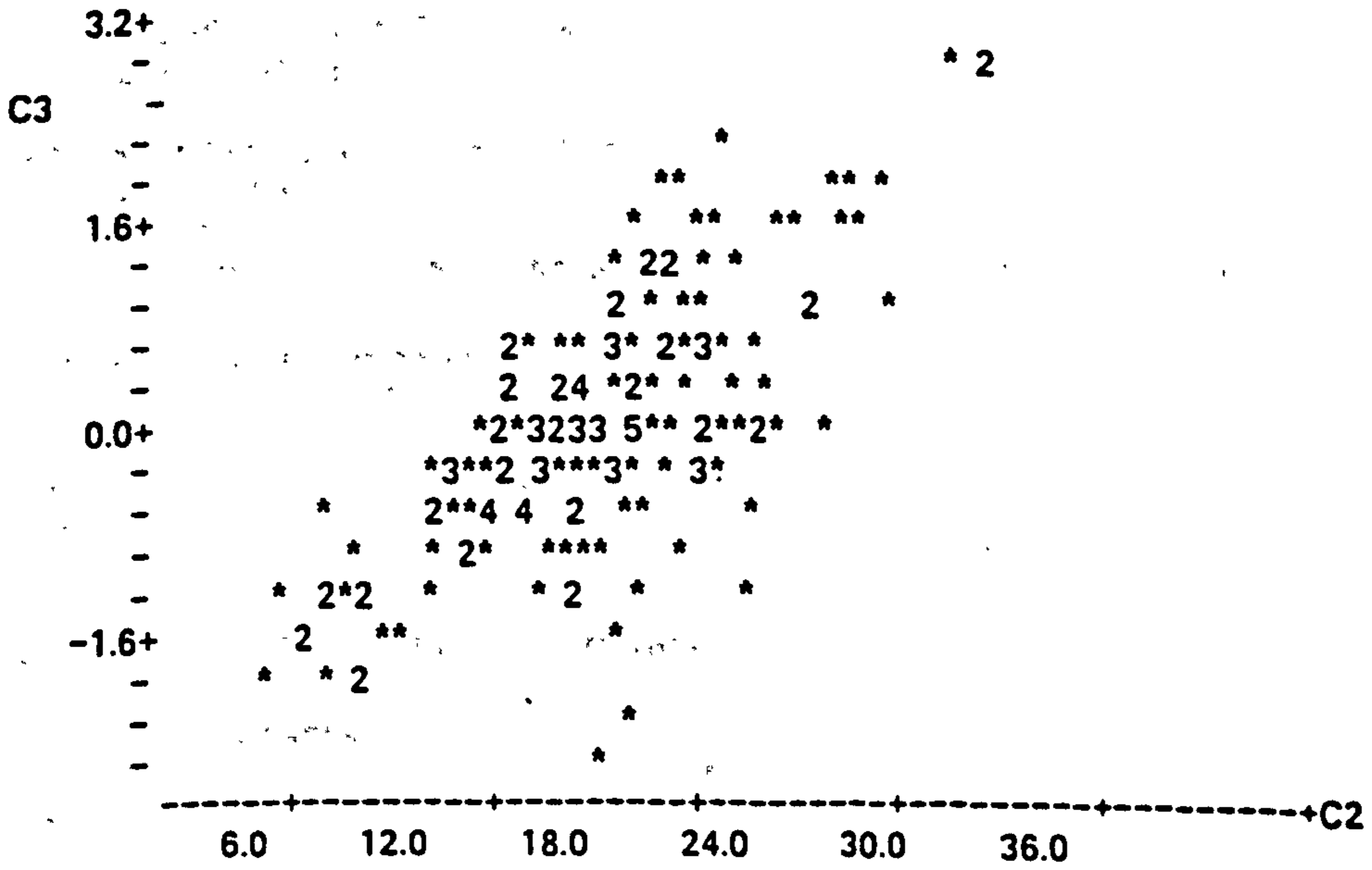
Table A25 - Results of walls and stack bond prisms.  
(after James<sup>[38,39,40,41,43,44,45]</sup>)



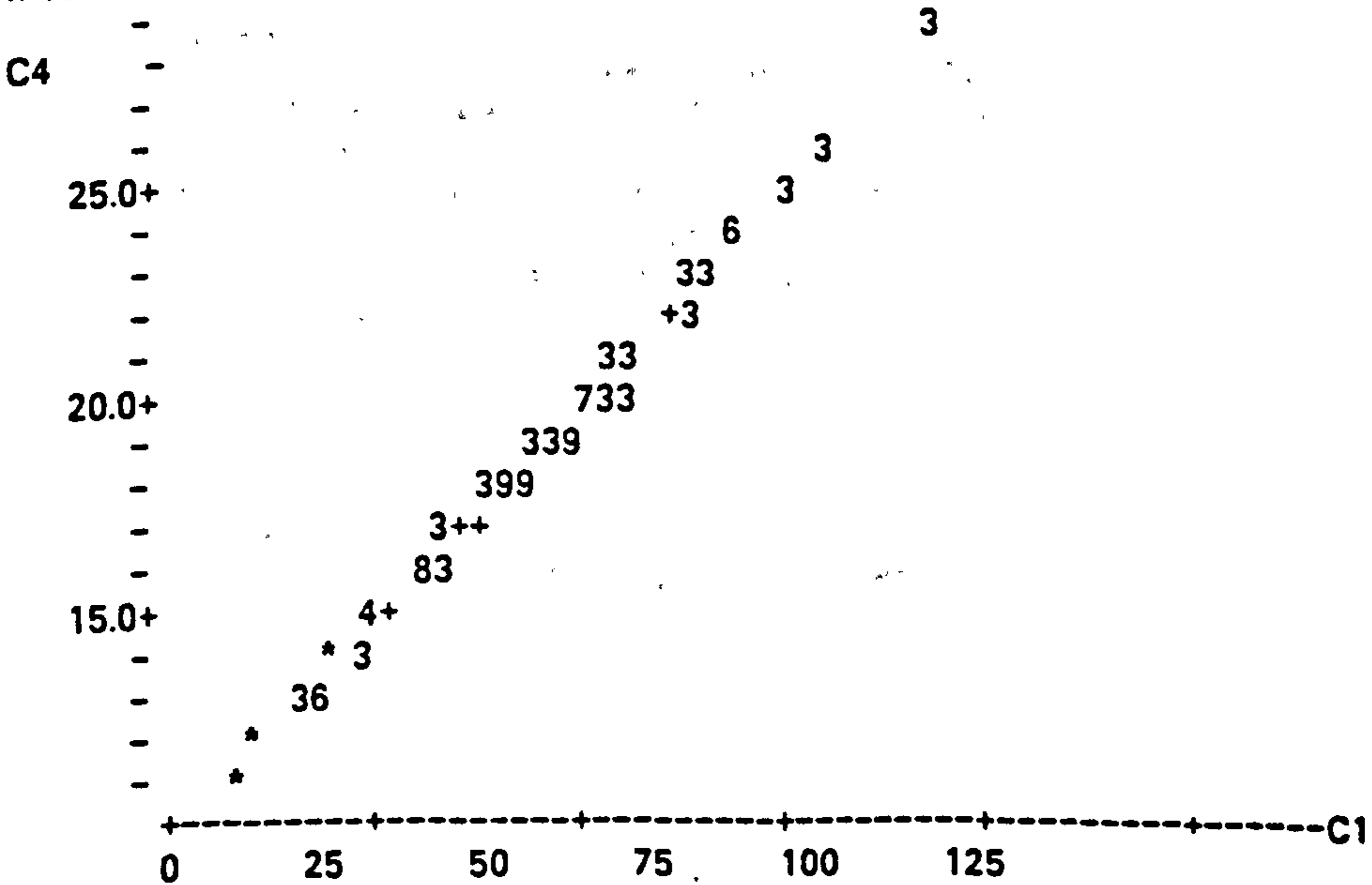
MTB > PLOT C3 C1



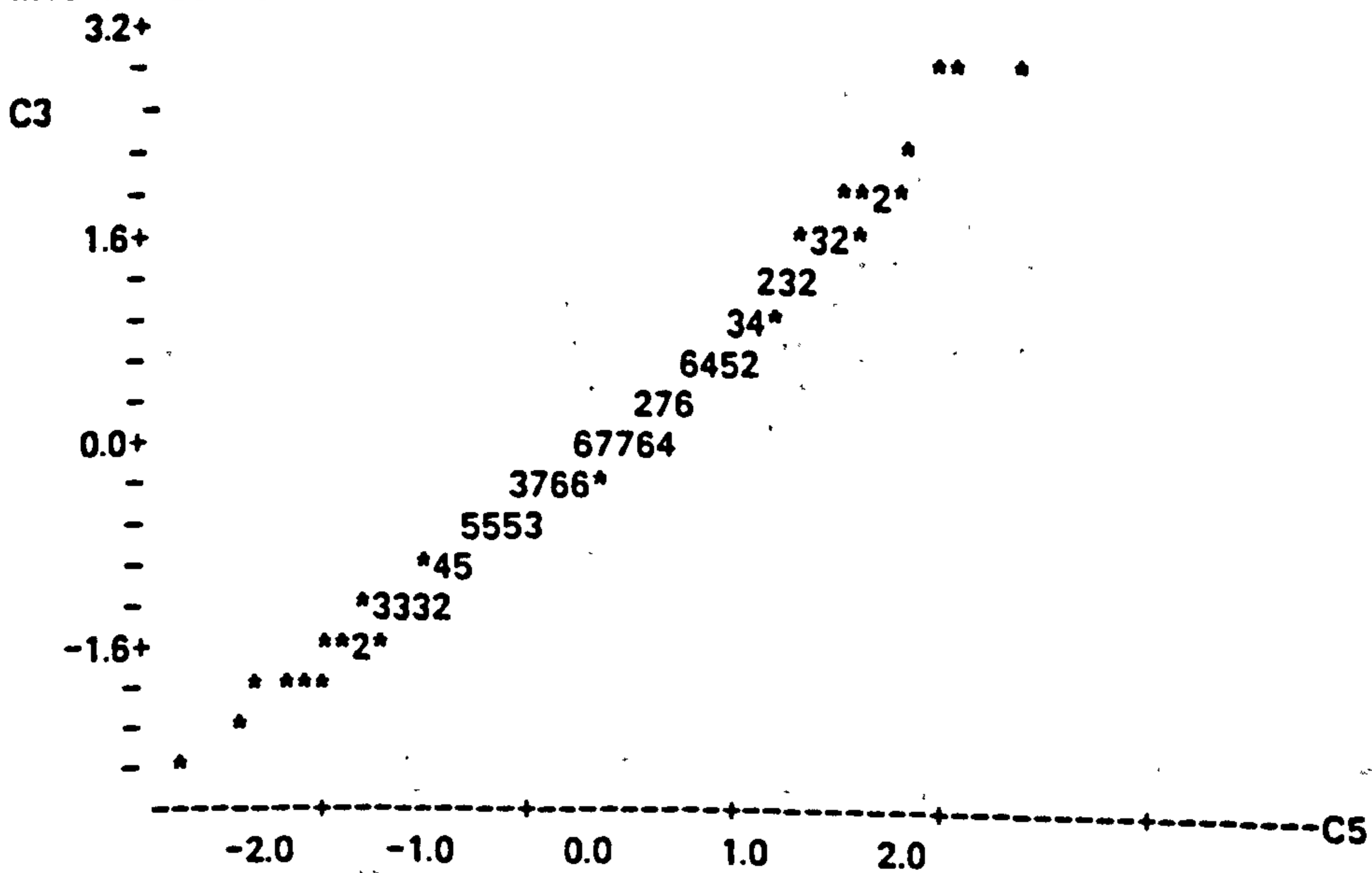
MTB > PLOT C3 C2



MTB > PLOT C4 C1



MTB > NSCOR C3 C5  
 MTB > PLOT C3 C5



MTB > CORRELATION OF C3 C5  
 Correlation of C3 and C5 = 0.993

MTB > NOTE\*\*\*LOGARITHMIC FIT\*\*\*  
 MTB > LET C80=LOGE(C1)  
 MTB > LET C81=C2  
 MTB > REGRESS C81 ON 1 PREDICTOR C80 RESIDS IN C83 FIT IN C84

The regression equation is  
 $C81 = -14.0 + 8.24 C80$

Predictor	Coef	Stdev	t-ratio
Constant	-14.003	2.720	-5.15
C80	8.2427	0.6866	12.01

s = 3.866      R-sq = 46.6%      R-sq(adj) = 46.3%

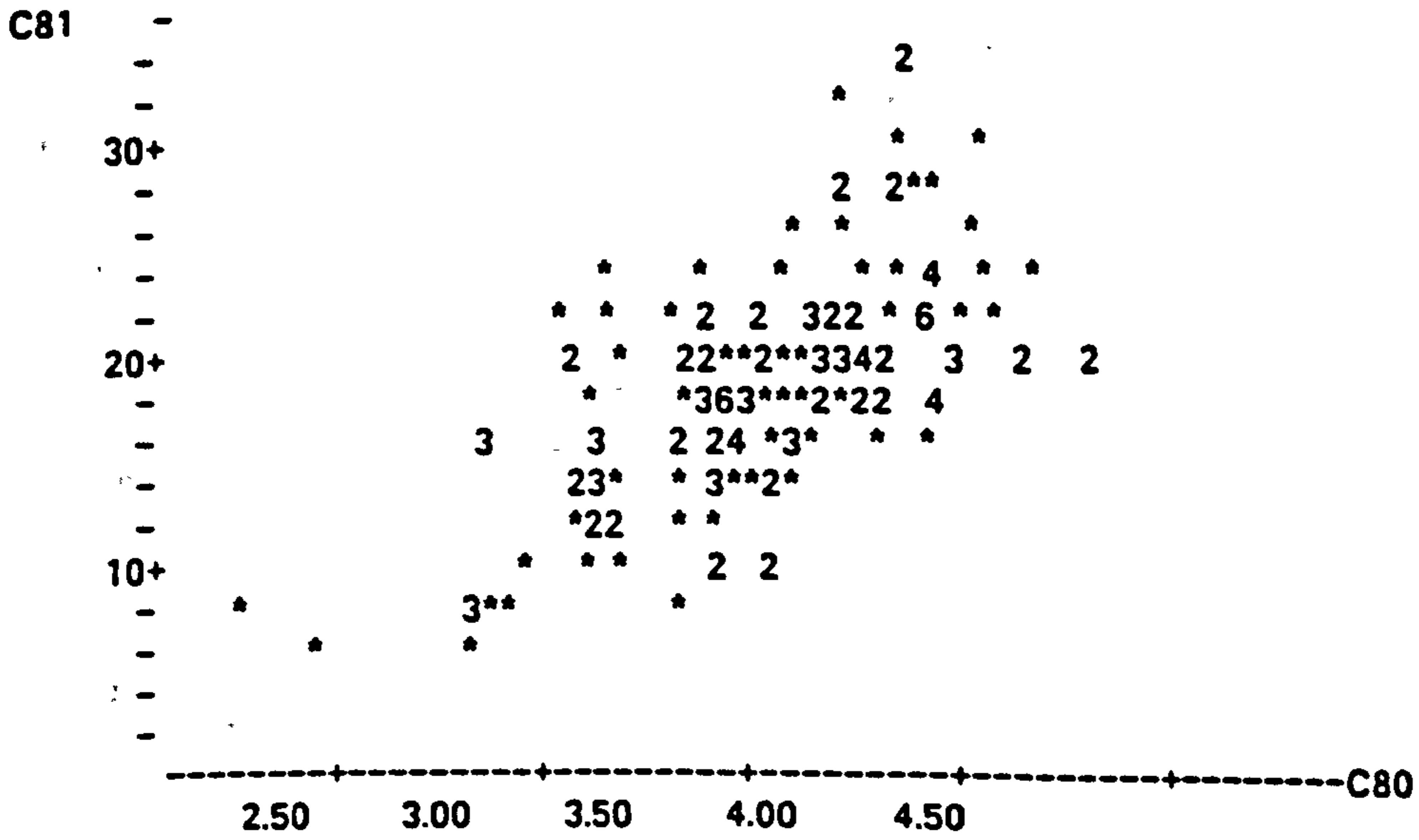
Analysis of Variance			
SOURCE	DF	SS	MS
Regression	1	2154.6	2154.6
Error	165	2466.7	14.9
Total	166	4621.2	

Unusual Observations						
Obs.	C80	C81	Fit	Stdev.Fit	Residual	St.Resid
1	2.29	8.270	4.860	1.171	3.410	0.93 X
2	2.55	6.840	7.024	0.998	-0.184	-0.05 X
14	3.36	21.500	13.695	0.496	7.805	2.04R
35	3.51	23.700	14.941	0.418	8.759	2.28R
80	3.94	9.860	18.475	0.299	-8.615	-2.23R
82	3.94	9.790	18.475	0.299	-8.685	-2.25R
123	4.23	28.680	20.883	0.361	7.797	2.03R
129	4.27	32.750	21.188	0.376	11.562	3.00R
151	4.45	34.130	22.697	0.463	11.433	2.98R
152	4.45	34.470	22.697	0.463	11.773	3.07R

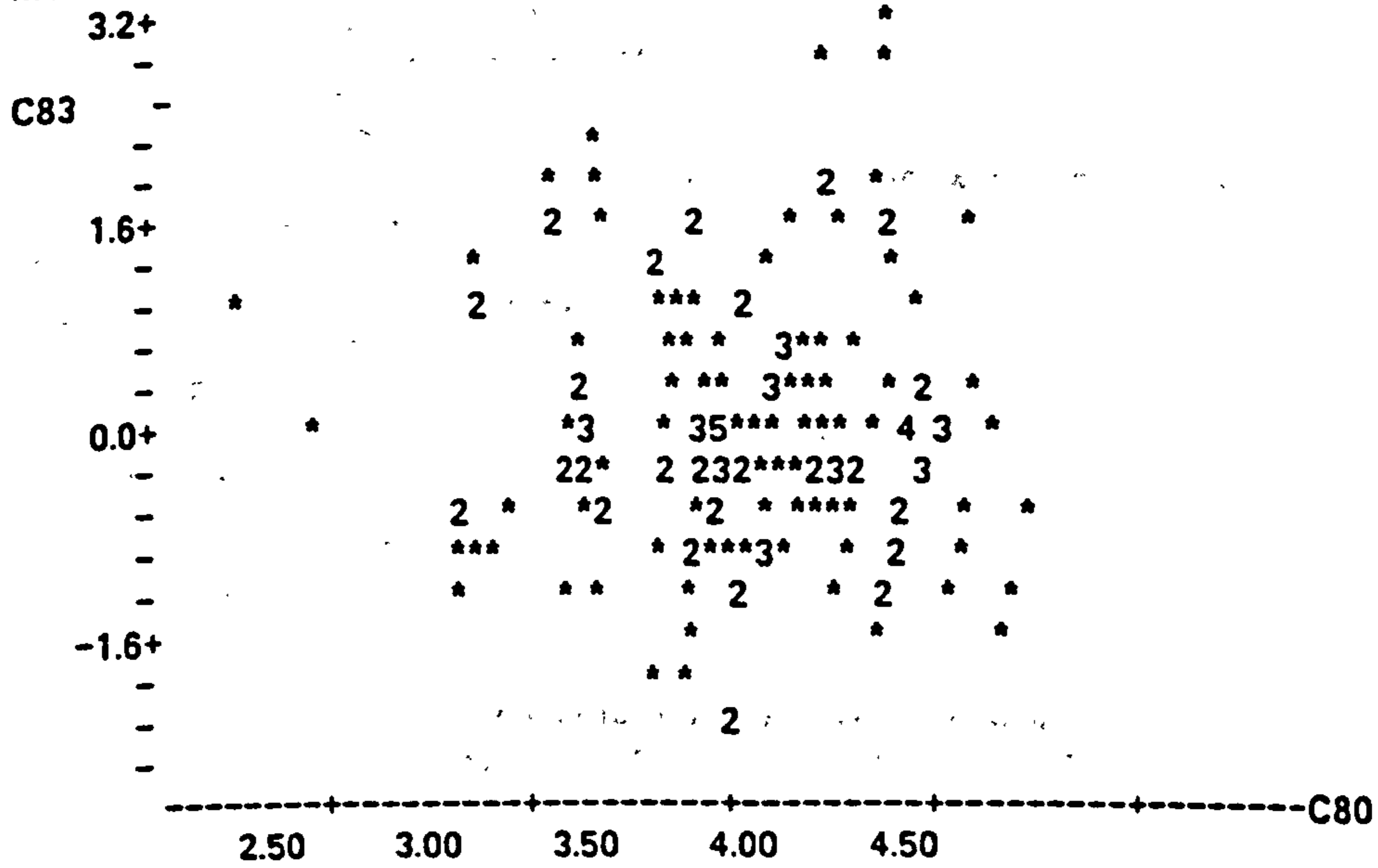
R denotes an obs. with a large st. resid.  
 X denotes an obs. whose X value gives it large influence.



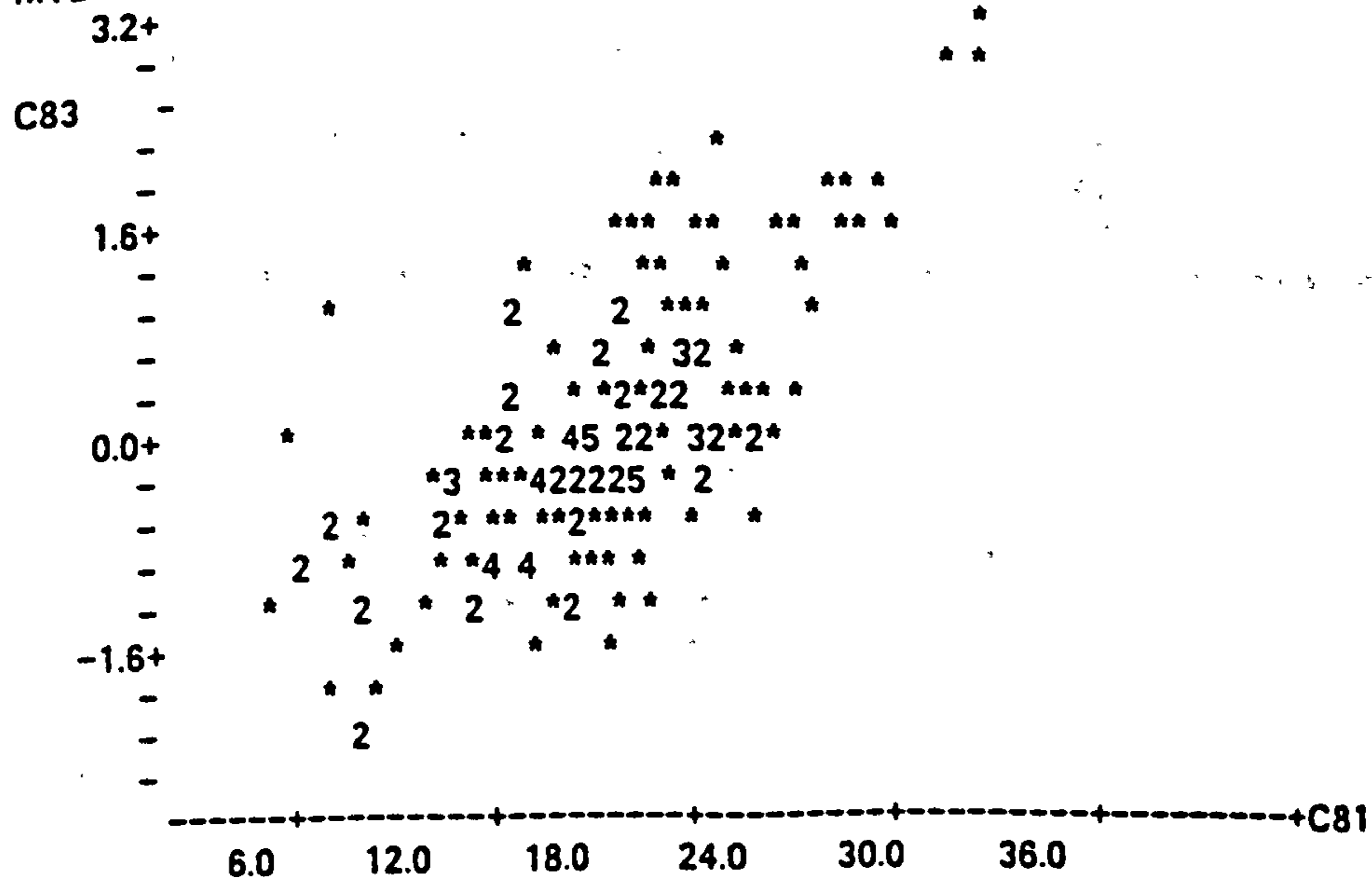
MTB > PLOT C81 C80



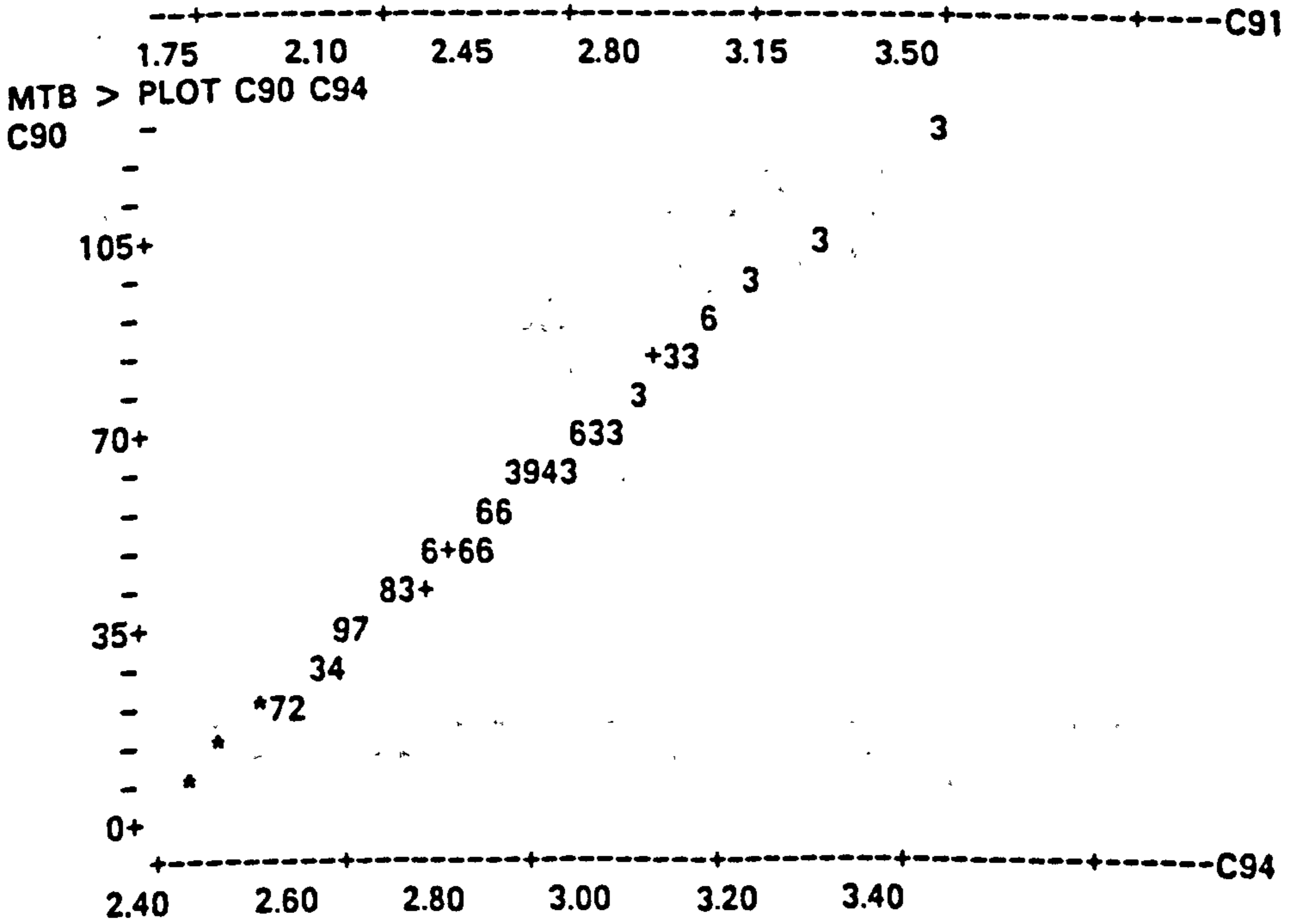
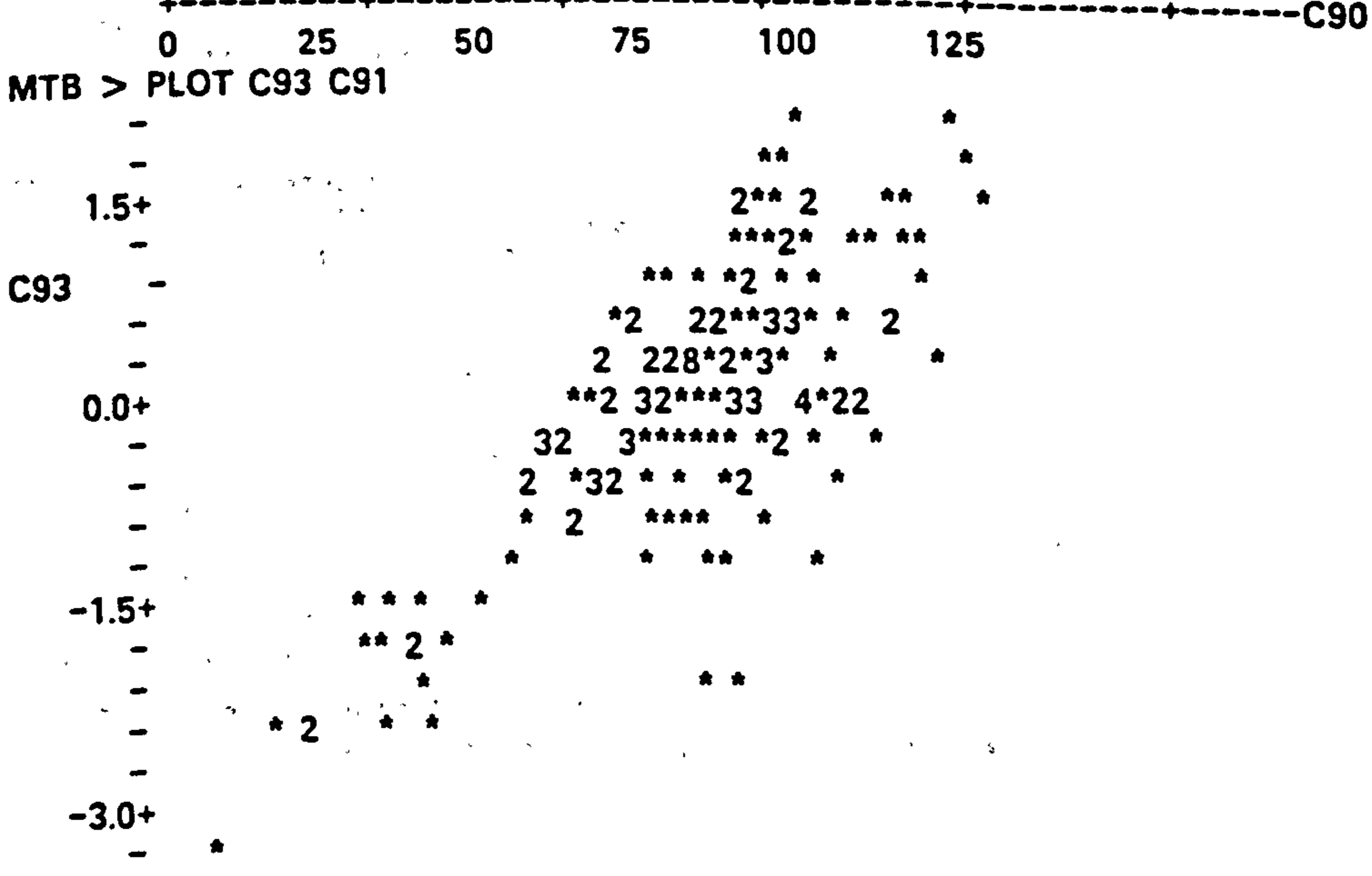
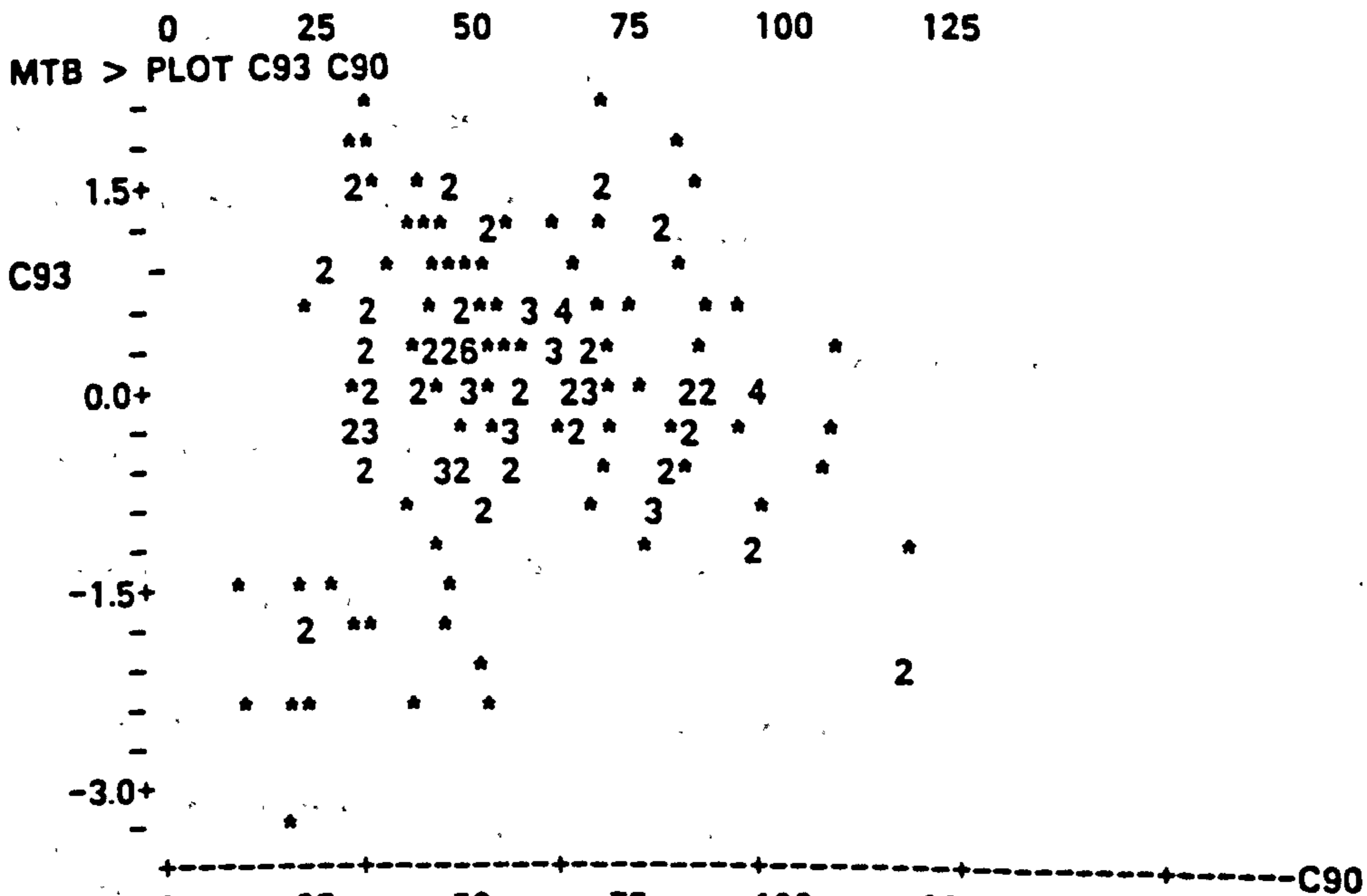
MTB > PLOT C83 C80



MTB > PLOT C83 C81







MTB > NSCOR C93 C95  
 MTB > CORRELATION OF C93 C95  
 Correlation of C93 and C95 = 0.987

MTB > NOTE\*\*\*POWER FIT\*\*\*  
 MTB > NOTE\*\*\*NORMAL DISTRIBUTION\*\*\*\*  
 MTB > LET C11=LOGE(C1)  
 MTB > LET C22=LOGE(C2)  
 MTB > REGRESS C22 ON 1 PRED C11 RESID IN C23 FIT C24

The regression equation is  
 C22 = 0.838 + 0.516 C11

Predictor	Coef	Stdev	t-ratio
Constant	0.8381	0.1572	5.33
C11	0.51591	0.03969	13.00

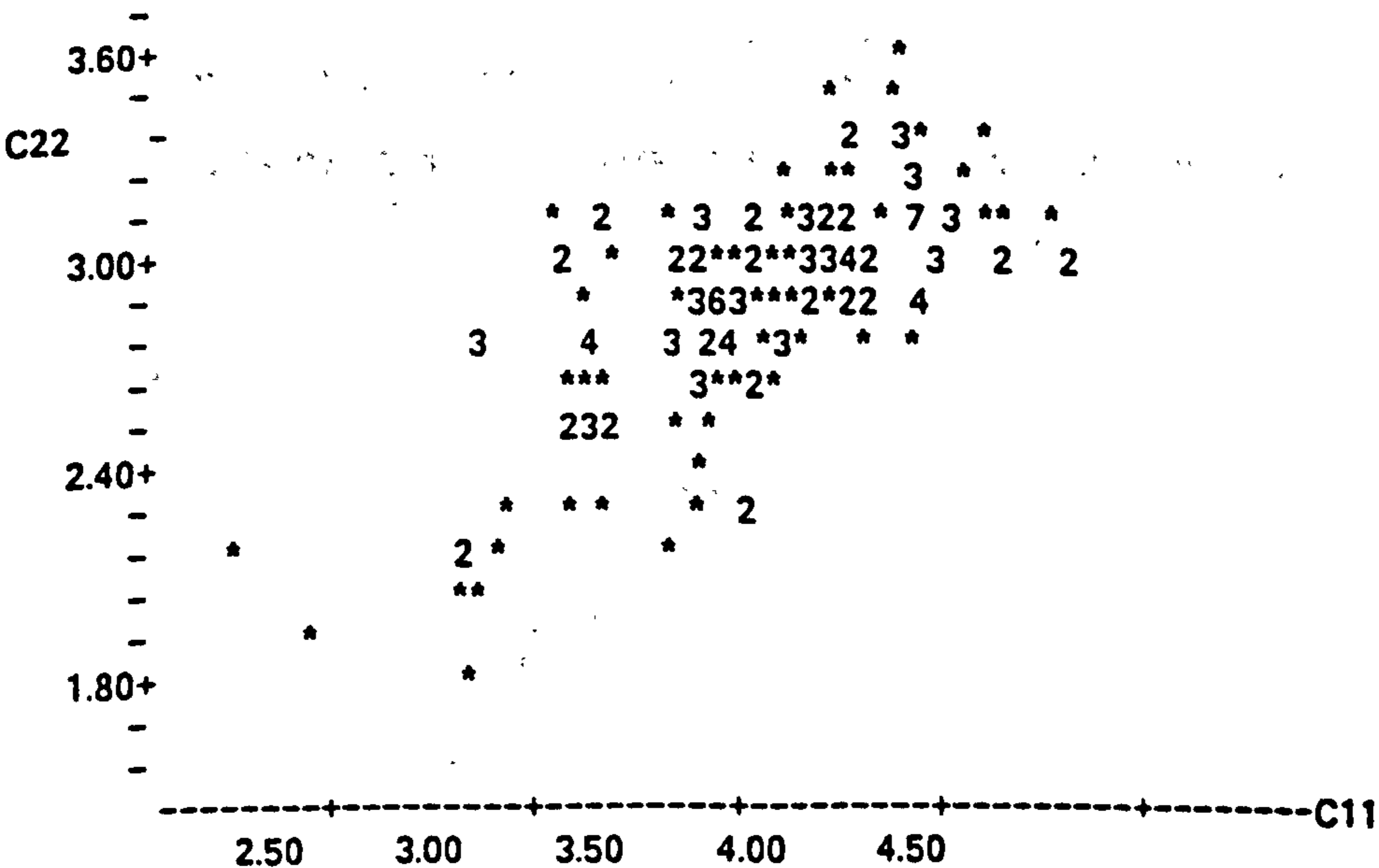
s = 0.2235      R-sq = 50.6%      R-sq(adj) = 50.3%

Analysis of Variance			
SOURCE	DF	SS	MS
Regression	1	8.4408	8.4408
Error	165	8.2417	0.0499
Total	166	16.6824	

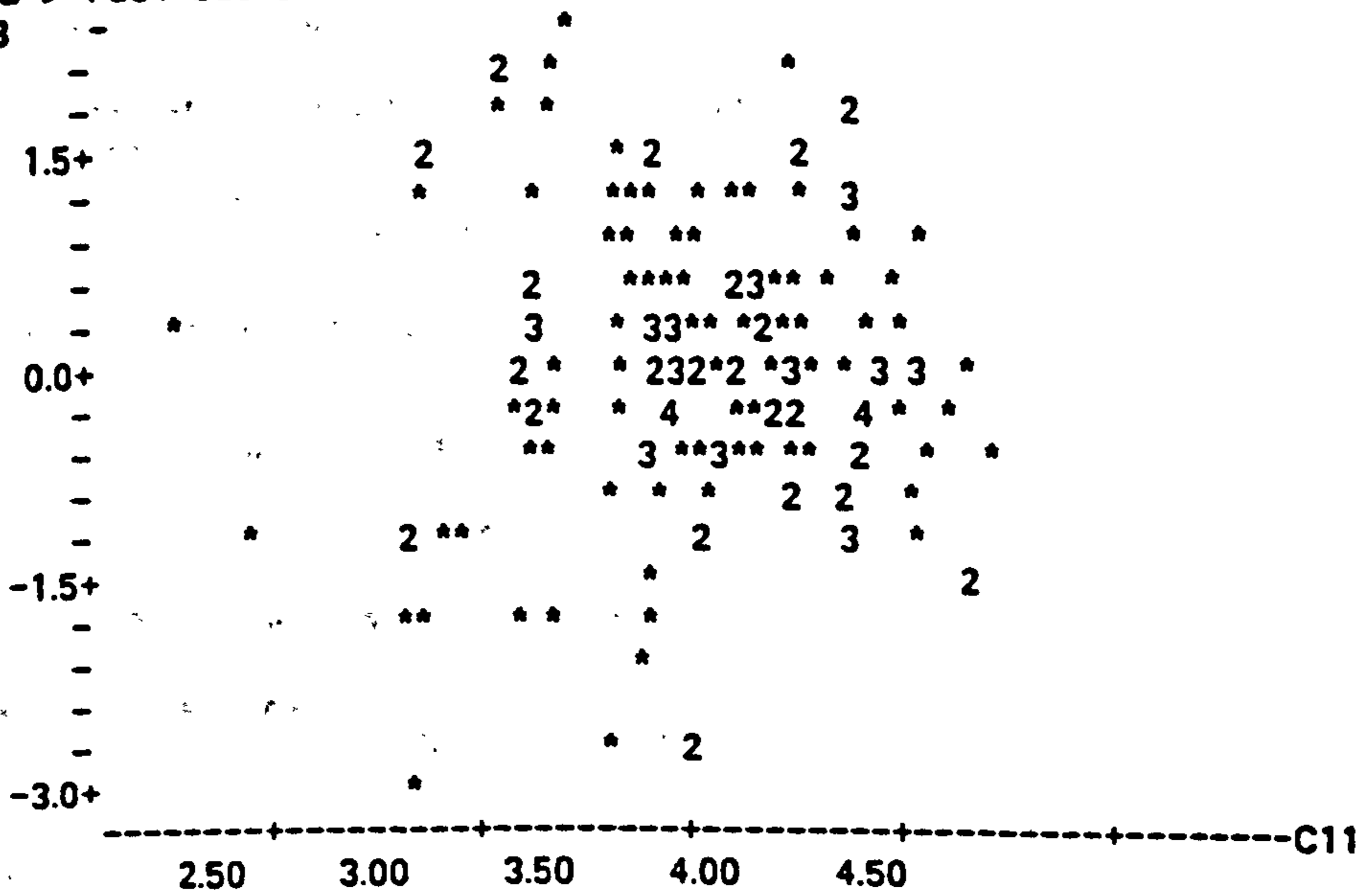
Unusual Observations						
Obs.	C11	C22	Fit	Stdev.Fit	Residual	St.Resid
1	2.29	2.1126	2.0188	0.0677	0.0938	0.44 X
2	2.55	1.9228	2.1542	0.0577	-0.2314	-1.07 X
4	3.05	1.7750	2.4113	0.0393	-0.6363	-2.89R
14	3.36	3.0681	2.5718	0.0287	0.4963	2.24R
34	3.51	3.1091	2.6498	0.0242	0.4593	2.07R
35	3.51	3.1655	2.6498	0.0242	0.5157	2.32R
37	3.68	2.1622	2.7358	0.0201	-0.5737	-2.58R
51	3.79	2.3125	2.7935	0.0183	-0.4810	-2.16R
80	3.94	2.2885	2.8709	0.0173	-0.5825	-2.61R
82	3.94	2.2814	2.8709	0.0173	-0.5896	-2.65R
129	4.27	3.4889	3.0408	0.0217	0.4481	2.01R

R denotes an obs. with a large st. resid.  
 X denotes an obs. whose X value gives it large influence.

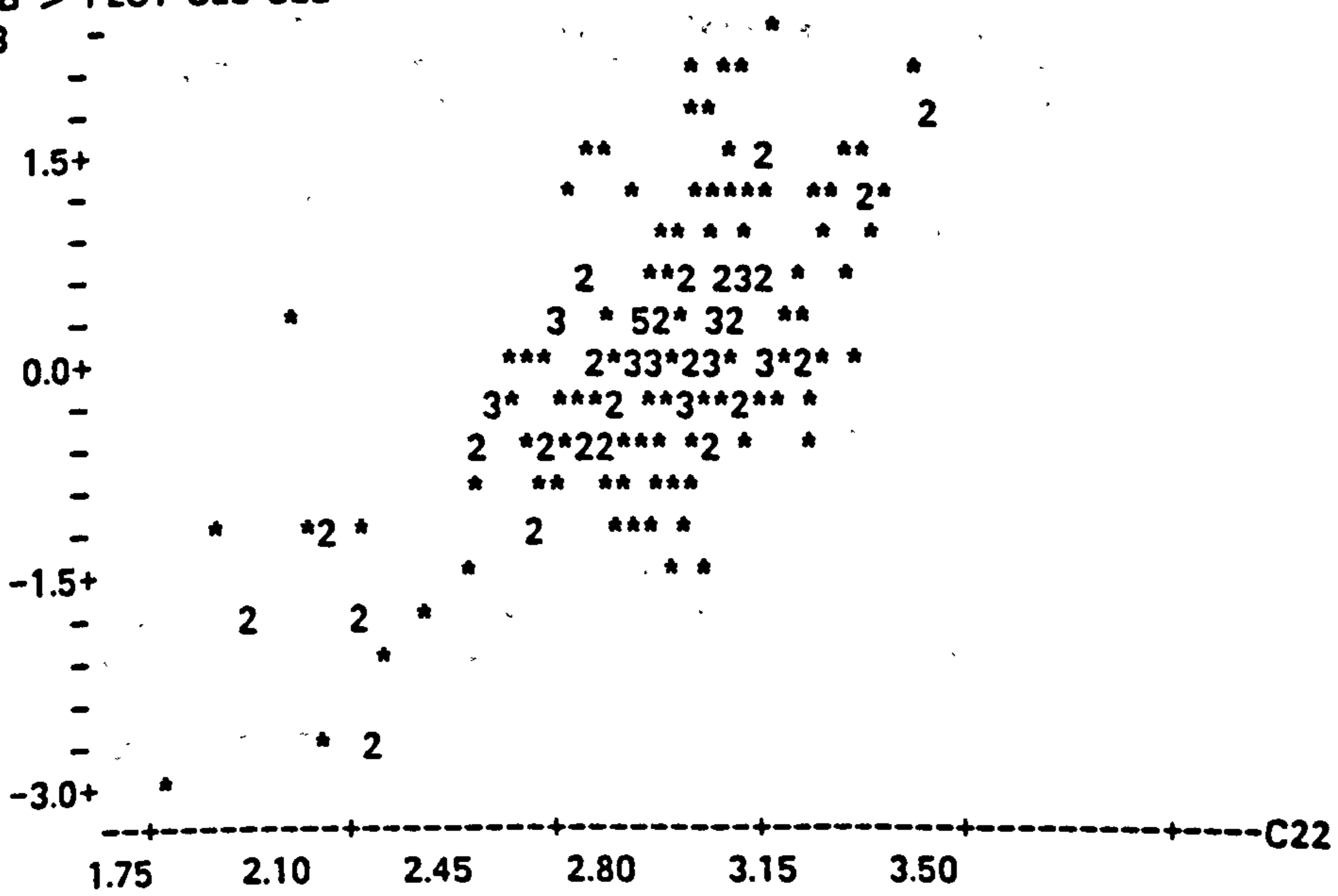
MTB > PLOT C22 C11



MTB > PLOT C23 C11  
C23

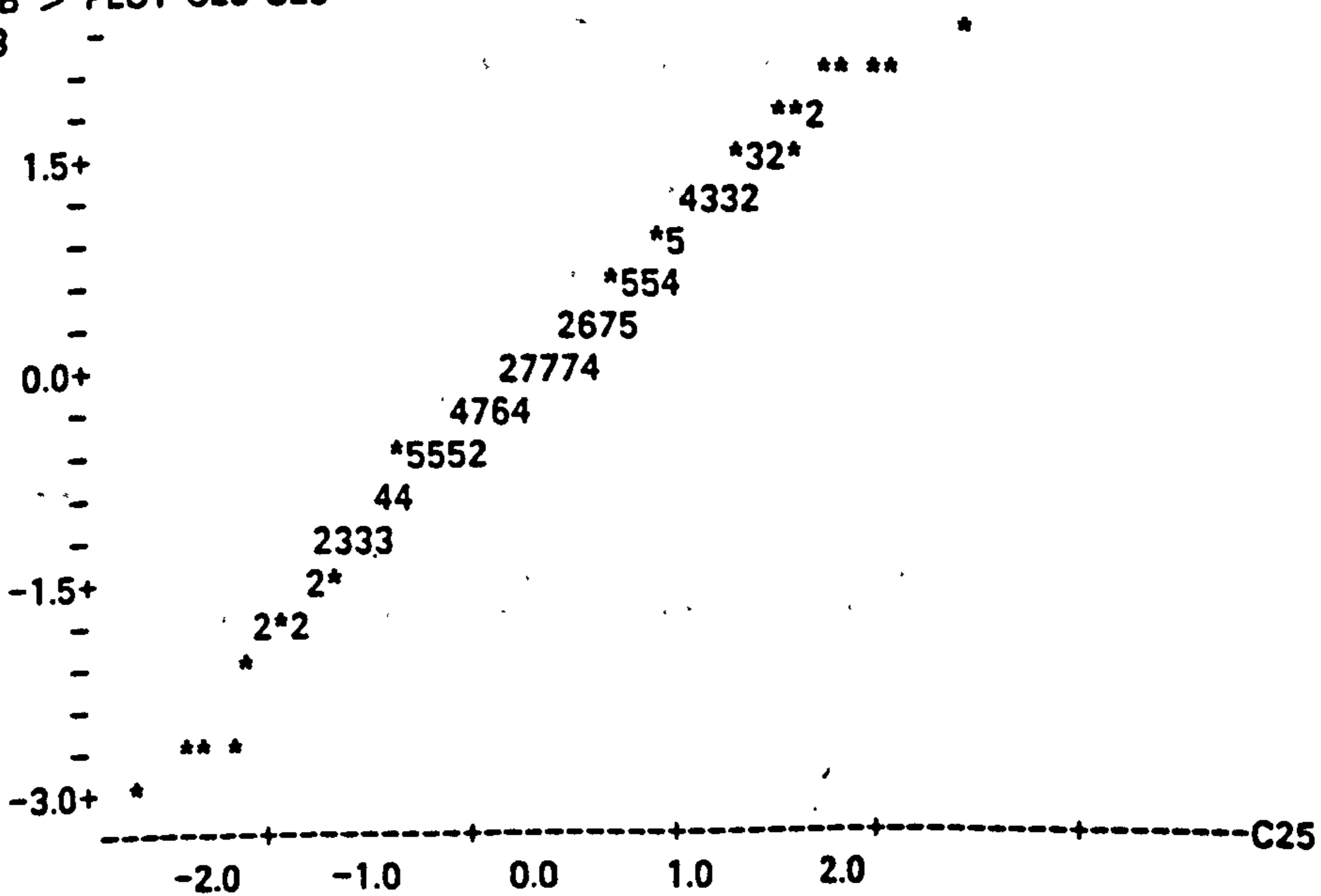


MTB > PLOT C23 C22  
C23



MTB > NSCOR C23 C25  
MTB > PLOT C23 C25  
C23

NOTE\*\*\*TEST FOR NORMAL DISTRIBUTION\*\*\*



MTB > CORRELATION OF C23 C25  
 Correlation of C23 and C25 = 0.994

MTB > NOTE\*\*\*LOGNORMAL DISTRIBUTION\*\*\*  
 MTB > LET C50=LOGE(C11)  
 MTB > LET C51=LOGE(C22)  
 MTB > REGRESS C51 ON 1 PRED C50 RESID IN C54 FIT C55

The regression equation is  
 C51 = 0.0540 + 0.728 C50

Predictor	Coef	Stdev	t-ratio
Constant	0.05399	0.07482	0.72
C50	0.72839	0.05466	13.33

s = 0.08270    R-sq = 51.8%    R-sq(adj) = 51.5%

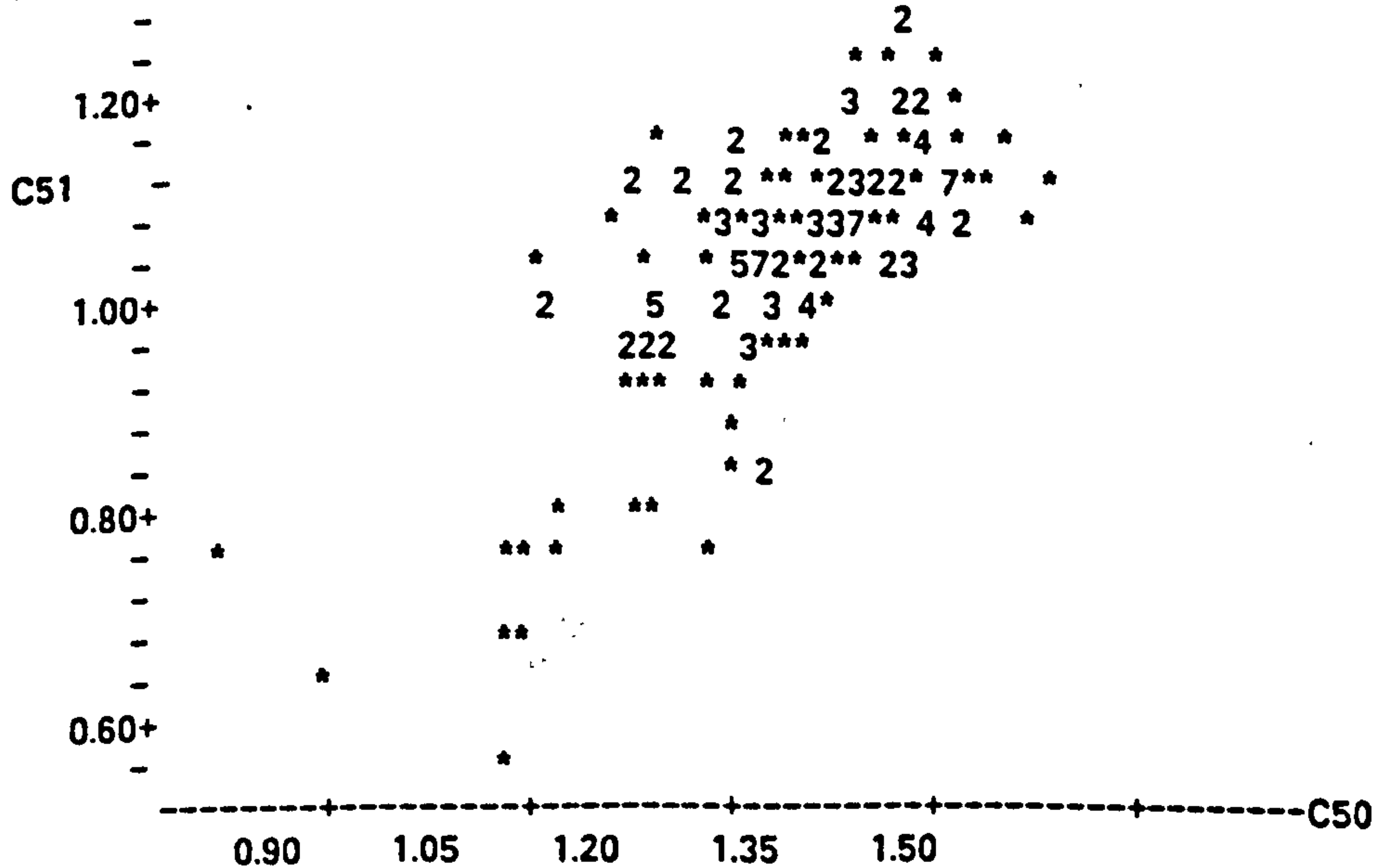
Analysis of Variance			
SOURCE	DF	SS	MS
Regression	1	1.2145	1.2145
Error	165	1.1284	0.0068
Total	166	2.3430	

Unusual Observations

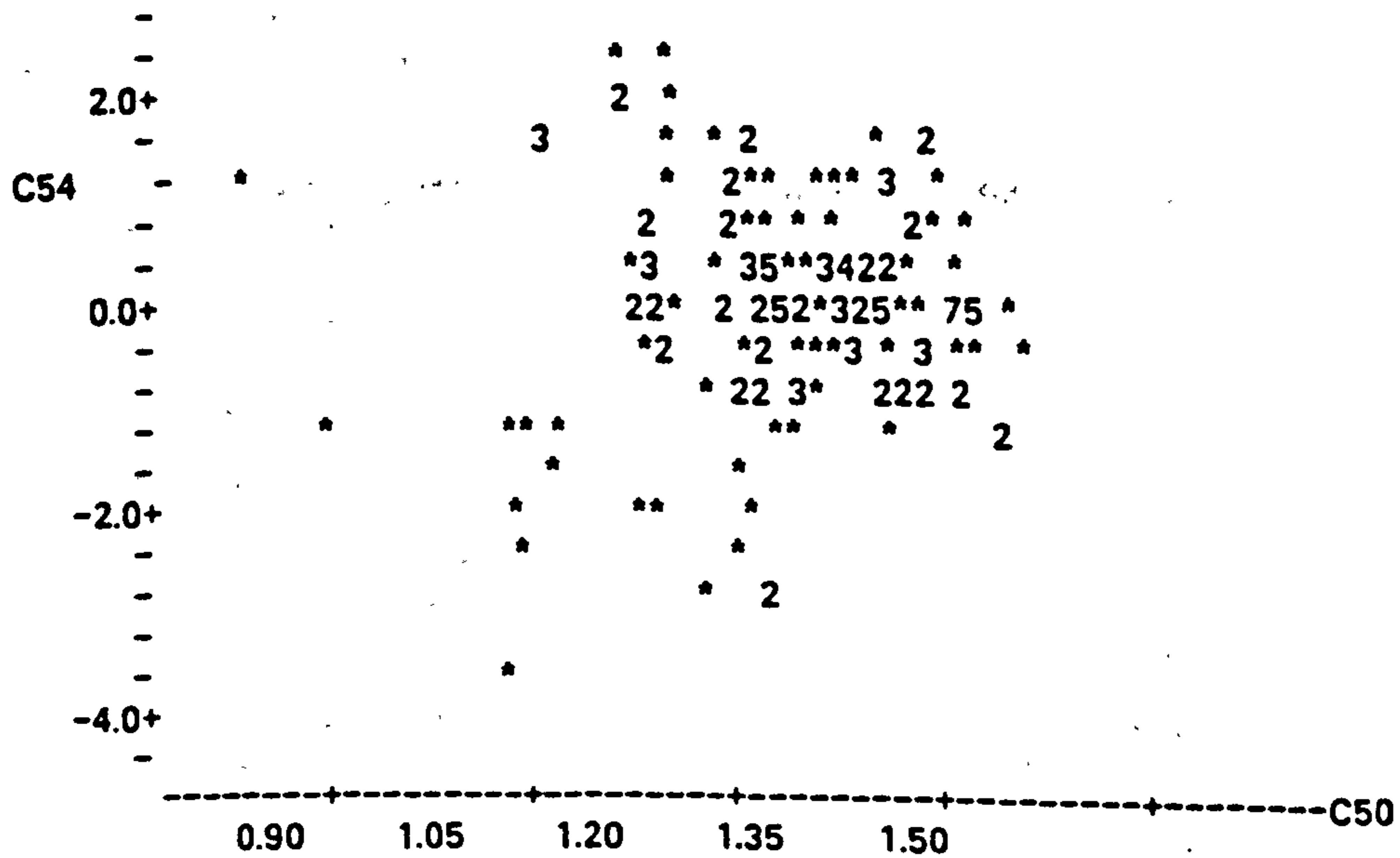
Obs.	C50	C51	Fit	Stdev.Fit	Residual	St.Resid
1	0.83	0.74794	0.65702	0.02999	0.09092	1.18 X
2	0.94	0.65378	0.73612	0.02422	-0.08235	-1.04 X
4	1.11	0.57377	0.86608	0.01504	-0.29230	-3.59R
5	1.11	0.68775	0.86608	0.01504	-0.17832	-2.19R
7	1.13	0.69725	0.87663	0.01433	-0.17938	-2.20R
13	1.21	1.10215	0.93684	0.01048	0.16531	2.02R
14	1.21	1.12104	0.93684	0.01048	0.18420	2.25R
34	1.26	1.13432	0.96889	0.00870	0.16543	2.01R
35	1.26	1.15230	0.96889	0.00870	0.18341	2.23R
37	1.30	0.77111	1.00269	0.00723	-0.23157	-2.81R
51	1.33	0.83834	1.02449	0.00663	-0.18614	-2.26R
80	1.37	0.82789	1.05279	0.00641	-0.22490	-2.73R
82	1.37	0.82477	1.05279	0.00641	-0.22801	-2.77R

R denotes an obs. with a large st. resid.  
 X denotes an obs. whose X value gives it large influence.

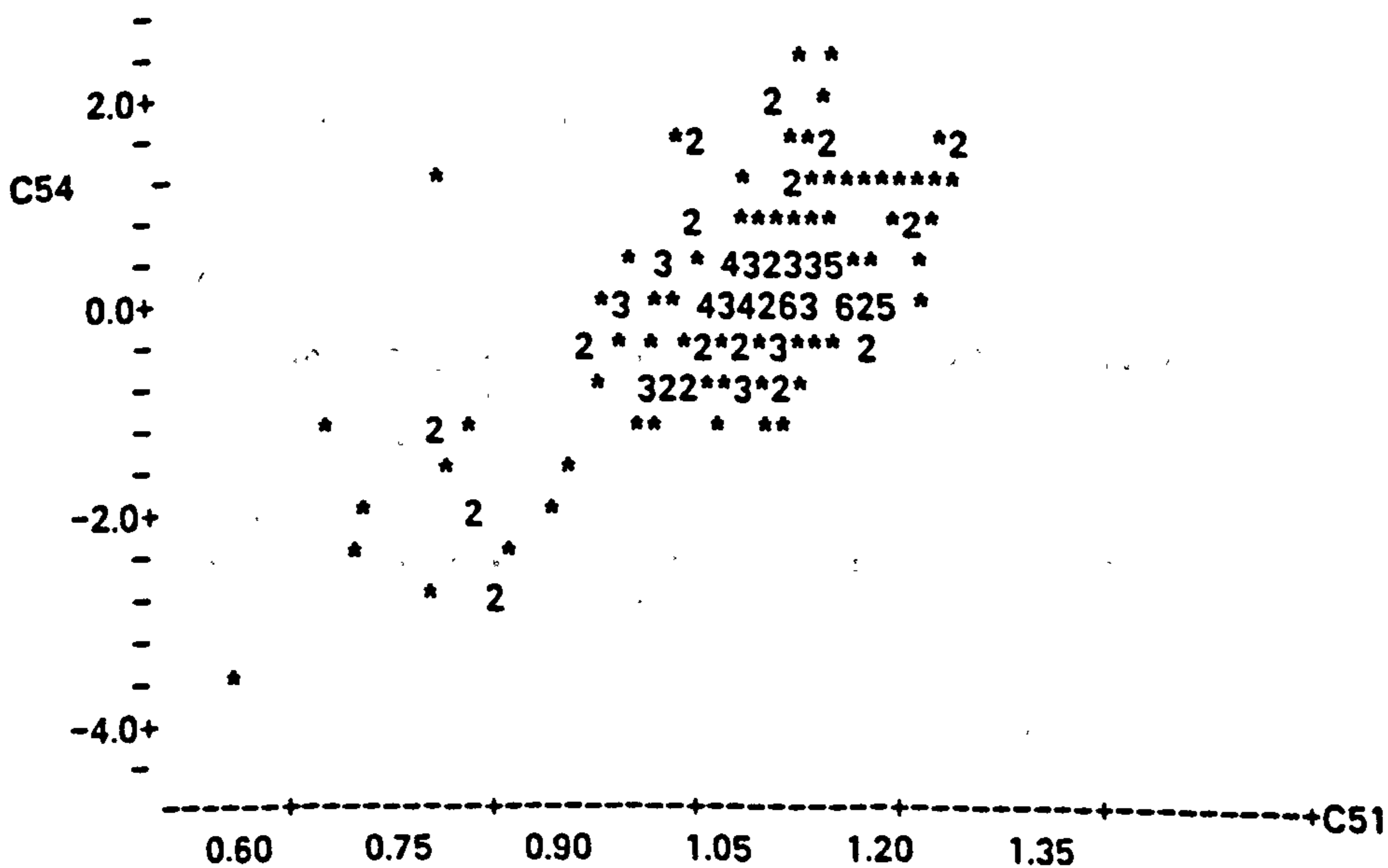
MTB > PLOT C51 C50



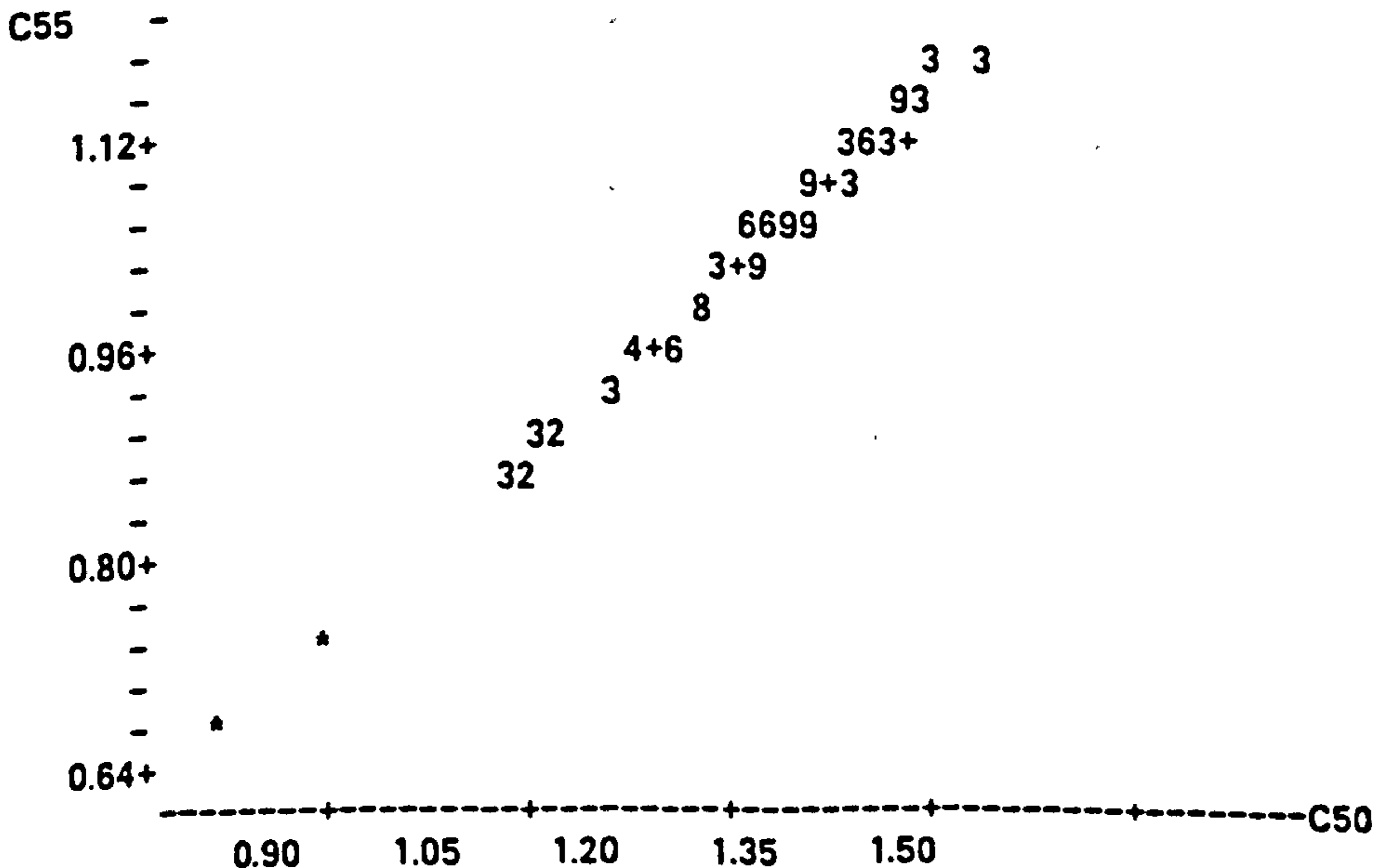
MTB > PLOT C54 C50



MTB > PLOT C54 C51



MTB > PLOT C55 C50



MTB > NSCOR C54 C56 NOTE\*\*\*TEST FOR LOGNORMAL DISTRIBUTION\*\*\*  
 MTB > CORRELATION OF C54 C56  
 Correlation of C54 and C56 = 0.987

MTB > NOTE\*\*\*CALCULATION OF CHARACTERISTIC STRENGTH\*\*\*

MTB > LET C30=C24-1.645\*0.2235

MTB > LET C31=EXPONENTIAL(C30)

MTB > PRINT C30

C30

1.65114	1.78657	2.03326	2.04364	2.04364	2.05020	2.06659
2.07907	2.07907	2.07907	2.09790	2.11286	2.20414	2.20414
2.20414	2.22863	2.22863	2.22863	2.23676	2.25168	2.25168
2.25168	2.25526	2.25526	2.25526	2.25526	2.25526	2.25526
2.26506	2.27904	2.27904	2.27904	2.28213	2.28213	2.28213
2.36817	2.36817	2.37168	2.37168	2.37168	2.37619	2.37619
2.37619	2.39608	2.39608	2.39608	2.41938	2.41938	2.41938
2.42583	2.42583	2.42583	2.42665	2.42665	2.42665	2.43209
2.43209	2.43209	2.44325	2.44325	2.44325	2.45627	2.45627
2.45627	2.46087	2.46087	2.46087	2.46757	2.46757	2.46757
2.46908	2.46908	2.46908	2.47345	2.47345	2.47345	2.49214
2.49214	2.49214	2.50329	2.50329	2.50329	2.51086	2.51086
2.51086	2.51155	2.51155	2.51155	2.52768	2.52768	2.52768
2.54583	2.54583	2.54583	2.54831	2.54831	2.54831	2.55152
2.55152	2.55152	2.58504	2.58504	2.58504	2.59730	2.59730
2.59730	2.59730	2.59730	2.59730	2.60362	2.60362	2.60362
2.61594	2.61594	2.61763	2.61763	2.62860	2.62860	2.62860
2.64089	2.64089	2.64089	2.65401	2.65401	2.65401	2.66827
2.66827	2.66827	2.67313	2.68750	2.68750	2.72844	2.72844
2.72844	2.73463	2.73463	2.73463	2.73463	2.73463	2.73463
2.73597	2.73597	2.73597	2.74428	2.74428	2.74428	2.74772
2.74772	2.74772	2.76757	2.76757	2.76757	2.79027	2.79027
2.79027	2.79228	2.79228	2.79228	2.83180	2.83180	2.83180
2.86782	2.86782	2.86782	2.95231	2.95231	2.95231	

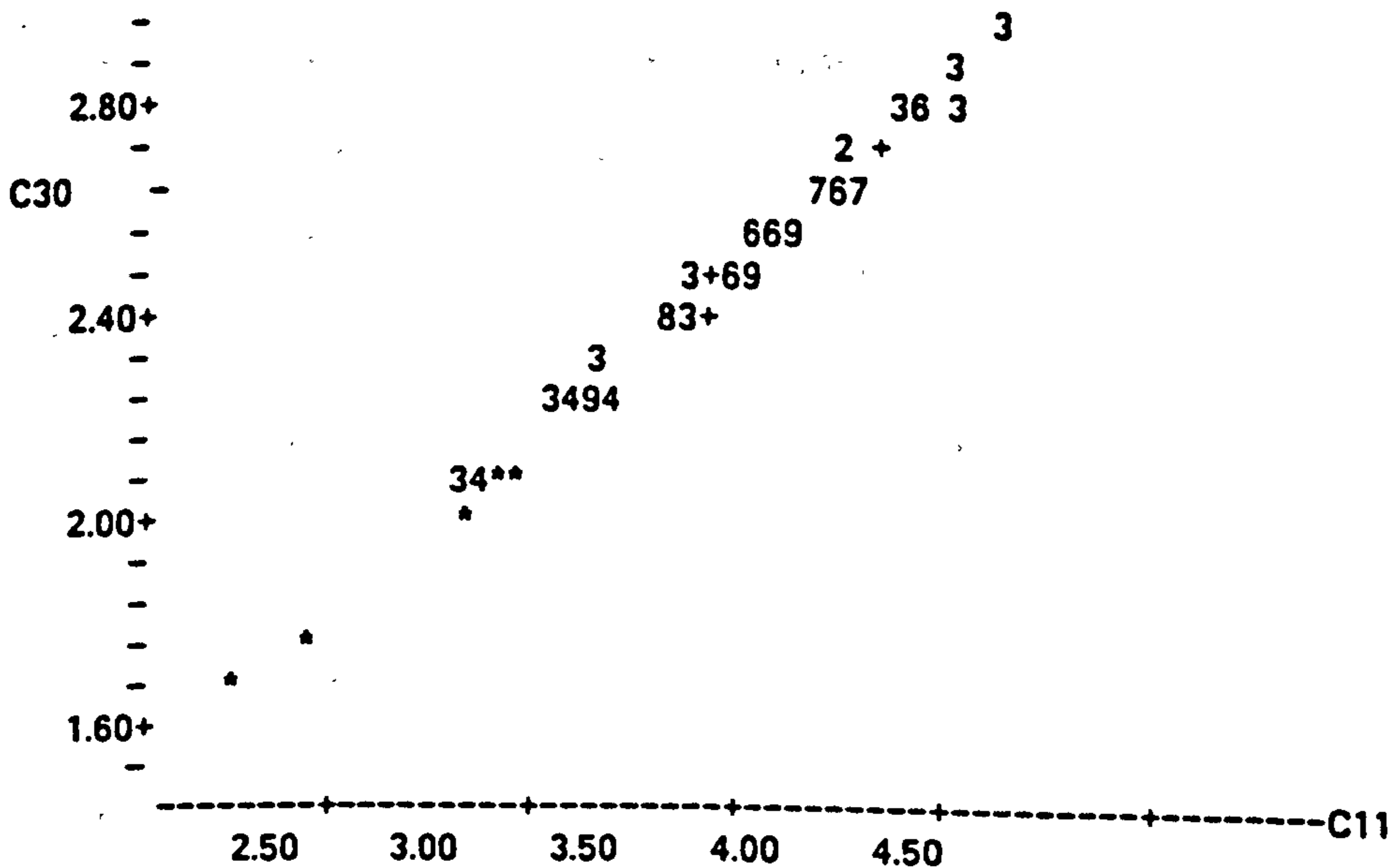
MTB > PRINT C31

C31

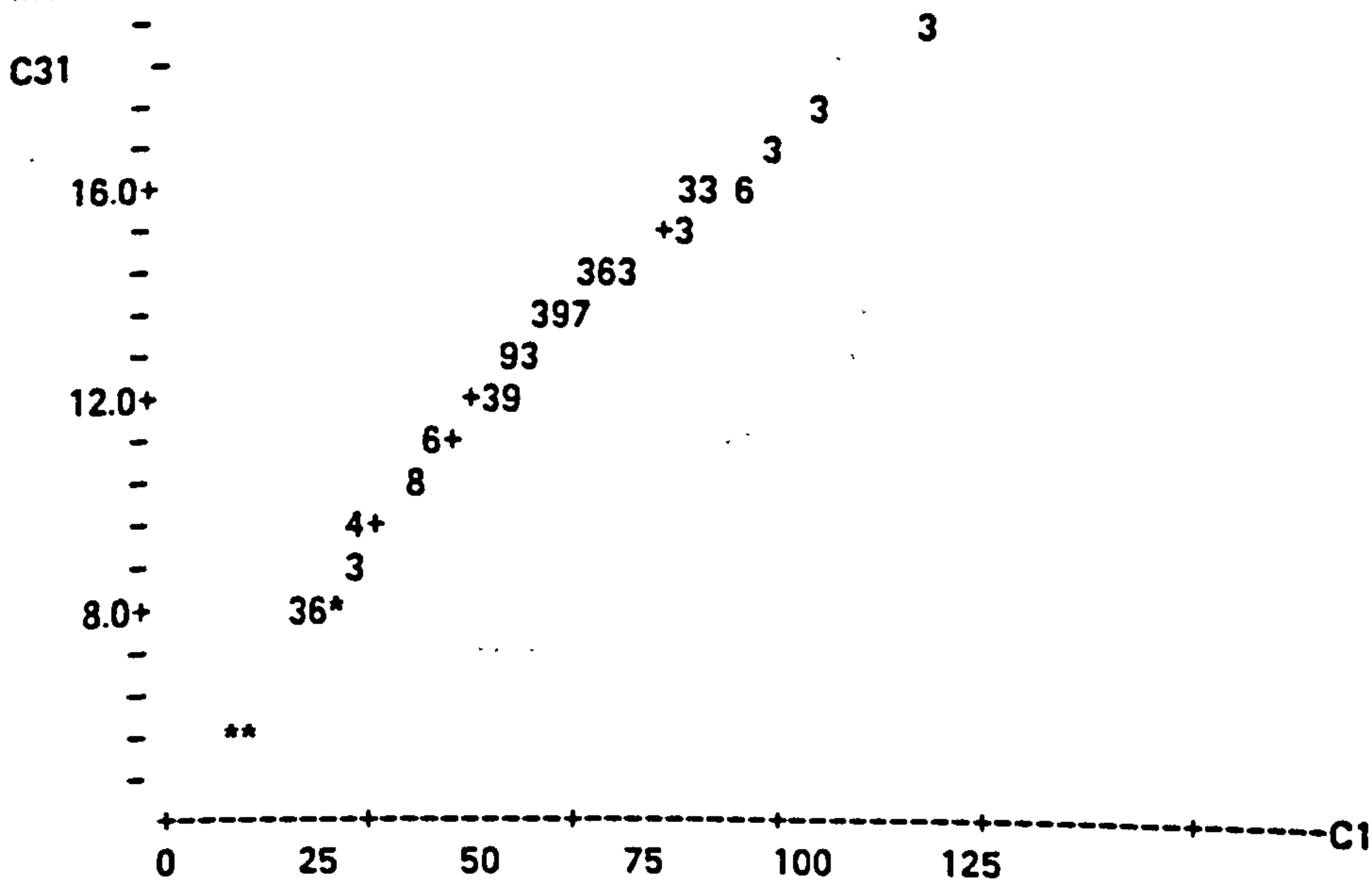
5.2129	5.9690	7.6390	7.7186	7.7186	7.7694	7.8979
7.9970	7.9970	7.9970	8.1490	8.2719	9.0624	9.0624
9.0624	9.2871	9.2871	9.2871	9.3630	9.5037	9.5037
9.5037	9.5378	9.5378	9.5378	9.5378	9.5378	9.5378
9.6317	9.7673	9.7673	9.7673	9.7975	9.7975	9.7975
10.6779	10.6779	10.7154	10.7154	10.7154	10.7638	10.7638
10.7638	10.9801	10.9801	10.9801	11.2389	11.2389	11.2389
11.3116	11.3116	11.3116	11.3208	11.3208	11.3208	11.3826
11.3826	11.3826	11.5104	11.5104	11.5104	11.6612	11.6612
11.6612	11.7149	11.7149	11.7149	11.7938	11.7938	11.7938
11.8115	11.8115	11.8115	11.8633	11.8633	11.8633	12.0871
12.0871	12.0871	12.2226	12.2226	12.2226	12.3155	12.3155
12.3155	12.3240	12.3240	12.3240	12.5244	12.5244	12.5244
12.7538	12.7538	12.7538	12.7855	12.7855	12.7855	12.8266
12.8266	12.8266	13.2638	13.2638	13.2638	13.4275	13.4275
13.4275	13.4275	13.4275	13.4275	13.5125	13.5125	13.5125
13.6801	13.6801	13.7032	13.7032	13.8544	13.8544	13.8544
14.0257	14.0257	14.0257	14.2109	14.2109	14.2109	14.4150
14.4150	14.4150	14.4852	14.6950	14.6950	15.3090	15.3090
15.3090	15.4041	15.4041	15.4041	15.4041	15.4041	15.4041
15.4248	15.4248	15.4248	15.5534	15.5534	15.5534	15.6071
15.6071	15.6071	15.9200	15.9200	15.9200	16.2854	16.2854
16.2854	16.3181	16.3181	16.3181	16.9760	16.9760	16.9760
17.5986	17.5986	17.5986	19.1501	19.1501	19.1501	



MTB > PLOT C30 C11



MTB > PLOT C31 C1



MTB > NOTE\*\*\*EQUATION OF CHARACTERISTIC CURVE\*\*\*  
 MTB > REGRESS C30 ON 1 PRED C11 RESID IN C32 FIT C33

The regression equation is  
 $C30 = 0.470 + 0.516 C11$

Predictor	Coef	Stdev	t-ratio
Constant	0.470472	0.000000	*
C11	0.515915	0.000000	*

s = 0      R-sq = 100.0%      R-sq(adj) = 100.0%

Analysis of Variance			
SOURCE	DF	SS	MS
Regression	1	8.4408	8.4408
Error	165	0.0000	0.0000
Total	166	8.4408	

Unusual Observations

Obs.	C11	C30	Fit	Stdev.Fit	Residual	St.Resid
1	2.29	1.65114	1.65113	0.00000	0.00000	* X
2	2.55	1.78657	1.78657	0.00000	0.00000	* X

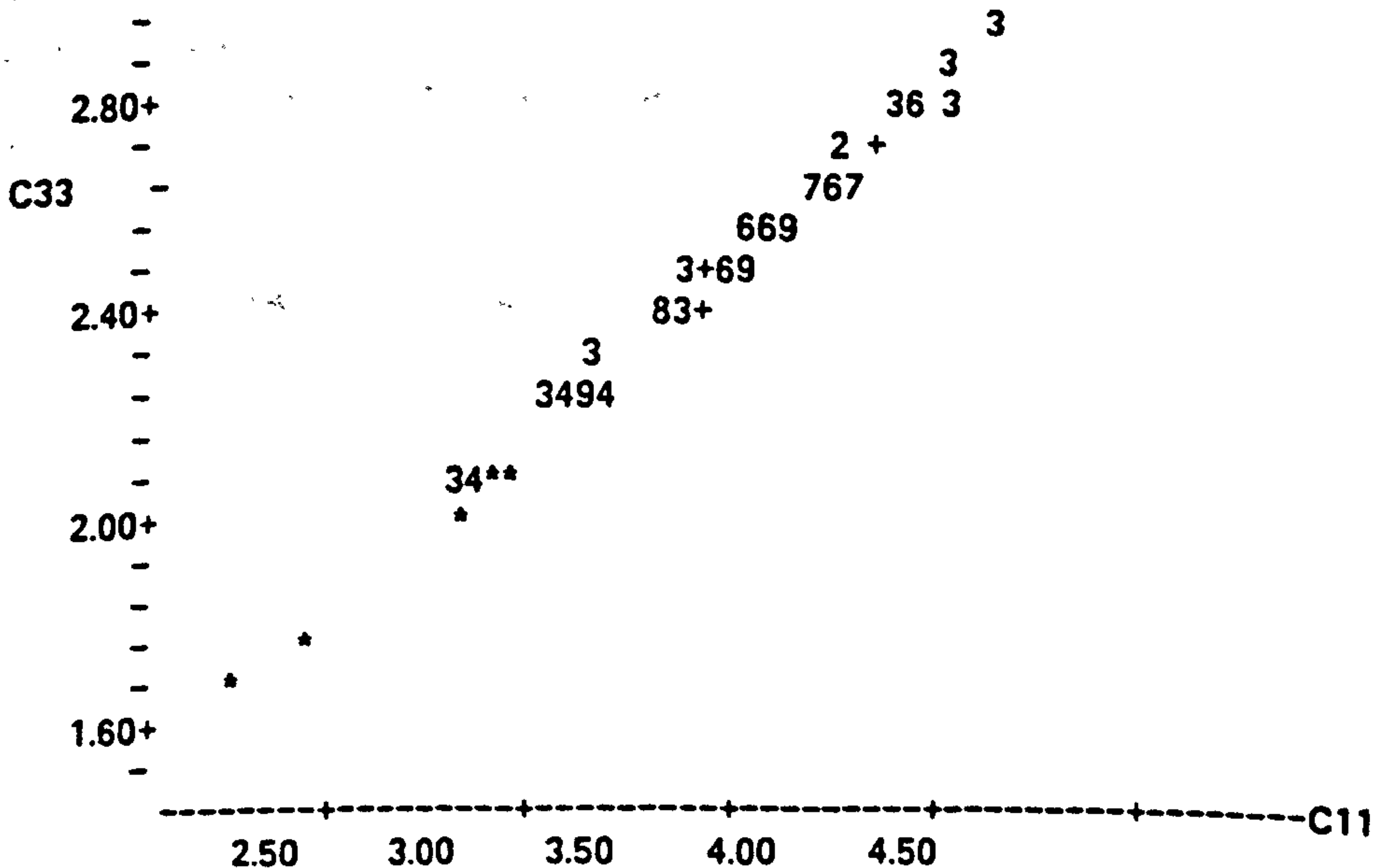
X denotes an obs. whose X value gives it large influence.

MTB > PRINT C33

C33

1.65113	1.78657	2.03326	2.04364	2.04364	2.05020	2.06659
2.07907	2.07907	2.07907	2.09790	2.11286	2.20414	2.20414
2.20414	2.22863	2.22863	2.22863	2.23676	2.25168	2.25168
2.25168	2.25526	2.25526	2.25526	2.25526	2.25526	2.25526
2.26506	2.27904	2.27904	2.27904	2.28213	2.28213	2.28213
2.36817	2.36817	2.37168	2.37168	2.37168	2.37619	2.37619
2.37619	2.39608	2.39608	2.39608	2.41938	2.41938	2.41938
2.42583	2.42583	2.42583	2.42665	2.42665	2.42665	2.43209
2.43209	2.43209	2.44325	2.44325	2.44325	2.45627	2.45627
2.45627	2.46087	2.46087	2.46087	2.46757	2.46757	2.46757
2.46908	2.46908	2.46908	2.47345	2.47345	2.47345	2.49214
2.49214	2.49214	2.50329	2.50329	2.50329	2.51086	2.51086
2.51086	2.51155	2.51155	2.51155	2.52768	2.52768	2.52768
2.54583	2.54583	2.54583	2.54831	2.54831	2.54831	2.55152
2.55152	2.55152	2.58504	2.58504	2.58504	2.59730	2.59730
2.59730	2.59730	2.59730	2.59730	2.60362	2.60362	2.60362
2.61594	2.61594	2.61763	2.61763	2.62860	2.62860	2.62860
2.64089	2.64089	2.64089	2.65401	2.65401	2.65401	2.66827
2.66827	2.66827	2.67313	2.68750	2.68750	2.72844	2.72844
2.72844	2.73463	2.73463	2.73463	2.73463	2.73463	2.73463
2.73597	2.73597	2.73597	2.74428	2.74428	2.74428	2.74772
2.74772	2.74772	2.76757	2.76757	2.76757	2.79027	2.79027
2.79027	2.79228	2.79228	2.79228	2.83180	2.83180	2.83180
2.86782	2.86782	2.86782	2.95231	2.95231	2.95231	

MTB > PLOT C33 C11



MTB > LET C35=EXPONENTIATE(C33)

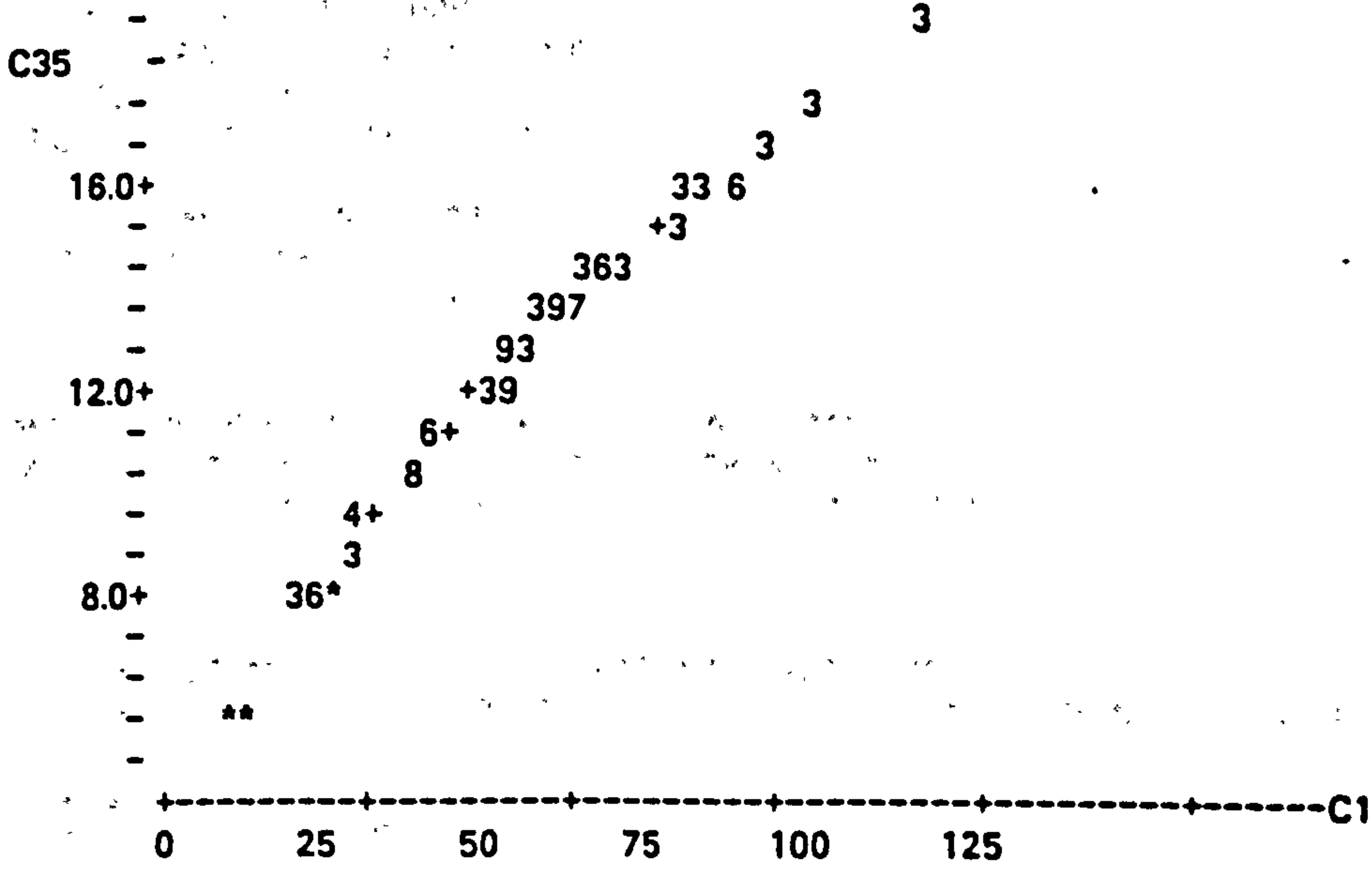
MTB > PRINT C35

C35

5.2129	5.9690	7.6390	7.7186	7.7186	7.7694	7.8979
7.9970	7.9970	7.9970	8.1490	8.2719	9.0624	9.0624
9.0624	9.2871	9.2871	9.2871	9.3630	9.5037	9.5037
9.5037	9.5378	9.5378	9.5378	9.5378	9.5378	9.5378
9.6317	9.7673	9.7673	9.7673	9.7975	9.7975	9.7975
10.6779	10.6779	10.7154	10.7154	10.7154	10.7638	10.7638
10.7638	10.9801	10.9801	10.9801	11.2389	11.2389	11.2389
11.3116	11.3116	11.3116	11.3208	11.3208	11.3208	11.3826
11.3826	11.3826	11.5104	11.5104	11.5104	11.6612	11.6612
11.6612	11.7149	11.7149	11.7149	11.7938	11.7938	11.7938
11.8115	11.8115	11.8115	11.8633	11.8633	11.8633	12.0871
12.0871	12.0871	12.2226	12.2226	12.2226	12.3155	12.3155
12.3155	12.3240	12.3240	12.3240	12.5244	12.5244	12.5244
12.7538	12.7538	12.7538	12.7855	12.7855	12.7855	12.8266
12.8266	12.8266	13.2638	13.2638	13.2638	13.4275	13.4275
13.4275	13.4275	13.4275	13.4275	13.5125	13.5125	13.5125
13.6801	13.6801	13.7032	13.7032	13.8544	13.8544	13.8544
14.0257	14.0257	14.0257	14.2109	14.2109	14.2109	14.4150
14.4150	14.4150	14.4852	14.6950	14.6950	15.3090	15.3090

15.3090	15.4040	15.4040	15.4040	15.4040	15.4040	15.4040
15.4248	15.4248	15.4248	15.5534	15.5534	15.5534	15.6071
15.6071	15.6071	15.9200	15.9200	15.9200	16.2854	16.2854
16.2854	16.3181	16.3181	16.3181	16.9760	16.9760	16.9760
17.5986	17.5986	17.5986	19.1501	19.1501	19.1501	

MTB > PLOT C35 C1



MTB > STOP

\*\*\* Minitab Release 5.1 \*\*\* Minitab, Inc. \*\*\*  
Storage available 10000

End of MINITAB run: Completed

# I.V. STATISTICAL ANALYSIS OF BRICKWORK WALL STRENGTH IN TERMS OF UNIT BRICK AND MORTAR CUBE STRENGTHS

Command:MINITAB  
 MINITAB RELEASE 5.1 \*\*\* COPYRIGHT - MINITAB, INC. 1985  
 STORAGE AVAILABLE 10000  
 MTB > READ 'CHAR\_X1' C1 C2 C3  
 372 ROWS READ

ROW	C1	C2	C3
1	9.86	15.65	8.27
2	12.82	18.62	6.84
3	20.68	16.55	8.62
4	21.10	16.27	5.90

MTB > NOTE\*\*\*C1 = UNIT BRICK STRENGTH\*\*\*  
 MTB > NOTE\*\*\*C2 = MORTAR CUBE STRENGTH\*\*\*  
 MTB > NOTE\*\*\*C3 = BRICKWORK WALL STRENGTH\*\*\*  
 MTB > LET C11=LOGE(C1)  
 MTB > LET C12=LOGE(C2)  
 MTB > LET C13=LOGE(C3)  
 MTB > NOTE\*\*\*EQUATION OF MEAN STRENGTH \*\*\*  
 MTB > REGRESS C13 ON 2 PRED C11 C12 STORE ST RESID IN C20 VALUES IN C21

The regression equation is  
 $C13 = 0.217 + 0.531 C11 + 0.208 C12$

Predictor	Coef	Stdev	t-ratio
Constant	0.2171	0.1285	1.69
C11	0.53079	0.03119	17.02
C12	0.20767	0.02148	9.67

s = 0.2772      R-sq = 53.1%      R-sq(adj) = 52.8%

Analysis of Variance

SOURCE	DF	SS	MS
Regression	2	31.354	15.677
Error	361	27.743	0.077
Total	363	59.097	

SOURCE	DF	SEQ SS
C11	1	24.174
C12	1	7.180

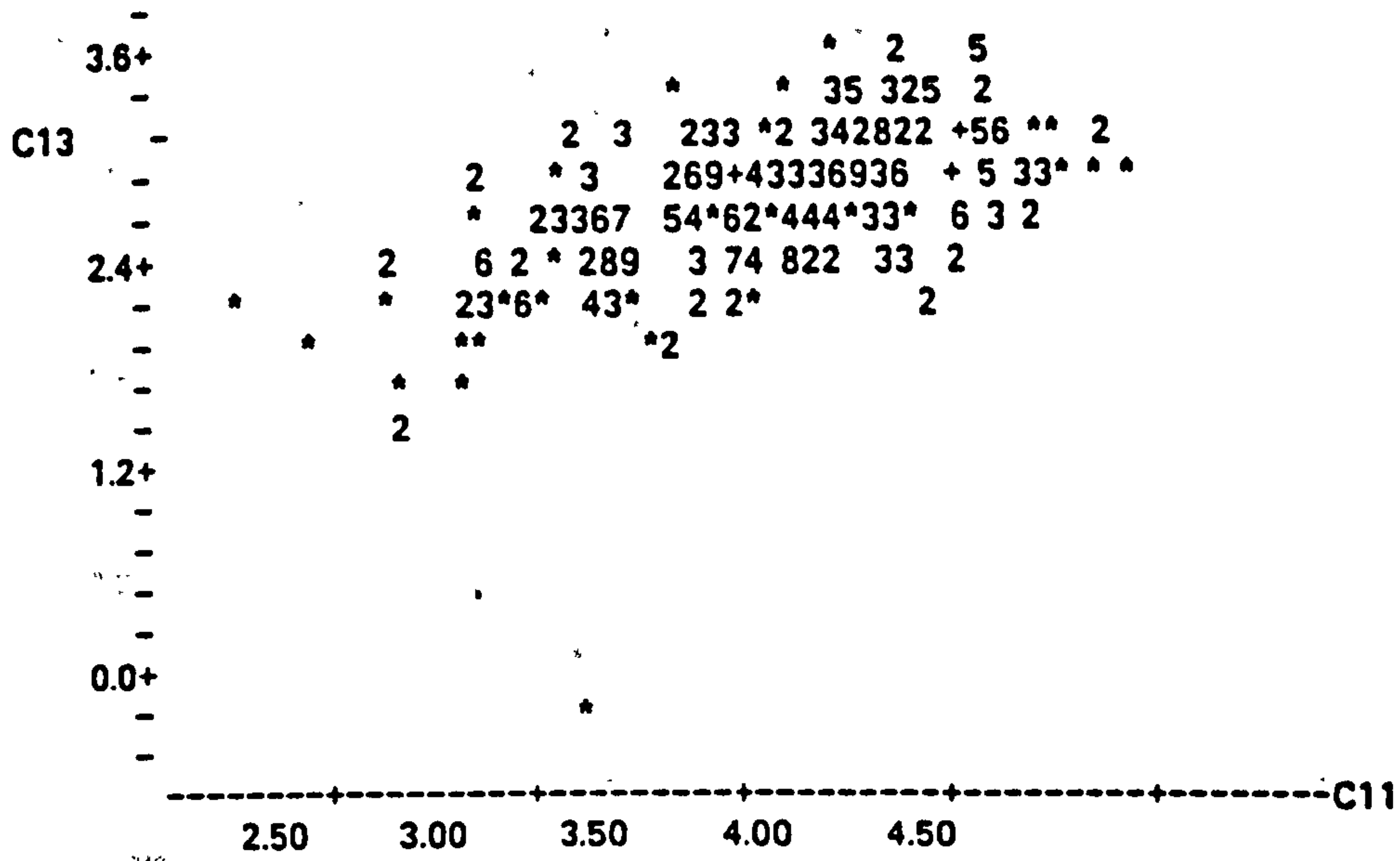
Unusual Observations

Obs.	C11	C13	Fit	Stdev.Fit	Residual	St.Resid
1	2.29	2.1126	2.0029	0.0560	0.1097	0.40 X
2	2.55	1.9228	2.1784	0.0499	-0.2556	-0.94 X
4	3.05	1.7750	2.4148	0.0354	-0.6399	-2.33R
82	3.94	2.2814	2.8513	0.0183	-0.5699	-2.06R
165	4.81	3.1693	2.9265	0.0436	0.2428	0.89 X
174	4.07	2.4006	2.9548	0.0210	-0.5542	-2.00R
176	4.18	2.4006	2.9562	0.0184	-0.5555	-2.01R
198	2.87	1.5665	2.1579	0.0361	-0.5913	-2.15R
199	2.87	1.4996	2.1745	0.0362	-0.6748	-2.46R
200	2.87	1.5304	2.1727	0.0361	-0.6423	-2.34R
247	3.66	1.8421	2.5930	0.0168	-0.7509	-2.71R
318	4.39	2.1702	2.8905	0.0228	-0.7203	-2.61R
319	4.39	2.0882	2.8696	0.0239	-0.7815	-2.83R
358	3.12	2.1041	1.9562	0.0452	0.1479	0.54 X
360	3.12	2.1633	1.9506	0.0457	0.2127	0.78 X
363	3.46	2.1748	2.0912	0.0451	0.0836	0.31 X
365	3.46	-0.2107	2.1509	0.0397	-2.3616	-8.61R

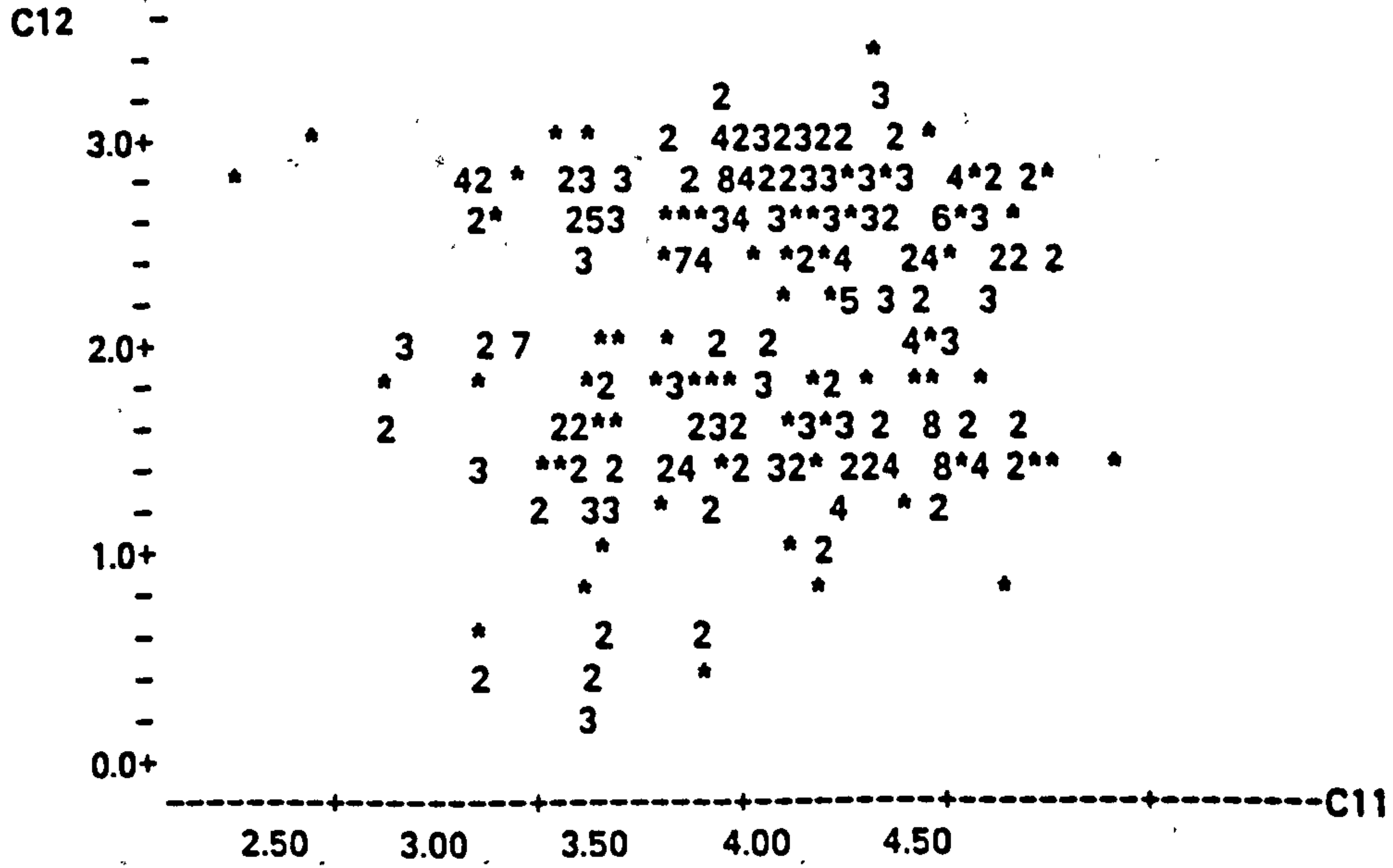
R denotes an obs. with a large st. resid.

X denotes an obs. whose X value gives it large influence.

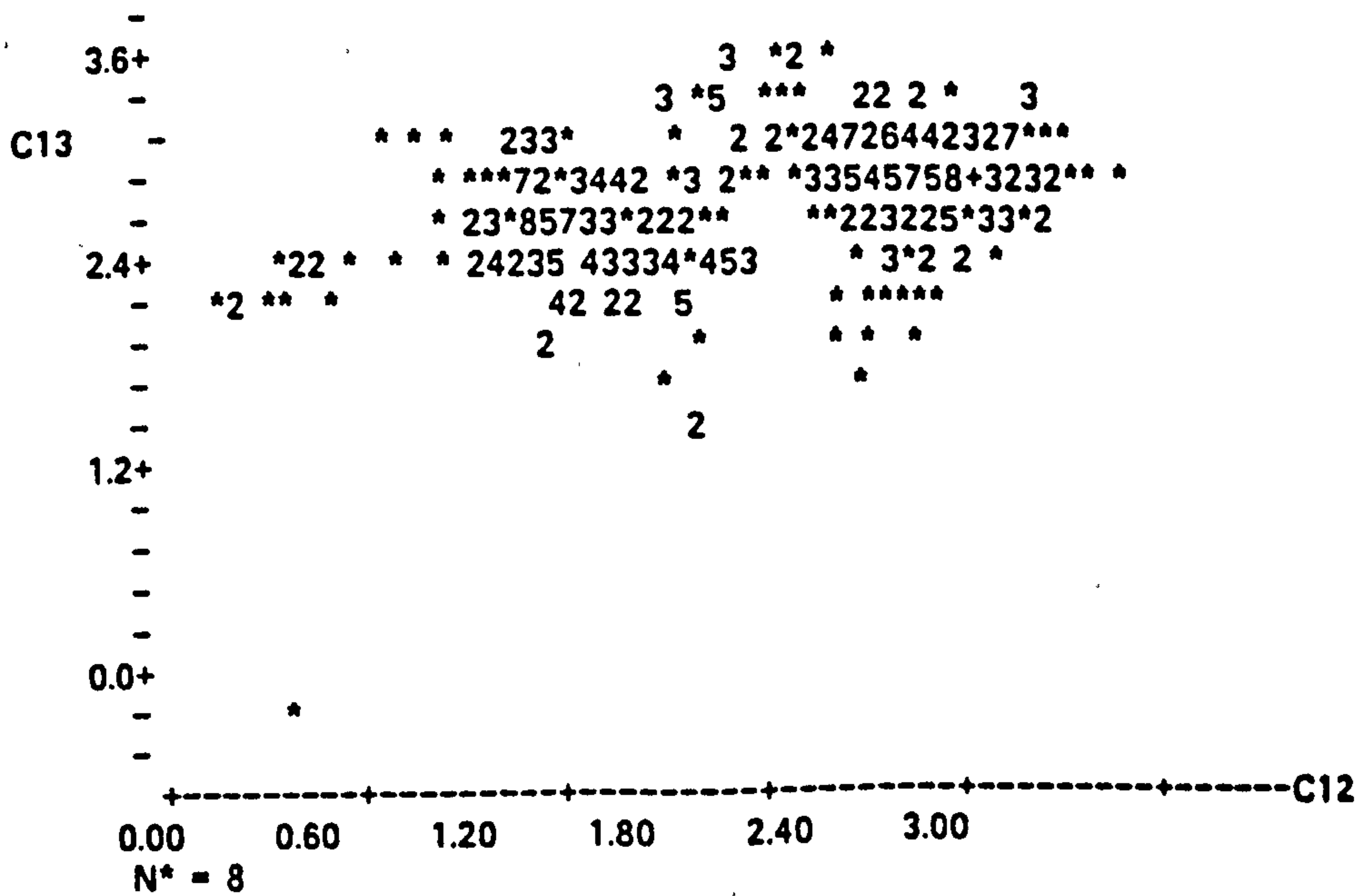
MTB > PLOT C13 C11



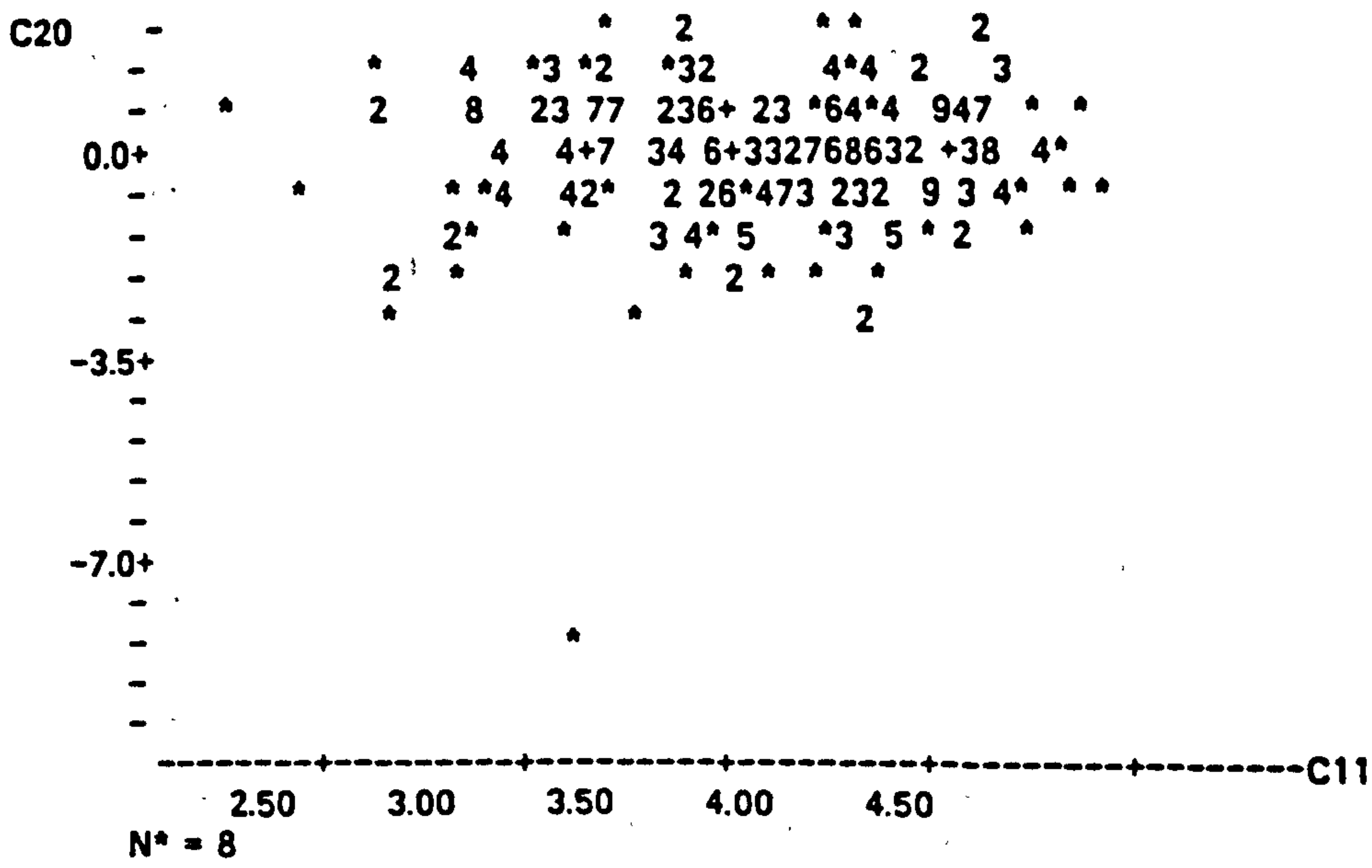
MTB > PLOT C12 C11



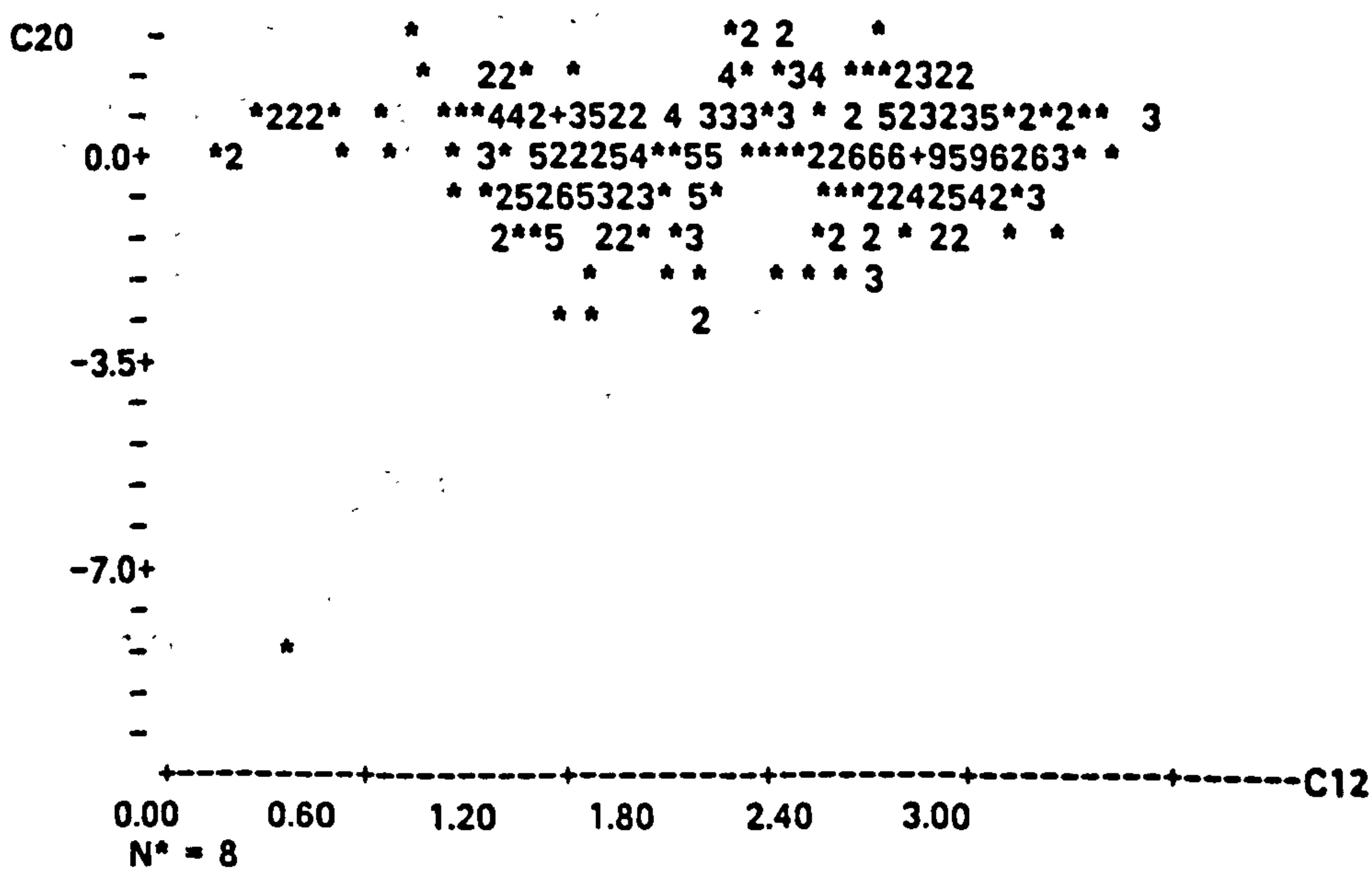
N\* = 8  
MTB > PLOT C13 C12



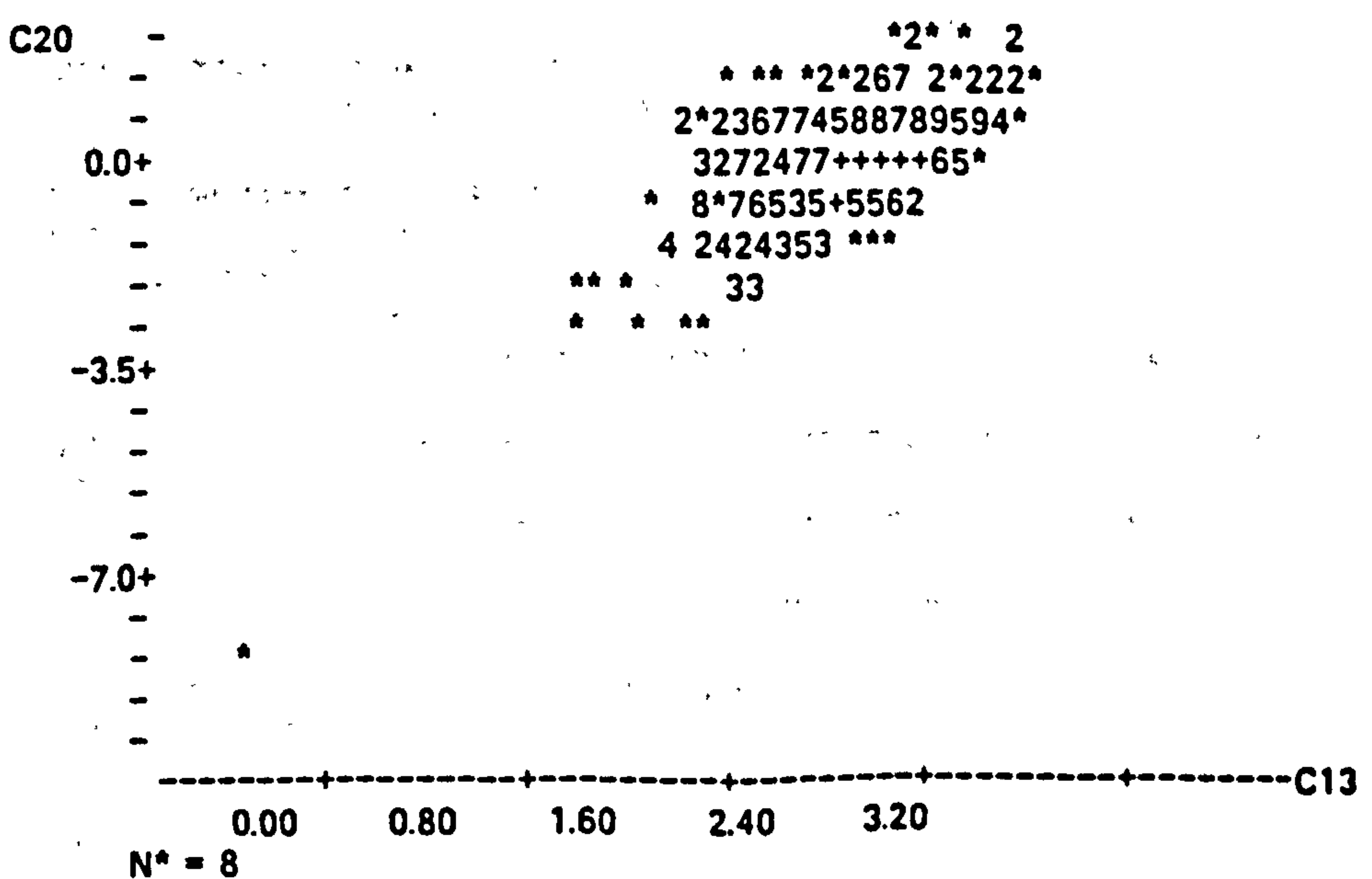
MTB > PLOT C20 C11



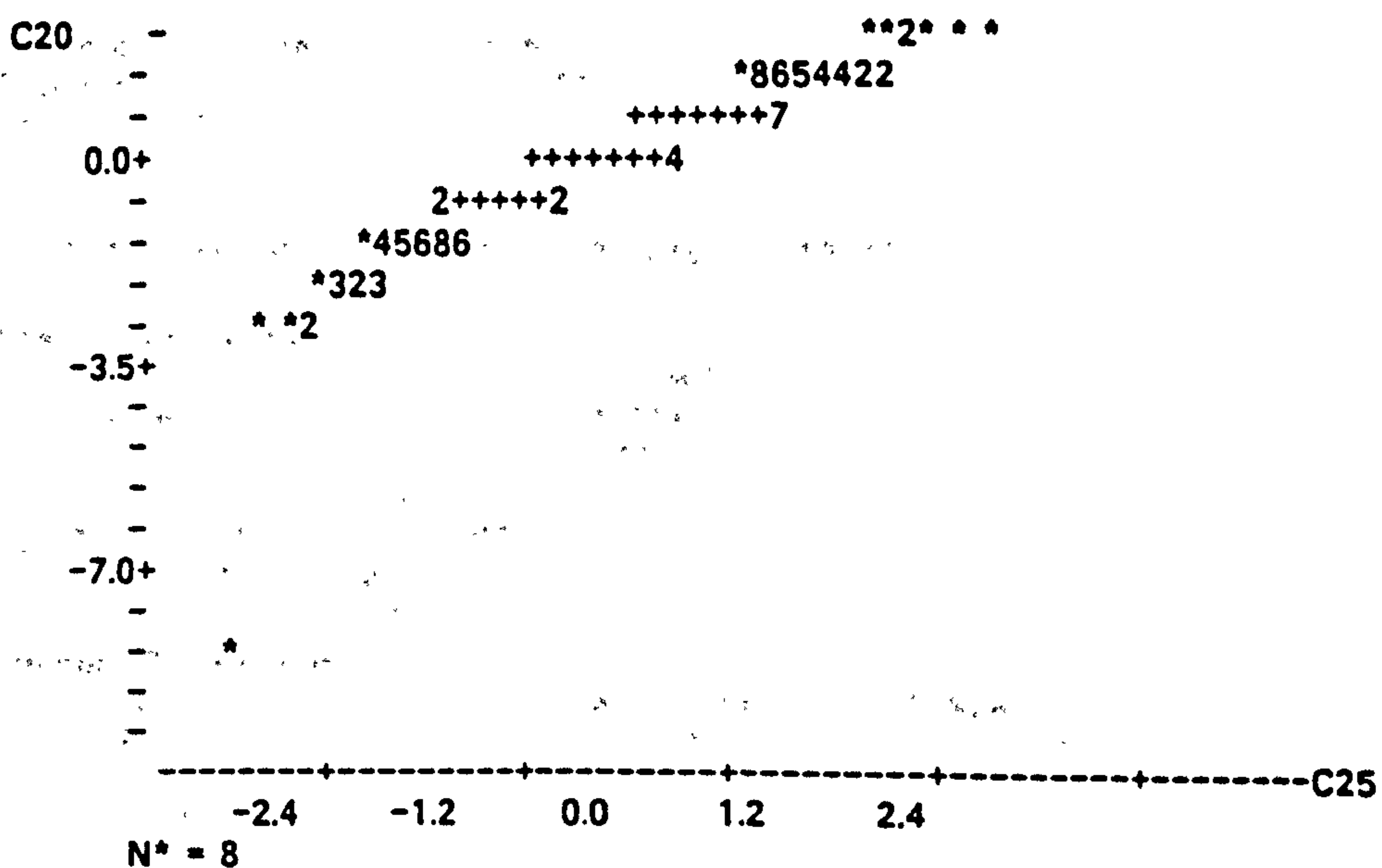
MTB > PLOT C20 C12



MTB > PLOT C20 C13

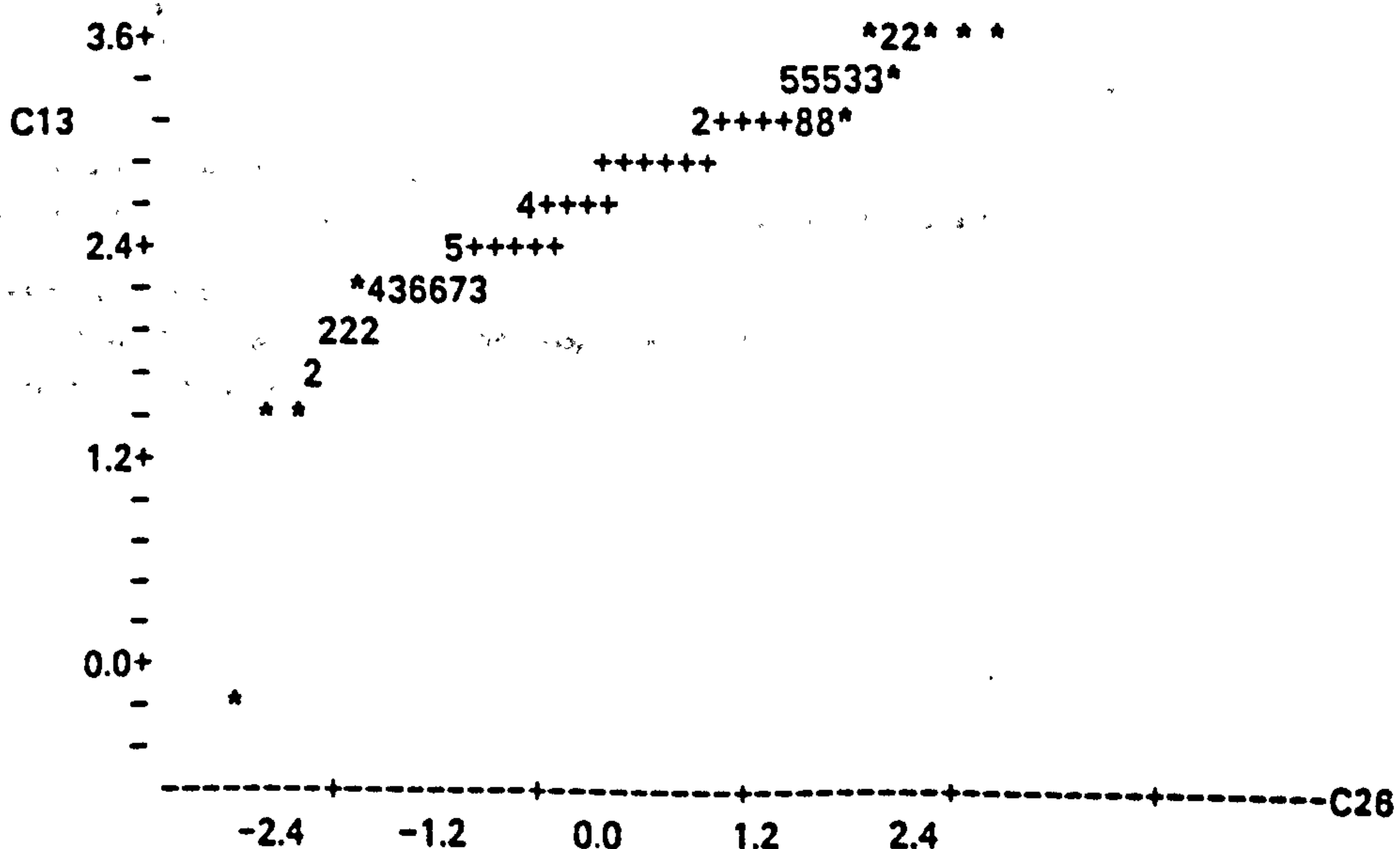


MTB > NSCOR C20 C25  
 MTB > PLOT C20 C25



MTB > CORRELATION OF C20 C25  
 Correlation of C20 and C25 = 0.945

MTB > NSCOR C13 C26  
 MTB > PLOT C13 C26



MTB > CORRELATION OF C13 C26  
 Correlation of C13 and C26 = 0.967

MTB > NOTE\*\*\*C30 = RESIDUAL e \*\*\*  
 MTB > LET C30=C13-C21  
 MTB > NOTE\*\*\*C31 = + OR - S.D.(e) \*\*\*  
 MTB > LET C31=C30/C20  
 MTB > NOTE\*\*\* K1 = SUM OF SQUARES/DEGREES OF FREEDOM \*\*\*  
 MTB > LET K1=27.743/361  
 MTB > NOTE\*\*\*C32 = VARIANCE OF PREDICTED VALUE OF WALL STRENGTH \*\*\*  
 MTB > LET C32=K1-(C31\*\*2)  
 MTB > NOTE\*\*\*C33 = STAND. DEV. OF PREDICTED WALL STRENGTH \*\*\*  
 MTB > LET C33=SQRT(C32+K1)  
 MTB > NOTE\*\*\*C34 = THE LOWER 95% CONFIDENCE LINE ON ln(f mw)&(f b) GRAPH \*\*\*  
 MTB > LET C34=C21-(1.645\*C33)  
 MTB > NOTE\*\*\*EQUATION OF CHARACTERISTIC STRENGTH \*\*\*  
 MTB > REGRESS C34 ON 2 PRED C11 C12 FIT IN C35

The regression equation is  
 $C34 = -0.245 + 0.532 C11 + 0.208 C12$

Predictor	Coef	Stdev	t-ratio
Constant	-0.244783	0.000451	-542.44
C11	0.531567	0.000110	4852.58
C12	0.208094	0.000075	2757.88

s = 0.0009736 R-sq = 100.0% R-sq(adj) = 100.0%

Analysis of Variance

SOURCE	DF	SS	MS
Regression	2	31.455	15.728
Error	361	0.000	0.000
Total	363	31.455	

SOURCE	DF	SEQ SS
C11	1	24.246
C12	1	7.209

Unusual Observations

Obs.	C11	C34	Fit	Stdev.Fit	Residual	St.Resid
1	2.29	1.53770	1.54406	0.00020	-0.00636	-6.67RX
2	2.55	1.71502	1.71976	0.00018	-0.00475	-4.96RX
141	4.39	2.77348	2.77553	0.00011	-0.00204	-2.11R
142	4.39	2.78010	2.78227	0.00011	-0.00216	-2.24R
143	4.39	2.77059	2.77258	0.00011	-0.00200	-2.06R
165	4.81	2.46487	2.46871	0.00015	-0.00385	-4.00RX
357	4.89	2.63809	2.64076	0.00013	-0.00267	-2.76R
358	3.12	1.49419	1.49699	0.00016	-0.00280	-2.92RX
359	3.12	1.53162	1.53377	0.00015	-0.00215	-2.23R
360	3.12	1.48846	1.49137	0.00016	-0.00291	-3.03RX
361	3.46	1.67656	1.67853	0.00014	-0.00197	-2.04R
362	3.46	1.64618	1.64875	0.00015	-0.00257	-2.67R
363	3.46	1.62916	1.63209	0.00016	-0.00293	-3.05RX
366	3.46	1.64618	1.64875	0.00015	-0.00257	-2.67R

R denotes an obs. with a large st. resid.

X denotes an obs. whose X value gives it large influence.

MTB > STOP

\*\*\* Minitab Release 5.1 \*\*\* Minitab, Inc. \*\*\*

Storage available 10000



**I.V. STATISTICAL ANALYSES OF MORTAR CUBES STRENGTHS**

**Mortar 1:1/4:3, cement:lime:sand mix by volume**

MTB > READ 'CHAR\_M1' C1  
331 ROWS READ

C1  
14.30 11.60 10.90 14.00 . . .

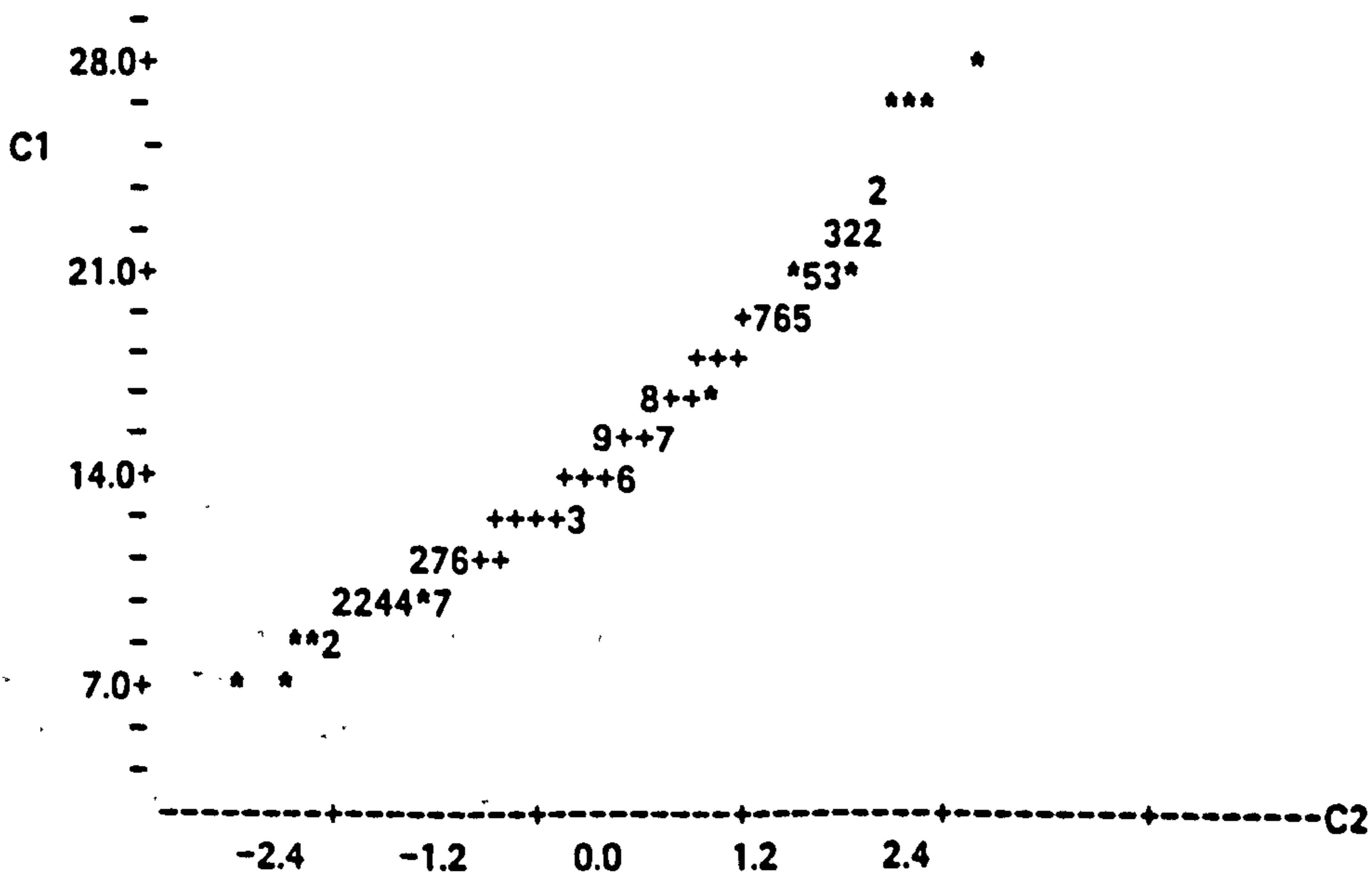
MTB > HISTOGRAM OF C1  
Histogram of C1 N = 331  
Each \* represents 2 obs.

Midpoint	Count
6	1 *
8	4 **
10	36 *****
12	61 *****
14	72 *****
16	65 *****
18	42 *****
20	31 *****
22	13 *****
24	2 *
26	2 *
28	2 *

MTB > AVERAGE THE VALUES IN C1  
MEAN = 15.110

MTB > STANDARD DEVIATION OF C1  
ST.DEV. = 3.5637

MTB > NSCOR OF C1, PUT INTO C2  
MTB > PLOT C1 C2



MTB > CORRELATION OF C1 C2  
Correlation of C1 and C2 = 0.990

MTB > TINTERVAL WITH 95 PERCENT CONFIDENCE FOR DATA IN C1

	N	MEAN	STDEV	SE MEAN	95.0 PERCENT C.I.
C1	331	15.110	3.564	0.196	( 14.725, 15.496)

Mortar 1:0.5:4.5, cement:lime:sand mix by volume

MTB > READ 'CHAR\_M2' C1  
110 ROWS READ

C1  
8.33 8.33 7.08 7.08 . . .

MTB > HISTOGRAM OF C1  
Histogram of C1 N = 110

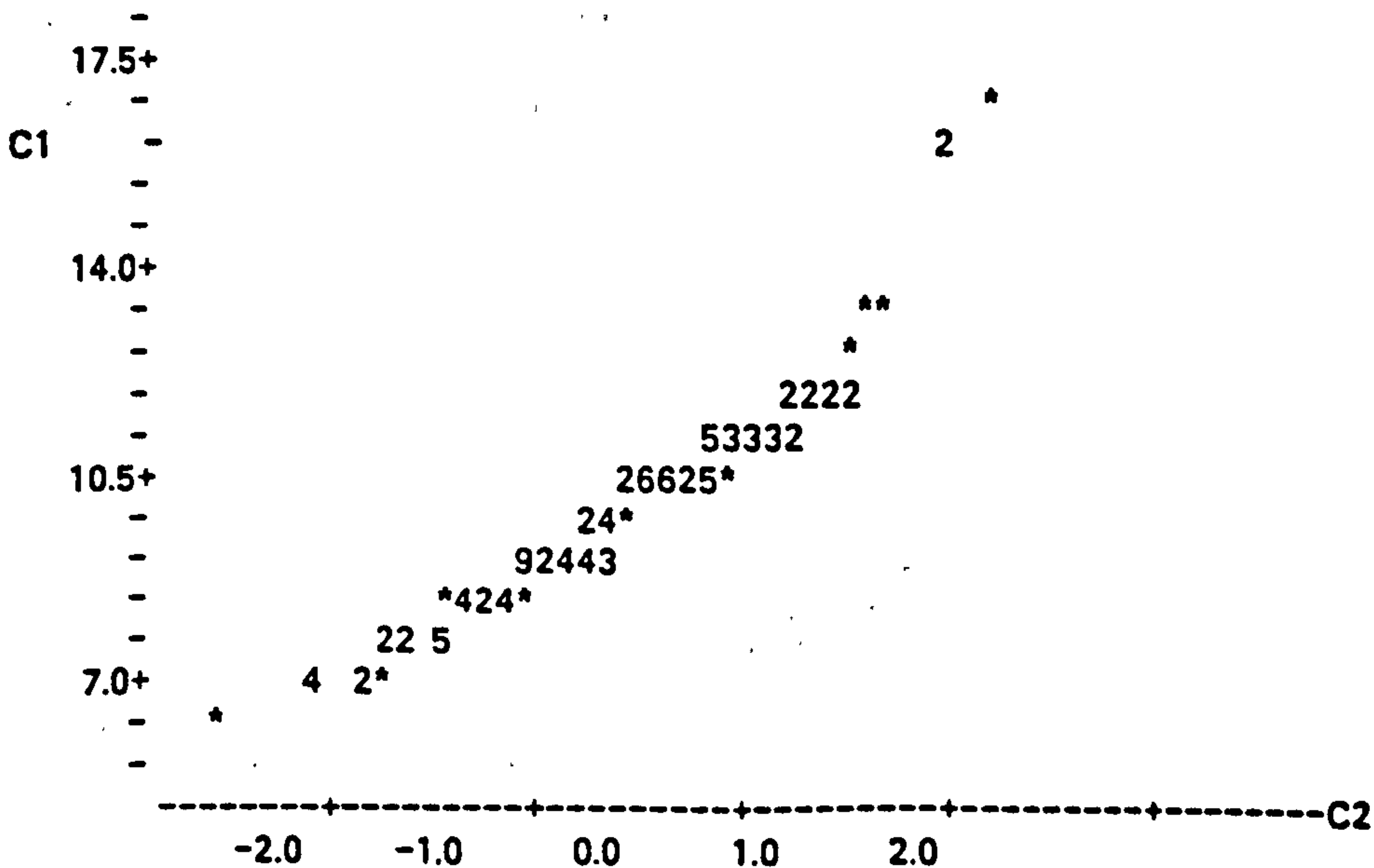
Midpoint	Count
6	1 *
7	7 *****
8	19 *****
9	25 *****
10	14 *****
11	29 *****
12	9 *****
13	3 ***
14	0
15	0
16	2 **
17	1 *

MTB > AVERAGE THE VALUES IN C1  
MEAN = 9.8645

MTB > STANDARD DEVIATION OF C1  
ST.DEV. = 1.8943

MTB > NSCOR OF C1, PUT INTO C2

MTB > PLOT C1 C2



MTB > CORRELATION OF C1 C2  
Correlation of C1 and C2 = 0.963

MTB > TINTERVAL WITH 95 PERCENT CONFIDENCE FOR DATA IN C1

	N	MEAN	STDEV	SE MEAN	95.0 PERCENT C.I.
C1	110	9.864	1.894	0.181	( 9.506, 10.222)

Mortar 1:1:6, cement:lime:sand mix by volume

MTB > READ 'CHAR\_M3' C1  
279 ROWS READ

C1  
9.14 7.61 8.36 4.47 . . .

MTB > HISTOGRAM OF C1  
Histogram of C1 N = 279  
Each \* represents 2 obs.

Midpoint	Count
2	3 **
3	43 *****
4	94 *****
5	56 *****
6	30 *****
7	27 *****
8	21 *****
9	2 *
10	0
11	0
12	1 *
13	0
14	1 *
15	0
16	1 *

MTB > AVERAGE THE VALUES IN C1

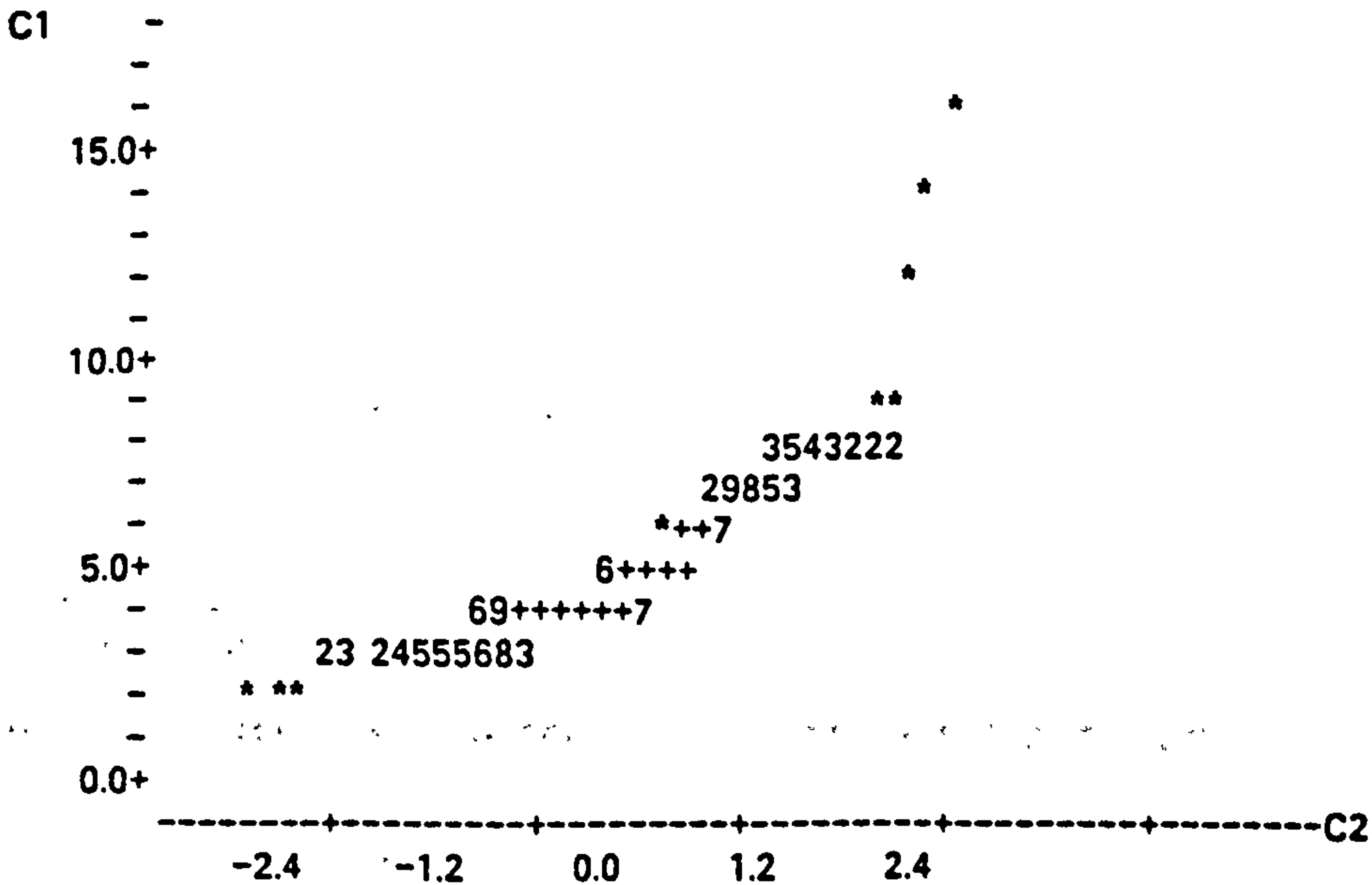
MEAN = 4.9420

MTB > STANDARD DEVIATION OF C1

ST.DEV. = 1.7604

MTB > NSCOR OF C1, PUT INTO C2

MTB > PLOT C1 C2



MTB > CORRELATION OF C1 C2  
Correlation of C1 and C2 = 0.922

MTB > TINTERVAL WITH 95 PERCENT CONFIDENCE FOR DATA IN C1

	N	MEAN	STDEV	SE MEAN	95.0 PERCENT C.I.
C1	279	4.942	1.760	0.105	( 4.734, 5.150)

Mortar 1:2:9, cement:lime:sand mix by volume

MTB > READ 'CHAR\_M4' C1  
15 ROWS READ

C1  
2.74 1.94 1.72 1.66 . . .

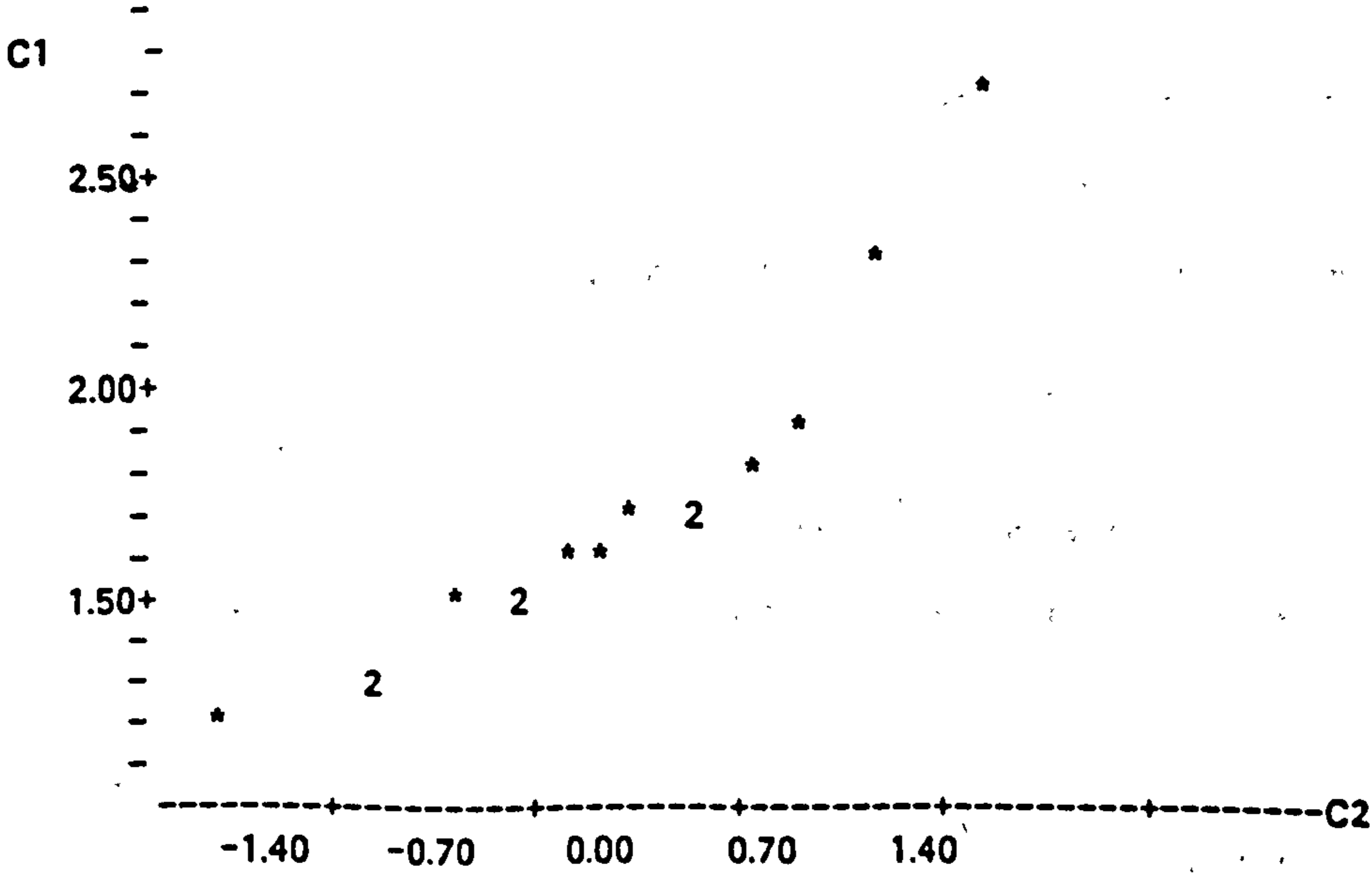
MTB > HISTOGRAM OF C1  
Histogram of C1 N = 15

Midpoint	Count
1.2	1 *
1.4	3 ***
1.6	5 *****
1.8	3 ***
2.0	1 *
2.2	0
2.4	1 *
2.6	0
2.8	1 *

MTB > AVERAGE THE VALUES IN C1  
MEAN = 1.6880

MTB > STANDARD DEVIATION OF C1  
ST.DEV. = 0.39975

MTB > NSCOR OF C1, PUT INTO C2  
MTB > PLOT C1 C2



MTB > CORRELATION OF C1 C2  
Correlation of C1 and C2 = 0.932

MTB > TINTERVAL WITH 95 PERCENT CONFIDENCE FOR DATA IN C1

	N	MEAN	STDEV	SE MEAN	95.0 PERCENT C.I.
C1	15	1.688	0.400	0.103	( 1.467, 1.909)

## II. APPENDIX B

### III. RESULTS OF TESTS ON BRICKWORK UNDER CONCENTRATED LOAD

Wall No.	Age at test (days)	Wall dimens. h x l x t (mm)	Plate dimens. a x b (mm)	Edge dist. d (mm)	$A_r$	d/l	b/t	l/a	$f_{cb}$ (Nmm <sup>-2</sup> )	$\zeta$
M 3	14	590x665x215.0	215x 50	107.50	0.075	0.162	0.233	3.09	32.09	2.79
M14	30								37.40	3.25
M 1	14	590x665x215.0	215x105	107.50	0.158	0.162	0.488	3.09	15.28	1.33
M18	55								17.63	1.53
M 2	15	590x665x215.0	215x160	107.50	0.241	0.162	0.744	3.09	19.33	1.68
M11	38								20.35	1.77
M19	53								23.66	2.06
M 7	18	590x665x215.0	215x 50	166.25	0.075	0.250	0.233	3.09	32.56	2.83
M15	30								36.28	3.15
M 8	35	590x665x215.0	215x105	166.25	0.158	0.250	0.488	3.09	23.48	2.04
M17	55								26.00	2.26
M10	35	590x665x215.0	215x160	166.25	0.241	0.250	0.744	3.09	21.80	1.90
M 9	36								20.20	1.76
M21	53								18.63	1.62
M 6	18	590x665x215.0	215x 50	332.50	0.075	0.500	0.233	3.09	28.38	2.47
M13	29								40.47	3.52
M 5	15	590x665x215.0	215x105	332.50	0.158	0.500	0.488	3.09	19.29	1.68
M16	30								30.12	2.62
M 4	17	590x665x215.0	215x160	332.50	0.241	0.500	0.744	3.09	14.46	1.26
M12	38								22.09	1.92
M20	53								16.86	1.47

$$f_b = 72.70 \text{ Nmm}^{-2}$$

Mortar mix by volume 1:1/4:3;  $f_m = 12.69 \text{ Nmm}^{-2}$  cured hydrally

$f_m = 22.97 \text{ Nmm}^{-2}$  cured by covering in Polyethene sheet (same as masonry)

$$f_k = 11.50 \text{ Nmm}^{-2}$$

Prism strength:

$$f_p = 20.53 \text{ Nmm}^{-2}$$

$$f_{kp} = 13.60 \text{ Nmm}^{-2}$$

$$f_p = 23.54 \text{ Nmm}^{-2}$$

$$f_{kp} = 20.00 \text{ Nmm}^{-2}$$

$$f_p = 14.45 \text{ Nmm}^{-2}$$

$$f_{kp} = 12.50 \text{ Nmm}^{-2}$$

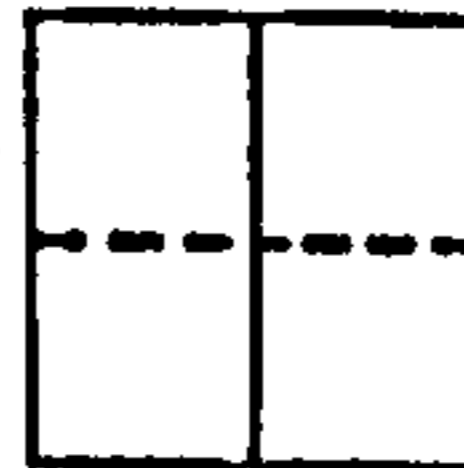
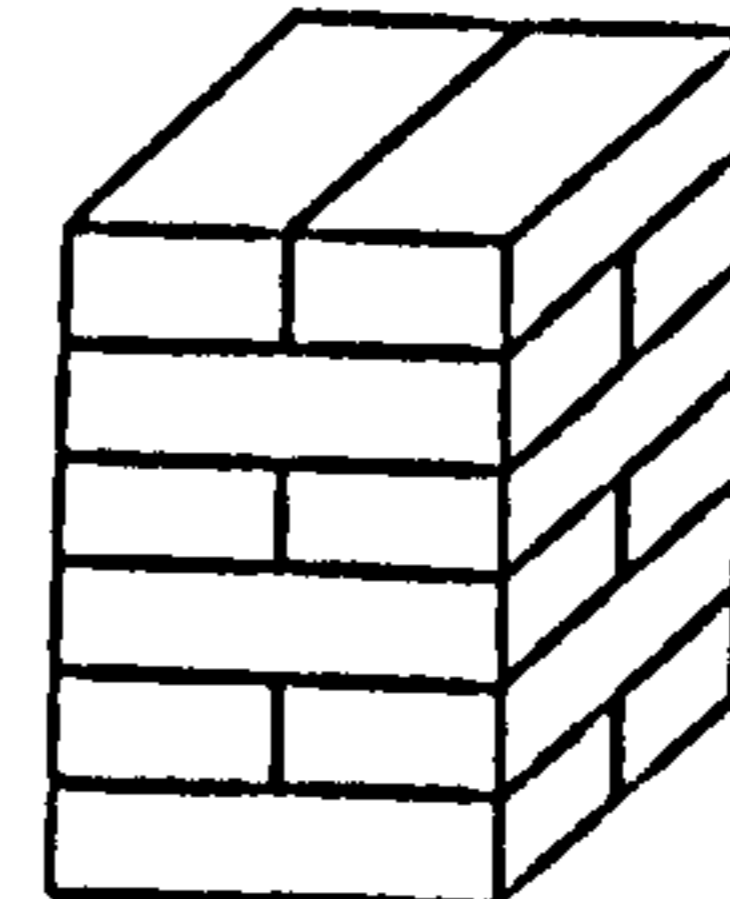
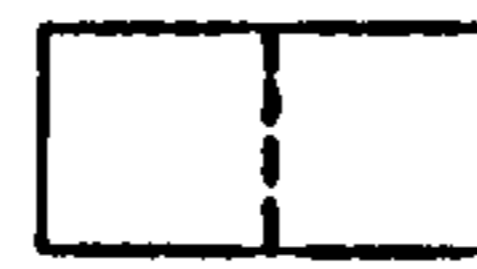
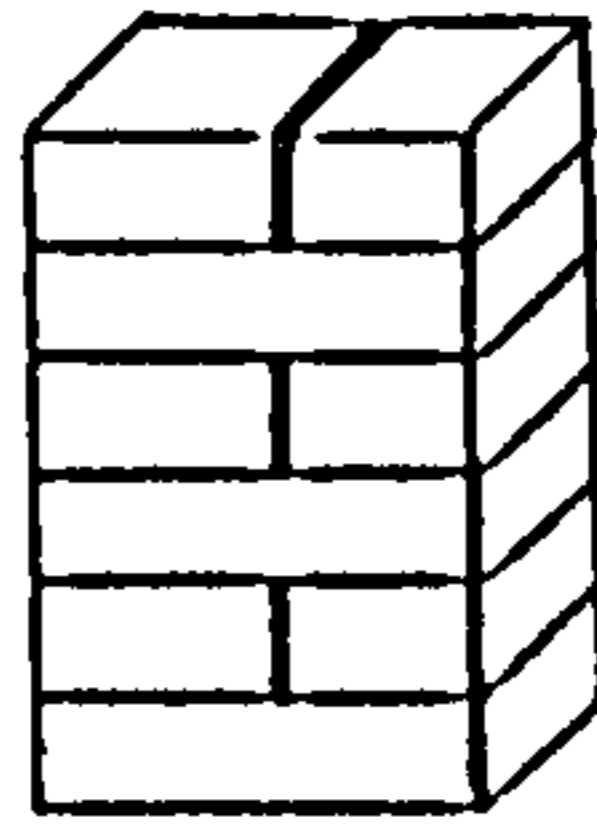
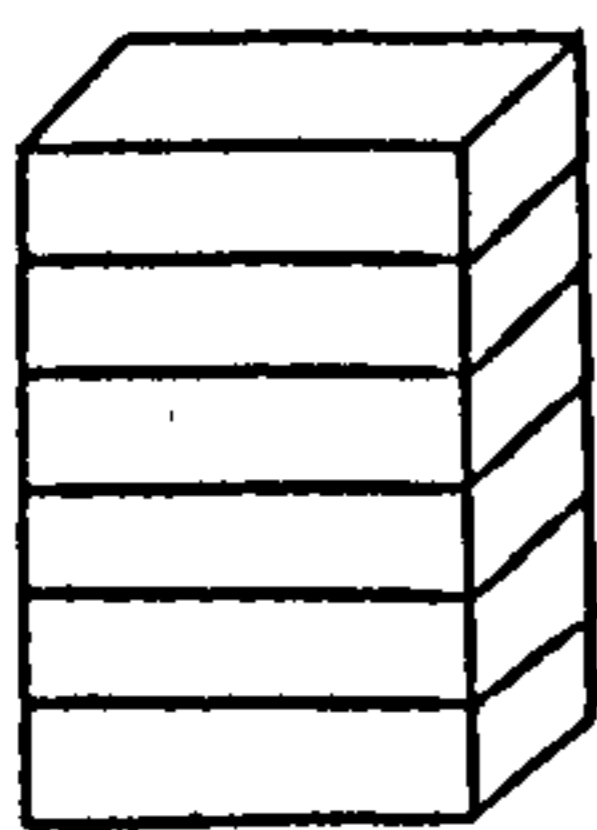


Table B1 - Test results of 215mm thick masonry type M under concentrated edge loading.

(after Malek<sup>[67]</sup>)

Wall No.	Age at test (days)	Wall dimens. h x l x t (mm)	Plate dimens. a x b (mm)	Edge dist. d (mm)	$A_r$	d/l	b/t	l/a	$f_{cb}$ (Nmm <sup>-2</sup> )	$\zeta$
H 1	32	590x665x215.0	50x215	25.00	0.075	0.038	1.0	13.30	28.65	2.49
H 2	32		50x215	25.00	0.075	0.038	1.0	13.30	32.37	2.81
H 1	40		105x215	52.50	0.158	0.079	1.0	6.33	28.22	2.45
H 8	39		105x215	52.50	0.158	0.079	1.0	6.33	21.97	1.91
H13	26		160x215	80.00	0.241	0.120	1.0	4.16	15.81	1.37
H14	31	160x215	80.00	0.241	0.120	1.0	4.16	19.83	1.72	
H 3	28	590x665x215.0	50x215	166.25	0.075	0.250	1.0	13.30	33.12	2.88
H 4	28		50x215	166.25	0.075	0.250	1.0	13.30	37.49	3.28
H 9	38	590x665x215.0	105x215	166.25	0.158	0.250	1.0	6.33	22.77	1.98
H10	39		105x215	166.25	0.158	0.250	1.0	6.33	29.46	2.56
H 5	27	590x665x215.0	50x215	332.50	0.075	0.500	1.0	13.30	23.91	2.08
H 6	27		50x215	332.50	0.075	0.500	1.0	13.30	26.14	2.27
H11	38	590x665x215.0	105x215	332.50	0.158	0.500	1.0	6.33	24.98	2.17
H15	30		160x215	332.50	0.241	0.500	1.0	4.16	23.87	2.08
H16	33		160x215	332.50	0.241	0.500	1.0	4.16	23.87	2.08
			160x215	332.50	0.241	0.500	1.0	4.16	24.53	2.13

$$f_b = 72.70 \text{ Nmm}^{-2}$$

Mortar mix by volume 1:1/4:3

$$f_k = 11.50 \text{ Nmm}^{-2}$$

Table B2 - Test results of 215mm thick masonry under concentrated strip concentrated strip loading.

(after Hendry<sup>[unpublished]</sup>).

Wall No.	Age at test (days)	Wall dimens. h x l x t (mm)	Plate dimens. a x b (mm)	Edge dist. d (mm)	$A_r$	d/l	b/t	l/a	$f_{cb}$ (Nmm <sup>-2</sup> )	$\zeta$
L 1	30	590x665x102.5	50x102.5	25.00	0.075	0.038	1.0	13.30	17.48	1.94
L 9	31		50x102.5	25.00	0.075	0.038	1.0	13.30	19.14	2.13
L 4	29		105x102.5	52.50	0.158	0.079	1.0	6.33	11.92	1.32
L17	28		105x102.5	52.50	0.158	0.079	1.0	6.33	12.51	1.39
L14	28	590x665x102.5	160x102.5	80.00	0.241	0.120	1.0	4.16	13.95	1.55
L16	28		160x102.5	80.00	0.241	0.120	1.0	4.16	12.27	1.36
L 2	29	590x665x102.5	50x102.5	166.25	0.075	0.250	1.0	13.30	22.70	2.52
L12	28		50x102.5	166.25	0.075	0.250	1.0	13.30	24.82	2.76
L 5	29	590x665x102.5	105x102.5	166.25	0.158	0.250	1.0	6.33	17.23	1.91
L13	28		105x102.5	166.25	0.158	0.250	1.0	6.33	14.27	1.59
L18	28	590x665x102.5	160x102.5	166.25	0.241	0.250	1.0	4.16	13.81	1.53
L20	29		160x102.5	166.25	0.241	0.250	1.0	4.16	14.74	1.64
L 3	29	590x665x102.5	50x102.5	332.50	0.075	0.500	1.0	13.30	23.86	2.65
L 7	31		50x102.5	332.50	0.075	0.500	1.0	13.30	22.68	2.52
L15	28		50x102.5	332.50	0.075	0.500	1.0	13.30	24.67	2.74
L 6	28		105x102.5	332.50	0.158	0.500	1.0	6.33	20.48	2.28
L 8	31	590x665x102.5	105x102.5	332.50	0.158	0.500	1.0	6.33	19.33	2.15
L19	28		105x102.5	332.50	0.158	0.500	1.0	6.33	18.97	2.11
L10	28	590x665x102.5	160x102.5	332.50	0.241	0.500	1.0	4.16	12.76	1.42
L16	33		160x102.5	332.50	0.241	0.500	1.0	4.16	24.53	1.38

$$f_b = 33.02 \text{ Nmm}^{-2}$$

Mortar mix by volume 1:1:6;  $f_m = 6.22 \text{ Nmm}^{-2}$  cured hydrallycally

$f_m = 6.41 \text{ Nmm}^{-2}$  cured by covering in Polyethene sheet (same as masonry)

$$f_k = 9.0 \text{ Nmm}^{-2}$$

Prism strength:  
 $f_p = 8.35 \text{ Nmm}^{-2}$

$$f_{kp} = 6.60 \text{ Nmm}^{-2}$$

$$f_p = 8.47 \text{ Nmm}^{-2}$$

$$f_{kp} = 6.35 \text{ Nmm}^{-2}$$

$$f_p = 7.68 \text{ Nmm}^{-2}$$

$$f_{kp} = 5.85 \text{ Nmm}^{-2}$$

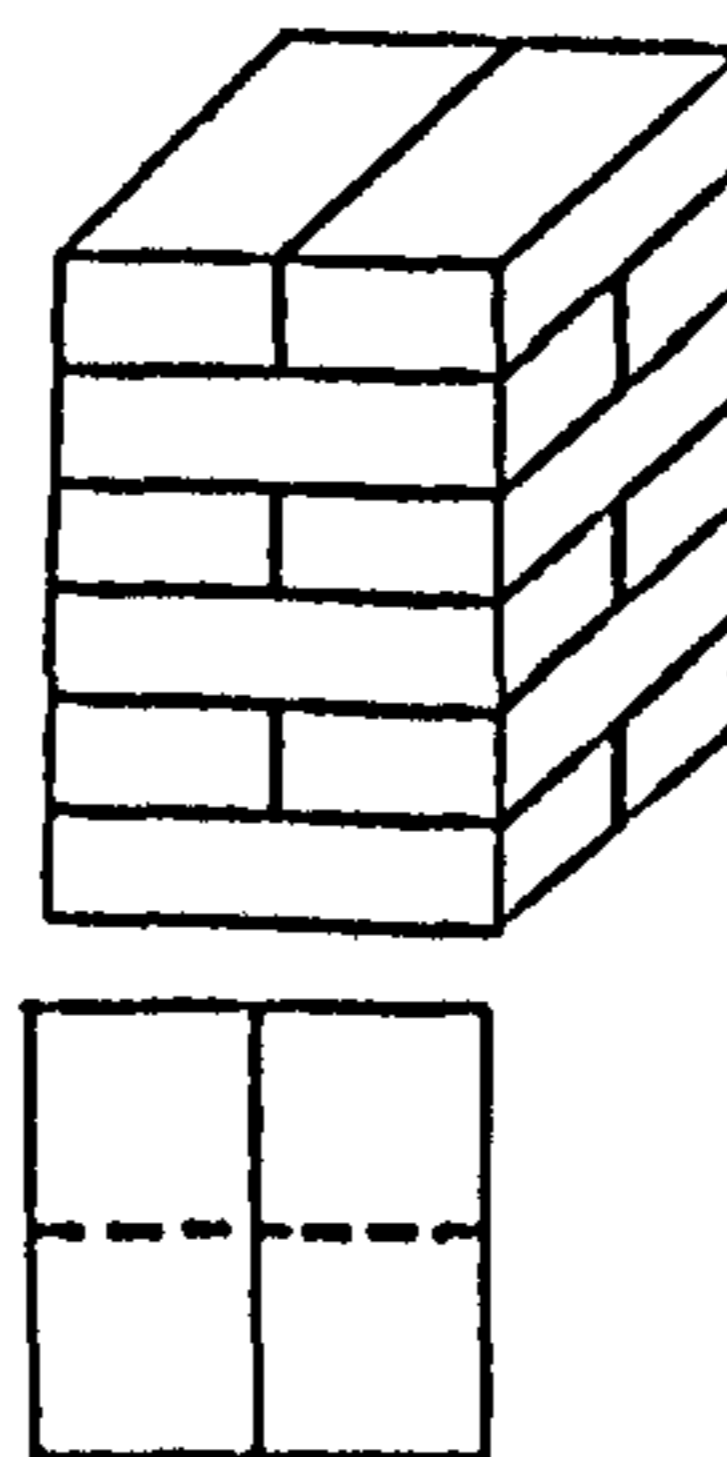
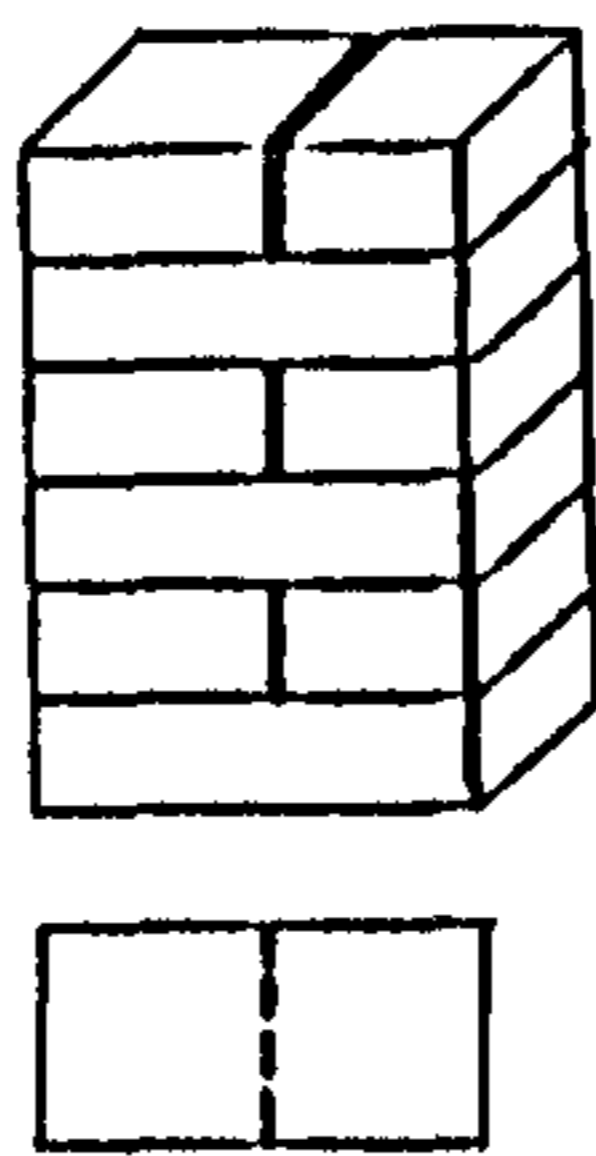
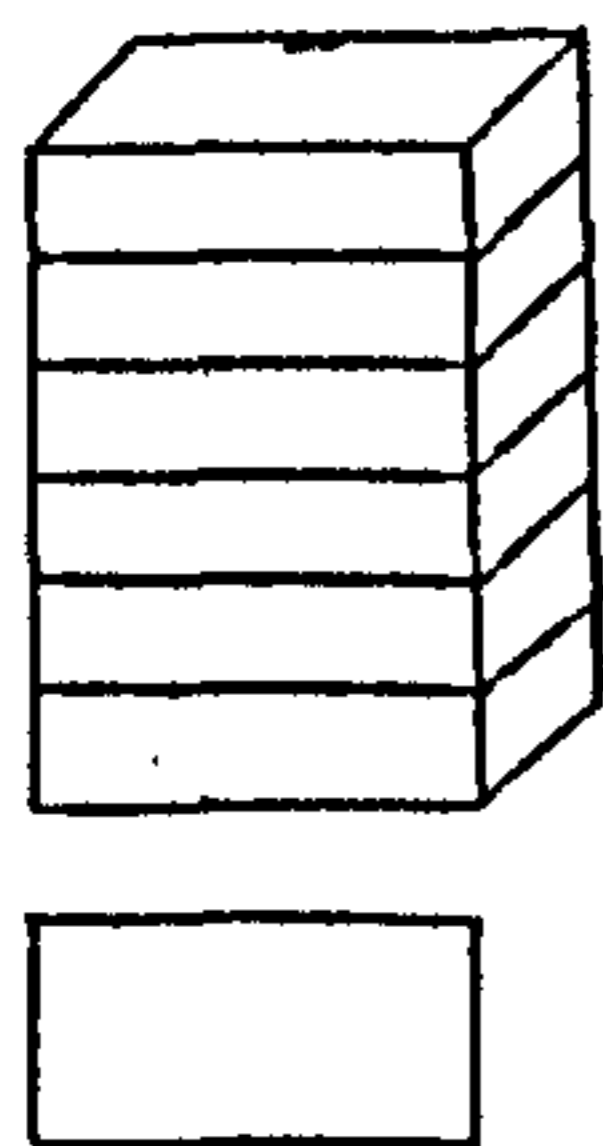


Table B3 - Test results of 102.5mm thick masonry type L under concentrated strip loading.

(after Hendry<sup>[unpublished]</sup>).